WAVE-INDUCED CURRENTS AND SEDIMENT TRANSPORT ON GRAVEL AND MIXED BEACHES

A thesis submitted to the Cardiff University

In candidature for the degree of

Doctor of Philosophy

by

Christos Antoniadis

B.Eng., M.Eng.

Division of Civil Engineering, Cardiff School of Engineering

Cardiff University

September 2008

ProQuest LLC
789 East Eisenhower Parkway
P.O. Box 1346
Ann Arbor, MI 48106-1346

This is purely a specimen sample layout for Declaration/Statements to be included in Higher Degree Theses.

****

DECLARATION

This work has not previously been accepted in substance for any degree and is not being concurrently submitted in candidature for any degree.

Signed.....(Candidate)

Date.....30-9-08.....

STATEMENT 1

This thesis is the result of my own investigations, except where otherwise stated. Other sources are acknowledged by footnotes giving explicit references. A bibliography is appended.

Signed.....(Candidate)

Date.....30-9-08.....

STATEMENT 2

I hereby give consent for my thesis, to be available for photocopying and for inter-library loan, and for the title and summary to be made available to outside organisations.

Signed.....(Candidate)

Date.....30-9-08.....

Candidates on whose behalf a bar on access has been approved by the University should use the following version of Statement 2.

I herby give consent for my thesis, if accepted, to be available for photocopying and for inter-library loans **after expiry of a bar on access approved by the University of Wales on the special recommendation of the Constituent Institution/University College concerned.**

Signed.....(Candidate)

Date.....30-9-08.....

ABSTRACT

During the last few years the interest on the behaviour of both gravel and mixed beaches has increased because of the interest in soft coastal engineering measures for combating erosion. In contrast to gravel beaches, little research has been devoted to the sediment transport of beaches containing a mixture of both sand and gravel sediment (Mason and Coates, 2001). Thus, because of the limited understanding surrounding these beaches, mixed sand and gravel coastlines have a lot of research potential for both coastal resource management and scientific reasons. In recognition of this, a series of 3-dimensional physical model tests has been undertaken in order to examine the behaviour of gravel and mixed beaches more closely.

The 3-D physical model tests were carried out in the 3-D wave basin located at Franzius-Institute (Marienwerder) of University of Hannover, at a nominal scale of 1:1. During the study, measurements of beach profiles and of cross-shore and long-shore current data were taken, generated by oblique wave attack, along gravel and mixed beaches with a uniform slope and a trench.

New formulae for predicting wave breaking depth index, breaking depth and height, undertow velocity, long-shore current velocity and step and berm elevation have been proposed. A new parametric profile model has been developed in order to predict the beach profile changes of gravel and mixed beaches with a uniform slope and a trench due to sediment transport.

The results of the new parametric profile model and of the refined parametric model SHINGLE have been validated against field and experimental data. The results of this validation were encouraging for the refined model, showing better accuracy than the SHINGLE model and showing that it has the potential to be a valuable tool in the design and management of gravel and mixed beaches.

ACKNOWLEDGMENTS

I would like to express my sincere gratitude to my supervisor Professor Binliang Lin, for his help, encouragement, guidance and support during this research project.

I would also like to express my earnest gratitude to Professor Roger A. Falconer for his support.

I am eternally grateful to my brother (Ανέστη Αντωνιάδη), my mother (Δήμητρα Τζελεπάκη) and my father (Κώστα Αντωνιάδη) for their unbounded love and support. I would like to thank my grandparents (Χρήστο Τζελεπάκη και Δέσποινα Μαλάκη) and my aunt (Τένια Τζελεπάκη) for their enormous support during this period.

I would like to thank all the people below (with no specific order) for their support:

Manos Orfanoudakis (Έτσι να γουστάρουμε, τί λέμε τωρα), Antonis Karantzas (or Andi Karanxha, a.k.a The Boss), Dionysis Pantazis (a.k.a. Gianluca), the tenants of 301 Cowley Road (Salar, Paola, Annabelle, Marco, Orestis, Eleni), Chris Lee, Dr. Belen Lopez De San Roman Blanco, Dr. Tim Pullen, Dr. Alan Brampton, Dr. Isabel Garcia-Hermosa, Jean-Philippe Vidal, Ronan Hock Lee, Dr. Saied Mortazavy Dorcheh, Dr. Umme Kulsum Navera, Dr. Theo Grammenos, Dr. John Ortiz, Andrews, Allan Davies, and last but not least Dr. Pumpkins.

Last but not least I would like to thank all the people below (with no specific order) for their comments and their suggestions relating to my thesis:

Prof. William Allsop, Dr. Keith Powell, Dr. Phil Besley, Dr. Maree Hemmingsen, Prof. Andrew Chadwick, Dr. Charlotte Obhrai, Dr. Iain Dawe, Dr. Leont'yev I.O., Prof. N.Kobayashi, Prof.G.F.Bullock, Prof. Tai-Wen Hsu, Dr. M. Kleinhans, Dr. Stephen Richardson, Dr. Sebastien Dupray, Dr. Karambas Theofanis, Dr. Adrian Pedrozo-Acuña, Dr. Tobias Linke, Andrew Steele, Dr. Tom Coates, Dr. Richard Whitehouse, Dr. James Sutherland and Dr. Terry Stewart.

DEDICATED

TO MY GRANDPARENTS

CHRISTO TZELEPAKI AND DESPOINA MALAKI

ΑΦΙΕΡΩΜΕΝΟ

ΣΤΟΝ ΠΑΠΠΟΥ ΚΑΙ ΤΗΝ ΓΙΑΓΙΑ ΜΟΥ

ΧΡΗΣΤΟ ΤΖΕΛΕΠΑΚΗ ΚΑΙ ΔΕΣΠΟΙΝΑ ΜΑΛΑΚΗ

TABLE OF CONTENTS

LIST OF FIGURES

LIST OF TABLES

NOTATION/SYMBOLS

A	Archimedes buoyancy index
A	coefficient (=0.12)
A, A_p	sediment scale parameter
BSS	Brier Skill Score
$B(t)$	instantaneous total height of the active profile above the water level
B_h	elevation of the berm
C	Chézy coefficient
c	computed (index)
c	wave celerity
c_b	phase velocity at the breaking point
c_g	group velocity
d	characteristic diameter of sediment
d	water depth measured from the level at rest
d/L	relative water depth
d/L_0	relative deep water depth
D_{15F}	grain size diameter of the filter where 15% by weight of the soil particles are smaller in diameter
D_{16}	grain size diameter where 16% by weight of the soil particles are smaller in diameter

D_5	grain size diameter where 5% by weight of the soil particles are smaller in diameter
D_{50}	diameter of the median-grain size of the sediment particle
D_{50}	median diameter of the sediment particle
D_{84}	grain size diameter where 84% by weight of the soil particles are smaller in diameter
D_{85B}	grain size diameter where 85% of the base or filter soil is smaller in diameter
D_{95}	grain size diameter where 95% by weight of the soil particles are smaller in diameter
D_B	time-averaged rate of energy dissipation per unit horizontal area due to wave breaking
D_b	schematised distance from the point, where the local water depth is equal to the still water level, to the breaking point
d_b	wave breaking depth
D_F	effective thickness of beach material measured relative to the initial slope
D_f	time-averaged rate of energy dissipation per unit horizontal area due to bottom friction
D_i	schematised distance from the point, where the local water depth is equal to the still water level, to the point of interest
D_t	schematised distance between the breaking point and the point of interest

D_w	depth of water at beach toe
E	wave energy
f	frequency
f	friction factor
f	empirical Darcy-Weisbach friction factor
F_x, F_y	time-averaged energy flux per unit width in the x and y-directions, respectively
g	acceleration due to gravity (=9.81 m/s^2)
h	still water depth
h	elevation of the water table above a given datum
H	wave height
h_*	offshore depth of closure
H/L	wave steepness
h_0	asymptotic depth at a great offshore distance
H_{0x}	deep water significant wave height
$H_{1/10}$	mean height of 10% highest waves
$H_{1/3}$	mean height of 33% highest waves
h_b	breaking depth
H_b	breaking wave height
h_i	schematised local water depth
h_j	schematised depth above still water depth
H_m	zeroth-moment wave height

H_{m0}	estimation of the significant wave height from spectral analysis
H_{max}	maximum wave height
H_{mean}	mean wave height
H_o	nominal deepwater wave height
H_o'	unrefracted deepwater wave height
H_{rms}	root-mean-square wave height
H_s	significant wave height
h_t	schematised height of the trench
h_w	still water depth
k	decay constant
K	hydraulic conductivity (permeability)
k	wave number (=2π/L)
k_b	wave number at the breaking point
K_R	refraction coefficient
k_s	Nikuradse roughness
K_S	shoaling coefficient
L	wavelength
L_i	the length from the origin to the beach profile of interest
L_t	the total length of the beach
L_0	nominal deepwater wavelength
L_b	wavelength at breaking
L_m	wave length based on T_m

m	measured (index)
m	linear beach-face slope
m	suffix to model
m_0	beach face slope
m_0/k	equilibrium depth
m_o	total spectral variance
N	constant (=0.016)
n	constant (=2/3)
p	suffix to prototype
q_t	total average load in the submerged part of the beach
q_x, q_y	cross-shore and longshore volumetric sediment fluxes (per unit width in the direction normal to the sediment flux component)
R	coefficient which is accomplished by linear squares fitting with the available topographical data
R_{oo}	shoreline recession
R_r	long-shore force on the water column
S	sea level rise
s	specific yield (dimensionless)
S.W.L.	still water level
S_{xx}, S_{xy}, S_{yy}	time-averaged momentum fluxes similar to radiation stresses
$S_{xy}^{\cdot}$	radiation stress component
t	time

T	wave period
$\tan\beta$	beach slope
$TH_{1/10}$	mean period of mean wave height of 10% highest waves
$TH_{1/3}$	mean period of mean wave height of 33% highest waves
TH_{max}	mean period of maximum wave height
T_m	average wave period
T_p	peak spectral period
U	current velocity in x-direction
u_a	reference horizontal velocity at the elevation given by z_a (z_a=-0.531h)
u_b	wave orbital velocity under the wave breaking point
Uo	undertow
V	current velocity in y-direction
v_b	long-shore velocity at the breaking point
V_s	fall velocity of a beach material particle of size D_{50}
$\bar{v}_l$	mean longshore velocity at the breaker zone
w, w_f	fall velocity
W_b	surf zone width
w_t	schematised width of the trench
x	horizontal distance from the shoreline
x_0	point midway between the shoreline and the position of the first breaking point of the incident wave

x_b	horizontal distance to the breaker line from shore
X_b	schematised distance from the origin to the breaking point
X_e	schematised distance from the origin to the end of the beach
X_h	schematised distance from the origin to the point of the highest h_j
X_i	schematised distance from the origin to the local point of interest
X_w	schematised distance from the origin to the point where $Y_i=h_w$
y	still-water depth (vertical distance)
Y_i	schematised local bed level
Y_p	predicted local bed level
z_b	bed level
z_b	bottom elevation
$z_{b,0}$	initial bed level
z_{step}	elevation of the step
α	cubic velocity profile parameter
γ	breaking depth index
Δ	relative density of sediment
δ	roller thickness
$\Delta z_{b,m}$	error of measured bed level
Δy(-ve)	retreat of the shoreline
ε_m	coefficient (=2.0)
ε_v	eddy viscosity
ζ	free surface elevation

ζ	wave setup
η	elevation of the water level due to the wave setup/setdown
$\bar{\eta}$	wave set-up
θ	angle of wave attack
θ_0	deepwater wave angle
θ_b	wave angle at the breaking point
κ	breaker index
ν	kinematic viscosity of water
ξ	Iribarren number
ρ	density of liquid
ρ_s	density of sediment
σ	sorting index
τ_{bx}	x components of bottom shear stress
τ_{by}	y components of bottom shear stress
φ	angle of the wave attack
Ω_b	breaker height index
$\lvert\ \rvert$	absolute value
<..>	averaging procedure over time series

CHAPTER 1

INTRODUCTION

1.0 BACKGROUND

Due to global warming and climate change, there is increased storminess and sea level and as a result erosion of the world's coastlines has become a well-know phenomena. A coastal protection with an economical solution is needed. Coastal managers and coastal engineers are beginning to give attention to gravel and mixed beaches due to the fact that they are two of the most effective natural sea defences.

Over the past years the majority of existing coastal research has been conducted on sand beaches. Comparatively little research was carried out using gravel beaches and even less research conducted with mixed (gravel and sand) beaches. As a result, this research field is at its early stages. These beach types show important differences in their morphodynamic responses to environmental conditions despite the fact that there are general principles that can be applied to them. The differential sediment sizes within mixed beaches, makes them more complex than the gravel beaches.

Despite their neglected status, gravel beaches are an important landform, and due to their distinct properties, have a number of applications for coastal management. With continued research, gravel beaches should become more widely recognised for the role they play as a highly effective and dynamic buffer against the forces of the sea. Gravel beaches are highly efficient dissipators of wave action and they can provide excellent natural or managed defence systems. They are particularly efficient since their high permeability enables energy loss through percolation within the beach.

The dissipation of the mixed beaches depends on the proportion of sand compared to gravel. Because of the limited understanding surrounding these beaches, mixed (sand and gravel) coastlines have a lot of research potential for both coastal resource management and scientific reasons. Mixed sediment beaches occur commonly around the shores of regions where the effects of glacitation have provided an abundant source of sand and gravels for subsequent re-working by Holocene rising sea levels (Mason & Coates, 2001).

However these beaches (gravel and mixed) in common with other types of beach will suffer erosion under extreme conditions of storm events with high water level. Therefore, predicting their evolution is very important issue due to the fact that pattern of accumulation or erosion can be identified and calculated. Thus, an accurate assessment and maintenance of the beach structure can be done and the beach failure can be prevented.

Therefore, there is a need, from a scientific and coastal management perspective to have a deeper understanding of how gravel and mixed beaches operate.

1.1 AIM AND OBJECTIVES OF THE RESEARCH STUDY

The main aim of the present research study is to understand the dynamics of gravel and mixed beaches. In order to achieve that, the study had to be related to up to date research done on gravel and mixed beaches and it had to focus on the following main objectives which were to:

- investigate the hydrodynamics and the cross-shore sediment transport of gravel and mixed beaches evolved by oblique wave attack,
- examine the influence of a feature (trench) in their behaviour,
- identify similarities and differences between them,
- assess the effectiveness of commonly used beach profile response models for use in gravel and mixed beaches,
- develop new beach profile response model for both beach types and,
- verify and calibrate the new model against laboratory and field data.

1.2 THESIS STRUCTURE

The thesis is divided into eight chapters, which can be summarised as follows:

Chapter II describes and explains the nature and the characteristics of gravel and mixed (gravel and sand) beaches and their differences. A review of previous models/studies about the characteristics of the sedimentation and the beach profile prediction (by numerical or parametric models) of both types of beach is undertaken. These reviews could give an overall idea of the research done in the coastal hydrodynamic processes and the mechanics of sediment transport of both types of beach and also outline the basis for the current research work.

Chapter III provides descriptions of what kinds of experiments were undertaken and how the gravel and mixed beach were represented. Furthermore, it presents the facility where the experiments took place, the instrumentation that was used during the experiments and how it was calibrated and used.

Chapter IV describes the range of wave conditions that were used during the experimental tests. The evolvement of the beach profiles, of both types of beach, in the experiments was presented. Moreover, it describes the influence of the different wave parameters and the influence of the different beach materials during the tests and also how both types of beach did compare.

Chapter V presents the analysis of the results from the experimental tests. It introduces new formulae for wave breaking, undertow current and long-shore current. A comparison between the tests with previous models was undertaken and new formulae for berm and step elevation were presented. Finally, the sediment balance of both types of beach was described.

Chapter VI consists of the development of a new equilibrium beach profile model. It presents the parameters that were used in the model and also the comparison between the new parametric model, the leading parametric model available (for predicting the profile development of gravel and dissimilar sediment beaches) and the results from the experimental tests.

Chapter VII describes the application of the new parametric model to a physical shingle beach, namely Chesil Beach. A detailed analysis was undertaken. The model was calibrated and verified against different sets of field data from December 1993 to May 1996.

Chapter VIII provides a summary of the main findings/ conclusions of the study including the presentation of the new formulae and of the new parametric model for gravel and mixed beach. This is followed citing recommendations for future research.

CHAPTER 2

LITERATURE REVIEW

2.0 INTRODUCTION

In the CIRIA Beach Management Manual (Simm et al., 1996), a beach is defined *as a deposit of non-cohesive material (e.g. sand, gravel) situated on the interface between dry land and the sea (or other large expanses of water) and actively "worked" by present-day hydrodynamic processes (i.e. waves, tides and currents) and sometimes by winds*. The three types of beach are: sand beach, shingle or gravel beach and coarse grained beach.

1. Sand beaches are formed of non-cohesive sediment between about 63μm and 2mm, and have slopes range typically about 1:100 to 1:12. Sand can be transported by both waves and tidal currents. Despite the fact that sand is permeable, the interstices in the swash zone are rapidly saturated leaving an essentially impermeable surface.
2. Shingle/gravel beaches comprise material greater than 2mm (up to about 256mm) and have slopes range typically about 1:8 to 1:2. Gravel can be transported mainly by waves and only during storms some of its materials become mobile. Gravel is very permeable and tends to be sorted by size across shore with large material thrown up to form a steep storm crests.
3. Coarse grained beaches consist of steeply inclined gravel or cobbles. Additionally, coarse grained beaches are formed of a less steep upper beach of mixed sand and gravel which fronted by a wide lower foreshore of sand or a rock platform. Despite the fact that mixed beaches have the characteristics of the first two types of beach, they are totally different to sand and gravel beaches from a coastal process perspective.

Moreover, beaches have also divided into those which are dissipative and those which are reflective beaches. Dissipative beaches characterised by a wide surf zone and normally numerous spilling lines of breakers, and reflective beaches characterised by a steep beach-face and mostly surging or plunging waves. These beaches have different morphodynamics and sediment transport related to each one (Lopez de San Roman-Blanco, 2003).

By considering the differences between the types of beach, it can be found that (Lopez de San Roman-Blanco, 2003):

- the permeability of shingle is higher than mixed beaches and both are relatively higher than sand beaches,
- gravel beaches are reflective and sand beaches are normally dissipative,
- gravel and mixed beaches respond to waves by forming a crest/step profile whereas sand beaches respond by creating a bar/trough profile,

Throughout this thesis, the two types of beach that will be examined are the shingle/gravel and coarse grained beaches. Moreover, from coarse grained beaches, consideration will be given to those consisting of mixed sand and gravel (mixed beaches).

During the last few years the interest of the behaviour of both gravel and mixed beaches has increased due to the interest on soft coastal engineering measures to combat erosion (for example : renourishment of beaches).

2.1 SHINGLE/GRAVEL BEACHES

According to Sherman (1991), gravel is made up of sediment particles in the 4 to 256 mm size range but the term can also refer to particles which are greater than 2mm.

In the UK, one third of the coastline is projected by shingle, or gravel, beaches. This type of beaches can have many differences based on the range of form and on the composition. Some beaches in the UK consist entirely of shingle and some others have a high sand content either within the interstices of the shingle or on the lower foreshore. Nevertheless, despite all that, all shingle beaches have the same responses and are following the same processes.

Shingle beaches respond rapidly to changes in the wave conditions making uncertain the fully form of a bar. The hydraulic conductivity of shingle beaches is very high and permits rapid and, occasionally, turbulent infiltration into the bed. This is one significant reason why shingle beaches are capable of dissipating in excess of 90% of all incident wave energy. Shingle beaches are known to be an efficient form of natural sea defence and, efficient and practical forms of coast protection with a high amenity and aesthetic value.

Moreover, gravel beaches are most common along the Pacific coast of the USA, Japan, Argentina and Canada, which is largely due to the fact of glacial activity. (Van Wellen et al, 2000).

Gravel beaches are often related with glacial activity (Forbes et al, 1995: Isla, 1993; Carter and Orford, 1984). The coarse sediment found on these beaches may have been the result of the deposition of entrained materials through current glacial actions or even from reworked sedimentary deposits of past glacial activity (Forbes et al, 1995; Carter and Orford, 1984). Gravel beaches can also be the result of the

fluvial deposition of glacial outwash (Forbes et al, 1995). As glacial activity is a source of beach gravel, gravel beaches are most commonly found in latitudes greater than 40 ((Forbes et al, 1995; Sherman, 1991).

Furthermore, there can be other reasons for the existence of gravel beaches, such as marine reworking of gravel transported via fluvial processes from mountain ranges (Isla, 1993) or they can be found in tectonically active areas (Forbes et al, 1995), or even on a local scale, they can be derived from the erosion of nearby cliffs (Bluck, 1967).

Despite their neglected status, gravel beaches are an important landform, and due to their distinct properties, have a number of applications for coastal management. With continued research, gravel beaches should become more widely recognised for the role they play as a highly effective and dynamic buffer against the forces of the sea.

2.1.1 Gravel beach sedimentation

As far as the sediment transport characteristics of a shingle beach are concerned, they are very different to those of a sand beach. Shingle supports a steep gradient (typically of the order 1:8) which allows waves to progress much closer inshore before breaking. The sediment transport within the swash zone is of more significance on a shingle beach than on a sand beach (Lawrence et al., 2003). In addition, Pedrono-Acuna et al. (2006), based on large-scale experiments stated that the most profile change on gravel beaches occur in the swash zone, especially above and below SWL (Sea Water Level).

Gravel beaches are highly efficient dissipators of wave action and they can provide excellent natural or managed defence systems. Gravel beaches are particularly efficient since their high permeability enables energy loss through percolation

within the beach. Gravel is very permeable and its transport is heavily dominated by wave action.

Gravel beaches and barriers develop distinctive patterns of sedimentation (Forbes et al, 1995) which function to minimise further sediment transport and reworking, develop both across (Bluck, 1967; Orford, 1975) and along the shore (Carr, 1969), with their relative importance dependant upon whether the beach is swash aligned or drift aligned (Forbes et al, 1995). These patterns appear, as sediment of a particular size tends to move across a beach until it reaches a position in which it is in equilibrium with the waves and flows acting upon it (Horn, 1992). Patterns in sedimentation also reflect sediment supply, developing only when the influx of new material is low (Sherman et al, 1993).

Bluck (1967) created a model of beach sedimentation (one of the first attempts describing cross-shore sedimentation), which was based on the selective sorting of beach pebbles according to shape, with spheres accumulating at the base of the beach, while discs tended to accumulate at the top. Bluck (1967) supported that, variations in wave energy across the foreshore profile, and to particles of various shapes reacting differently to the flow of water resulted in selective sorting, which creates a series of sedimentation zones across the beach parallel to the shore.

Sherman, (1991), suggested that Bluck's model was found to be both oversimplified and non-universal by various authors, even though later studies have supported the importance of shape in particle sorting, with the exception of Carr (1971). Further research undertaken by Orford (1975) and Williams and Caldwell (1988), indicates that particle shape and size were both important in determining the response of particles to swash and backwash processes as well as, the subsequent formation of depositional zones on the beach. Orford (1975) found that maximum zonation appears in swell wave conditions whereas, Williams and Caldwell (1988) suggest

that size determines particle sorting at high energies, with shape determining sorting at low energies.

Bluck (1999) admits the importance of size as well as shape in particle sorting and modifies his 1967 model, describing particle selection and rejection as being a largely self-regulating process that is driven by turbulent energy derived from backwash over the sediment floor, which as it becomes better sorted, it also becomes more selective. Bluck also acknowledges the role of cusps in sediment sorting in response to the work of Sherman et al (1993).

Shulmeister and Kirk (1997) showed that the sorting of sediment according to size and shape is capable of converting sandy beaches with minor gravel components into gravel dominated beaches. Isla and Bujalesky (1993) supported that spherical particles are preferentially set into saltation, leaving laminar, disc-shaped and flattened particles to dominate the bed.

The phenomenon of armouring on gravel beaches has been researched by Isla (1993) but there is little mention on armouring by other researchers. Isla describes the development of armouring as being the result of the continued rolling and subsequent deposition of large rounded particles during backwash over smaller particles that have already ceased movement. Although Isla's (1993) armouring model represents further particle sorting in relation to shape and size, it appears to conflict with models proposed by Bluck (1999; 1967) for gravel beach sedimentation.

Additionally, Matthews (1983) has shown that under high-energy conditions, attrition, which is the result of the opposing processes of breakage and abrasion, can result in a particle weight loss of 41 percent per year that may account for a predominance of granules over pebbles on many beaches and as suggested by Kirk (1980) an accumulation of fine sands and silts on the inner shelf. Matthews (1983)

suggests that lithology, particle size and the texture of associated sediments are also important to rates of attrition.

Finally, the development of shingle beach profile under wave action maybe influenced by a number of variables including:

1. Wave height
2. Wave period
3. Wave duration
4. Beach material size
5. Beach material grading
6. Effective depth of beach material (Effective beach thickness)
7. Foreshore level
8. Water level
9. Angle of wave attack
10. Spectral shape
11. Initial beach profile

2.1.1.1 *Influence of wave height and period*

Variations in both parameters (wave height and period) have a substantial effect upon the resulting beach profiles. On one hand, an increase of the wave height results in an increase of the surf zone width and hence increasing levels of wave energy (Powell, 1990). Consequently, the extra surf zone volume necessary to dissipate an increased incident wave energy is obtained by a lengthening of the surf zone rather than by a change in profile (Hughes and Chiu, 1981).

On the other hand, an increase of the wave period results in the increase of the beach crest elevation and, as a consequence, the volume of material above the still water-line. This is matched by a respective increase in the erosion of the beach

profile below the step position, and therefore a seaward displacement of the lower limit of profile deformation (Powell, 1990).

2.1.1.2 *Influence of wave duration*

The development of the beach profile is very rapid in the early stages of a wave attack (during the first 500 waves) and the main features of a particular profile quickly become apparent. Subsequent wave action, as a consequence, serves only to hone the final profile shape (Powell, 1990).

2.1.1.3 *Influence of beach material size and grading*

The influence of the beach material size (D_{50}) is more important than the influence of the grading (D_{85}/D_{15}) with respect to the beach profile change. Powell (1990) suggested that this importance is partly dependent upon the characteristic steepness of the incident wave field. Therefore, the greatest deviations between two 'corresponding' profiles are seen to occur under the steeper wave conditions.

In agreement with Powel (1990), Van der Meer (1988) found that the nominal diameter had an influence on the profile. Nevertheless, for small diameters in the range of materials that Van der Meer (1988) tested, the material size did not influence some parts of the profile, such as the crest height.

As far as the sediment grading is concerned, there is little or no variation in beach profile response other than an apparent reduction in the crest elevation as the beach grading narrows (Powell, 1990 and Van der Meer, 1988).

2.1.1.4 *Influence of effective beach thickness*

The effect of restricting the natural development of flow fields within the beach structure by incorporating an impermeable membrane parallel to the initial beach slope may be considered representative of natural beaches overlying sloping sea walls or containing compacted cores of finer (lower permeability) material. This situation was used by Powell (1990) in order to test the influence of the effective beach thickness upon the development of shingle beach profile under wave action.

In each case (model tests), Powell has used D_B as the effective thickness of beach material measured relative to the initial slope and D_{50} as the median diameter of the sediment particles. The results of the model tests have shown that the influence of D_B/ D_{50} on the beach profiles was largely confined to the horizontal profile displacements, at least for within the tested range (values of 29.4, 41.2, 52.9 and >95), and was most pronounced above the still water level. Additionally, the general trends across different wave conditions appeared to show a partial wave steepness dependency.

2.1.1.5 *Influence of foreshore level*

The majority of beaches are usually fronted by a sand foreshore located in relatively shallow water. Van de Meer (1988) carried out a number of tests (covering the range $0.56<H_s/D_w<0.74$, where D_w is depth of water at beach toe) and found that the effect of a reduced foreshore depth manifested itself in a shortening of the beach profile below still water level. Above the still water level there was no apparent effect on the profile.

Moreover, Powell (1990) and an earlier, unpublished, study carried out at Hydraulics Research Station (Wallingford) with a range of $0.8<H_s/D_w<2.5$ have indicated that profiles formed above a depth limited foreshore do not exhibit a distinctive step feature below the still water line. Therefore, the step normally forms

at the position of, and in response to, wave breaking. However, on a depth limited foreshore this breaking occurs seaward of the beach structure and consequently the conditions responsible for step formation on a beach are removed.

Powell (1990) suggested that with the elevated foreshore there is also a reduction in profile dimensions above the shoreline. Even though this suggestion was in contrast with van der Meer's (1988) results, it was perhaps given that crest dimensions are largely determined by wave run-up, which will itself be limited by the increased energy losses associated with wave action in depth limited conditions.

2.1.1.6 *Influence of water level*

Despite the fact that tides plays a significant part in the development of natural beach profiles, in field studies of beach profiles the effect of tidal action is often neglected.

The introduction of tides, regardless of range or duration, does not materially affect the shape or slopes of the resulting beach profiles. The only exception occurs when the changes in wave steepness, induced by the varying water depth in the wave channel, span the critical value for the transformation from accretion to erosion profiles (Watts and Dearduff, 1954).

Natural shingle beaches react far more rapidly to tidal changes than sand beaches do, the profiles appearing to move up and down the beach with the tide (Kemp, 1963 and van Hijum and Pilarczyk, 1982). Moreover, the beach profile respond immediately to changes in water level but the profile shape at the end of each tide is generally unaffected (van der Meer, 1988 and Powell, 1986).

It may therefore be concluded that gradually varying water levels do not affect the shape or slope of beach profiles. They will however determine the location of the profile on the beach face.

2.1.1.7 *Influence of the angle of wave attack*

The influence of the angle of the wave attack (φ) on the development of beach profiles has been examined by some researchers for both regular and random waves.

The dimensions of beach profiles formed under oblique wave attack are less than those formed under normally incident waves by a factor. This factor was firstly described to be equivalent to $(\cos\varphi)^{1/2}$ by van Hijum and Pilarczyk (1982), however, van der Meer (1988) has indicated that this factor was more closely described as $\cos\varphi$. Furthermore, the position of the beach crest relative to the shoreline is unaffected by the angle of wave attack.

It may be concluded that oblique wave action restricts the full development of at least part of the profile.

2.1.1.8 *Influence of the spectral shape*

Van der Meer and Pilarczyk (1986) compared profiles formed under a very narrow spectrum with those formed under a much wider Pierson Moskowitz spectrum in order to evaluate the influence of spectral type on the development of beach profiles.

On the basis of these tests they concluded that spectral shape had only minor influence on the beach profiles provided that the average zero-crossing period, T_m (and not the peak spectral period T_p) was used to compare the profile.

2.1.1.9 *Influence of the initial beach slope*

The influence of the initial beach slope on the development of the beach profile was the debate of many researchers through the years. Initial slopes from 1:5 to 1:30 were found to have no effect on the final profiles other than determining whether the upper beach was formed by erosion or accretion for 0.21mm to 3.44mm sand (Rector, 1954; Nicholson, 1968; Dalrymple and Thompson, 1976), with material from 1.8mm to 16.5mm (Van Hijum, 1974) and with much coarser material and random waves (van der Meer, 1988). Nevertheless, the direction of material transport and hence the mode of profile formation varied with slope.

Despite all the above, it was found that the final profile shape formed in 0.2mm and 0.7mm sands was influenced by the initial slopes of 1:10, 1:20, 1:30 (Sunamura and Horikawa, 1974) and when the latter was changed from 1:10 to 1:20 (Chesnutt, 1975). Gourlay (1980) concluded that the initial slope did not affect the shape of the beach profile when the former was steep, but could have an effect if the initial slope was very gentle.

Moreover, King (1972) observed that the initial gradient modified the critical wave steepness which effectively divides breaking and non-breaking sea states; critical steepness being higher for steeper beaches than shallow beaches. Nevertheless, any increase in beach slope will produce a slight change in the type of characteristic breaking wave even if the wave steepness remains constant. In the extreme case, this change will be from spilling through plunging and collapsing to surging. Thus a wave steepness that is critical on a steep slope (collapsing/plunging waves) might well result in spilling waves on a shallow slope where the critical value is in fact much lower. The variation in profile shapes obtained by different investigations, on different slopes, may therefore be partly explained by Kings' observation, particularly if the wave steepness is close to the critical values. (Powell, 1990)

As a result, Powell (1990) concluded that whilst the initial beach slope does not necessarily affect the form of the active length of beach profile it does affect its mode if formation.

2.1.1.10 Summary of findings

According to Powell (1990) and Van der Meer (1988), the main factors influencing gravel beach profiles are wave duration, wave period, wave height, beach material and angle of wave attack. Additional factors which play secondary role in profile development are the beach thickness, material shape and grading, and foreshore level.

Despite the fact of all the advantages of a shingle beach, it can still suffer erosion such as the other types of beach. Therefore, an efficient management of the shingle beach is required. However, the tools of such a beach management are currently limited. Most of predictions of the erosion/accretion, future shape/profile of shingle beaches are using numerical methods.

These methods/models are generally not very accurate when they provide information above the still water level. Each of them has its own limitations for application. The majority of shingle beach profile models are of the parametric type (due to the fact that the surface of a shingle beach, by exhibiting a number of readily identifiable features (steps & bars), is particularly amenable to a parametric description (Powell, 1990)).

Many different formulae are found to estimate/predict the shape/development of a beach profile. Formulae based on theoretical or experimental study tend to give the best result for their studied case. There are as many experiments or case studies as formulae. Generally, only a small percent of these formulae can be applied for all different wave/sediment conditions but with, of course, their own individual

limitations. Some of formulae used for the estimation/prediction of the shape/development of a beach profile are discussed in the following section.

2.1.2 Background of previous theories

2.1.2.1 *Equilibrium Beach Profile (methods)*

Observations of similarities in the shape of coastal profiles, since the start of the century, have led to the concept that for given conditions, profiles tend towards equilibrium. This concept called the equilibrium profile concept. The concept of an equilibrium beach profile provides a basis for assessing a characteristic shape to a beach in design and analysis situations, thus is of central importance to coastal engineers. Moreover, the equilibrium concept is valid for varying forcing conditions over different time scales (Larson et al., 1999). This concept has been applied by Edelman (1968, 1972) in order to predict dune erosion during a severe storm. Edelman's method was improved on a large number of scale experiments (Van de Graaf, 1997 and Vellinga, 1982) from where Vellinga (1982) derived scale relations, which can be used to design laboratory experiments or to assess the erosion for a particular profile and storm.

Many authors have commented upon the equilibrium profile of beaches. Bruun (1954) and Dean (1977, 1991) proposed that beach profiles develop a characteristic parabolic equilibrium beach shape given by

Eq.2-1 $$y = Ax^n$$

where,

y = still-water depth (vertical distance)

x = horizontal distance from the shoreline

A = a dimensional parameter related to sediment characteristics

n = 2/3

Bruun (1954) showed that Eq.2-1 fit to beach profile data obtained from the North Sea coast of Denmark and from Mission Bay, California. Dean (1977) also found that Eq.2-1 fit over 500 beaches profiles collected by Hayden et al. (1975) along the U.S. east coast and the Gulf of Mexico.

Numerous studies have developed conceptual models to explain the form of Eq.2-1. An early paper by Keulegan and Krumbein (1949) concluded that a shoaling solitary wave would produce an equilibrium profile of the shape given by Eq.2-1 with n=2/5. Dean (1977) considered dissipation of shallow-water linear waves and showed that if equilibrium is associated with wave energy per unit area of bed, then n=2/5. However, if equilibrium is associated with wave energy per unit volume of the water column, then n=2/3. Dean (1977) and Hughes and Chiu (1978) concluded that n=2/3 led to the best fit to the data in the majority of cases, including field data profiles.

Hallermeier (1981a) have developed equations that relate the fall velocity with the sediment diameter. Hallermeier gives fall-velocity equations for a wide range of beach sand, temperature, and both fresh and salt water. For the case of common beach sand with diameters in the range of 0.15mm to 0.85mm and temperature form 15 to 25^{0}C, Hallermeier's equations can be reduced to give the following fall-velocity relationship:

Eq.2-2 $$w = 14 D_{50}^{1.1}$$

where w (fall velocity) has units of cm/s and D_{50} is the diameter of the median-grain size of sediment with units of mm.

Moore (1982) and Dean (1987) have provided representations for the sediment scale parameter, A, as a function of sediment size, D_{50}, and fall velocity, w_f. Dean (1987) has shown that A can be related to fall velocity of sediment by the following:

Eq.2-3 $$A = 0.067 w^{0.44}$$

and also by using the Hallermeier's equation (Eq.2-2), A can be expressed then as

Eq.2-4 $$A = 0.21 D_{50}^{0.48}$$

Kriebel et al. (1991) have found another relationship between the sediment scale parameter and the sediment fall velocity

Eq.2-5 $$A = 2.25\left(\frac{w_f^{\,2}}{g}\right)^{\frac{1}{3}}$$

where,

g=acceleration due to gravity (=9.81 m/s^2)

Hughes (1994) have also suggested this dependence of the sediment scale parameter, A, on the sediment fall velocity, w_f, to the 2/3 power.

Moreover, a simple and very accurate prediction equation where the sediment scale parameter can be calculated is given by (Ahrens, 2003)

Eq.2-6 $$A_p / d^{1/3} = 2.23 \exp\left(-1.24 / A^{1/3}\right)$$

where A_p is the sediment scale parameter, d is the characteristic diameter of sediment and A is the Archimedes buoyancy index. The symbol A is the Archimedes buoyancy index which is given by

Eq.2-7 $$A = \Delta g d^3 / \nu$$

where g=acceleration of gravity, ν=kinematic viscosity of water, Δ=relative density of sediment, $\Delta=(\rho_s-\rho)\rho$, (ρ=density of water; ρ_s=density of sediment)
There are, however, two inherent disadvantages of Eq.2-1 with an exponent of 2/3. The slope of the beach profile at the water line (y=0) is infinite and the form is monotonic, i.e., it cannot represent bars. It has been shown that the first shortcoming can be overcome by recognising that gravity is also a significant destabilising force when the profile becomes steep. In this case the form is (Liu, 1994)

Eq.2-8 $$y = \frac{h}{m} + \left(\frac{h}{A}\right)^{3/2}$$

which unfortunately is significant more cumbersome to apply. In Eq.2-8, h is the depth, m is the linear beach-face slope and A is the sediment scale parameter.
Larson (1988) and Larson and Kraus (1989) have shown that an equilibrium beach profile of the form of Eq.2-8 results by replacing the simple breaking wave model leading to Eq.2-1 (with an exponent of 2/3) by the more complex breaking model of Dally et al. (1985).

Bodge (1992) and Komar and McDougal (1994) have proposed slightly different forms of an equilibrium profile based on an exponential form. Bodge proposed

Eq.2-9 $$h(y) = h_0(1 - e^{-ky})$$

in which h_o is the asymptotic depth at a great offshore distance, and k is a decay constant.

The form suggested by Komar and McDougal is quite similar

Eq.2-10 $$h(y) = \frac{m_0}{k}(1 - e^{-ky})$$

in which $\frac{m_0}{k}$ is the equilibrium depth and m_0 can be shown to be the beach face slope

Eq.2-11 $$\frac{\partial h}{\partial y} = m_0, y = 0$$

Bodge fitted his recommended form to the averages to the ten data sets provided by Dean (1977) and found that the majority (60% to 71%) were fitted better by the exponential fit compared to the Ax^n relationship and that 80% to 86% of the data sets were fit better than the $Ax^{2/3}$ expression. The exponential forms have two free constants which are determined to provide the best fit and thus should agree better in general than for the case in which n is constrained to the 2/3 value. Komar fitted his form to a single Nile Delta profile. Since the exponential profile forms require determination of the two free parameters from the individual profile being represented, they can be applied in a diagnostic manner but not prognostically (Liu, 1994).

In another approach Inman et al. (1993) examine the fitting of compound beach profile to a number of beaches. The curve-fitting approach needs up to seven free parameters and appears to require subjectivity in parameter choice. This method can not be applied in a prognostic manner.

Moreover, Vellinga (1983, 1986) has recommended an equilibrium beach profile based on a series of small and large scale model tests and comparisons with field data. This equilibrium profile was the basis for an update method for dune erosion prediction in the Netherlands. Based on the model tests, the equilibrium beach profile was determined to be

Eq.2-12 $$\left(\frac{7.6}{H_{0,}}\right)h = 0.47\left[\left(\frac{7.6}{H_{0,}}\right)^{1.28}\left(\frac{w_f}{0.0268}\right)^{0.56} y + 18\right]^{0.5} - 2.0$$

in which all units are metric and H_{o_s} is the deep water significant wave height corresponding to the breaking wave height as calculated using linear wave theory. The profile equilibrated out to a depth equal to approximately $0.75\,H_{o_s}$.

It is of interest that the equilibrium beach profile developed by Vellinga is somewhat similar to that represented by Eq.2-1 with an exponent of 2/3. One difference is the Vellinga's equation depends on both the sediment characteristics and the wave height, whereas Eq.2-1 is a function of only the sediment characteristics. It can be shown that the Vellinga's equation predicts that an increase in wave height causes a milder beach face slope which is in according with nature.

Furthermore, Vellinga (1984) based on an extensive investigation into the scale factors pertaining to the laboratory modelling of sand dune erosion under storm surges, he have derived an empirical scale factor through curve fitting of the dune erosion profiles and erosion quantities:

Eq.2-13 $$\frac{y_p}{y_m} = \left(\frac{x_p}{x_m}\right)^{0.78}$$

where the suffixes p and m refer to prototype and model respectively.

This equation can be written also as

Eq.2-14 $$y = Ax^{0.78}$$

,assuming that the erosion profiles can be described by a power curve of the form of Eq.2-1. However, Eq.2-14 gives poor results for shingle beaches.

There are some equations that are in disagreement with each other (example, Hughes and Chiu's (1978) equation with the equations of Vellinga (1984) and Bruun (1954). This occurs due to the fact of the difference in wave climates in various places in the world where there would appear also to be a steepness effect.

Vellinga (1984) attempted to establish the form of this steepness effect assuming that only the coefficient described the steepness effect. Furthermore, he attempted to add the effect of material size within the coefficient A and derived a universal erosion profile of the form of

Eq.2-15 $$y = 0.7\left(\frac{H_0}{L_0}\right)^{0.17} V_s^{0.44} x^{0.78}$$

where V_s is the fall velocity of a beach material particle of size D_{50}, H_0 is the nominal deepwater wave height and L_0 is the nominal deepwater wavelength.

This equation is applicable only below the still water level and gives reasonable results in the field for conditions with $0.025<H_0/L_0<0.04$ and $0.16mm<D_{50}<0.4mm$. Additional, for sand beaches with $D_{50}=0.225mm$ and $H_0/L_0=0.034$, Eq.2-15 becomes,

Eq.2-16 $$y = 0.08x^{0.78}$$

The curve obtained by Eq.2-16 is in close agreement with that obtained by Bruun (1954) for the very similar Danish beaches.

In concern of the prediction of the equilibrium beach profile, Romanczyk et al. (2005) proposed a class of shape functions f that can describe both the very nearshore area and the deeper portion of the littoral zone. Inman et al. (1993), Pruszak et al. (1997) and Larson et al. (1999) explored the idea of splitting the nearshore profile into two parts. The proposal of Romanczyk et al. (2005) was:

Eq.2-17 $$f(x) = \begin{cases} f_1(x) = -Ax^{2/3} & \text{for } x \geq x_0 \\ f_2(x) = -Ax_0^{2/3} + \frac{2}{3}Ax_0^{-2/3} + R(x_0 - x)^2 & \text{for } x < x_o \end{cases}$$

where x_0 is the point midway between the shoreline and the position of the first breaking point of the incident wave, and R is a coefficient which is accomplished by linear squares fitting with the available topographical data. The scheme of the

coordinate system of the proposal of Romanczyk et al. (2005) can be seen in the following figure.

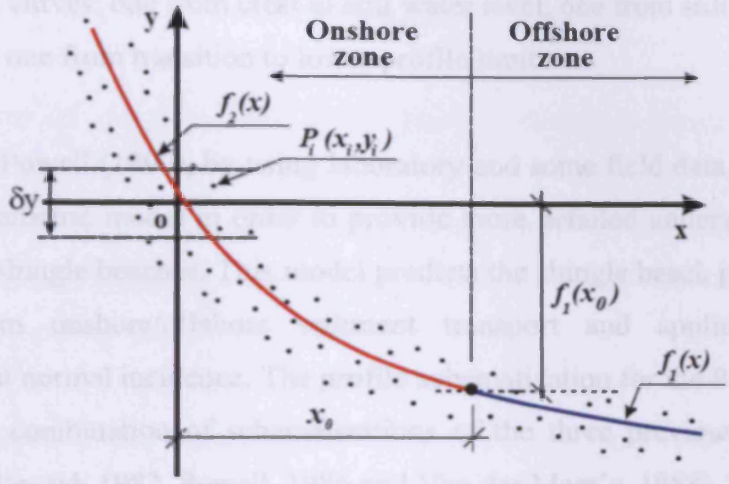

Figure 2-1 Scheme of the coordinate system (taken from Romanczyk et al., 2005)

Finally, several numerical models have been developed according to equilibrium beach profile concepts. Some of these are: EDUNE (Kriebel, 1982, Kriebel and Dean, 1985, Kriebel, 1986), SBEACH (Larson and Kraus, 1989, Larson et al., 1989, 1996), the model used in establishing a coastal hazard zone in Florida, termed the Coastal Construction Control Line (CCCL) (Chiu and Dean, 1984, 1986) and the non-linear model CROSS (Zheng and Dean, 1997).

2.1.2.2 *Shingle Beach Profile (models)*

Van Hijum and Pilarczyk (1982) and Powell (1986) have attempted to describe shingle beach profiles based on results of physical model tests. Their profiles were schematised as two hyperbolic curves: one from the beach crest to the step and one from the step to lower profile limit. The equations that they have obtained, which were in good agreement with the model results, were based mainly on regular waves and were not directly applicable for the field conditions.

Moreover, Van der Meer's (1988) profiles, based on the work undertaking on the dynamic stability of rock slopes to natural gravel beaches, were schematised as three separate curves: one from crest to still water level, one from still water level to transition and one from transition to lower profile limit.

Furthermore, Powell (1990), by using laboratory and some field data, developed an improved parametric model in order to provide more detailed understanding of the behaviour of shingle beaches. This model predicts the shingle beach profile changes resulting from onshore/offshore sediment transport and applies for waves approaching at normal incidence. The profile schematization for the Powell's (1990) model was a combination of schematizations of the three previous studies (Van Hijum and Pilarczyk 1982, Powell, 1986 and Van der Meer's, 1988). The model has employed three hyperbolic curves between the prescribed limits of:

1. Beach crest and still water level shoreline,
2. Still water level shoreline and top edge of step, and
3. Top edge of step and lower limit of profile deformation, i.e. wave base.

2.1.2.3 *Beach Profile Response (static models)*

One class of profile evolution models is that of static or geometric models. In this class, an equilibrium profile is established and the profile responds to the forcing function, usually an increased water level and wave height by satisfying the conservation equation and the landward and seaward limits of profile mobilisation. Because the models are static, a sediment transport distribution is not required. Bruun (1962) proposed the following relationship for shoreline response to sea level rise, (S)

Eq.2-18 $$R_\infty = S\frac{L_*}{h_* + B}$$

in which R_∞ is the shoreline recession (-Δy), L_* and (h_*+B) are the width and vertical extent of the active profile. The basis of this equation is seen in Figure 2-2 in which the two components of the response are:

1. a retreat of the shoreline, -Δy, which produces a sediment "yield" – Δy(h_*+B) and
2. an increase in elevation of the equilibrium profile by an amount of the sea level rise, S, which causes a sediment "demand" equal to SW_*. Equating the demand and the yield results in Eq.2-18.

Eq.2-18 is known as the "Bruun Rule". It is noted that the Bruun Rule does not depend on the particular profile shape. Dean and Maurmeyer (1983) later extended Bruun's result to apply to the case of barrier island in the form

Eq.2-19 $$R_\infty = S\frac{L_* + L_w + L_L}{h_* - h_L}$$

and the various terms are explained in Figure 2-3.

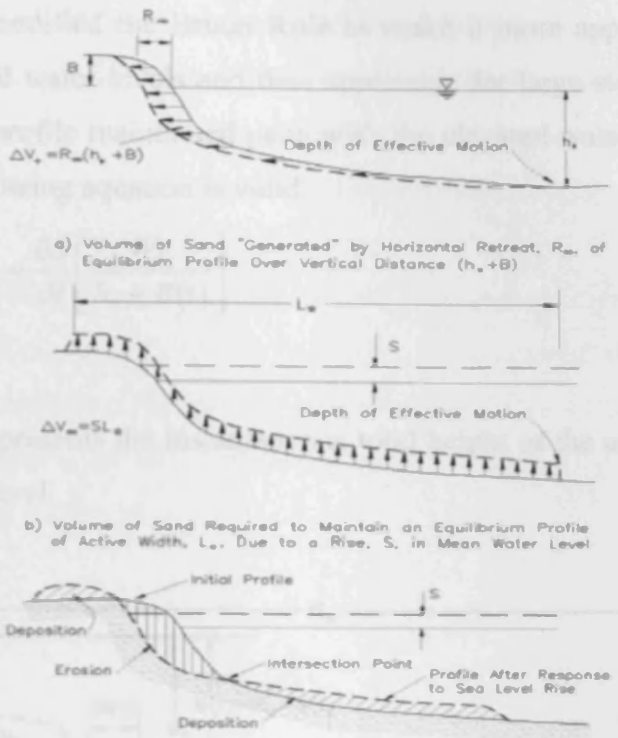

Figure 2-2 Components of sand volume balance due to the sea level rise and associated profile retreat according to the Bruun Rule (taken from Dean et al., 2002)

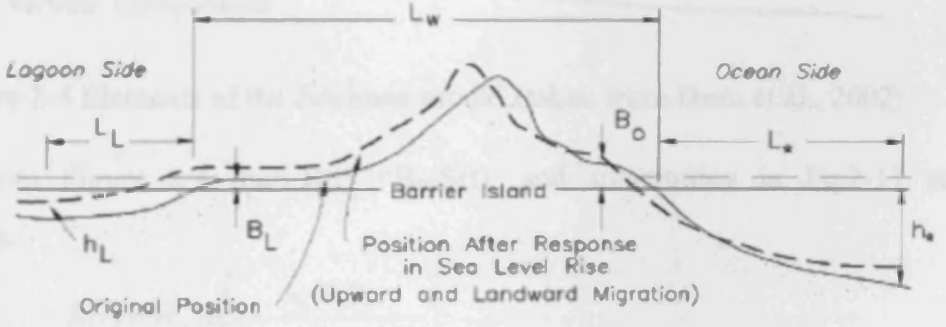

Figure 2-3 The Bruun Rule generalised for the case of a barrier island that maintains its form relative to the adjacent ocean and lagoon (taken from Dean and Maurmeyer, 1983)

Edelman (1972) modified the Bruun Rule to make it more appropriate for larger values of increased water levels and thus applicable for large storm surges. It was assumed that the profile maintained pace with the elevated water level and thus at each time, the following equation is valid

Eq.2-20 $$\frac{\partial R}{\partial t} = \frac{\partial S}{\partial t}\left[\frac{W_*}{h_* + B(t)}\right]$$

where now B(t) represents the instantaneous total height of the active profile above the current water level.

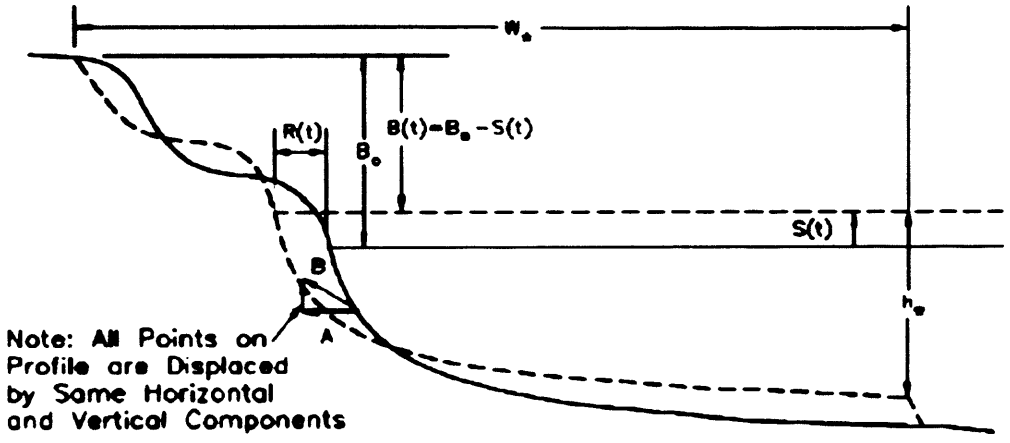

Figure 2-4 Elements of the Edelman model (taken from Dean et al., 2002)

Noting from Figure 2-4 that $B(t) = B_0 - S(t)$, and substituting in Eq.2-17 and integrating,

Eq.2-21 $$R(t) = W_* \ln\left[\frac{h_* + B_0}{h_* + B_0 - S(t)}\right]$$

Using the small argument approximation for the natural logarithm

Eq.2-22 $$\ln(1+z) \approx z - \frac{z^2}{2} + \frac{z^3}{3} + \ldots$$

it is readily shown that to the first approximation, Edelman's equation (Eq.2-21) is the same as the Bruun Rule (Eq.2-18). Additionally, for application to storm events, Edelman adopted at his equations the breaking depth h_b and surf zone width W_b rather than the offshore depth of closure h_* and corresponding W_b.

Moreover, Dean (1991), based on theoretical pre- and post-storm profile forms given by the equilibrium beach profile in Eq.2-1, have derived similar solutions for storm-induced berm retreat. An approximate solution for the steady-state erosion for the case where water levels are elevated by both a storm surge and by breaking-induced wave setup is give as

Eq.2-23 $$R_\infty = (S + 0.068H_b)\frac{W_b}{B + h_b}$$

where H_b is the breaking wave height and W_b is the width of the surf zone, defined for the equilibrium profile as

Eq.2-24 $$W_b = \left(\frac{h_b}{A}\right)^{\frac{3}{2}}$$

The solution for erosion due to combined storm surge and wave setup is similar in form to the Bruun Rule in Eq.2-18.

Furthermore, Kriebel and Dean (1993), assuming that beach response is driven primarily by storm surge, have established a simple analytical solution (convolution method) to estimate the equilibrium berm recession due to storm surge level. For the derivation of that solution, Kriebel and Dean (1993) did not include the wave setup effects due to the fact that storm surge has a much larger effect than wave setup. They have considered also both profiles with a vertical face at the water line and profiles with a sloping beach face. The three types of maximum potential (cross-

shore) equilibrium-profile response for severe storm conditions (and especially for water level rise), which they have calculated, are the following:

1) Response of Equilibrium Profile with Square Berm,
2) Response of Equilibrium Profile with Sloping Beach Face and
3) Response of Equilibrium Profile with Dunes

2.2 COARSE SEDIMENT BEACHES

Coarse sediment beaches are a feature of many coastal landscapes and provide a fine example of natural shoreline protection, acting as a highly responsive buffer between land and the sea (Sherman, 1991; Williams and Caldwell, 1988). Despite their useful properties, coarse sediment beaches remain however, a neglected feature compared with sand dominated beaches (Bluck, 1999; Sherman, 1991; Williams and Caldwell, 1988; Kirk, 1980). As a consequence, much of our understanding of these environments is comparatively rudimentary (Sherman, 1991).

Throughout this thesis consideration will be given to beaches consisting of mixed sand and gravel (mixed beaches) which are type of coarse sediment beaches.

2.3 MIXED BEACHES

The majority of research associated with sediment transport and coastal hydrodynamics has been focused with a single sediment type beach (sand or gravel) leaving beaches containing a mixture of both sand and gravel (mixed beach). Thus, because of the limited understanding surrounding these beaches, mixed sand and

gravel coastlines have a lot of research potential for both coastal resource management and scientific reasons.

Despite the fact that these beaches are found rare on a world-wide scale, mixed sediment beaches occur commonly around the shores of regions where the effects of glacitation have provided an abundant source of sand and gravels for subsequent re-working by Holocene rising sea levels (Mason & Coates, 2001), including the UK, Eire, Canada and the Artic Sea coast (e.g. Carter et al., 1990a; Finkelstein, 1982; Hill, 1990), Tierra del Fuego (Bujalesky and Gonzalez-Bonorino, 1991), New Zealand (e.g. Kirk, 1969) and Greece (Moutzouris, 1991). Figure 2-5 show some examples of mixed beaches around Europe.

According to the modified Folk scheme (BGS, 1987), mixed sediments are usually classified whereby the proportions of mud (<62.5μm), sand (62.5 to 2000 μm) and gravel (2 to 64mm) are expressed as the ratio of sand to mud and the percentage of gravel. Additionally, mixed beaches defined by Coates and Damgaard (1999) as those including sediment sizes ranging over three orders of magnitude from fine sand (100 μm), though gravels (2-64mm) right up to small boulders (>256mm).

Mixed beaches are divided into two categories where their division is often marked by an abrupt change of bed slope. The first category is a composite-type beach, where a wide, sandy, inter-tidal terrace is flanked by a shingle ridge and the second is a homogeneous mixture of sand and shingle. Both types may have a complex vertical sedimentary structure where, below the surface layer of cobbles and pebbles, layers of mixed pebble sizes are supported by a sand matrix and underlain by sand. (Mason et al., 1997)

Sicily, Italy

Ventimiglia, Italy

Hayling Island, UK

Seaford, UK.

Amorgos Island, Greece

Playa del Albir, Spain

Figure 2-5 Examples of mixed beaches around Europe (taken from Lopez de San Roman–Blanco et al., 2003)

2.3.1 Mixed Beach Sedimentation

Mixed beaches, from a coastal processes perspective, are distinctly different to sand or gravel beaches, but with characteristics from both forms. Moreover, mixed beaches are very high energy environments and they are more complex morphologically than either sand or gravel beaches. A study by Lopez de San Blanco and Holmes (2002) on the behaviour of mixed and gravel beaches found that the profile development of the mixed beach is more irregular and less predictable than that of the gravel beach. Lopez de San Roman–Blanco et al. (2002) stated that the main difference of these beach materials is not in their nominal diameter, but in the amount of sand present and this has an influence on the porosity, permeability and ultimately in the internal pressures.

The distribution of the mixed beach material may vary across shore, along shore, vertically through the beach and over time, both seasonally and over longer time scales. Leaving the visible part as gravel, the sand and gravel may be mixed below the surface with a coarsening of material towards the beach crest. Transport of the sand may be influenced by non-wave induce currents, being carried as both suspended and bed slope, while gravel is primarily as bed load driven by wave action in the surf and swash zones. Coarse material may be lifted into temporary suspension during storms where wave action alone will not normally cause gravel to be drawn seaward across typical low tide sand platforms, so the content of the beach may change as sand is drawn down by storms or returned shoreward by lower swell waves. Mixed beach transport mechanisms can lead to complex littoral drift regimes, with different sediment sizes moving at different rates and even in different directions.

From the results of a DEFRA's (2003) funded research project it was found that the overall composition of mixed beaches is very variable spatially (alongshore, across-shore and in depth within the sediment) and temporally (in different time-scales: daily and seasonally). DEFRA (2003) recognised two basic foreshore types:

- typical of meso and macro tidal conditions, lower sand platform and a steep upper gravel ridge with a very variable area of mixing at the boundary and also,
- typical of micro and meso tidal conditions, fully mixed beaches with a variable cross-shore sediment distribution ranging from a higher percentage of sand across the lower beach to predominantly coarse gravel and cobbles along the storm crest.

The behaviour of mixed beaches is influenced by the amount of sand that it contains. It might probably be the process of sand beach sedimentation (rather gravel beach sedimentation) that can help to understand the processes that influence the sediment transport on mixed beaches. However, there is limited literature on the basic factors that distinguish the processes of sediment transport on mixed beaches from the processes on single sediment beaches. Despite that, Mason and Coates (2001) stated factors that may influence the sediment transport of mixed beach. They considered to be first or second order factors. These factors are:

First Order

- Hydraulic Conductivity
- Groundwater and Infiltration
- Wave Reflection
- Threshold of Motion

and

Second Order

- Clast shape
- Tidal Range
- Specific Gravity
- Armouring
- Chemical processes

The first order of factors that may influence the sediment transport of mixed beach are described below.

2.3.1.1 *Hydraulic Conductivity*

Hydraulic conductivity is the most characteristic property which differentiates a mixed beach. The hydraulic conductivity, K (m/s), or permeability, measures how easily the fluid flows through a permeable material and also has an important influence on sediment transport process and swash zone hydrodynamics. This influence on sediment transport is related by the beach profile and the groundwater flow. The conceptual classification of beach composition and permeability suggested by Lopez B. et al. (2003) is shown in Figure 2- 6.

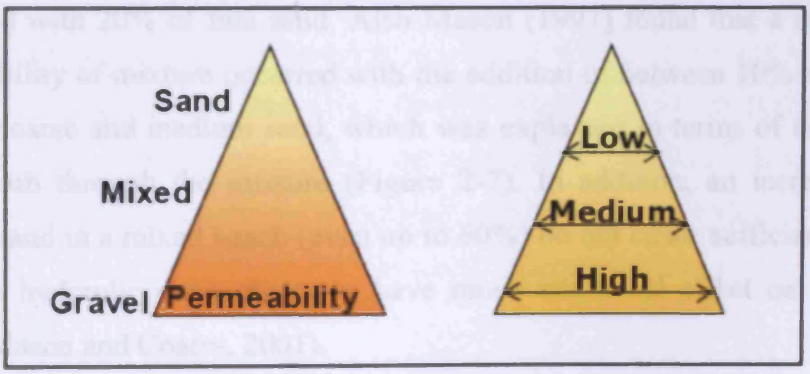

Figure 2- 6 The behaviour of permeability for each type of sediment beach (taken from Lopez B. et al., 2003)

Lopez de San Roman-Blanco (2003) stated that the factors that the permeability of mixed beaches depends on are:

- the type of sediment mix, gap-graded or well-graded
- the sizes of the sediments and
- the percentage of these sediments

Researches show that the amount of sand in a mixed beach influences (by reducing) the hydraulic conductivity and consequently the profile response of the beach. The percentage of sand required to produce a given reduction in hydraulic conductivity will vary with both the size and grading of the gravel material, since both properties determine the void ratio of the bulk sediment (Mason and Coates, 2001).

Mixed beach profile response is not the same as a gravel beach when it contains greater than about 25% sand by weight (or 20% for fine sand) in the sediments within a metre or so from the surface(Mason and Coates, 2001).

Mason (1997) found that the permeability of the shingle reduced by 65% with a mixture of only 20% medium sand and shingle, and this decrease was almost 90% when mixed with 20% of fine sand. Also Mason (1997) found that a reduction of the permeability of mixture occurred with the addition of between 10% and 60% of shingle to coarse and medium sand, which was explained in terms of tortuosity of the fluid path through the mixture (Figure 2-7). In addition, an increase of the amount of sand in a mixed beach (even up to 60%) do not cause sufficiently further decrease in hydraulic conductivity to have much additional effect on the profile response (Mason and Coates, 2001).

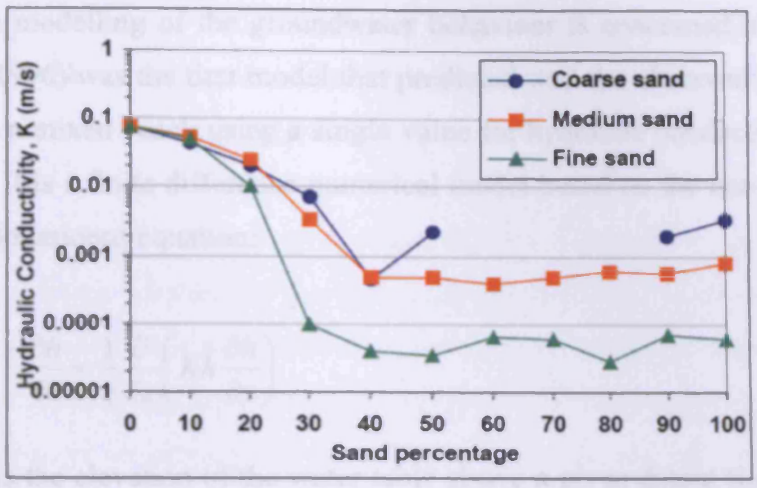

Figure 2-7 Mason's (1997) hydraulic conductivity results

2.3.1.2 *Groundwater and Infiltration*

The beach groundwater is important for the sediment transport and more research has been undertaken especially on sandy beaches. In a similar manner to sandy beaches, Kirk (1975) identified the influence of beach groundwater levels on the net sediment transport budget of mixed beaches. The groundwater response of the mixed beach is not significantly different to that of a sand beach. By comparison of gravel with mixed beaches, it is found (DEFRA, 2003) that the speed of the groundwater response in gravel beaches is quicker with a maximum value of the order of 1m/s compared with the mixed beaches which was of the order of 0.8m/s. From the same comparison, the groundwater response is cumulative in time because of the lower drainage capacity of the mixed beaches in comparison to the gravel beaches, "*as if the water table had a "memory" for the previous wave conditions*" (DEFRA, 2003).

Moreover, the elevation and shape of the beach water table depend on the characteristics of the beach material (size, shape range, porosity and permeability) and the hydraulic conditions (waves and tides).

As far as the modelling of the groundwater behaviour is concerned, the model of Baird et al. (1996) was the first model that predicted well the observed groundwater behaviour on a mixed beach using a single value for hydraulic conductivity (Mason et al., 1997). It is a finite difference numerical model based on the one-dimensional form of the Boussinesq equation:

Eq.2-25 $$\frac{\partial h}{\partial t} = \frac{1}{s}\frac{\partial}{\partial x}\left(Kh\frac{\partial h}{\partial x}\right)$$

where h (L) is the elevation of the water table above a given datum (i.e. the aquifer depth), K (LT^{-1}) is the hydraulic conductivity, s (dimensionless) is the specific yield, x (L) is the distance and t is the time. Moreover, in order to include the groundwater fluctuations due to set-up the model has been developed subsequently (Baird et al., 1997).

Furthermore, in mixed beaches infiltration is more important than in sand beaches. Therefore, an important part of the development of sediment beach modelling for mixed beaches is the swash/backwash module. During both swash and backwash on beaches with high hydraulic conductivity, the infiltration should be high.

Nevertheless, there are no laboratory or field experiments which have measured differential infiltration during swash and backwash and nor techniques have been developed sufficiently to measure this. Mason and Coates (2001) state that the principal drawbacks to quantifying the effects of sediment mixture on swash/backwash and wave run-up are:

- *the spatial and temporal variations in sediment mixture*
- *the mobility of the sediment and often complex beach profile, both of which generally preclude the use of run-up wires*

- *reversing flows in shallow water, high levels of turbulence and an inhospitable environment, which make the field deployment of electronic instruments extremely difficult and expensive.*

Mason and Coates (2001) also concluded that any overlying gravel can not dissipate much energy through percolation if a mixed sand/gravel layer exists below surface at an elevation greater than the tidally-induced fluctuations of the water table. This happen due to the fact that both the hydraulic conductivity and specific retention of the mixed sediment determined largely by the sand fraction, so that gravel/sand mixtures remain saturated for longer than gravel.

2.3.1.3 *Wave Reflection*

Another important factor that influences the mixed sediment transport is the wave reflection. However, little research has been undertaken on wave reflection from mixed beaches.

Davidson et al. (1994) and Mason (1997) observe, for the swell wave component ($0.05 < f < 0.1$ Hz), that the reflection from mixed beach varied with tidal stage with the reflection coefficients increased from the steeper upper beach gradient. Nevertheless, for the wind waves the reflection coefficients stay constant independently from the change in beach gradient.

Lopez B. et al. (2003) conclude that there are two aspects influencing reflection on mixed beaches:

- reflection on a mixed beach will reduce by the milder beach slope in comparison with a gravel beach and,
- reflection might be influenced, by the greater permeability of gravel beaches in comparison with mixed beaches, by reducing the amount of energy available for reflection.

Furthermore, Mason (1997) concluded that the mixed sand/shingle beach reflects more energy than a sandy beach due to a steeper surface gradient and more than a gravel beach due to less energy dissipation through infiltration.

2.3.1.4 *Threshold Motion*

Threshold motion is generally related to sediment size, which makes it difficult to describe for mixed sediment. The value of threshold motion for sand is much lower than the value of threshold motion for gravel. As a result the sand starts moving earlier than the gravel in gravel-sand mixed sediment.

An important factor of the threshold motion is the effect of bed slope. Besides, establishing critical threshold of motion for mixed sediments is complicated by the relative protrusion into the flow, the angle of repose and the pivoting angle. Despite that, some research is in contrast in the role of these processes. Fenton and Abbot (1977) and Naden (1987) suggested that larger clasts, due to their higher protrusion into the flow, are entrained more easily, whereas Komar and Li (1986) reported that granules within a mixed gravel-sized bed, since their critical threshold is lower, are removed first.

By laboratory work for mixed beaches, Kuhnle (1994) suggested that with low percentage of sand on the mixture, the sand would become trapped within the interstices and not be available for transport, so that the effective transport rates of sand would be low even at high flow velocities. Accordingly to Parker and Klingeman (1982) study, the proportion of coarser grains exposed to the flow is increased and the near equal mobility of coarser sizes is restored, once the surface layer of sand is removed. As a result, due to the high percentage of sand, the coarsening process is inhibited.

As far as field observations (which are few) of gravel/mixed sediment transport is concerned, the field report of Walker et al. (1991) and the results of a funded research project, managed by HR Wallingford (Van Wellen et al., 1997; HR Wallingford, 1999) measured threshold velocity of about 1.6 m/sec for gravel of 5 to 200mm with no preferential transport of differing sizes.

2.3.2 Background of previous models/studies

Little research has been devoted to develop numerical methods /models for predicting the morphological behaviour of mixed beaches. There are no parametric models, for mixed beaches, existing at the moment. Moreover, attempts to extend the numerical models that have been derived for sand beaches into numerical models for mixed beaches arise problems (Mason and Coates, 2001, Lopez San de Roman-Blanco, 2000). However, the main problem arises from the assumption of having a single nominal diameter for the whole mixed beach ignoring flows within the beach face (Lopez San Roman-Blanco et al., 2006).

As well, less research has been devoted to cross-shore numerical modelling of mixed beaches. In addition, there is no process-based model available to predict the response of a mixed beach to a given hydrodynamic forcing. The limited success of these models is the result of the inability to understand or model the governing physical processes adequately (Lopez de San Roman-Blanco, 2003).

The research work has been limited into the experiments of some members of research teams such as the HR Wallingford team and the team of the University of Plymouth. Clarke and Damgaard (2002) have worked on the extension of OTTP-1D towards a morphological capability and Lawrence et al. (2003) have worked on the coupling of a 1-D phase resolving numerical wave model with a sediment transport module and a morphodynamic module.

In order to develop models for use on mixed beaches, it requires input of data obtained from field experiments; however, it is difficult to deploy instrumentation on mixed beaches. Usually, these models require data obtained from sensitive instruments placed in the breaker zone. Placing such delicate instruments in the breaker zone of a mixed sand and gravel beach would have them destroyed almost immediately. Therefore, the instruments have to be built and placed in such a way in order to survive the battering they receive by gravel and waves.

As a result, only few field experiments have taken place on mixed beaches. Kirk (1969, 1980) reported that most field evidence suggests that the majority of transport on mixed beaches takes place in the inner surf/swash zone. Moreover, Pontee (1996), by examining the profile response and sedimentary characteristics along the Suffolk coast, concluded that the sand content increased by increasing wave height and period, although he came across a great variability in sediment composition over a range of time scales under similar wave conditions. Furthermore, Mason (1997) described a field investigation of a micro-tidal, ridge and runnel composite mixed beach at Morfa Dyffryn, North Wales. Mason (1997) concluded that the sand/shingle mixture had a significant ability to maintain a steeper slope than would be supported by a sand beach, in relation to the morphodynamic response of the ridge. Additionally, since the sand content dominated the groundwater behaviour, Mason (1997) found that through swell wave reflection, the steep beach slope exerted greater control on the hydrodynamics than did energy dissipation through infiltration.

As far as the laboratory experiments for shingle/sand beach are concerned, there are three recent reports of laboratory studies (Petrov, 1989; Quick and Dyksterhuis, 1994; Lopez San Roman-Blanco et al., 2006).

Petrov (1989) examined three dimensional hydraulically-induced sorting of mixed gravel and sand sediment (i.e. cross-shore, alongshore and vertically through the beach). In the experiments, only one sediment mixture (D_{50} of just over 5mm at a

nominal scale of 1:25) has been used and the waves approached at an angle of 15^0. In agreement with the field observations of Orford (1975), the more spherical particles, in the Petrov's (1989) laboratory experiments, were transported seawards while the flatter particles moved landwards. In the meantime, an immobile layer of finer size fractions has been produced by the removal of the sand fraction from the surface sediments (both by transport alongshore and by sinking into the sediments below). Due to Petrov (1989), the kinetic sieving induced by wave action was the reason of the downwards translation of smaller particles in his experiments although Mason and Coates (2001) believed that it might be also result from simple downwashing by infiltrating water.

The laboratory experiments of Quick and Dyksterhuis (1994) have been taken place in a small, regular wave flume (approx. 1:40 scale) and were focused on the profile response of sand with D_{50}=900μm, fine gravel with D_{50}=3.4mm and a 50:50 mixture. Each of these sediment was subjected to low, medium and high energy conditions. Quick and Dyksterhuis (1994) concluded that due to the hydraulic conductivity, the beach steepness is controlled by sand and the profile change is achieved though the effect of wave height, infiltration and bed roughness. Finally, by using equations derived by Quick (1991), Quick and Dyksterhuis (1994) produced an analytical equation which predicts a new equilibrium profile by taking an existing profile, two sediment parameters (D_{60} and D_{10}) and a wave height.

Lopez San Roman-Blanco (2003) took part of an EU project named "Large Scale Modelling of Coarse Grained Beaches", which was undertaken at the Large Wave Channel (GWK) of FZK in Hannover between March and May 2002. Two beaches (Beach I-gravel only with D_{50}=21mm and Beach II- sand/gravel with a 30:70 mixture) were constructed with an initial profile of 1:8 and were placed over an asphalt permanent slope of 1:6. This EU project has provided useful data for further development of numerical models describing the profile evolution of mixed sediment and coarse grained beaches.

Lopez San Roman-Blanco (2003) based on the research of the GWK experiments, proposed new formulations for both gravel and mixed beaches. These formulations referred to the calculation of the berm elevation, the step elevation, the dependency of the set-up at the shoreline/of the asymptotic over-height and of the coefficient of reflection on wave and sediment characteristics.

2.4 MORPHODYNAMICS

Coarse sediment beaches display distinct morphodynamic features but as Forbes et al, (1995) suggest, a comparable understanding of coarse sediment beaches has been slow to evolve, whereas, conceptual models for sandy beach morphodynamics have been developed.

Lopez and Holmes (2002) noted that in both mixed and gravel beaches, the response of the initial profile to the wave action leads to the building up of material above the SWL forming a crest or ridge and therefore erosion occurs below the SWL, especially below the step or breaking step. The main morphological differences between them are that the chainage of the beach at the SWL is always "landwards" and the profile change is smaller for the mixed beaches.

According to Forbes et al, (1995) one of the distinctive features of coarse sediment beaches is a steep reflective beachface, (often with a low angle platform or apron at the base) which allows waves to progress close to the shore before breaking into either plunging or surging breakers (Morfett, 1990; Sherman et al, 1993). On coarse sediment beaches, energy dissipation through breaking waves is concentrated on a much narrower area than occurs on sandy beaches, which causes sediment transport to occur primarily within the swash zone (Van Wellan et al, 2000; Forbes et al, 1995; Kirk, 1980). Van Wellan et al, (2000), suggest that, steep beach gradients have the effect of concentrating refraction processes into a narrow zone resulting in

incomplete refraction, with waves arriving at the beachface at a substantial angle which according to Kirk (1980) has implications for sediment transport.

A portion of the incident wave energy reaching steep coarse sediment beaches is reflected as edge waves (Forbes et al, 1995; Sherman et al, 1993). The presence of edge waves leads to the formation of cusps, which are commonly found on coarse sediment beaches (Forbes et al, 1995; Sherman et al, 1993; Carter and Orford, 1984). Cusps (beach cusps) are the formations that beaches show of regularly spaced, crescentic accumulations of materials, ranging from sand to cobbles (Figure 2- 8). Although Carter and Orford (1984) have found the development of edge waves to be particularly prevalent during long period (10-20s) swells, Sherman et al (1993) have interpreted cusps as being the products of progressively diminishing setup and runup as wave energy and period diminish at the end of major storms.

Figure 2- 8 Beach cusps

Cusps develop as part of a process of self-organization involving sediment transport and sorting that brings the active beachface into equilibrium with the prevailing wave and swash conditions. If the gravel is either sufficiently coarse or present in very large volumes, then cusps and berms may be very stable and persist for some

time, where through a process of feedback, they continue to influence surf and swash dynamics (Forbes et al, 1995; Carter and Orford, 1984). From studies of Kirk (1975) and Nolan et al. (1999), it concluded that cusp elevation is controlled by breaker height, through swash length, on mixed sand and gravel beaches. Moreover, on mixed beaches, cusps having particular spacings form at distinct elevations on the beachface, with the largest spacings occurring at the highest levels on the beachface (Nolan et al., 1999).

Cusps are also the sites in which the run-up of swash attains its maximum limit (Sherman et al, 1993). Having been accentuated by edge waves, high swash run-up may lead to either barrier crest sedimentation of marine gravels (Carter and Orford, 1984), or berm overtopping and breaching (Short, 1979), the latter contributing to either shoreline migration (Carter and Orford, 1981), or landward migration in the case of gravel barriers (Ciavola, 1997; Forbes et al, 1995; Carter and Orford, 1984).

As coarse sediment beaches are highly permeable they allow swash infiltration and seepage to occur (Forbes et al, 1995), which according to Inman and Bagnold (1966), exerts a primary control on beach slope and as Van Wellan et al, (2000) indicate is probably also responsible for the berm found at maximum swash run-up. A study conducted on mixed sand and gravel beach, found that, due to the enhanced permeability, beach gradient steepness with an increase in sediment size and sorting, (McLean and Kirk, 1969), however Van Wellan et al, (2000) suggest that once the volume of sand in a mixed sand and gravel beach exceeds about 30 percent by weight hydraulic conductivity is reduced to about that for a sand beach. That, as indicated by Carter and Orford, (1984), brings a corresponding decrease in beach slope sufficient for the transition from a stable reflective beach to one more likely to pass through intermediate, and even dissipative stages.

As confirmed by Masselink and Li (2001) swash infiltration has a dominant role in determining the gradient of coarse sediment beaches, as it increases onshore swash

asymmetry that enhances onshore sediment transport creating a steep beach slope. Carter and Orford (1984) in a study regarding gravel barriers found that shoreward barrier migration occurred because of a lack of tidal passes, as very little sediment is transported seaward, with swash infiltration.

Finally, in terms of morphological response, very little has been done to establish cyclic patterns in the profiles of gravel beaches (Sherman, 1991). However, Sherman (1991) and Caldwell and Williams (1986) have shown that a cyclic model of beach profile response, based on the development of characteristic storm and swell morphologies as originally described for sand beaches, is applicable to gravel beaches.

2.5 POTENTIAL NUMERICAL MODELS

This section will introduce some of the existing models that could be used /modified in order to describe the behaviour of the gravel and mixed beaches (especially for cross-shore sediment transport).

Kobayashi et al. (1997) have developed a numerical model, which applied on regular and random waves, for obliquely incident shallow-water waves with small incident angles to elucidate the dispersion effects due to the vertical variations of instantaneous horizontal fluid velocities on the depth-integrated continuity, cross-shore and alongshore momentum equations:

Eq.2-26 $$\frac{\partial h}{\partial t}+\frac{\partial}{\partial x}(hU)=0$$

Eq.2-27 $$\frac{\partial}{\partial t}(hU)+\frac{\partial}{\partial x}(hU^2+m)=-h\frac{\partial \eta}{\partial x}-\tau_{b_x}$$

Eq.2-28 $$\frac{\partial}{\partial t}(hV)+\frac{\partial}{\partial x}(hUV+n)=-h\frac{\partial \eta}{\partial y}-\tau_{b_y}$$

where,

t is the time, h is the still water depth, U is the current velocity in x-direction, V is the current velocity in y-direction, η is the elevation of the water level due to the wave setup/setdown, τ_{bx} and τ_{by} is the x and y components of bottom shear stress respectively. The time-averaged alongshore momentum equation was obtained from Eq.2-27 for the case of alongshore uniformity:

Eq.2-29 $$\frac{d}{dx}(S_{xy}) + \frac{d\tilde{n}}{dx} = -\tilde{\tau}_{by}$$

where,

S_{xy} is the radiation stress component

The dispersion terms m and n in these equations express the additional cross-shore and alongshore momentum fluxes, respectively. The equations for m and n derived from the depth-dependent cross-shore and alongshore momentum equations.

In addition, Leont'yev (1999) has introduced an approach that implied the modelling of the whole suite of elementary processes responsible for changes in nearshore bottom topography during a given storm. The hydrodynamic governing equations (momentum, continuity and energy) that Leont'yev (1999) used were:

Eq.2-30 $$\frac{\partial M_x}{\partial t} + \frac{\partial M_x^2 / h}{\partial x} + \frac{\partial M_x M_y / h}{\partial y} + gh\frac{\partial \zeta}{\partial x} + \frac{F_x}{\rho} + \frac{\tau_{bx}}{\rho} - \frac{1}{\rho}\frac{\partial \tau_l}{\partial y} = 0$$

Eq.2-31 $$\frac{\partial M_y}{\partial t} + \frac{\partial M_x M_y / h}{\partial x} + \frac{\partial M_y^2 / h}{\partial y} + gh\frac{\partial \zeta}{\partial y} + \frac{F_y}{\rho} + \frac{\tau_{by}}{\rho} - \frac{1}{\rho}\frac{\partial \tau_l}{\partial x} = 0$$

Eq.2-32 $$\frac{\partial \zeta}{\partial t} + \frac{\partial M_x}{\partial x} + \frac{\partial M_y}{\partial y} = 0$$

where ζ is the wave setup, F_x and F_y represent the forcing terms (in x- and y-direction) caused by the radiation stress and stresses due to rollers in breaking

waves, τ_l is the Reynolds stress value due to turbulent mixing, M_x=Uh and M_y=Vh and the energy equation :

Eq.2-33 $$\frac{\partial}{\partial x}(EC_g \cos\theta) + \frac{\partial}{\partial y}(EC_g \sin\theta) = -D$$

where, C_g is group velocity.

Furthermore, Kobayashi and Karjadi (2001) have developed a two-dimensional, time-dependent numerical model for finite-amplitude, shallow water waves with arbitrary incident angles in order to examine oblique wave dynamics on steep rough slopes.

The time-averaged continuity, momentum and energy equations that were used to check the accuracy of the numerical model as well as to examine the cross-shore variations of wave setup, return current, longshore current, momentum fluxes, energy fluxes and dissipation rates were the followings.

The time-averaged continuity and momentum equations:

Eq.2-34 $$\frac{\partial}{\partial x}(\overline{hU}) + \frac{\partial}{\partial y}(\overline{hV}) = 0$$

Eq.2-35 $$\frac{\partial}{\partial x}(S_{xx}) + \frac{\partial}{\partial y}(S_{xy}) = -\bar{h}\frac{\partial \bar{\eta}}{\partial x} - \tau_{bx}$$

Eq.2-36 $$\frac{\partial}{\partial x}(S_{xy}) + \frac{\partial}{\partial y}(S_{yy}) = -\bar{h}\frac{\partial \bar{\eta}}{\partial y} - \tau_{by}$$

with

$$S_{xx} = \overline{hU^2} + \frac{1}{2}\overline{(\eta - \bar{\eta})^2}; S_{xy} = \overline{hUV};$$

$$S_{yy} = \overline{hV^2} + \frac{1}{2}\overline{(\eta - \bar{\eta})^2}$$

$$\tau_{bx} = f\overline{(U^2 + V^2)^{1/2}U}; \tau_{by} = f\overline{(U^2 + V^2)^{1/2}V}$$

where f is the friction factor and S_{xx}, S_{xy} and S_{yy} = time-averaged momentum fluxes similar to radiation stresses (Longuet-Higgins, 1970).

Also, the time-averaging normalized energy equation:

Eq.2-37 $$\frac{\partial}{\partial x}(F_x)+\frac{\partial}{\partial y}(F_y)=-D_f-D_B$$

with

$$F_x=\overline{hU\left[\eta+\frac{1}{2}(U^2+V^2)\right]};F_y=\overline{hV\left[\eta+\frac{1}{2}(U^2+V^2)\right]};$$
$$D_f=\overline{f(U^2+V^2)^{1.5}}$$

where F_x and F_y = time-averaged energy flux per unit width in the x and y-directions, respectively; and D_f and D_B = time-averaged rate of energy dissipation per unit horizontal area due to bottom friction and wave breaking, respectively. The dissipation rate D_B is related to the vertical variations of horizontal velocities and shear stresses outside the bottom boundary layer which were not predicted in that two-dimensional model.

As far as the morphodynamic models are concerned, Lee et al. (1996) have developed a robust and efficient beach-erosion prediction model based on the inhomogeneous diffusion equation (Kobayashi, 1987) that was implemented with moving boundary conditions. This numerical model was used to investigate beach evolution, dune recession, and offshore movement of the breaking point for various initial profiles and time-varying storm conditions.

Moreover, the governing equation for on-offshore sediment transport had the form of:

Eq.2-38 $$\frac{\partial h}{\partial t}=\frac{\partial}{\partial x}\left[D(h)\frac{\partial h}{\partial x}-K(h)\right]+\frac{\partial S}{\partial t},0\le h\le h_b$$

where, S= sea level rise; $D(h) = \alpha\sqrt{h}; K = \frac{2}{3}\alpha A^{3/2}$, α is the cubic velocity profile parameter and h_b = breaking water depth.

Furthermore, Lee et al. (1999) have adopted this approach (Eq.2-38) in order to investigate the generation of nearshore bars by multi-domain hybrid numerical model. Similar equation with Eq.2-38 was used in the numerical model of Lawrence et al. (2003) who have investigated the cross-shore sediment transport on mixed coarse grain sized beaches.

Karambas and Koutitas (2002) have developed a nonlinear breaking wave model in order to compute the nonlinear wave transformation in the surf and swash zone. With the aim of computing the changes in beach profile, they use the conservation equation of the sediment mass, given a form of:

Eq.2-39 $$\frac{\partial z_b}{\partial t} = -\frac{\partial}{\partial x}\left(q_t - \varepsilon_m |q_t| \frac{\partial z_b}{\partial x}\right)$$

where z_b =bottom elevation and the value of coefficient ε_m was set to a value of 2.0 and q_t is the total average load in the submerged part of the beach.

Leont'yev (2003) has developed a numerical model in order to compute the morphological response in coastal zone for different temporal scales. His model was based on this original one (Leont'yev, 1996) describing the whole sediment transport in the nearshore area. Leont'yev's (2003) model, in contrast with previous models, has included the influence of the longshore flux in the cross-shore sediment transport (Figure 2-9).

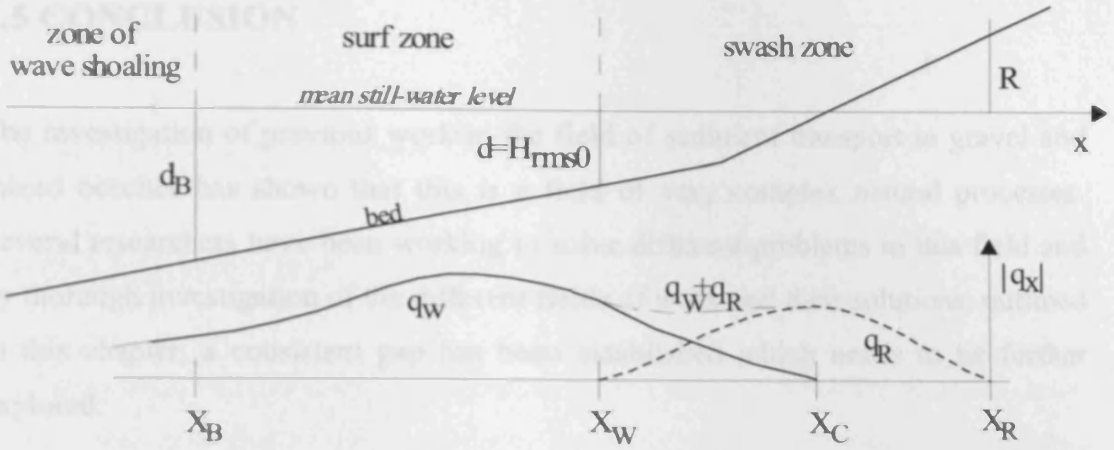

Figure 2-9 Scheme of nearshore zone (taken from Leont'yev, 2003)

The continuity equation for sediment transport for his morphodynamic model had the form of:

Eq.2-40 $$\frac{\partial d}{\partial t} = \frac{\partial q_x}{\partial x} + \frac{\partial q_y}{\partial y}$$

where d is the water depth measured from the level at rest, t denotes time, q_x and q_y are the cross-shore and longshore volumetric sediment fluxes (per unit width in the direction normal to the sediment flux component), and the coordinate axes OX and OY are shore-normal and shore-parallel respectively. In Eq.2-40, temporal changes in the local depths are determined by spatial gradients of the sediment flux. The contribution of the cross-shore (q_x) and longshore (q_y) components depends, among others, on the choice of the temporal scale of the considered process. For instance, the long-term evolution of a coastal zone with groin-type structures is mainly influenced by gradients of the longshore sediment flux. By contrast, the shoreline displacement and evolution of a coastal profile during a storm event depends mainly on the gradients of the cross-shore sediment transport flux.

2.5 CONCLUSION

The investigation of previous work in the field of sediment transport in gravel and mixed beaches has shown that this is a field of very complex natural processes. Several researchers have been working to solve different problems in this field and by thorough investigation of the different fields of work and their solutions, outlined in this chapter, a consistent gap has been established which needs to be further explored.

The majority of existing research on beach processes and morphodynamics has concentrated upon sandy beaches, however gravel and especially mixed beaches are only just beginning to receive attention in the research field. There are a number of numerical and parametric models that can predict the sediment transport of gravel beaches and none that can predict accurately the sediment transport of mixed beaches. Most of the models that are used in predicting the profile response of gravel or mixed beaches are based on laboratory/field tests with wave conditions and with normal wave angles.

A more detailed research on beach processes and morphodynamics of gravel and mixed beaches has been the primary objective of this thesis. This research was undertaken based on laboratory tests on gravel and mixed beaches with uniform slope and a trench. The establishment of a parametric model which can be applied to predict the breach profile of both gravel and mixed beaches being attacked by oblique waves has been established as the secondary objective of the thesis.

CHAPTER 3

EXPERIMENTAL SET-UP

3.0 INTRODUCTION

The importance of laboratory experiment is well known for scientific research, since experiments give rise to the opportunity to check on the accuracy of theoretical models, and also improve on the understanding of the physical processes involved in the theoretical model.

The laboratory experiments have the advantage of creating controlled conditions. With the help of highly sensitive equipments, laboratory experiments can facilitate accurate measurements and reduce significantly the cost in comparison with the field studies. Despite that, laboratory experiment is not a field experiment; meaning that it can not replicate exactly real natural conditions. Because of that, extensive care is taken when constructing the basin geometry and the boundaries, so that the designed wave current system is not significantly affected by scaling.

For the purpose of the thesis, an experiment was carried out in the three-dimensional wave basin located at Franzius-Institute (Marienwerder), Hannover University. The experiment ran for nearly 70 days and was undertaken for a beach model which consisted first of gravel sediment and secondly of mixed (gravel and sand) sediment.

The objective of the experiment was to gain understanding of the mechanism of the cross-shore distribution of wave-induced currents in mixed and gravel beaches. Comparative results between the gravel and mixed beaches help to understand their differences and similarities.

This chapter summarises the procedure and set-up of the experiment relevant to the thesis.

3.1 THE WAVE BASIN

The wave basin was requested and granted as a substitution of an old wave basin. It is sufficiently dimensioned for three-dimensional swell investigations. The wave basin had a length of 40 m, width of 24 m and could be filled up, to a maximum depth of water of 0.7 m (Figure 3-1).

Experiences from past models of wave production required that the plant was controlled by separated mobile individual components with a total width of about 25 m. The wave machine plates implemented a pure translation movement (piston type) and could be used in water depths to about 0.7 m.

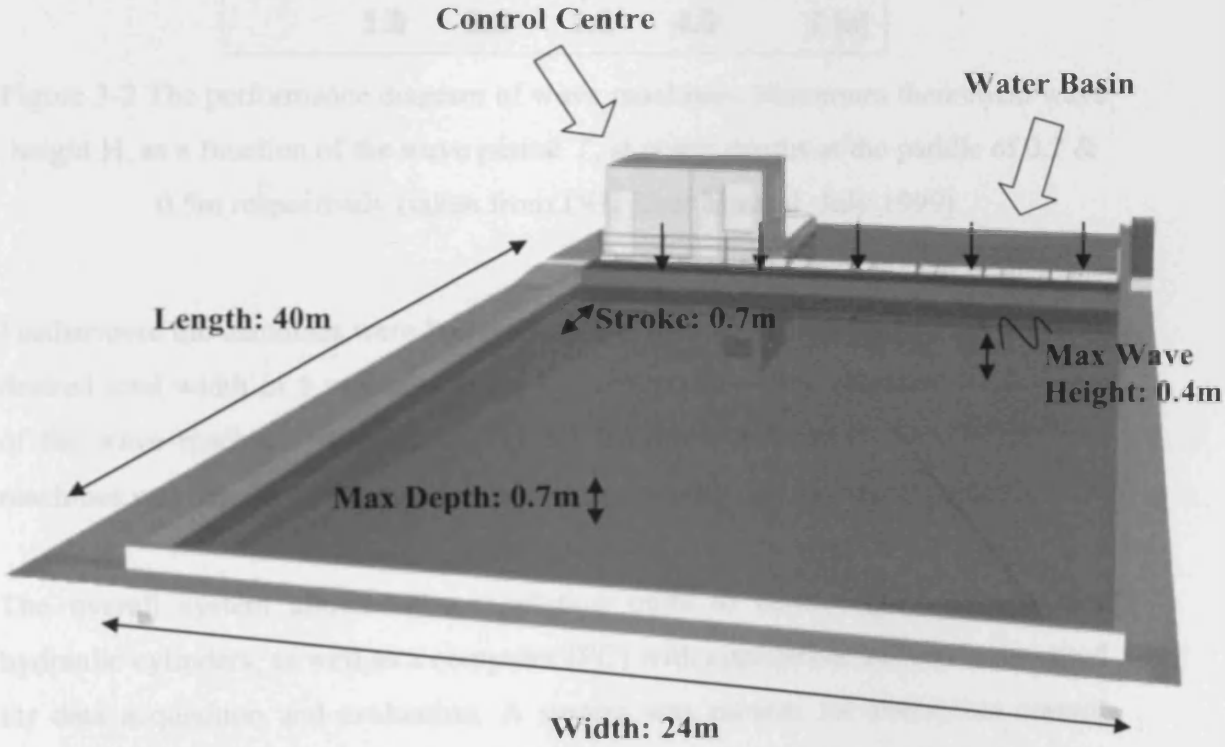

Figure 3-1 Dimensions of the new wave basin (taken from Zimmermann C. et al., Jun'99–Feb'00)

To have better absorption control within the long-periodic range, first the stroke (moving range of the plates of the wave machines) of 0.6 m (standard) was increased to 0.7 m because of better efficiency of a control with consideration to components bound to it. The performance diagram of the wave machines (Figure 3-2) shows that wave heights, to approximately 0.33 m, can be produced with a water level of 0.5 m.

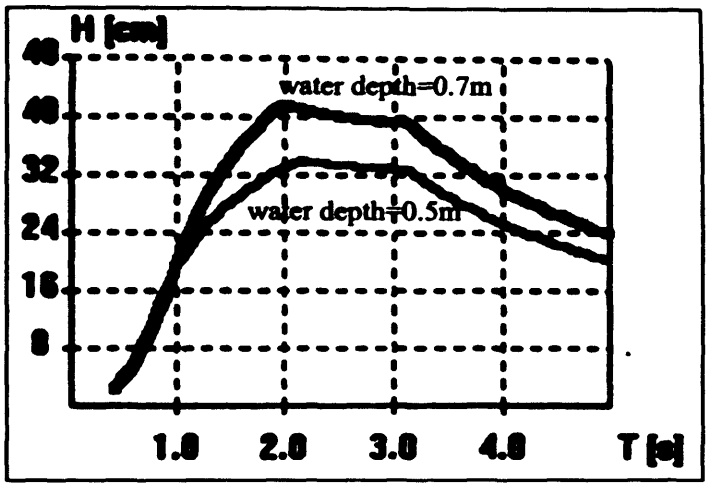

Figure 3-2 The performance diagram of wave machines. Maximum theoretical wave height H, as a function of the wave period T, at water depths at the paddle of 0.7 & 0.5m respectively (taken from DHI User Manual, July 1999)

Furthermore the machines were built with basic width of 3 m (standard 5.5 m). The desired total width of 5 m was reached by (removable) wing elements. The plates of the wave machines were moved by oil hydraulic cylinders. Each of the two machines was supplied with the intended capacity range by a pressure station.

The overall system allowed the regulation units to control the valves of the hydraulic cylinders, as well as a computer (PC) with appropriate software, also used for data acquisition and evaluation. A system was present for absorption control (absorption of reflected waves at the wave machine). Also, at the end of the wave basin, around 6 tonnes of gravel were placed in order to absorb the wave energy and diminish the reflected waves.

3.2 THE PHYSICAL MODEL

3.2.1 The beach model

A beach model of 8m x 7m x 0.7m (width x length x depth) was set up in the middle of the wave basin. It was open to the side from which the generated waves were approaching to (Figure 3-3). The beach was oriented in such a way that waves, generated by the wave paddle, were always approaching with an angle of 15^0 to the beach (Figure 3-4). The bathymetry of the beach consisted of a uniform slope beach (straight-line parallel contour) and a trench (curved contour) with a width of 2m, as shown in Figure 3-5.

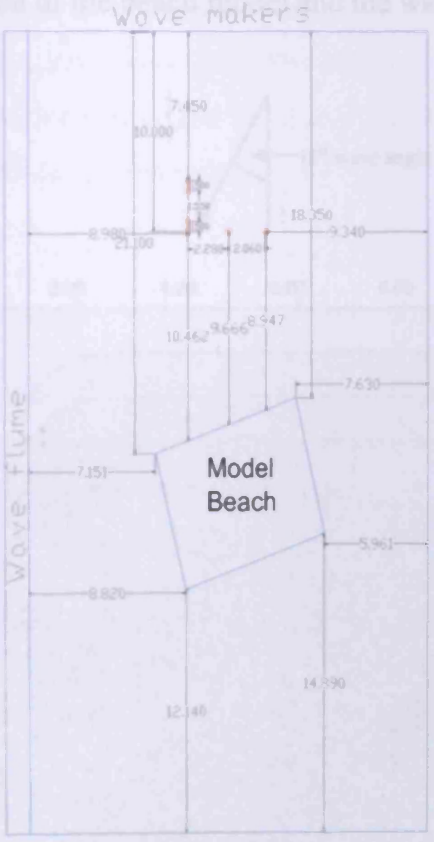

Figure 3-3 Plan view of the wave basin

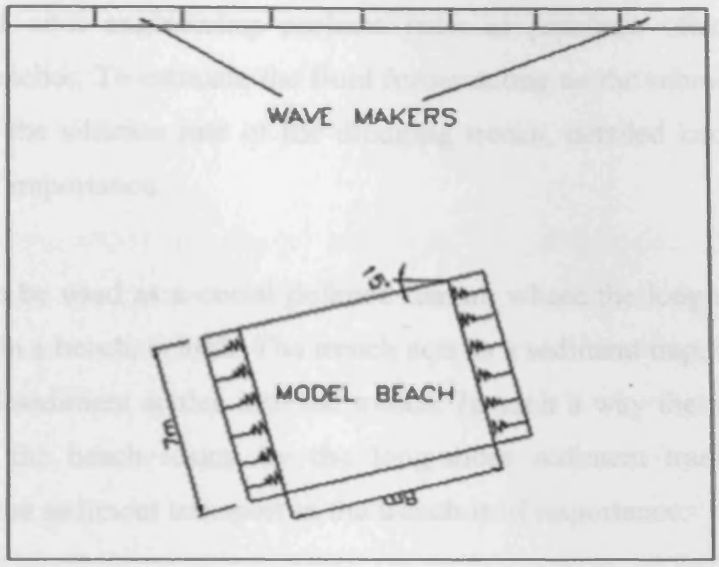

Figure 3-4 Orientation of the beach model and the wave angle

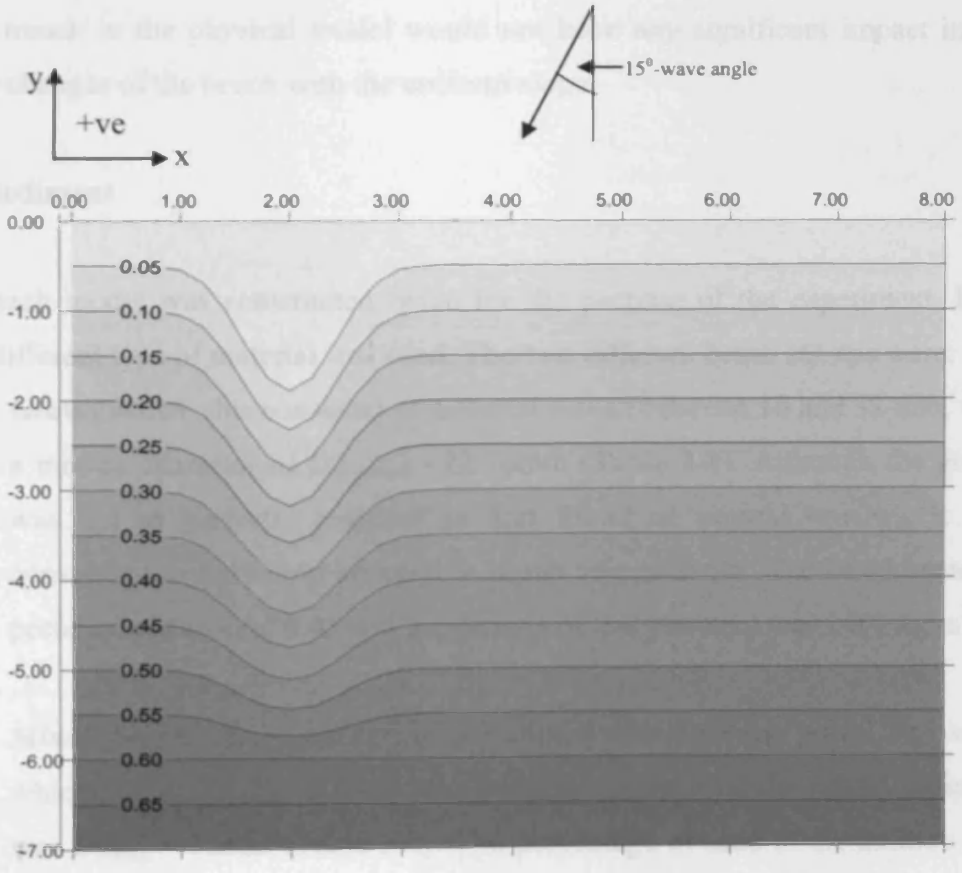

Figure 3-5 Bathymetry of the beach model (units in meters)

The design of civil engineering projects such as pipelines often requires the dredging of trenches. To estimate the fluid forces acting on the submerged structure or to compute the siltation rate of the dredging trench, detailed knowledge of the flow field is of importance.

The trench can be used as a costal defence feature where the long-shore sediment transport rate, in a beach, is high. The trench acts as a sediment trap, where bed load and suspended sediment settles into the trench. In such a way the trench traps the sediment that the beach losing by the long-shore sediment transport. Detailed knowledge of the sediment transport in the trench is of importance.

Therefore, it is important to include the trench in to the beach model to investigate its hydrodynamic and morphodynamic behaviour. The location and the dimensions of the trench in the physical model would not have any significant impact in the profile changes of the beach with the uniform slope.

3.2.2 Sediment

The beach model was constructed twice for the purpose of the experiment. Both times different type of material was used. The two different beach set-ups were:

1. ***Gravel beach***: this consisted of material sieved between 16 and 32 mm, with a median diameter of $D_{50gravel}$ =22.76mm (Table 3-1). Although the gravel was not as perfectly rounded as that found on natural beaches, it was considered to be within acceptable limits of angularity. The beach material porosity was around 0.45 and the density of the sediment was 2450 kg/m^3.

2. ***Mixed beach***: this consisted of a bimodal mix between gravel and sand, which had a D_{50sand} =300μm. The median diameter of the mixed sediment was D_{50mix} = 12mm (Table 3-1). The percentage of sand in the mixture was around 40%. The sediment was thoroughly mixed prior to beach

construction outside the wave basin and during beach construction within the wave basin. For the mixed beach, the porosity was far lower than for the gravel beach of around 0.2 and the density of the sediment was 2580 kg/m^3.

Figure 3-6 below shows the initial sediment size distribution for both beach materials. Initially, the beaches were constructed at a 1:10 slope but they were not reshaped during the experiment procedure (except when the sediment changed), so that the initial condition for each test was the final profile from the previous test. Reshaping the beach in such a large facility would have been very time consuming and therefore not practical, and there are also uncertainties as to what should be an appropriate initial condition in any event. The beaches were conducted at this slope due to the fact that firstly, the gravel beaches are steep, in general steeper than about 1:10 and secondly, the mixed sand and gravel beaches can be steep reflective beaches which have in generally a beach slope of the range of 1:10.

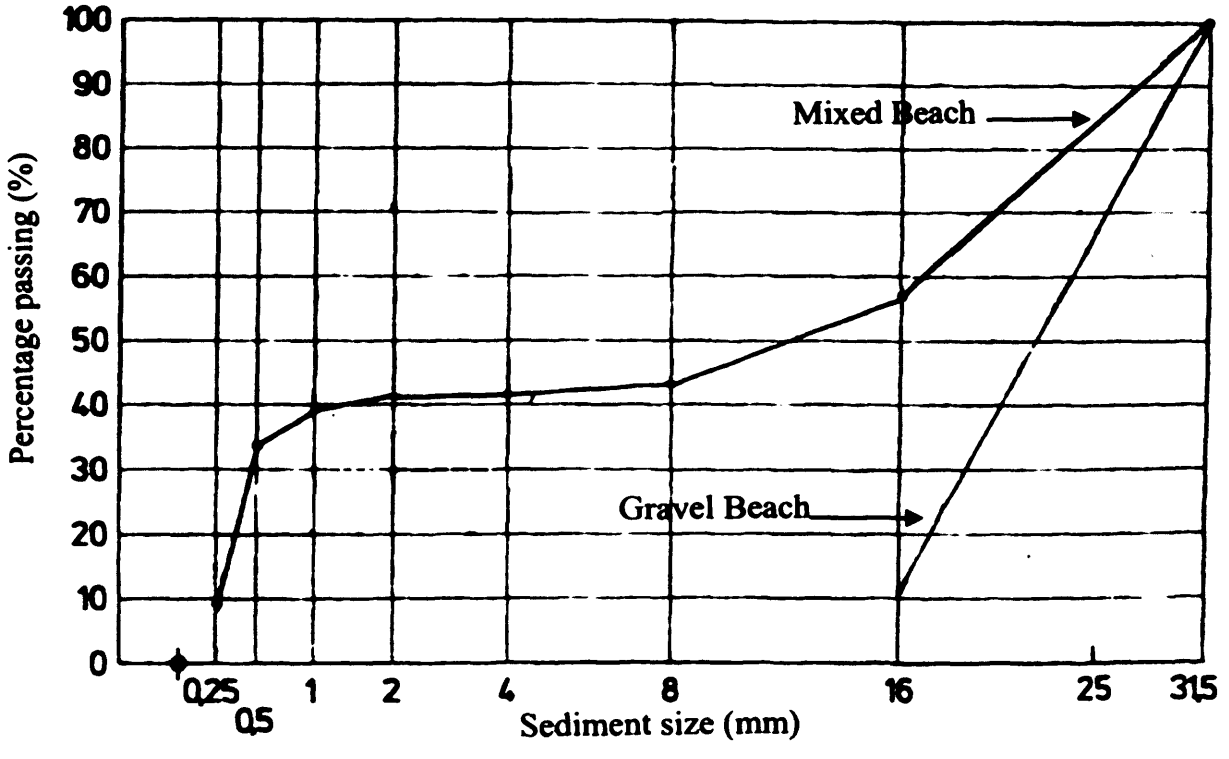

Figure 3-6 Initial sediment particle size distributions for gravel and mixed beach material

Table 3-1 The different particle sizes of the sediments

Type of Beach	D_5 (mm)	D_{15} (mm)	D_{16} (mm)	D_{50} (mm)	D_{84} (mm)	D_{85} (mm)	D_{90} (mm)	D_{94} (mm)
Gravel Beach	15.35	16.66	16.83	22.76	28.38	28.86	29.59	30.50
Mixed Beach	0.21	0.32	0.33	12	25.20	25.9	27.31	29.19

3.2.3 Construction issues

A number of factors had to be considered for the construction of the beach model. These factors are discussed below:

- Compaction: In preventing different compaction of the sediments along the beach due to the machinery, resulting irregularities across the beach during the experiment, the sediments were compacted manually.
- Settlement: Mixed Beach appeared to be quite compacted at the end of the construction. However the basin was filled with water over 8 hours before carrying out the instrument calibrations. During this time, it was apparent that some settlement had taken place especially at the rear (at y=-7m) of the beach.

3.2.4 The Reinforcement

Due to the fact of the size of the waves, and as consequently the high energy, that would be produced by the wave paddles and would impact on the beach, the model had to be reinforced on its three sides (at y=-7m, x=0m, and x=8m) in order to withstand the wave breaking and to become more stable. After various tests with different wave periods and wave heights, it was concluded to reinforce the model with 3 layers of stones on each of the three sides.

For the rear sides of the model, the layers were consisted of stones with dimensions of 23.6 x 37 x 23.6 cm (height x length x width). The rear side was more reinforced by 10 small stone towers placed at equal distances from each other. The small stone towers, which had the same dimensions with the stones the sides of the model at x=0m and x=8m, were placed to prevent the beach to move backwards. Furthermore, several stones were placed at the corners of the rear side in order to prevent the small stone towers and the layers to be destroyed from the phenomenon of the diffraction.

As far as the other sides (x=0m and x=8m) were concerned, the layers consisted of stones with dimensions of 23.8 x 37 x 17.2 cm. Several stones were placed along the sides in order to make them solid and to prevent the stones to fall into the beach. Finally, the model was braced along the sides, at x=0m and x=8m, with gravel in order to be stable. The reinforcement was arranged in such a way in order the model to be safe since the instability would slow down the progress of the experiment.

3.2.5 Additional structure

The size of the beach required the construction of a structure with the aim of taking measurements safely and accurately. The structure had a height of 1.7m and was mainly made of steel. It consisted of two steel trusses that were connected with a scaffold which played the role of a walkway for the technician and the researcher. Two steel bars with dimensions of 8cm x 6m x 6cm were placed above the trusses with a 3.9m distance from each other. The steel bars played the role of the rails of the wheels of a steel hollow section. The steel hollow section had dimensions of 9.5cm x 1.6m x 4m x 5cm (height x length x width x thickness) and could move at the vertical direction of the beach. Two steel bars were placed at both sides of the hollow section with the intention of placing the ADV and have the opportunity to take measurements at the horizontal direction of the beach. At that place, the ADV could also be moved upwards and downward to take measurements in z direction.

Furthermore, a steel gantry was placed at the steel hollow section in order the technician or the researcher to sit and use the ADV. A plan view of the beach model with the additional structure can be seen in the
Figure 3- 7.

Due to the fact that the model was at the centre of the basin another walkway was needed to be constructed. The new walkway connected the structure with the side of the wave basin where the computer, at which the data was stored, was.

The additional structure, the wave basin and the construction of both beach models can be seen in Appendix I (A1).

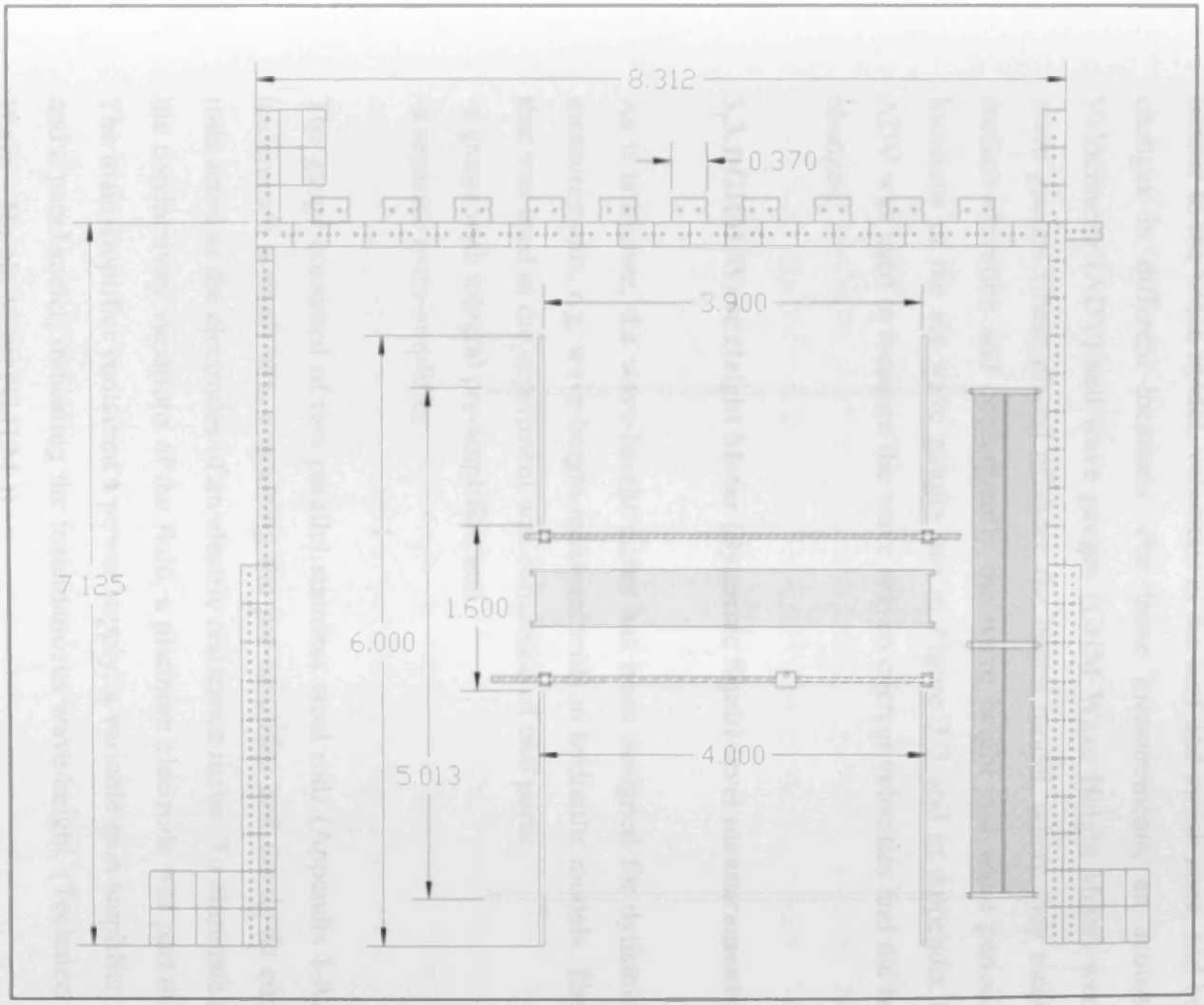

Figure 3- 7 Plan view of the wave basin and of the additional structure (units in meters)

3.3 INSTRUMENTATION

During the experiment measurements have been taken of water surface elevation further to the beach model, velocities at the surf and swash zone, and beach profile changes in different locations. For these measurements, an acoustic Doppler Velocimeter (ADV) and wave gauges (GHM Wave Height Meter) were used. Six wave gauges where placed offshore the beach model, where they measured water surface elevation and consequently the wave height and wave period. The exact locations of the six wave gauges are in Figure 3-3 and in Appendix I (A2). The ADV was used to measure the wave driven current velocities and the beach profile changes.

3.3.1 GHM Wave Height Meter (dynamic liquid-level measurements)

As it is known, the wave-height meter has been designed for dynamic fluid level measurements, e.g. wave-height measurements in hydraulic models. The instrument that was used in the experiment was composed of two parts:
-a gauge with integral pre-amplifier, and
-a separate main-amplifier

The gauge consisted of two parallel stainless steel rods (Appendix I-A2), mounted underneath a small box, containing the pre-amplifier and the dc-dc converter. The rods acted as the electrodes of an electric resistance meter. To eliminate the effect of the conductivity variations of the fluid, a platinum electrode was part of the system. The main-amplifier contained a power supply, a variable gain amplifier, a zero-shift and a panel-meter, indicating the instantaneous wave-height. (Technical Manual for Wave – Height Meter (G.H.M.))

The probe was connected by means of the measuring-cable supplied, to the connector at the rear of the cabinet, at the same side of the control-unit to be used. Power for the probe was supplied also via this cable.

Before the measurements started, the probe was attached to e.g. a point-gauge for calibration and fixed position for measurements. The depth was chosen in such a way that, during calibration and measurement the top of the reference-electrode is at least 4cm under the water-surface. The electronics housing kept dry under all conditions. The immersion-depth that started with the calibrations was half the value indicated on the switch "Range" +4cm. measured from the top of the reference-electrode. With the multi-turn dial "Zero" the pointer of the indicating meter (and also the output-voltage) was adjusted to its center-scale position (= 0V output) and then the calibration was made.

After calibration the gauge was placed at the measuring-point, taking care that the wave crest met both rods simultaneously. There was no objection to execute/perform the calibration on the measuring-point, provided the water level remained sufficiently constant. When several Wave Height Meters are used close to each other, a certain mutual influence can be experienced, but because distances in the experiment were more than 20cm, this influence was neglected.

Finally the procedure for wave spectrum calibration was split into two parts, the first to record the spectral properties and to obtain the appropriate gain setting on the wave maker machine, and secondly to record the statistical properties of the spectrum over at least 1000 waves. During testing, a similar procedure was used, usually, only statistical data was likely to be recorded. For both cases there was a consistency in recording.

3.3.2 ADV (Acoustic Doppler Velocimeter)

Acoustic Doppler Velocimeter (ADV) was developed to satisfy the need for an accurate current meter that can measure 3D dynamic velocity in physical models. ADV can replace several types of flow measurement instrument and therefore simplifying procedures for technicians/researchers while providing continuous digital records at user-specified sampling rates.

3.3.2.1 *ADV- The Instrument*

Figure 3-8 shows an overview of the ADV that was used in the experiment. The system had four main modules: the ADV sensor, the ADV probe, the ADV signal conditioning module and the ADV processor.

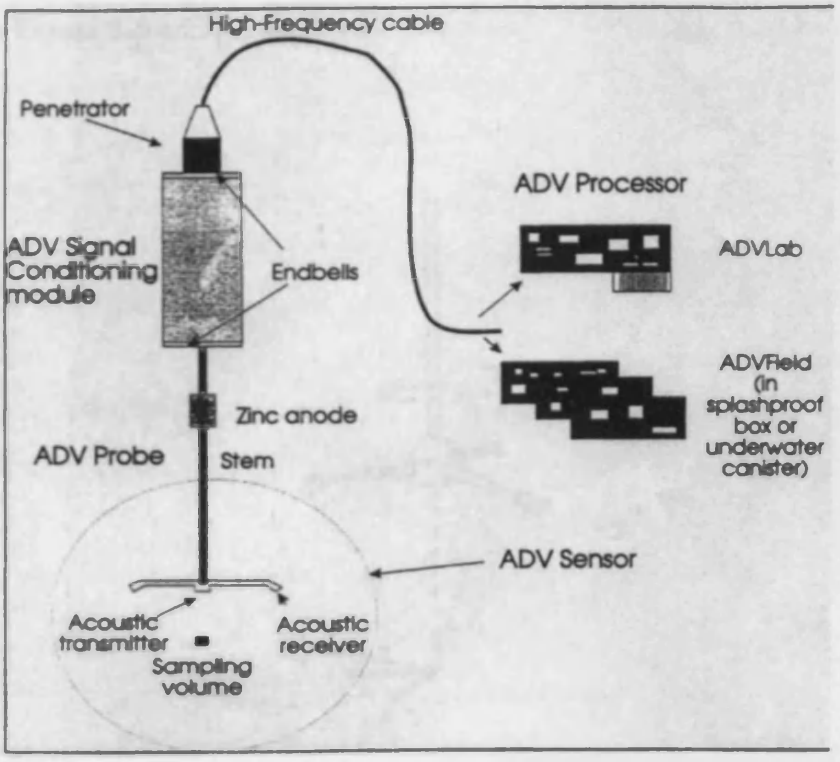

Figure 3-8 Naming convection for the ADV (ADV Operation Manual, 1997)

- The ADV sensor comprised of two acoustic or three acoustic receivers and a transmitter.
- The ADV probe was attached to the ADV signal conditioning module and was assembled by the sensor, a stem and an endbell.
- The ADV signal conditioning module holden the receiver. A penetrator was attached permanently with a high-frequency cable.
- The ADV processor, which is connected with the ADV signal conditioning module through the high-frequency cable, consists of a PC-card or a set of three cards enclosed in an underwater housing or in a splash-proof enclosure. The ADV processor that was used in the experiment consisted of only a PC-card.

3.3.2.2 *The use of the ADV in the experiment*

The type of probe that was used in the experiment was a 3D down-looking probe as sketched in Figure 3-9 and Figure 3-10.

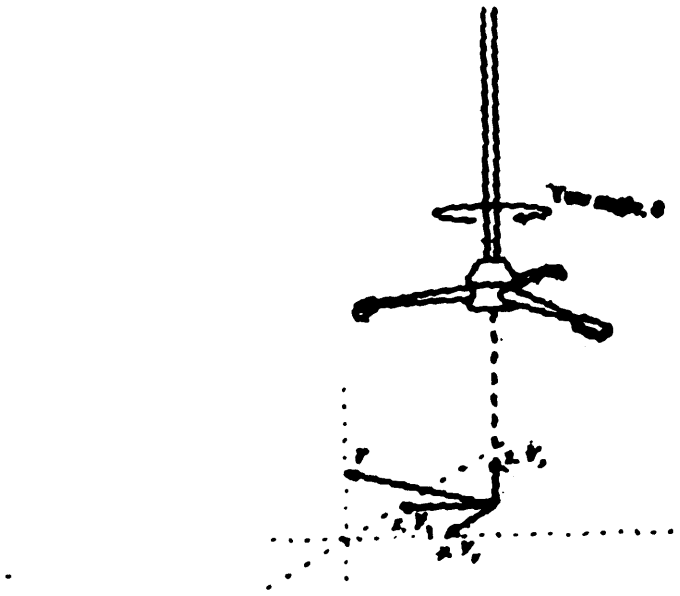

Figure 3-9 Sketch of ADV Probe and its Coordinate System

(Snyder and Castro, 1999)

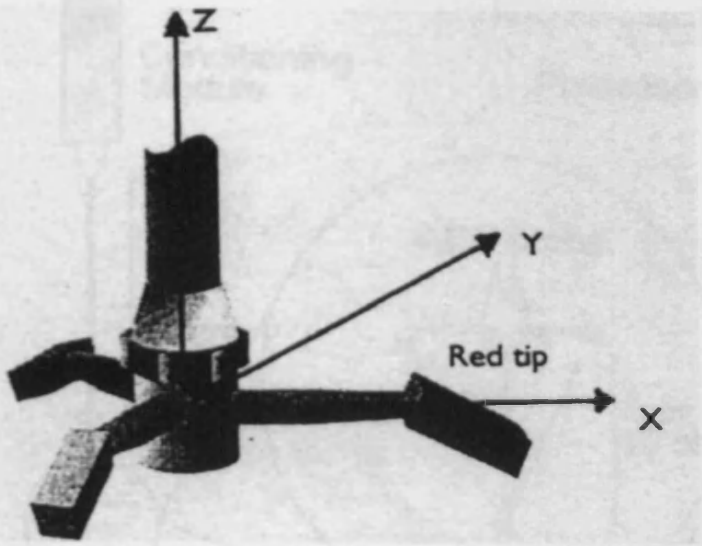

Figure 3-10 Standard, 3D down-looking probe (ADV Operation Manual, 1997)

In Figure 3-10, the red receiver arm in the direction of the x-axis and the velocity V_x in the software refers to the velocity along this axis. The direction of the y-axis and the z-axis are based on the definition of a right-handed coordinate system where z is pointing upwards (towards the conditioning module).

For the duration of the experiment, the probe was most of the time submerged in the flow and the receivers were slanted at 30^0 from the axis of the transmit transducer and focus on a common sampling. In general, the volume was located either 5 or 10cm from the probe to reduce flow interference (Figure 3- 11). During the experiment the sample volume was located 5cm away from the transducer. The sampling rate was fixed at 25Hz and also the velocity range was set at $\pm$ 30cm/s before data collection was started.

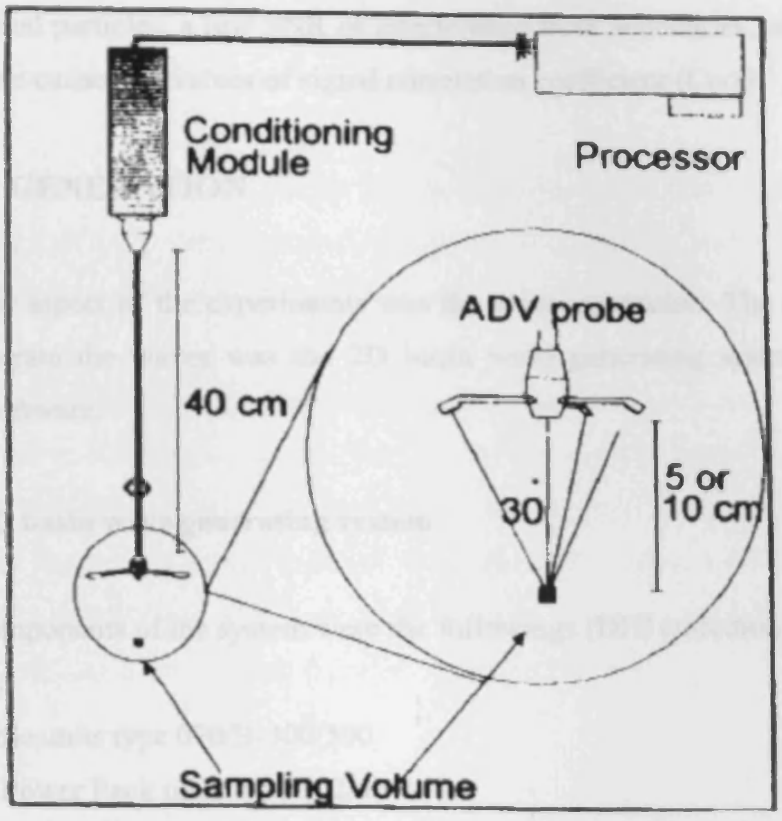

Figure 3- 11 Measuring volume of ADV (taken from Lohrmann et al., 1994)

The processor output was RS-422 compatible, and the software used for the data acquisition was version ADV 2.6 (Nortek). Using the software ADV 2.6, the three velocity components (V_x,V_y,V_z), their standard deviations (σV_x,σV_y,σV_z), the signal-to-noise ratio (SNR1/2/3) measured at each of the three receivers in ADV and the signal correlation coefficient (Corr 1/2/3) of the receivers can be displayed at all time during the experiment.

The correlation coefficient output with each ADV sample, is a control parameter that indicates the degree to which all particles within the sampling volume are moving in exactly the same way. Ideal values of the correlation parameter should be between 70 and 100. Generally, the higher the SNR, the higher the correlation and the more reliable the velocity measurement is. However, the presence of bubbles or

large individual particles, a low SNR or interference from boundaries, or even high turbulence can cause low values of signal correlation coefficient (Corr).

3.4 WAVE GENERATION

An important aspect of the experiments was the wave generation. The system that used to generate the waves was the 2D basin wave generating system with the WAVEPC software.

3.4.1 The 2D basin wave generating system

The main components of the system were the followings (DHI quotation, 1998):

5 Wave paddle units type 070/B-300/500
3 Hydraulic Power Pack units type 302/45-140
2 Wave Controllers type 414/2
1 Wave Synthesizer package type 452/16
1 AWACS (Active Wave Absorption Control System)

A description of the wave paddles and the AWACS is following. The rest of the components of the wave generating system including the software used for generation and storing data, are described in Appendix I (A3).

3.4.1.1 *The Wave paddles*

The 5 movable basin wave paddles were able to generate 2D regular and random waves. The wave paddle was of the piston type. Any number of wave paddles could be synchronized and thereby provide the required overall wave front length. The stroke of the wave paddle was 700mm and the paddle height was 1.00m. The base

width of the wave paddle was 3.00m. Additionally, two attachable/detachable wing elements enabled the paddle width to be extended to 5.00m.

Moreover, the wave paddle was driven by a hydraulic actuator. The hydraulic servo actuator consisted of a double-ended, symmetrical hydraulic piston which was trunnion mounted to allow unrestricted movements in all directions.

Furthermore, the five wave paddles were controlled by two wave controllers. Each wave paddle/servo actuator was controlled by a servo amplifier module. Easy access was provided for adjustment of the servo gain. In addition to the servo amplifier modules, the wave controller featured a signal generation module for easy generation of regular waves. For generation of random waves, the wave controller received the relevant control signal from the Wave Synthesizer.

3.4.1.2 *The Active Wave Absorption Control System (AWACS)*

The AWACS was a digital control system that enabled wave paddles to simultaneously generate the desired waves and to absorb online spurious waves reflected from the flume back to the wave paddle. Re-reflection from the paddle was virtually eliminated. Hereby, the desired incoming wave field was controlled with superior precision, notable if reflection from the flume is significant. The AWACS worked equally well for regular and random waves.

The system made use of digital recursive filters designed to ensure excellent performance for a broad frequency range. The AWACS, in conjunction with a standard wave paddle, practically eliminated the problem of re-reflection by absorbing the reflected waves.

CHAPTER 4

THE EXPERIMENTAL TESTS AND RESULTS

4.0 INTRODUCTION

As the construction of the beach model finished, the experimental tests began. The experiment comprised of ten tests, which were mainly focused on the profile and wave current measurements across the gravel and mixed beach.

However, the experiment involved making measurements of wave height and wave period. These measurements were carried out with the use of the six wave gauges (probes) at locations which have been in Chapter 3.

Moreover, the wave driven current (for all the dimensions) measurements were carried out with an ADV. The observations started 10 minutes after the first wave was generated. These 10 minutes were sufficient to eliminate long-periodic start-related variations in wave fields. The current velocity observations were done at various levels in the horizontal and vertical direction. This allows an estimate of the vertical structure of the time-averaged velocity and a more accurate determination of the depth-averaged current velocities than measurements taken at a single elevation. The accuracy of the present current velocity data is good mainly because is due to the large number of observations per measuring point. The data presented here are not just for application in this thesis alone, but could be used by others as well.

The ADV was also used to measure the profile development of the beach. Due to the fact that ADV can only take measurements below water, its measurements were related to the submerged part of the beach. For the remaining part of the beach, the profile measurements were carried out with the use of a measuring stick.

The profile and wave driven current measurements were taken at three cross-shore sections of the beach. The first was at the curved beach section (at x=2.0m) and the other two at the straight beach section (at x=4.0m and at x=5.64m). These sections had a length of approximately 5.4m and their location can be seen in Figure 4-1 below. In Figure 4-1 these sections are shown as lines and that's how they will be mentioned in the thesis. In this figure the coordination of the positive x and y direction has been indicated.

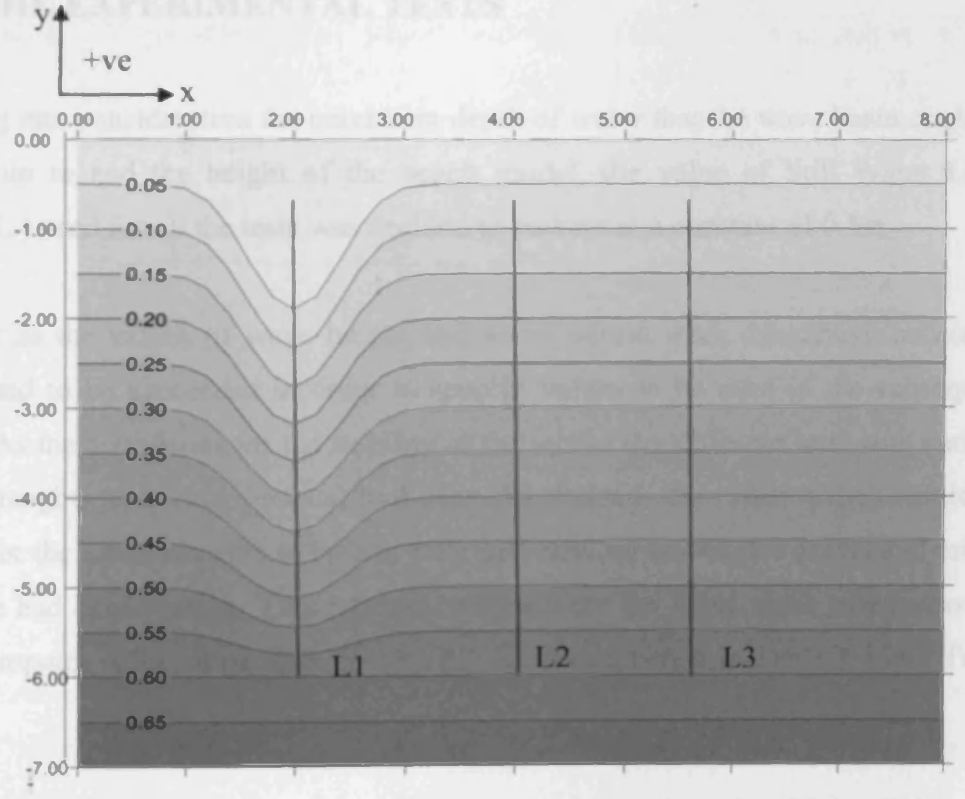

Figure 4-1 Locations of measurements (the three lines: L1, L2 and L3)

The bathymetry of the beach with the uniform slope is replicate by using Eq.4- 1 , whether the bathymetry of the trench can be replicate by Eq.4- 2.

Eq.4- 1 $h(x,y) = sx$ for $0 \leq x < 1m$ and $3m < x \leq 8$

Eq.4- 2 $h(x,y) = s\left[1.0 - \cos\left(\frac{2\pi(x(i)-(10\times dx))}{(20\times dx)}\right)\right] \times 1.5$ for $1m \leq x \leq 3m$

where, s = slope = 0.01

x(i) = distance from origin for longshore distance

dx = 0.1m, grid spacing

4.1 THE EXPERIMENTAL TESTS

Taking into consideration the maximum depth of water that the wave basin could be filled up to and the height of the beach model, the value of Still Water Level (S.W.L.) used for all the tests was decided to be kept at a constant of 0.5m.

As far as the values of wave height and wave period were concerned, resistance tests had to be proceeded in order to specify values to be used in the subsequent tests. As the boundaries for the stability of the model (by different tests with various wave heights and wave periods) had been determined, the values which would be used for the measurements of both regular and random waves (for gravel and mixed beach) had been chosen. These values, which were the input wave parameters for the computer software package WAVEPC, are listed below in Table 4-1 and Table 4-2.

Table 4-1 WAVEPC input wave parameters for tests with regular waves

REGULAR WAVES			
Test Number	**Type of Beach**	**Wave Height (H)**	**Wave Period (T)**
1	Gravel	24cm	2sec
2	Gravel	24cm	3sec
3	Gravel	8.4cm	2sec
4	Gravel	8.4cm	3sec
7	Mixed	8.4cm	2sec
8	Mixed	8.4cm	3sec

Table 4-2 WAVEPC wave parameters for tests with random waves

RANDOM WAVES			
Test Number	**Type of Beach**	**Significant Wave Height (H_s)**	**Spectral Peak Period (T_p)**
5	Gravel	12cm	2sec
6	Gravel	12cm	3sec
9	Mixed	12cm	2sec
10	Mixed	12cm	3sec

4.1.1 The chosen values

The author used the values in Table 4-1 and Table 4-2 for both types of beach, in order for them to be in a scale that could be matched to real field conditions. Moreover, as it can be seen in the above Tables, both types of beach had the same values of wave height in all tests (except for Tests 1 and 2, where the wave height

was 24cm and applied only on gravel beach). The reason behind that is to compare the two beach models and understand their similarities and differences.
The maximum wave height that wave paddles could produce was 24cm for the given S.W.L. and it was also the maximum wave height that could be generated without the beach being destroyed. The generation of this wave height gave the opportunity to the author to observe the clear movement of the gravel material. However, the value of this wave height could generate high wave energy, which could move the sand very fast so it wasn't suitable for observing and measuring the wave currents and beach profile of mixed beach. Consequently, it was only used in gravel beach.

The optimum value of wave height, with which both the movement of the sand and the slight movement of the gravel could be observed, was 8.4cm. This value of wave height was used for both beach models.

The value of the significant wave height that was used for both beach models was 12cm. This value of the significant wave height was different from the value of the wave height for the case of regular waves. This occurred due to the fact that the author wanted to have the same wave energy produced for both regular and random waves.

4.1.2 The duration of tests

The number of waves and its duration for each test that generated can be shown in Table 4- 3 below. With respect to the random waves, the wave paddles generated sequenced batches (C) with same wave spectra (JOHSWAP type) where each batch contained 116 waves.

Table 4- 3 The time duration and the number of waves generated for each test

	Number of waves	Time Duration
Test 1-G	33,600	18h 40m
Test 2-G	18,250	15h 13m
Test 3-G	14,400	8h 00m
Test 4-G	7,450	6h 13m
Test 5-G	18,328 (C=158)	10h 32m
Test 6-G	12,412 (C=107)	10h 42m
Test 7-M	12,000	6h 40m
Test 8-M	7,900	6h 35m
Test 9-M	17,748 (C=153)	10h 12m
Test 10-M	12,644 (C=109)	10h 54m

4.2 THE EXPERIMENTAL RESULTS

In this section, the results of the experiments can be observed. The numerical results can be seen in Appendix II. It has to be mentioned that measurements with correlation less than 70% were not included in these numerical results. The results for both regular and random waves have been divided into three categories:

1. Wave parameters
2. Wave-induced current velocities
3. Cross-shore beach profiles

4.2.1 Wave parameters

Table 4-1 and Table 4-2 show the input wave parameters that were used in WAVEPC in order the wave paddles to generate the various wave heights and wave

periods. During the generation of the waves, the six wave gauges/probes took measurements for various wave parameters.

In deep water $H_{1/3}$ and H_{m0} are very close in value and are both considered good estimates of H_s (significant wave height). In fact, all modern wave forecast models report H_{m0} as the significant wave height. Similarly, the H_s values recorded from wave gauge records is also H_{m0}. It is worth noting, however, that in shallow water $H_{1/3}$ may be significantly larger than H_{m0}, especially for low-frequency waves. Therefore, in the case of the irregular waves more consideration was given to the values of H_{m0}.

The numerical presentation of the wave parameters measured at the wave probes can be seen in Appendix II (A1). From a quick look of the tables in Appendix II (A1), it can be seen that the results from the wave measurements were close to the input wave parameters of the WAVEPC.

For the purpose of the analysis of the results, a selection of a representative probe had to be chosen. The chosen probe was number 9 (P09) due to its location. It was close enough to the beach in order to have a representative incoming wave height and also far enough in order not to be affected from the reflective waves compared to the other probes. Table 4-4 shows a comparison/error difference between the input and measured values of wave height and wave period at probe 9, where the input values were the wave conditions specified for the wave paddle and the measured values were the actual conditions in the wave basin that were the ones used in all subsequent analysis.

Table 4-4 Comparison between input and measured wave parameters at probe 9

TESTS	Wave Height			Wave Period		
	Input (cm)	Measured (cm)	Error. Diff. (%)	Input (sec)	Measured (sec)	Error. Diff. (%)
Test 1-G	24	25.3	-5.4	2	2	0
Test 2-G	24	21.8	9.2	3	3	0
Test 3-G	8.4	8.6	-2.4	2	2	0
Test 4-G	8.4	9.2	-9.5	3	3	0
Test 5-G	12	10.8	10.0	2	2.3	-15.0
Test 6-G	12	11	8.3	3	3.2	-6.7
Test 7-M	8.4	8.6	-2.4	2	2	0
Test 8-M	8.4	7.7	8.3	3	3	0
Test 9-M	12	11	8.3	2	2.3	-15.0
Test 10-M	12	11.7	2.5	3	3.1	-3.3

From the values of Table 4-4, the following conclusions can be drawn:

- With respect to the wave heights, the input values were always larger (except Test 1, 3, 4 and 7) than those measured at the probe. The highest percentage error difference for gravel beach can be observed at Test 4 and 5 and for mixed beach at Tests 8 and 9. Moreover, under random wave conditions, the measured values for mixed beach (8.3% and 2.5%) were closer to the input values rather than the measured values for gravel beach (10.0% and 8.3%).

- With respect to the wave periods, the agreement was satisfactory. Most of the tests have the same input and measured values. However, at tests relating to the random wave conditions, for both types of beach, there were discrepancies between the input and measured values. The highest percentage error difference, with respect to the wave periods, appeared to be

at the same Tests where the highest error difference with respect to the wave heights occurred (Tests 5 and 9).

The measured wave heights were used, rather than the input wave height, for the analysis of the results.

Based on the measured values from probe 9 and the angle at which the waves approached (15^0), some wave parameters could be calculated. These are: deep water wave height (L_0), wavelength (L), relative deep water depth (d/L_0), relative water depth (d/L), and wave steepness (H/L). The summary of all these wave parameters can be found in Table 4-5 below.

Table 4-5 Summary of calculated wave parameters

	H (m)	T (sec)	L_o (m)	d/L_o	d/L	L (m)	H/L
Test 1-G	0.253	2	6.245	0.080	0.123	4.056	0.062
Test 2-G	0.218	3	14.052	0.036	0.078	6.396	0.034
Test 3-G	0.086	2	6.245	0.080	0.123	4.056	0.021
Test 4-G	0.092	3	14.052	0.036	0.078	6.396	0.014
Test 5-G	0.108	2.3	8.259	0.061	0.105	4.770	0.023
Test 6-G	0.110	3.2	15.988	0.031	0.073	6.854	0.016
Test 7-M	0.086	2	6.245	0.080	0.123	4.056	0.021
Test 8-M	0.077	3	14.052	0.036	0.078	6.396	0.012
Test 9-M	0.110	2.3	8.259	0.061	0.105	4.770	0.023
Test 10-M	0.117	3.1	15.004	0.033	0.075	6.625	0.018

Observing the values at Table 4-5, the following conclusions can be drawn:

- Examining the relative water depth (d/L), the values which were between 0.04 and 0.05 showed that the waves were in transitional water depth. This is the zone between deep water and shallow water: that is, $0.5 > d/L > 0.04$. In this zone there are characteristics of both deep and shallow water waves.

Celerity depends on both water depth and wavelength. Moreover, the orbits of the particles become progressively flattened with depth.

- Examining the wave steepness (H/L), the values were smaller than $\frac{1}{7}$ meaning that no wave broke before reaching the beach.

4.2.2 Wave-induced Current velocities

The observations started 10 minutes after the first wave was generated. These 10 minutes were sufficient to eliminate long-periodic start-related variations in wave fields.

As it was mentioned previously an ADV had been used to take measurements for long-shore and cross-shore currents generated by regular and random waves. The measurements of the currents started 30 minutes after the first wave was generated for both regular and random waves. These 30 minutes were sufficient to eliminate bed level changes during the measurements which will influence the currents. However, for the mixed beach, the sand was moved slightly after the 30 minutes without any sufficient influence in the measurements. The currents had been measured at the three lines, one at the trench and the other two at uniform slope beach section, for all the three directions (x, y, z) V_x, V_y and V_z. The positive direction of V_x and V_y was the same with the positive direction of x and y at Figure 4-1. As for V_z, the positive direction was upwards. The three lines had coordinates of:

- At x-direction : x=2.0m (Line 1), x=4.0m (Line 2) and x=5.64m (Line 3), and
- At y-direction: from y=-0.6m until y=-6m for each line.

As far as the current velocities were concerned, the measurements had reached the maximum of -4.7m at y-direction due to the fact that the ADV can work only at submerged sections. Despite that, the number of current velocity measurements that was taken was satisfactory. The total number of points (measurements) of current velocities that were taken at the three cross-shore sections is shown below (Table 4-6 and Table 4-7).

Table 4-6 Points taken for current velocities (Regular waves)

Gravel Beach			
TESTS	**LINE 1**	**LINE 2**	**LINE 3**
Test 1	330	182	176
Test 2	246	183	201
Test 3	114	82	87
Test 4	114	83	87
Total Points for all the lines which were equivalent for each V_x, V_y and V_z separately: **1885**			
Mixed Beach			
TESTS	**LINE 1**	**LINE 2**	**LINE 3**
Test 7	103	93	92
Test 8	105	94	92
Total Points for all the lines which were equivalent for each V_x, V_y and V_z separately: **579**			

Table 4-7 Points taken for current velocities (Random waves)

Gravel Beach			
TESTS	**LINE 1**	**LINE 2**	**LINE 3**
Test 5	64	50	48
Test 6	62	39	46
Total Points for all the lines which were equivalent for each V_x, V_y and V_z separately: **309**			
Mixed Beach			
TESTS	**LINE 1**	**LINE 2**	**LINE 3**
Test 9	59	54	53
Test 10	64	59	60
Total Points for all the lines which were equivalent for each V_x, V_y and V_z separately: **349**			

The current velocity measurements were carried out at various levels in the z direction. At each level, the current velocity measurements were taken over duration of 60 seconds. The observations for regular waves started at the surface (point 1) and deepened with a constant 5cm integral until the maximum point at each measurement was reached. The maximum point was the point at which the ADV could take logical measurements, usually that was between five and ten cm from the bed level. The deepest point of measurement was 35cm below water surface.

The same procedure was followed for random waves but with a 10cm integral. The deepest point of measurement for random waves was 30cm below the water surface. This procedure allowed an estimate of the vertical structure of the time-averaged velocity and a more accurate determination of the depth-averaged current velocities than measurements taken at a single elevation. The depth-averaged current velocity V was determined as:

Eq.4- 3 $$V = \frac{(V_{surface} + 2V_{mid-depth} + V_{bottom})}{4}$$

Moreover, the current velocity measurements were also carried out in various locations in the y direction. As mentioned previously, the locations of measurements varied from y=-0.6m to maximum y=-4.7m. At Line 1 for wave height of 24 cm with wave period of 2sec, the measurements started at y=-0.6m, sustained with an integral of 5cm until y=-1.8m and then continued with an integral of 10cm until y=-4.7m. For the other two lines on the same test, the integral was 10cm which was also adopted for all the three lines with wave conditions of H=24cm and T=3sec. However, the integral was finally increased to 20cm for all the other tests of regular and random waves.

The graphical presentation of the results of the wave-induced current velocity measurements, for all the tests, can be seen in Figure 4-2 to Figure 4-31 below. Each point of V_x, V_y and V_z at the graphs represents the time- and depth-averaged current velocity of the location.

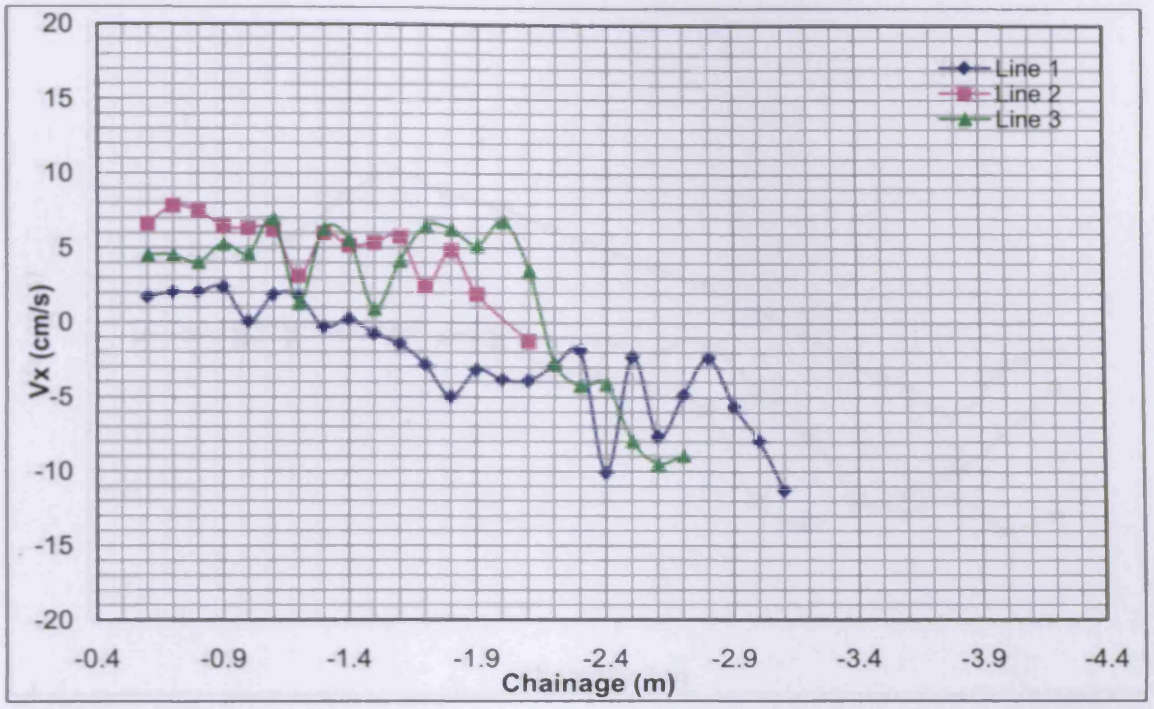

Figure 4-2 Long-shore current velocity (Test 1)

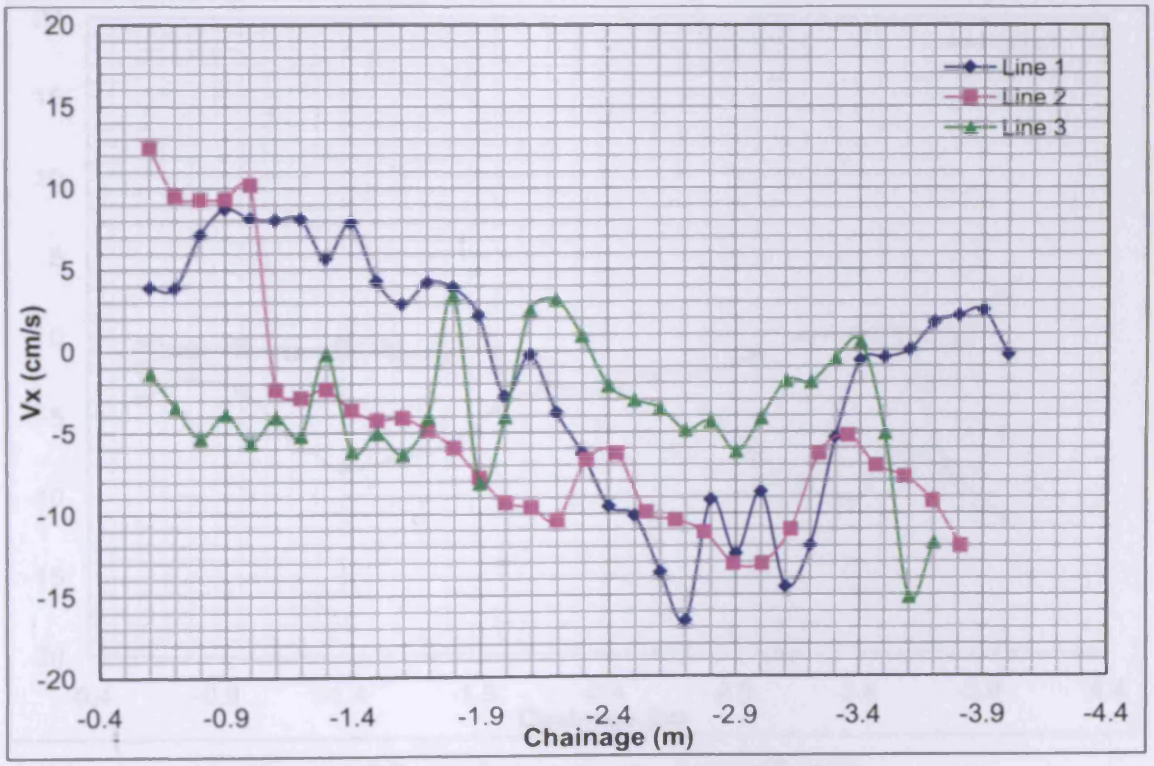

Figure 4-3 Long-cross current velocity (Test 2)

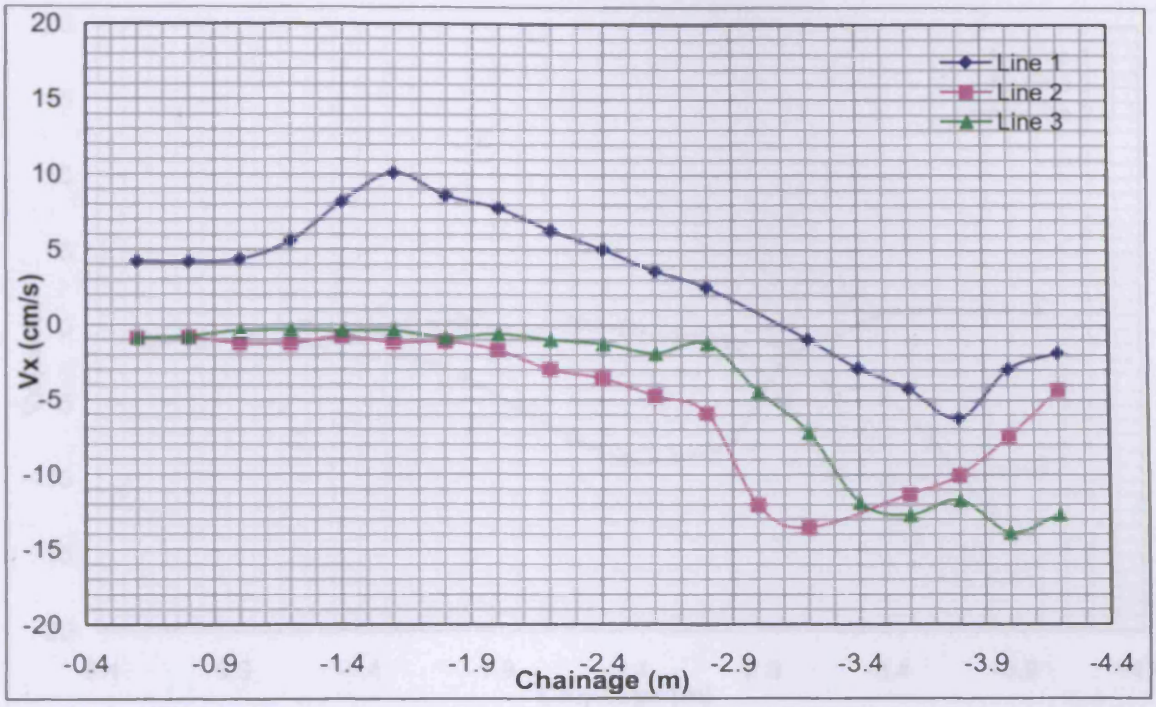

Figure 4-4 Long-shore current velocity (Test 3)

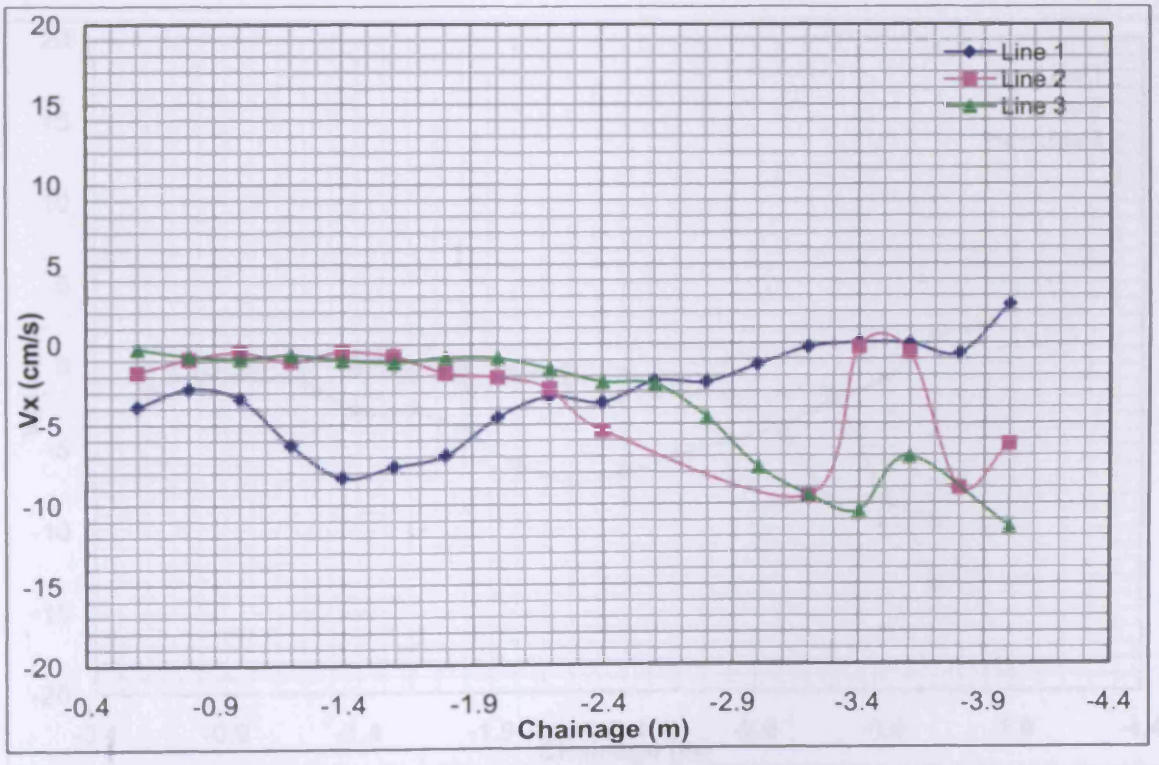

Figure 4-5 Long-shore current velocity (Test 4)

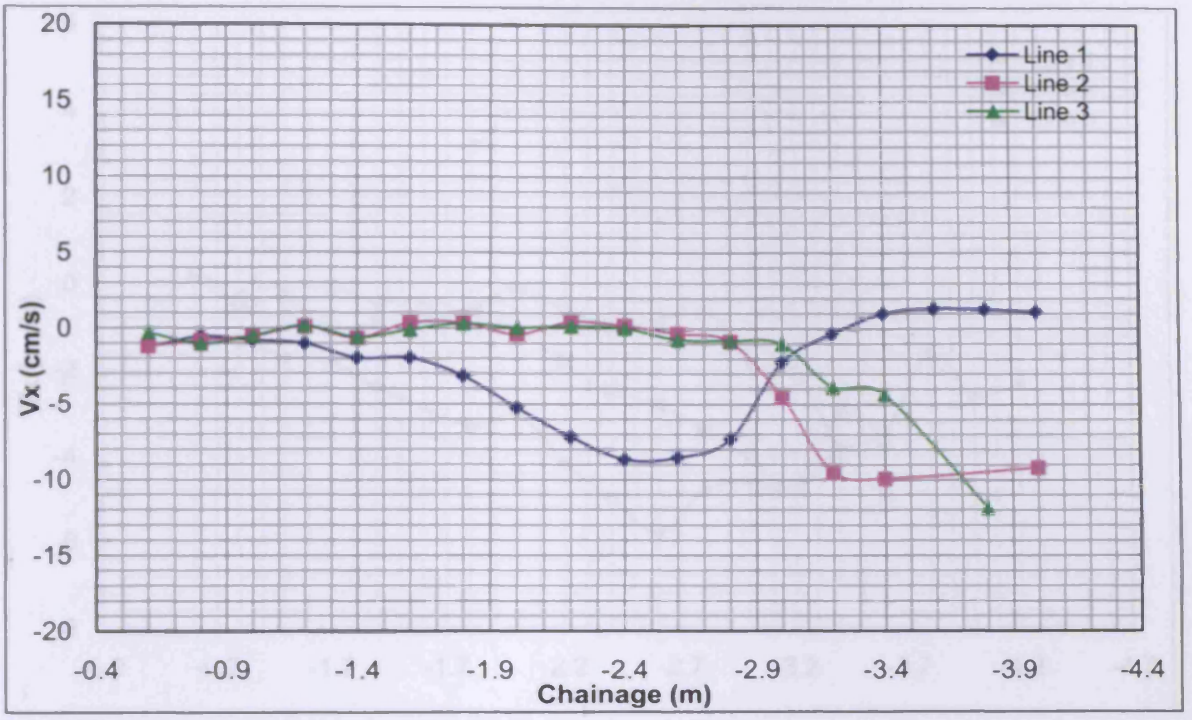

Figure 4-6 Long-shore current velocity (Test 7)

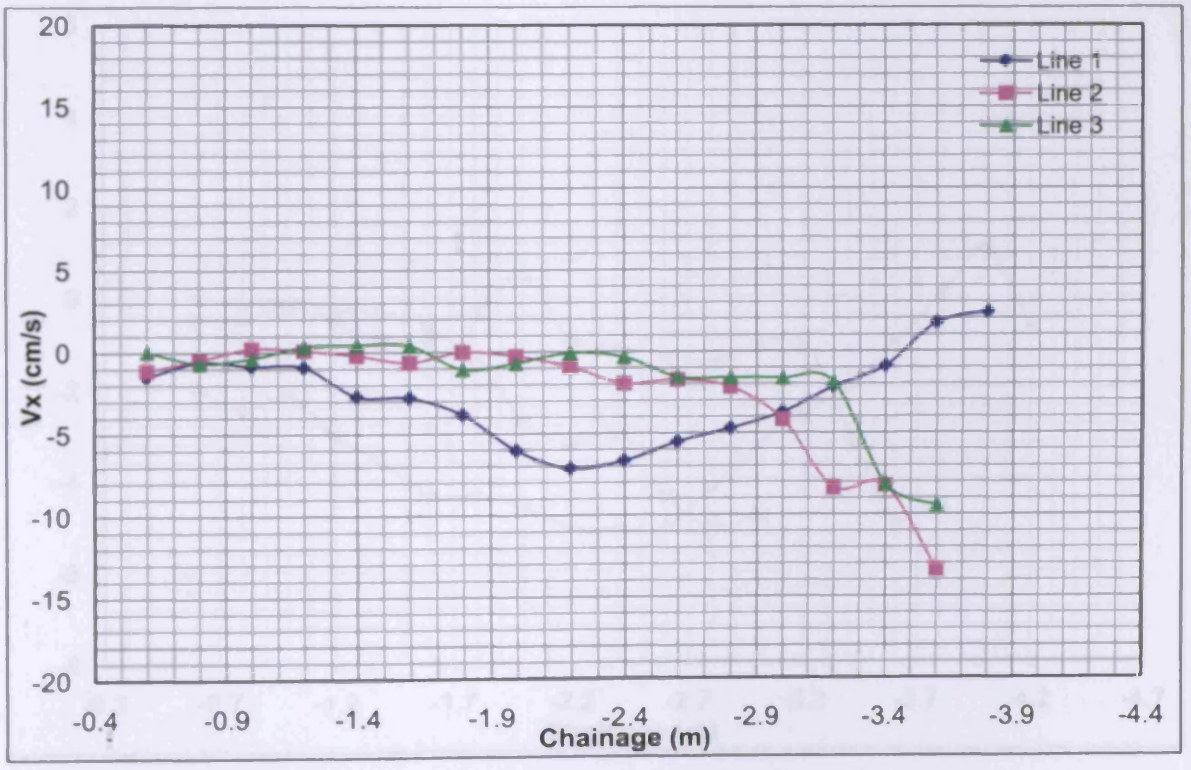

Figure 4-7 Long-shore current velocity (Test 8)

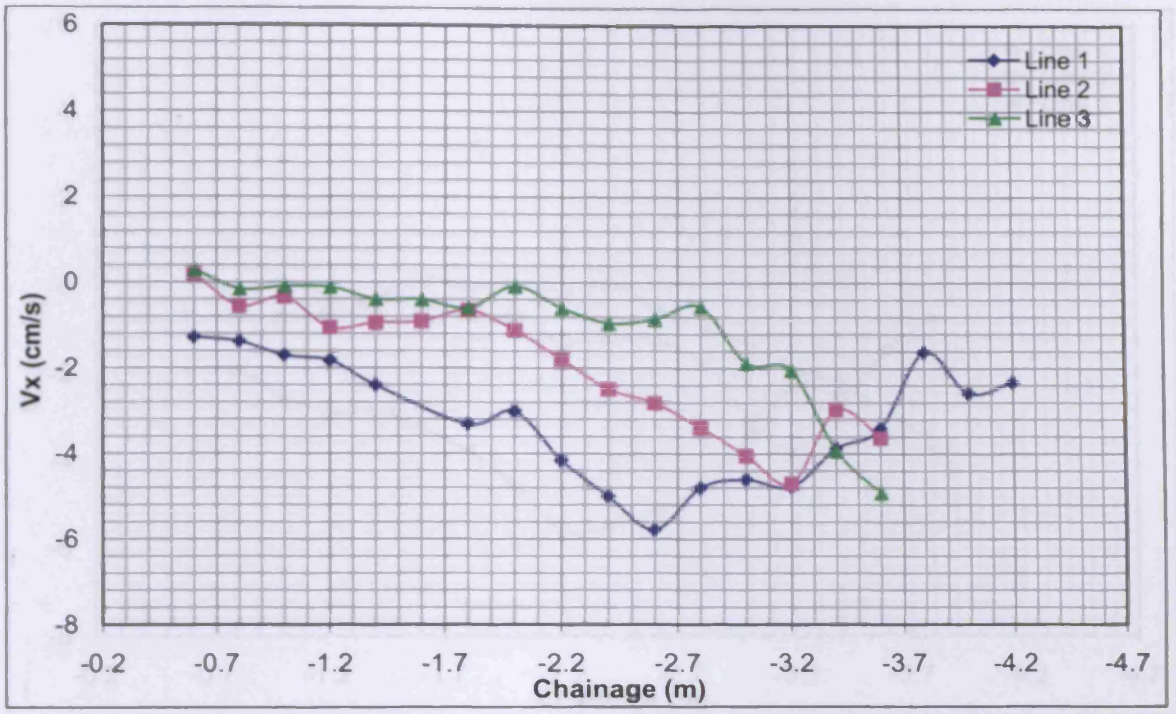

Figure 4-8 Long-shore current velocity (Test 5)

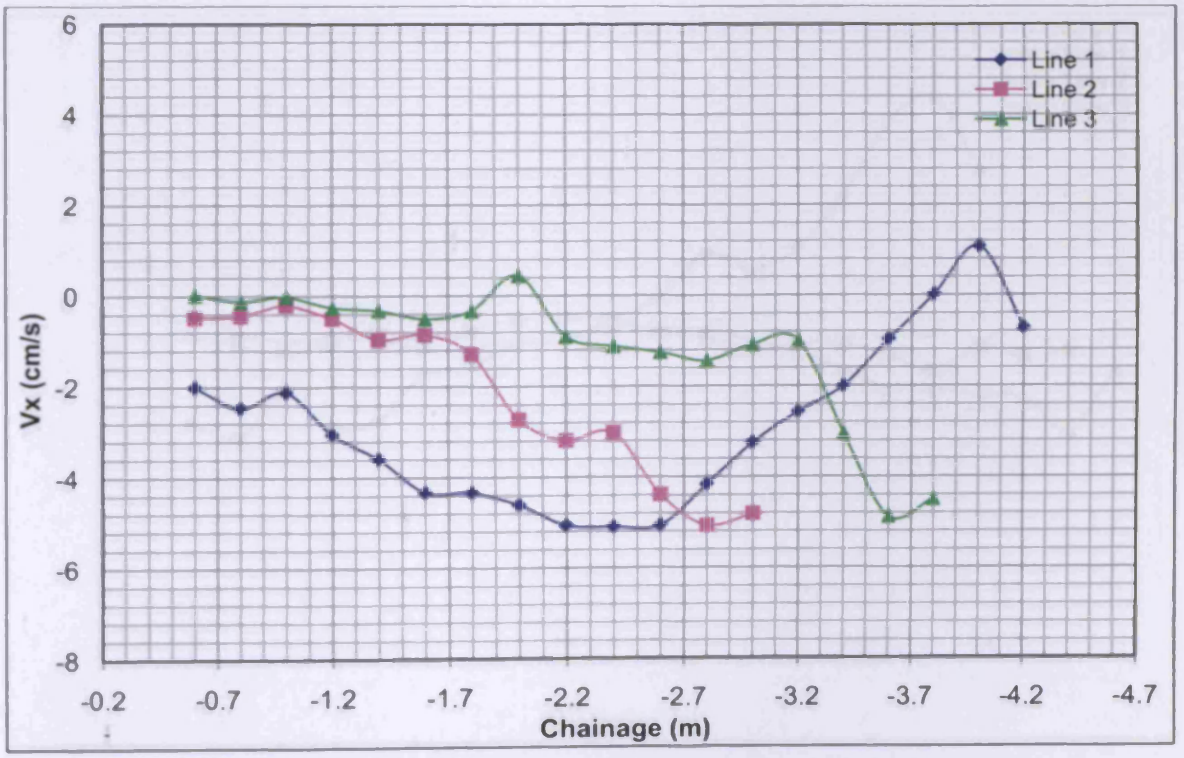

Figure 4-9 Long-shore current velocity (Test 6)

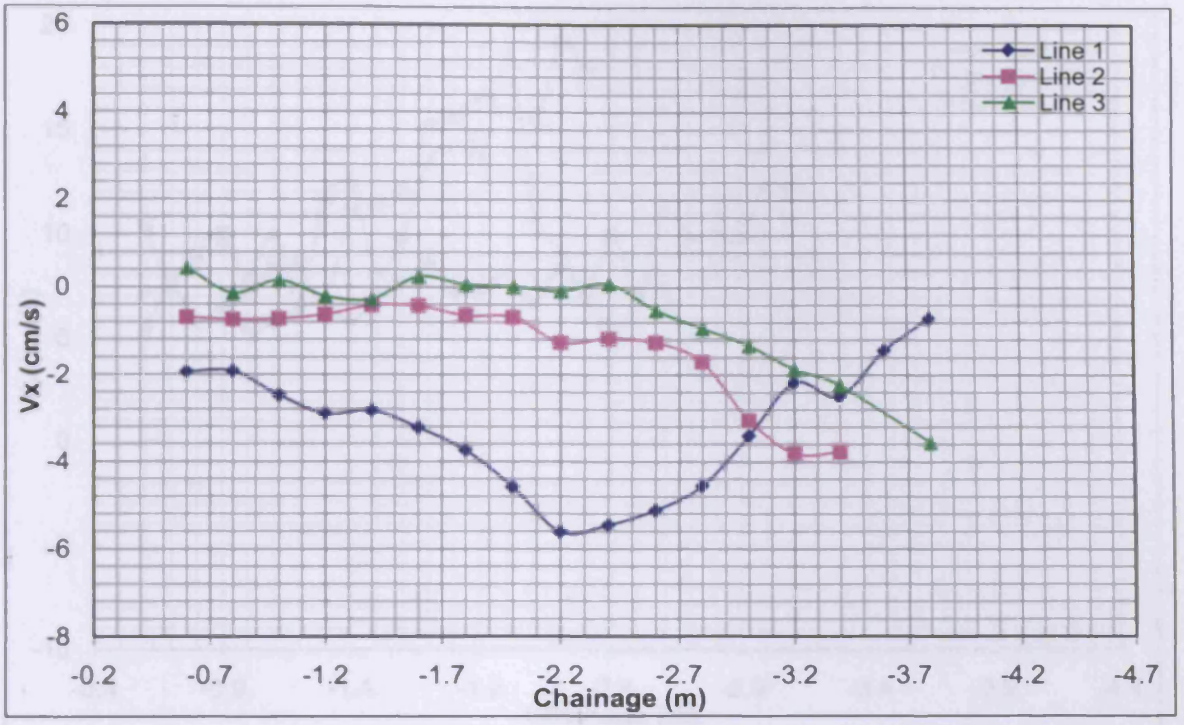

Figure 4-10 Long-shore current velocity (Test 9)

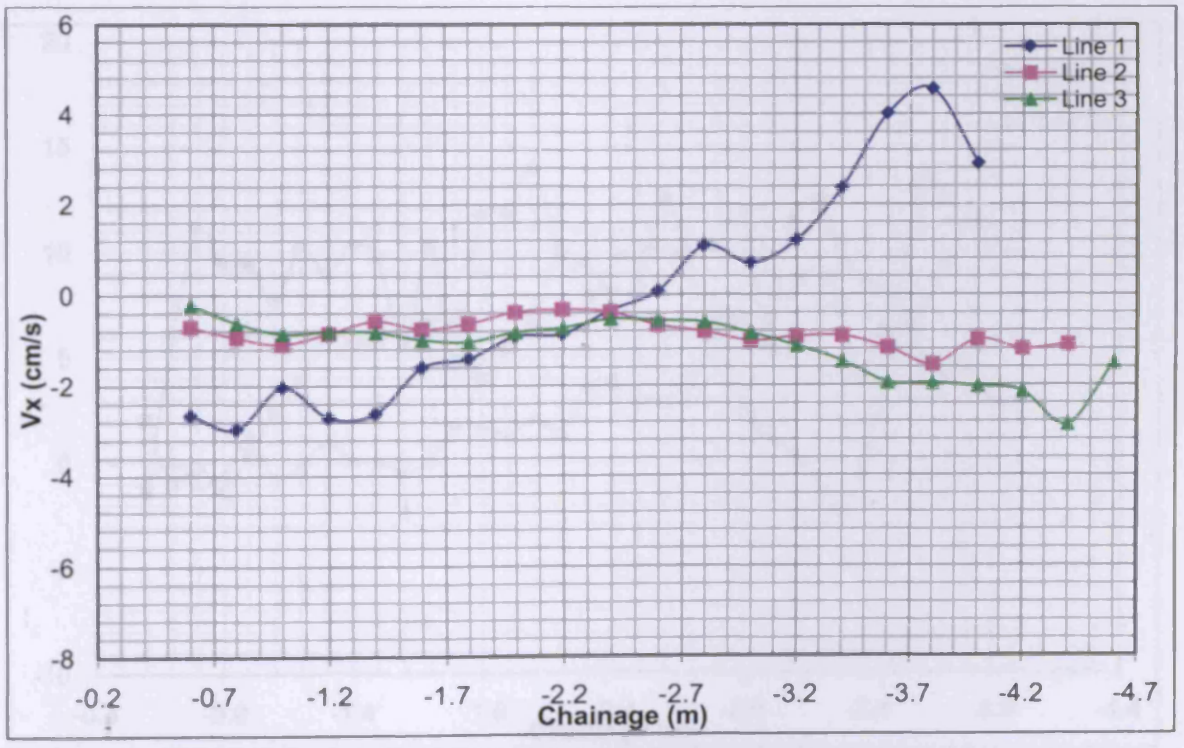

Figure 4-11 Long-shore current velocity (Test 10)

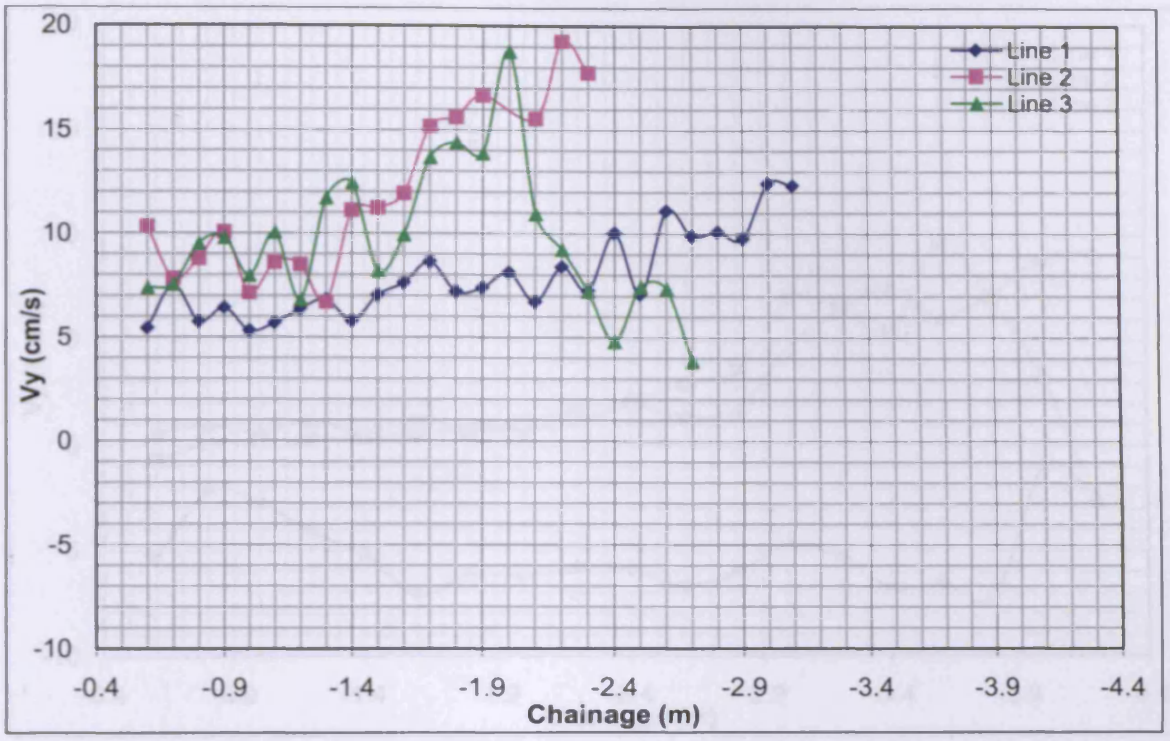

Figure 4-12 Cross-shore current velocity (Test 1)

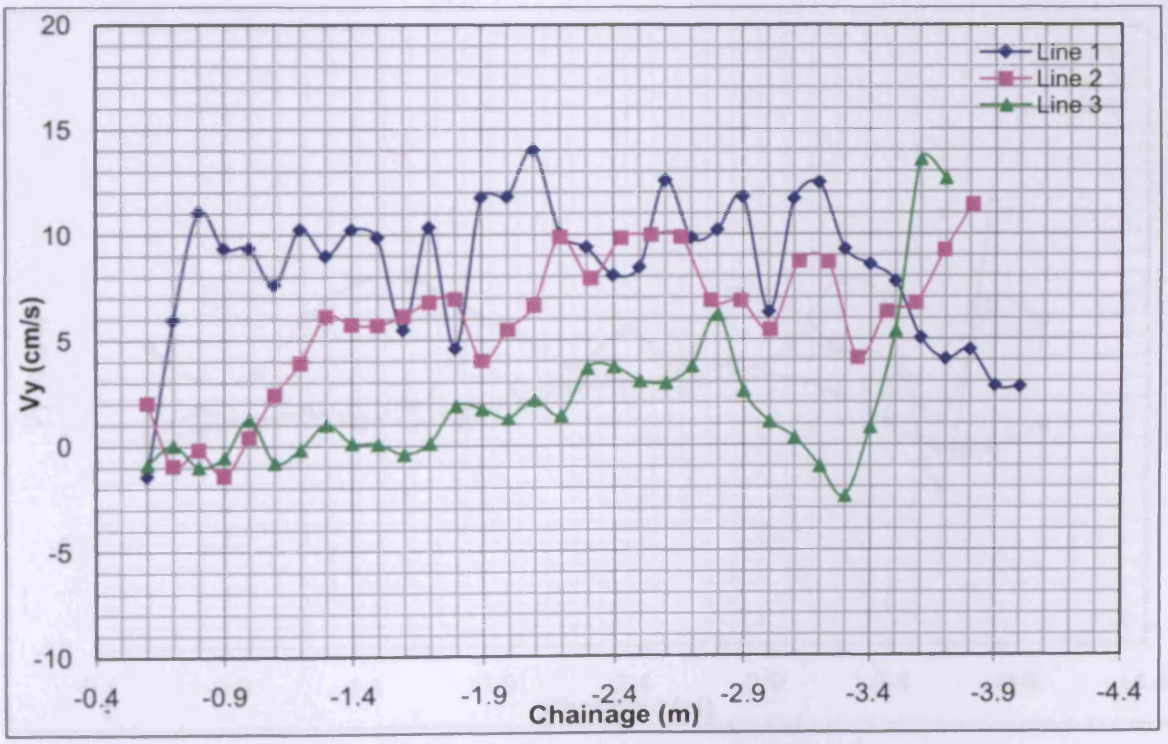

Figure 4-13 Cross-shore current velocity (Test 2)

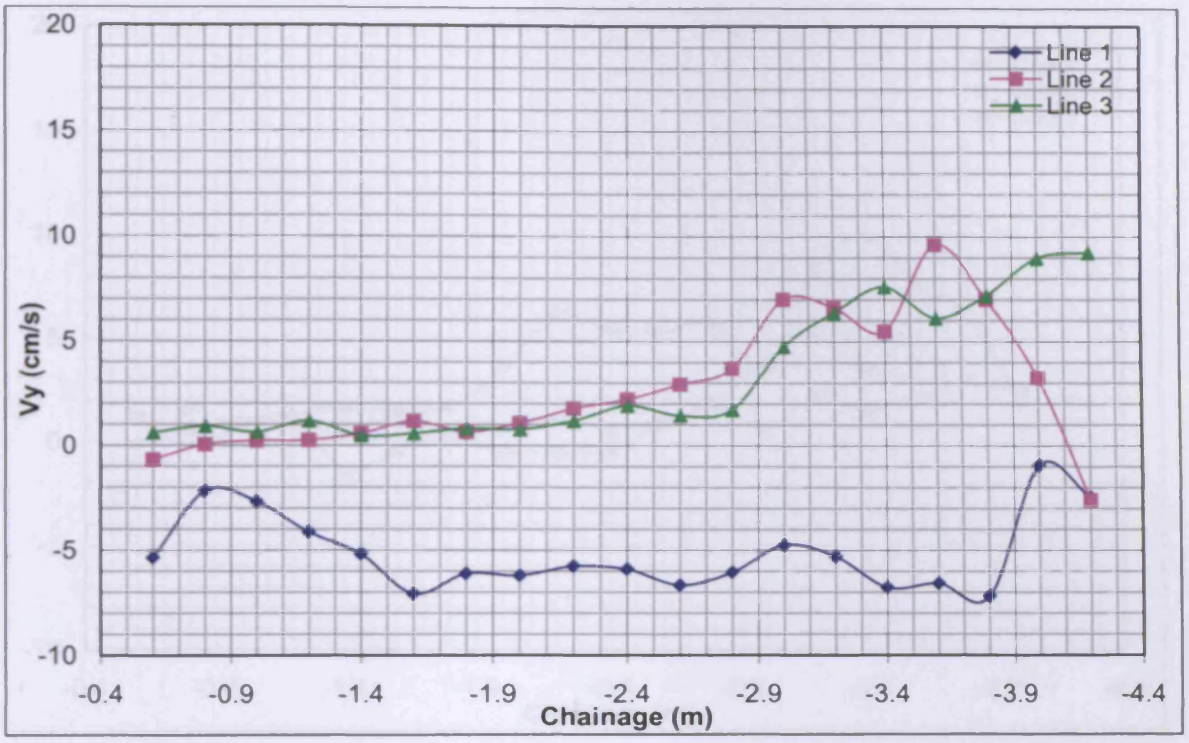

Figure 4-14 Cross-shore current velocity (Test 3)

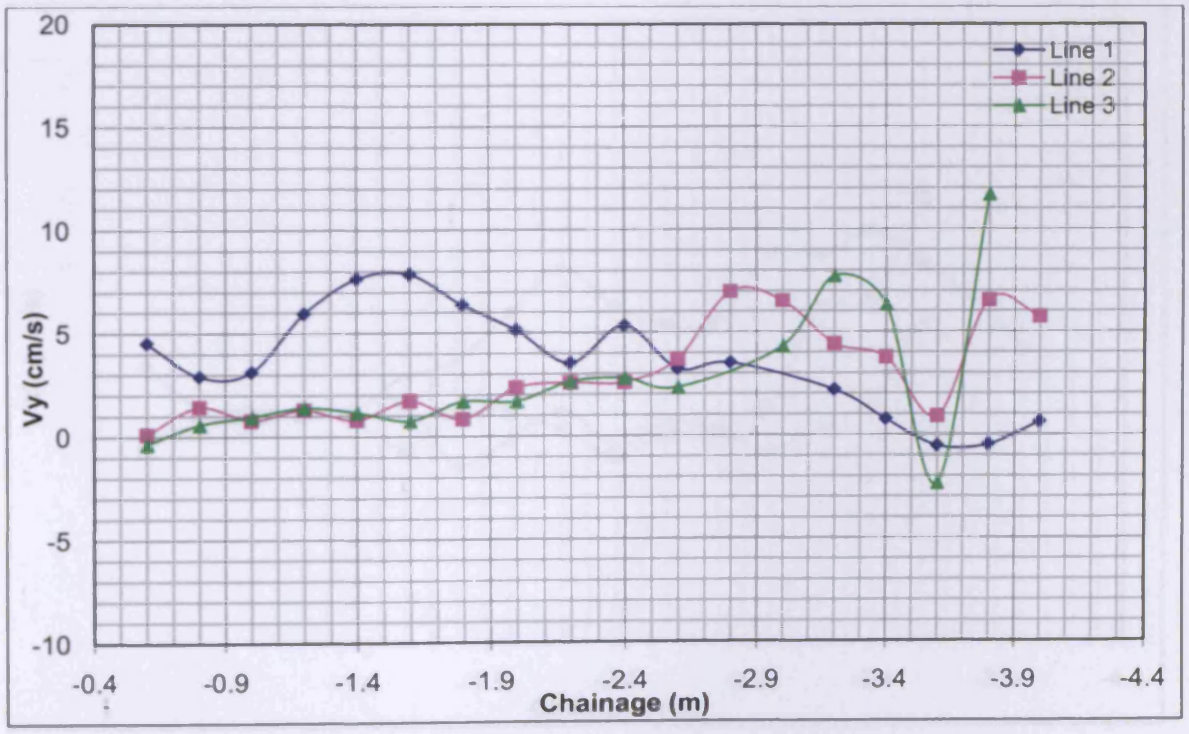

Figure 4-15 Cross-shore current velocity (Test 4)

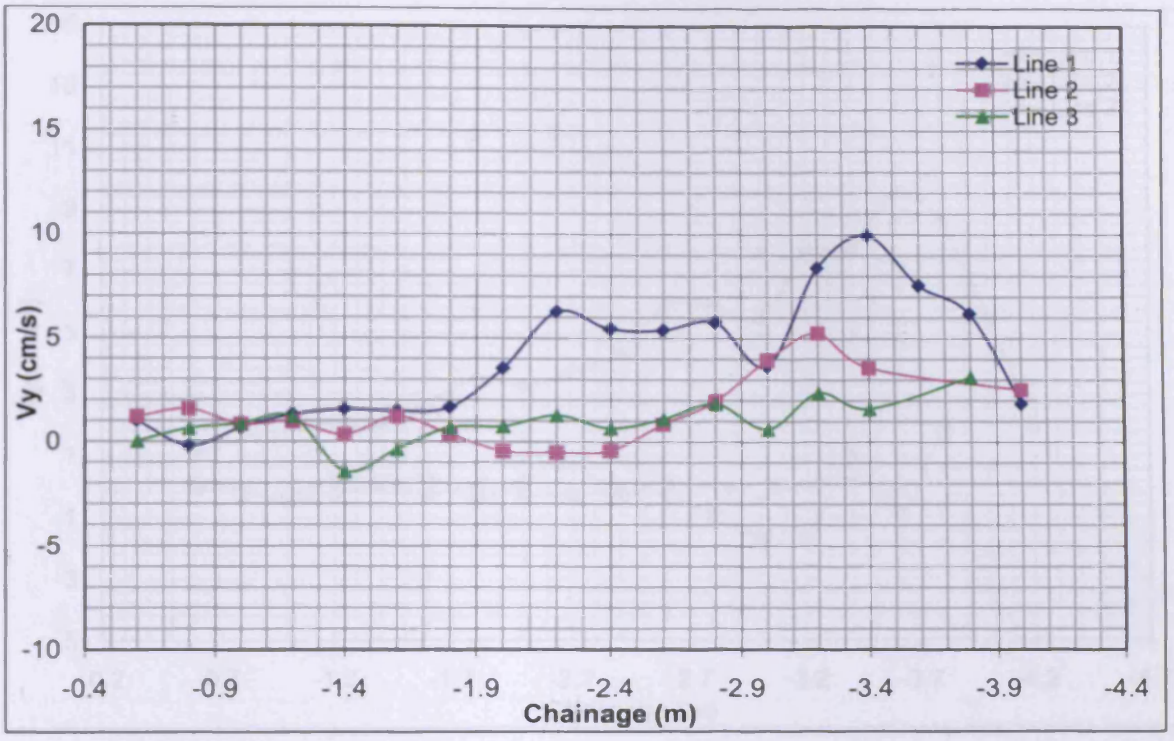

Figure 4-16 Cross-shore current velocity (Test 7)

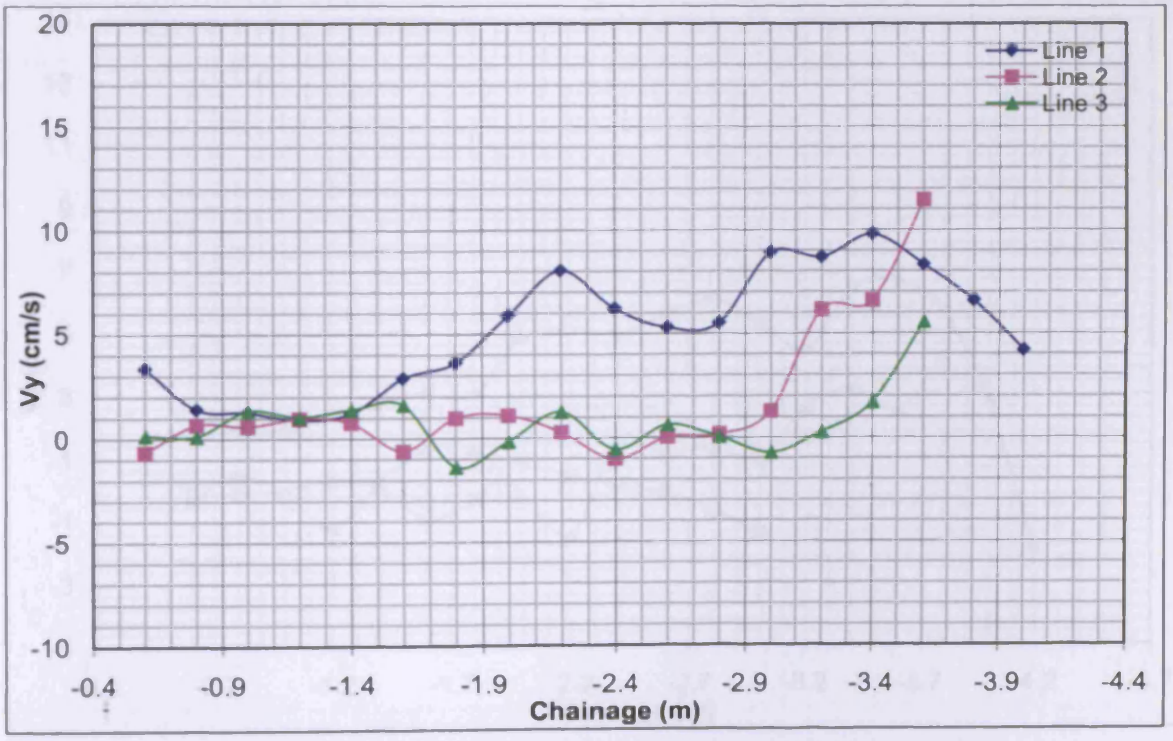

Figure 4-17 Cross-shore current velocity (Test 8)

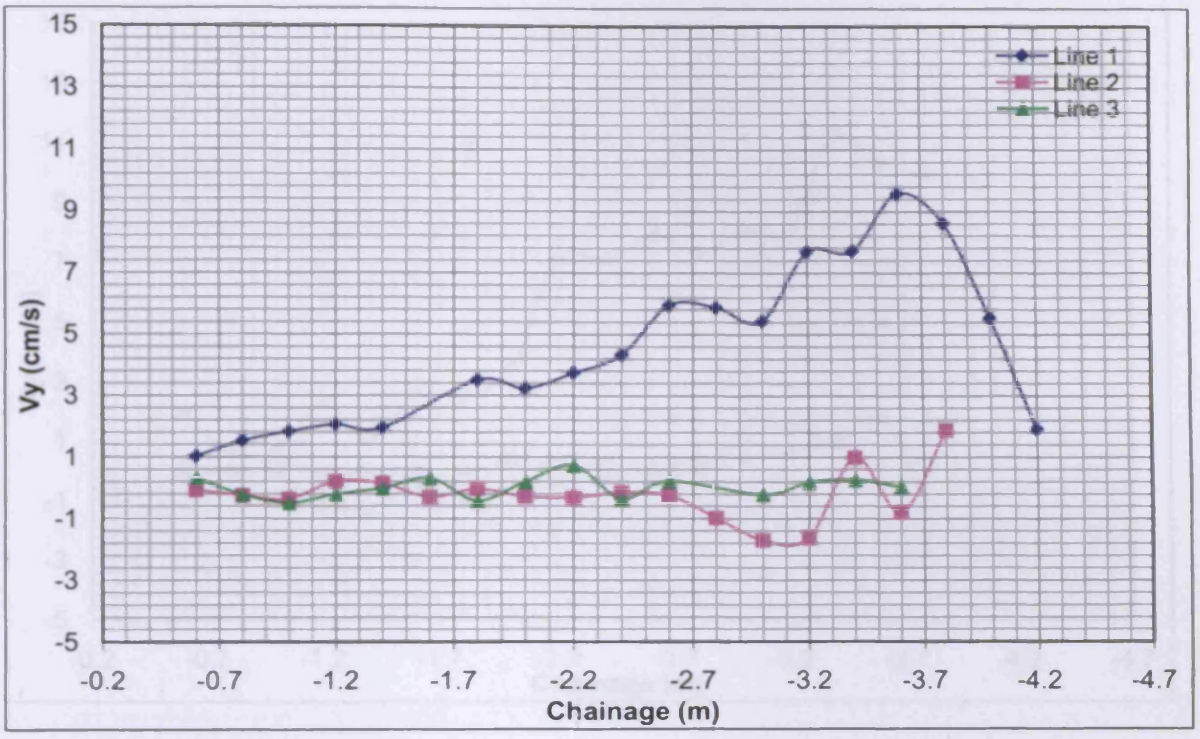

Figure 4-18 Cross-shore current velocity (Test 5)

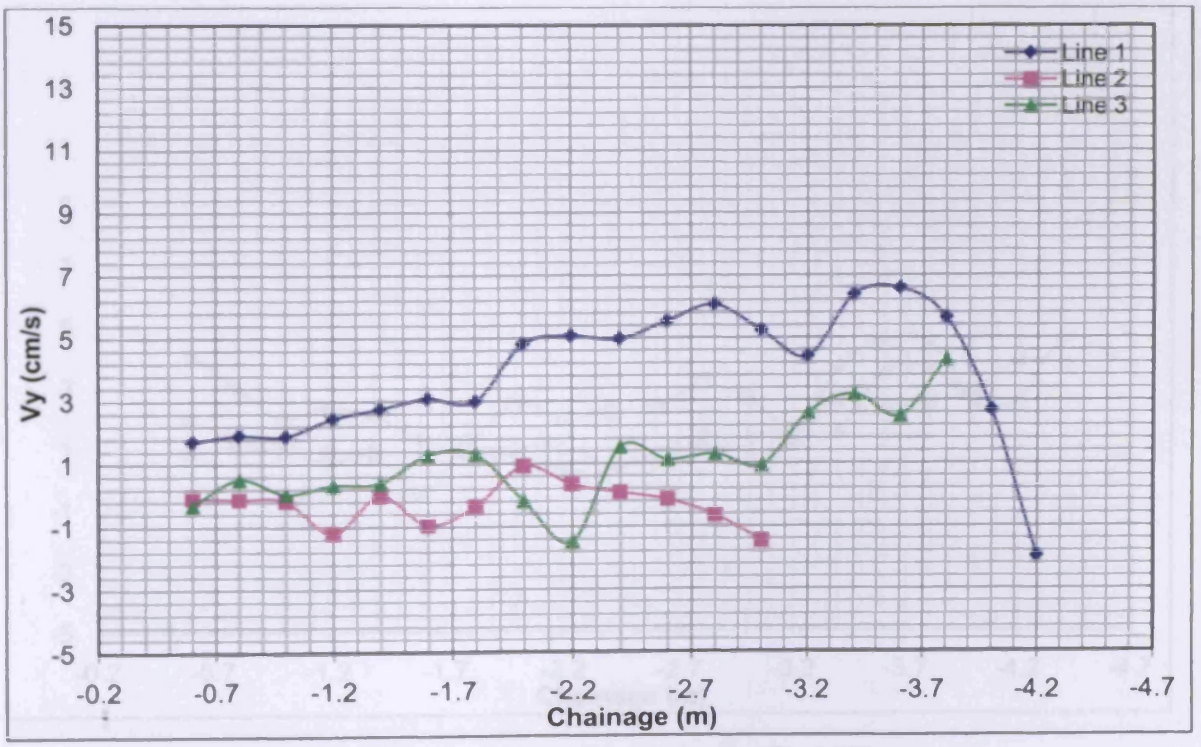

Figure 4-19 Cross-shore current velocity (Test 6)

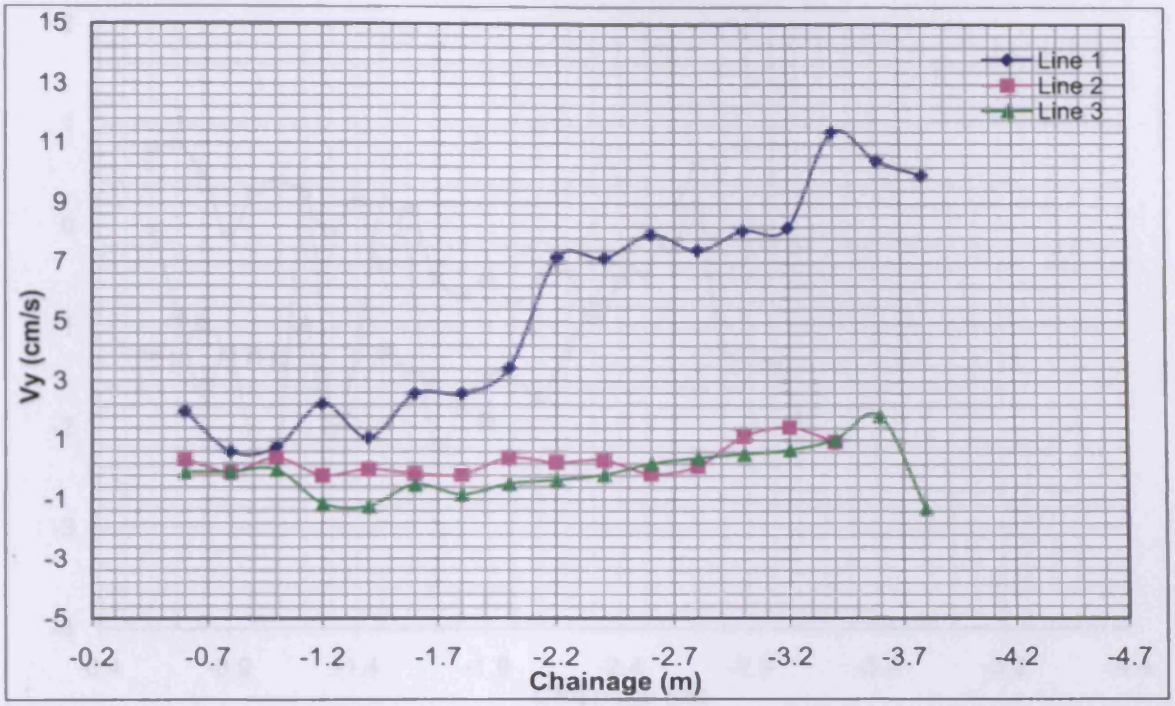

Figure 4-20 Cross-shore current velocity (Test 9)

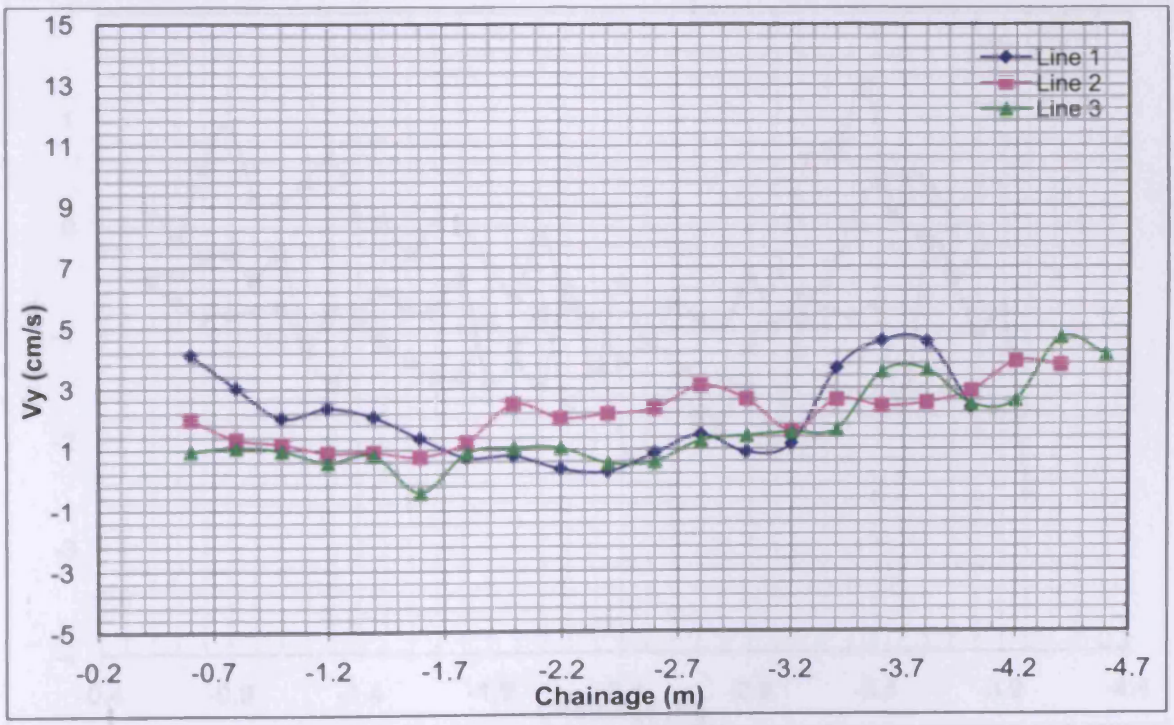

Figure 4-21 Cross-shore current velocity (Test 10)

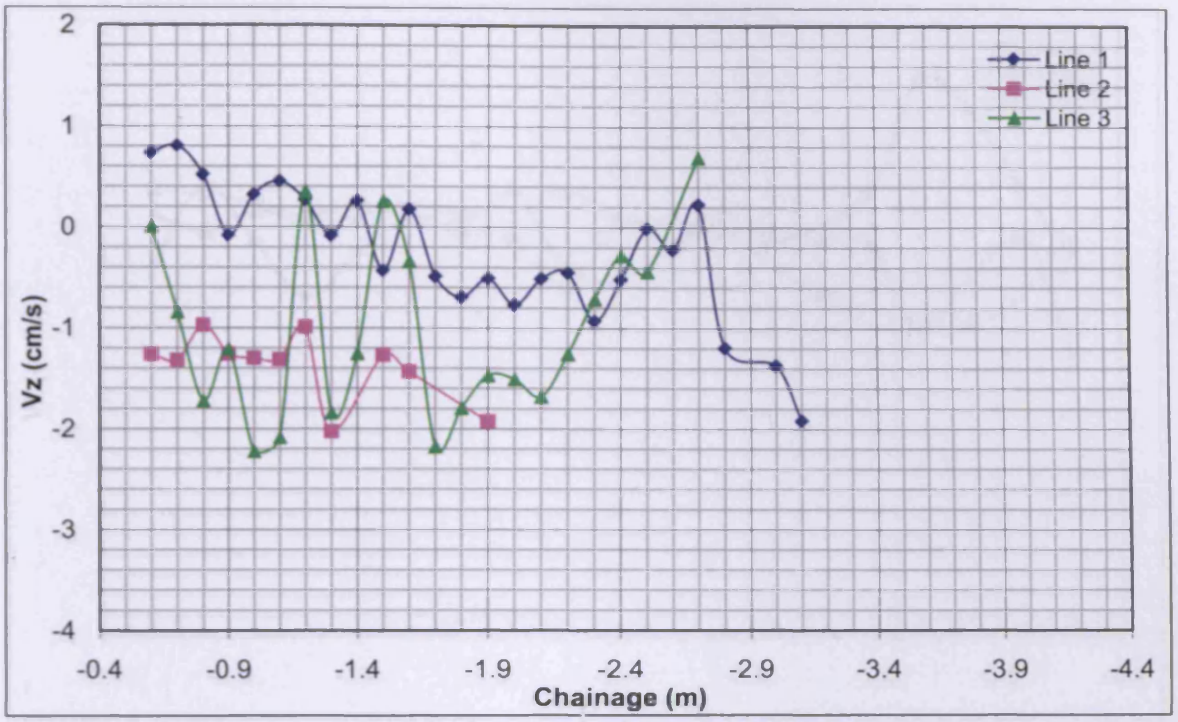

Figure 4-22 Wave-induced current velocity at z-direction (Test 1)

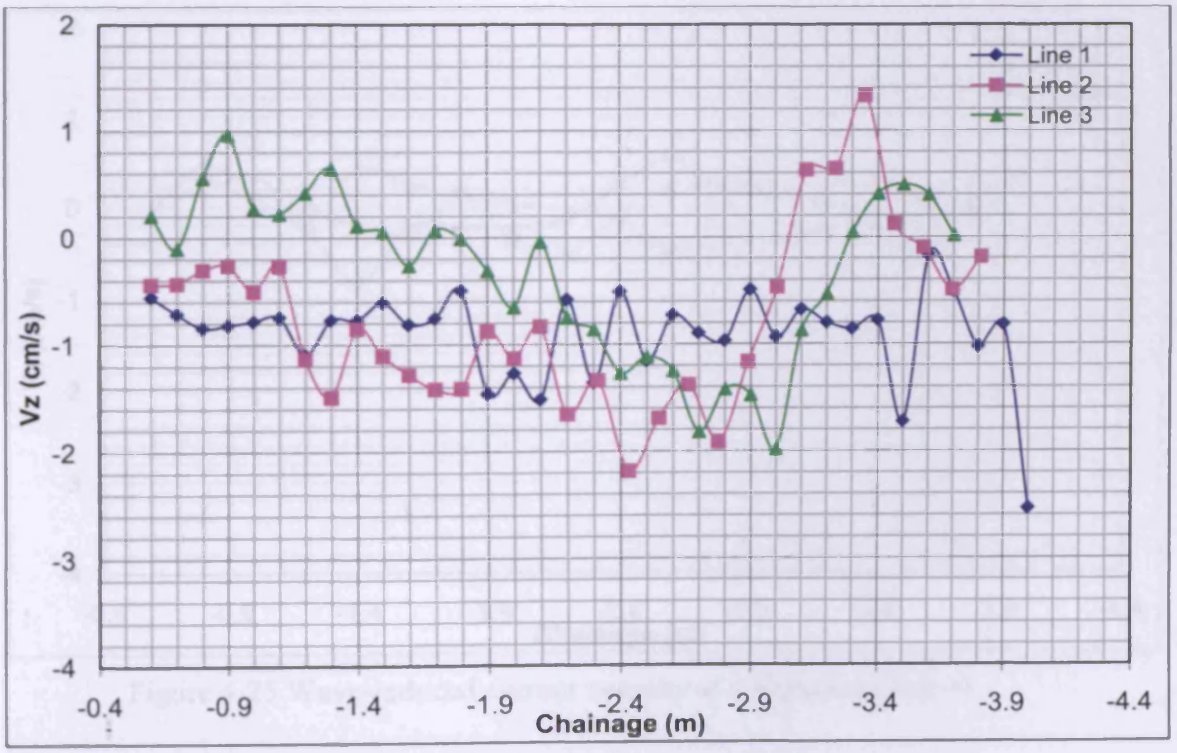

Figure 4-23 Wave-induced current velocity at z-direction (Test 2)

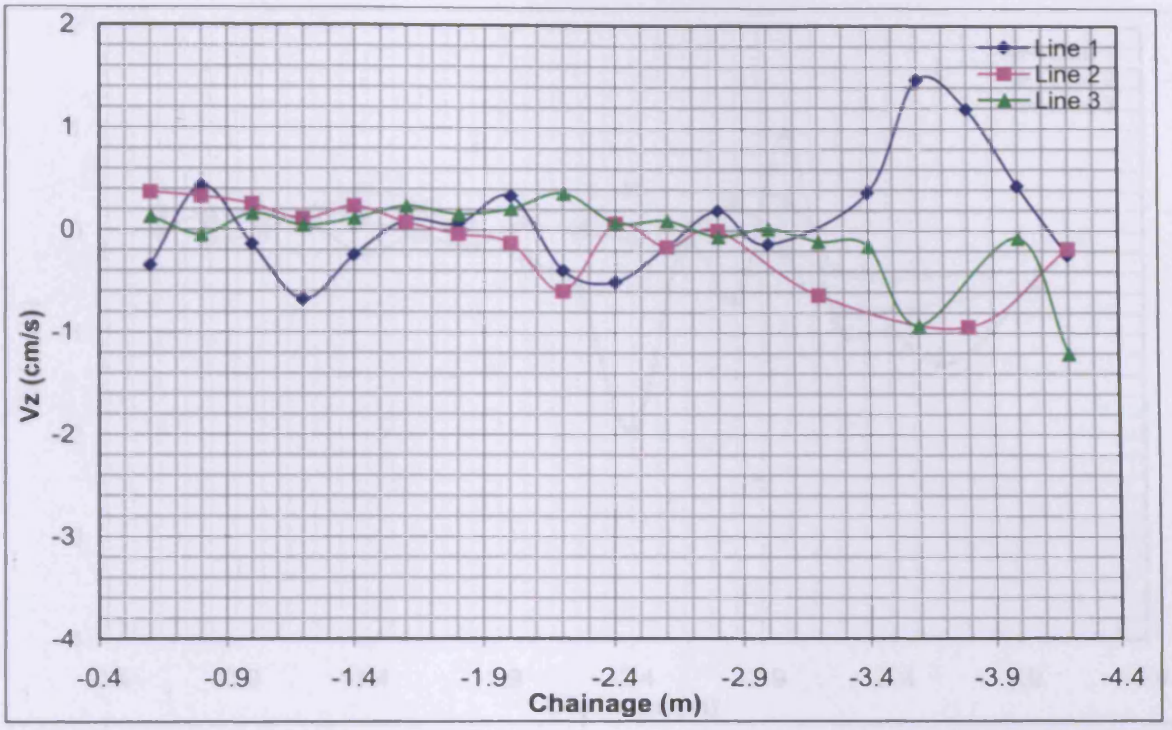

Figure 4-24 Wave-induced current velocity at z-direction (Test 3)

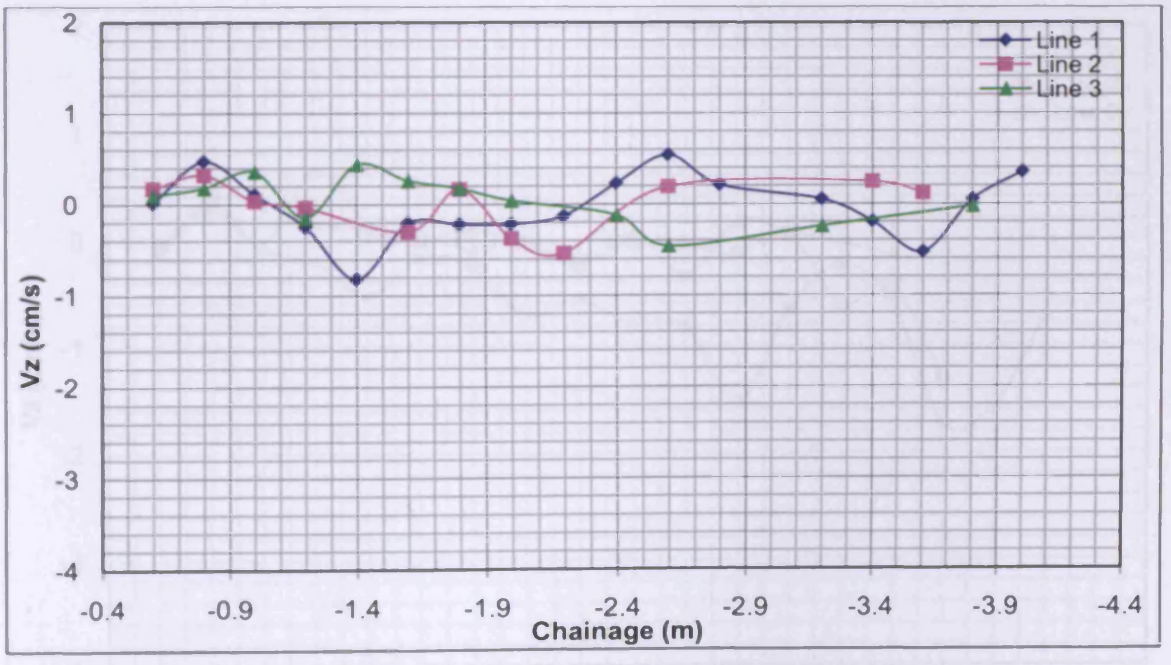

Figure 4-25 Wave-induced current velocity at z-direction (Test 4)

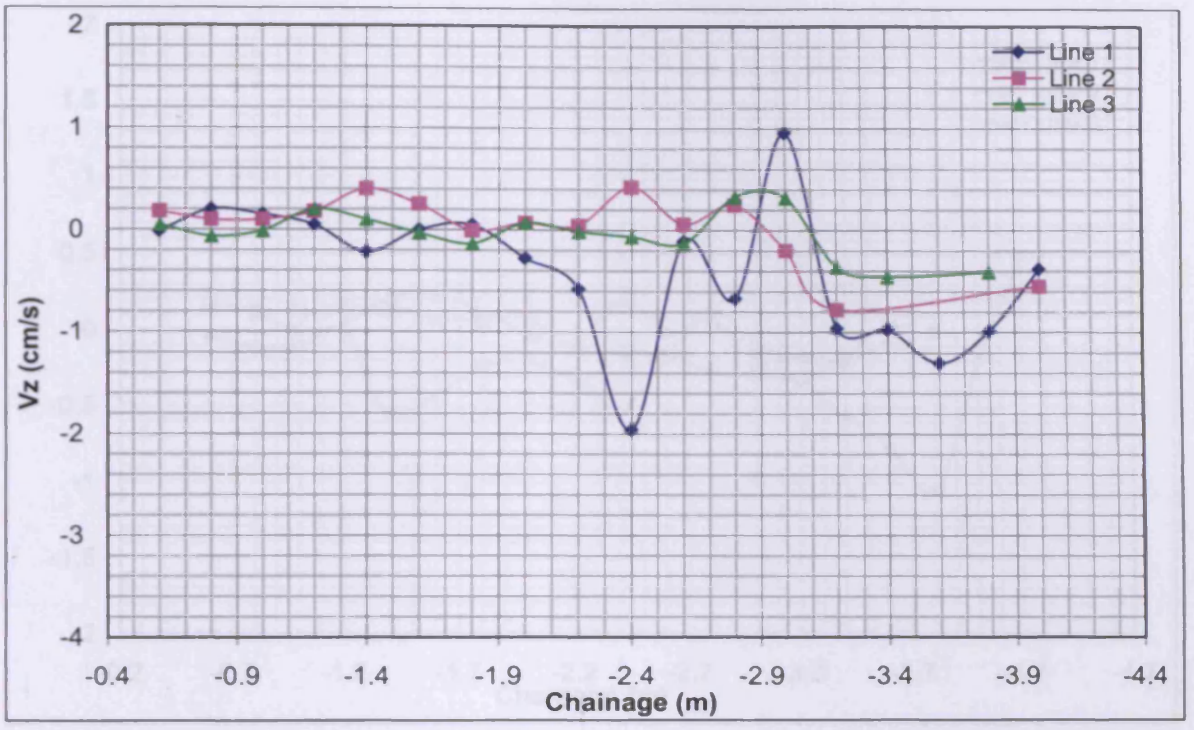

Figure 4-26 Wave-induced current velocity at z-direction (Test 7)

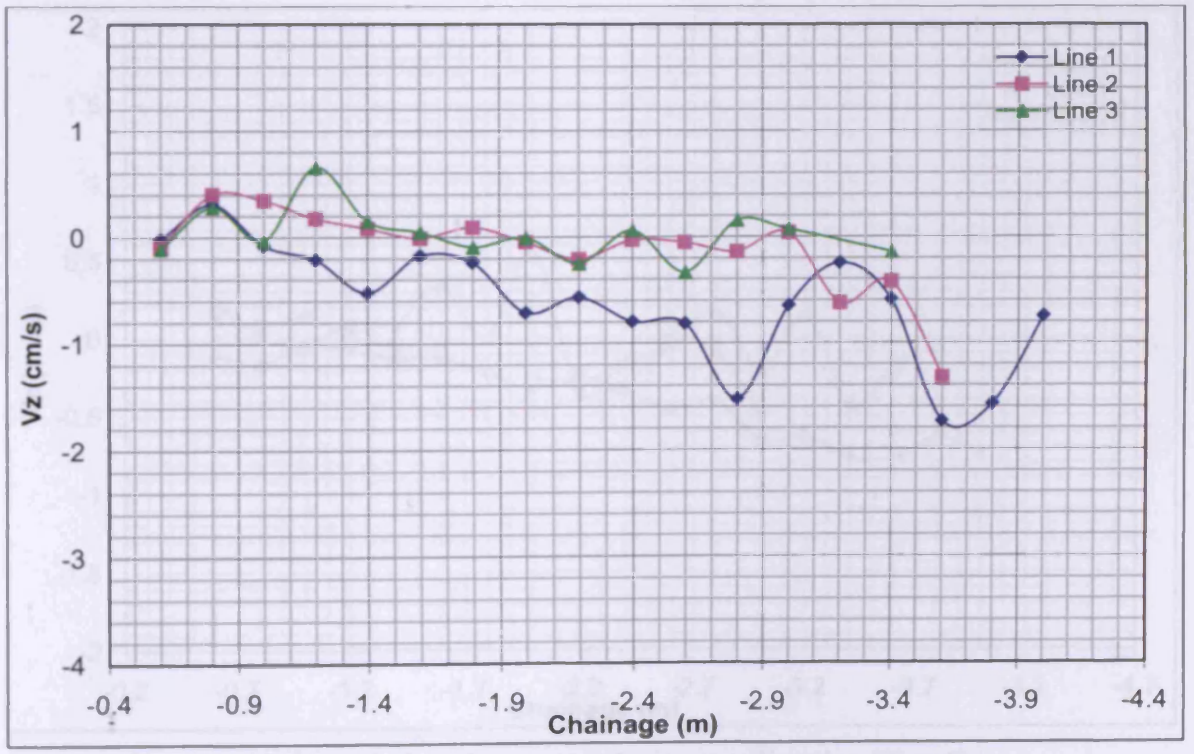

Figure 4-27 Wave-induced current velocity at z-direction (Test 8)

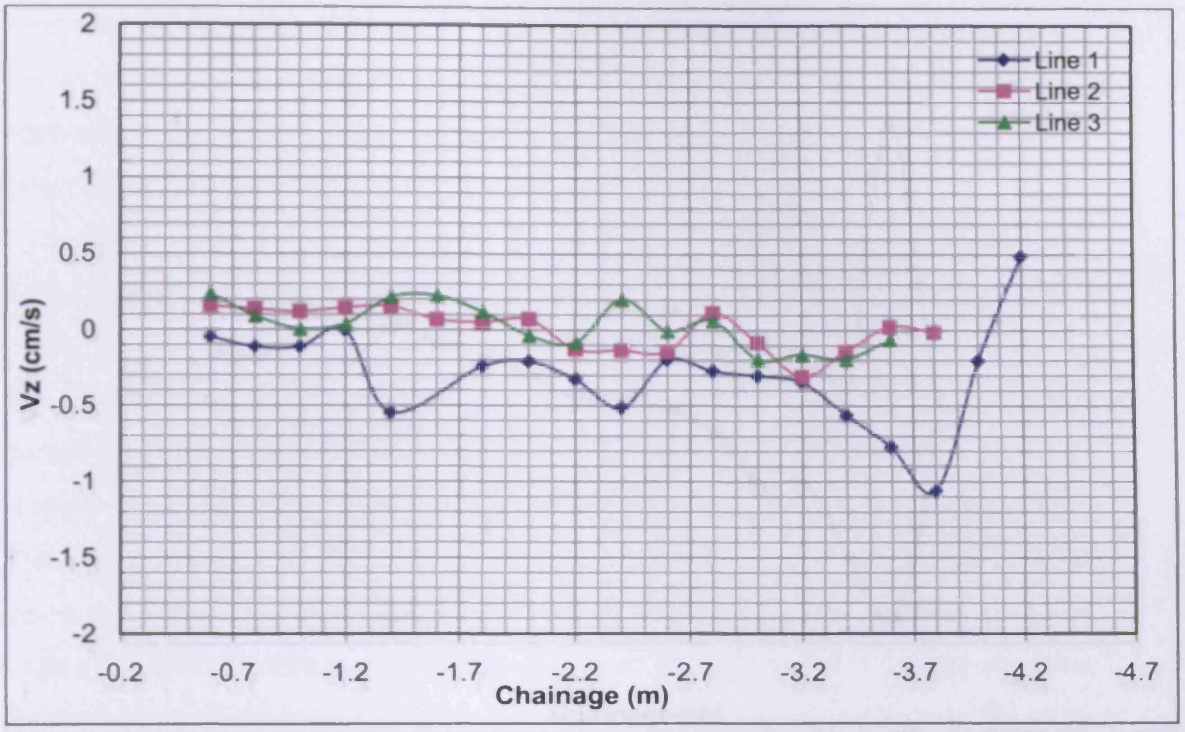

Figure 4-28 Wave-induced current velocity at z-direction (Test 5)

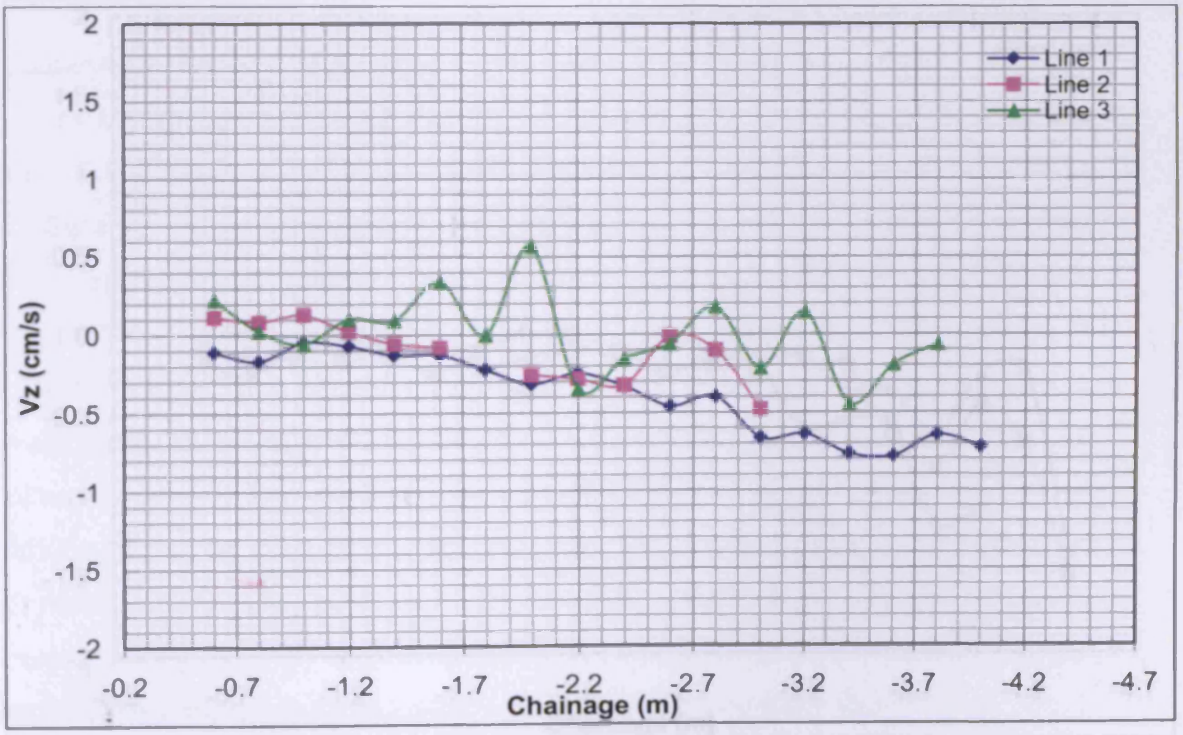

Figure 4-29 Wave-induced current velocity at z-direction (Test 6)

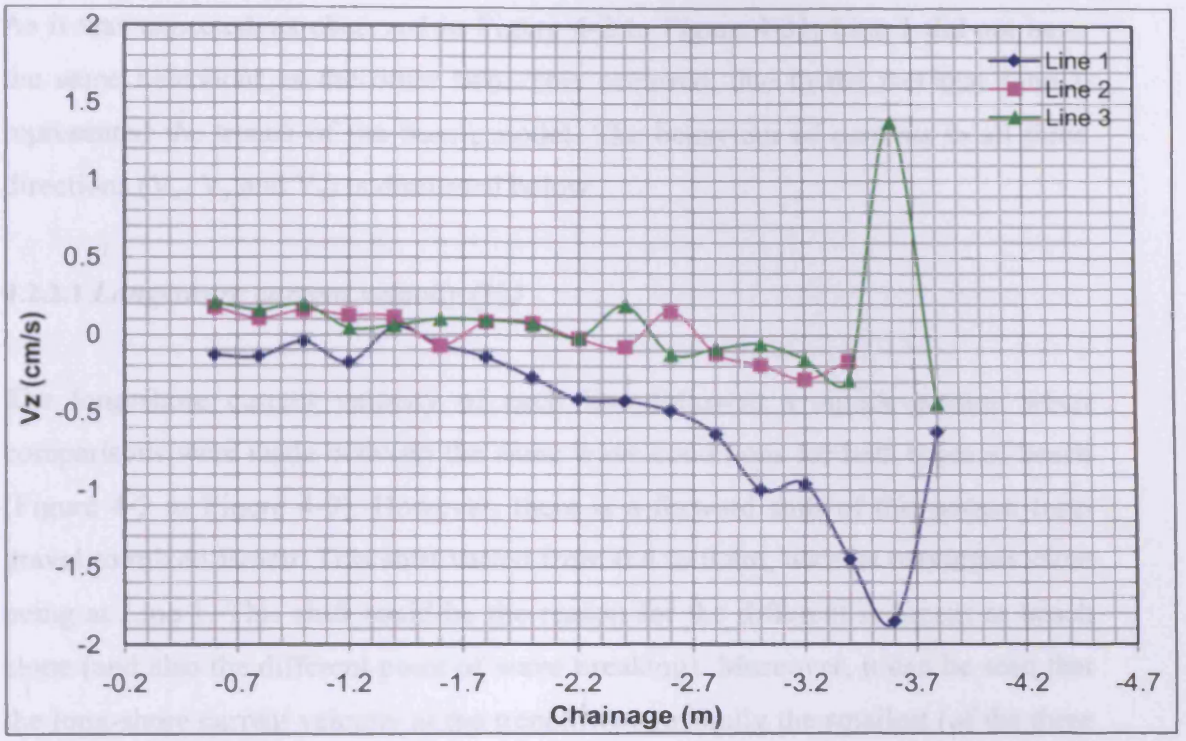

Figure 4-30 Wave-induced current velocity at z-direction (Test 9)

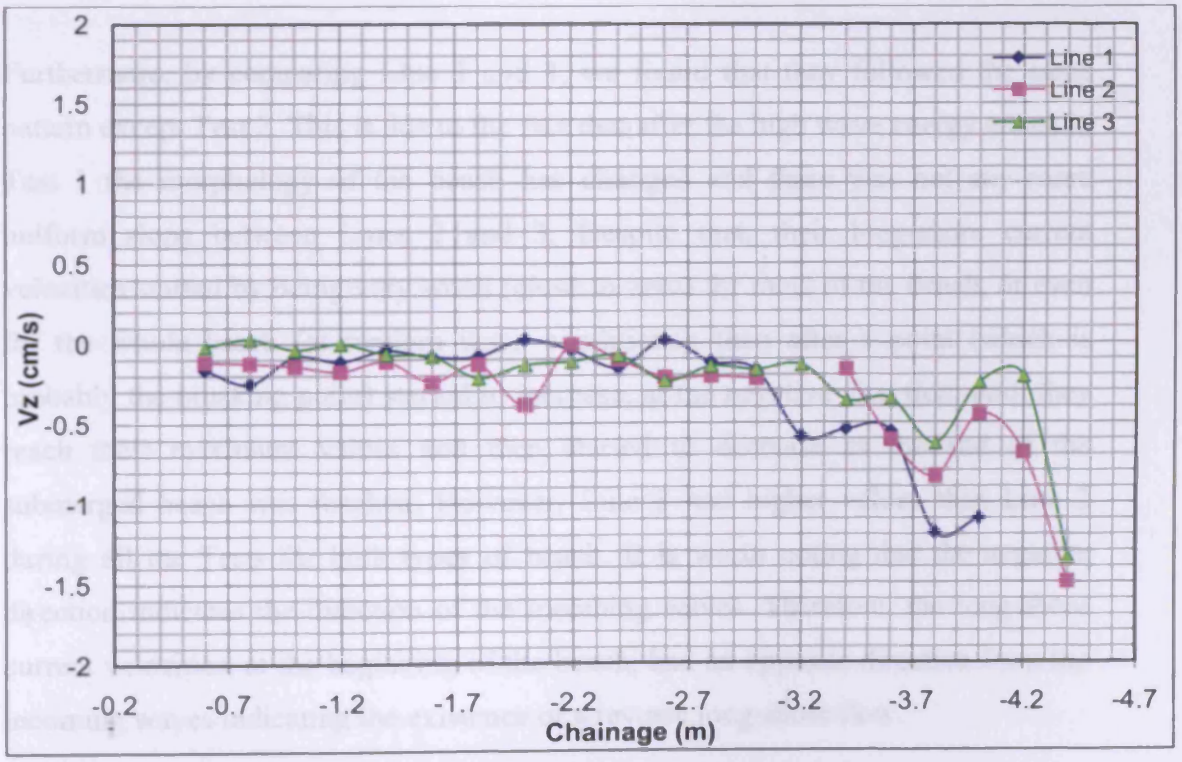

Figure 4-31 Wave-induced current velocity at z-direction (Test 10)

As it was expected, as observed in Figure 4-2 to Figure 4-31, Line 1 did not have the same behaviour as the other two. This occurred, due to the fact that Line 1 represented the trench of the beach model. The behaviour of currents in all three directions (V_x, V_y and V_z) is discussed below.

4.2.2.1 *Long-shore current velocity (V_x)*

The long-shore current velocity of each line followed a similar pattern when comparisons were made between the same wave conditions for both types of beach (Figure 4-2 to Figure 4-9). However, there is a forward shift of this pattern from gravel to mixed Beach. This shift varied from 0.4 to 0.8m, with its maximum value being at Line 1. This shift could be the reason for the different sediment or beach slope (and also the different point of wave breaking). Moreover, it can be seen that the long-shore current velocity at the trench was generally the smallest (of the three lines) at the beginning of the beach due to the beach slope at that location.

Furthermore, by comparing Line 2 and 3, we found that they followed the same pattern except Test 2. This is due to the fact that after the high wave energy attack in Test 1 the morphology of the beach has changed and there was not any more uniform slope between Lines 2 and 3. Despite that, their long-shore current velocities started by being very small (close to zero) for most of the beach, or even for the whole beach (at random wave conditions), then after a point (which is probably the breaking point) started to increase, at the negative direction, until they reach their maximum values and then started to decrease as the end of the submerged beach was reached. However, Line 3 had higher values than Line 2 during all the Tests for both types of beach. It is worth noting that the negative direction indicates the direction of the incoming waves. Therefore, the long-shore current velocities, at the beginning of the beach, had an opposite direction from the incoming waves indicating the existence of a reverse long-shore flow.

Nevertheless, at trench (Line 1) the long-shore current velocities were not very small (except at some points at random wave conditions). They started to increase earlier compare with the V_x of the other two lines.

As far as the first two tests are concerned, the values of long-shore current velocity were the highest of all the tests. At Test 1, all lines followed the same pattern which was a gradual decrease of the values of V_x. Moreover, at Test 2, Line 1 and 2 followed the same pattern as at Test 1. Line 3 shows to have a fluctuation of values of V_x with mainly negative direction.

Comparison between regular and random wave conditions shows that the long-shore current velocity profile was smoother in random waves than in regular. This can be explained due to the fact that at random wave conditions the incoming waves have different heights which result to break at different water depths. Therefore, the long-shore driving force and the dissipation energy will be more distributed than at regular wave conditions where the distribution of the driving force is discontinuous at the breaking point.

4.2.2.2 *Cross-shore current velocity (V_y)*

In all tests and lines at each individual measured point, the cross-shore current velocity increased when the long-shore decreased and it decreased when the long-shore increased (Figure 4-12 to Figure 4-21). In contrast with long-shore current velocity, cross-shore current velocity was different for both gravel and mixed beach for Line 1 (trench). However, Line 2 and 3 followed the same pattern (with a small shift between them) for all the tests (except Test 2, for the same reason as in long-shore current velocity), with Line 2 having often (except at Test 5 and 6) higher values than Line 3. During regular wave conditions, Line 2 and 3 increased their values rapidly where this behaviour starting at Tests 3 and 4 from y=-2.4m. Line 1 had, in general, the highest values of cross-shore current velocity of all the lines

(except at Test 1, 4 and 8). Frequently all lines had positive values of V_y. This pointed to an existence of a cross-shore flow with an offshore direction (reverse cross-shore flow).

As mentioned previously, the behaviour of cross-shore current velocity is different for both gravel and mixed beaches for Line 1. However, it can be told that at random waves for both gravel and mixed beach (for Tests 5 and 9) the V_y followed the same pattern in Line 1. This was not the case for the other tests. Comparing the tests from gravel and mixed beach, it can be seen that whenever the V_y remains constant or decreased (Tests 3 and 4), the V_y for mixed beach (Tests 7 and 8) started to increased. Moreover, whenever V_y (Test 6) started to increase, the V_y for mixed beach became constant or even decreased (Test 10). Furthermore, it is worth noting, that for regular wave conditions (Tests 3 and 4) the V_y changed behaviour at y=-1.6m whereas the V_y in Tests 7 and 8 changed at y=-2.2.

As far as Tests 1 and 2 are concerned, the three lines had similar pattern and only a small shift occurred between them. At Test 1, Line 1 had the lowest values whereas at Test 2 had the highest.

4.2.2.3 *Current velocity at z direction (V_z)*

The current velocity at z direction was approximately the same for both gravel and mixed beach for random wave conditions for all lines (Figure 4-22 to Figure 4-31). For all other tests comparing gravel and mixed beach, V_z was different and especially at Line 1. All lines had almost the same pattern, some with slightly different shifts and some with slightly different peaks, especially at Line 1, from y=-2.4m to y=-3.4m.

The V_z for both gravel and mixed beach, tended to have negative direction except at regular wave conditions (Tests 3 and 7) whereas the V_z had a fluctuation of directions.

4.2.3 Cross-shore beach profiles

As mentioned before, the bed level had been measured at the selected cross-shore sections. The observations of the beach development were carried out in y direction from y=-0.6m to y=-6.0m with an integral of 10cm.

Moreover, in the previous chapter, it was pointed out that the (gravel & mixed) beaches were initially constructed at a 1:10 slope but they were not reshaped during the experiment procedure (except for when the sediment changed), so that the initial condition for each test was the final profile from the previous test. As result, the measurements were taken place in 3 stages:

1. Before the generation of the waves (Original Profile).

2. At the end of the generation of waves for the initial test (the test with input wave period of 2sec) and.

3. At the end of the generation of waves for the second test (the test with input wave period of 3sec).

The beach was reconstructed every time at its original shape after the completion of measurements at stage 3. Consequently, the beach was reconstructed five times in its original shape for both regular and random wave conditions. The graphical presentation of the cross-shore profiles for all the tests and for all the three lines can be seen in Figure 4-32 to Figure 4-46.

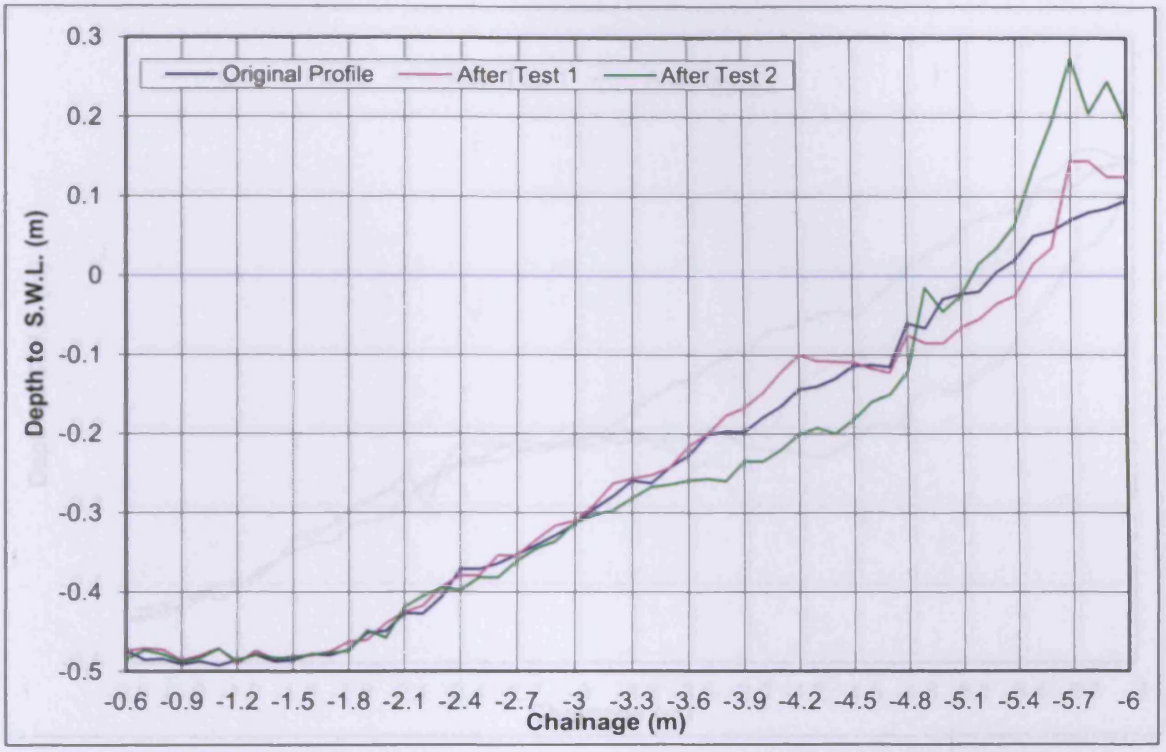

Figure 4-32 Cross-shore profile changes during Test 1 and Test 2 (Line 1)

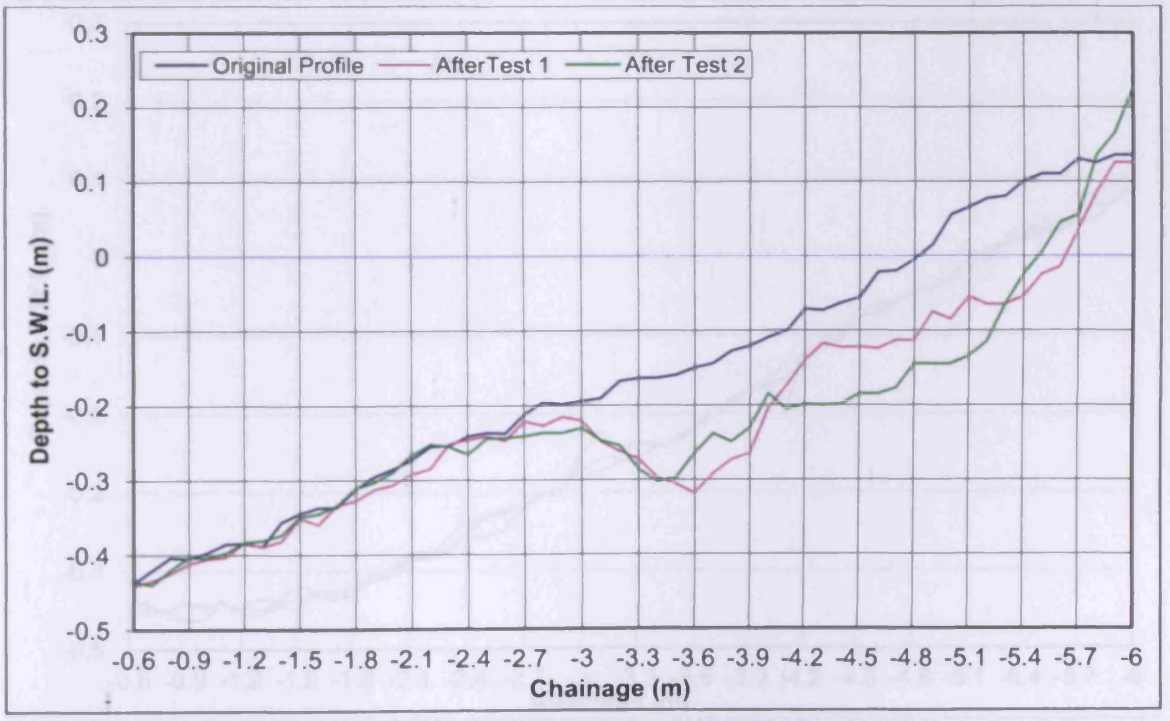

Figure 4-33 Cross-shore profile changes during Test 1 and Test 2 (Line 2)

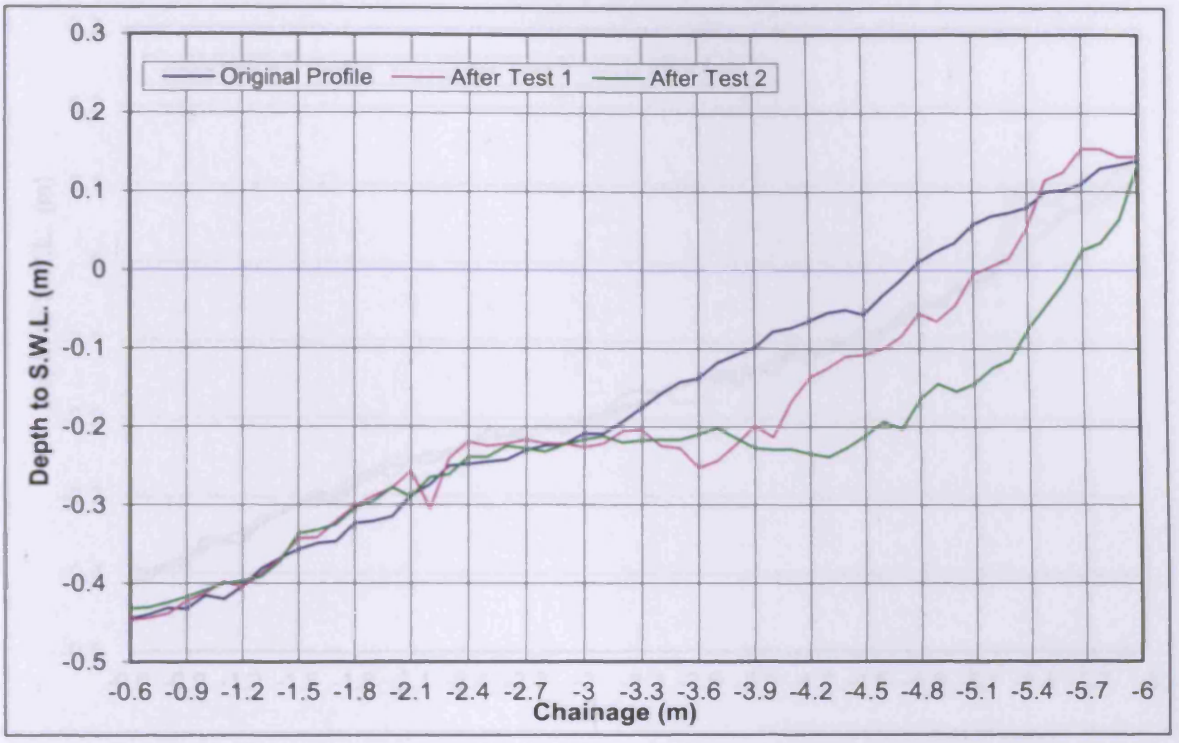

Figure 4-34 Cross-shore profile changes for Test 1 and Test 2 (Line 3)

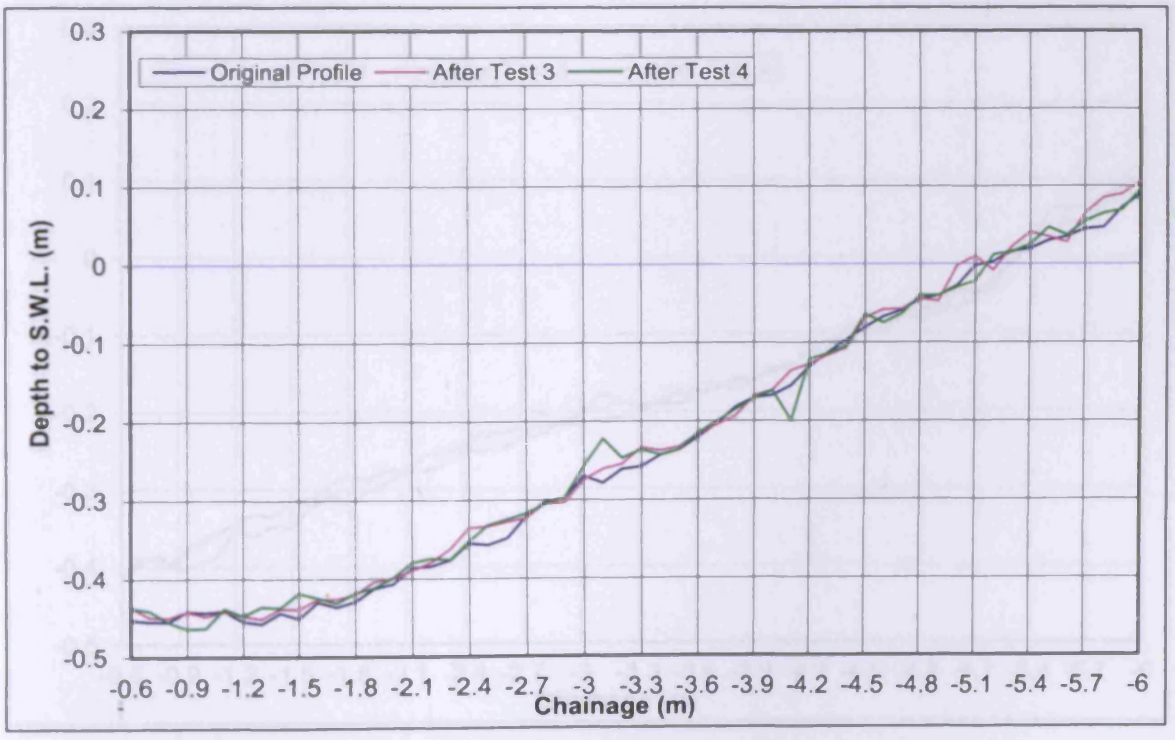

Figure 4-35 Cross-shore profile changes during Test 3 and Test 4 (Line 1)

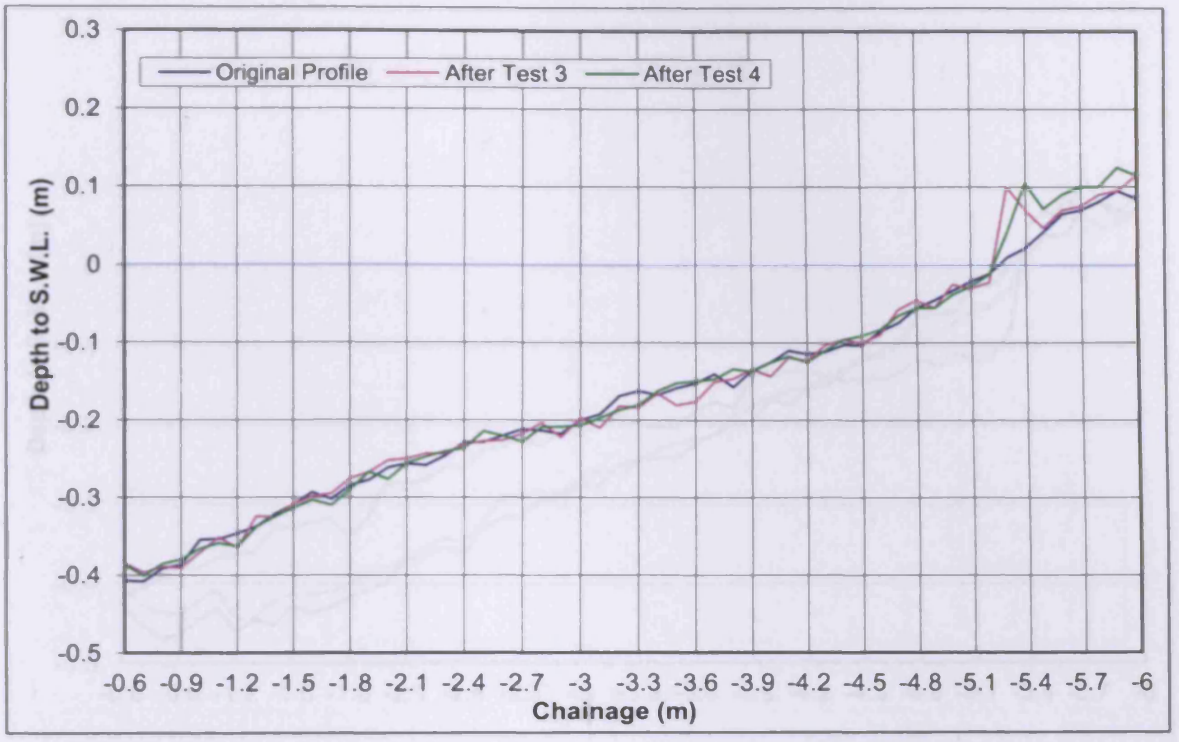

Figure 4-36 Cross-shore profile changes during Test 3 and Test 4 (Line 2)

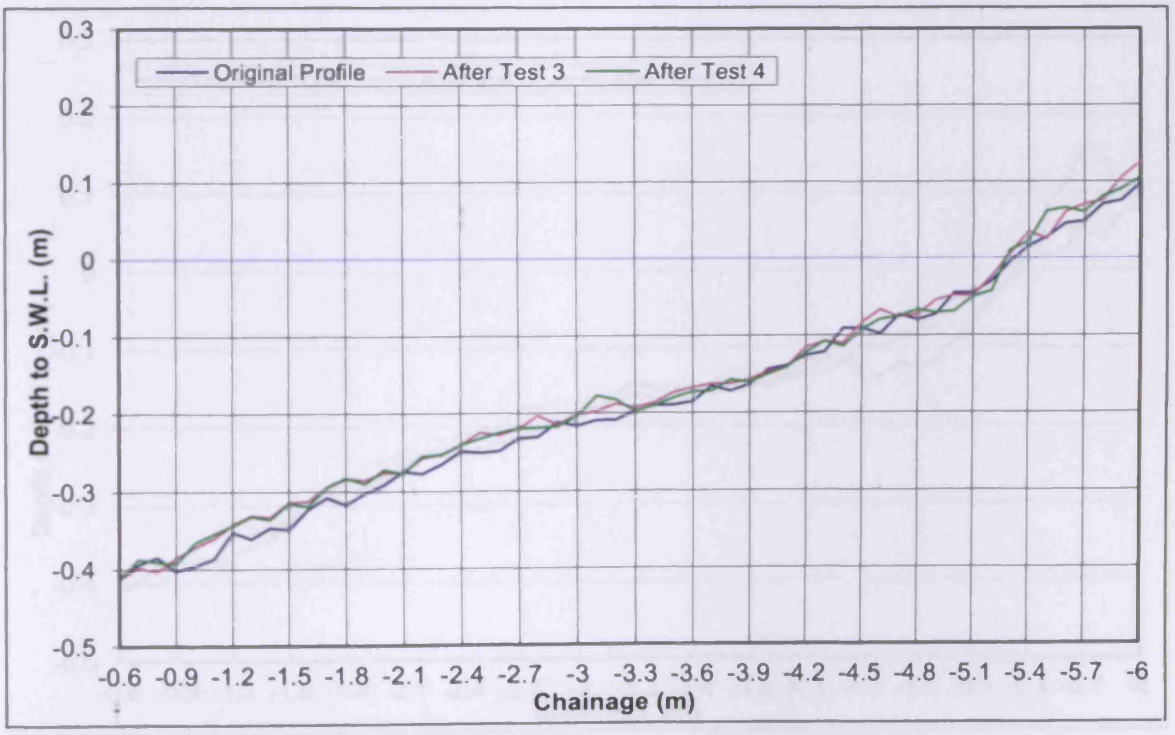

Figure 4-37 Cross-shore profile changes during Test 3 and Test 4 (Line 3)

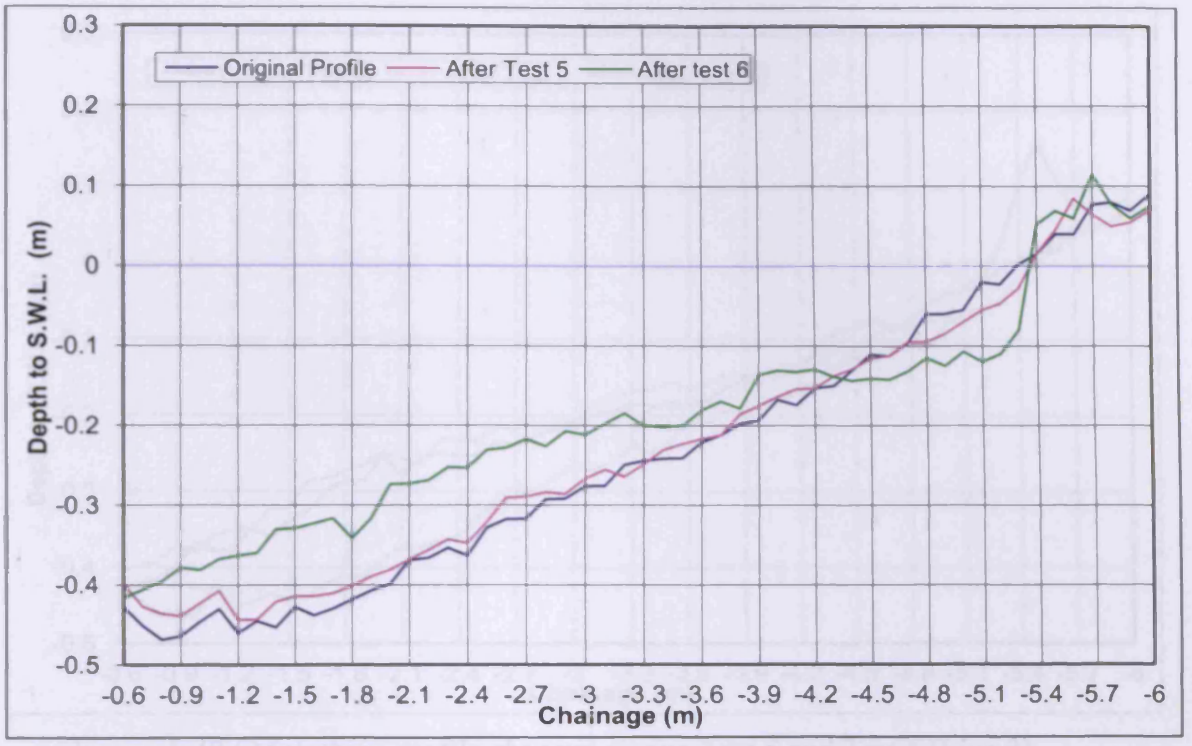

Figure 4-38 Cross-shore profile changes during Test 5 and Test 6 (Line 1)

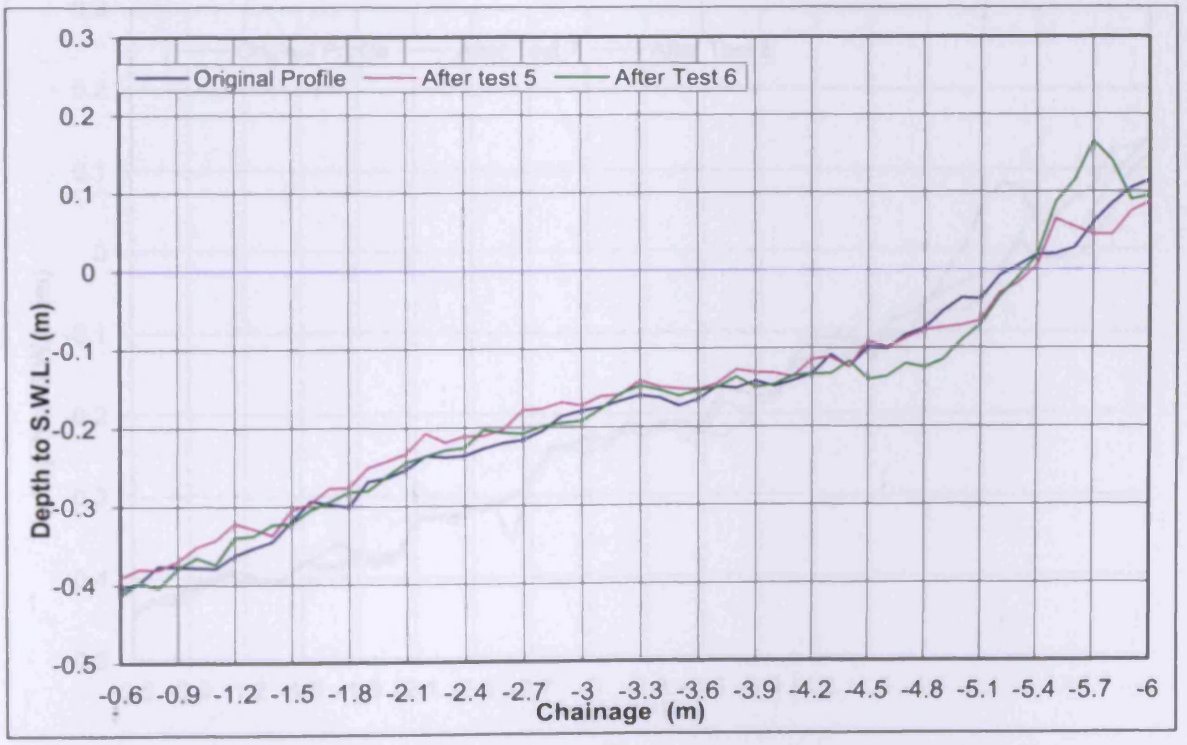

Figure 4-39 Cross-shore profile changes during Test 5 and Test 6 (Line 2)

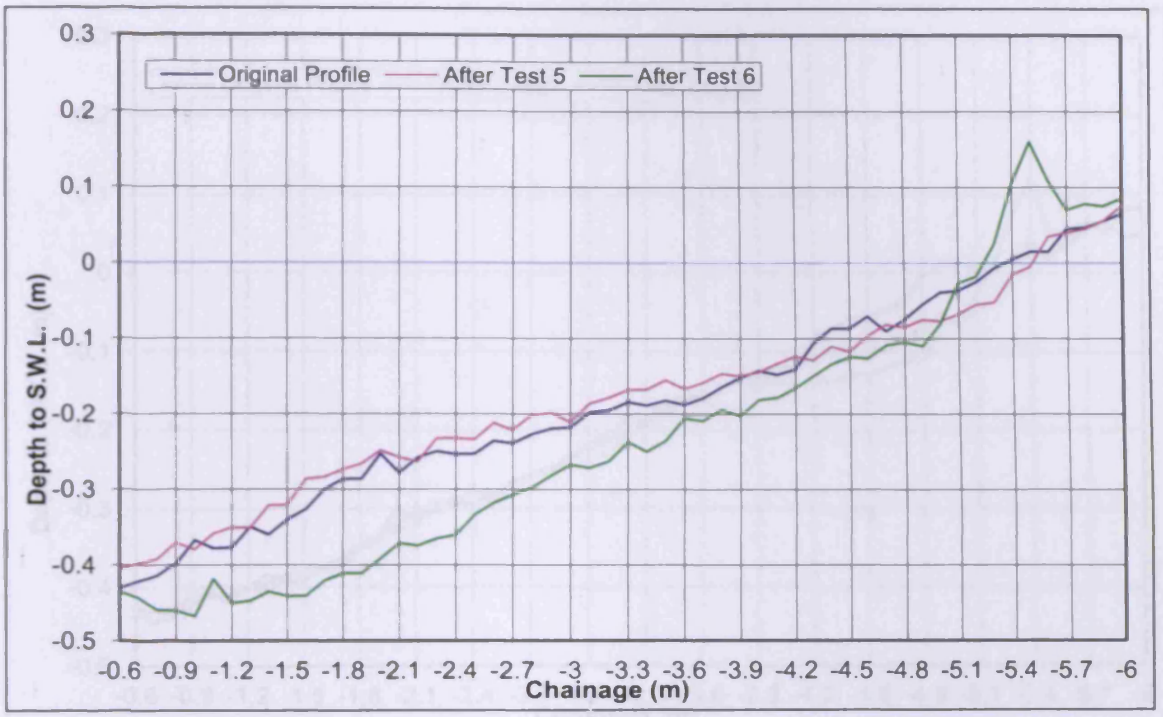

Figure 4-40 Cross-shore profile changes during Test 5 and Test 6 (Line 3)

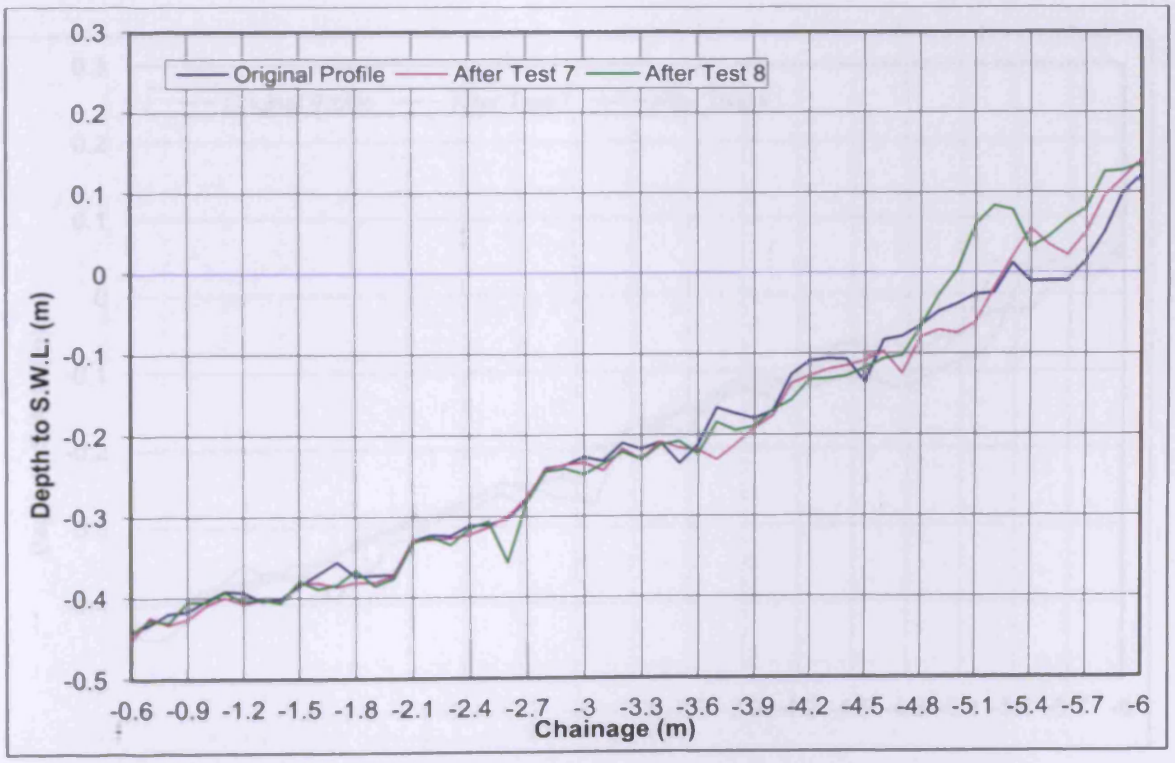

Figure 4-41 Cross-shore profile changes during Test 7 and Test8 (Line 1)

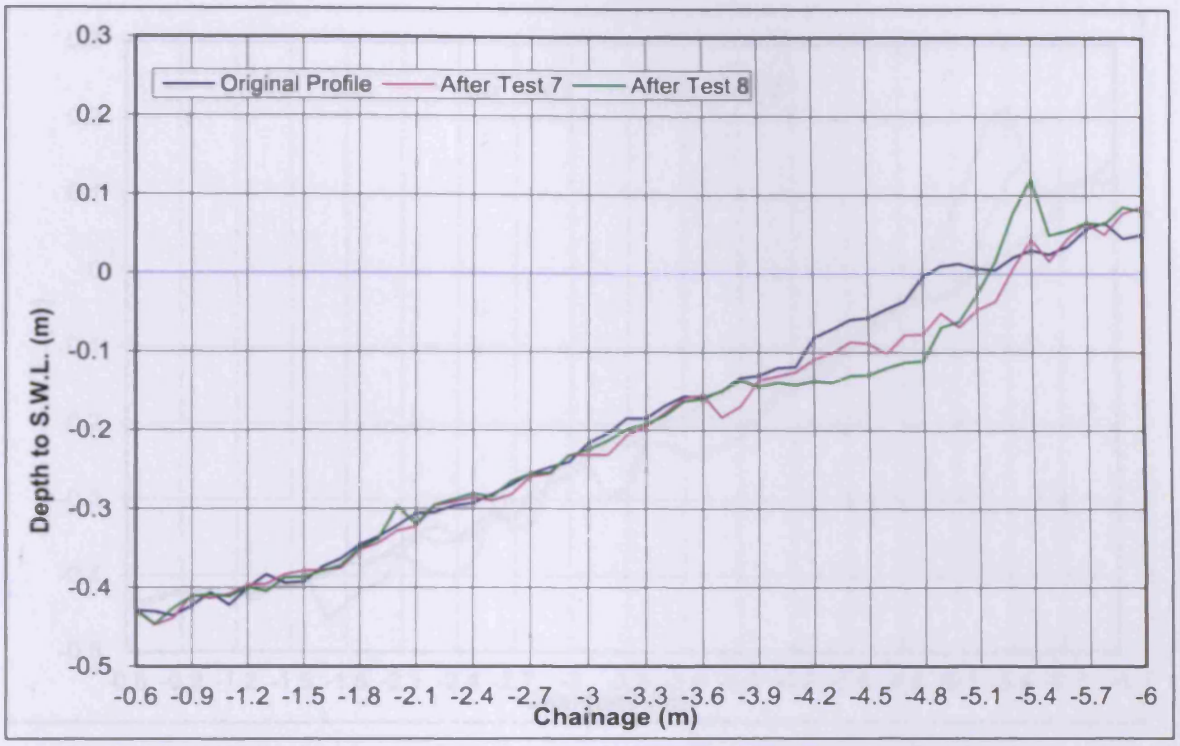

Figure 4-42 Cross-shore profile changes during Test 7 and Test 8 (Line 2)

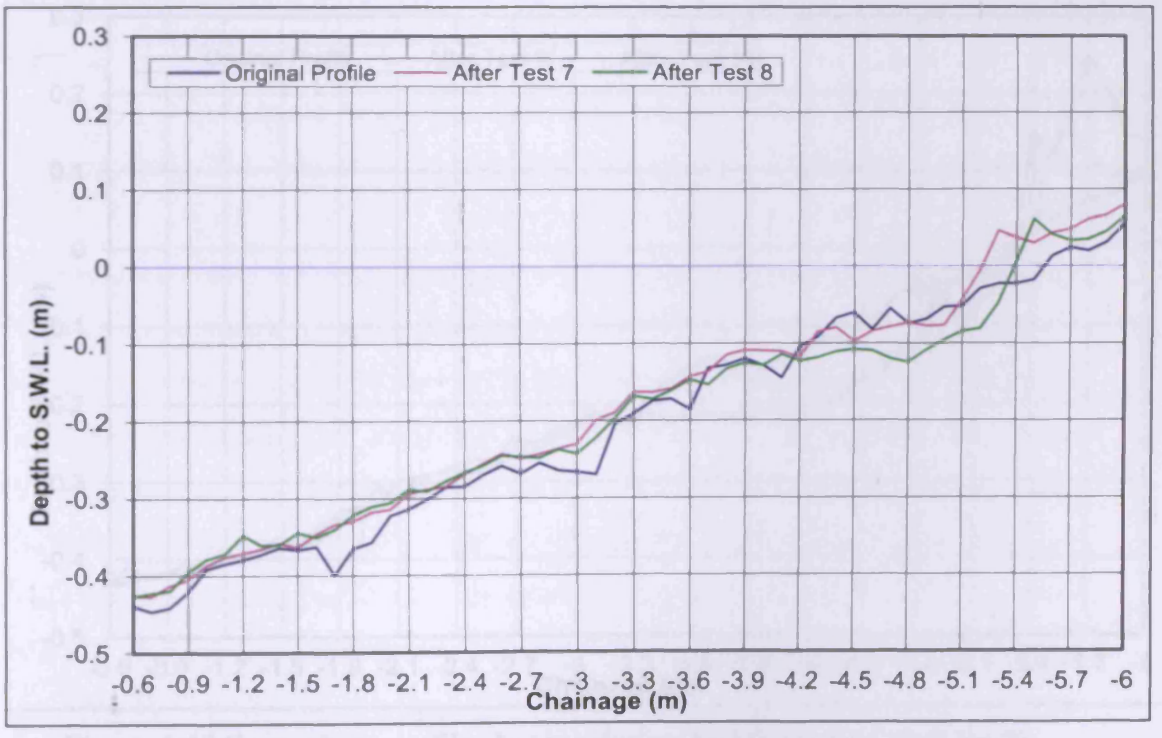

Figure 4-43 Cross-shore profile changes during Test 7 and Test 8 (Line 3)

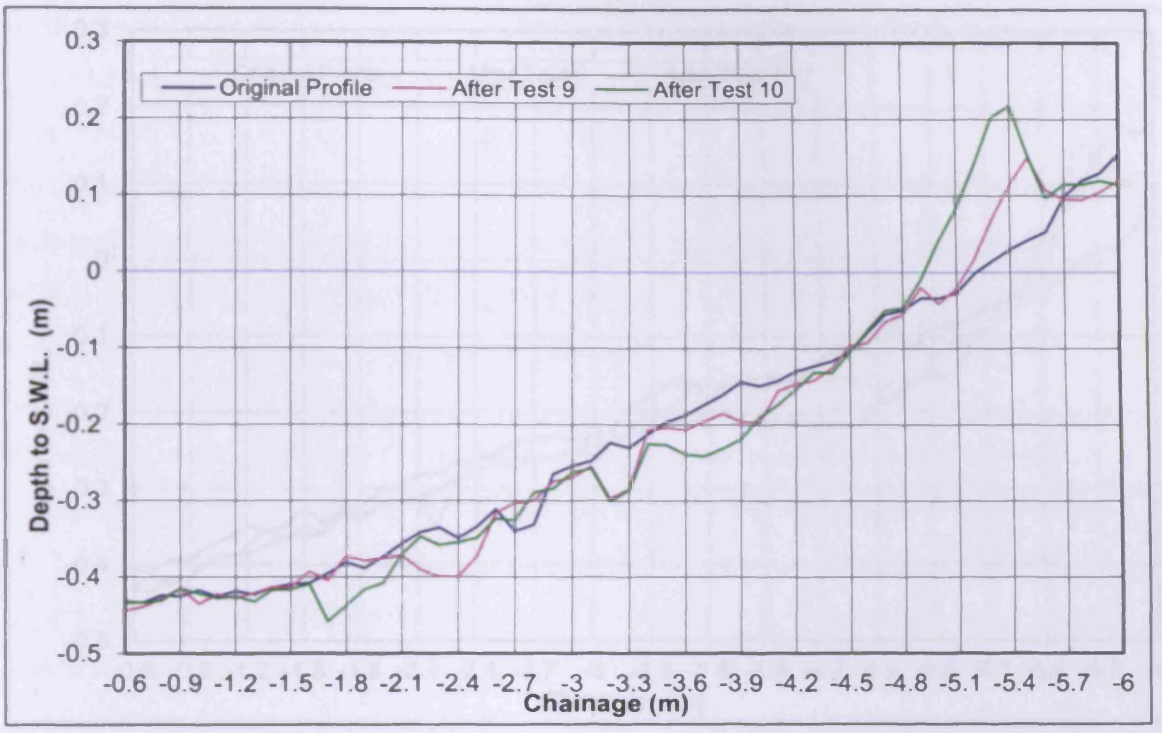

Figure 4-44 Cross-shore profile changes during Test 9 and Test 10 (Line 1)

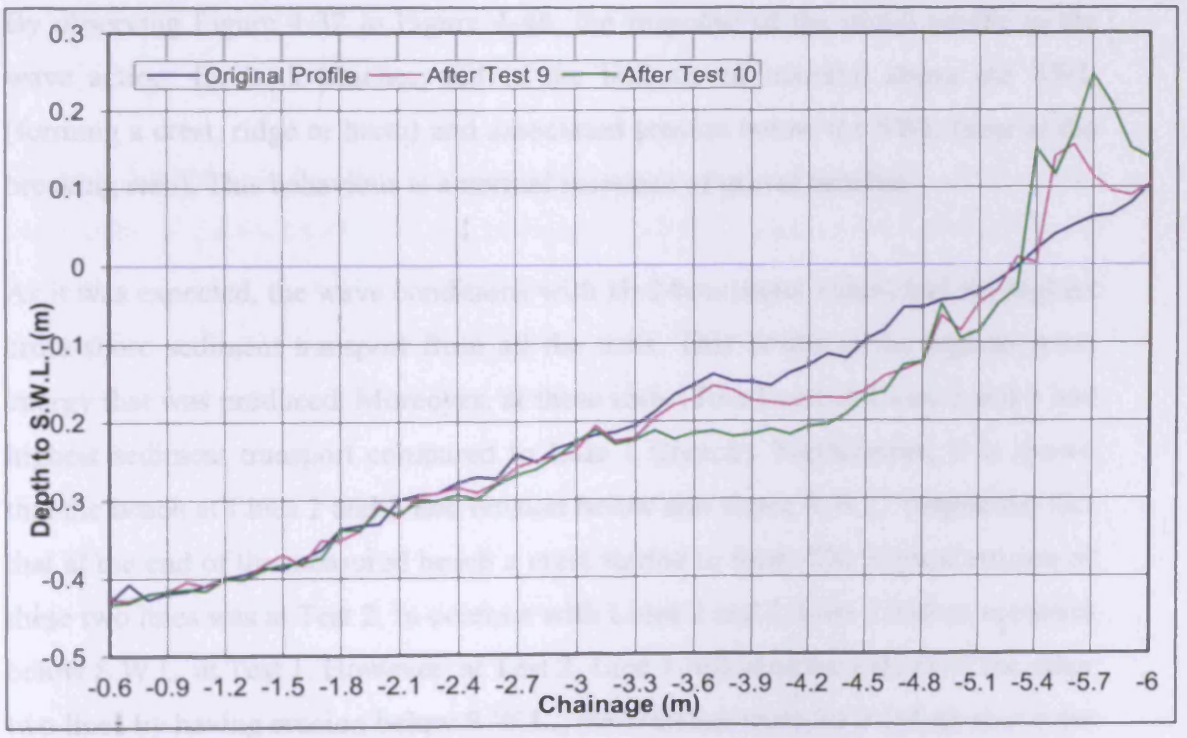

Figure 4-45 Cross-shore profile changes during Test 9 and Test 10 (Line 2)

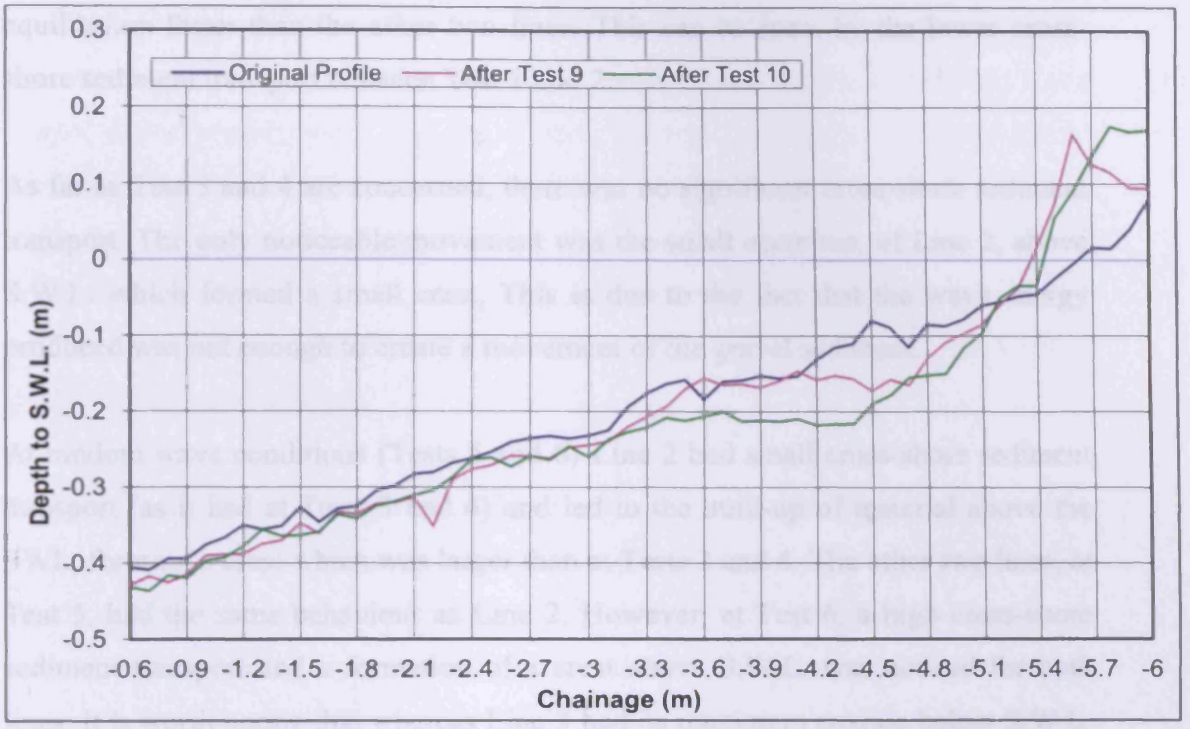

Figure 4-46 Cross-shore profile changes during Test 9 and Test 10 (Line 3)

By observing Figure 4-32 to Figure 4-46, the response of the initial profile to the wave action, for both beaches, led to the built-up of material above the SWL (forming a crest, ridge or berm) and associated erosion below the SWL (near at the breaking step). This behaviour is a normal response of gravel beaches.

As it was expected, the wave conditions with H=24cm (input value) had the highest cross-shore sediment transport from all the tests. This is due to the highest wave energy that was produced. Moreover, at these tests (Test 1 and 2) Lines 2 and 3 had highest sediment transport compared to Line 1 (trench). Furthermore, it is shown that the beach at Lines 2 and 3 had erosion below and above S.W.L. despite the fact that at the end of the measured beach a crest started to form. The highest erosion of these two lines was at Test 2. In contrast with Lines 2 and 3, Line 1 had an accretion below S.W.L. at Test 1. However, at Test 2, Line 1 followed the pattern of the other two lines by having erosion below S.W.L., nevertheless material build-up above the S.W.L. formed the highest crest of all lines. Finally, Line 2 reached the beach

equilibrium faster than the other two lines. This can be seen, by the lower cross-shore sediment transport between Test 1 and 2.

As far as Test 3 and 4 are concerned, there was no significant cross-shore sediment transport. The only noticeable movement was the small accretion, of Line 2, above S.W.L. which formed a small crest. This is due to the fact that the wave energy produced was not enough to create a movement of the gravel sediment.

At random wave conditions (Tests 5 and 6) Line 2 had small cross-shore sediment transport (as it had at Tests 3 and 4) and led to the built-up of material above the SWL, forming a crest which was larger than at Tests 3 and 4. The other two lines, at Test 5, had the same behaviour as Line 2. However, at Test 6, a high cross-shore sediment transport and a formation of a crest above S.W.L. was noticed for both lines. It is worth noting that whereas Line 3 had its maximum erosion below S.W.L. Line 1 had its maximum accretion below S.W.L. This difference indicates that there is movement of sediment from Line 3 to Line 1. However, the fact that Line 2 hasn't been influenced by this movement is quite interesting.

Considering the tests that were based on the mixed beach (Tests 7-10), there was a settlement of the sediment. The original profile of the mixed beach was built based on Figure 1. However, after pumping water into the wave basin in order to reach the preferred S.W.L. of 0.5m, there was a settlement of the sediment especially at the rear back as it was mentioned in the previous chapter.

At these tests, all three lines followed similar pattern of bed level change having the highest and form of crest (above S.W.L.) at random wave conditions, especially at Test 10. The only difference between the lines, was a small shift of the form of the crest which was related to the location of each line individually.

As mentioned previously in the literature review, according to Powell (1990) and Van der Meer (1988), the main factors influencing gravel beach profiles are wave height, wave period, wave duration, beach material and angle of wave attack. Moreover, Mason and Coates (2001) stated the factors that may influence the sediment transport of mixed beach are the hydraulic conductivity, groundwater and infiltration, wave reflection, threshold of motion. In accordance with the measurements taken through the experiment, only the three factors influencing gravel beach can be studied.

With the exception of wave attack and wave duration, the other three factors will be studied on gravel and on mixed beach. Moreover a comparison will be made between them. However, in order for the three factors to be studied, it had to be ensured that the beach slopes were the same for all the tests that would be compared (Figure 4-47 to Figure 4-58).

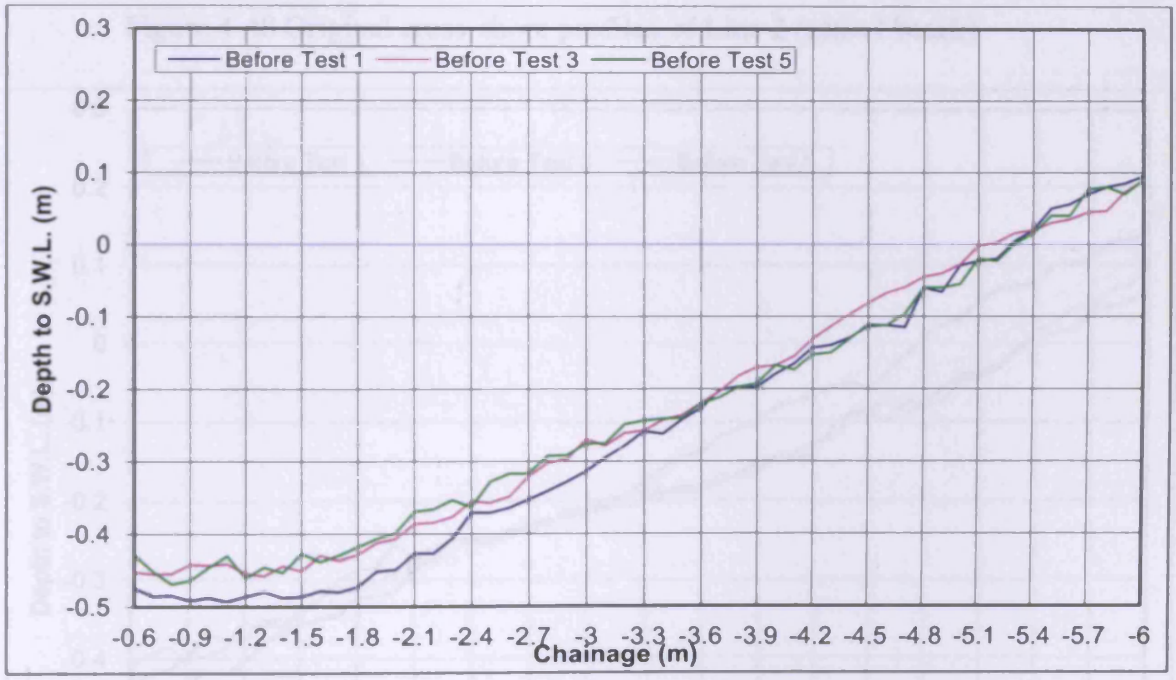

Figure 4-47 Original cross-shore profiles of Line 1 (gravel beach)

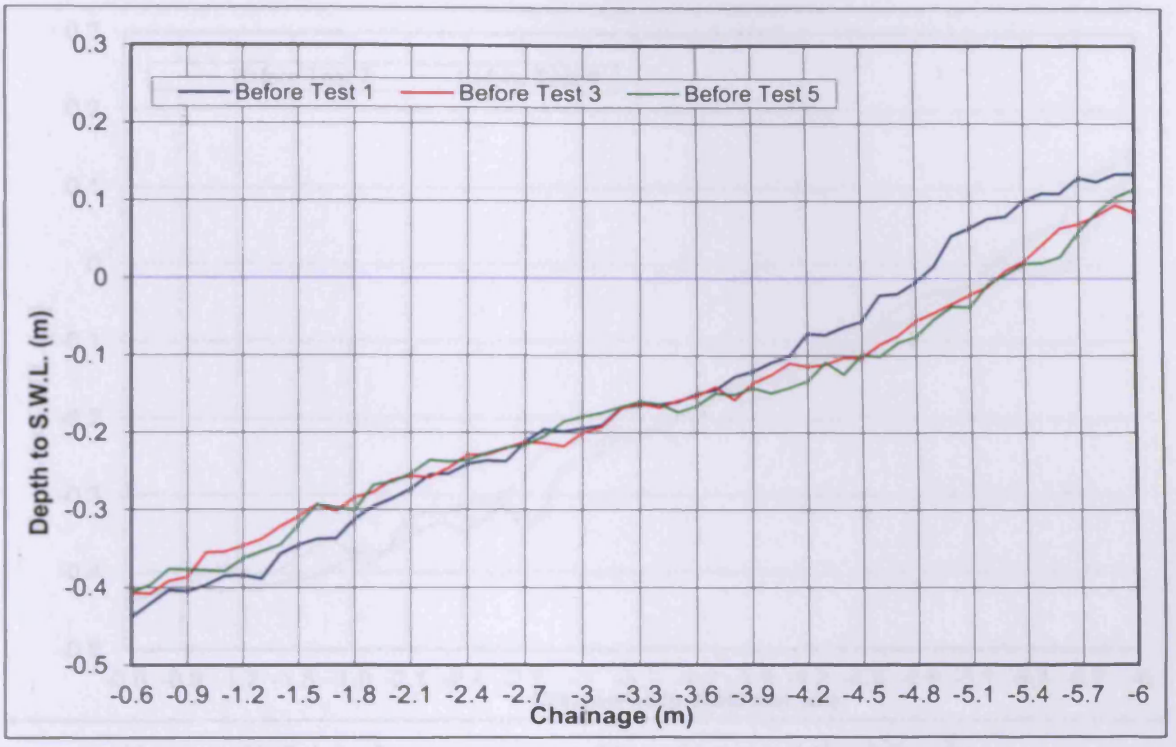

Figure 4-48 Original cross-shore profiles of Line 2 (gravel beach)

Figure 4-49 Original cross-shore profiles of Line 3 (gravel beach)

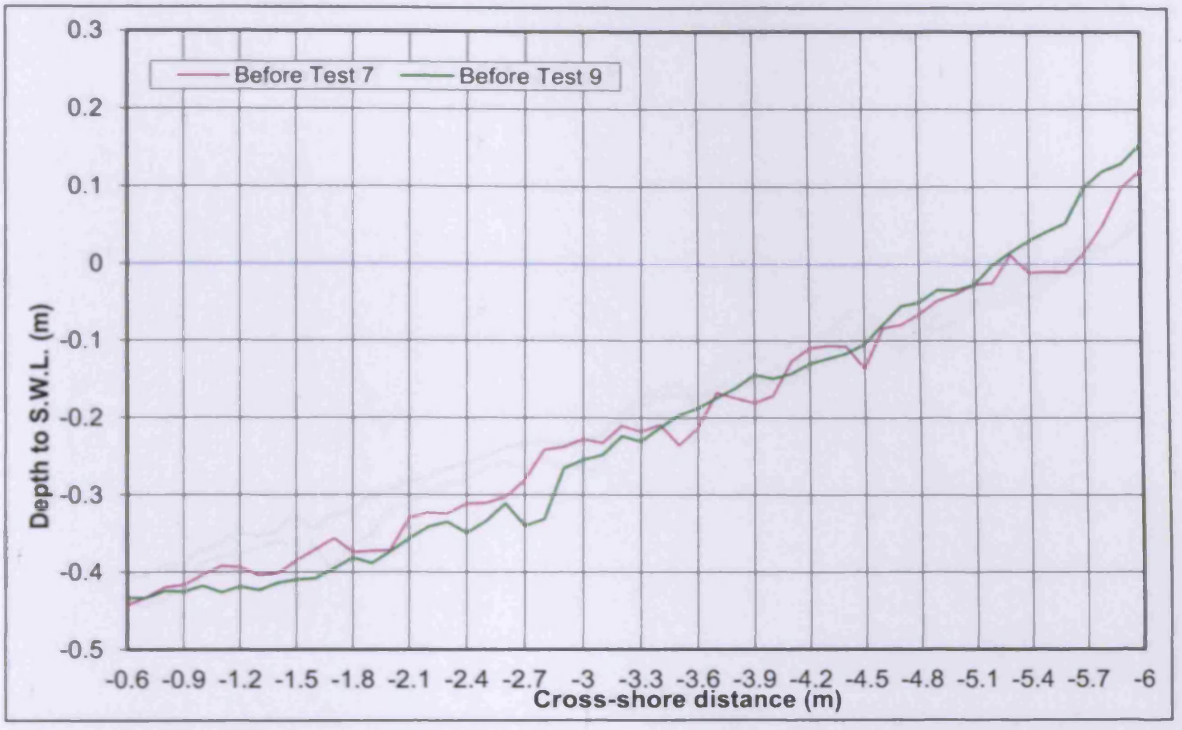

Figure 4-50 Original cross-shore profiles of Line 1 (Mixed Beach)

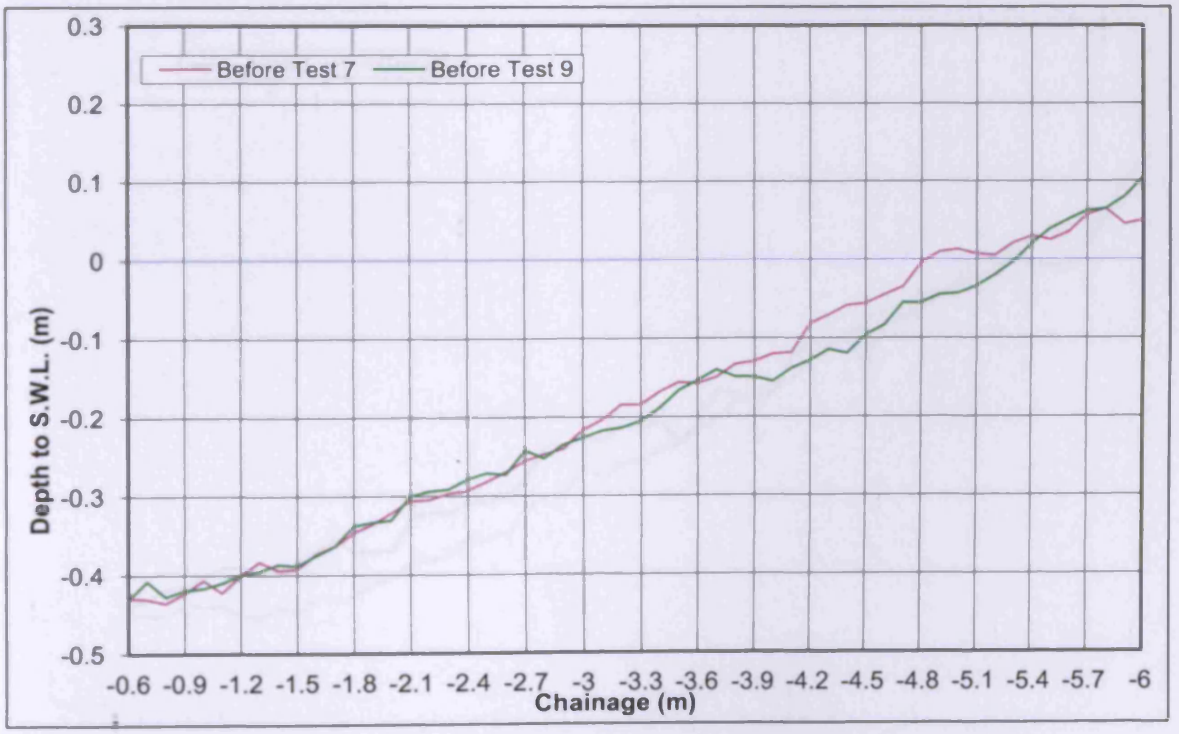

Figure 4-51 Original cross-shore profiles of Line 2 (Mixed Beach)

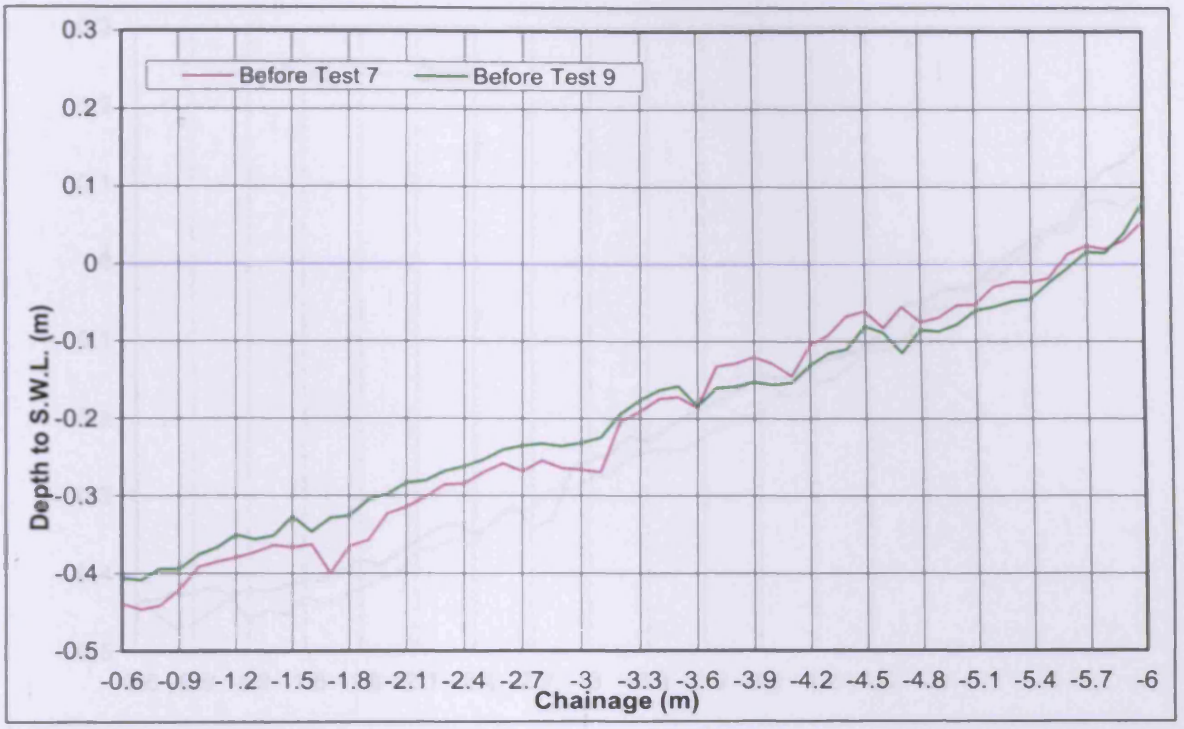

Figure 4-52 Original cross-shore profiles of Line 3 (Mixed Beach)

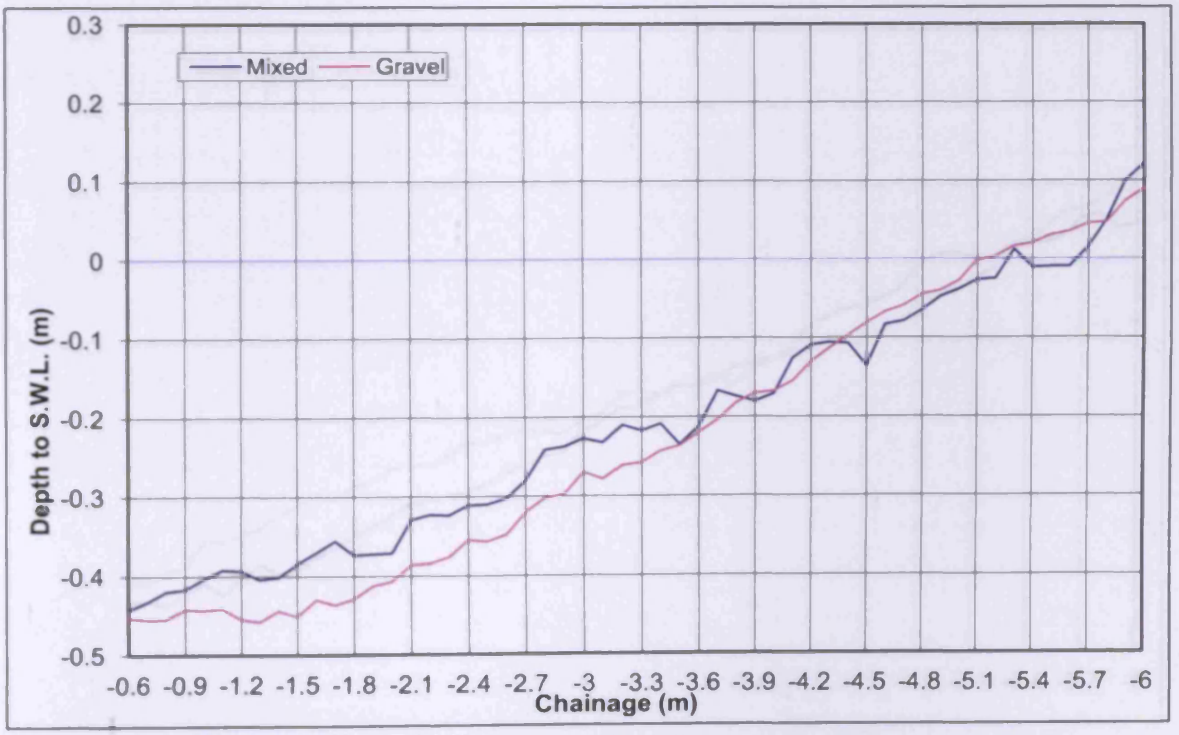

Figure 4-53 Original cross-shore profiles of Line 1 (Regular Waves)

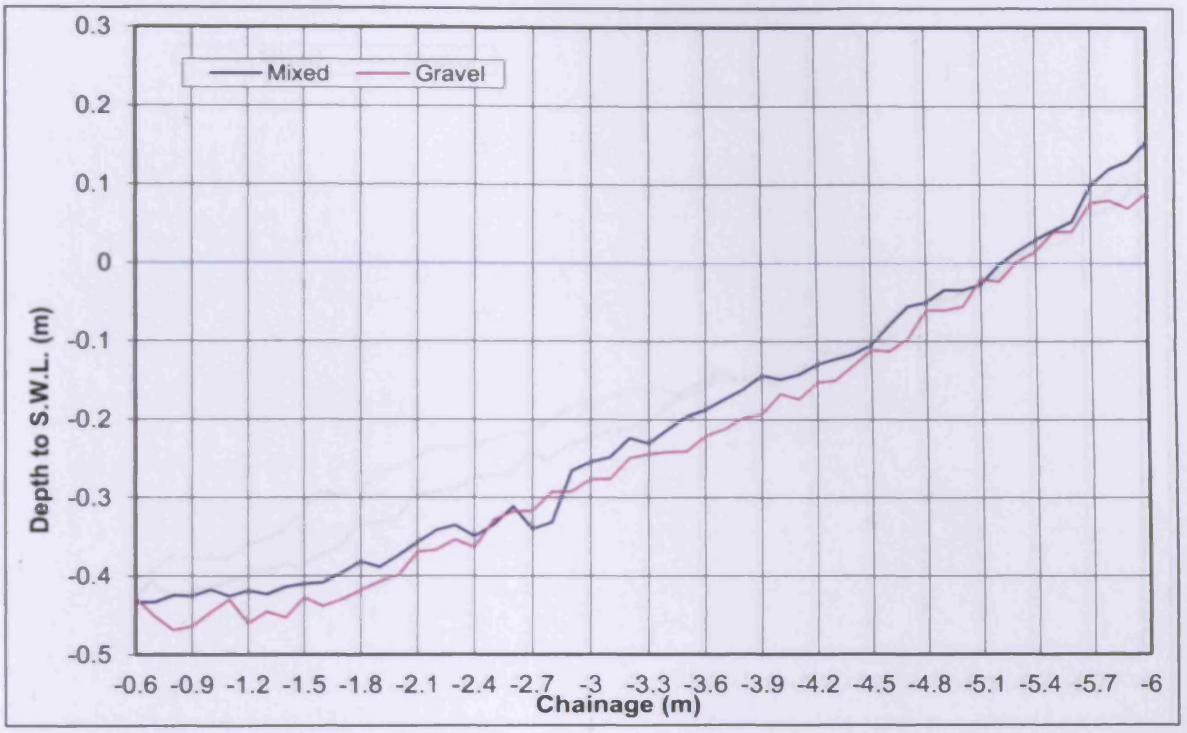

Figure 4-54 Original cross-shore profiles of Line 1 (Random Waves)

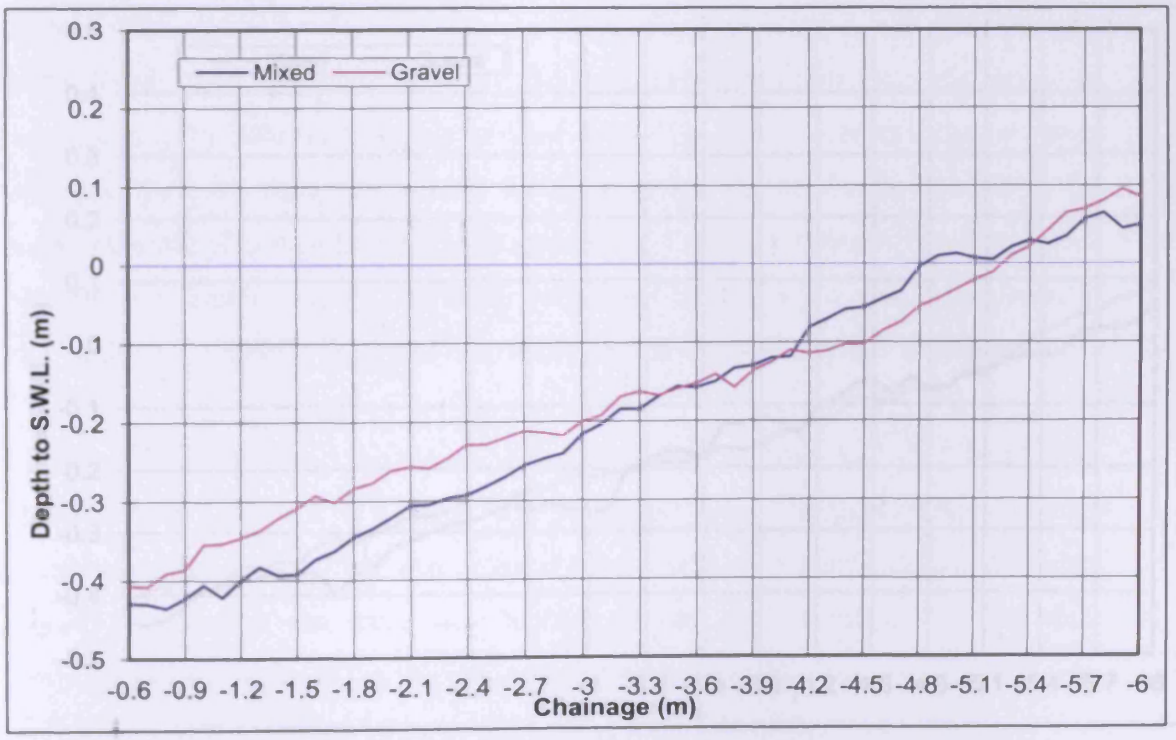

Figure 4-55 Original cross-shore profiles of Line 2 (Regular Waves)

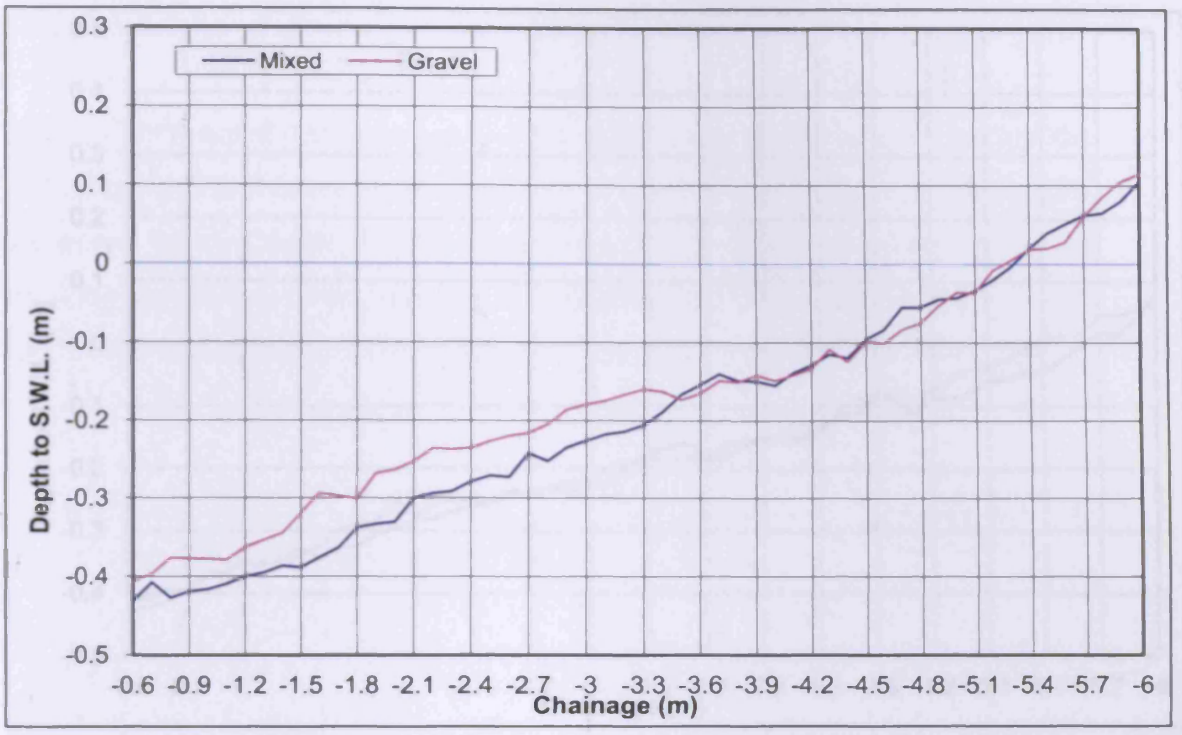

Figure 4-56 Original cross-shore profiles of Line 2 (Random Waves)

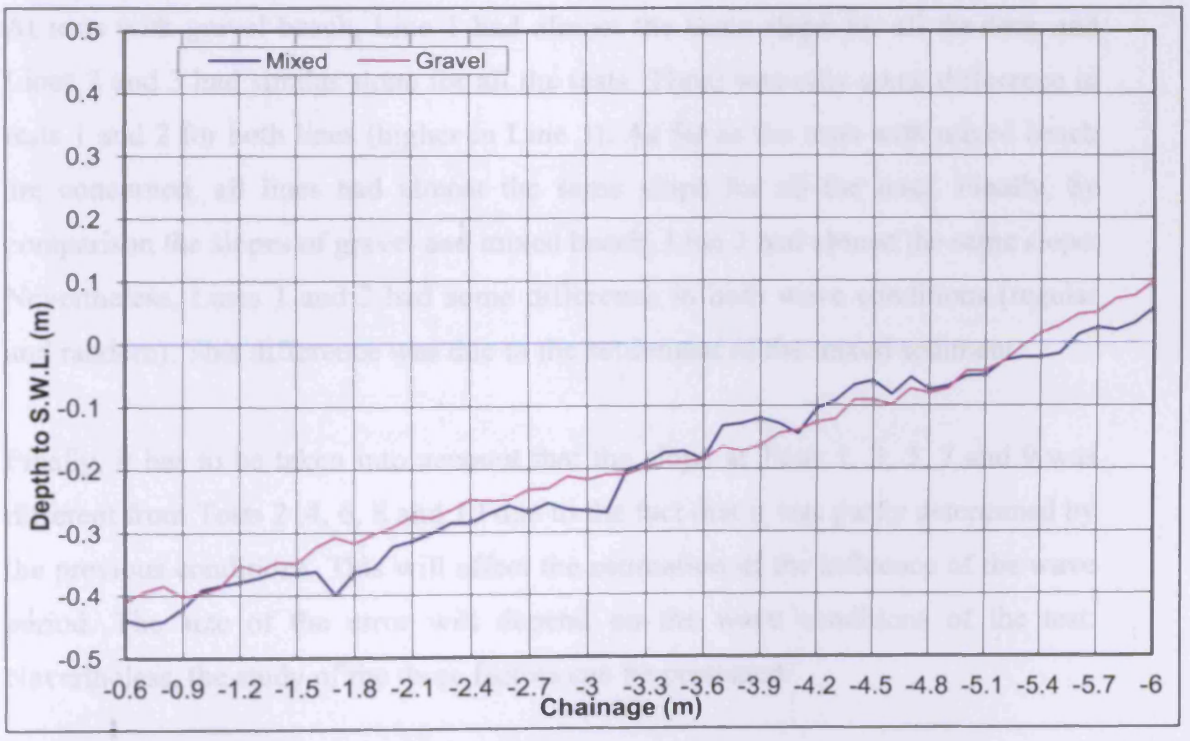

Figure 4-57 Original cross-shore profiles of Line 3 (Regular Waves)

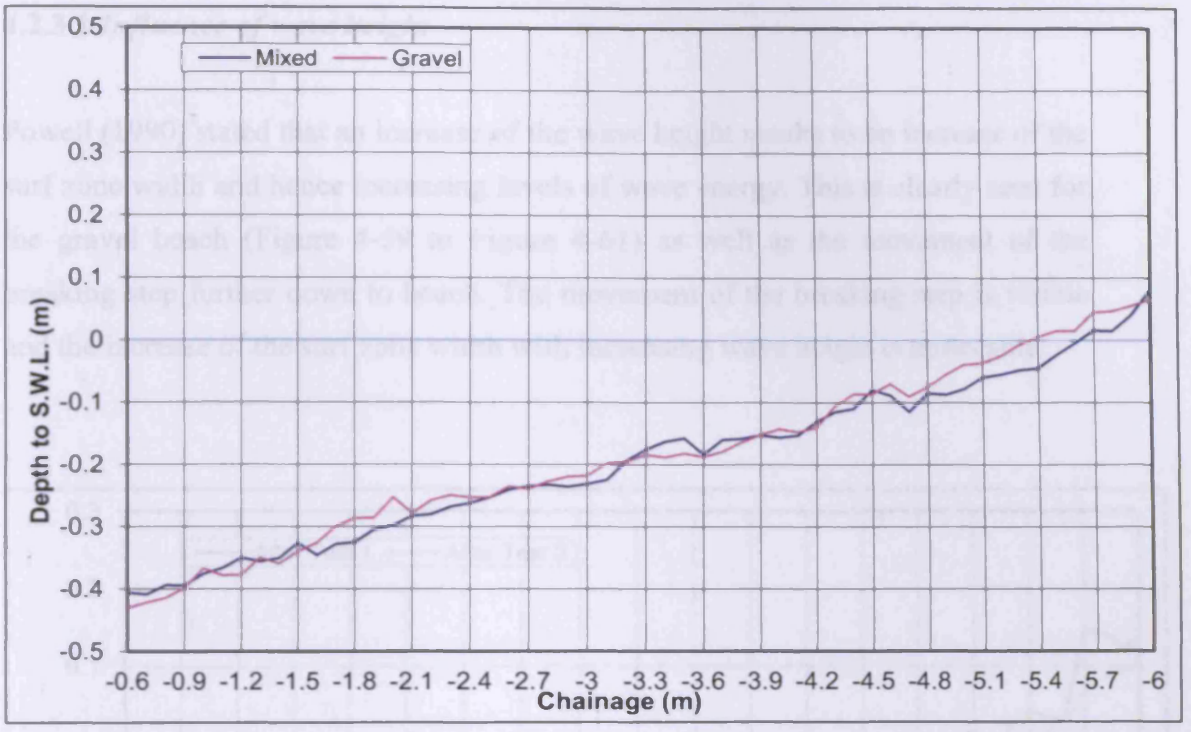

Figure 4-58 Original cross-shore profiles of Line 3 (Random Waves)

At tests with gravel beach, Line 1 had almost the same slope for all the tests and Lines 2 and 3 had similar slope for all the tests. There was only some difference in tests 1 and 2 for both lines (higher in Line 3). As far as the tests with mixed beach are concerned, all lines had almost the same slope for all the tests. Finally, by comparison the slopes of gravel and mixed beach, Line 3 had almost the same slope. Nevertheless, Lines 1 and 2 had some difference in both wave conditions (regular and random). This difference was due to the settlement of the mixed sediment.

Finally, it has to be taken into account that the slope at Tests 1, 3, 5, 7 and 9 was different from Tests 2 ,4, 6, 8 and 10 due to the fact that it was partly determined by the previous conditions. This will affect the estimation of the influence of the wave period. The size of the error will depend on the wave conditions of the test. Nevertheless, the study of the three factors can be presented.

4.2.3.1 *Influence of wave height*

Powell (1990) stated that an increase of the wave height results to an increase of the surf zone width and hence increasing levels of wave energy. This is clearly seen for the gravel beach (Figure 4-59 to Figure 4-61) as well as the movement of the breaking step further down to beach. The movement of the breaking step is visible and the increase of the surf zone width with increasing wave height is noticeable.

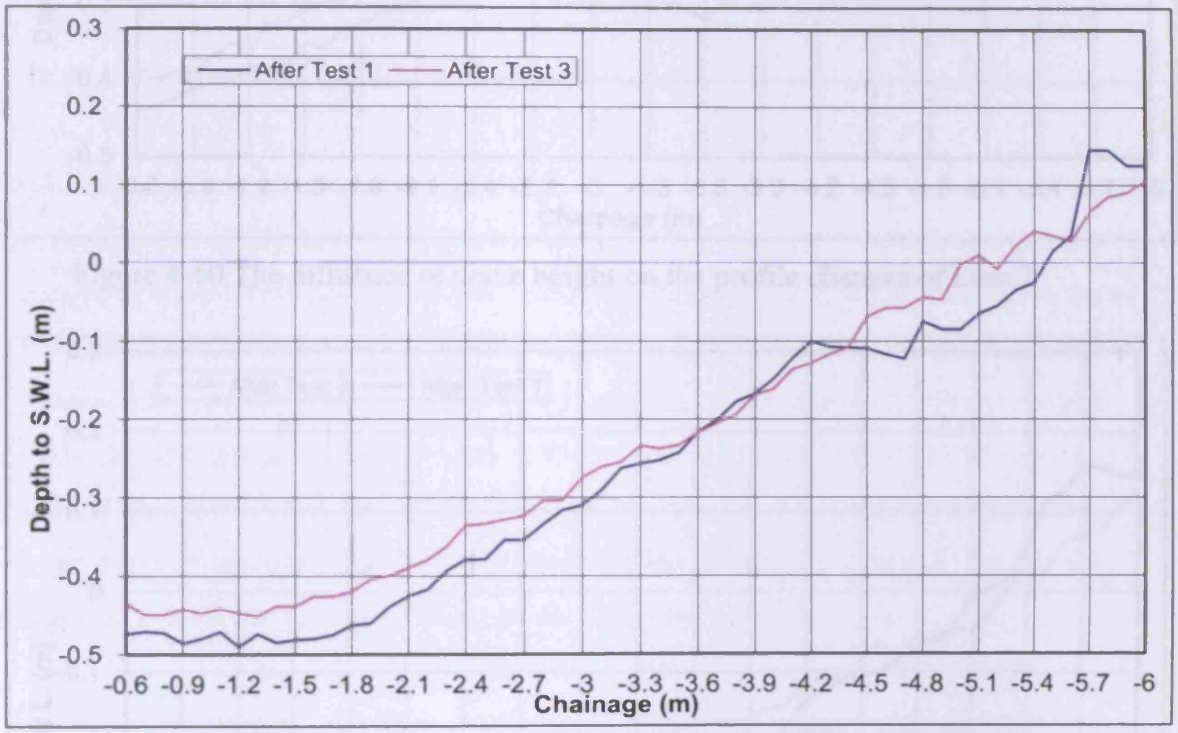

Figure 4-59 The influence of wave height on the profile changes of Line 1

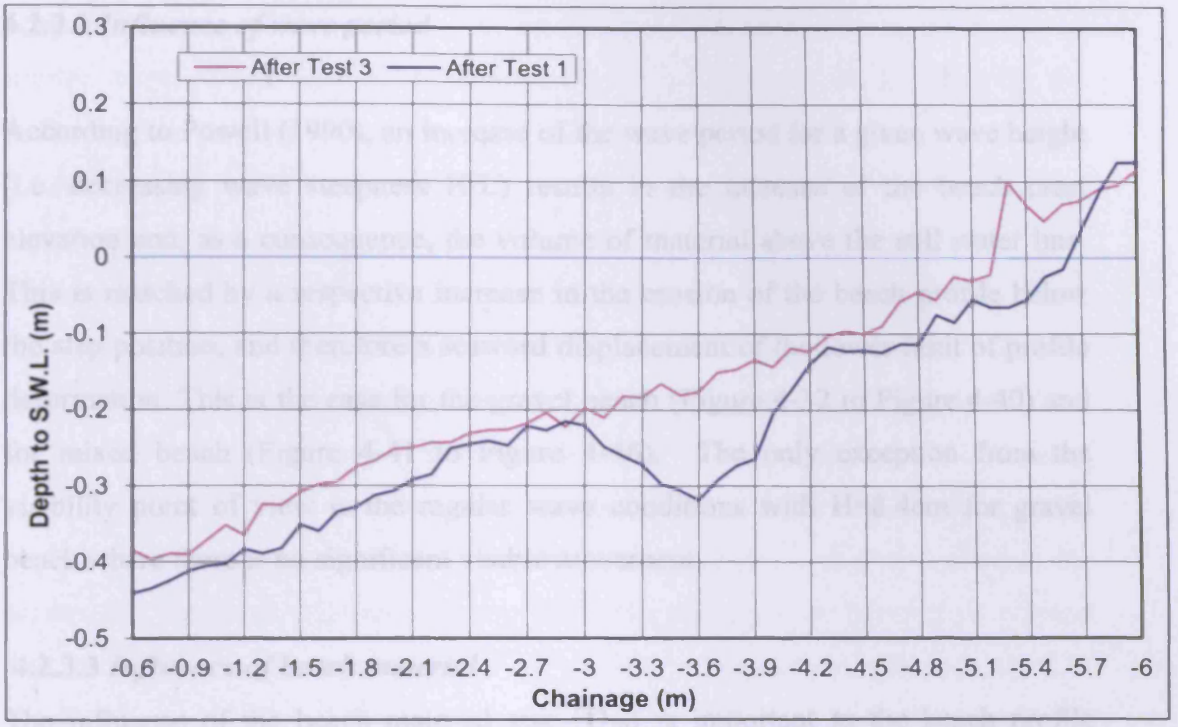

Figure 4-60 The influence of wave height on the profile changes of Line 2

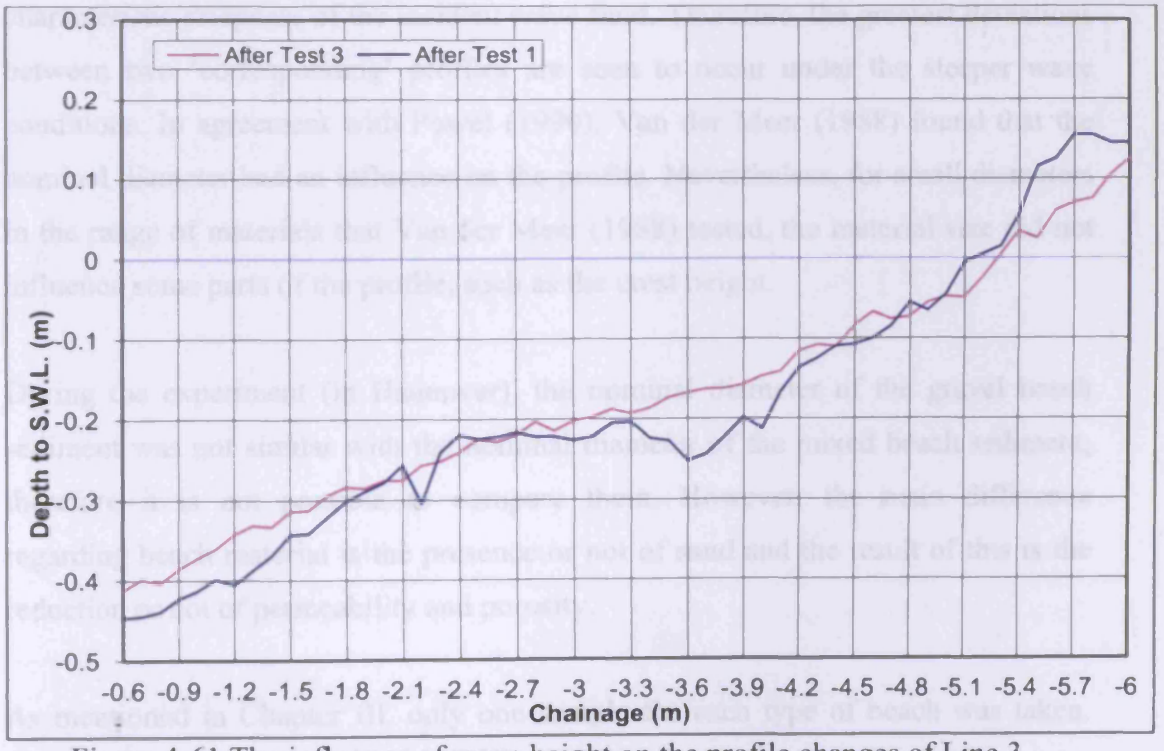

Figure 4-61 The influence of wave height on the profile changes of Line 3

4.2.3.2 *Influence of wave period*

According to Powell (1990), an increase of the wave period for a given wave height (i.e. decreasing wave steepness H/L) results in the increase of the beach crest elevation and, as a consequence, the volume of material above the still water line. This is matched by a respective increase in the erosion of the beach profile below the step position, and therefore a seaward displacement of the lower limit of profile deformation. This is the case for the gravel beach (Figure 4-32 to Figure 4-40) and for mixed beach (Figure 4-41 to Figure 4-46). The only exception from the visibility point of view is the regular wave conditions with H=8.4cm for gravel beach where there is no significant visible movement.

4.2.3.3 *Influence of beach material*

The influence of the beach material size (D_{50}) is important to the beach profile change. Powell (1990) suggested that this importance is partly dependent upon the characteristic steepness of the incident wave field. Therefore, the greatest deviations between two 'corresponding' profiles are seen to occur under the steeper wave conditions. In agreement with Powel (1990), Van der Meer (1988) found that the nominal diameter had an influence on the profile. Nevertheless, for small diameters in the range of materials that Van der Meer (1988) tested, the material size did not influence some parts of the profile, such as the crest height.

During the experiment (in Hannover), the nominal diameter of the gravel beach sediment was not similar with the nominal diameter of the mixed beach sediment; therefore it is not possible to compare them. However, the main difference regarding beach material is the presence or not of sand and the result of this is the reduction or not of permeability and porosity.

As mentioned in Chapter III, only one sample for each type of beach was taken. These samples were taken at the crest. It must be noted that the sampling of the

beaches was a secondary objective of the test and, due to time restrictions, was of limited scope. Despite the fact that there were no further records taken for the sediment compositions during the experiment, there were visual observations done for both gravel and mixed beach sediment. It was noted that as the experimental tests with gravel beach progressed, the step and the crest tend to be composed with the coarsest material whether the SWL and the area seawards the step with the finest material. During the experimental tests with mixed beach, the observations were focused on whether the composition of gravel/sand changed. The general trend shown that at the surface of the crest, step and SWL the sediment was composed only with gravel. There was no sand that can be observed; on the contrary, at the surface of the area seawards the step the percentage of sand was similar to the percentage of gravel. Moreover, at the area after the crest the percentage of sand was even higher to the percentage of gravel. The comparison of the two types of beach is shown in Figure 4-62 to Figure 4-73.

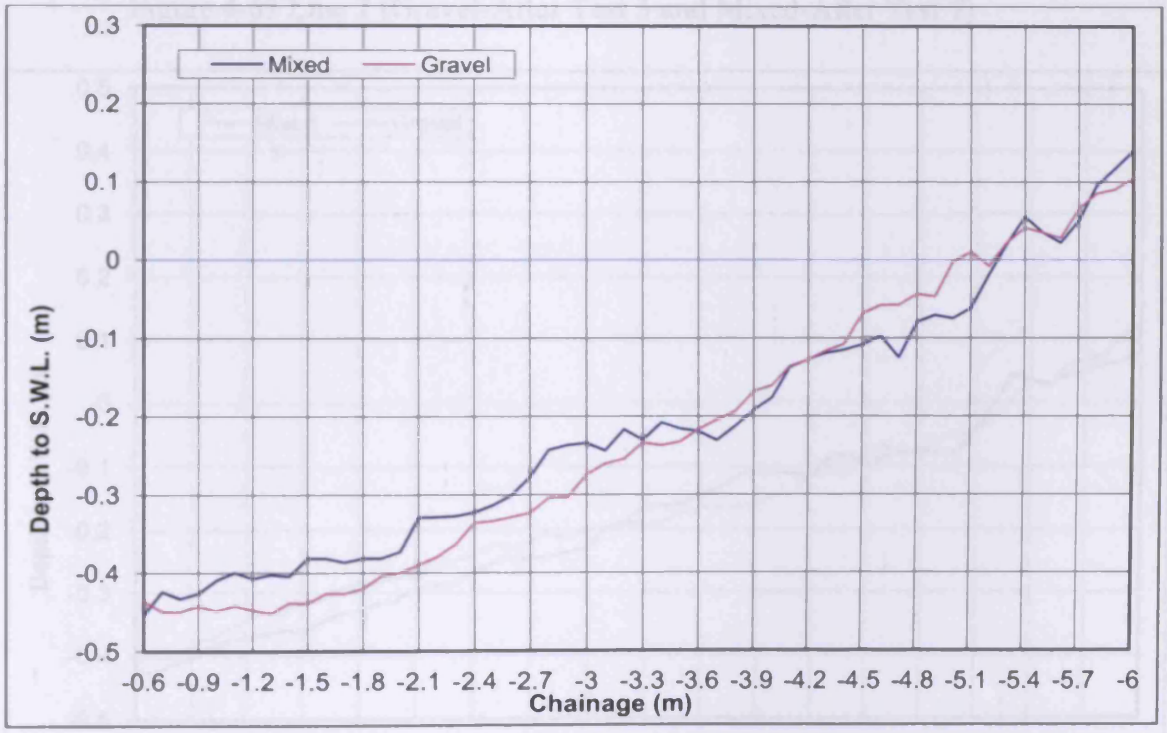

Figure 4-62 Line 1 (Gravel-After Test 3 and Mixed-After Test 7)

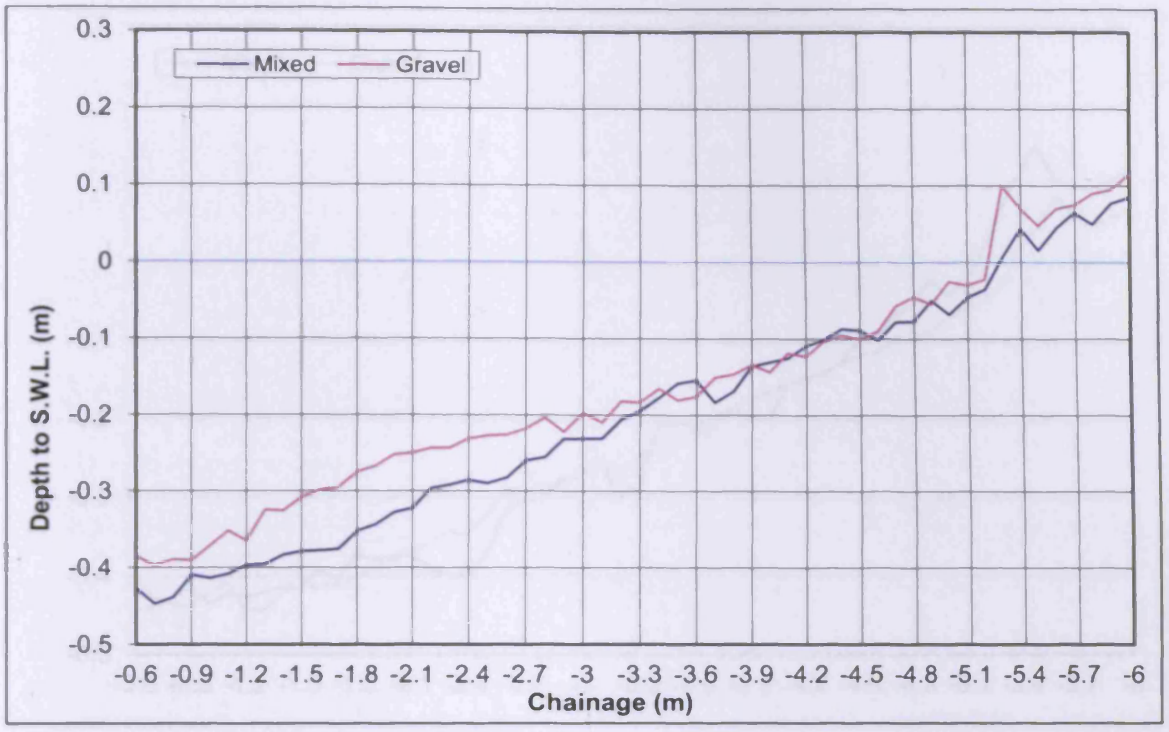

Figure 4-63 Line 2 (Gravel-After Test 3 and Mixed-After Test 7)

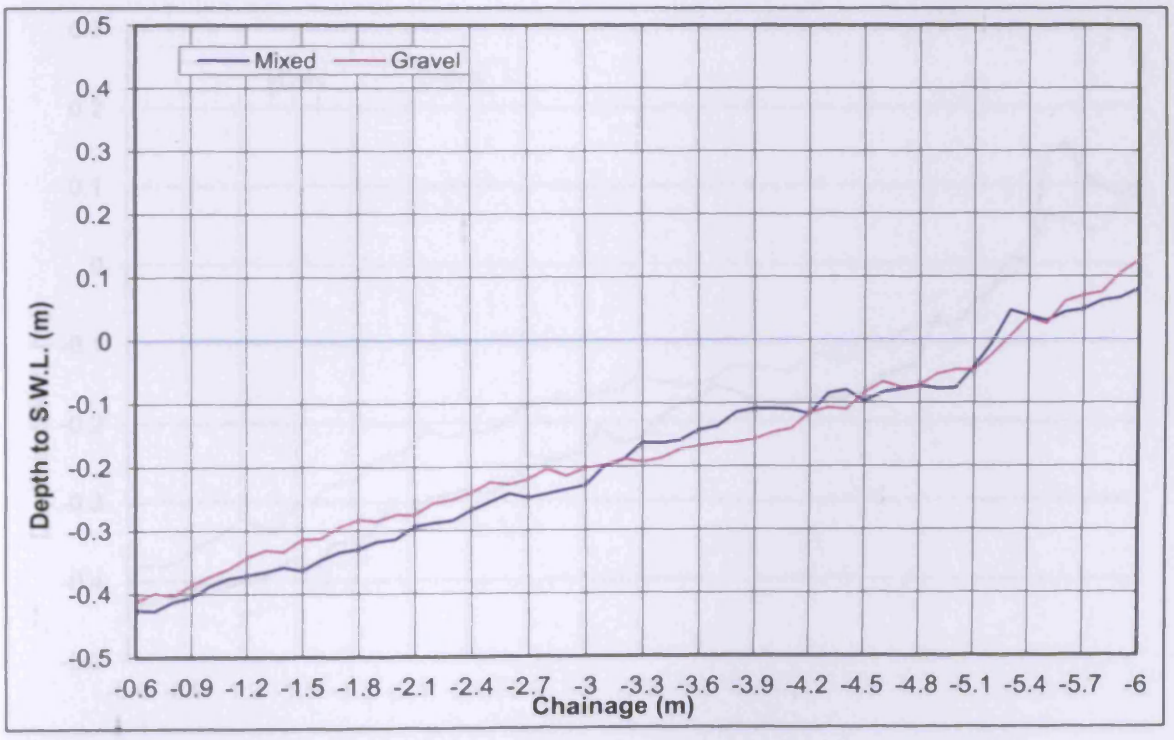

Figure 4-64 Line 3 (Gravel- After Test 3 and Mixed- After Test 7)

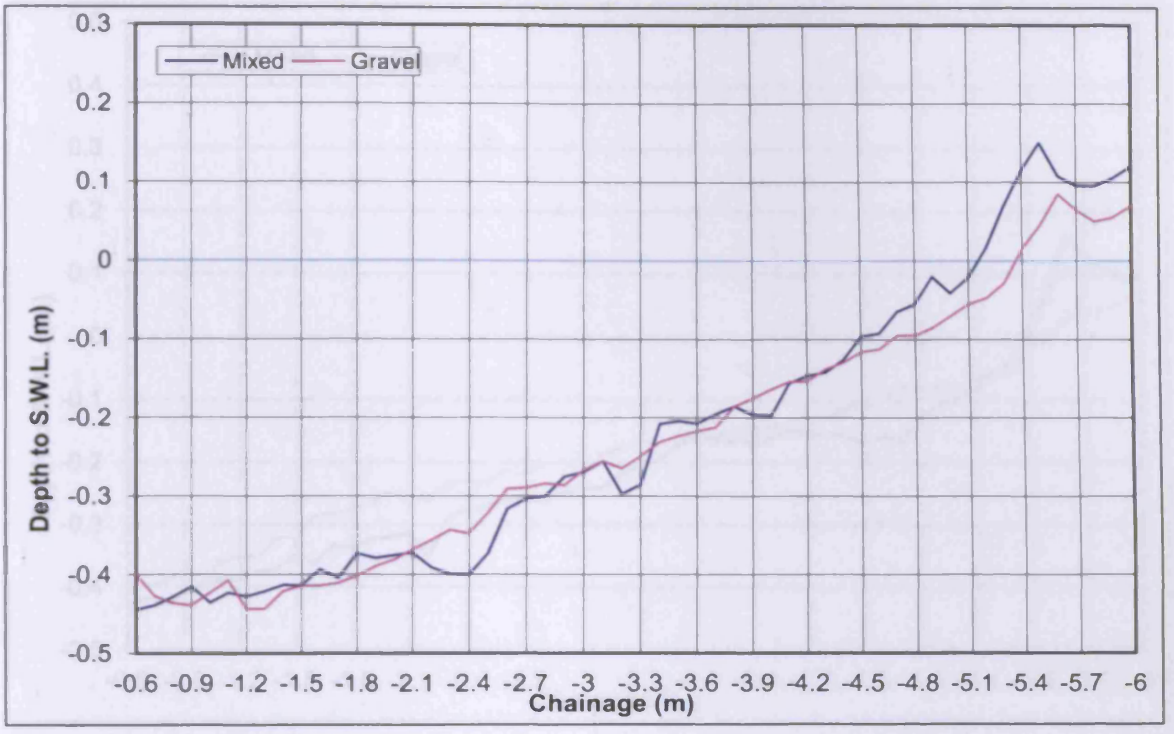

Figure 4-65 Line 1 (Gravel-After Test 5 and Mixed-After Test 9)

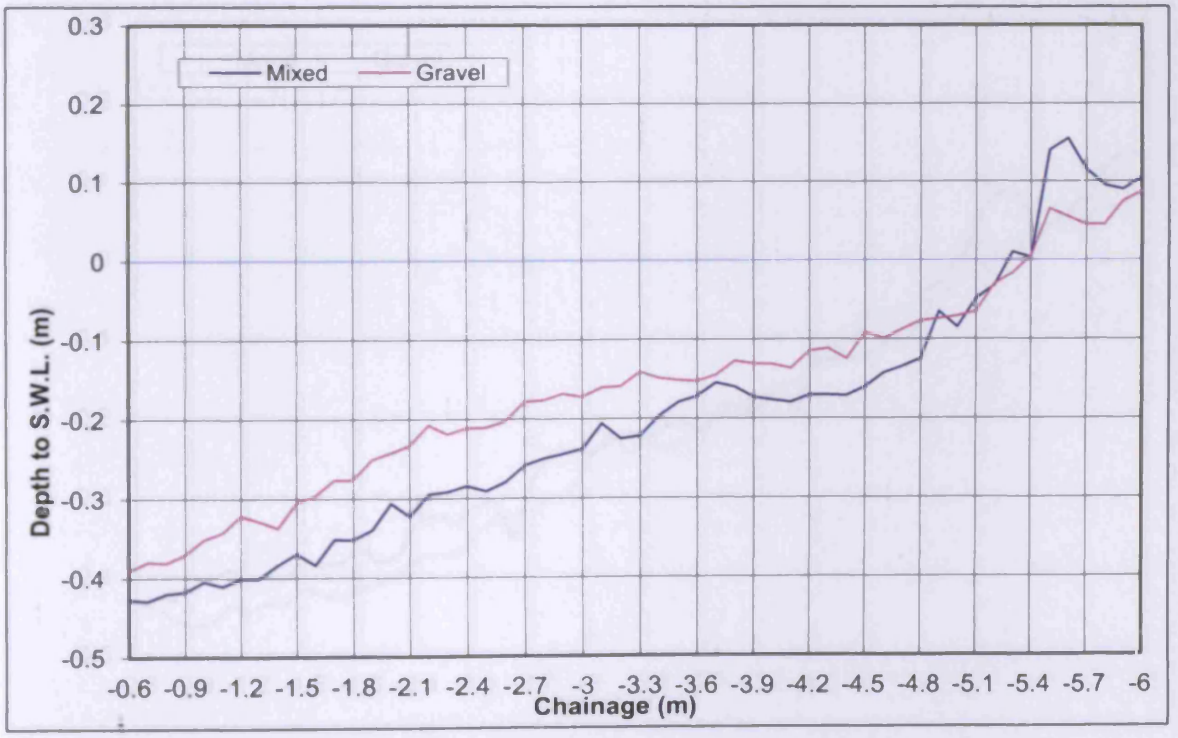

Figure 4-66 Line 2 (Gravel-After Test 5 and Mixed-After Test 9)

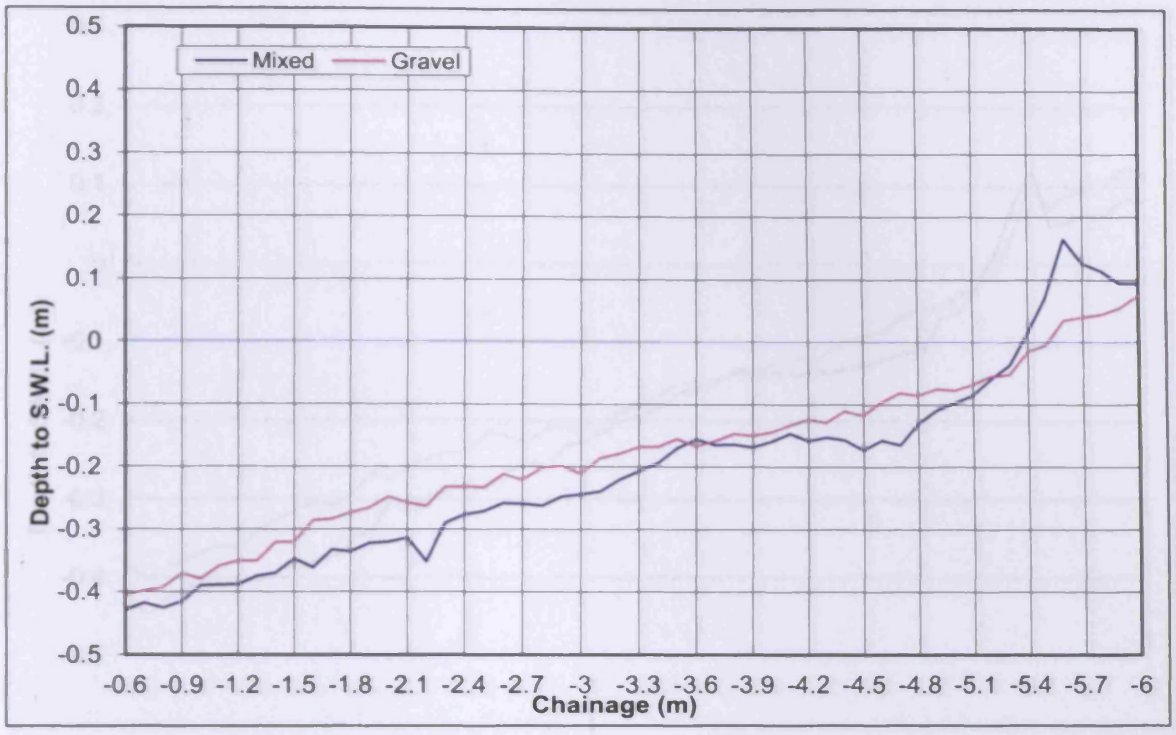

Figure 4-67 Line 3 (Gravel-After Test 5 and Mixed-After Test 9)

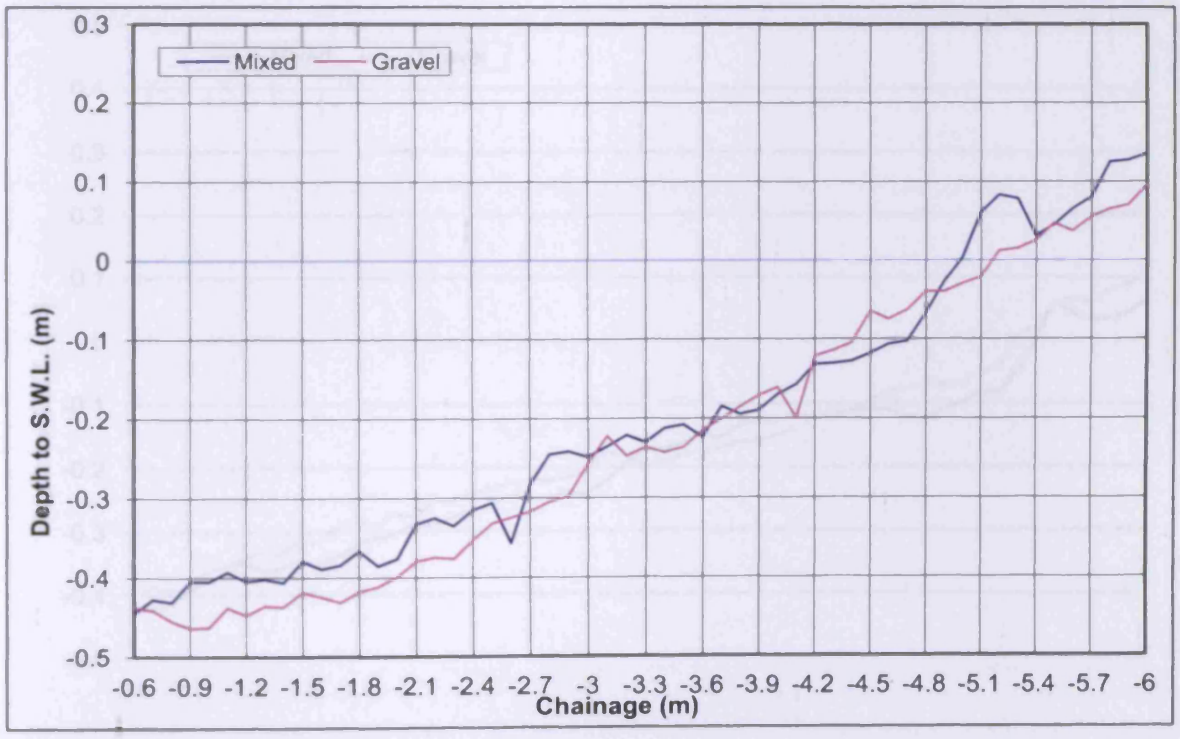

Figure 4-68 Line 1 (Gravel- After Test 4 and Mixed- After Test 8)

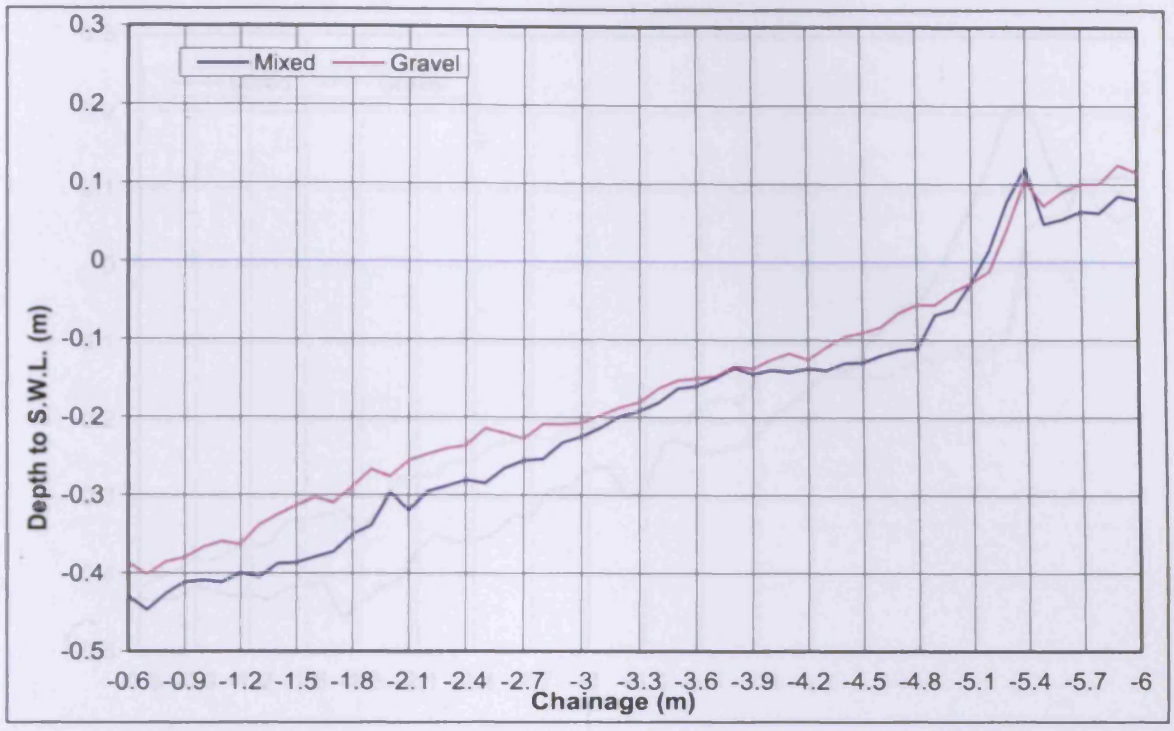

Figure 4-69 Line 2 (Gravel- After Test 4 and Mixed- After Test 8)

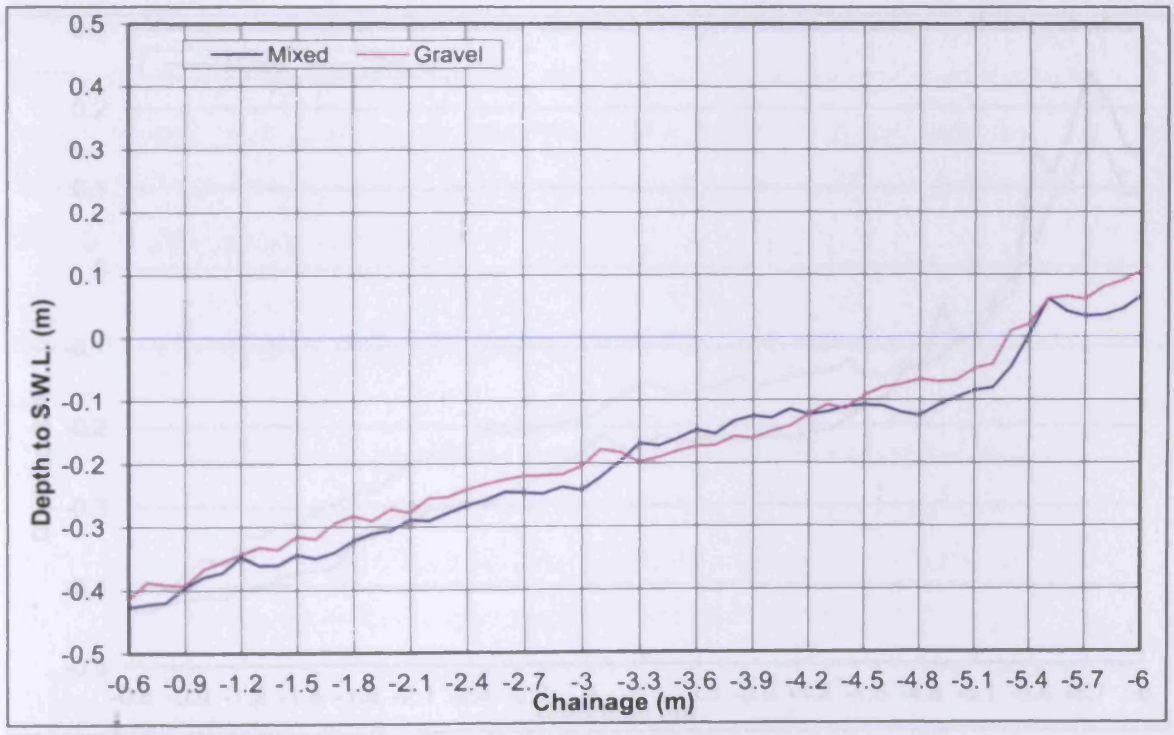

Figure 4-70 Line 3 (Gravel- After Test 4 and Mixed- After Test 8)

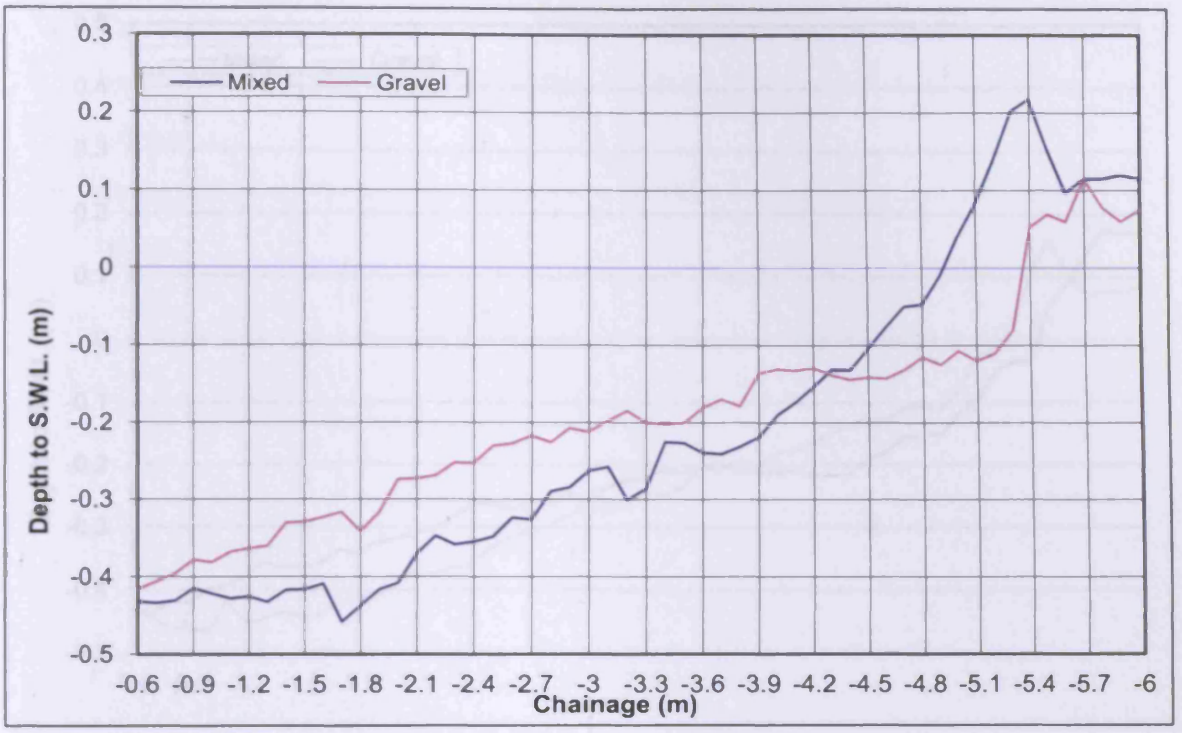

Figure 4-71 Line 1 (Gravel- After Test 6 and Mixed- After Test 10)

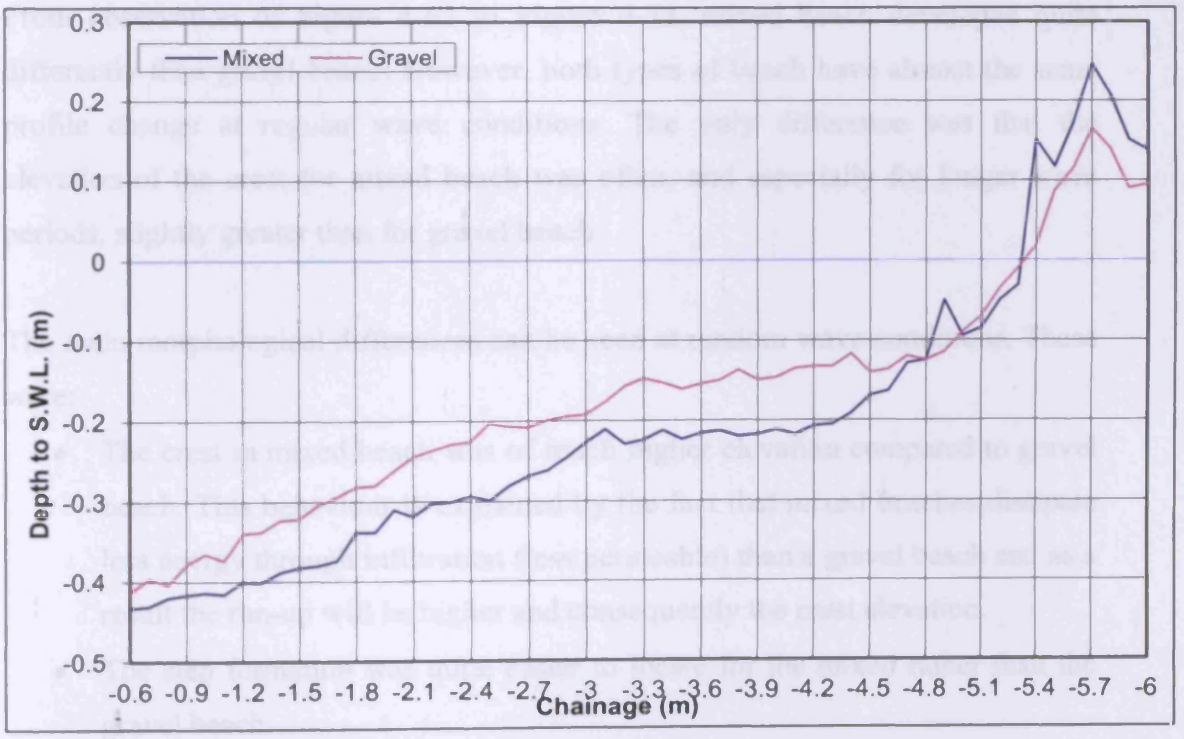

Figure 4-72 Line 2 (Gravel- After Test 6 and Mixed- After Test 10)

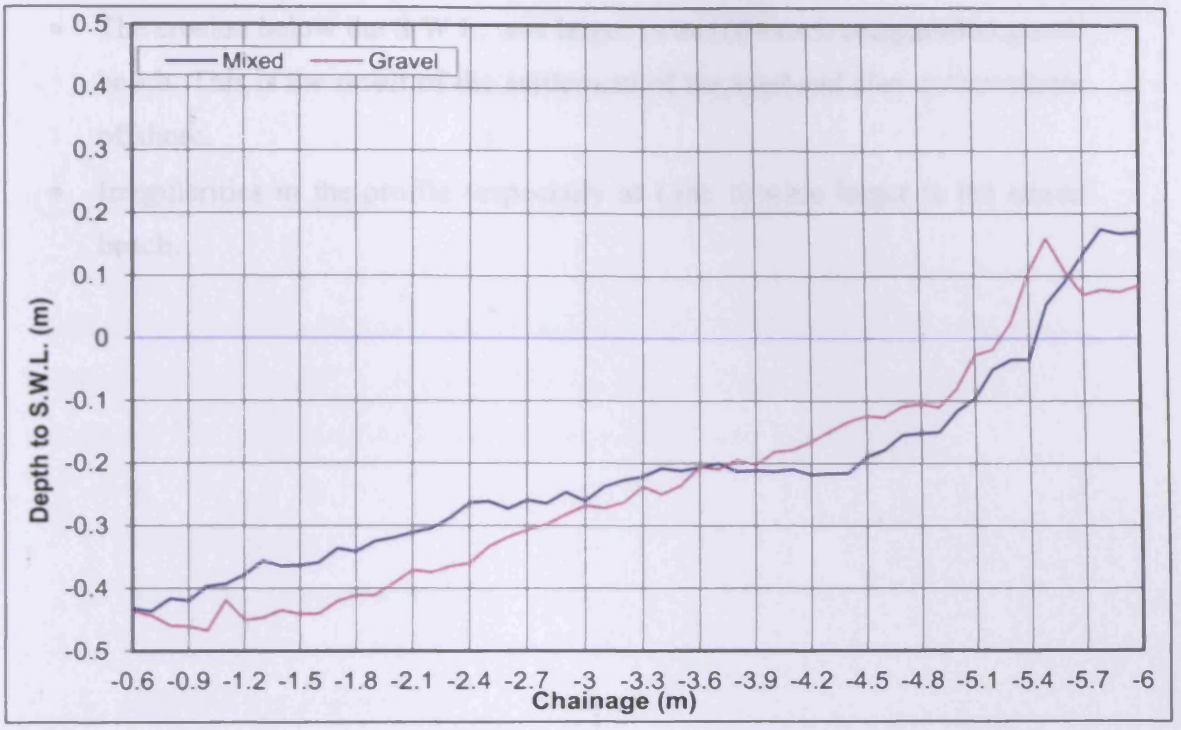

Figure 4-73 Line 3 (Gravel- After Test 6 and Mixed- After Test 10)

From observation of Figure 4-62 to Figure 4-73, mixed beach developed quite differently than gravel beach. However, both types of beach have almost the same profile change at regular wave conditions. The only difference was that the elevation of the crest for mixed beach was often, and especially for longer wave periods, slightly greater than for gravel beach.

The main morphological differences can be seen at random wave conditions. These were:

- The crest in mixed beach was of much higher elevation compared to gravel beach. This behaviour is explained by the fact that mixed beaches dissipate less energy through infiltration (less permeable) than a gravel beach and as a result the run-up will be higher and consequently the crest elevation.
- The step formation was quite easier to locate for the mixed rather than the gravel beach.

- The erosion below the S.W.L. was larger in mixed beach compared to gravel beach. This is the result of the settlement of the sand and also its movement offshore.
- Irregularities in the profile (especially at Line 1) were larger in the mixed beach.

CHAPTER 5

ANALYSIS OF THE EXPERIMENTAL RESULTS

5.0 INTRODUCTION

In this Chapter, the results of the experiment will be analysed and compared with existing methods. A modification of the existing methods will also be attempted. The main categories that will be analysed are listed below:

1. Wave breaking
2. Wave-induced currents
3. Profile response
4. Step and Berm elevation
5. Sediment balance

5.1 WAVE BREAKING

Wave breaking is the dominant process in the dynamics of nearshore water movements resulting in sediment transport. Wave breaking can be defined as the transformation of particle motion from irrotational to rotational generating vorticity and turbulence. The location in space where some part of the front face of the wave first becomes vertical or overturns, or both, is herein defined as the wave breaking point. Moreover, the breaking point can be referred, for waves shoaling up a beach, as the location where the maximum wave height is achieved.

Wave breaking depends on the nature of the bottom slope and the characteristics of the wave. Waves break as they reach a limiting steepness which is a function of the relative depth (d/L) and the beach slope ($\tan\beta$). Wave breaking may be classified in four types (Galvin 1968): as spilling, plunging, collapsing, and

surging. Breaker type may be identified according to the surf similarity parameter (Iribarren number) ξ_0, defined as

Eq.5-1 $$\xi_0 = \frac{\tan\beta}{\sqrt{\frac{H_0}{L_0}}}$$

where the subscript 0 denotes the deepwater condition (Galvin 1968, Battjes 1974).

On a uniformly sloping beach, breaker type is estimated by

Surging/collapsing $\xi_0 > 3.3$

Plunging $0.5 < \xi_0 < 3.3$ and,

Spilling $\xi_0 < 0.5$

As it is shown further, the breaker type of the waves generated at the experiments in Hannover was plunging. Plunging breakers occurs on steeper beaches and are classically characterized by a large-scale, visible, curling over of the wave with an inner air core and falling jet impacting on the preceding trough. A sudden, violent transition from irrotational to rotational motion results over the entire water column. An identifiable time and distance are required for the wave to curl over before reaching the initial jet impact point or plunge point (Basco, 1985).

Furthermore, the depth (d_B) and the height (H_B) of breaking waves are important factors. The term "breaker index" is used to describe non-dimensional breaker height. The four common indices are in the form of H_b/d_b, H_b/H_0, H_b/L_b and H_b/L_0 (where the subscript b denotes the breaking condition). The first two indices are the breaker depth index (γ) and the breaker height index (Ω_b), respectively.

Rattanapitikon and Shibayama (2000) examined the applicability of 24 existing formulas, for computing breaking wave height of regular wave, by wide range and large amount of published laboratory data (574 cases collected from 24 sources). They found that the formula of Komar and Gaughan (1973) gives the

best prediction, among 24 existing formulas, over a wide range of experiments. Komar and Gaughan (1973) used linear wave theory to derive the breaker height formula from energy flux conservation and assumed a constant H_b/d_b. After calibrating the formula to the laboratory data of Iversen (1952), Galvin (1969), unpublished data of Komar and Simons (1968), and the field data of Munk (1949), the formula proposed was

Eq.5-2 $$H_b = 0.56 H_o \left(\frac{H_o'}{L_o}\right)^{-\frac{1}{5}} \text{ or } \Omega_b = 0.56 \left(\frac{H_o'}{L_o}\right)^{-\frac{1}{5}}$$

where H_o' is the equivalent unrefracted deepwater wave height.

Rattanapitikon and Shibayama (2000) showed that the ER (root mean square relative error) of most formulae varies with the bottom slope, and it was expected that incorporating the new form of bottom slope effect into the formulas could improve the accuracy of the formulae. They therefore modified the three most accurate prediction formulae, concluding that the modified formula of Goda (1970) gives the best prediction for the general case (ER=10.7%).

The formula of Goda (1970) was modified to be

Eq.5-3 $$H_b = 0.17 L_0 \left\{1 - \exp\left[\frac{\pi d_b}{L_o}(16.21(\tan\beta)^2 - 7.07\tan\beta - 1.55)\right]\right\}$$

The breaking depth, and consequently the breaking point, is also determined by using the Eq.5-3 together with the linear wave theory. It is necessary that the breaking point is predicted accurately, in order for an accurate computation of the wave field or other wave-induced phenomena (e.g., undertow, sediment transport and beach deformation) to be concluded.

It is well known that the wave height, just before the breaking point, is underestimated by linear wave theory. Consequently, the predicted breaking point will shift on shoreward of the real one when the breaker height formula is used together with the linear wave shoaling (Isobe, 1987). As a result, the computation of wave height transformation will not be predicted accurately.

Two methods are known for dealing with the problem of underestimating the linear wave theory. The first method computes wave shoaling by using nonlinear wave theories (e.g. Stoke, 1847; Dean, 1965; Shuto, 1974; and Isobe, 1985) and the second method by using linear wave theory. The second method also uses other variables, rather than breaker height, to compute the breaking point (e.g. Watanabe et al., 1984; Isobe, 1987; Rattanapitikon, 1995 and Rattanapitikon and Shibayama, 2006).

Rattanapitikon and Shibayama (2006), by following the second method, undertook a study to find out the suitable breaking wave formulas for computing breaker depth, and corresponding assumed orbital to phase velocity ratio and breaker height converted with linear wave theory. A total of 695 cases collected from 26 sources of published laboratory data were used. All data referred to experiments that were performed on regular waves. The formulae of Rattanapitikon and Shibayama (2006) gave satisfactory predictions over a wide range of experimental conditions. Their formulae for breaking depth and breaking wave height were:

Eq.5-4a $$h_b = (3.86m^2 - 1.98m + 0.88)H_0\left(\frac{H_0}{L_0}\right)^{-0.16} \text{ for } \frac{H_0}{L_0} \leq 0.1$$

Eq.5-4b $$h_b = (3.86m^2 - 1.98m + 0.88)H_0\left(\frac{H_0}{L_0}\right)^{-0.34} \text{ for } \frac{H_0}{L_0} > 0.1$$

and

Eq.5-5 $$H_b = (-0.57m^2 + 0.31m + 0.58)L_0\left(\frac{H_0}{L_0}\right)^{0.83}$$

where m is the bed slope.

Random waves consist of incoming waves which have different wave height and they break in different water depths. Therefore, the wave breaking takes place in a relatively wide zone (surf zone) of variable water depth. Goda's breaking method (Goda, 1985) is the most widely applied method for estimating significant wave heights ($H_{1/3}$) within the surf zone. Goda (1970) proposed a diagram, presenting criterion for predicting breaking wave height, based on the analysis of several sets of laboratory data of breaking waves on slopes obtained

by several researchers (Iversen, 1952; Mitsuyasu, 1962; and Goda, 1964). Goda gave an approximate expression of the diagram as

Eq.5-6 $$H_b = AL_0\left\{1 - \exp\left[-1.5\frac{\pi d_b}{L_o}\left(1 + 15(\tan\beta)^{\frac{4}{3}}\right)\right]\right\}$$

where A= a coefficient (=0.12)

The breaking point is defined as the maximum wave height admissible for a given water depth (Torrini and Allsop, 1999).

5.1.1 Calculation of the long-shore velocity at the breaking point (v_b)

The breaking of obliquely waves generates currents which usually dominate in and near the surf zone on open coasts. These wave driven currents have long-shore and cross-shore components. In this section, the long-shore velocity (v_b) at the breaking point has been calculated in order to be compared with the results of the experimental tests for both gravel and mixed beaches.

For the theoretical approximation of the v_b the wave refraction and shoaling were included. Moreover, the seabed contours were assumed to be straight and parallel for both trench and beach with uniform slope. Despite the fact that trench usually does not have straight and parallel contour, this assumption was adopted through the whole thesis. Moreover, approaches and equations that derived for planar beach, in their original form, were applied also at the trench. However, these approaches and equations, used for trench, were modified in order the effect of the complex sea bed contour to be reduced as more as possible.

5.1.1.1 *Regular Waves*

The following procedure relates to the estimation of breaking wave height and depth and is applied to regular waves. The deep water wavelength and celerity are calculated by:

Eq.5-7 $$L_0 = \frac{C_0}{T}$$

Eq.5-8 $$C_0 = \frac{gT}{2\pi}$$

the water wavelength by,

Eq.5-9 $$L = \frac{gT^2}{2\pi}\tanh\left(\frac{2\pi d}{L}\right)$$

The shoaling coefficient K_S and refraction coefficient K_R can be estimated from,

Eq.5-10 $$K_S = \left(\frac{C_0}{C\left[\frac{2kd}{\sinh 2kd}\right]}\right)^{\frac{1}{2}}$$

and

Eq.5-11 $$K_R = \left(\frac{\cos\theta_0}{\cos\theta}\right)^{\frac{1}{2}}$$

where θ_0 is the deepwater wave angle, where the wave number k is equal to $2\pi/L$.

Assuming that a refraction analysis gives a refraction coefficient K_R at the point where breaking is expected to occur, and that the equivalent unrefracted deepwater wave height can be found from the refraction coefficient

Eq.5-12 $H_o' = K_R H_0$, consequently $H = H_o' K_S$

Then by estimating the breaking wave height, the breaking depth can be calculated by corresponding equation.

The initial value selected for the refraction coefficient would be checked to determine if it is correct for the actual breaker location. If necessary, a corrected refraction coefficient should be used to recompute the breaking wave height and depth.

Longuet-Higgins (1970) formed an expression for the mean longshore velocity ($\bar{v}_l$) at the breaker zone, of a planar beach, which was modified by Komar (1976) and took the form of:

Eq.5-13 $$\bar{v}_l = 2.7 u_b \sin\theta_b \cos\theta_b$$

where θ_b= the wave angle at the breaking point

u_b= the wave orbital velocity under the wave breaking point, which is calculated by

Eq.5-14 $$u_b = \frac{\gamma}{2}\sqrt{g d_B}$$

where γ= breaking depth index (H_b/d_b)

Longuet-Higgins (1972) stated that the longshore velocity at the breaking point (v_B) is usually about $0.2\overline{v_l}$. Therefore, knowing the breaking depth and height, the longshore velocity at the breaking point can be estimated by

Eq.5-15 $$v_B = 0.54\frac{\gamma}{2}\sqrt{gd_B}\sin\theta_b\cos\theta_b$$

Moreover for a plane beach where d = xtanβ (tanβ is the beach slope), the distance to the breaker line from shore is

Eq.5-16 $$x_B = \frac{d_B}{\tan\beta}$$

Using the above equations, v_B was calculated for all the tests with regular waves. The slope between Lines 2 and 3 was approximately the same. Test 2 wasn't taken into consideration for the calculations due to the fact that the slope changed significantly after test 1. However, Eq.5-14 was not based on a wave breaking equation that includes the influence of the slope. Therefore, the three lines will be considered as one. The wave conditions for both gravel and mixed beaches were not exactly the same (except the Tests with wave height H=0.086m). Consequently, the longshore velocity at the breaking point would be similar for both types of beach, only in Tests 3 and 7. The results of the calculations are shown in Table 5-1 below.

Table 5-1 The results of the calculations of v_B for the tests with regular waves

H (m)	T (sec)	θ (°)	d_B (m)	v_B (cm/s)
0.253 (G)	2.016	15	0.326	5.20
0.086 (G)	2.016	15	0.132	2.19
0.092 (G)	3.009	15	0.161	1.81
0.086 (M)	2.015	15	0.131	2.18
0.077 (M)	3.005	15	0.139	1.57

It has to be mentioned that the equation of Longuet-Higgins (1972) did not take into consideration the spatial and temporal variability. The beach profile of each line has been changed through time. There was a longshore sediment transport that made that change. Therefore, the break point of each line changed and consequently v_B changed. However, for the purpose of the comparison and the analysis of the equation of Longuet-Higgins (1972), it was assumed that there were not any spatial and temporal variability.

Results from the calculation of the longshore velocity at the breaking point (Table 5- 1) show that all the breaking waves were plunging (Table 5-4). Moreover, as it was expected, the waves with less wave height (H=0.086m) broke further onshore and with less v_b than the waves with same wave period but greater wave height (H=0.253m).

In order to compare the estimated values of v_B with the measured v_B from experimental results (for both types of beach), the data have been tabulated and presented in the following Tables (Table 5-2 and Table 5-3). It has to be mentioned that when the column of measured v_b had negative values, it meant that the longshore current velocity was in opposite direction with the incoming wave direction and where the column has no number, it meant that there were no measurements (or measurements with less than 70% correlation) at that point.

Table 5-2 The measured and estimated v_B at the tests with gravel beach

H (m)	T (sec)	d_B (m)	v_B (cm/s) estimated	v_B (cm/s) measured
0.253 (L1)	2.016	0.326	5.20	2.36
0.253 (L2)	2.016	0.326	5.20	-4.85
0.253 (L3)	2.016	0.326	5.20	-6.52
0.086 (L1)	2.016	0.132	2.19	2.51
0.086 (L2)	2.016	0.132	2.19	7.45
0.086 (L3)	2.016	0.132	2.19	12.65
0.092 (L1)	3.009	0.161	1.81	-2.41
0.092 (L2)	3.009	0.161	1.81	0.26
0.092 (L3)	3.009	0.161	1.81	-

Table 5-3 The measured and estimated v_B at the tests for the mixed beach

H (m)	T (sec)	d_B (m)	v_B (cm/s) estimated	v_B (cm/s) measured
0.086 (L1)	2.015	0.131	2.18	-
0.086 (L2)	2.015	0.131	2.18	9.19
0.086 (L3)	2.015	0.131	2.18	-
0.077 (L1)	3.005	0.139	1.57	-
0.077 (L2)	3.005	0.139	1.57	-
0.077 (L3)	3.005	0.139	1.57	10.13

The breaking longshore velocity has been chosen based on the value of the estimated breaking depth. It must be mentioned that the accuracy of the measurements of the ADV is ±0.5%.

Looking at Table 5-2 and Table 5-3, overall, the estimated v_B from Longuet-Higgins (1972) equation did not predict accurate results. Generally, it underestimated the measured v_B. At some tests/lines the estimated v_B was 9 times greater than the measured v_B and at some others it was 7 times smaller. The estimated v_B was similar to the measured v_B, only in Tests 1, 3 and 4 (especially for Line 1). At these tests, the magnitude of the v_B was similar but not its direction. At the tests related to the mixed beach, there were only few available locations to compare with. Based on the theory that the longshore velocity at the breaking point would be the same for both types of beach, if both types of beach have the same wave conditions, the measured longshore velocity at the breaking point for Line 3 gave similar values for both types of beach for Tests 3 and 7. However, based on the assumption that the estimated breaking depth was accurate, it can be seen that the measured longshore "breaking" velocity had different values for all three lines.

This might have happened due to the fact that the estimated v_B of Longuet-Higgins (1972) was based on a wave breaking equation that did not take into consideration the influence of the bottom slope (H_d=0.78d_b). Therefore, in order

to include the influence of the bottom slope, the estimated breaking depth of Eq.5-3 were used into Eq.5-11. The longshore "breaking" velocities of Lines 2 and 3 were calculated as one due to the fact that the bottom slopes of both lines were approximately the same.

At the trench (Line 1), the calculation of the breaking depth, and consequently of v_B, based on different bottom slope from the other two Lines (Line 2 and Line 3). Furthermore, Line 1 had two bottom slopes where x=-1.6m was the point where the two slopes changed. The first slope was nearly horizontal. Based on the wave conditions in the tests, the first slope wouldn't affect the breaking depth and breaking height. Therefore, the second bottom slope has been used for the calculation of d_B. As previously, Test 2 wasn't considered in the calculations due to the fact that the bottom slope changed significantly after Test 1. The results of the calculations for Lines 2 and 3 are shown in Table 5-4 below.

Table 5-4 The results of the calculations of v_B for the tests with regular waves (Line 2 and Line 3)

H (m)	T (sec)	θ (°)	ξ	d_B (m)	v_B (cm/s)
0.253 (G)	2.016	15	0.55 (plunging breaker)	0.266	5.45
0.086 (G)	2.016	15	0.77 (plunging breaker)	0.104	2.31
0.092 (G)	3.009	15	1.11 (plunging breaker)	0.125	1.93
0.086 (M)	2.015	15	0.85 (plunging breaker)	0.102	2.32
0.077 (M)	3.005	15	1.22 (plunging breaker)	0.108	1.67

In order to compare the estimated values of v_B with the measured v_B from experimental results (for both types of beach), the data have been tabulated and presented at the following Tables.

Table 5-5 The measured v_B at the tests with gravel beach (Line 2 and Line 3)

H (m)	T (sec)	d_B (m)	v_B (cm/s) estimated	v_B (cm/s) measured
0.253 (L2)	2.016	0.266	5.45	-
0.253 (L3)	2.016	0.266	5.45	-3.54
0.086 (L2)	2.016	0.104	2.31	-
0.086 (L3)	2.016	0.104	2.31	-
0.092 (L2)	3.009	0.125	1.93	6.31
0.092 (L3)	3.009	0.125	1.93	-

Table 5-6 The measured v_B at the tests with mixed beach (Line 2 and Line 3)

H (m)	T (sec)	d_B (m)	v_B (cm/s) estimated	v_B (cm/s) measured
0.086 (L2)	2.015	0.102	2.32	-
0.086 (L3)	2.015	0.102	2.32	-
0.077 (L2)	3.005	0.108	1.67	-
0.077 (L3)	3.005	0.108	1.67	-

The results of the calculations for Line 1 are shown in Table 5-7.

Table 5-7 The results for the calculations of v_B for the tests with regular waves (Line 1)

H (m)	T (sec)	θ (°)	ξ	d_B (m)	v_B (cm/s)
0.253 (G)	2.016	15	0.65 (plunging breaker)	0.259	5.48
0.086 (G)	2.016	15	1.02 (plunging breaker)	0.100	2.34
0.092 (G)	3.009	15	1.48 (plunging breaker)	0.120	1.95
0.086 (M)	2.015	15	0.85 (plunging breaker)	0.102	2.32
0.077 (M)	3.005	15	1.35 (plunging breaker)	0.106	1.68

In order to compare the estimated values of v_B with the measured v_B from experimental results (for both types of beach), the data have been tabulated and presented at the following Tables.

Table 5-8 The measured v_B at the tests with gravel beach (Line 1)

H (m)	T (sec)	d_B (m)	v_B (cm/s) estimated	v_B (cm/s) measured
0.253 (L1)	2.016	0.259	5.48	-
0.086 (L1)	2.016	0.100	2.34	-
0.092 (L1)	3.009	0.120	1.95	-

Table 5-9 The measured v_B at the tests with mixed beach (Line 1)

H (m)	T (sec)	d_B (m)	v_B (cm/s) estimated	v_B (cm/s) measured
0.086 (L1)	2.015	0.102	2.32	-
0.077 (L1)	3.005	0.106	1.68	-

Despite the fact that the new estimated v_B had few available locations to compare with, especially for tests with mixed beach where there were not any measurements at these breaking depths for both trench and uniform slope, it gave slightly better results than the previous estimated v_B of Longuet-Higgins equation. There were not any available measurements for trench for both types of beach. In general, the estimated value of v_B was still not close enough to the measured v_B.

Rattanapitikon and Shibayama (2006) undertook a study to find out the suitable breaking wave formulas for computing breaker depth, and corresponding orbital to phase velocity ratio and breaker height converted with linear wave theory. A total of 695 cases collected from 26 sources of published laboratory data were used.

With regard to assumed orbital to phase velocity, only the formula of Isobe (1987) was available. Rattanapitikon and Shibayama (2006) developed a new formula by reanalysis of the Isobe's (1987) formula. The new formula gave excellent predictions for all conditions (ER_{avg}=3%). The assumed orbital velocity ($\widehat{u_b}$) formula of Rattanapitikon and Shibayama (2006) was written as:

Eq.5-17 $$\widehat{u_b} = \frac{(-0.57m^2+0.31m+0.58)\pi c_b}{\tanh^2(k_b h_b)}\left(\frac{H_0}{L_0}\right)^{0.83}$$

where,

c_b is the phase velocity at the breaking point, k_b is the wave number at the breaking point, m is the bottom slope and h_b is the breaker depth (Eq.5-4). Eq.5-14 was substituted by Eq.5-17 in the Longuet-Higgins's (1972) equation. The new equation has the form of:

Eq.5-18 $$\overline{v_l} = 2.7\widehat{u_b}\sin\theta_b\cos\theta_b$$

and consequently,

Eq.5-19 $$v_B = 0.54\widehat{u_b}\sin\theta_b\cos\theta_b$$

The results of the calculations, by using Eq.5-17 and Eq.5-19, for Lines 2 and 3 are shown in Table 5-10 below.

Table 5-10 The results for the calculations of v_B for the tests with regular waves (Line 2 and Line 3)

H (m)	T (sec)	θ (°)	ξ	d_B (m)	$\widehat{u_b}$ (m/s)	v_B (cm/s)
0.253 (G)	2.016	15	0.55 (plunging breaker)	0.301	0.841	6.04
0.086 (G)	2.016	15	0.77 (plunging breaker)	0.126	0.497	2.39
0.092 (G)	3.009	15	1.11 (plunging breaker)	0.151	0.539	1.92
0.086 (M)	2.015	15	0.85 (plunging breaker)	0.123	0.502	2.39
0.077 (M)	3.005	15	1.22 (plunging breaker)	0.130	0.498	1.65

In order to compare the estimated values of v_B with the measured v_B from experimental results (for both types of beach), the data have been tabulated and presented in the following Tables.

Table 5-11 The measured v_B at the tests with gravel beach (Line 2 and Line 3)

H (m)	T (sec)	d_B (m)	v_B (cm/s) estimated	v_B (cm/s) measured
0.253 (L2)	2.016	0.300	6.04	1.25
0.253 (L3)	2.016	0.300	6.04	-6.29
0.086 (L2)	2.016	0.125	2.39	4.31
0.086 (L3)	2.016	0.125	2.39	12.65
0.092 (L2)	3.009	0.151	1.92	0.59
0.092 (L3)	3.009	0.151	1.92	-

Table 5-12 The measured v_B at the tests with mixed beach (Line 2 and Line 3)

H (m)	T (sec)	d_B (m)	v_B (cm/s) estimated	v_B (cm/s) measured
0.086 (L2)	2.015	0.123	2.39	-
0.086 (L3)	2.015	0.123	2.39	11.86
0.077 (L2)	3.005	0.130	1.65	-
0.077 (L3)	3.005	0.130	1.65	-

The results of the calculations, by using equations Eq.5-18 and Eq.5-19, for Line 1 are shown in Table 5-13 below.

Table 5-13 The results for the calculations of v_B for the tests with regular waves (Line 1)

H (m)	T (sec)	θ (°)	ξ	d_B (m)	$\hat{u}_b$ (m/s)	v_B (cm/s)
0.253 (G)	2.016	15	0.65 (plunging breaker)	0.292	0.856	6.07
0.086 (G)	2.016	15	1.02 (plunging breaker)	0.120	0.513	2.41
0.092 (G)	3.009	15	1.48 (plunging breaker)	0.144	0.557	1.94
0.086 (M)	2.015	15	0.85 (plunging breaker)	0.123	0.502	2.39
0.077 (M)	3.005	15	1.35 (plunging breaker)	0.127	0.504	1.66

In order to compare the estimated values of v_B with the measured v_B from experimental results (for both types of beach), the data have been tabulated and presented at the following Tables.

Table 5-14 The measured v_B at the tests with gravel beach (Line 1)

H (m)	T (sec)	d_B (m)	v_B (cm/s) estimated	v_B (cm/s) measured
0.253 (L1)	2.016	0.291	6.07	7.95
0.086 (L1)	2.016	0.119	2.41	-1.86
0.092 (L1)	3.009	0.144	1.94	-

Table 5-15 The measured v_B at the tests with mixed beach (Line 1)

H (m)	T (sec)	d_B (m)	v_B (cm/s) estimated	v_B (cm/s) measured
0.086 (L1)	2.015	0.123	2.39	-
0.077 (L1)	3.005	0.128	1.66	-

The values of estimated v_B were close to the values of measured v_B for Line 1 (for both types of beach) and for Line 3 (for gravel beach). It estimated quite accurately the magnitude of the v_B for few tests. However, it also underestimated, as in the previous approaches, the value of v_B in some occasions. Overall, Eq.5-19 gave much more accurate results than the previous equations.

Based on the present experimental results and results of Eq.5-19, five equations are proposed for estimation of the mean longshore velocity at the breaking point. A linear regression has been fitted to the data and the proposed fits are given by the following equations:

For gravel beach-trench,

Eq.5- 20a $v_B = 0.554\widehat{u_b}\sin\theta_b\cos\theta_b$ (R^2=0.548)

For mixed beach-uniform slope

Eq.5- 20b $v_B = 2.68\widehat{u_b}\sin\theta_b\cos\theta_b$ (R^2=1)

The range of applicability of Eq.5- 20a and Eq.5- 20b is the test series of the experiment for regular waves (for both gravel and mixed beach). The two equations should be quite reliable when used within the limits of applicability.

5.1.1.2 *Random Waves*

The procedure of estimating the breaking wave height and depth for random waves is described in Appendix III (A1). In this section, Eq.5-19 was used to estimate the mean long-shore current at the breaking point as it was the most accurate equation for regular waves. However, the breaking depth will not be calculated by Eq.5-4 but with Eq.5-6.

The results of the calculations, by using Eq.5-19 with Eq.5-6, for Lines 2 and 3 are shown in Table 5-16 below.

Table 5-16 The results for the calculations of v_B for the tests with random waves (Line 2 and Line 3)

H (m)	T_s (sec)	θ (°)	ξ	d_B (m)	$\hat{u}_b$ (m/s)	v_B (cm/s)
0.108 (G)	2.264	15	0.77 (plunging breaker)	0.183	0.696	3.72
0.110 (G)	3.244	15	1.10 (plunging breaker)	0.222	0.852	3.53
0.110 (M)	2.278	15	0.86 (plunging breaker)	0.179	0.724	3.81
0.117 (M)	3.053	15	1.45 (plunging breaker)	0.200	0.964	4.03

In order to compare the estimated values of v_B with the measured v_B from experimental results (for both types of beach), the data have been tabulated and presented at the following Tables.

Table 5-17 The measured v_B at the tests with gravel beach (Line 2 and Line 3)

H (m)	T_s (sec)	d_B (m)	v_B (cm/s) estimated	v_B (cm/s) measured
0.108 (L2)	2.264	0.183	3.72	3.63
0.108 (L3)	2.264	0.183	3.72	2.04
0.110 (L2)	3.244	0.222	3.53	3.03
0.110 (L3)	3.244	0.222	3.53	3.05

Table 5-18 The measured v_B at the tests with mixed beach (Line 2 and Line 3)

H (m)	T_s (sec)	d_B (m)	v_B (cm/s) estimated	v_B (cm/s) measured
0.110 (L2)	2.278	0.179	3.81	-
0.110 (L3)	2.278	0.179	3.81	-
0.117 (L2)	3.053	0.200	4.03	1.21
0.117 (L3)	3.053	0.200	4.03	1.95

The results of the calculations, by using Eq.5-19 with Eq.5-6, for Line1 are shown in Table 5-19 below.

Table 5-19 The results for the calculations of v_B for the tests with random waves (Line 1)

H (m)	T_s (sec)	θ (°)	ξ	d_B (m)	$\hat{u}_b$ (m/s)	v_B (cm/s)
0.108 (G)	2.264	15	0.95 (plunging breaker)	0.172	0.746	3.87
0.110 (G)	3.244	15	1.46 (plunging breaker)	0.203	0.947	3.76
0.110 (M)	2.278	15	0.94 (plunging breaker)	0.174	0.750	3.89
0.117 (M)	3.053	15	1.67 (plunging breaker)	0.190	1.03	4.19

In order to compare the estimated values of v_B with the measured v_B from experimental results (for both types of beach), the data have been tabulated and presented at the following Tables.

Table 5-20 The measured v_B at the tests with gravel beach (Line 1)

H (m)	T_s (sec)	d_B (m)	v_B (cm/s) estimated	v_B (cm/s) measured
0.108 (L1)	2.264	0.172	3.87	2.58
0.110 (L1)	3.244	0.203	3.76	3.25

Table 5-21 The measured v_B at the tests with mixed beach (Line 1)

H (m)	T_s (sec)	d_B (m)	v_B (cm/s) estimated	v_B (cm/s) measured
0.110 (L1)	2.278	0.174	3.89	-
0.117 (L1)	3.053	0.190	4.19	-2.90

It can be seen that Eq.5-19 gave satisfactory results for gravel beach. The v_B was often overestimated for mixed Beach.

Based on the present experimental results and results of Eq.5-19, three equations are proposed for the mean longshore velocity at the breaking point for random waves. A linear regression has been fitted to the data and the proposed fit is given by the following equation:

For gravel beach-uniform slope

Eq.5-21a $v_B = 0.438\widehat{u_b}\sin\theta_b\cos\theta_b$ (R^2=0.666)

For mixed beach-uniform slope

Eq.5-21b $v_B = 0.212\widehat{u_b}\sin\theta_b\cos\theta_b$ (R^2=0.434)

For gravel beach-trench

Eq.5-21c $v_B = 0.412\widehat{u_b}\sin\theta_b\cos\theta_b$ (R^2=0.267)

The range of applicability of Eq.5-21a, Eq.5-21b and Eq.5- 20c is the test series of the experiment for random waves (for both gravel and mixed beach). The three equations should be quite reliable when used within the limits of applicability.

5.1.2 Theoretical approaches of calculating γ, H_b and d_b

Based on the assumption that the estimated breaking depth and height of Eq.5-3 were accurate, new theoretical equations of breaker depth index (γ), breaking height (H_b) and breaking depth (d_b) have been put forward. Firstly, the influence of four parameters (θ, T, H_o and m) on γ, d_B and H_B has been investigated. The influence of each parameter on the breaking depth and height, and consequently on γ, has been investigated separately from the other parameters, while the other three parameters remained constant. The values of these parameters was chosen in such a way in order to cover the whole range from normal wave attack to more oblique and from no slope to very steep slope. The values of wave height and wave period were chosen in such a way that the wave steepness remained

less than 1/7 (no wave breaking before reach the slope). The breaking depth and breaking height, in Table 5-22 to Table 5-25, were calculated based on Eq.5-3 where the breaking depth index (γ) was calculated by H_B/d_B. The Iribarren number was calculated based on the Eq.5-1.

5.1.2.1 *Incident deepwater wave angle*

Various incident wave angles, normal to the shoreline, have been used in order to calculate the d_B, H_B and γ. The results of the calculations are shown in Table 5-22 below.

Table 5-22 The influence of incident wave angle

Number of scenario	θ (°)	$\cos\theta_0$	m	H_0 (m)	T (sec)	ξ	H_B (m)	d_B (m)	γ
1	0	1.000	0.1	0.24	2	0.510	0.254	0.259	0.979
2	10	0.985	0.1	0.24	2	0.510	0.251	0.256	0.980
3	15	0.966	0.1	0.24	2	0.510	0.251	0.256	0.980
4	30	0.866	0.1	0.24	2	0.510	0.242	0.245	0.986
5	45	0.707	0.1	0.24	2	0.510	0.225	0.226	0.996
6	50	0.643	0.1	0.24	2	0.510	0.217	0.217	1.000
7	60	0.500	0.1	0.24	2	0.510	0.197	0.194	1.012
8	75	0.259	0.1	0.24	2	0.510	0.150	0.144	1.038
9	80	0.174	0.1	0.24	2	0.510	0.127	0.121	1.050
10	89	0.017	0.1	0.24	2	0.510	0.050	0.045	1.092

It can be seen that the incident deepwater wave angle is inversely proportional to breaking height and depth, and proportional to the breaker depth index.

5.1.2.2 *Wave period (T)*

Various wave periods have been used in order to calculate d_B, H_B and γ.The results of the calculations are shown in Table 5-23 below.

Table 5-23 The influence of wave period

Number of scenario	T (sec)	θ (°)	$\cos\theta_0$	m	H_0 (m)	ξ	H_B (m)	d_B (m)	γ
11	1.8	15	0.966	0.1	0.24	0.459	0.242	0.254	0.953
12	2	15	0.966	0.1	0.24	0.510	0.251	0.256	0.981
13	3	15	0.966	0.1	0.24	0.765	0.291	0.277	1.049
14	4	15	0.966	0.1	0.24	1.020	0.324	0.301	1.076
15	5	15	0.966	0.1	0.24	1.275	0.354	0.325	1.089
16	6	15	0.966	0.1	0.24	1.530	0.380	0.347	1.096
17	7	15	0.966	0.1	0.24	1.785	0.405	0.367	1.101
18	8	15	0.966	0.1	0.24	2.040	0.428	0.388	1.105
19	9	15	0.966	0.1	0.24	2.296	0.451	0.408	1.107
20	10	15	0.966	0.1	0.24	2.551	0.475	0.428	1.109

It can be seen that the wave period is proportional to the Iribarren number, to breaking height, to the breaking depth and to breaker depth index.

5.1.2.3 *Deepwater wave height (H_o)*

Various deepwater wave heights have been used in order to calculate d_B, H_B and γ. The results of the calculations are shown in Table 5-24 below.

Table 5-24 The influence of deepwater wave height

Number of scenario	H_o (m)	θ (°)	$\cos\theta_o$	m	T (sec)	ξ	H_B (m)	d_B (m)	γ
21	0.025	15	0.966	0.1	2	1.581	0.041	0.037	1.097
22	0.05	15	0.966	0.1	2	1.118	0.070	0.065	1.082
23	0.075	15	0.966	0.1	2	0.913	0.097	0.091	1.067
24	0.08	15	0.966	0.1	2	0.884	0.102	0.096	1.064
25	0.1	15	0.966	0.1	2	0.790	0.122	0.116	1.053
26	0.25	15	0.966	0.1	2	0.500	0.259	0.266	0.976
27	0.5	15	0.966	0.1	2	0.353	0.467	0.551	0.849
28	0.75	15	0.966	0.1	2	0.289	0.681	0.973	0.700
29	0.8	15	0.966	0.1	2	0.279	0.727	1.096	0.663
30	0.85	15	0.966	0.1	2	0.271	0.777	1.251	0.622

It can be seen that the deepwater wave height is proportional to breaking height and depth, and inversely proportional to the breaker depth index.

5.1.2.4 *Bottom slope (m)*

Various bottom slopes have been used in order to calculate d_B, H_B and γ.The results of the calculations are shown in Table 5-25 below.

Table 5-25 The influence of bottom slope

Number of scenario	m	θ (°)	$\cos\theta_0$	H_0 (m)	T (sec)	ξ	H_B (m)	d_B (m)	γ
31	0.01	15	0.966	0.24	2	0.051	0.242	0.317	0.762
32	0.02	15	0.966	0.24	2	0.102	0.243	0.307	0.792
33	0.05	15	0.966	0.24	2	0.255	0.246	0.282	0.874
34	0.06	15	0.966	0.24	2	0.306	0.248	0.276	0.899
35	0.07	15	0.966	0.24	2	0.357	0.249	0.270	0.921
36	0.1	15	0.966	0.24	2	0.510	0.251	0.256	0.981
37	0.2	15	0.966	0.24	2	1.020	0.255	0.235	1.082

It can be seen that the bottom slope is inversely proportional to the breaking depth and proportional to the breaking height and the breaker depth index. It can be observed that the changes of the breaking height were not substantial, showing that the influence of the bottom slope was not so effective to H_b.

It has to be mentioned that after the sensitivity study of Eq.5-3, it found that it is sensitive to the wave angle and the wave steepness giving numbers of breaking index higher than 0.8. A modification of Eq.5-3 is needed to improve the applicability of the equation for more cases.

After a nonlinear regression of the data from Table 5-22 to Table 5-25, an equation with a complex form has been produced in order to estimate the breaker depth index. The equation includes the wave steepness and the product of the Iribarren number and $\cos\theta_0$. The equation is shown below.

Eq.5-22 $$\gamma = -14.22 + 0.2242\xi + 0.7682\xi^2 - 0.1143\xi^3 - 0.6504\xi^4 + 0.1423\xi^5 - 21.3294\ln\frac{H_0}{L_0} - 12.3056\left(\ln\frac{H_0}{L_0}\right)^2 - 3.5954\left(\ln\frac{H_0}{L_0}\right)^3 - 0.5309\left(\ln\frac{H_0}{L_0}\right)^4 - 0.0315\left(\ln\frac{H_0}{L_0}\right)^5$$

The equation has been plotted in order to investigate its correlation with the estimated breaking depth index (Figure 5-1). It can be seen that the scatter of the equation correlated with the estimated breaking depth index quite accurately.

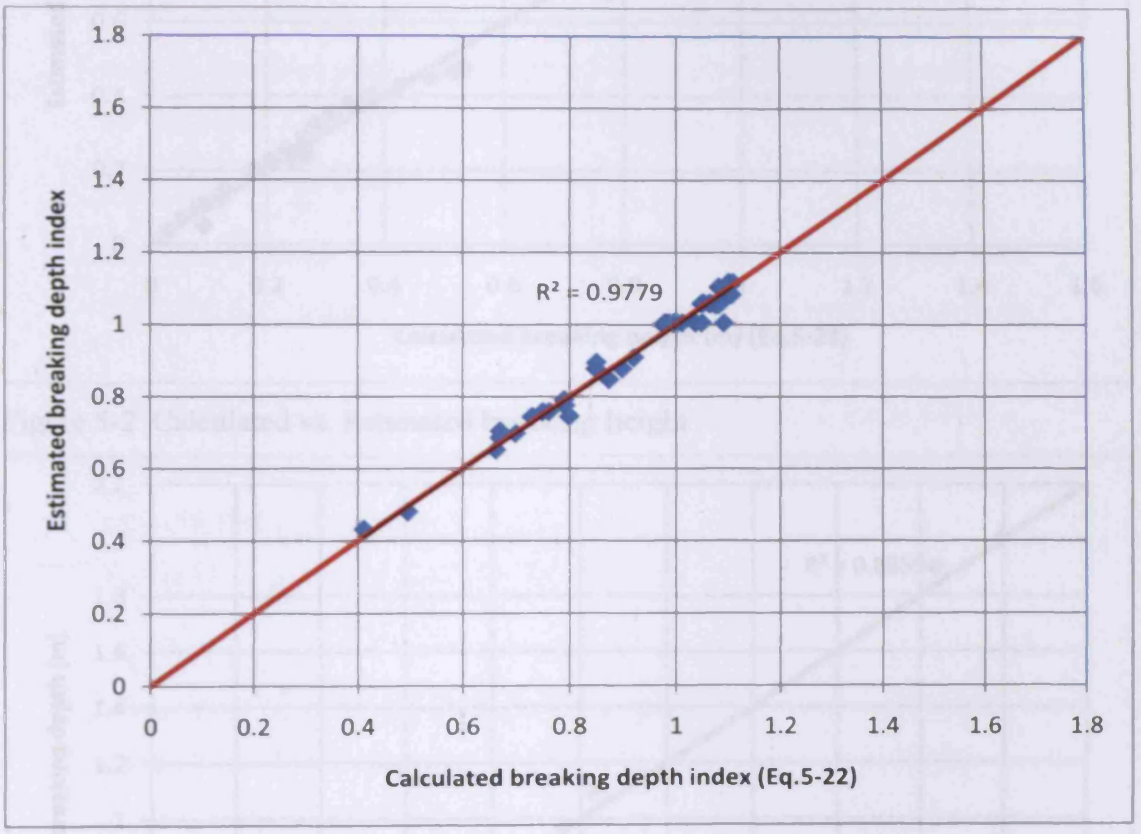

Figure 5-1 Calculated vs. Estimated breaking depth index

Moreover, after a nonlinear regression analysis, it is found that the best-fit equations for breaking depth and breaking height are the following:

Eq.5-23 $$H_b = 0.1657\cos\theta_0 - 0.1885m + 1.0284H_0 + 0.00189L_0 - 0.1504$$

Eq.5-24 $$d_b = -0.0466\cos\theta_0 - 0.5693m + 1.535H_0 - 1.4114\frac{H_0}{L_0} + 0.0853$$

The equations included all four parameters. Also, they have been plotted in order to investigate their correlation with the estimated breaking height and breaking depth (Figure 5-2 and Figure 5-3).

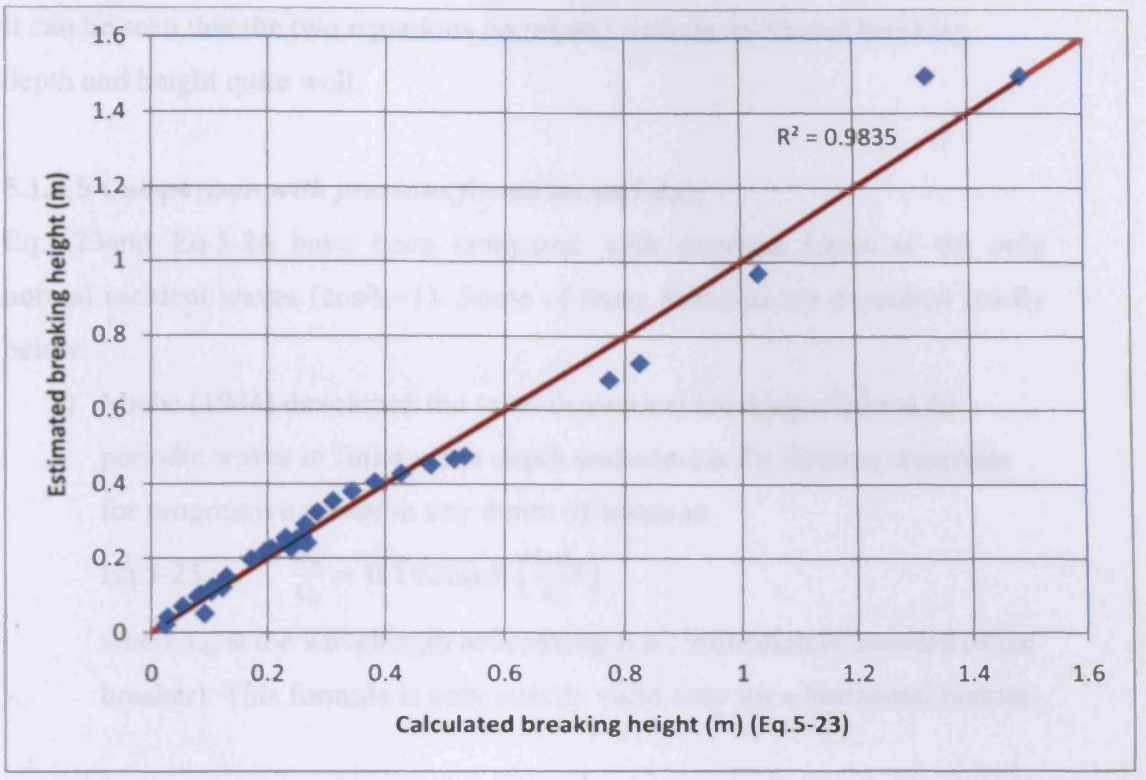

Figure 5-2 Calculated vs. Estimated breaking height

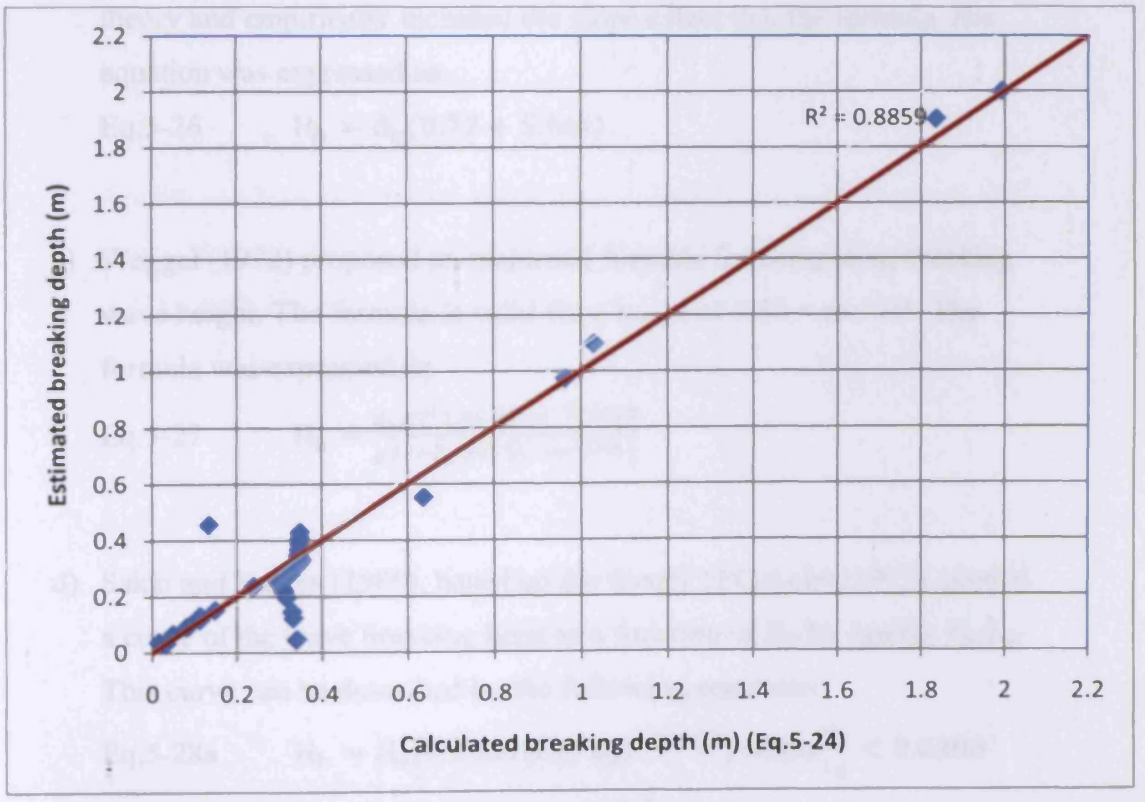

Figure 5-3 Calculated vs. Estimated breaking depth

It can be seen that the two equations correlated with the estimated breaking depth and height quite well.

5.1.2.5 *Comparison with previous formulae and data*

Eq.5-23and Eq.5-24 have been compared with previous formulae for only normal incident waves ($\cos\theta_0=1$). Some of these formulae are described briefly below:

a) Miche (1944) developed the semi-theoretical breaking criterion for periodic waves in finite water depth and express the limiting steepness for progressive waves in any depth of water as

Eq.5-25 $$\frac{H_b}{L_b} = 0.142\tanh\left(\frac{2\pi d_b}{L_b}\right)$$

where L_b is the wavelength at breaking (i.e., immediately seaward of the breaker). This formula is only strictly valid only for a horizontal bottom.

b) Collins (1970) produced a breaking height formula from linear wave theory and empirically included the slope effect into the formula. His equation was expressed as

Eq.5-26 $$H_b = d_b(0.72 + 5.6m)$$

c) Weggel (1972) proposed an empirical formula for computing breaking wave height. The formula is valid for a range of $1/50 < m < 1/5$. The formula was expressed as

Eq.5-27 $$H_b = \frac{d_b g T^2 1.56/[1+e^{-19.5m}]}{gT^2+d_b 43.75[1-e^{-19m}]}$$

d) Sakai and Battjes (1980), based on the theory of Cokelet (1977), plotted a curve of the wave breaking limit as a function of H_b/H_0 against H_0/L_0. This curve can be described by the following equations

Eq.5-28a $$H_b = H_0[0.3839(H_0/L_0)^{-0.3118}] \text{ when } \frac{H_0}{L_0} < 0.0208$$

Eq.5-28b $$H_b = H_0\left[0.6683\left(\frac{H_0}{L_0}\right)^{-0.1686}\right]$$

$$\text{when } 0.0208 \leq \frac{H_0}{L_0} < 0.1$$

Eq.5-28c $H_b = H_0$ when $0.1 \leq \frac{H_0}{L_0}$

The same curve in Sakai and Battjes (1980) also represents the ration of H_b/H_0 against d_b/L_0, which can be recast into the equations

Eq.5-29a $$H_b = H_0\left[27429\left(\frac{d_b}{L_0}\right)^2 - 773.71\left(\frac{d_b}{L_0}\right) + 7.4343\right]$$

$$\text{when } \frac{d_b}{L_0} < 0.011$$

Eq.5-29b $$H_b = H_0\left[0.3976\left(\frac{d_b}{L_0}\right)^{-0.3834}\right]$$

$$\text{when } 0.011 \leq \frac{d_b}{L_0} < 0.049$$

Eq.5-29c $$H_b = H_0\left[21.867\left(\frac{d_b}{L_0}\right)^2 - 7.06\left(\frac{d_b}{L_0}\right) + 1.5573\right]$$

$$\text{when } 0.049 \leq \frac{d_b}{L_0} < 0.6$$

Eq.5-29d $H_b = H_0$ when $0.6 \leq \frac{d_b}{L_0}$

e) Fenton and McKee (1990) determined the greatest unbroken wave that could exist as a function of both wavelength and depth over a nearly horizontal bottom as

Eq.5-30 $$H_b = d_b \frac{[0.141063(L_b/d_b)+0.0095721(L_b/d_b)^2+0.0077829(L_b/d_b)^3]}{[1+0.078834(L_b/d_b)+0.0317567(L_b/d_b)^2+0.0093407(L_b/d_b)^3]}$$

f) Kaminsky and Kraus (1993) ,based on the analysis of large data set on depth-limited breaking of regular waves incident to plane sloping beaches, derived a breaking height and a breaking depth formulae

Eq.5-31 $$H_b = 0.46H_0\left(\frac{H_0}{L_0}\right)^{-0.28}$$

Eq.5-32 $$d_b = 0.3m^{-0.25}H_0\left(\frac{H_0}{L_0}\right)^{-0.23}$$

g) Komar (1998) proposed two separate equations for H_b and d_b, respectively.

Eq.5-33 $$H_b = 0.39g^{0.2}(TH_0^2)^{0.4}$$

Eq.5-34 $$d_b = H_b\{1.2[m/(H_b/L_b)^{0.5}]^{0.27}\}$$

h) Rattanapitikon and Shibayama (2006) developed a breaking depth and wave height formulae (Eq.5-4 and Eq.5-5) based on the reanalysis of existing formulas which gave good predictions for small- and large-scale experiments.

i) Le Roux (2007) , proposed two separate equations for fully developed waves, H_b and d_b, respectively

Eq.5-35 $$H_b = L_0/24$$

Eq.5-36 $$d_b = L_0/20.0392$$

The comparison of Eq.5-23 and Eq.5-24 to the other formulae was based on the results taken from Table 2 of Le Roux (2007). The results from the comparison are presented in Table 5-26 and Table 5-27. The abbreviations in Table 5-26 and Table 5-27 are explained below:

Col = Collins (1970)

Mic = Miche (1944)

S&B1 = Eqs. (Eq.5- 28a - Eq.5- 28c) Sakai and Battjes (1980)

S&B2 = Eqs. (Eq.5- 29a - Eq.5- 29d), Sakai and Battjes (1980)

K&G = Komar and Gaughan (1973)

Kom = Komar (1998)

F&M = Frenton and McKee (1990)

LR = Le Roux (2007)

Weg = Weggel (1972)

KK = Kaminsky and Kraus (1993)

RS = Rattanapitikon and Shibayama (2006)

Table 5-26 Comparison of wave breaking heights for fully developed waves (H_0/L_0=0.0354) with different wave periods over different slopes (taken from Le Roux, 2007)

T	Col	Mic	S&B1	S&B2	K&G	Kom	F&M	LR	KK	RS	Eq.5-23
1x10^{-6} ^{0}slope											
1.6	0.14	0.17	0.16	0.18	0.15	0.15	0.15	0.17	0.17	0.14	0.17
3.3	0.61	0.71	0.7	0.76	0.66	0.66	0.63	0.71	0.71	0.62	0.67
5.1	1.46	0.69	1.69	1.81	1.57	1.58	1.5	1.69	1.69	1.47	1.57
6.6	2.44	2.82	2.83	3.04	2.63	2.65	2.5	2.83	2.82	2.46	2.62
8.4	3.96	4.57	4.58	4.91	4.26	4.29	4.06	4.59	4.57	3.99	4.23
11.1	6.91	7.98	7.98	8.56	7.43	7.47	7.09	8.02	7.98	6.97	7.38
11.8	7.81	9.02	9.03	9.68	8.4	8.45	8.01	9.06	9.02	7.88	8.34
5^0 slope											
1.6	0.2	-	0.16	0.19	0.15	0.15	-	0.19	0.17	0.15	0.15
3.3	0.84	-	0.7	0.81	0.66	0.66	-	0.81	0.71	0.64	0.65
5.1	2	-	1.69	1.95	1.57	1.58	-	1.93	1.69	1.53	1.55
6.6	3.35	-	2.83	3.27	2.63	2.65	-	3.23	2.82	2.56	2.60
8.4	5.43	-	4.58	5.29	4.26	4.29	-	5.23	4.57	4.15	4.22
11.1	9.48	-	7.98	9.22	7.43	7.47	-	9.14	7.98	7.24	7.37
11.8	10.71	-	9.03	10.43	8.4	8.45	-	10.33	9.02	8.19	8.33
10^0 slope											
1.6	-	-	0.16	0.2	0.15	0.5	-	0.2	0.17	0.15	0.14
3.3	-	-	0.7	0.84	0.66	0.66	-	0.85	0.71	0.66	0.63
5.1	-	-	1.69	2	1.57	1.58	-	2.04	1.69	1.57	1.54
6.6	-	-	2.83	3.36	2.63	2.65	-	3.41	2.82	2.62	2.59
8.4	-	-	4.58	5.43	4.26	4.29	-	5.53	4.57	4.25	4.20
11.1	-	-	7.98	9.47	7.43	7.47	-	9.65	7.98	7.41	7.35
11.8	-	-	9.03	10.71	8.4	8.45	-	10.91	9.02	8.38	8.31

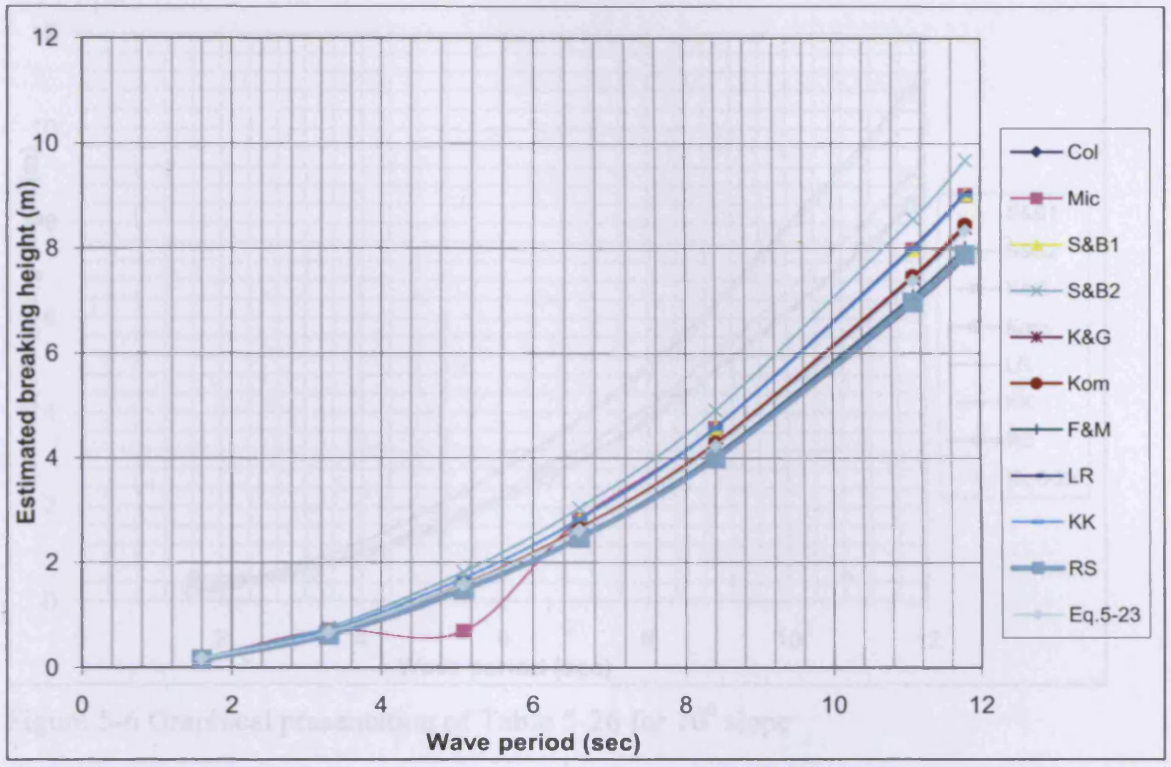

Figure 5-4 Graphical presentation of Table 5-26 for $1x10^{-6}$ ^{0}slope

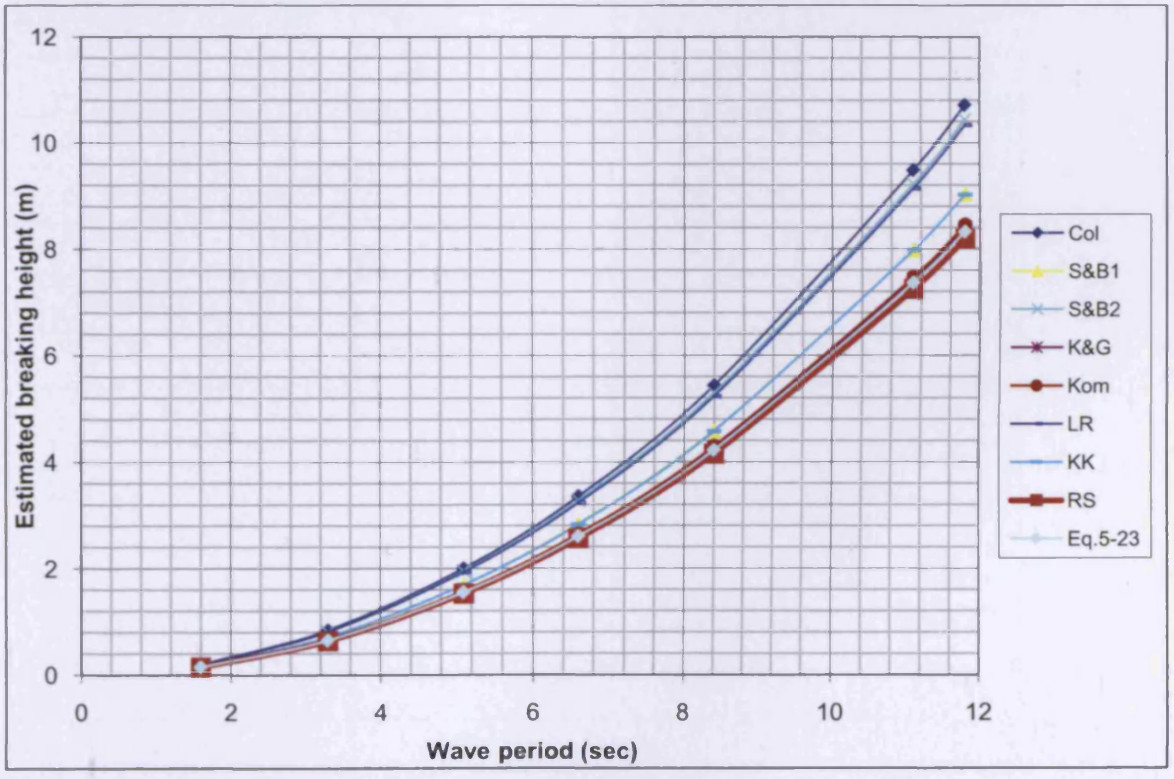

Figure 5-5 Graphical presentation of Table 5-26 for 5^0 slope

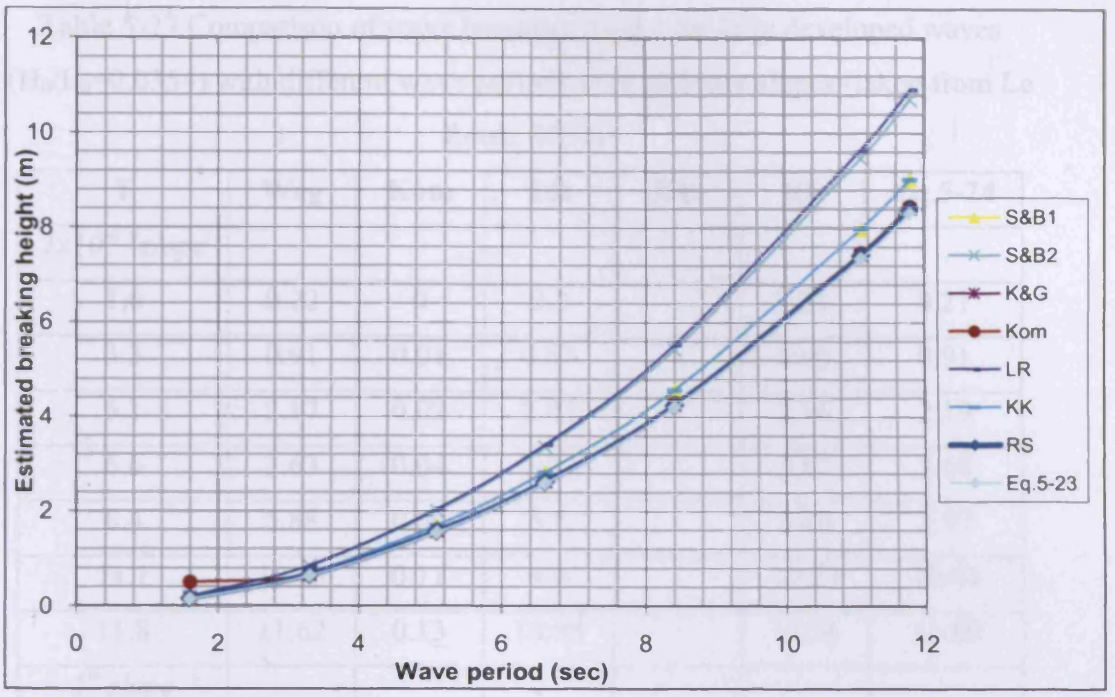

Figure 5-6 Graphical presentation of Table 5-26 for 10^0 slope

Table 5-27 Comparison of wave breaking depths for fully developed waves (H_0/L_0=0.0354) with different wave periods over different slopes (taken from Le Roux, 2007)

T	Weg	Kom	LR	KK	RS	Eq.5-24
1x10^{-6} ^{0}slope						
1.6	0.22	0	0.2	-	0.21	0.21
3.3	0.91	0.01	0.85	-	0.90	0.91
5.1	2.17	0.02	2.03	-	2.16	2.19
6.6	3.63	0.04	3.39	-	3.62	3.68
8.4	5.88	0.06	5.5	-	5.86	5.97
11.1	10.28	0.11	9.6	-	10.23	10.44
11.8	11.62	0.13	10.85	-	11.56	11.80
5^0 slope						
1.6	0.18	0.15	0.16	0.17	0.18	0.16
3.3	0.77	0.64	0.69	0.72	0.76	0.86
5.1	1.83	1.52	1.65	1.71	1.81	2.15
6.6	3.07	2.55	2.77	2.86	3.03	3.63
8.4	4.97	4.13	4.49	4.64	4.90	5.93
11.1	8.69	7.2	7.83	8.10	8.56	10.39
11.8	9.82	8.14	8.85	9.15	9.67	11.75
10^0 slope						
1.6	-	0.18	0.15	0.14	0.16	0.11
3.3	-	0.77	0.65	0.60	0.67	0.81
5.1	-	1.84	1.55	1.44	1.60	2.10
6.6	-	3.08	2.59	2.40	2.67	3.58
8.4	-	4.99	4.19	3.89	4.33	5.88
11.1	-	8.7	7.32	6.80	7.56	10.34
11.8	-	9.84	8.27	7.68	8.55	11.70

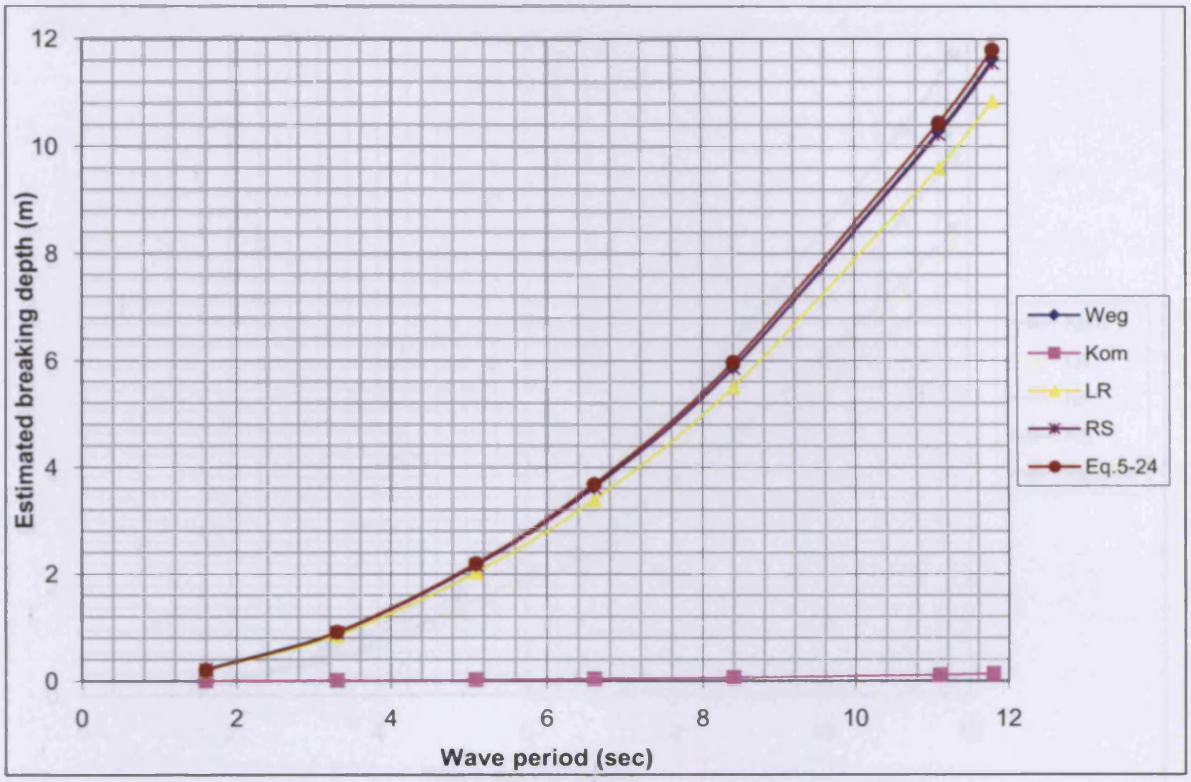

Figure 5-7 Graphical presentation of Table 5-27 for $1x10^{-6}$ ^{0}slope

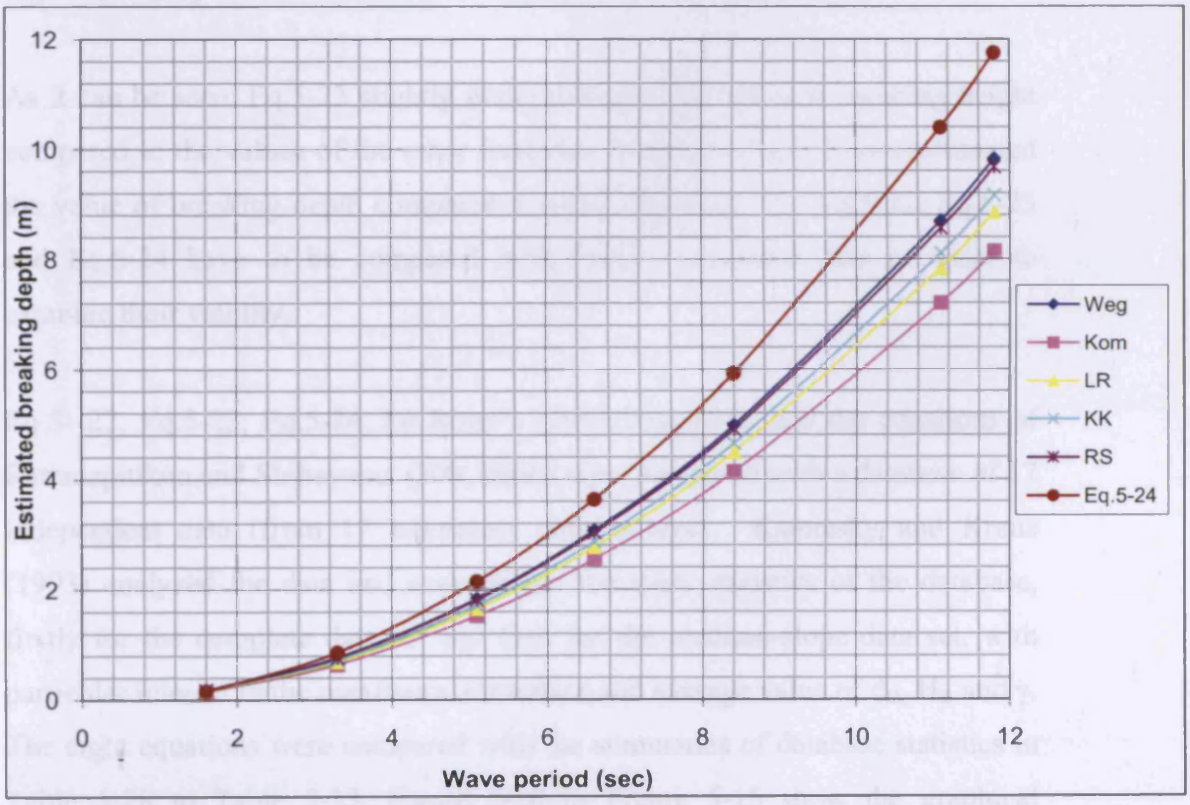

Figure 5-8 Graphical presentation of Table 5-27 for 5^0 slope

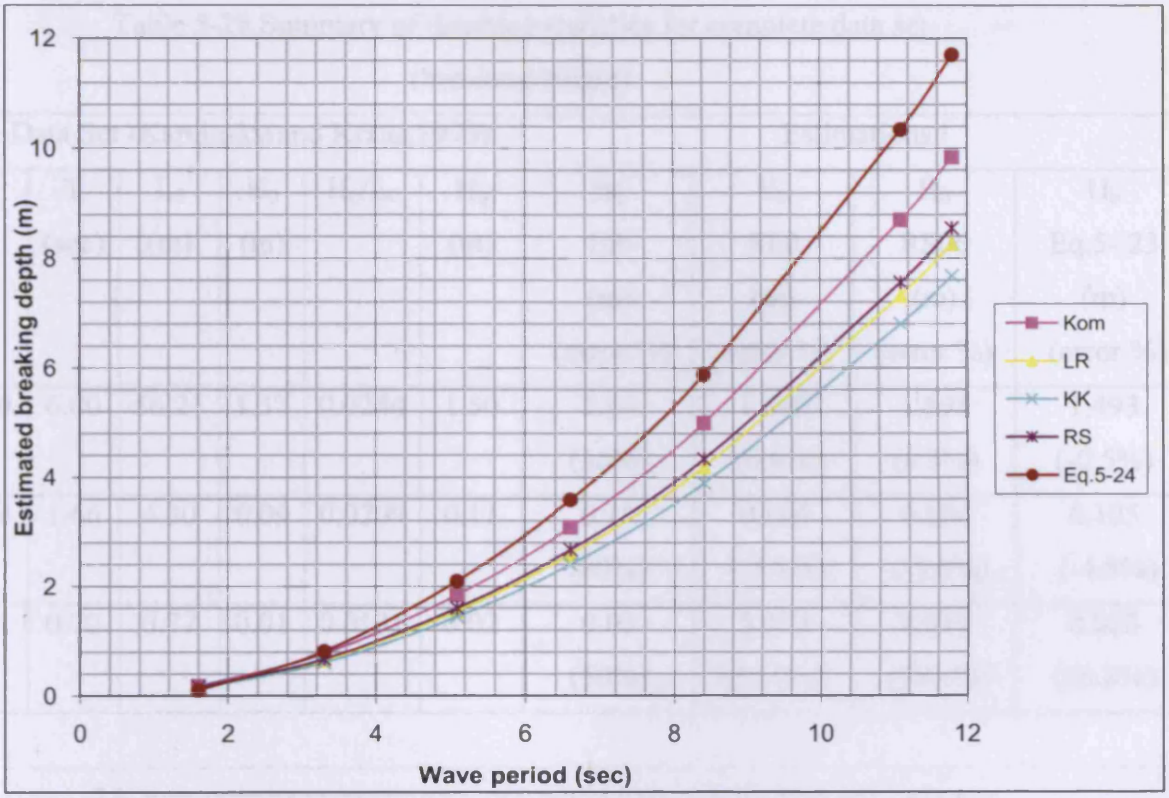

Figure 5-9 Graphical presentation of Table 5-27 for 10^0 slope

As it can be seen, Eq.5-23 slightly underestimated the value of breaking height compared to the values of the other formulae. However, Eq.5-24 overestimated the value of breaking depth compared to other formulae. The Eq.5-22, Eq.5-23 and Eq.5-24 have to be compared with further measured data in order to examine their validity.

Eq.5- 22, Eq.5-23, Eq.5-24, Le Roux's (2007) equations and the equations of Rattanapitikon and Shibayama (200, 2006) were compared with a database of 17 independent data (from 17 laboratory experiments). Kaminsky and Kraus (1993) analyzed the data and summarized the basic statistics of the database, firstly for the complete data set and then for the medium-slope data set, with particular interest in the maximum, minimum and average value of d_B, H_B and γ. The eight equations were compared with the summaries of database statistics in Table 5-28 to Table 5-33. Figure 5-10 to Figure 5-15 show the graphical presentation of this comparison.

Table 5-28 Summary of database statistics for complete data set (breaking height)

Complete Data Set (Kaminsky and Kraus,1993)							Estimations			
	m	T (sec)	L_0 (m)	H_0 (m)	H_0/L_0	H_b (m)	H_b LR (m) (error %)	H_b R00 (m) (error %)	H_b RS06 (m) (error %)	H_b Eq.5- 23 (m) (error %)
Max.	0.20	6.00	56.21	1.37	0.0244	1.50	2.34 (56%)	1.598 (6.6%)	1.595 (6.3%)	1.493 (-0.5%)
Avg.	0.06	1.66	4.30	0.09	0.0209	0.11	0.18 (80%)	0.104 (-5.1%)	0.104 (-5.8%)	0.105 (-4.8%)
Min.	0.01	0.70	0.77	0.01	0.0131	0.02	0.03 (50%)	0.012 (37.7%)	0.012 (39.1%)	0.025 (25.8%)

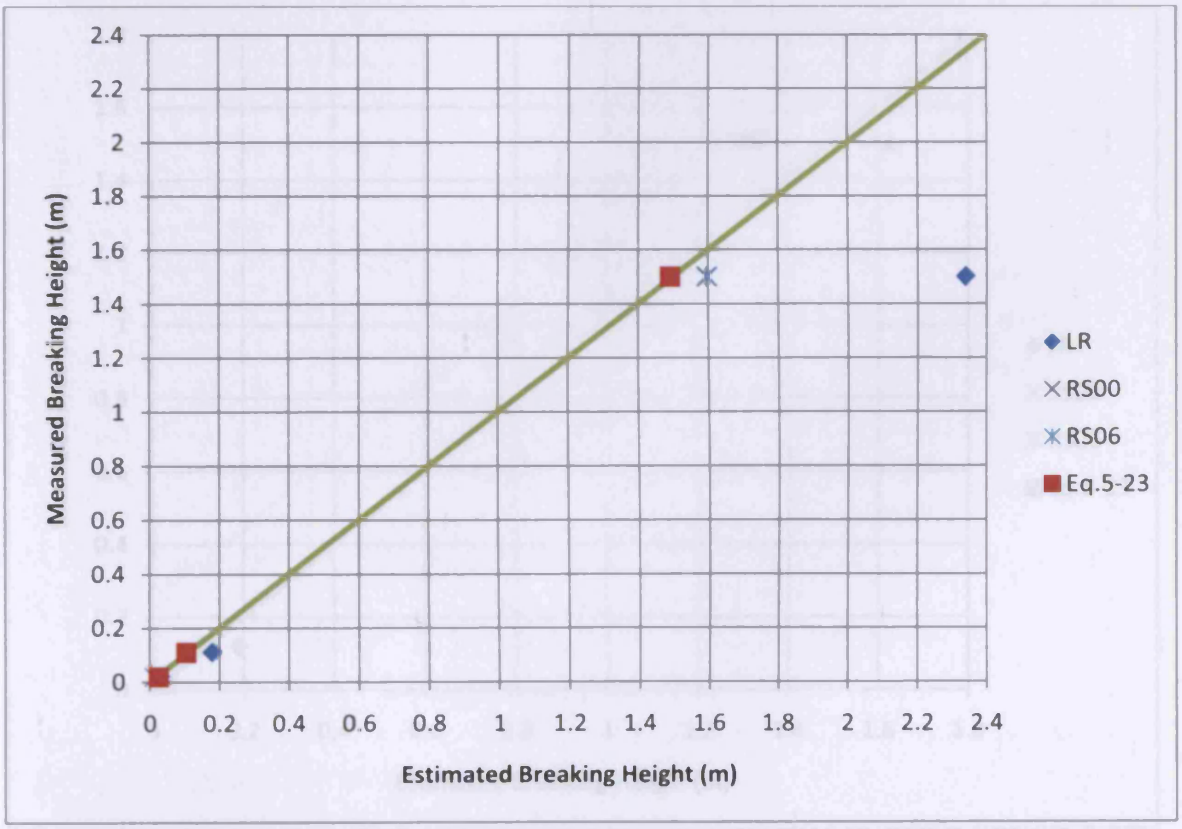

Figure 5-10 Graphical presentation of Table 5- 28

Table 5-29 Summary of database statistics for medium-slope data set (breaking height)

Medium-slope Data Set (Kaminsky and Kraus,1993)							Estimations			
	m	T (sec)	L_0 (m)	H_0 (m)	H_0/L_0	H_b (m)	H_b LR (m) (error %)	H_b R00 (m) (error %)	H_b RS06 (m) (error %)	H_b Eq.5- 23 (m) (error %)
Max.	0.03	5.00	39.03	1.21	0.0310	1.50	1.63 (8.7%)	1.291 (-13.9%)	1.286 (-14.3%)	1.328 (-11.5%)
Avg.	0.02	1.69	4.46	0.10	0.0224	0.12	0.19 (58.3%)	0.112 (-6.5%)	0.112 (-6.5%)	0.123 (2.4%)
Min.	0.01	0.78	0.95	0.01	0.0105	0.02	0.04 (100%)	0.013 (-34.7%)	0.013 (-34.7%)	0.025 (27.5%)

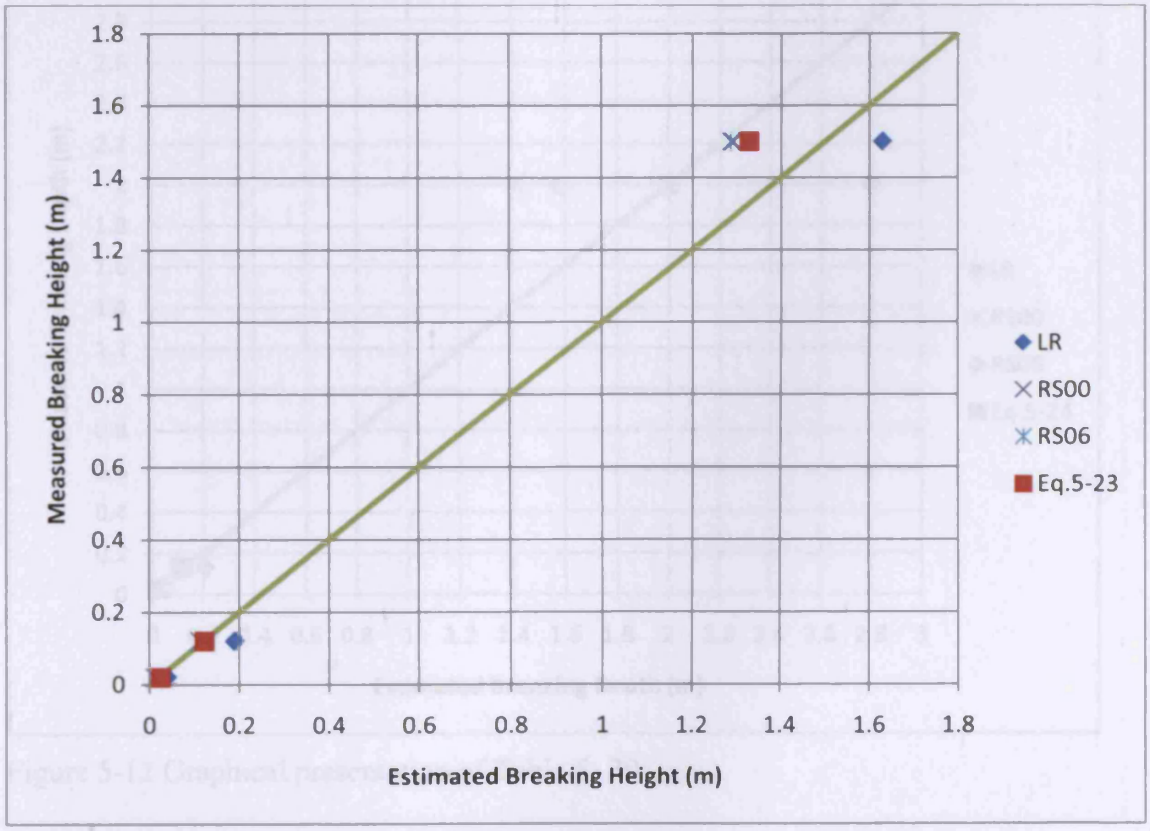

Figure 5-11 Graphical presentation of Table 5-29

Table 5-30 Summary of database statistics for complete data set (breaking depth)

Complete Data Set (Kaminsky and Kraus,1993)							Estimations			
	m	T (sec)	L_0 (m)	H_0 (m)	H_0/L_0	d_b (m)	d_b LR (m) (error %)	d_b R00 (m) (error %)	d_b RS06 (m) (error %)	d_b Eq.5- 24 (m) (error %)
Max.	0.20	6.00	56.21	1.37	0.0244	2	2.80 (40%)	1.414 (-29.3%)	1.585 (-20.8%)	1.994 (-0.3%)
Avg.	0.06	1.66	4.30	0.09	0.0209	0.13	0.21 (61.5%)	0.110 (-15.3%)	0.130 (0.0%)	0.113 (-13.2%)
Min.	0.01	0.70	0.77	0.01	0.0131	0.03	0.04 (33.3%)	0.015 (-49.5%)	0.017 (-42.6%)	0.029 (-2.5%)

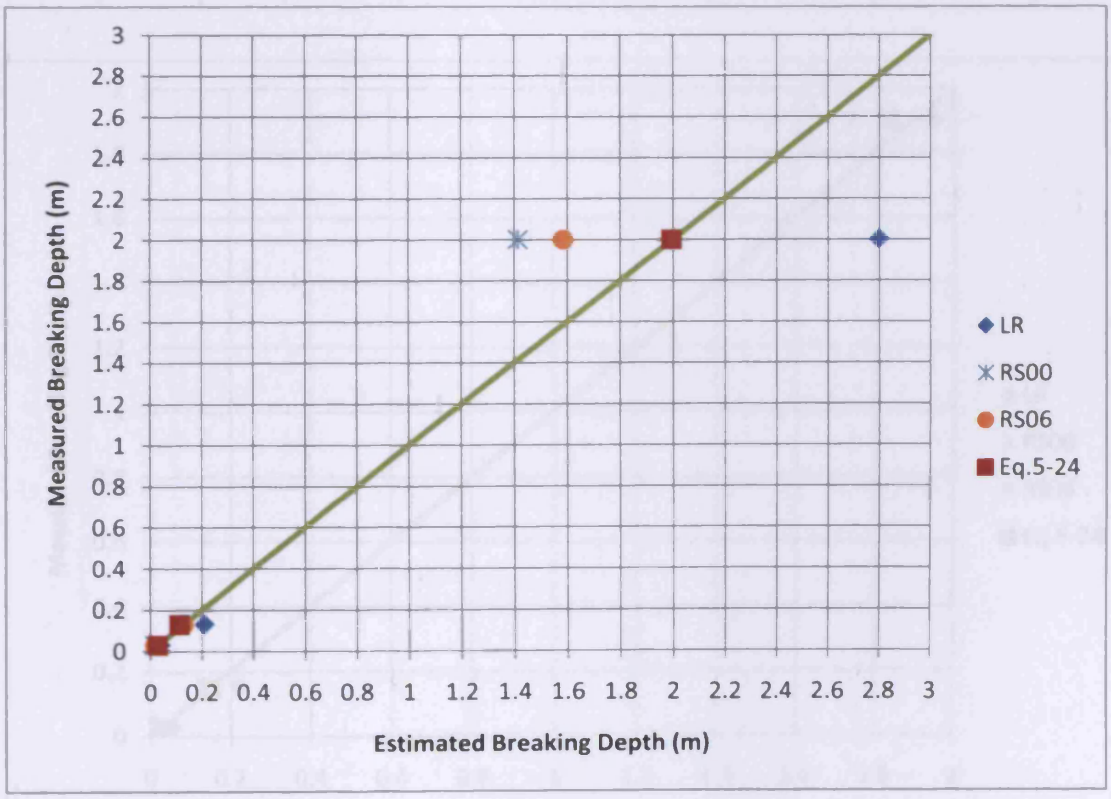

Figure 5-12 Graphical presentation of Table 5- 30

Table 5-31 Summary of database statistics for medium-slope data set (breaking depth)

Medium-slope Data Set (Kaminsky and Kraus,1993)							Estimations			
	m	T (sec)	L_0 (m)	H_0 (m)	H_0/L_0	d_b (m)	d_b LR (m) (error %)	d_b R00 (m) (error %)	d_b RS06 (m) (error %)	d_b Eq.5- 24 (m) (error %)
Max.	0.03	5.00	39.03	1.21	0.0310	1.9	1.95 (2.6%)	1.539 (19.0%)	1.738 (-8.5%)	1.835 (-3.4%)
Avg.	0.02	1.69	4.46	0.10	0.0224	0.15	0.22 (46.7%)	0.135 (-10.0%)	0.155 (3.1%)	0.149 (-0.9%)
Min.	0.01	0.78	0.95	0.01	0.0105	0.03	0.05 (66.7%)	0.016 (-47.5%)	0.018 (-40.6%)	0.033 (9.7%)

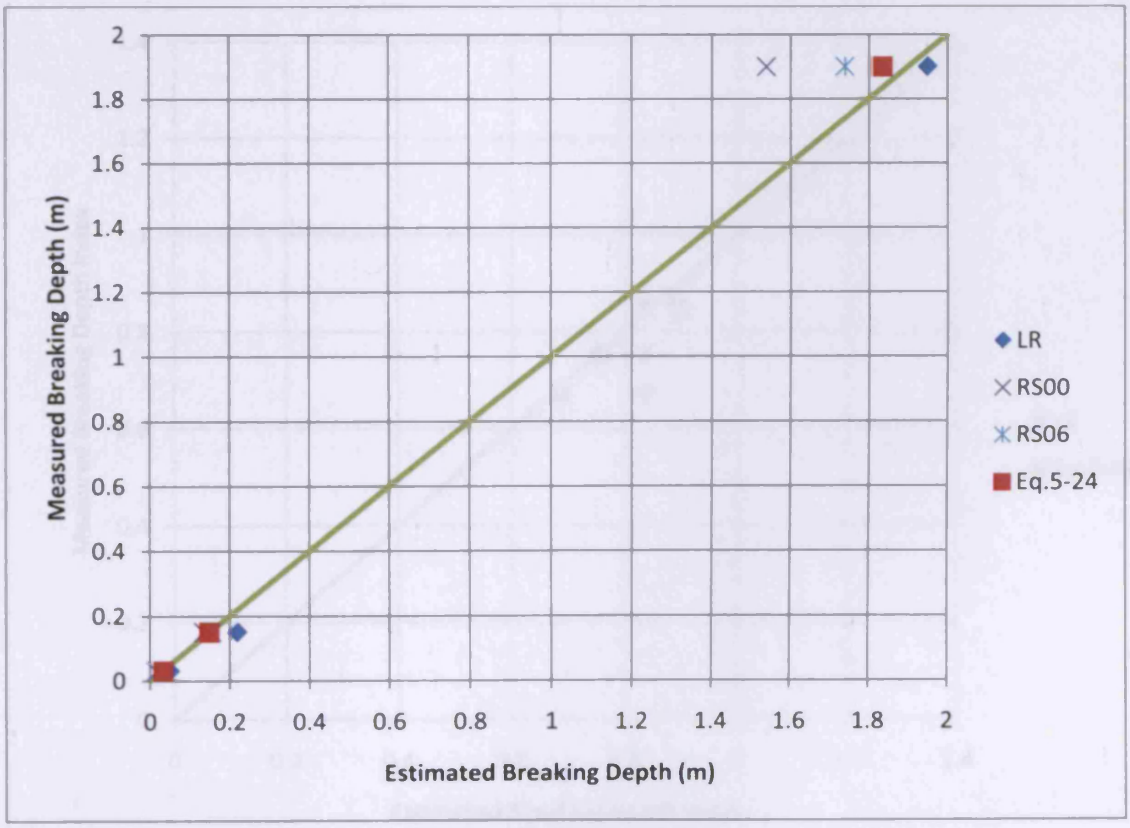

Figure 5-13 Graphical presentation of Table 5- 31

Table 5-32 Summary of database statistics for complete data set (breaking depth index)

Complete Data Set (Kaminsky and Kraus,1993)							Estimations	
	m	T (sec)	L_0 (m)	H_0 (m)	H_0/L_0	γ (m)	γ LR (m) (error %)	γ Eq.5- 22 (m) (error %)
Max.	0.20	6.00	56.21	1.37	0.0244	0.75	0.835 (-11.3%)	0.757 (0.9%)
Avg.	0.06	1.66	4.30	0.09	0.0209	0.85	0.835 (-1.3%)	0.894 (5.2%)
Min.	0.01	0.70	0.77	0.01	0.0131	0.67	0.835 (25.3%)	0.685 (2.2%)

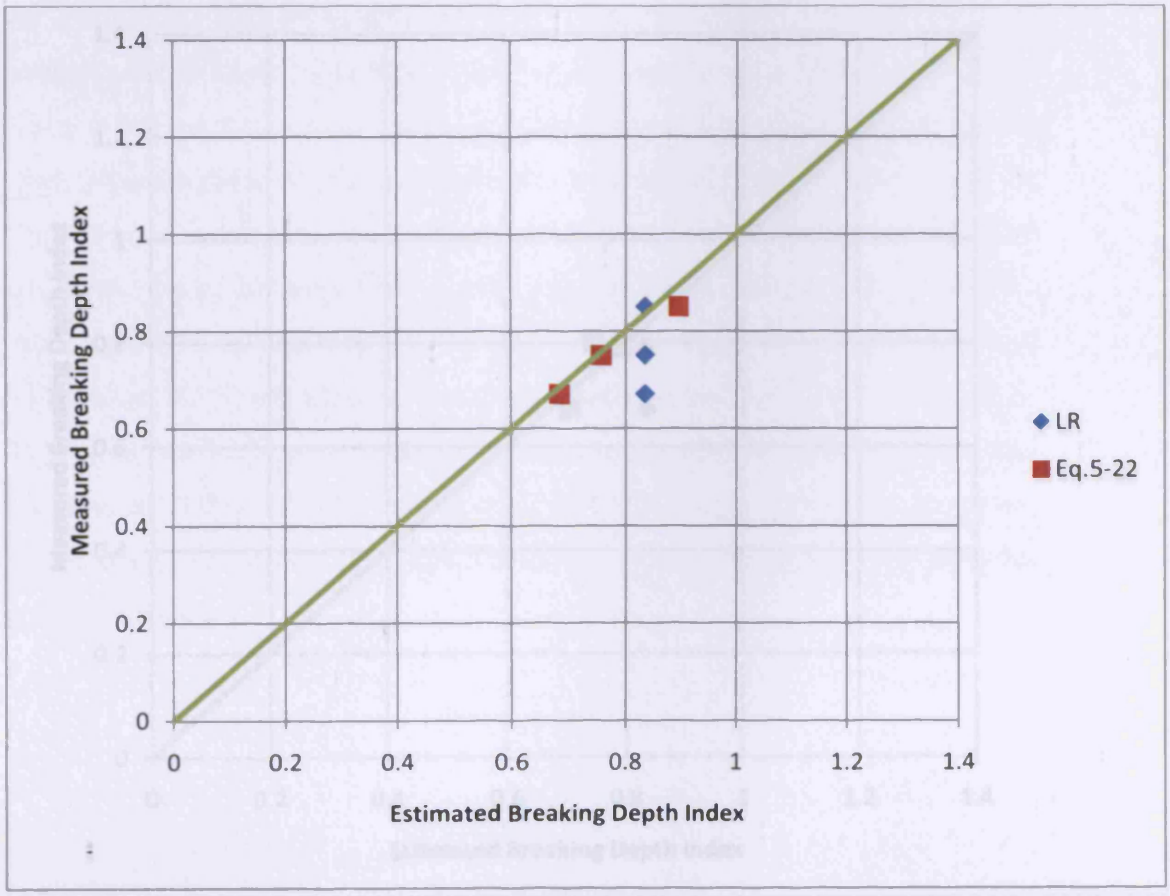

Figure 5-14 Graphical presentation of Table 5-32

Table 5-33 Summary of database statistics for medium-slope data set (breaking depth index)

Medium-slope Data Set (Kaminsky and Kraus,1993)							Estimations	
	m	T (sec)	L_0 (m)	H_0 (m)	H_0/L_0	γ (m)	γ LR (m) (error %)	γ Eq.5- 22 (m) (error %)
Max.	0.03	5.00	39.03	1.21	0.0310	0.79	0.835 (5.8%)	0.791 (0.1%)
Avg.	0.02	1.69	4.46	0.10	0.0224	0.80	0.835 (4.4%)	0.745 (-6.9%)
Min.	0.01	0.78	0.95	0.01	0.0105	0.67	0.835 (25.3%)	0.704 (5.1%)

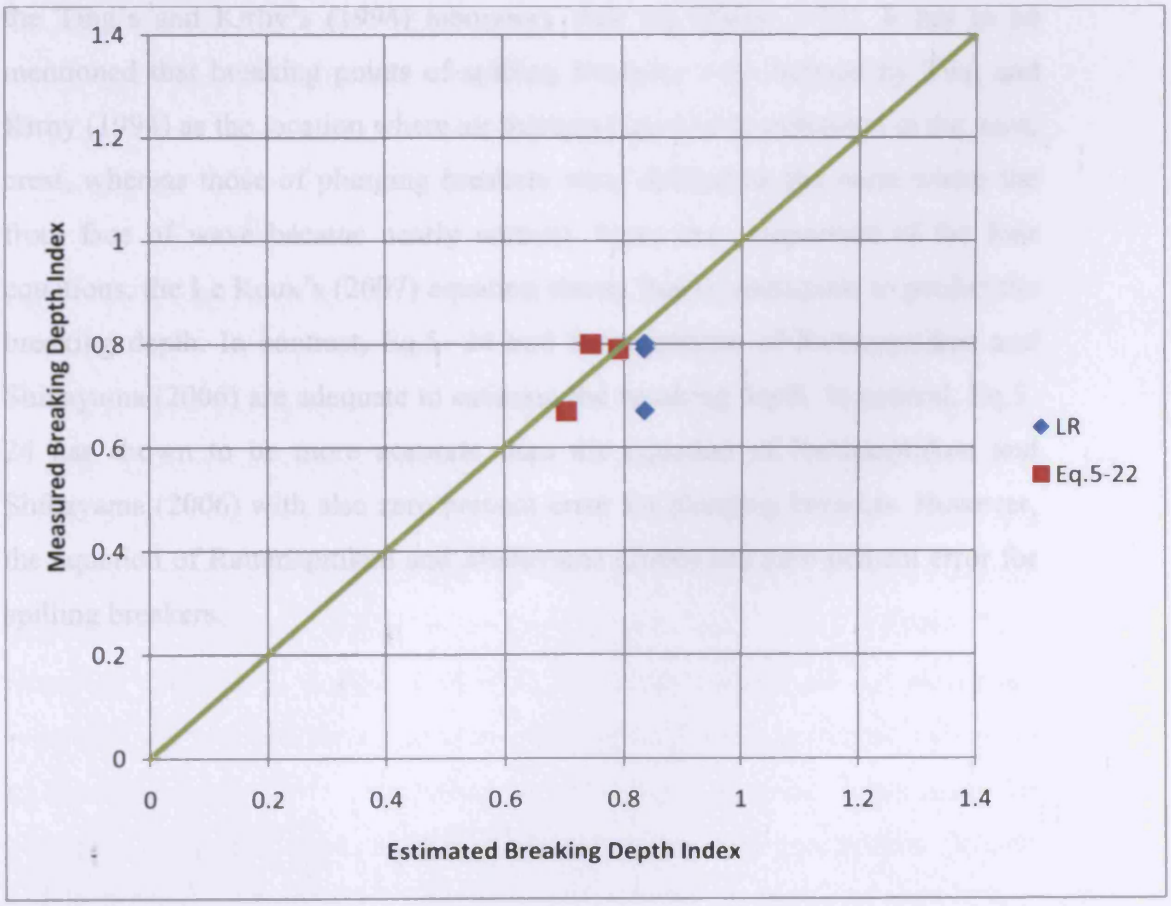

Figure 5-15 Graphical presentation of Table 5-33

The examination of the eight formulae shown Eq.5-22, Eq.5-23 and Eq.5-24 gave a satisfactory overall prediction for the complete and medium-slope data set. Eq.5-23 predicted the breaking height much more accurate than the other equations with a promising almost zero percentage error in the prediction of the maximum value of the complete data set.

Furthermore, Eq.5-24 was much more accurate in predicting the breaking depth, than the equations of Le Roux's (2007) and Rattanapitikon and Shibayama (2000, 2006), with most of its predictions having an under 5% error for both complete and medium-slope data set. The equation of Rattanapitikon and Shibayama (2006) also predicted the breaking depth accurately for the average values of both data sets with a zero percentage error for the complete data set.

The four equations, that estimate the breaking depth, have also been applied to the Ting's and Kirby's (1994) laboratory data set (Table 5-34). It has to be mentioned that breaking points of spilling breakers were defined by Ting and Kirby (1994) as the location where air bubbles began to be entrained in the wave crest, whereas those of plunging breakers were defined as the point where the front face of wave became nearly vertical. From the comparison of the four equations, the Le Roux's (2007) equation shows that is inadequate to predict the breaking depth. In contrast, Eq.5- 24 and the equations of Rattanapitikon and Shibayama (2006) are adequate to estimate the breaking depth. In general, Eq.5-24 has shown to be more accurate than the equation of Rattanapitikon and Shibayama (2006) with also zero percent error for plunging breakers. However, the equation of Rattanapitikon and Shibayama (2006) had zero percent error for spilling breakers.

Table 5-34 Comparison of breaking depth for laboratory data set

Complete Data Set (Kaminsky and Kraus,1993)							Estimations			
reaker Type	m	T (sec)	L_0 (m)	H_0 (m)	H_0/L_0	d_b (m)	d_b LR (m) (error %)	d_b R00 (m) (error %)	d_b RS06 (m) (error %)	d_b Eq.5- 24 (m) (error %)
pilling	1/35	2.00	6.25	0.127	0.020	0.196	2.80 (40%)	0.169 (-13.8%)	0.196 (0.0%)	0.189 (-3.6%)
unging	1/35	5.00	39.03	0.089	0.0023	0.156	0.21 (61.5%)	0.170 (9.0%)	0.195 (25.9%)	0.156 (0.0%)

As far as the breaker depth index was concerned, Eq.5-22 gave the best estimation. Eq.5-22 was very accurate in predicting the breaking depth index for the minimum and maximum values of the medium-slope data set. Overall it had less than seven percentage error, for either data set. The equation of Le Roux (2007) gave a constant value for all the cases and has shown its lack of estimating the value of γ for different wave conditions and slopes.

5.2 WAVE-INDUCED CURRENTS

As the oblique waves break to the shoreline two mean currents are generated flowing parallel (long-shore currents) and straight normal (cross-shore currents) to the coast. These two mean currents can be considered as components of a continuum flow field from which the resulting wave-induced mean current structure is illustrated in Figure 5-16 (Svendsen and Lorenz, 1989). These nearshore currents in combination with the stirring action of the waves are important for the sediment transport and therefore are significant factors in morphological changes. Consequently, they are of great importance for managers of coastal areas, coastal engineers and marine geologistics (Visser, 1991).

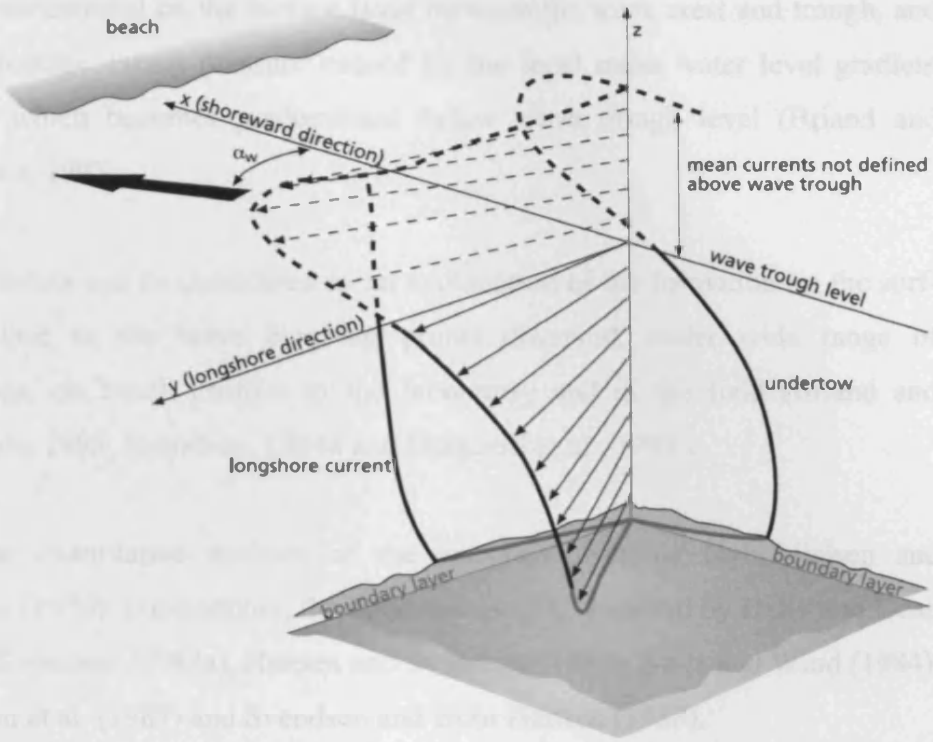

Figure 5-16 Schematic diagram of the vertical profile of the mean cross-shore and longshore current in the nearshore (from Svendsen and Lorenz, 1989)

5.2.1 Cross-shore Currents

Cross-shore currents are related to the mass compensation under breaking waves and they are not constant over depth (Coastal Engineering Manual, 2003). The main characteristic of the cross-shore current is the existence of the two-dimensional circulation in the surf zone known as "undertow current", which flows in the seawards direction from the shoreline. This current is directed offshore on the bottom, balanced with the onshore flow of water carried by the breaking waves. Closer to the water surface the resulting current is in the onshore direction. The undertow current may be relatively strong, being almost 8% to 10% of the wave celerity ($\sqrt{gd}$) near the bottom.

The undertow is the result of an imbalance between the excess momentum flux induced by the breaking wave, the mass flux of the carrier wave and the surface

roller, concentrated on the surface layer between the wave crest and trough, and the hydrostatic excess pressure caused by the local mean water level gradient (setup), which becomes predominant below wave trough level (Briand and Kamphuis, 1993).

The undertow can be considered as an explanation of bar formation (in the surf-zone, close to the wave breaking point) observed, under wide range of conditions, on beach profiles in the laboratory and in the field (Briand and Kamphuis, 1993; Svendsen, 1984a and Deigaard et al., 1991).

The first quantitative analysis of the undertow was by Dyhr-Nielsen and Sorensen (1970). Furthermore, the undertow profile is solved by Dally and Dean (1984), Svendsen (1984a), Hansen and Svendsen (1984), Stive and Wind (1984), Svendsen et al. (1987) and Svendsen and Buhr Hansen (1988).

5.2.1.1 *Analysis of the experimental results (cross-shore currents)*

The cross-shore currents, of each line and for each test, that measured from the experiments were analysed and can be observed at the Appendix III (A2). The reverse flow can clearly be seen at all lines for all tests. Most of the measurement points were before the breaking point but close enough the undertow current to be observed. The undertow was represented (in Appendix III-A2) by the seaward direction of the currents. Furthermore, at the trench, the seaward direction of the currents could represent rip currents, especially at Test 1 and Test 2 where the highest wave conditions of the experiment occurred.

Rip currents are usually confused with the undertow. As the waves move to the shoreline produces setup. Because of the inclination of the water level, the setup water is essentially piled up against the shoreline in an unstable condition. If this unstable condition exists along a barred coast or along some of the steeper coasts, the setup produces seaward flowing currents that are rather narrow and

that create circulation cells within the surf zone. These narrow currents are called rip currents.

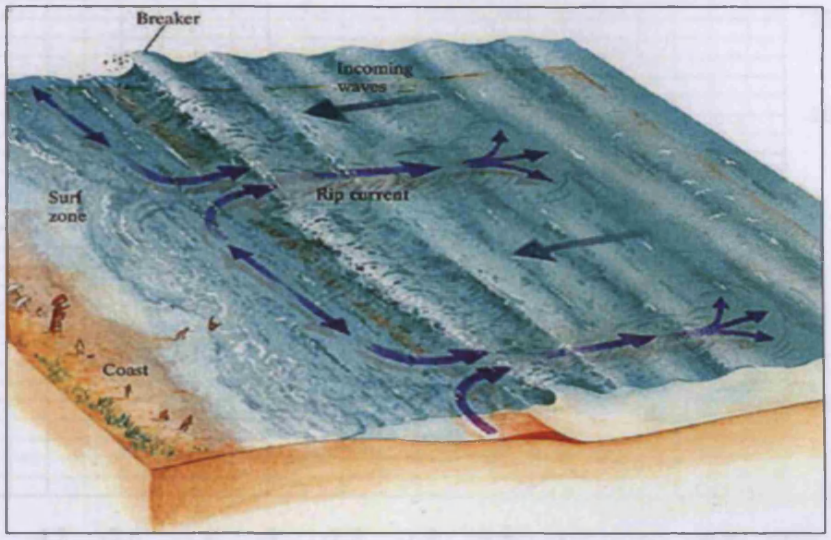

Figure 5- 17 Rip currents formation

When wind and waves push water towards the shore, the previous backwash is often pushed sideways by the oncoming waves. This water streams along the shoreline until it finds an exit back to the sea. The resulting rip current is usually narrow and located in a trench. In general, while a common misconception is that a rip occurring under the water, instead of on top — an undertow — is strong enough to drag people under the surface of the water; the current is actually strongest at the surface. In some areas, rip currents will persist during low- to moderate- energy wave conditions and then during high-energy wave conditions the rips will lose their definition and undertow will be primary mode of seaward return of water from unstable condition of setup.

Though, it has to be mentioned that at some locations, near the bed, the reverse current is replaced by a shoreward current. This behaviour of currents is carried out from Test 4 to Test 10 (especially at Lines 2 and 3). The shoreward direction of these currents also affected the sediment transport as the sediment showed to be slightly moved shoreward at the locations influenced by these currents. The cross-shore current velocities of all tests, near the bed, are presented at Figure 5-18 to Figure 5-27. In the y-direction, positive indicates seaward where negative indicates shoreward.

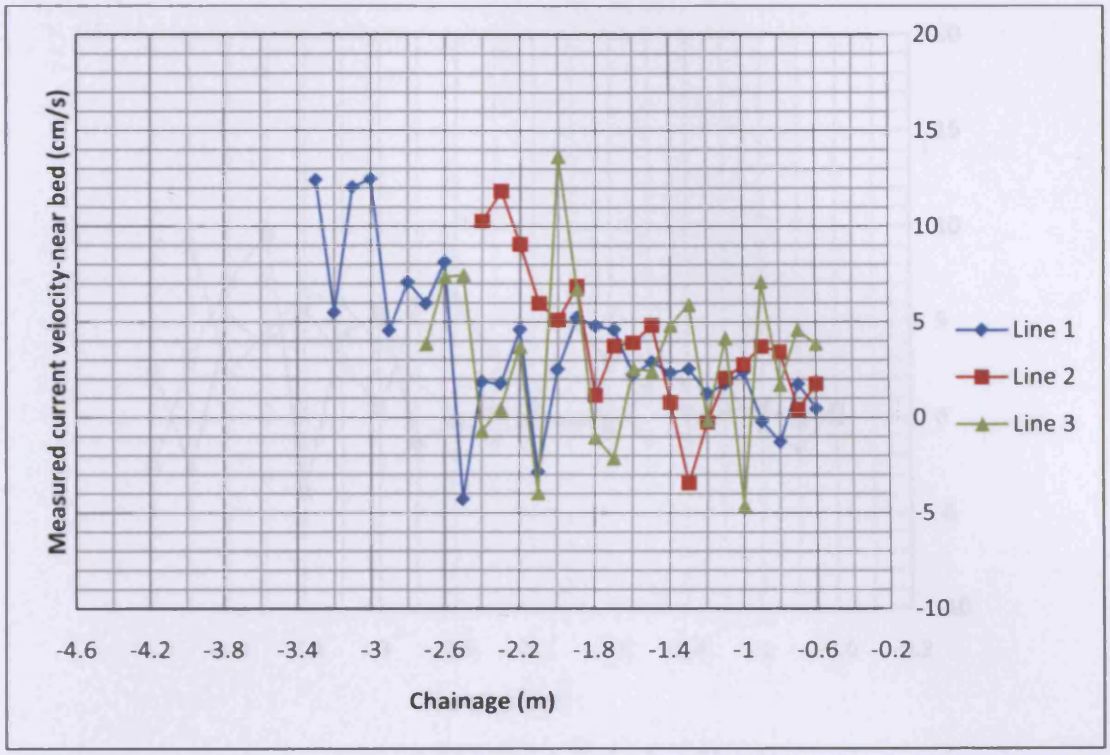

Figure 5-18 Near bed cross-shore current velocity (Test 1)

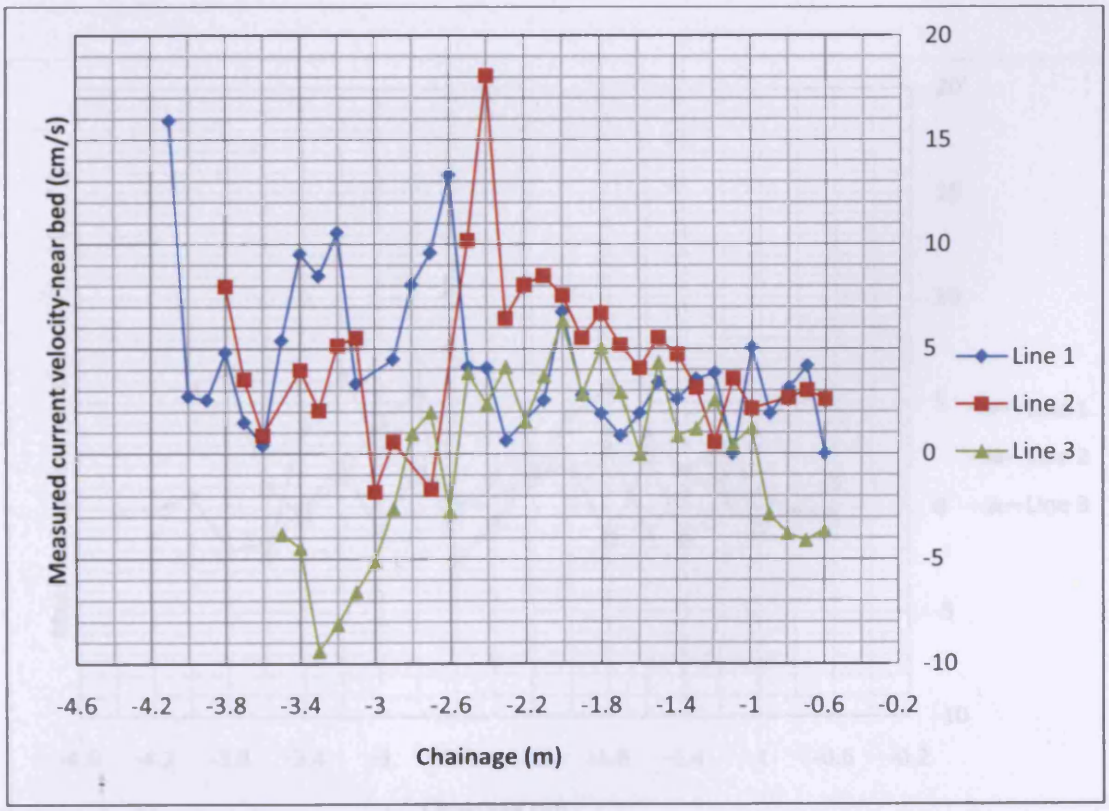

Figure 5-19 Near bed cross-shore current velocity (Test 2)

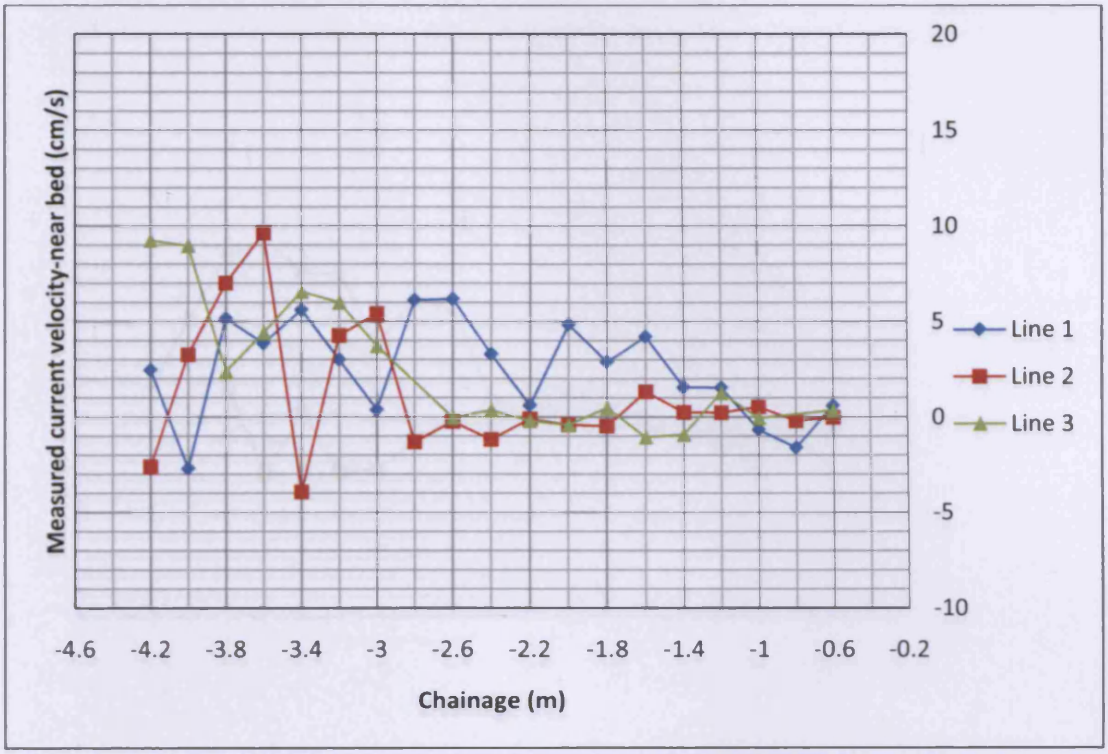

Figure 5-20 Near bed cross-shore current velocity (Test 3)

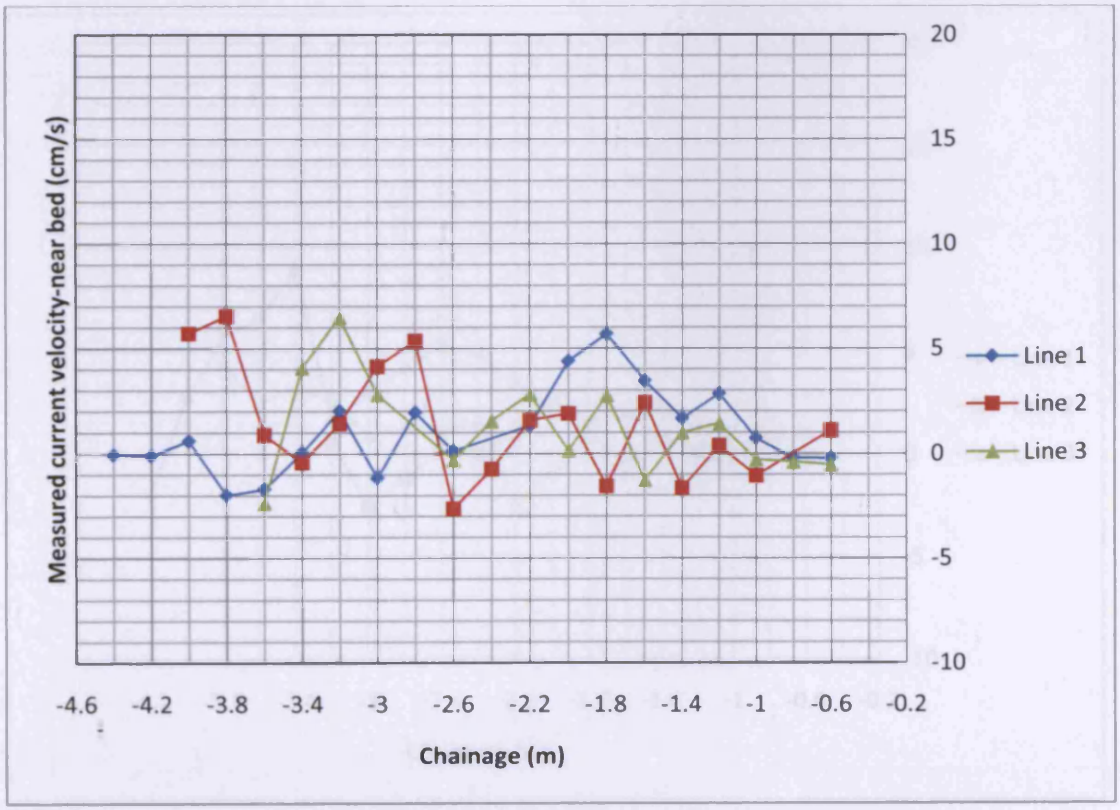

Figure 5-21 Near bed cross-shore current velocity (Test 4)

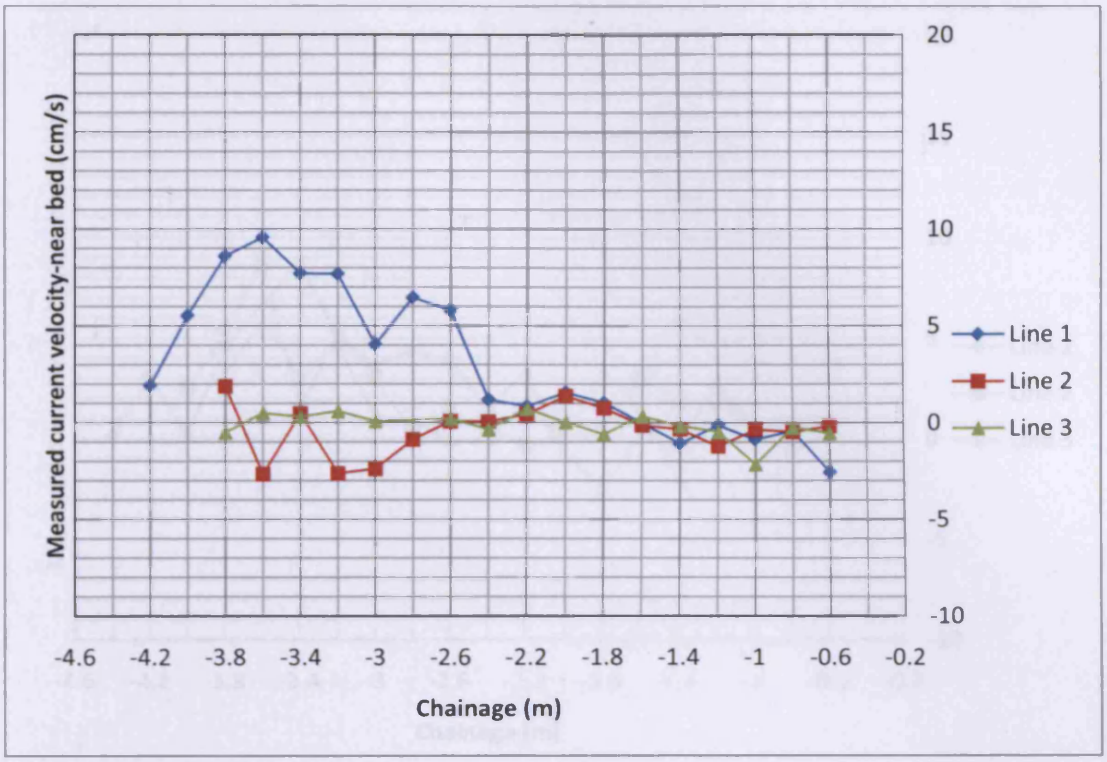

Figure 5-22 Near bed cross-shore current velocity (Test 5)

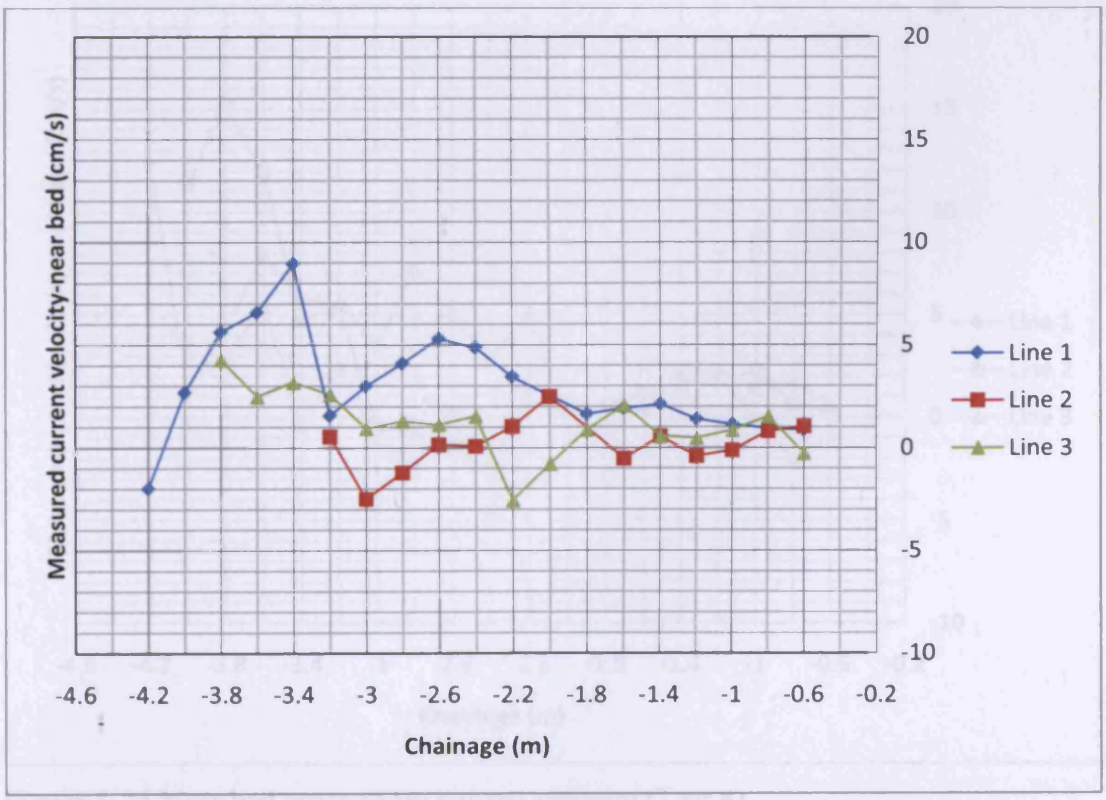

Figure 5-23 Near bed cross-shore current velocity (Test 6)

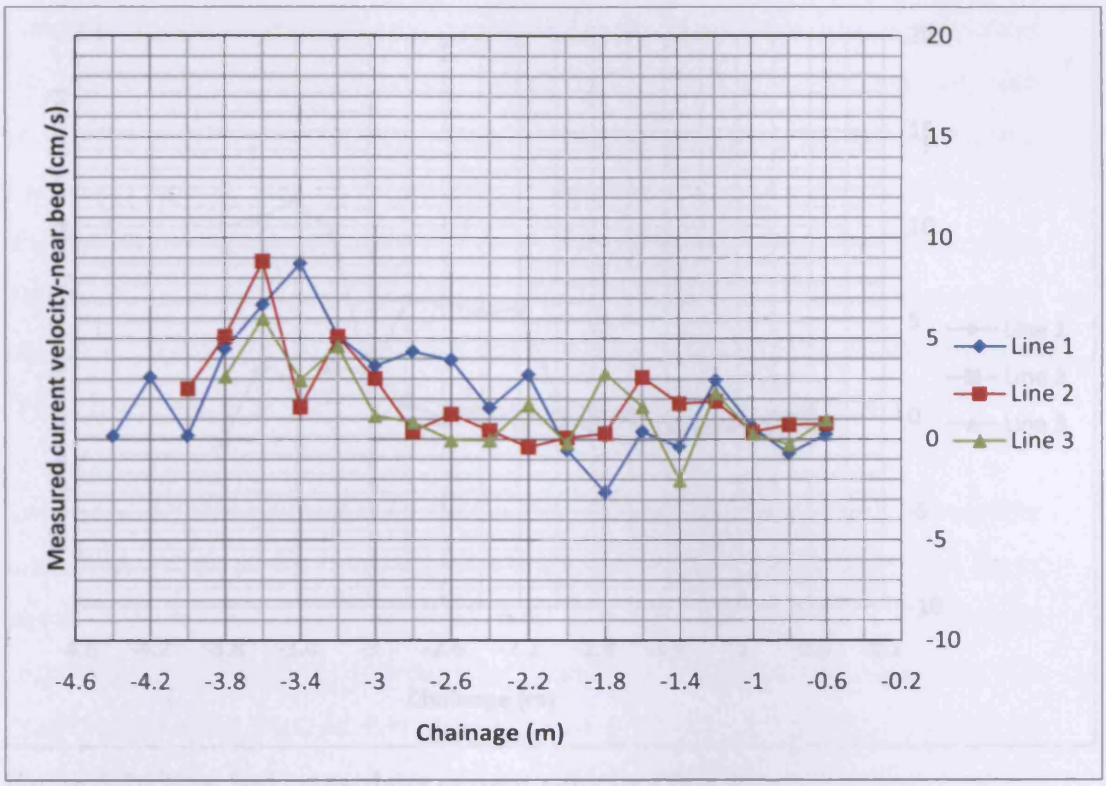

Figure 5-24 Near bed cross-shore current velocity (Test 7)

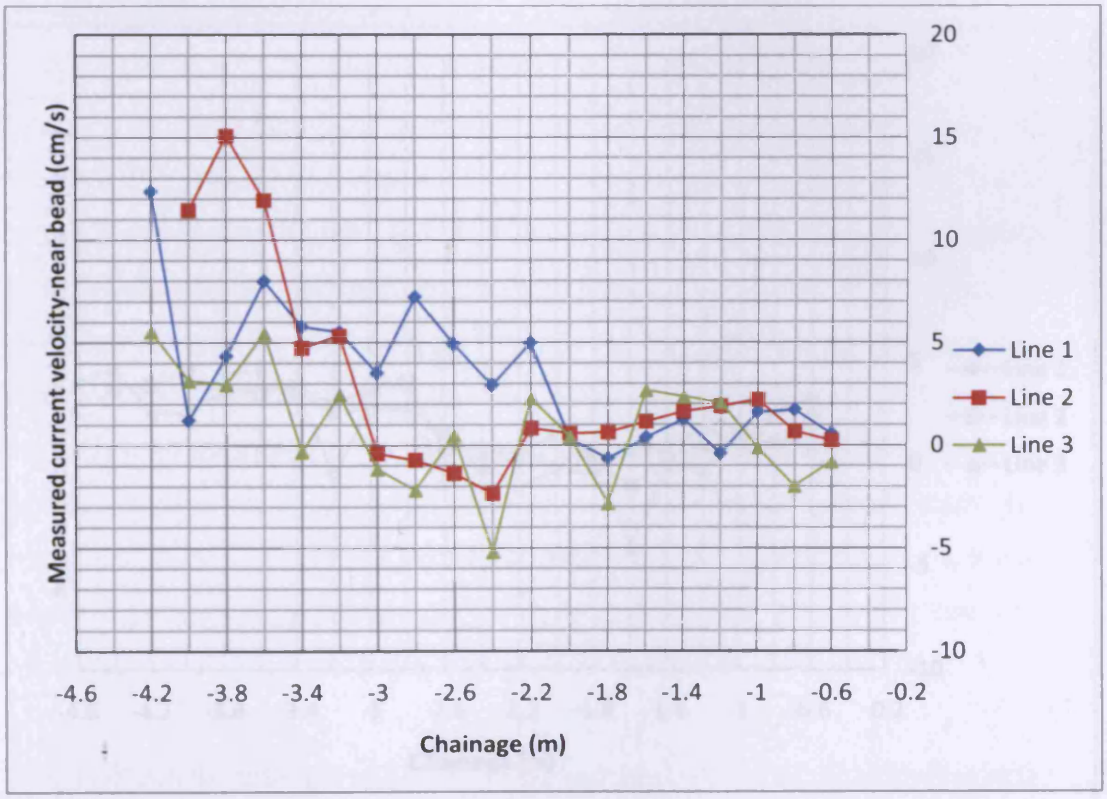

Figure 5-25 Near bed cross-shore current velocity (Test 8)

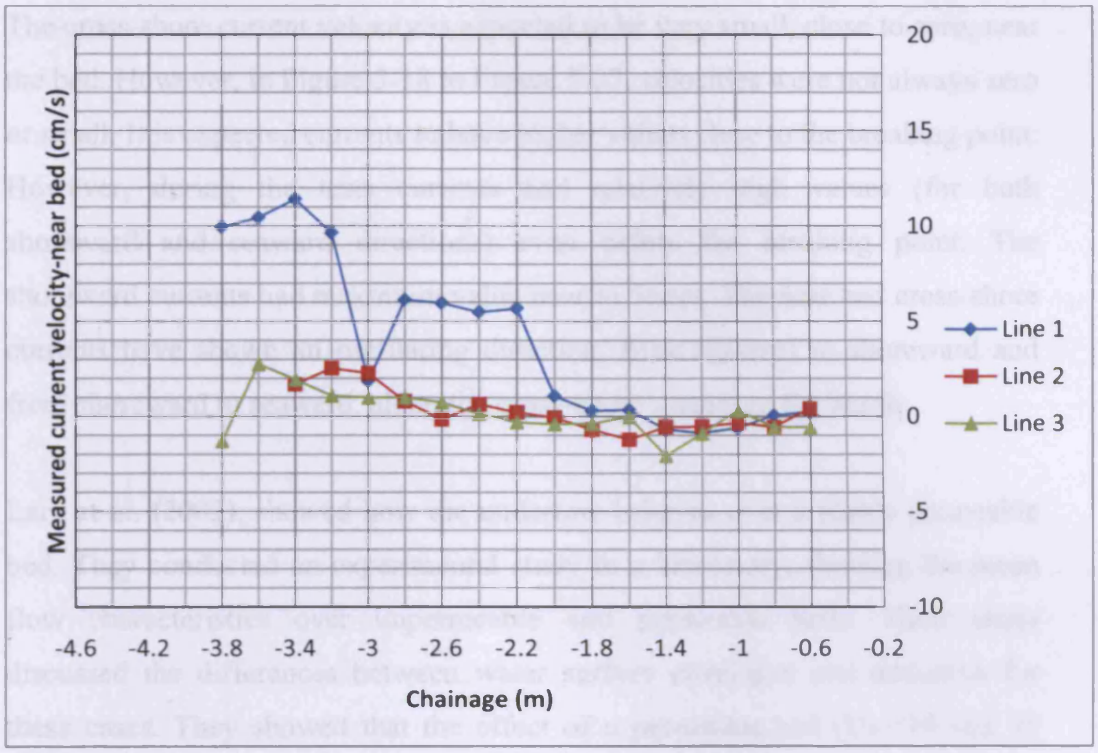

Figure 5-26 Near bed cross-shore current velocity (Test 9)

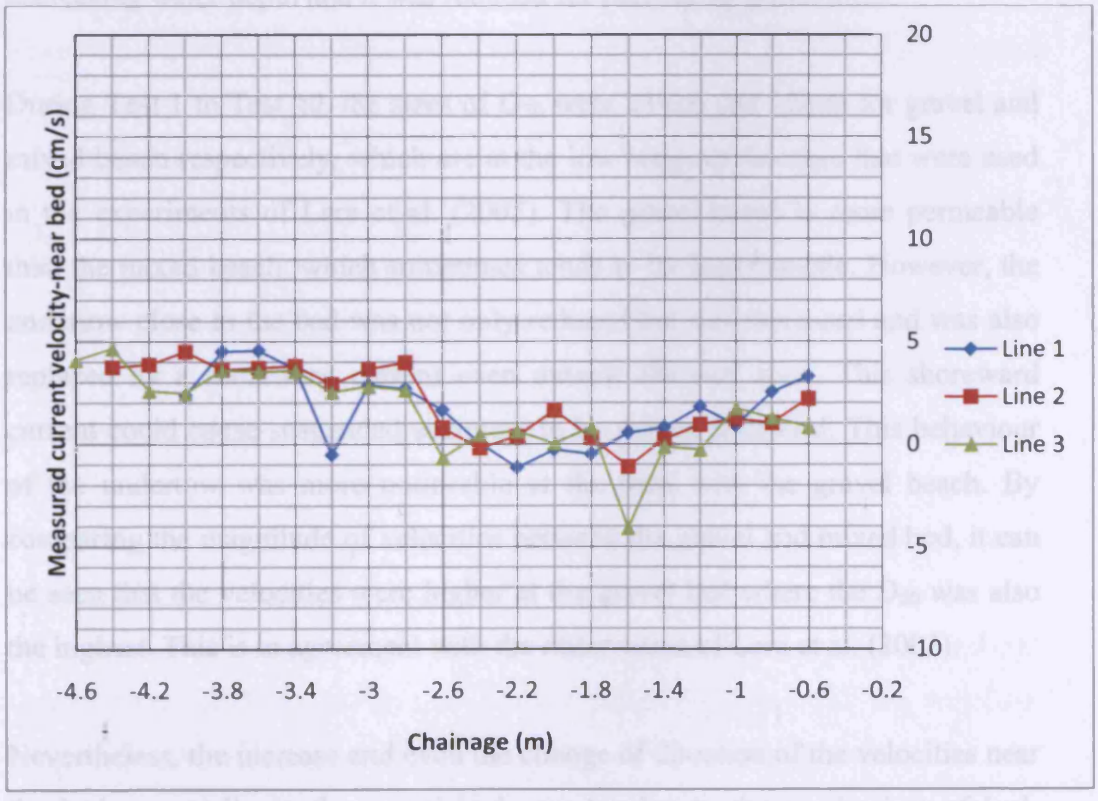

Figure 5-27 Near bed cross-shore current velocity (Test 10)

The cross-shore current velocity is expected to be very small, close to zero, near the bed. However, in Figure 5-18 to Figure 5-27, velocities were not always zero or small. It is expected currents to have higher values close to the breaking point. However, during the tests currents had relatively high values (for both shoreward and seaward directions) even before the breaking point. The shoreward currents had maximum value near to 5cm/s. The near bed cross-shore currents have shown an oscillating direction, from seaward to shoreward and from shoreward to seaward, along the cross-shore section of the beach.

Lara et al. (2002), showed how the undertow behaves over a highly permeable bed. They conducted an experimental study in a laboratory, showing the mean flow characteristics over impermeable and permeable beds. Their study discussed the differences between water surface envelopes and undertow for these cases. They showed that the effect of a permeable bed (D_{50}=19 and 39 mm) on the undertow is a change of the velocity profile, with the magnitude of undertow close to the seafloor reduced. This effect was more important in decreasing water depth and it was reduced for decreasing gravel size.

During Test 1 to Test 10, the sizes of D_{50} were 23mm and 12mm for gravel and mixed beach respectively, which are at the low range of the ones that were used in the experiments of Lara et al. (2002). The gravel beach is more permeable than the mixed beach, which sometimes tends to be impermeable. However, the undertow close to the bed was not only reduced but was increased and was also replaced by a shoreward current even outside the surf zone. This shoreward current could cause suspended sediment to be moved landward. This behaviour of the undertow was more noticeable at the tests with the gravel beach. By comparing the magnitude of velocities between the gravel and mixed bed, it can be seen that the velocities were higher at the gravel bed where the D_{50} was also the highest. This is in agreement with the observation of Lara et al. (2002).

Nevertheless, the increase and even the change of direction of the velocities near the bed, especially in the gravel bed, can be due to the mechanism of bed-

generated turbulence. Lara et al. (2002) stated that the gravel bed-generated turbulence characteristics depend on the gravel size and increasing gravel size results in an increase in the velocity gradient, which is the principal mechanism for the generation of larger-scale turbulence over the gravel bed. This mechanism of bed-generated turbulence has been noticed by Buffin-Bélanger et al. (2000) and Shvidchenko et al. (2001) over gravel bed rivers resulting in Reynolds stresses that have different signs, revealing different vortex orientation (Lara et al., 2002).

In the surf zone, the turbulence can be related to the type of breaking because partly or even the whole mechanism for the generation of turbulence is induced to the breaking process. The characteristics of turbulence structure and undertow are different in spilling and plunging breakers. Turbulent kinetic energy is transported seaward under the spilling breaker. This is different from the plunging breaker where turbulent kinetic energy is transported landward (Ting and Kirby, 1994).

Therefore, more experiments with different types of breaking, different water depths and different sizes of gravel and mixed (gravel and sand) could help in understanding this behaviour of the undertow, in depth.

5.2.1.2 *Comparison with other existing methods*

In this section, a comparison is given with other existing formulations that calculate the time-averaged and depth-averaged undertow. Various authors have presented models for predicting cross-shore currents, especially undertow.

Kuriyama and Nakatsukasa (2000) developed a one-dimensional model which predicts the time- and depth- averaged undertow velocities. The model was calibrated with field data obtained over longshore bars at Hazaki Oceanographical Research Station (HORS) and it predicted well the undertow over the longshore bars.

Grasmeijer and Ruessink (2003) presented a hydrodynamic model that can predict also the time-averaged cross-shore currents (undertow) in a parametric and probabilistic mode. The model was calibrated with laboratory and field experiments and it predicted well the undertow.

Recently, Tajima and Madsen (2006) developed a near-shore current model based on Tajima and Madsen's (2002, 2003) wave and surface roller models. There was a generally good agreement of predicted the undertow velocity profiles by using the model.

Pedrozo-Acuna et al. (2006) presented an estimation of the value of the undertow velocity from a Boussinesq model by explicitly allowing for the higher velocity in the roller region of a breaking wave front (e.g. Madsen et al., 1997). The value of undertow Uo was written as

Eq.5-37 $$U_o = \left\langle \frac{M - c\delta}{\zeta + h - \delta} \right\rangle$$

where,

Eq.5-38 $$M = (h+\zeta)\left[u_a + \left(\frac{1}{2}{z_a}^2 - \frac{1}{6}(\zeta^2 - \zeta h + h^2)\right)\nabla(\nabla u_a) + \left(z_a + \frac{1}{2}(h-\zeta)\right)\nabla[\nabla(h u_a)] \right].$$

ζ is the free surface elevation, h is the local water depth, u_a is the reference horizontal velocity at the elevation given by z_a (z_a=-0.531h, Nwogu,1993), c is the wave celerity and δ is the roller thickness. The roller contribution is minimal (Pedrozo-Acuna et al., 2006).

The experimental data was compared with the models of Kuriyama and Nakatsukasa (2000) and Grasmeijer and Ruessink (2003). The model of Grasmeijer and Ruessink (2003) was used in parametric mode as its authors stated that it would give the same accuracy with a computationally quicker approach than the probabilistic mode. The calculation procedures of both models are presented in Appendix III (A3 and A4).

Both models used the mass flux due to the wave motion and the mass flux due to the surface roller to estimate the undertow velocity. However, each of the models calculated these mass fluxes in a different way. The model of Kuriyama and Nakatsukasa (2000) did not include the angle of incidence; however, in the comparison with the experimental results, it was included. At the model of Grasmeijer and Ruessink (2003), the procedure of calculating the roller area was not described. However, in the comparison with the experimental results, the roller area was presented and calculated twice based on the following two equations:

Engelund (1981) made a simple dynamic model of a hydraulic jump, which is based on the depth-integrated horizontal momentum equation and gives the local thickness of the surface roller. Engelund assumed that the boundary between surface roller and the water below is a straight line. Using an analogy between the velocity distribution in separated diffuser flow and in the hydraulic jump, it was argued that the angle θ between this boundary and the horizontal is about 10^0. With accuracy within a few per cent the roller area obtained by the model of Engelund (1981) can be calculated as

Eq.5-39 $$A = \frac{H^2}{\tan\theta}\frac{H/h}{4}$$

Duncan (1981) has made measurements of rollers in waves that have been generated by a towel hydrofoil. Svendsen (1984b) approximated these results with the relation

Eq.5-40 $$A = 0.9H^2$$

The graphical presentations of the comparison of the experimental undertow velocities results, for all Lines and all tests, with the two models are shown in the following figures (the positive values represent the undertow velocities).

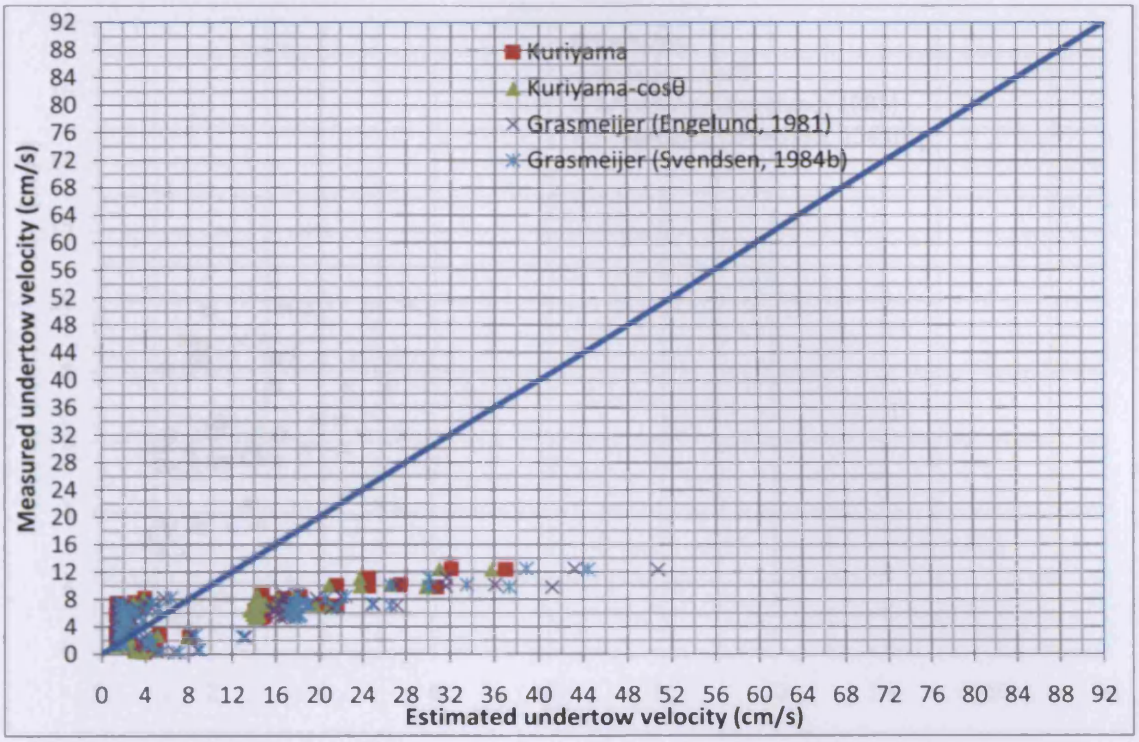

Figure 5-28 Estimated vs. Measured undertow velocity (Regular waves/gravel beach - Line1)

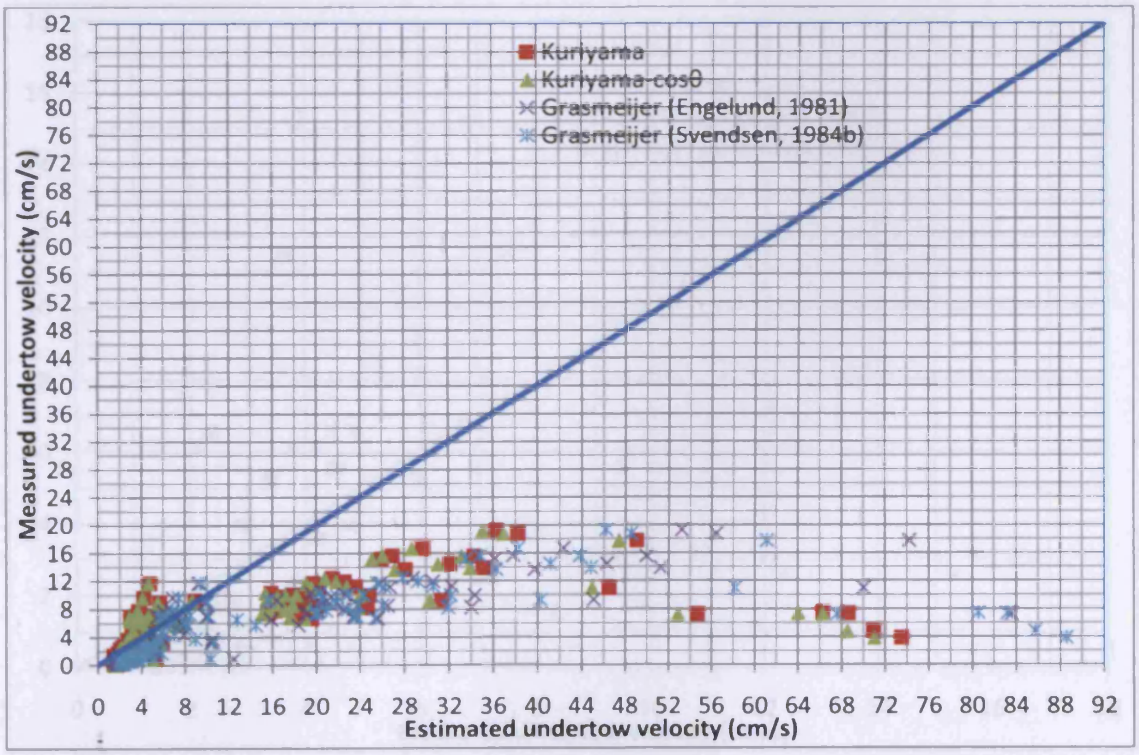

Figure 5-29 Estimated vs. Measured undertow velocity (Regular waves/gravel beach- Lines 2 & 3)

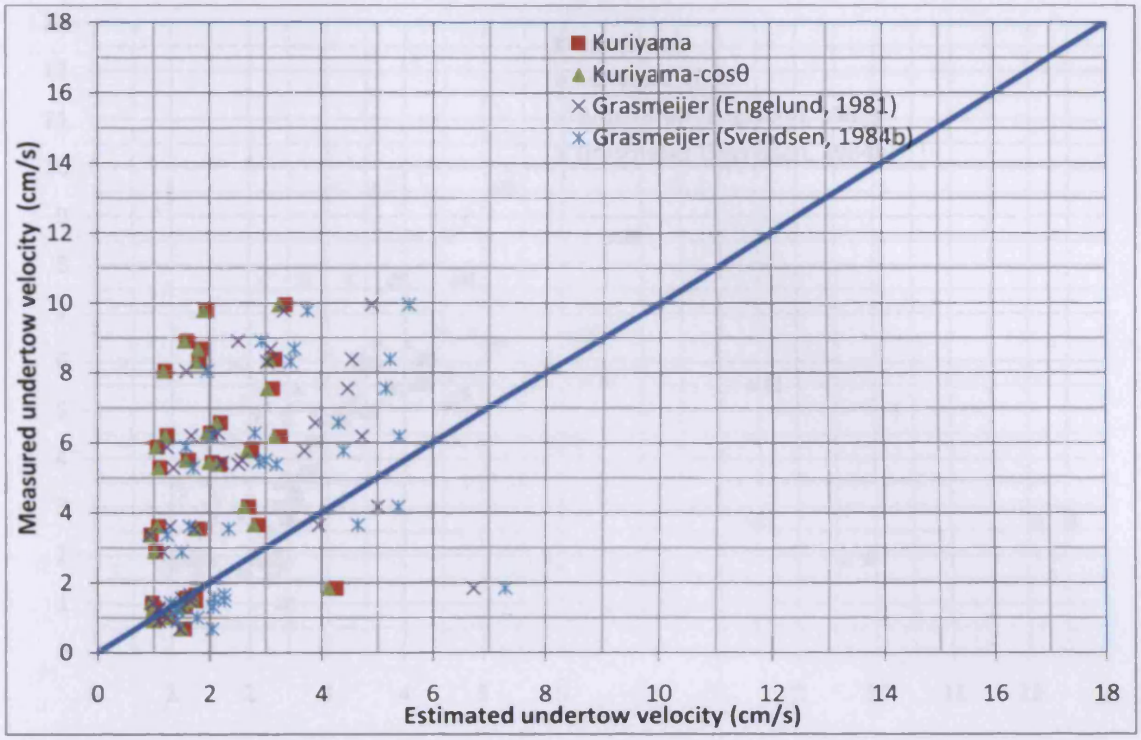

Figure 5-30 Estimated vs. Measured undertow velocity (Regular waves/mixed beach- Line1)

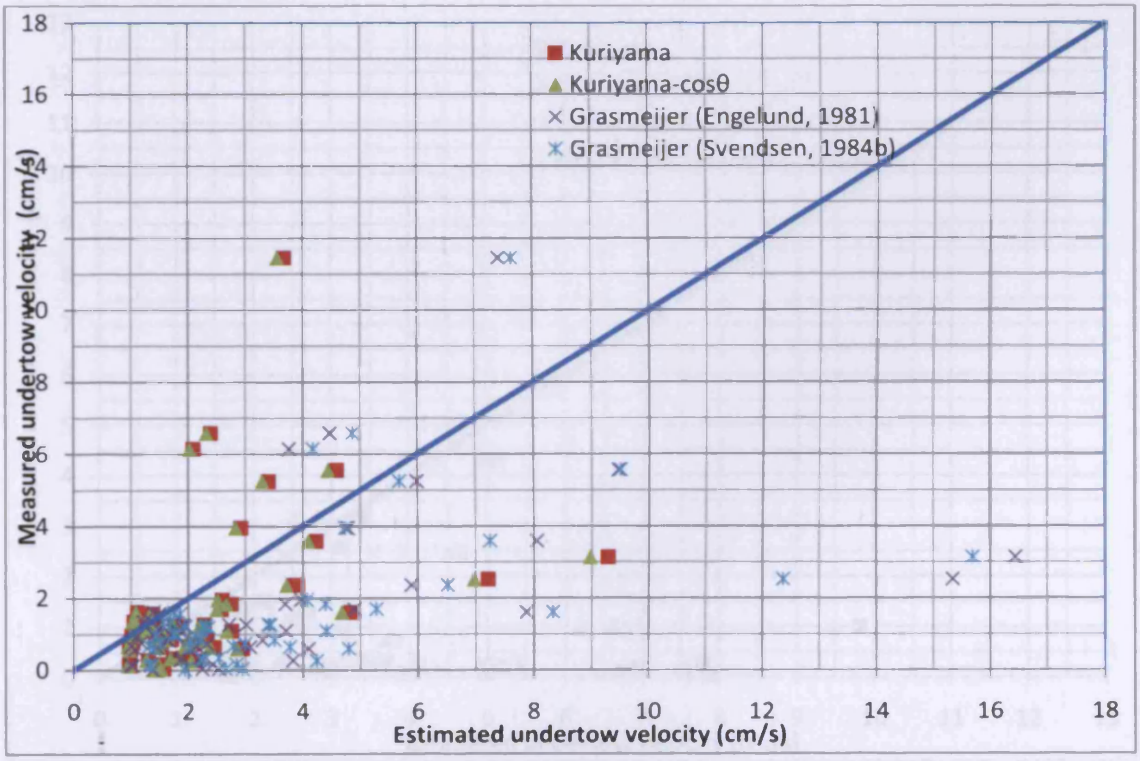

Figure 5-31 Estimated vs. Measured undertow velocity (Regular waves/mixed beach- Lines 2 & 3)

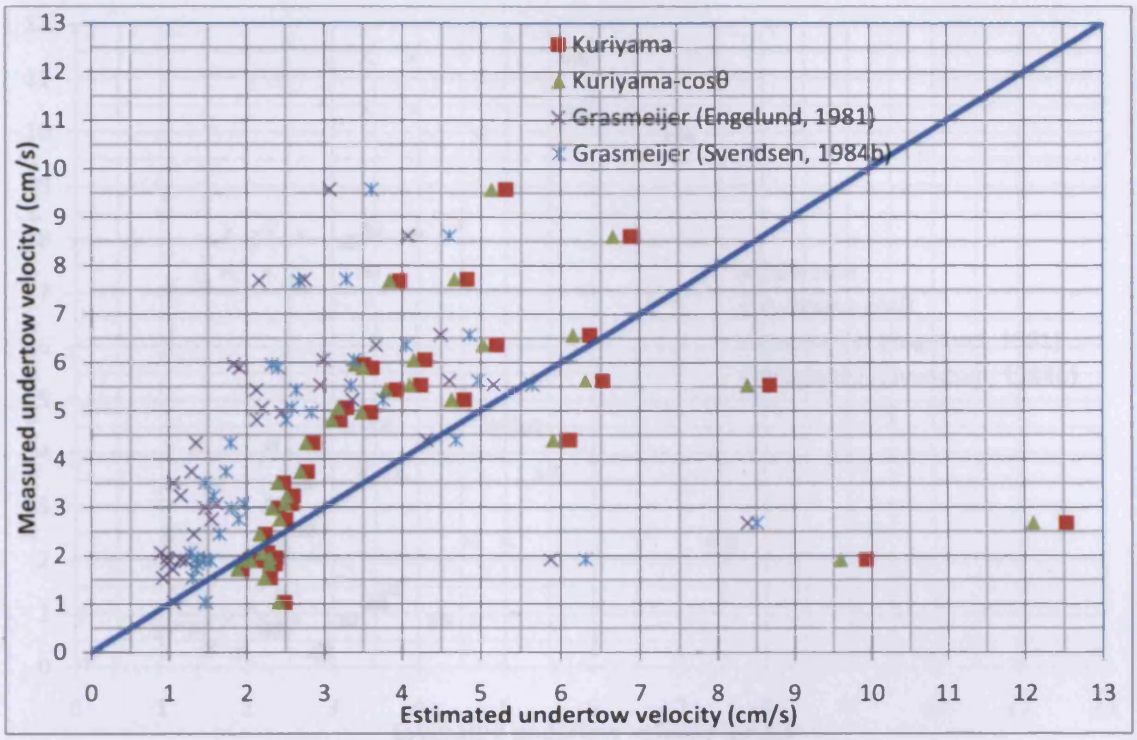

Figure 5-32 Estimated vs. Measured undertow velocity (Random waves/gravel beach- Line1)

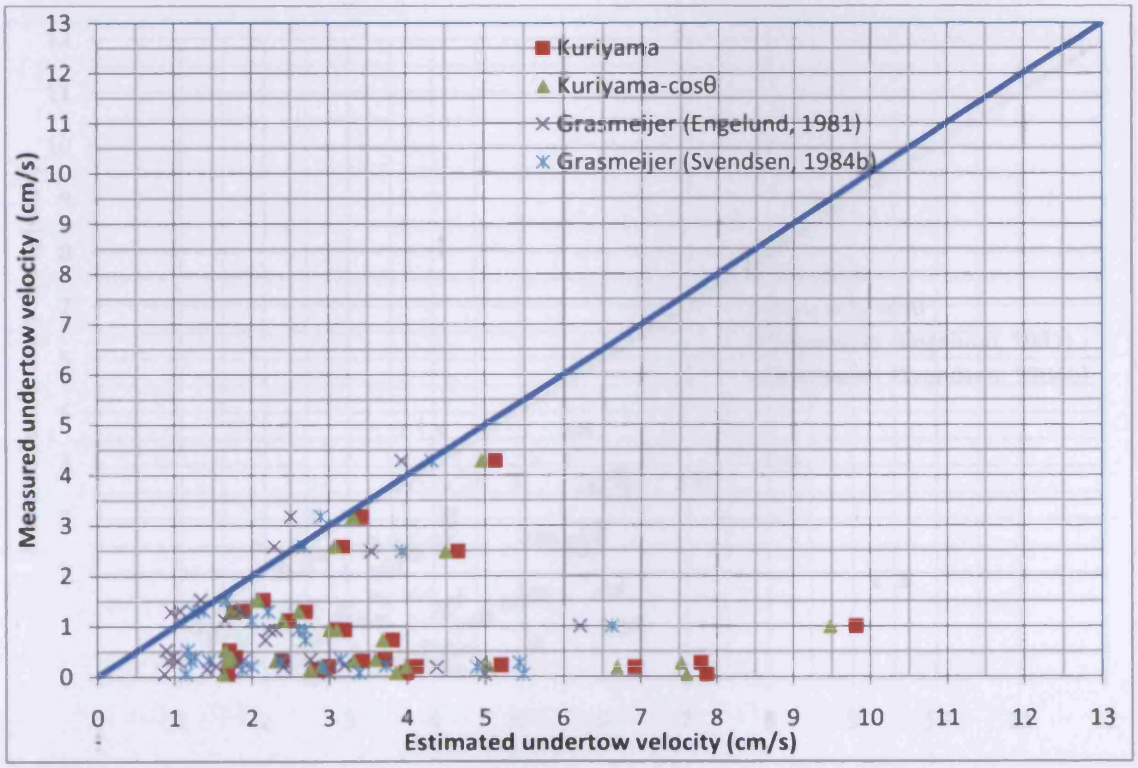

Figure 5-33 Estimated vs. Measured undertow velocity (Random waves/gravel beach- Lines 2 & 3)

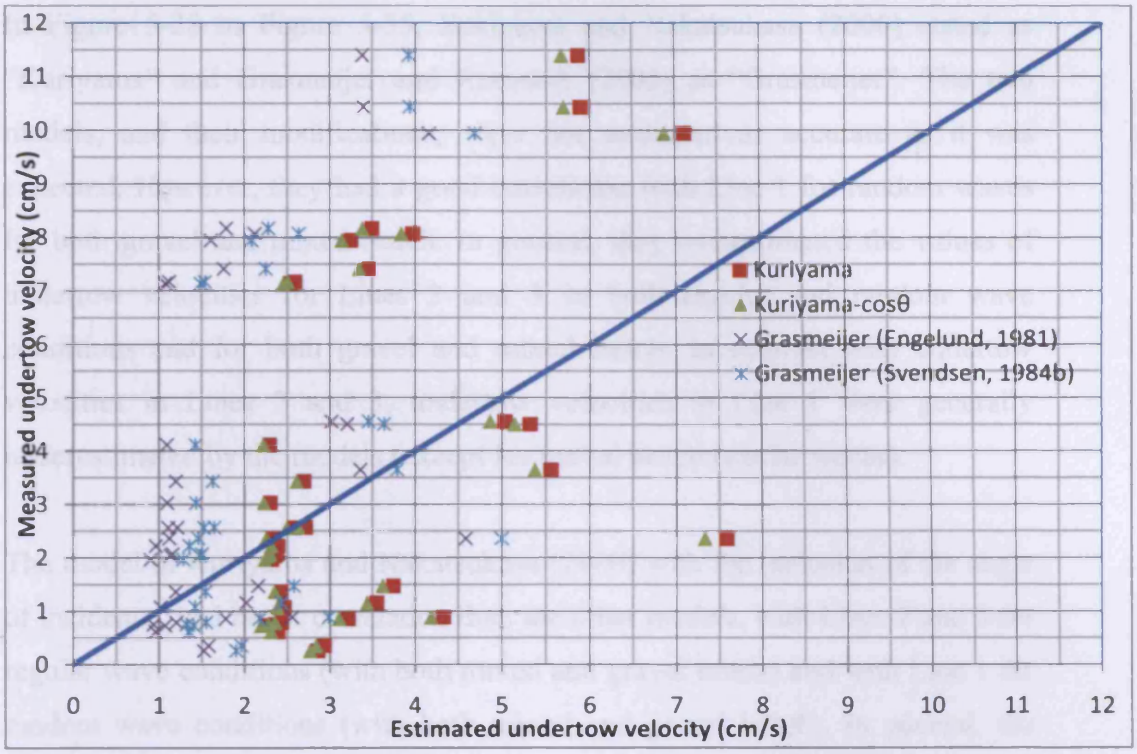

Figure 5-34 Estimated vs. Measured undertow velocity (Random waves/mixed beach- Line1)

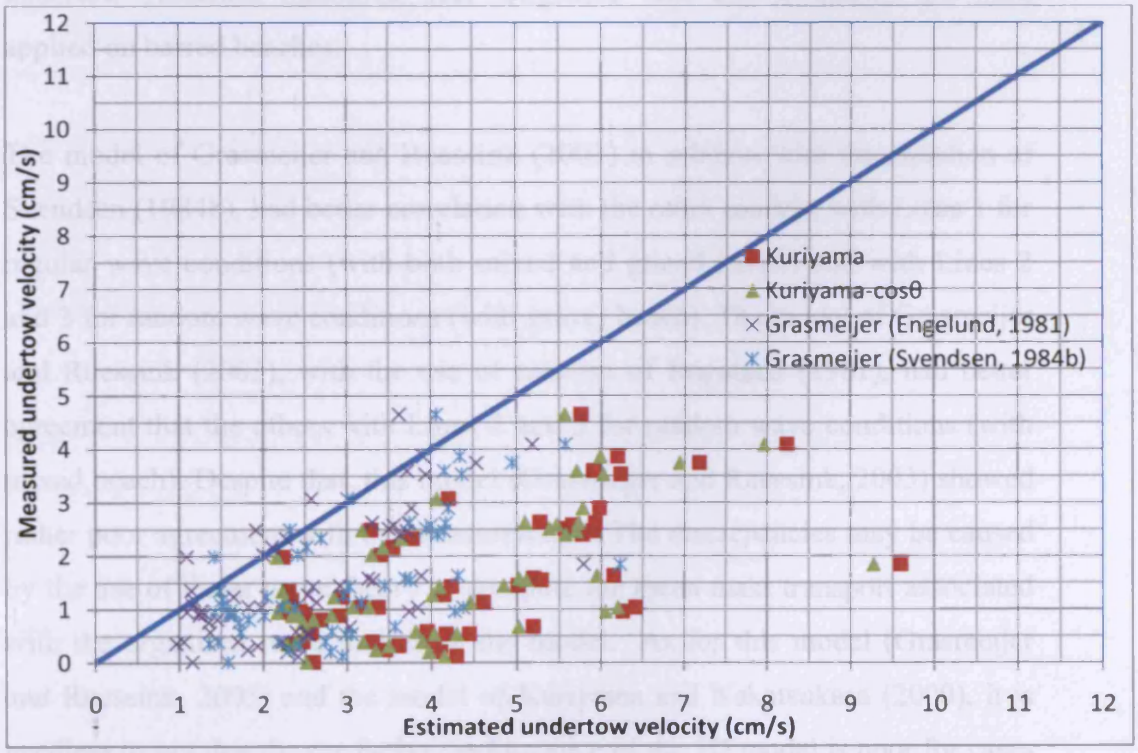

Figure 5-35 Estimated vs. Measured undertow velocity (Random waves/mixed beach- Lines 2 & 3)

In Figure 5-28 to Figure 5-35, Kuriyama and Nakatsukasa (2000) stated as "Kuriyama" and Grasmeijer and Ruessink (2003) as "Grasmeijer". The two models, and their modifications, were not estimated as accurate as it was expected. However, they had a good correlation with Line 1 for random waves for both gravel and mixed beach. In general, they overestimated the values of undertow velocities for Lines 2 and 3 in both regular and random wave conditions and for both gravel and mixed beach. In contrast with undertow velocities in Lines 2 and 3, undertow velocities in Line 1 were generally underestimated by the models (except for gravel beach-regular waves).

The model of Kuriyama and Nakatsukasa (2000) with the inclusion of the angle of incidence, had better correlation than the other models, with Lines 2 and 3 for regular wave conditions (with both mixed and gravel beach) and with Line 1 for random wave conditions (with both mixed and gravel beach). In general, the correlations of this model (Kuriyama and Nakatsukasa, 2000) with the measured data were poor because it was initially developed and calibrated with the undertow velocities measured over longshore bars and it mainly has been applied on barred beaches.

The model of Grasmeijer and Ruessink (2003) in relation with the equation of Svendsen (1984b), had better correlation with the other models, with Lines 1 for regular wave conditions (with both mixed and gravel beach) and with Lines 2 and 3 for random wave conditions (with gravel beach). The model of Grasmeijer and Ruessink (2003), with the use of relation of Engelund (1981), had better agreement that the others with Lines 2 and 3 for random wave conditions (with mixed beach). Despite that, this model (Grasmeijer and Ruessink, 2003) showed rather poor agreement with the measurements. The discrepancies may be caused by the use of linear wave theory to compute the mean mass transport associated with the organised wave motion in the model. As for this model (Grasmeijer and Ruessink, 2003) and the model of Kuriyama and Nakatsukasa (2000), it is needless to say that the predictive performance of the 2D model is poor for cases where 3D circulations are important.

Nevertheless, based on a non-linear regression analysis, an attempt has been made to generate empirical relations and to predict much more accurate experimental results. These empirical relations are based on the results of the model Grasmeijer and Ruessink (2003). The non-linear regression has been fitted to the data and the proposed fits are shown by the following equations:

-Regular Waves

For gravel beach (trench) $-R^2=0.998$

Eq.5-41 $$\frac{U}{u_{GB}} = -2278.898 + \frac{6828.806}{X} + 775.664A - \frac{6748.670}{X^2} - 87.836A^2 - 1563.506\frac{A}{X} + \frac{2199.256}{X^3} + 3.224A^3 + 89.543\frac{A^2}{X} + 776.899\frac{A}{X^2} + AX$$

For gravel beach (uniform slope) $-R^2=0.999$

Eq.5-42 $$\frac{U}{u_{GB}} = 0.333 + 2.815\ln(X) + 5.709\ln(X)^2 - 19.254\ln(X)^3 + 6.966\ln(X)^4 - 0.906\ln(X)^5 - 1.215A - 0.134A^2 + (4.4x10^{-3})A^3 + (2.86x10^{-4})A^4 - (2.729x10^{-7})A^5 + AX$$

For mixed beach (trench) $-R^2=0.999$

Eq.5-43 $$\frac{U}{u_{GB}} = -160.807 + 19.584X - 11.530X^2 + 2.695X^3 - 0.304X^4 + 0.01268X^5 + \frac{1933.442}{A} - \frac{10066.703}{A^2} + \frac{25203.259}{A^3} - \frac{29766.799}{A^4} + \frac{13102.164}{+A^5} + AX$$

For mixed beach (uniform slope) $-R^2=0.999$

Eq.5-44 $$\frac{U}{u_{GB}} = 0.135 + 1.015\ln(X) - 1.044A + 38.768\ln(X)^2 + 0.686A^2 - 11.093\ln(X)A + 1.734\ln(X)^3 - 0.13A^3 + 1.902\ln(X)A^2 - 8.27\ln(X)^2A + AX$$

-Random Waves

For gravel beach (trench) $-R^2=0.999$

Eq.5-45 $$\frac{U}{u_{GB}} = -53.142 + 127.971X - 112.891X^2 + 49.620X^3 - 11.038X^4 + 0.977X^5 - 1.873A + 0.0282A^2 - 0.016A^3 - 0.00124A^4 + 0.000155A^5 + AX$$

For gravel beach (uniform slope) $-R^2=0.998$

Eq.5- 46 $$\frac{U}{u_{GB}} = 592.981 - \frac{1632.502}{X} - 178.205A + \frac{1485.708}{X^2} + 16.502A^2 + 328.302\frac{A}{X} - \frac{445.855}{X^3} - 0.507A^3 - 15.449\frac{A^2}{X} - 150.941\frac{A}{X^2} + AX$$

For mixed beach (trench) $-R^2=0.990$

Eq.5- 47 $$\frac{U}{u_{GB}} = 33.472 - 64.842X + 47.024X^2 - 18.41X^3 + 3.42X^4 - 0.241X^5 + 4.626A - 2.842A^2 + 0.9A^3 - 0.133A^4 + 0.0068A^5 + AX$$

For mixed beach (uniform slope) $-R^2=0.999$

Eq.5- 48 $$\frac{U}{u_{GB}} = 0.533 + 3.881\ln(X) - 1.553A - 10.534\ln(X)^2 - 0.382A^2 + 3.182\ln(X)A - 127.824\ln(X)^3 + 0.481A^3 - 9.071\ln(X)A^2 + 57.488\ln(X)^2A + AX$$

where

U (cm/s) is the depth- and time-averaged undertow velocity with positive values for seaward direction,

u_{GB} (cm/s) is the value of the output of the model of Grasmeijer and Ruessink (2003),

X is the dimensional parameter which is equal to $\frac{D_i}{D_b}$, and

A is the dimensional parameter which is equal to $\frac{D_t}{h_i}$

The parameters D_i, D_b, D_t and h_i are shown in Figure 5- 36. The breaking depth for regular waves was calculated by Eq.5-4 and for random waves by Eq.5-6. The above equations should be quite reliable when used within the limits of applicability.

The graphical presentations of the comparison of the experimental depth- and time-averaged undertow velocities results, for all Lines and all tests, with the proposal equations (Eq.5-41 to Eq.5- 48) are shown in Figure 5- 37 to Figure 5- 44 (the positive values represent the undertow velocities). In these figures Eq.5-41 to Eq.5- 48 show a generally good agreement with the experimental data.

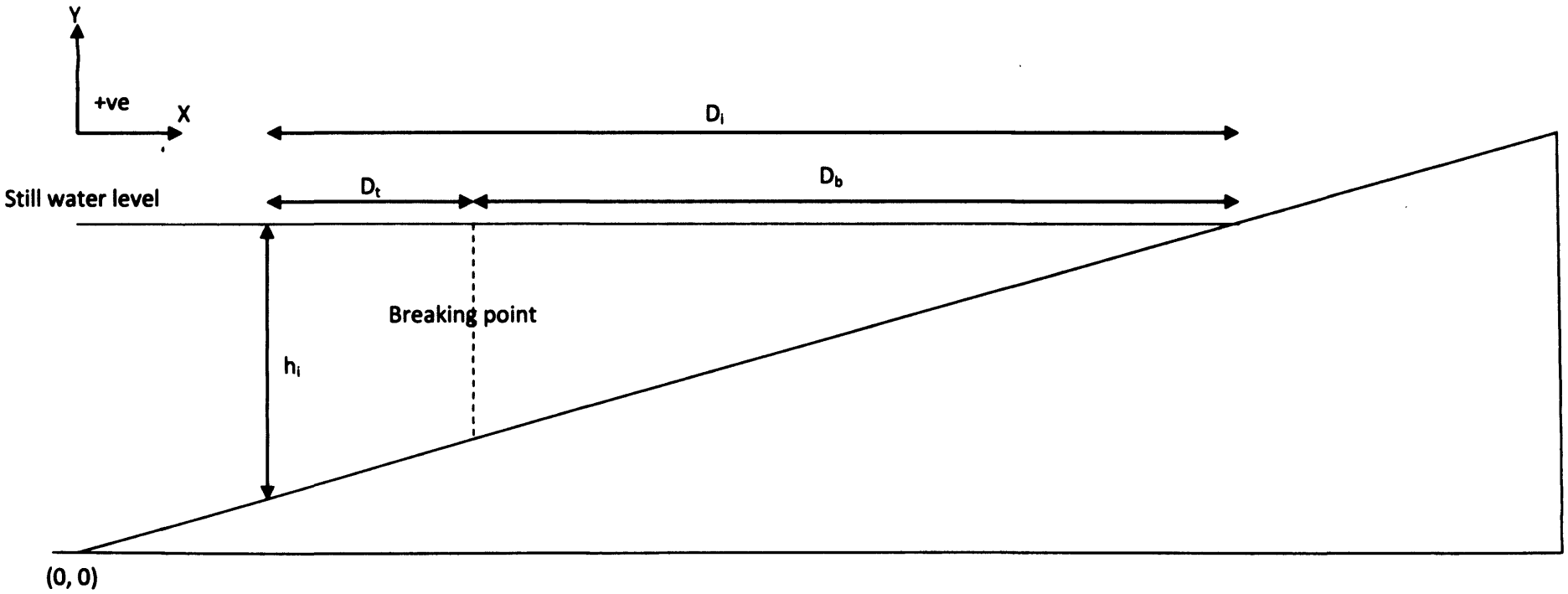

Figure 5- 36 Schematisation of the components of A and X

where,

h_i (m) is the local water depth,

D_t (m) is the distance between the breaking point and the point of interest

D_b (m) is the distance from the point, where the local water depth is equal to the still water level, to the breaking point

D_i (m) is the distance from the point, where the local water depth is equal to the still water level, to the point of interest

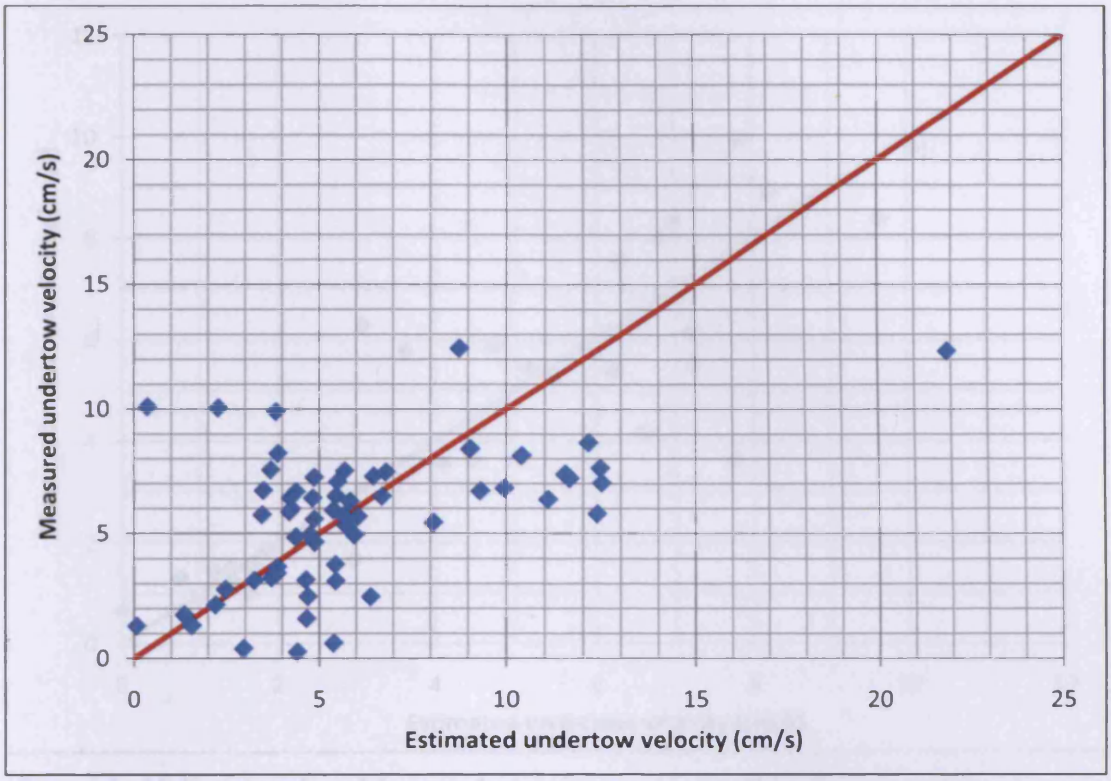

Figure 5- 37 Estimated vs. Measured undertow velocity (Regular waves/gravel beach - Line1)

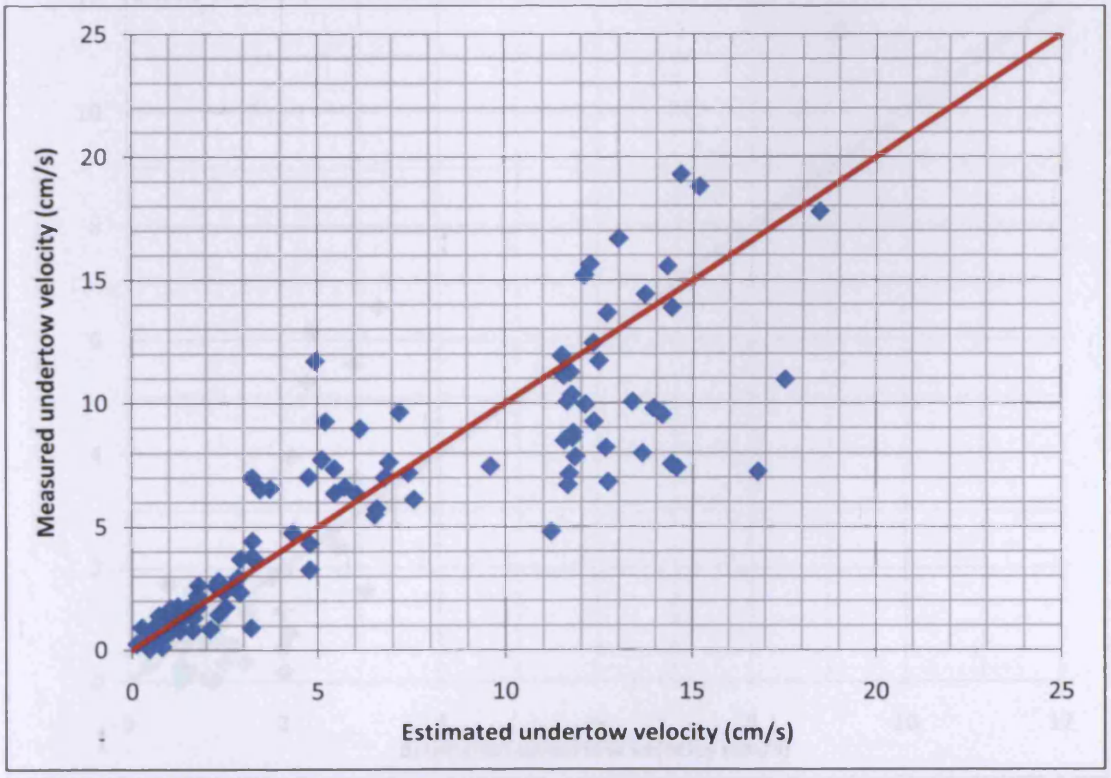

Figure 5- 38 Estimated vs. Measured undertow velocity (Regular waves/gravel beach – Lines 2& 3)

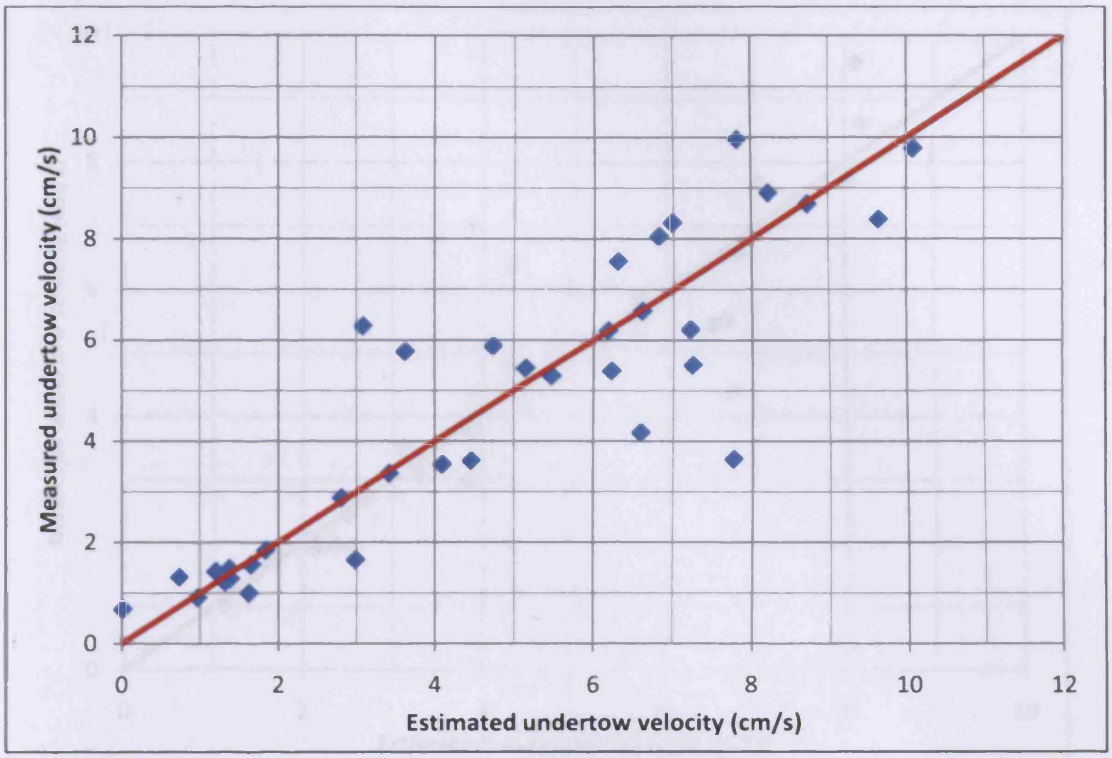

Figure 5- 39 Estimated vs. Measured undertow velocity (Regular waves/Mixed Beach - Line1)

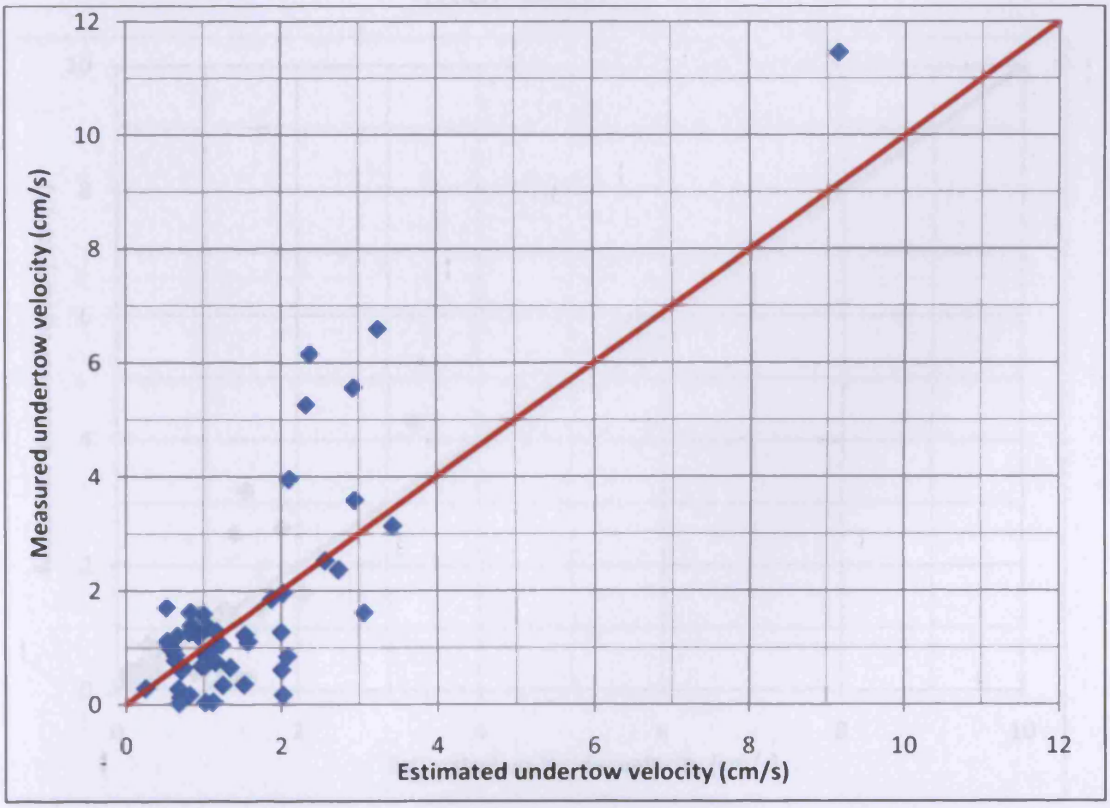

Figure 5- 40 Estimated vs. Measured undertow velocity (Regular waves/Mixed Beach – Lines 2& 3)

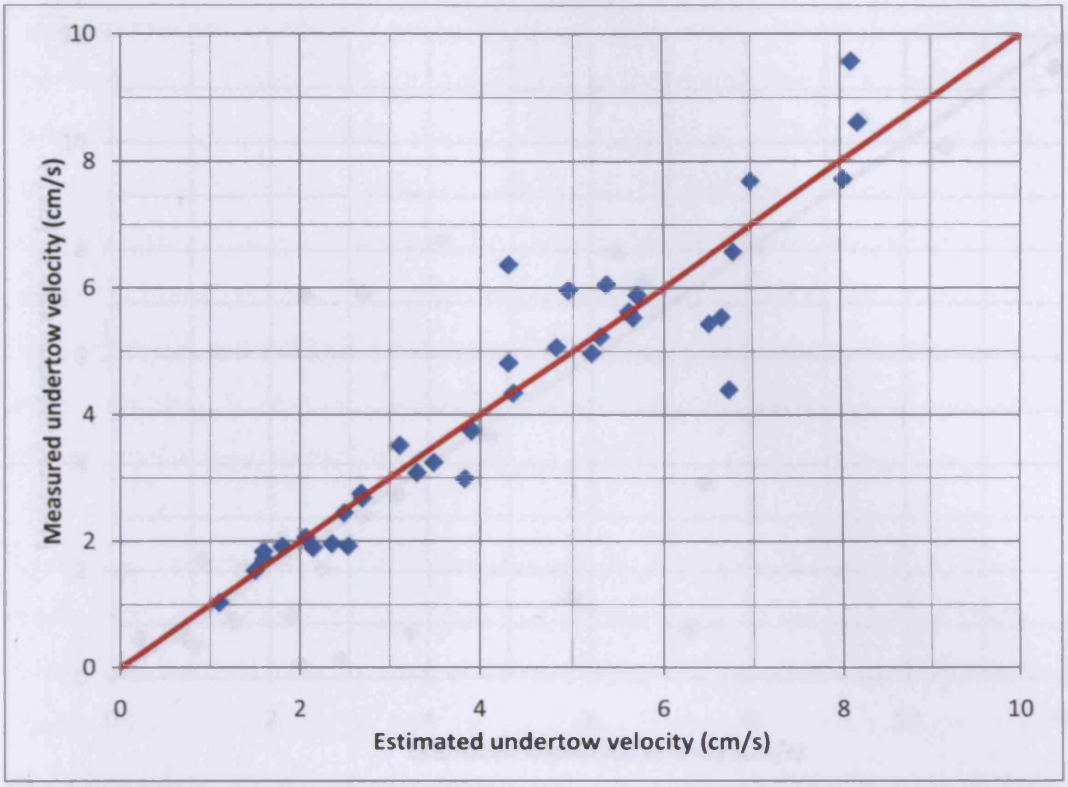

Figure 5- 41 Estimated vs. Measured undertow velocity (Random waves/gravel beach - Line1)

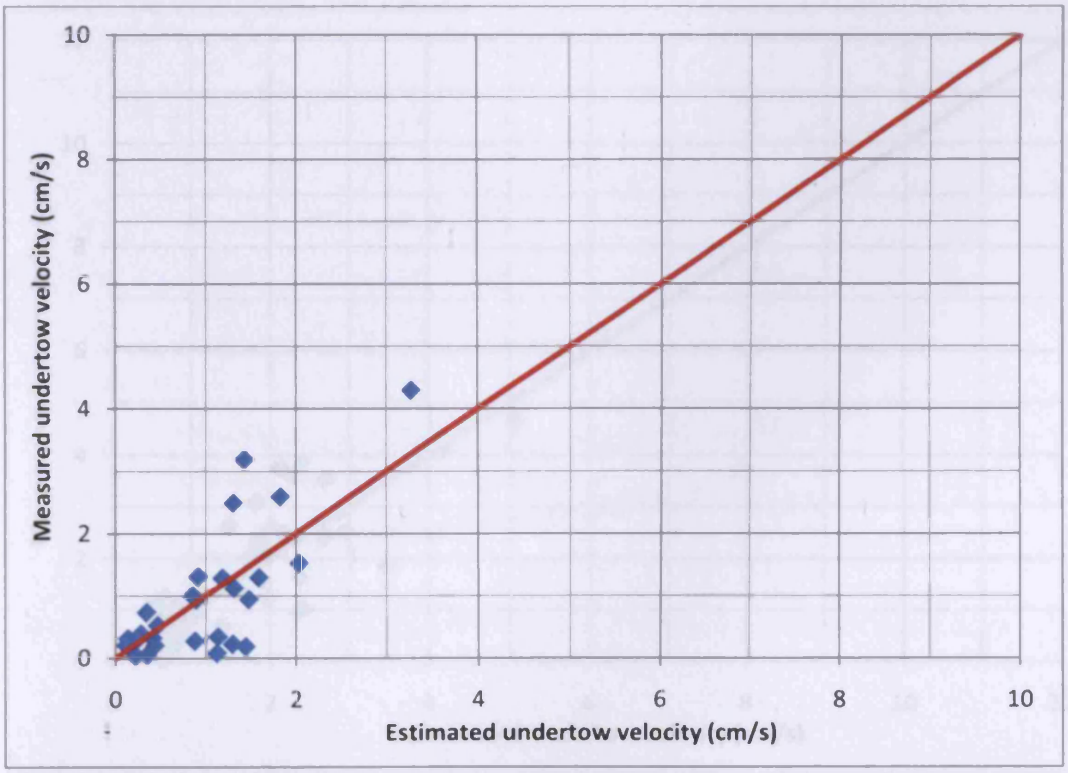

Figure 5- 42 Estimated vs. Measured undertow velocity (Random waves/gravel beach – Lines 2 & 3)

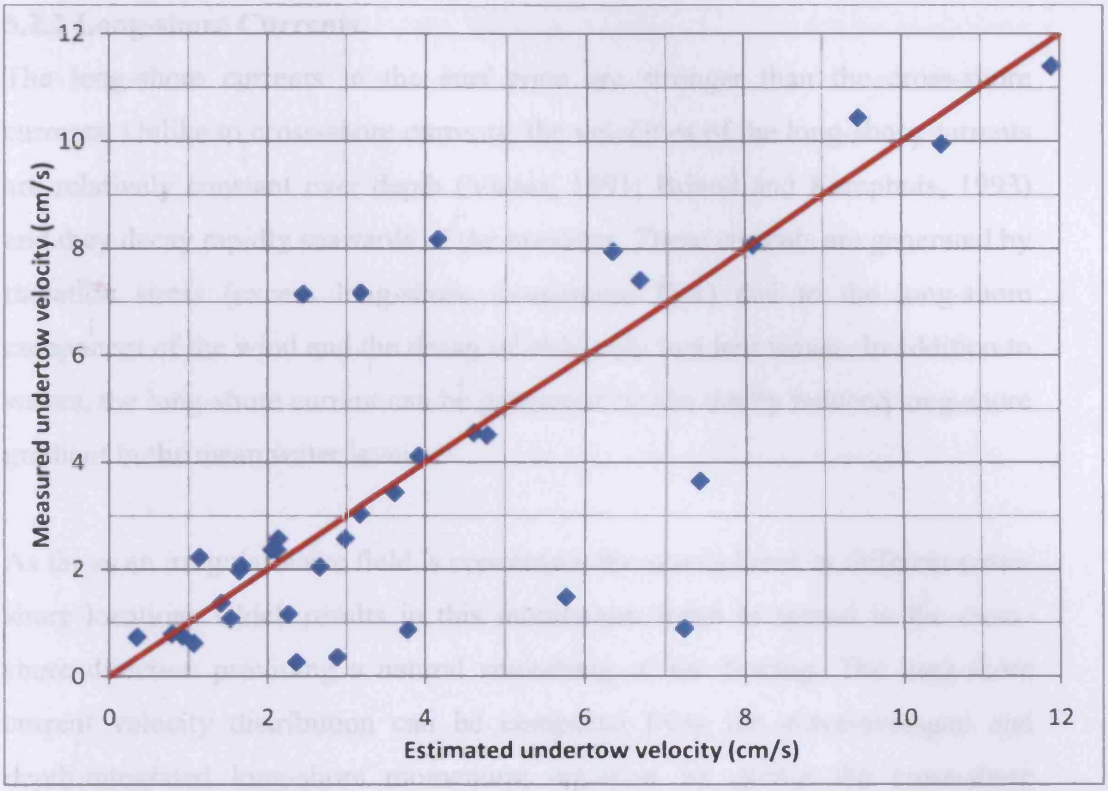

Figure 5- 43 Estimated vs. Measured undertow velocity (Random waves/Mixed Beach - Line1)

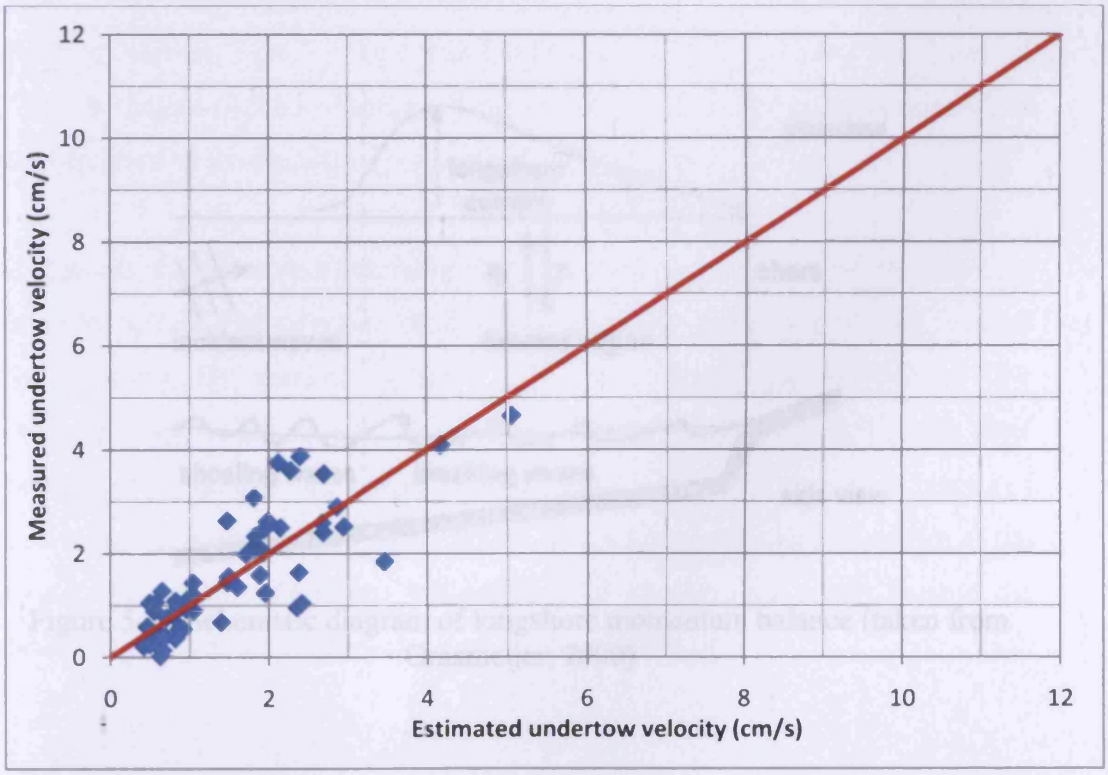

Figure 5- 44 Estimated vs. Measured undertow velocity (Random waves/Mixed Beach – Lines 2 & 3)

5.2.2 Long-shore Currents

The long-shore currents in the surf zone are stronger than the cross-shore currents. Unlike to cross-shore currents, the velocities of the long-shore currents are relatively constant over depth (Visser, 1991; Briand and Kamphuis, 1993) and they decay rapidly seawards of the breakers. These currents are generated by radiation stress (excess long-shore momentum flux) due to the long-shore component of the wind and the decay of obliquely incident waves. In addition to waves, the long-shore current can be generated by the tidally induced long-shore gradient in the mean water level.

As far as an irregular wave field is concerned, the waves break at different cross-shore locations which results in this momentum input to spread in the cross-shore direction providing a natural smoothing of the forcing. The long-shore current velocity distribution can be computed from the wave-averaged and depth-integrated long-shore momentum equation by giving the cross-shore distribution of the forcing due to the breaking waves (Figure 5-45).

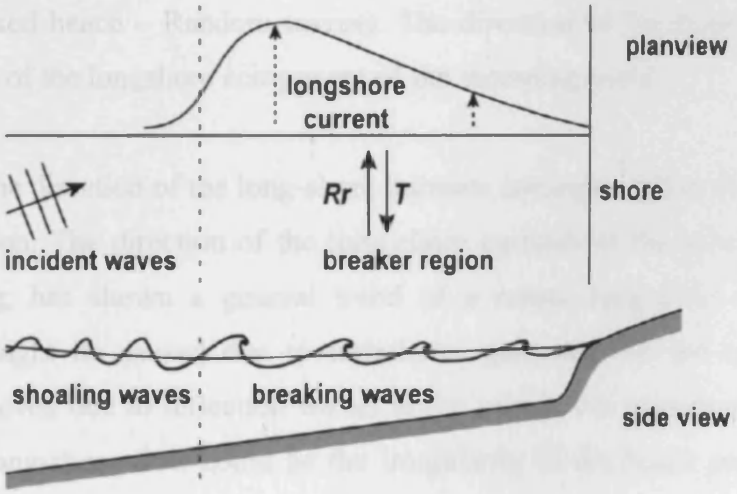

Figure 5-45 Schematic diagram of longshore momentum balance (taken from Grasmeijer, 2000)

A long-shore force R_r on the water column is induced by the excess long-shore momentum flux, and it is balanced by a shear force T which is brought about by a long-shore directed current velocity. The wave breaking produces a turbulence kinematic energy which brings momentum in the form of a roller. The dissipation of this roller is the reason that the mean flow forcing occurs. Svendsen (1984b) was the first to suggest the concept of this wave roller, which represents a region of intense turbulence that lies on and is advected with the steep face of the breaking waves. Thus, shoreward shifts in current forcing patterns can be brought about by the advection of the roller (Grasmeijer, 2000).

5.2.2.1 *Analysis of the experimental results (long-shore currents)*

The long-shore currents that were produced by the wave breaking during the experiment were analysed and can be observed from the two-dimensional presentation of the long-shore currents in Figure 5-46 to Figure 5-55, for all the tests : Test1-Test 4 (gravel beach-Regular waves), Test 5-Test 6 (gravel beach-Random waves), Test 7 – Test 8 (mixed beach –Regular waves) and Test 9 – Test 10 (mixed beach – Random waves). The direction of Vx corresponded to the direction of the longshore component of the incoming wave.

In general, the direction of the long-shore currents corresponded to the incoming wave direction. The direction of the long-shore currents at the trench, close to the breaking, has shown a general trend of a return long-shore flow. This behaviour might be caused due to turbulence generated on the trench after breaking or even due to reflection waves at the trench. An important reason of this return long-shore flow could be the irregularity of the beach profile at the trench. Moreover, this return long-shore flow can be seen partly (before the breaking point) at all the lines for both Test 1 and Test 2.

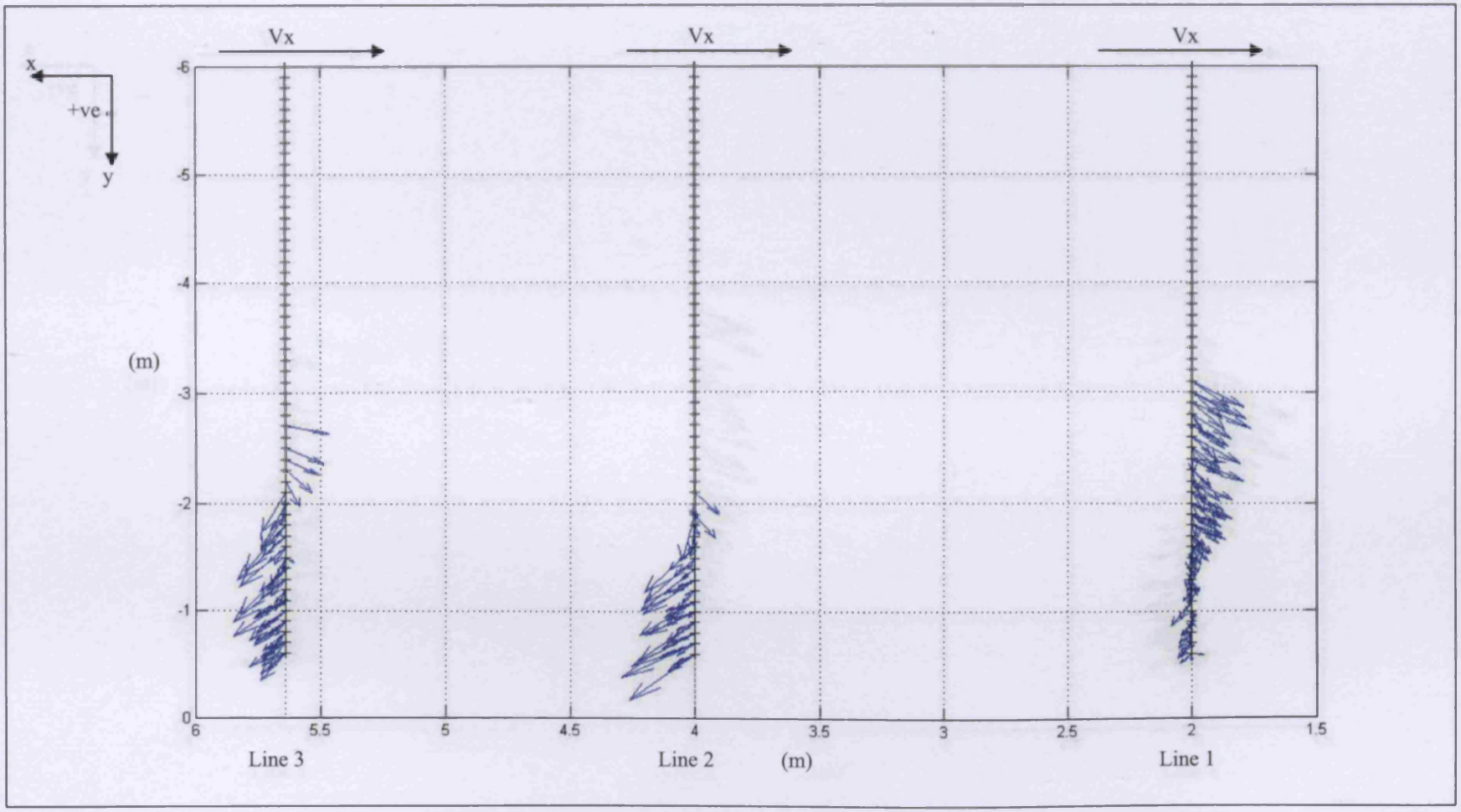

Figure 5-46 Two-dimensional presentation of the long-shore currents during Test 1 (plan view of the beach)

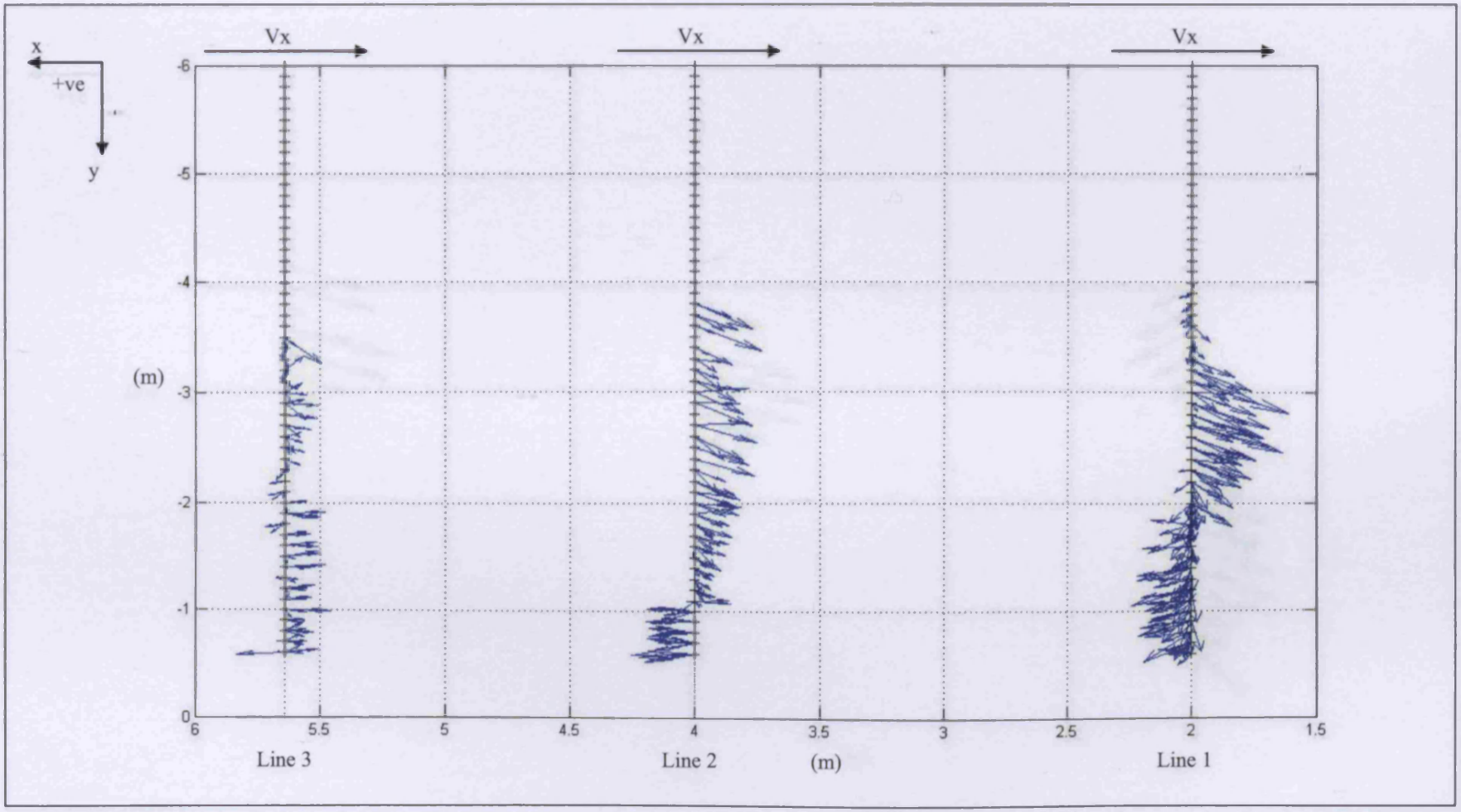

Figure 5-47 Two-dimensional presentation of the long-shore currents during Test 2 (plan view of the beach)

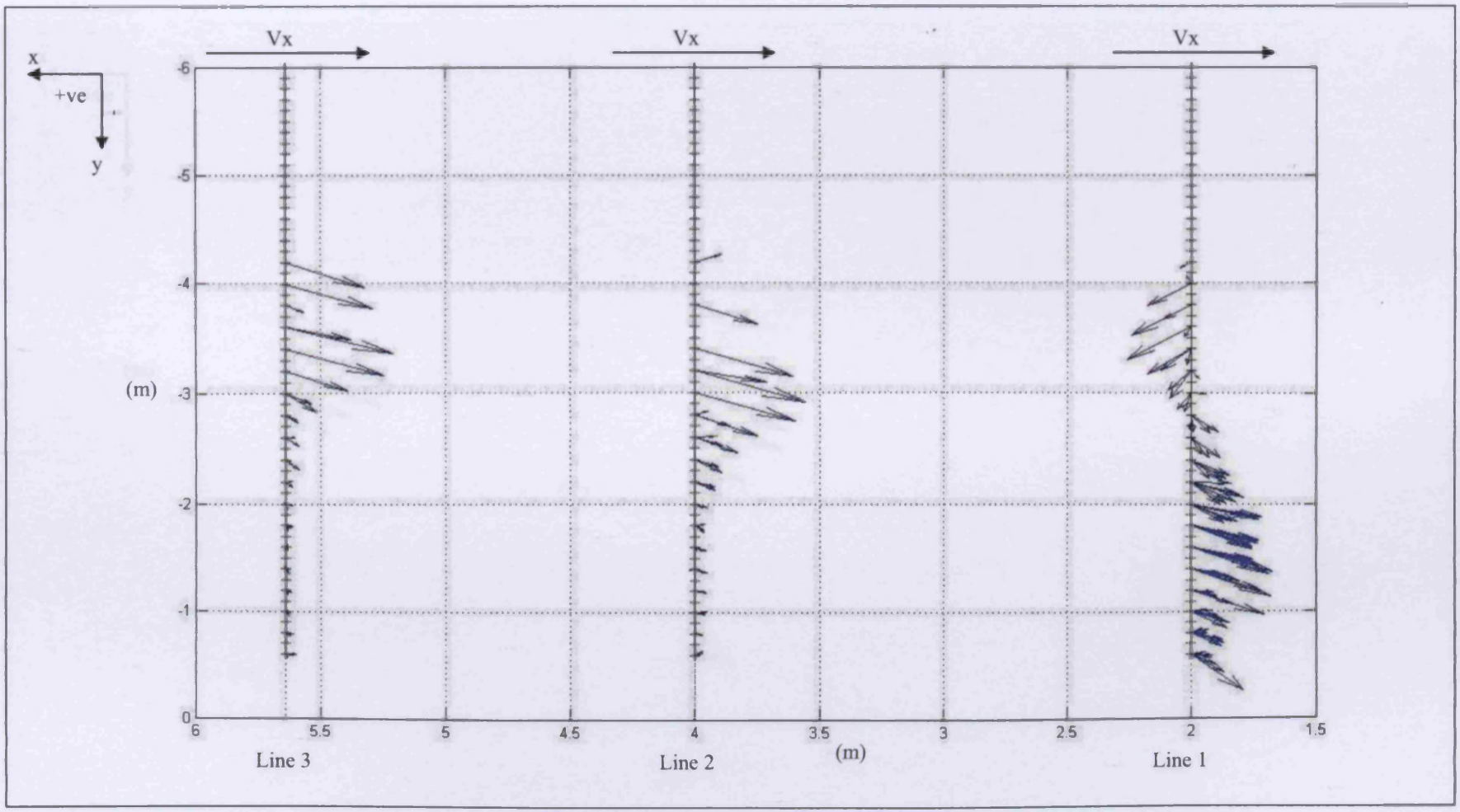

Figure 5-48 Two-dimensional presentation of the long-shore currents during Test 3 (plan view of the beach)

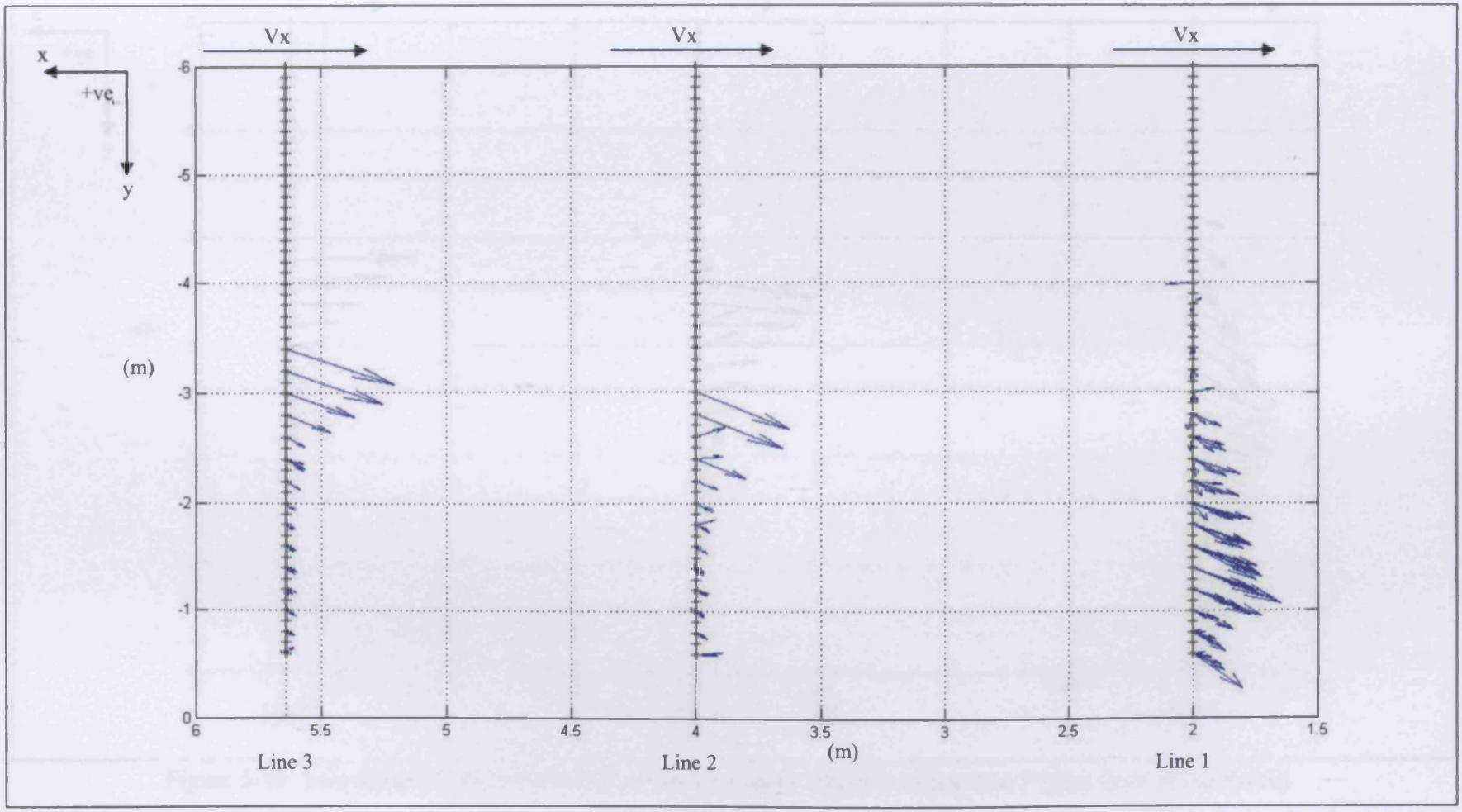

Figure 5-49 Two-dimensional presentation of the long-shore currents during Test 4 (plan view of the beach)

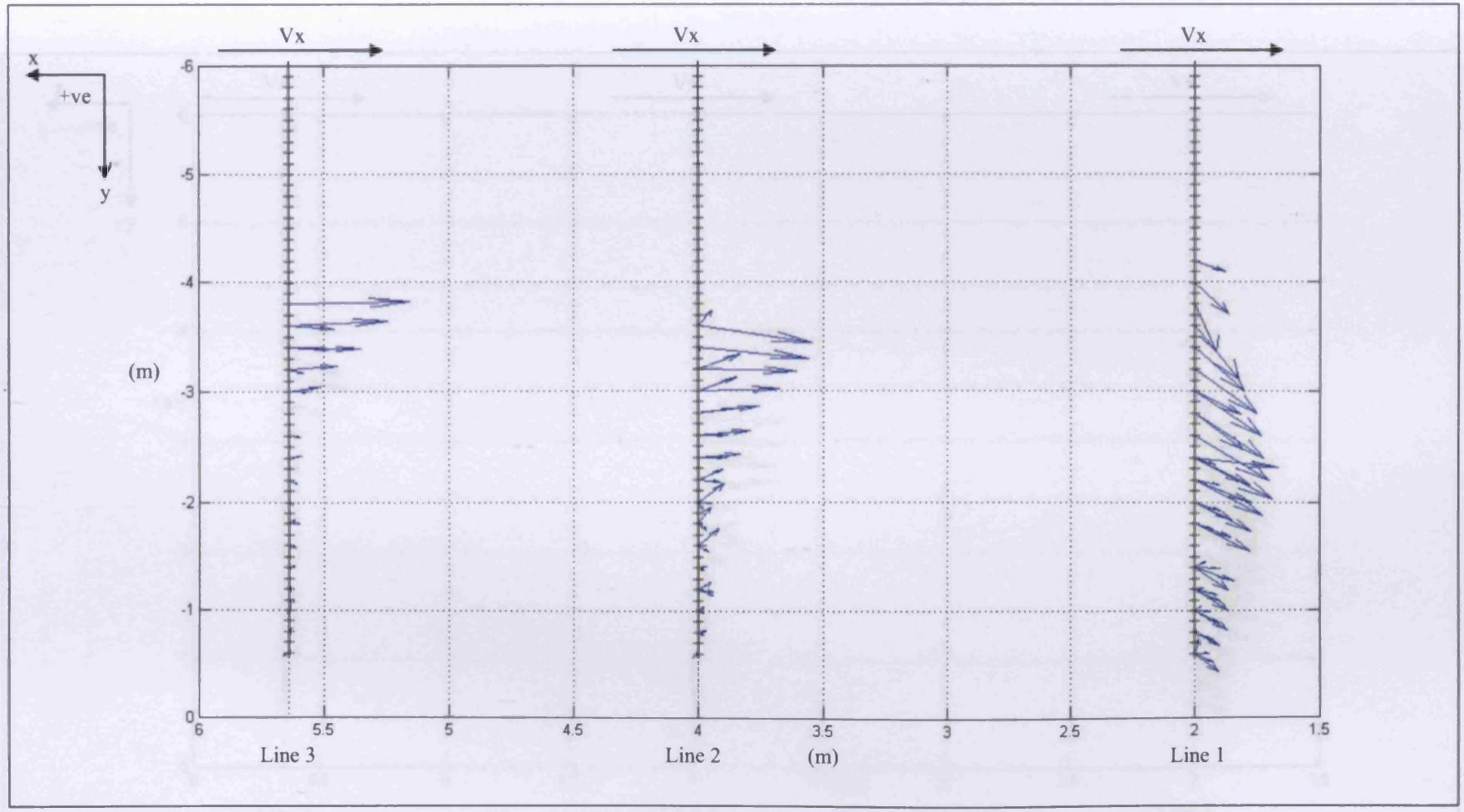

Figure 5-50 Two-dimensional presentation of the long-shore currents during Test 5 (plan view of the beach)

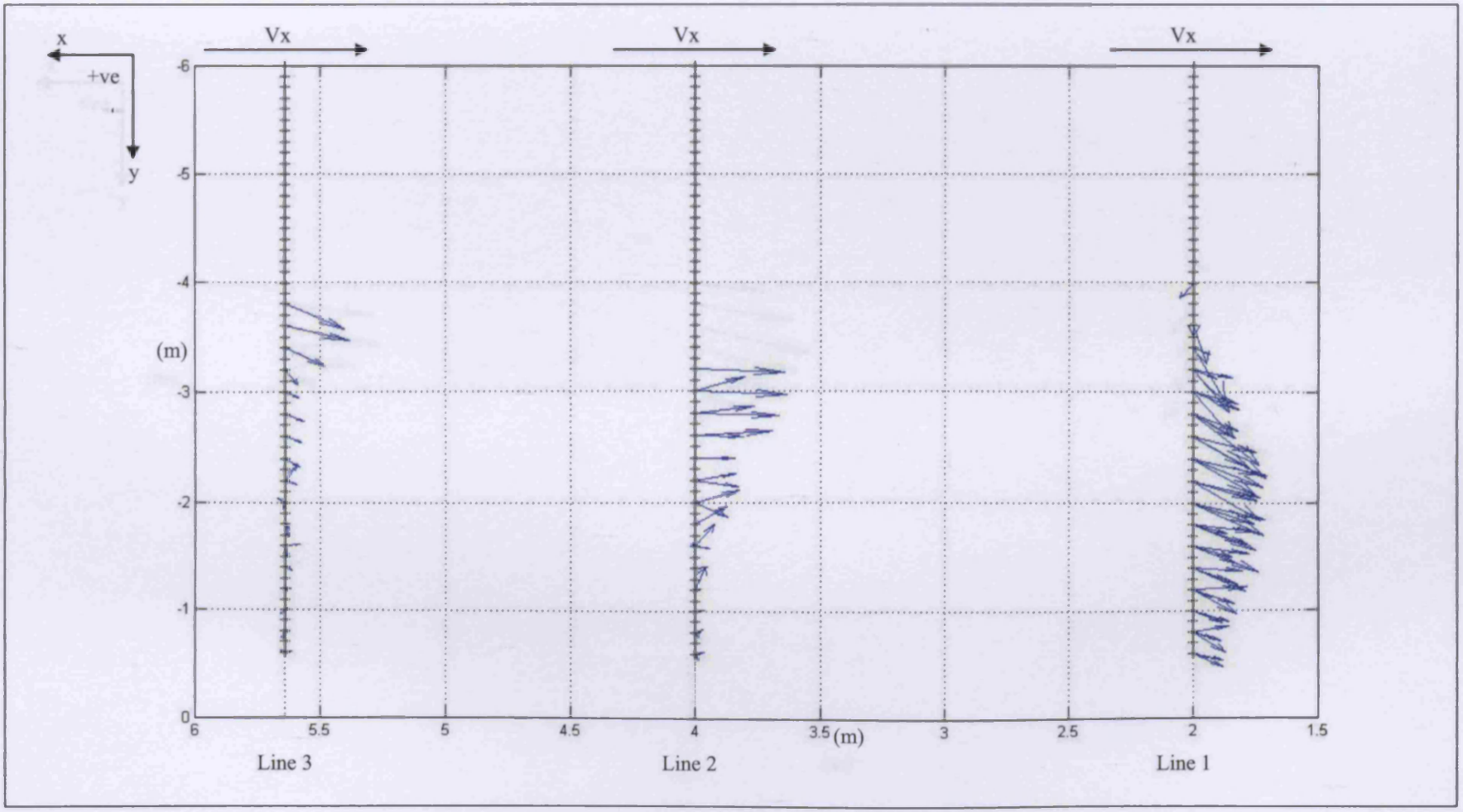

Figure 5-51 Two-dimensional presentation of the long-shore currents during Test 6 (plan view of the beach)

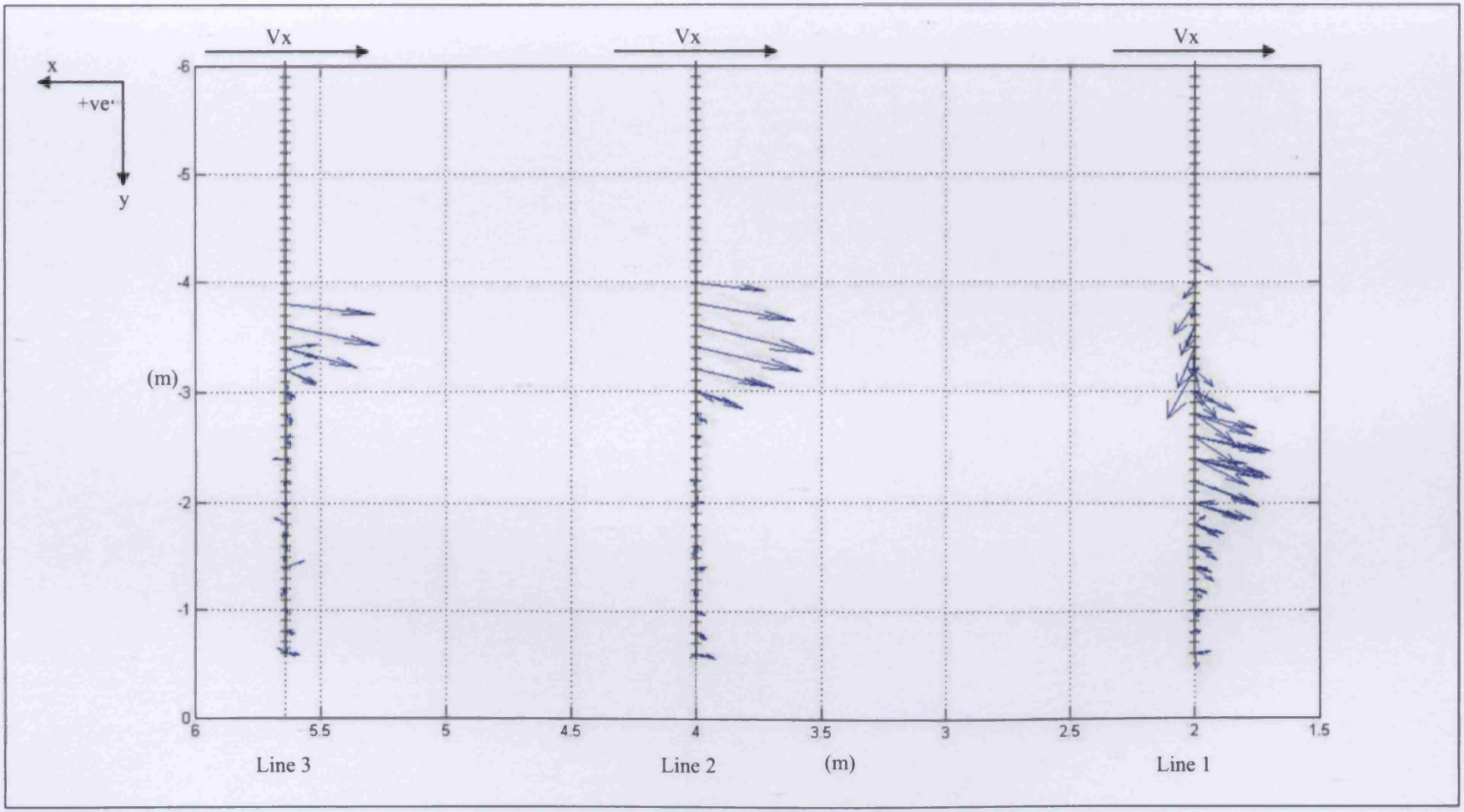

Figure 5-52 Two-dimensional presentation of the long-shore currents during Test 7 (plan view of the beach)

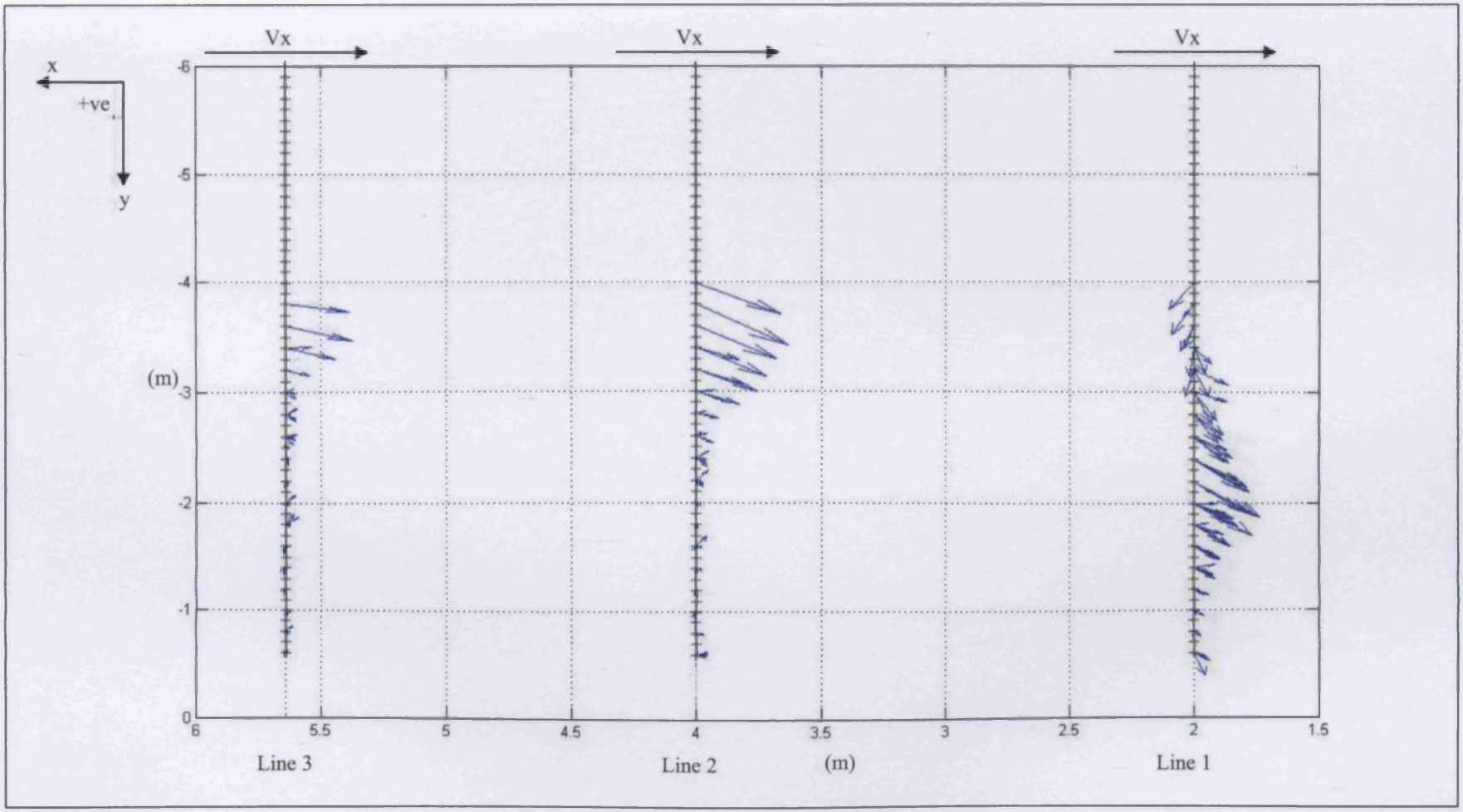

Figure 5-53 Two-dimensional presentation of the long-shore currents during Test 8 (plan view of the beach)

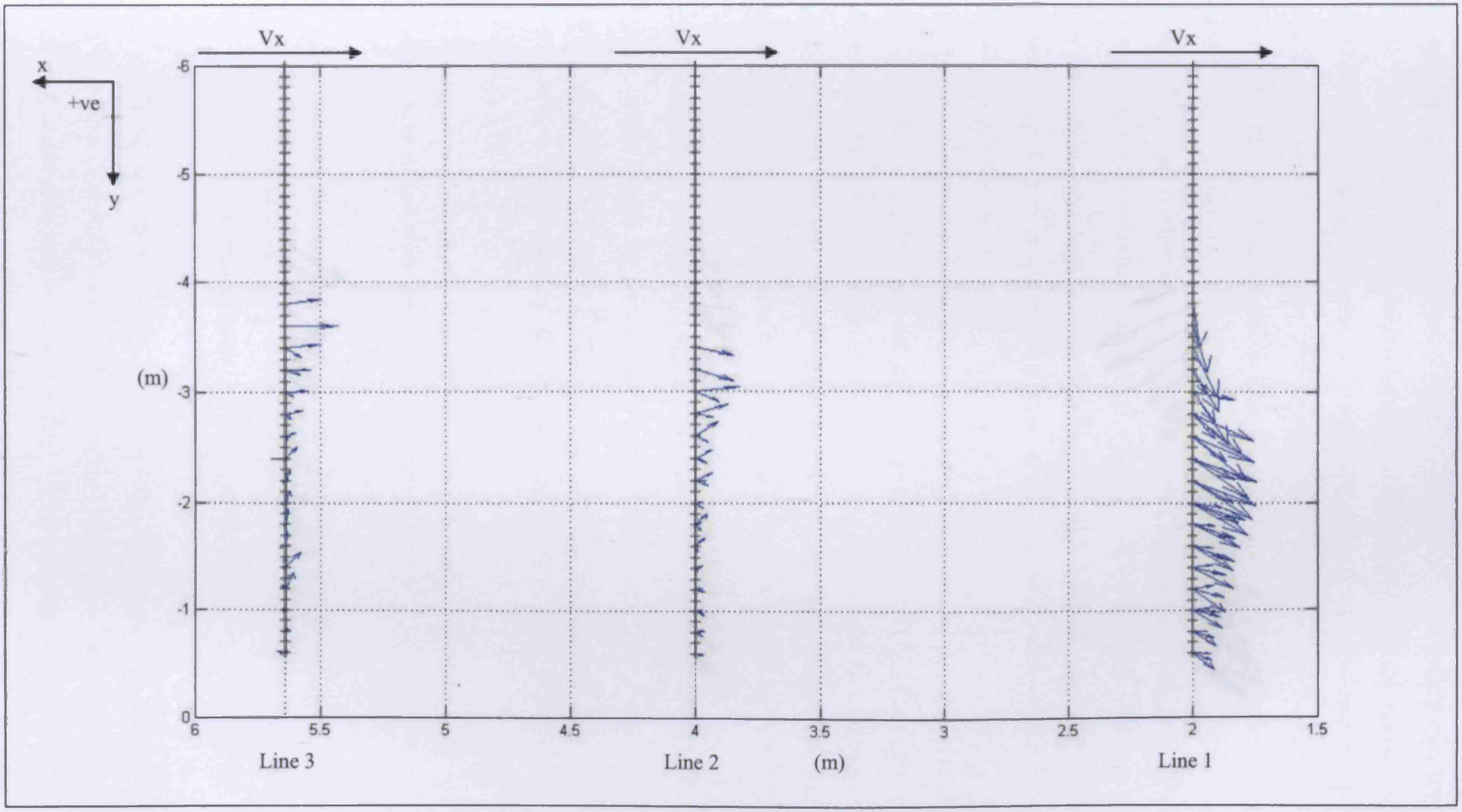

Figure 5-54 Two-dimensional presentation of the long-shore currents during Test 9 (plan view of the beach)

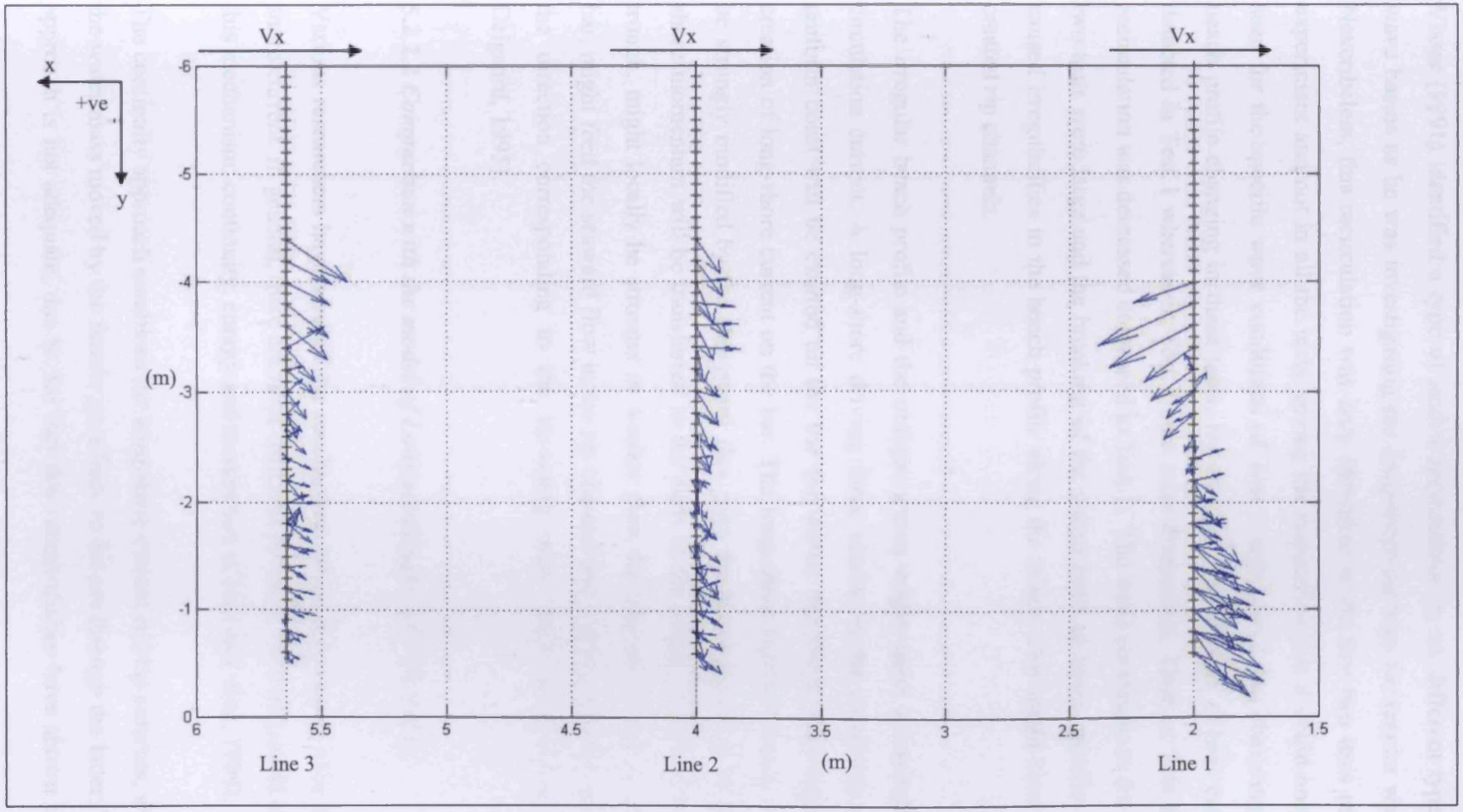

Figure 5-55 Two-dimensional presentation of the long-shore currents during Test 10 (plan view of the beach)

Visser (1991) identified a type of such a recirculation in six different types of wave basins as he was investigating the long-shore currents for regular waves. Nevertheless, this recirculation was only identified in the first two tests of the experiment and not in all the tests, giving the impression that it could only be seen for the specific wave conditions of Test 1 and Test 2. By observing the beach profile changing in these tests, for all lines, the creation of bars can be detected in Test 1 whereas in Test 2 bars were diminished. Thus, at Test 2 the recirculation was decreased compared to Test 1. The wave conditions in the first two tests were large and the breaking of the waves built up barred profiles and caused irregularities in the beach profile along the beach. This might have also created rip channels.

The irregular beach profile and the oblique waves might cause a wave-driven circulation current. A long-shore driving force similar to the conditions on a uniform coast will be exerted on the bar for waves that break, resulting in a creation of long-shore current on the bar. The long-shore current velocity could be strongly modified by the shoreward flux over the bar, and part of its long-shore momentum will be transferred to the flow in the trough. The flow in the trough, might locally be stronger or weaker than the long-shore flow over the bar, might feed the seaward flow in the rip channel and might go locally against the direction corresponding to the incoming wave direction (Fredsoe and Deigaard, 1995).

5.2.2.2 *Comparison with the model of Longuet-Higgins (1970a and b)*

Various researchers have studied the mechanism of the formulation of a long-shore current. In general, there are three different points of view that could study this mechanism: continuity, energy and momentum (Chien and Wan, 1999).

The continuity approach combines the long-shore current and rip currents, where the water mass moved by the former goes back to the sea through the latter. This approach is not adequate, due to the fact that recent studies have shown these

currents are generated by different mechanisms. The variation of wave height along the coastline affect the generation of the rip currents.

The energy approach suggests that, the long-shore currents are produced by the component of wave energy along the coastline which is dissipated by friction on the bottom during movement. This approach is not as satisfactory as the one that follows, because as the waves break, a portion of the wave energy is dissipated whereas the momentum remains unchanged. As a result, the momentum approach has been chosen to calculate the velocity of the long-shore current.

Longuet-Higgins (1970a and b,) derived in a widely used expression for estimating the velocity of the long-shore current, by using the momentum approach. The first solution of this expression had the form of (Dean and Dalrymple, 2002):

Eq.5-49 $$V(x) = \frac{5\pi g \kappa m^{*}(d+\bar{\eta})}{2f}\left(\frac{\sin\theta}{c}\right)$$

where,

κ is the breaker index $\left(=\frac{H_b}{d_b}\right)$, m^{*} is the modified slope $\left(=\frac{m}{1+\frac{3\kappa^2}{8}}\right)$, θ is the incident wave angle, c is the wave celerity $\left(=\sqrt{g(d+\bar{\eta})}\right)$, d is the water depth, $\bar{\eta}$ is the wave set-up and f is the empirical Darcy-Weisbach friction factor with a form of:

Eq.5-50 $$f = \frac{8g}{C^2}$$

where, C is the Chézy coefficient of the form:

Eq.5-51 $$C = 18\log\frac{12h}{k_s}$$

where, h is the water depth and k_s is Nikuradse roughness (k_s=D_{90}, Van Rijn,1993).

The equation applies within the surf zone, resulting in increasing velocity out to the breaker line and then the velocity is zero offshore. Eq.5-49 is valid for any monotonic beach profile when the lateral shear stress terms are negligible.

However, Eq.5-49 lacks the lateral shear stress, which could tend to smooth the breaker line discontinuity, which is not evident in laboratory experiments (Galvin and Eagleson, 1965). The second expression of Longuet-Higgins included a lateral shear stress term with an eddy viscosity of the form:

Eq.5-52 $$\varepsilon_v = Nx\sqrt{gh}$$

where, N is a constant with a typical approximation of about 0.016 (Greenwood and Sherman, 1986), h is the water depth and x is the distance offshore. The analysis of Longuet-Higgins yielded the following form of the long-shore current, which is non-dimensionalised by the values at the breaker line, $X=x/x_b$ and $V_0=V(x_b)$, given by Eq.5-49 :

Eq.5-53 $$\frac{v}{v_0} = \begin{cases} B_1 X^{p_1} + AX, & \text{for } 0 < X < 1 \\ B_2 X^{p_2}, & \text{for } X > 1 \end{cases}$$

where the coefficients and powers are

Eq.5-54 $$B_1 = \left(\frac{p_2 - 1}{p_1 - p_2}\right) A$$

Eq.5-55 $$B_2 = \left(\frac{p_1 - 1}{p_1 - p_2}\right) A$$

Eq.5-56 $$p_1 = -\frac{3}{4} + \sqrt{\left(\frac{9}{16} + \frac{1}{P}\right)}$$

Eq.5-57 $$p_2 = -\frac{3}{4} - \sqrt{\left(\frac{9}{16} + \frac{1}{P}\right)}$$

Eq.5-58 $$A = \frac{1}{\left(1 - \frac{5}{2}P\right)}$$

P is the variable that represents the ratio of the eddy viscosity to the bottom friction and having the following expression (Dean and Dalrymple, 2002):

Eq.5-59 $$P = \frac{8\pi mN}{\kappa f}$$

For P=0, the results will be the same as Eq.5-49 and for P=2/5 the following expression is applied:

Eq.5-60
$$\frac{V}{V_0} = \begin{cases} \frac{10}{49}X - \frac{5}{7}X\ln X, & \text{for } 0 < X < 1 \\ \frac{10}{49}X^{-\frac{5}{2}}, & \text{for } X > 1 \end{cases}$$

The second expression of Longuet-Higgins (1970a and b) was compared with the measured depth- and time-averaged long-shore current velocities. However, Eq.5-49 was substituted by Eq.5-19 as it was previously proved to give more accurate results. The graphical presentations of the comparison of the experimental depth- and time-averaged long-shore current velocities results, for all Lines and all tests, with the second expression of Longuet-Higgins are shown in Figure 5-56 to Figure 5-67 (the positive values represent the direction of the incoming waves). The red and green line correspond to the graphical presentation of the equation y=x and y=-x respectively. Test 1 and Test 2 were not included in this comparison.

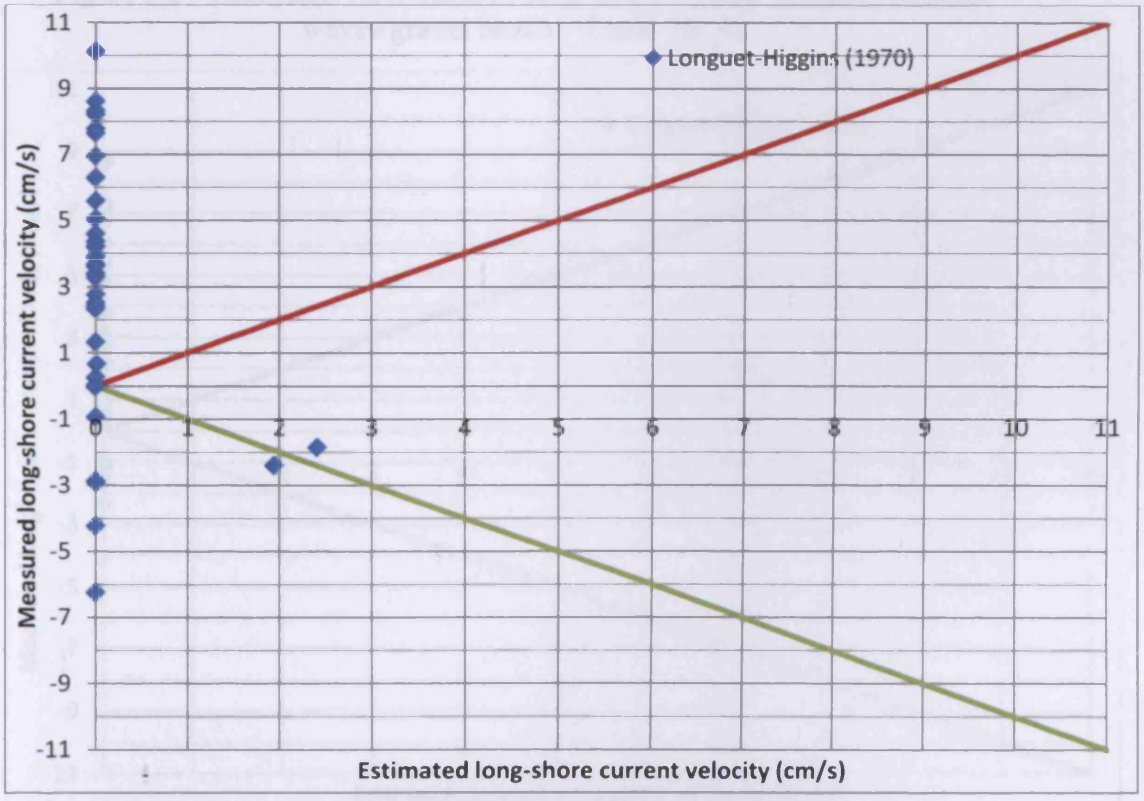

Figure 5-56 Estimated vs. Measured long-shore current velocity (Regular waves/gravel beach - Line1)

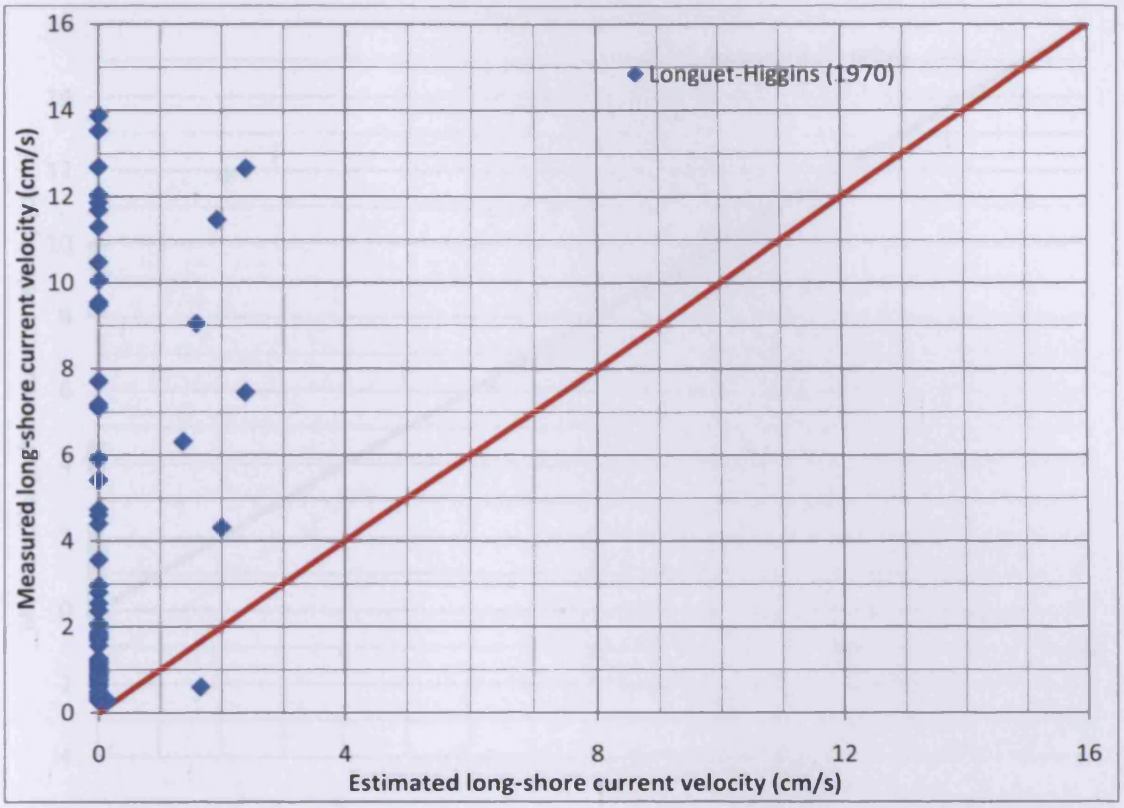

Figure 5-57 Estimated vs. Measured long-shore current velocity (Regular waves/gravel beach – Lines 2& 3)

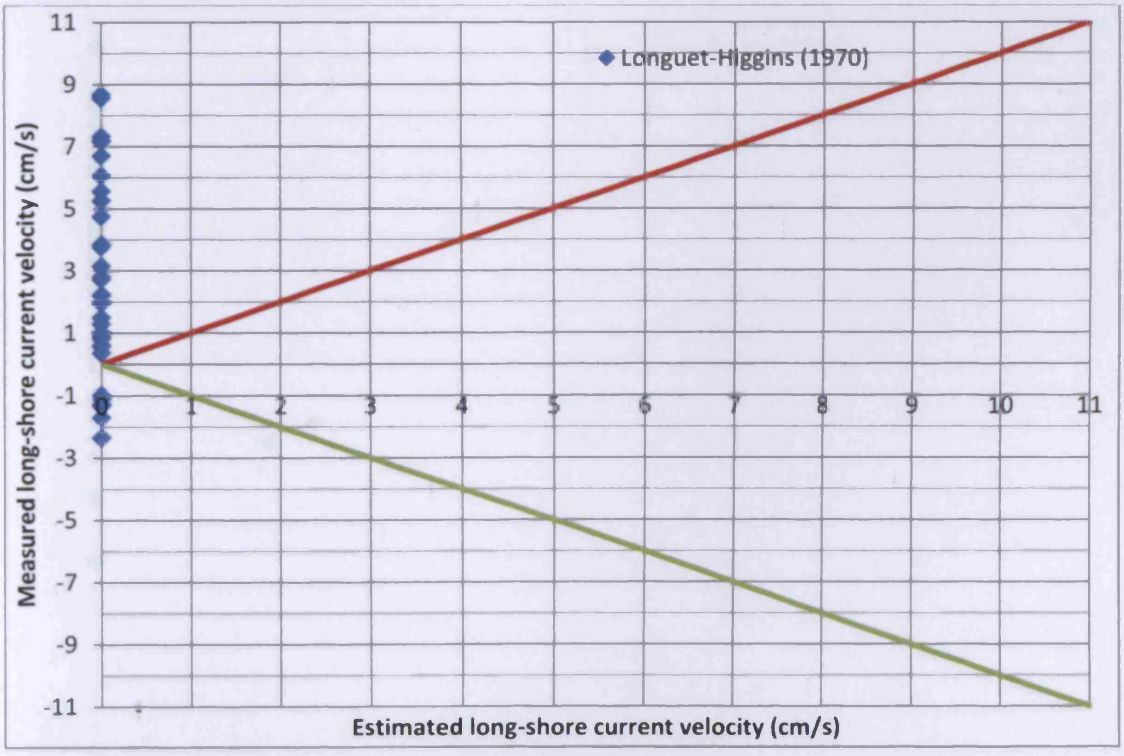

Figure 5-58 Estimated vs. Measured long-shore current velocity (Regular waves/mixed beach - Line1)

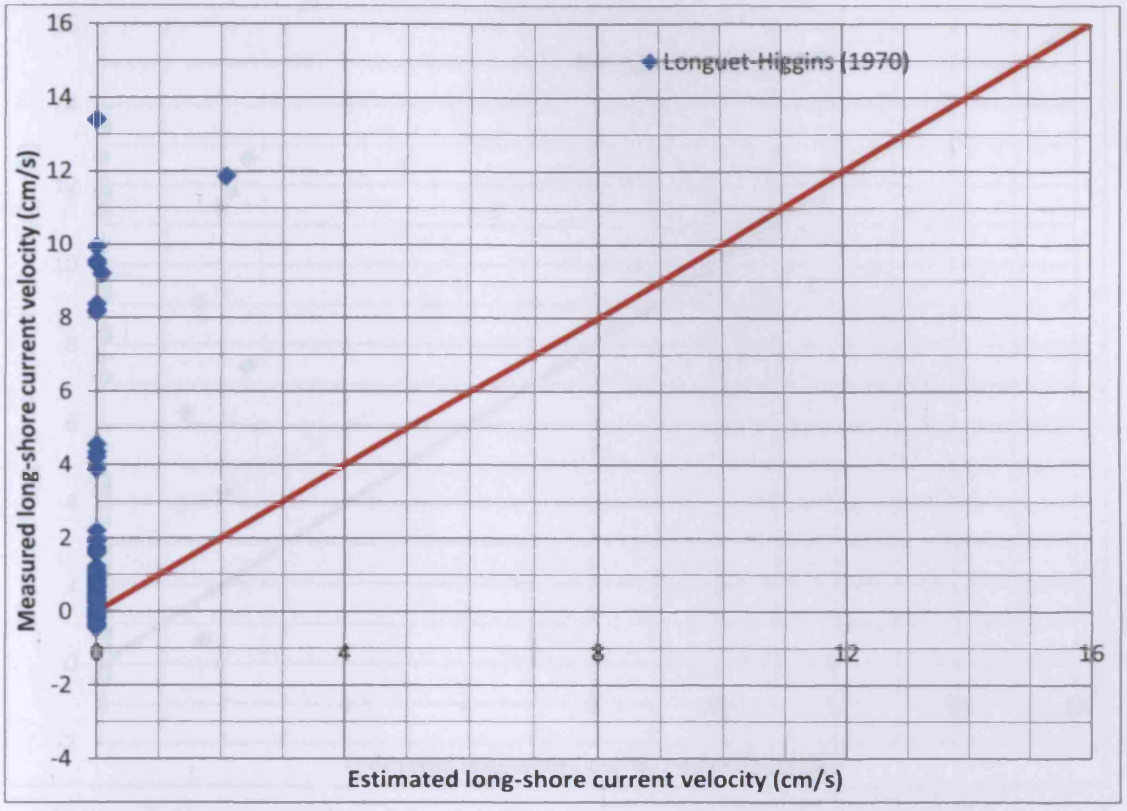

Figure 5-59 Estimated vs. Measured long-shore current velocity (Regular waves/mixed beach – Lines 2& 3)

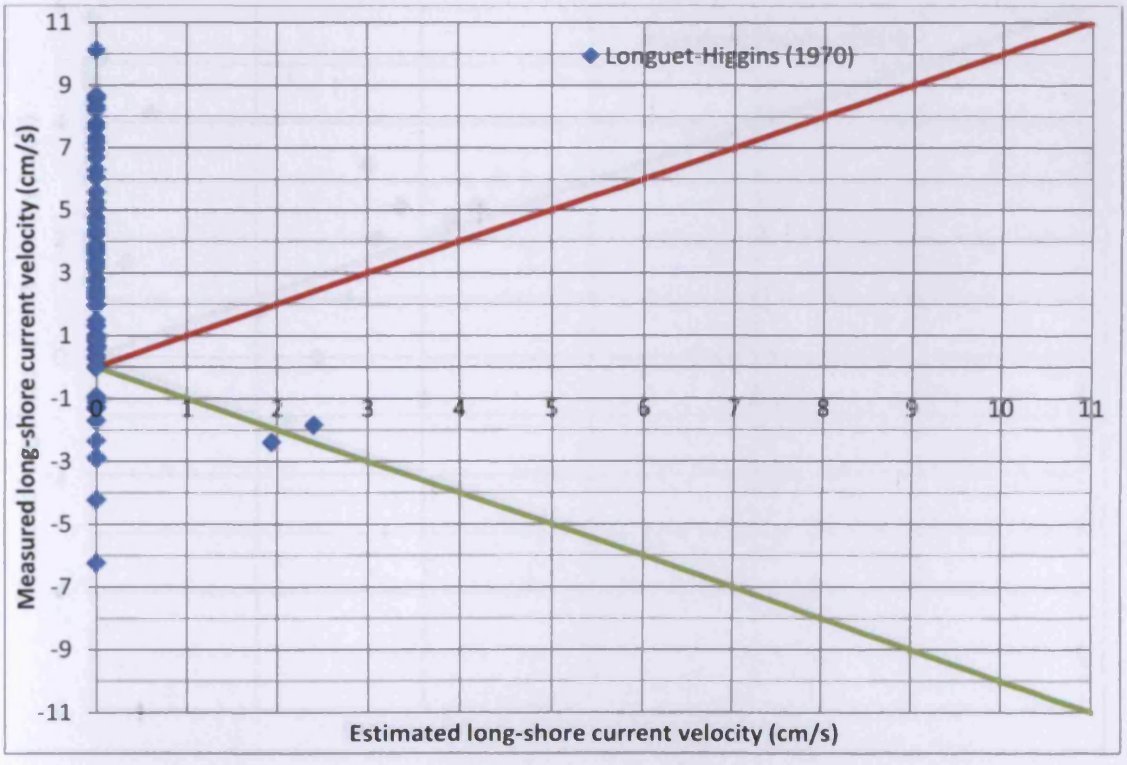

Figure 5-60 Estimated vs. Measured long-shore current velocity (Regular waves/gravel & mixed beach – Line 1)

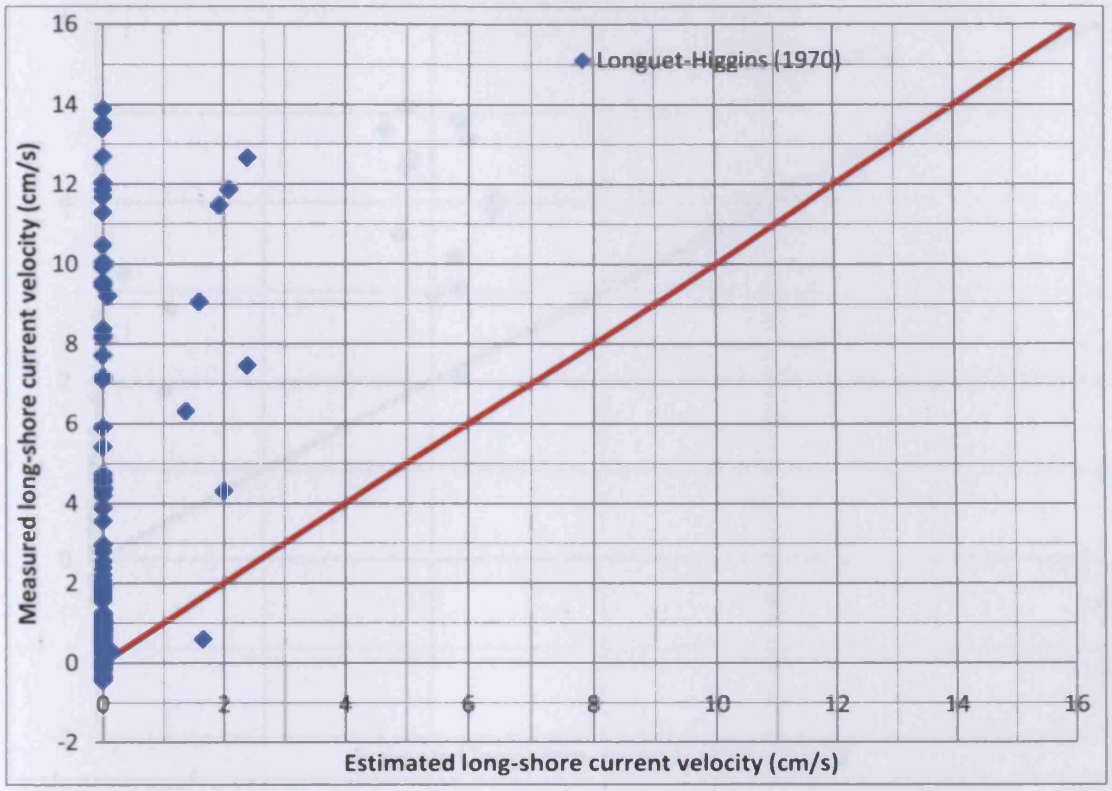

Figure 5-61 Estimated vs. Measured long-shore current velocity (Regular waves/gravel & mixed beach – Lines 2& 3)

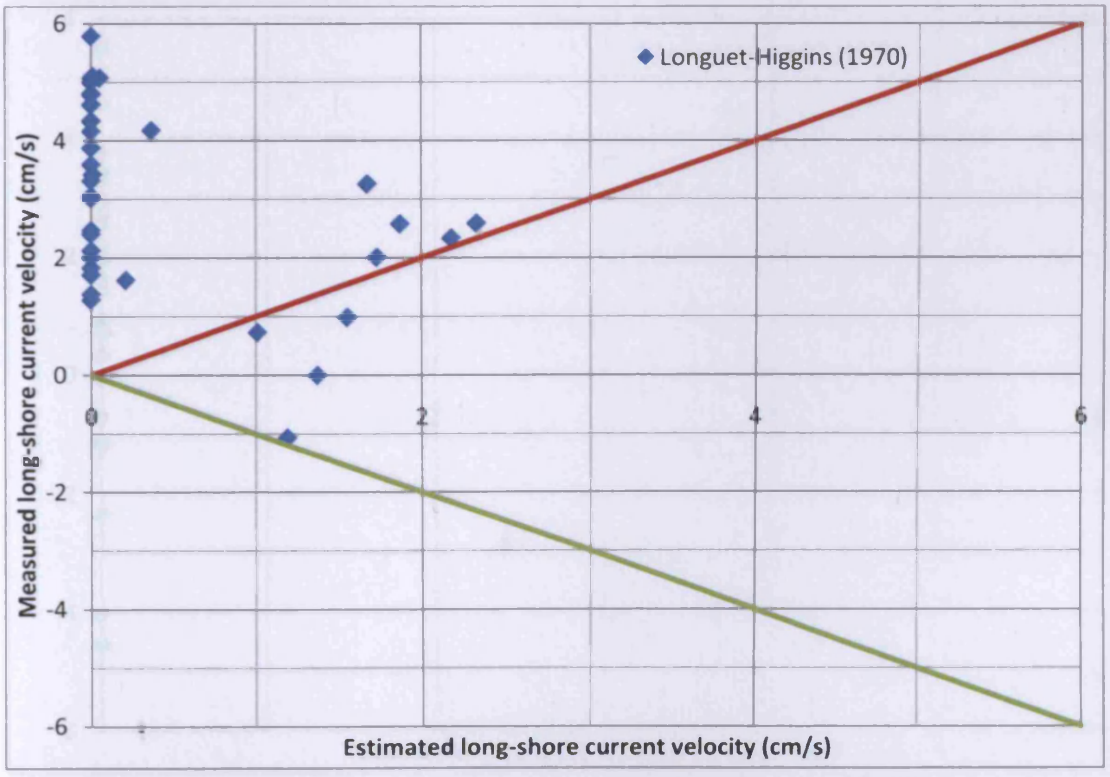

Figure 5-62 Estimated vs. Measured long-shore current velocity (Random waves/gravel beach - Line1)

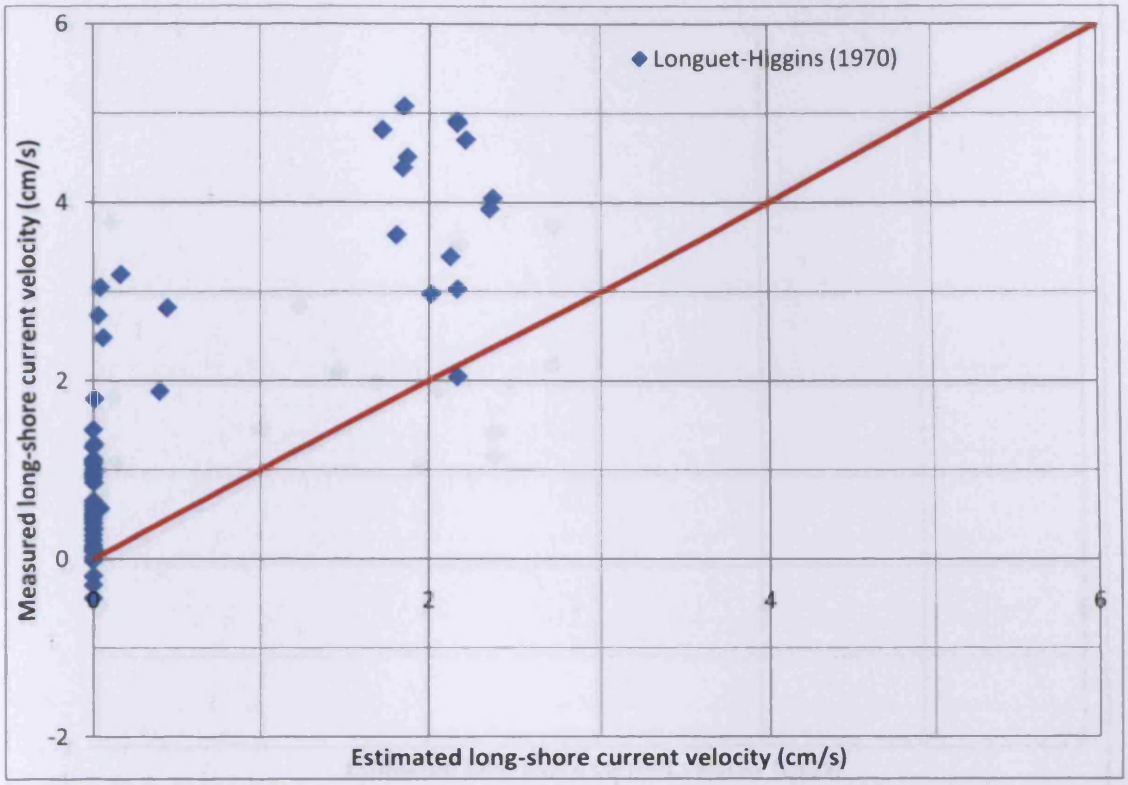

Figure 5-63 Estimated vs. Measured long-shore current velocity (Random waves/gravel beach – Lines 2 & 3)

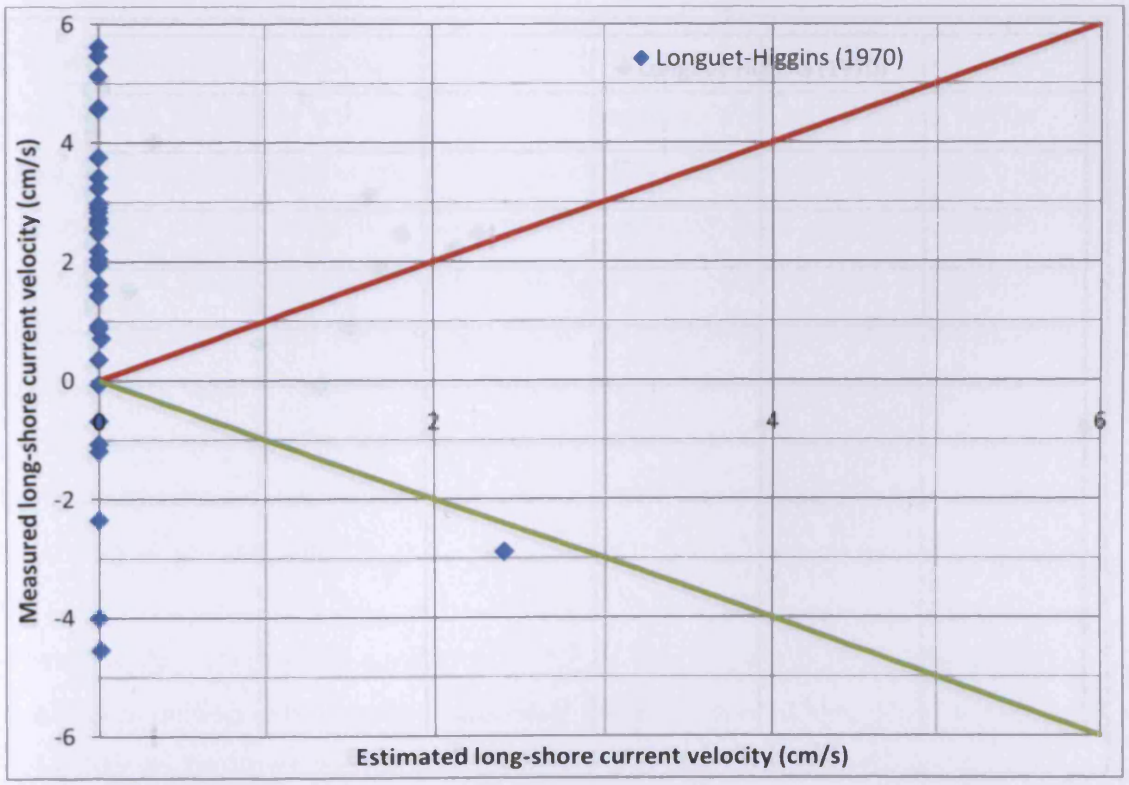

Figure 5-64 Estimated vs. Measured long-shore current velocity (Random waves/mixed beach - Line1)

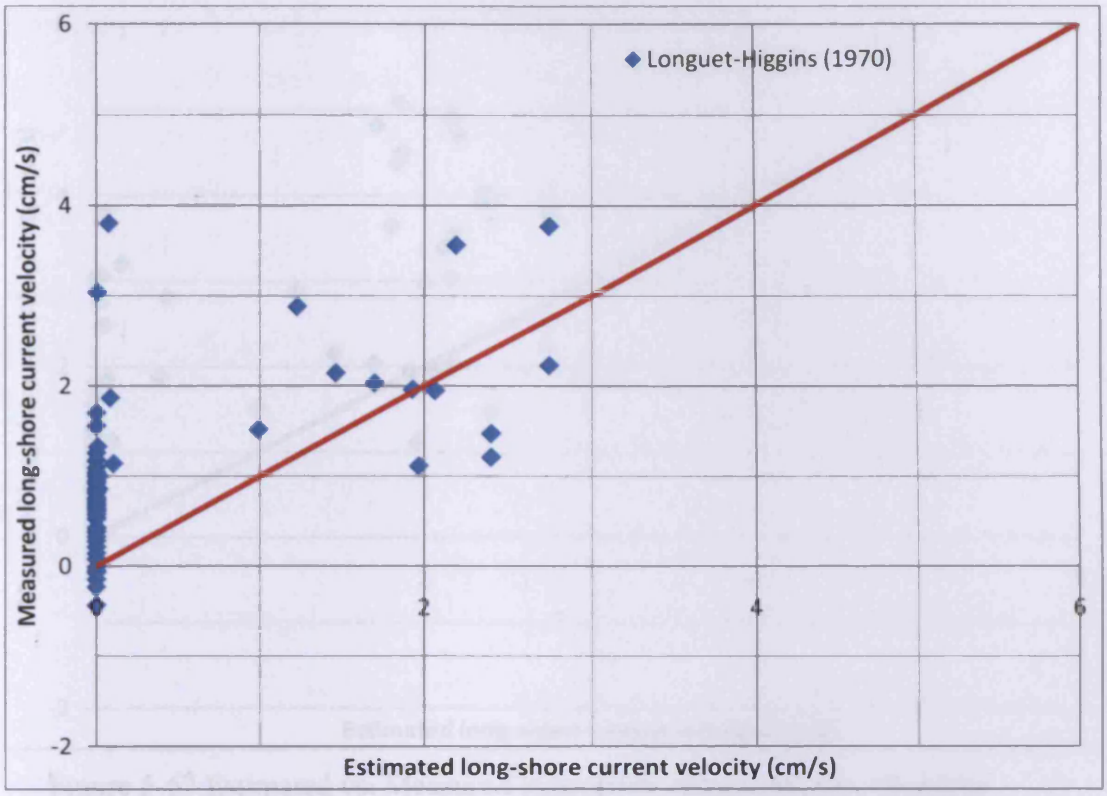

Figure 5-65 Estimated vs. Measured long-shore current velocity (Random waves/mixed beach – Lines 2 & 3)

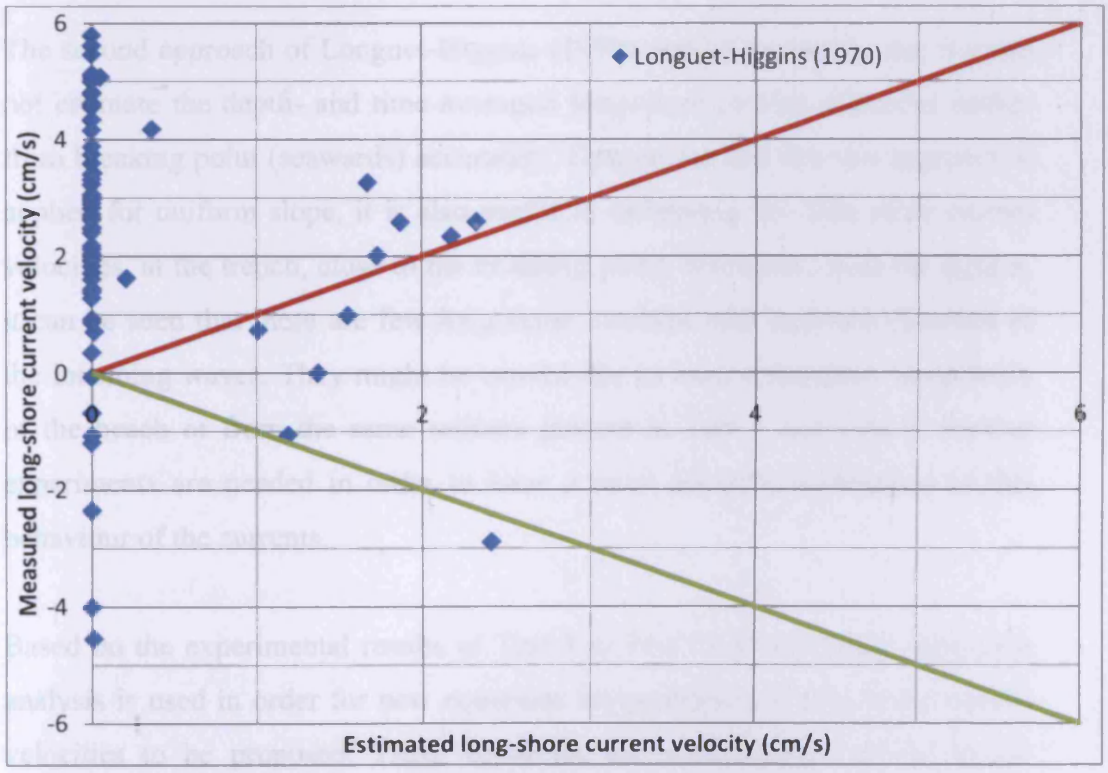

Figure 5-66 Estimated vs. Measured long-shore current velocity (Random waves/gravel & mixed beach- Line 1)

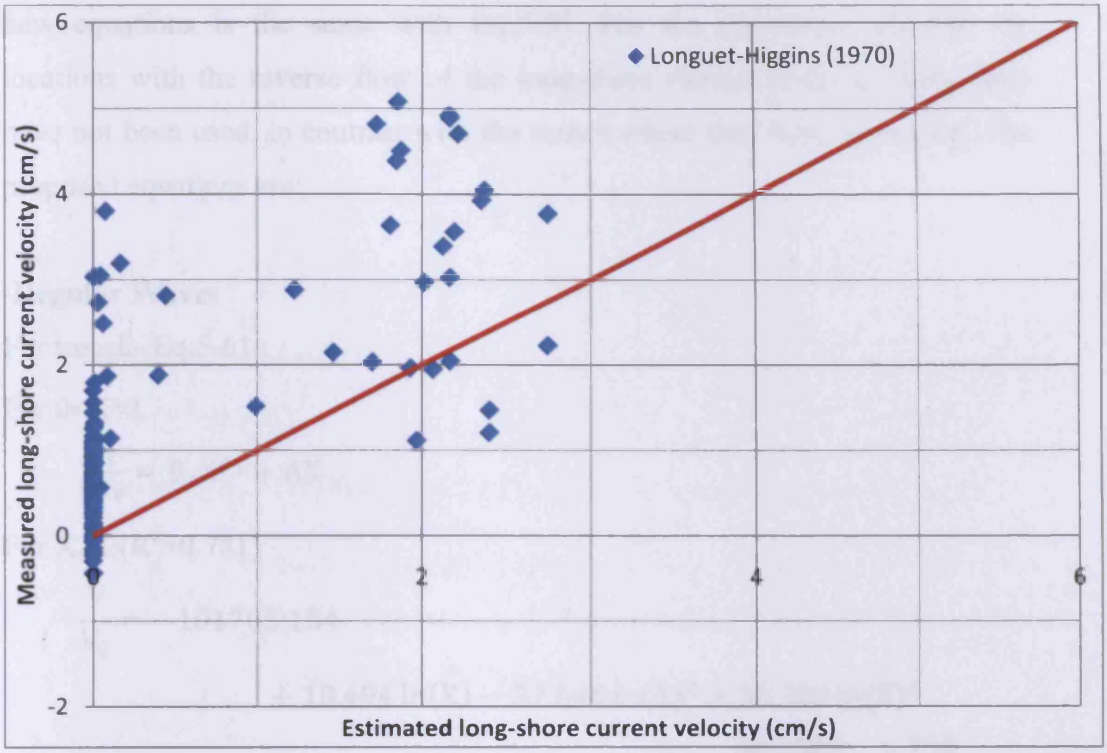

Figure 5-67 Estimated vs. Measured long-shore current velocity (Random waves/gravel & mixed beach – Lines 2 & 3)

The second approach of Longuet-Higgins (1970a and b) has shown that it could not estimate the depth- and time-averaged long-shore current velocities further from breaking point (seawards) accurately. Despite the fact that this approach is applied for uniform slope, it is also useful in estimating the long-shore current velocities, at the trench, close to the breaking point. Moreover, from the figures, it can be seen that there are few long-shore currents with opposite direction of the incoming waves. They might be caused due to local turbulence, irregularity of the beach or from the same reasons present in Test 1 and Test 2. Further experiments are needed in order to have a more accurate explanation of this behaviour of the currents.

Based on the experimental results of Test 3 to Test 10, a non-linear regression analysis is used in order for new equations for prediction of long-shore current velocities to be proposed. These equations are modifications of the second approach of Longuet-Higgins (1970). The eddy viscosity used in producing the

new equations is the same with Eq.5-55. For the regression analysis, the locations with the reverse flow of the long-shore current at the uniform slope have not been used, in contrast with the trench where they have been used. The proposed equations are:

-Regular Waves

For trench- Eq.5-61 :

For 0<X<1

$$\frac{V}{V_0} = B_1 X^{P1} + AX$$

For X>1 (R^2=0.781)

$$\frac{V}{V_0} = -101705.154 + 18.494\ln(X) - 37.546\ln(X)^2 + 35.384\ln(X)^3 - 15.066\ln(X)^4 + 2.341\ln(X)^5 + \frac{665.386}{P} - \frac{1.733}{P^2} + \frac{2.24x10^{-3}}{P^3} - \frac{1.45x10^{-4}}{P^4} + \frac{3.71x10^{-10}}{P^5}$$

For uniform slope- Eq.5-62 :

For 0<X<1 (R^2=0.861)

$$\frac{V}{V_0} = 70174.738Z^3 - 169318.731Z^2 + 135695.725Z - 36105.255$$

For X>1 (R^2=0.998)

$$\frac{V}{V_0} = -177.316 - \frac{860.318}{X} + \frac{1.01}{P} - \frac{339.42}{X^2} - \frac{1.66x10^{-3}}{P^2} + \frac{2.196}{XP} - \frac{100.535}{X^3} + \frac{8.42x10^{-7}}{P^3} - \frac{1.43x10^{-3}}{XP^2} + \frac{0.52}{X^2P}$$

-Random Waves

For trench- Eq.5-63 :

For 0<X<1 (R^2=0.999)

$$\frac{V}{V_0} = -5152513.157Z^7 + 25185233.7Z^6 - 52369077.84Z^5 + 60030146.93Z^4 - 40955313.23Z^3 + 16624677.17Z^2 - 3716458.238Z + 352848.033$$

For X>1 (R^2=0.675)

$$\frac{V}{V_0} = 820.091 - \frac{1047.845}{X} - 1169474.046P + \frac{264.861}{X^2} + 542259155.4P^2 + 1099136.529\frac{P}{X} - \frac{20.06}{X^3} - 81322770544P^3 - 284939904.4\frac{P^2}{X} - 142041.178\frac{P}{X^2}$$

For uniform slope- Eq.5-64 :

For 0<X<1 (R^2=0.807)

$$\frac{V}{V_0} = 80196.904 - 1089.686X + 3431.418X^2 - 5304.364X^3 + 4022.446X^4 - 1198.603X^5 - 291109103.436P + (4.21469x10^{11})P^2 - (3.03686x10^{14})P^3 + (1.08894236469046x10^{17})P^4 - (1.55460815105334x10^{19})P^5$$

For X>1 (R^2=0.665)

$$\frac{V}{V_0} = -8.869 - \frac{70.557}{X} + \frac{0.109}{P} - \frac{54.862}{X^2} - \frac{3.16x10^{-4}}{P^2} + \frac{0.317}{XP} - \frac{4.202}{X^3} + \frac{2.65x10^{-7}}{P^3} - \frac{3.38x10^{-4}}{XP^2} + \frac{0.102}{X^2P}$$

where,

$Z = B_1X^{P1} + AX$

The graphical presentations of the comparison of the experimental depth- and time-averaged long-shore current velocities results, for all Lines and all tests, with the modified second expression of Longuet-Higgins are shown in Figure 5-68 to Figure 5-71 (the positive values represent the direction of the incoming waves). For trench- Eq.5-61 to For uniform slope- Eq.5-64 shows a good agreement with the experimental results. They should be quite reliable when used within the limits of applicability.

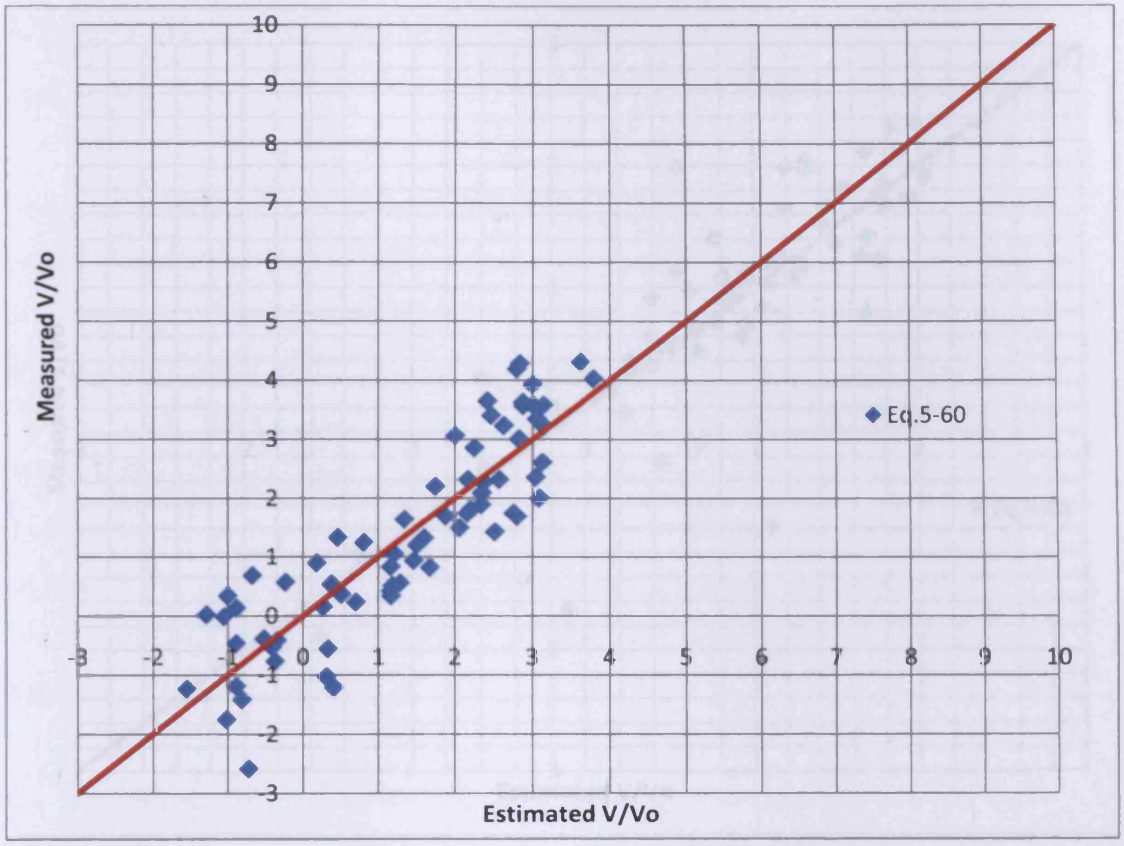

Figure 5-68 Estimated V/V_o vs. Measured V/V_o (Regular Beach - Line1)

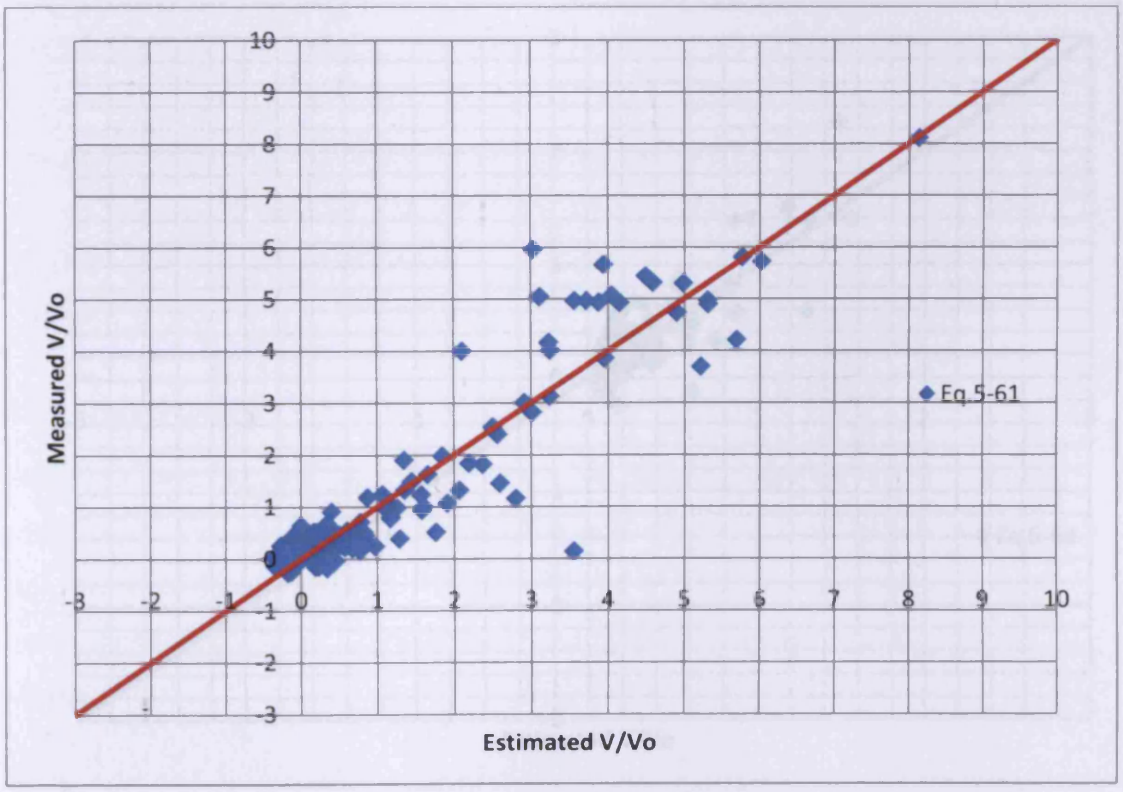

Figure 5-69 Estimated V/V_o vs. Measured V/V_o (Regular – Lines 2 & 3)

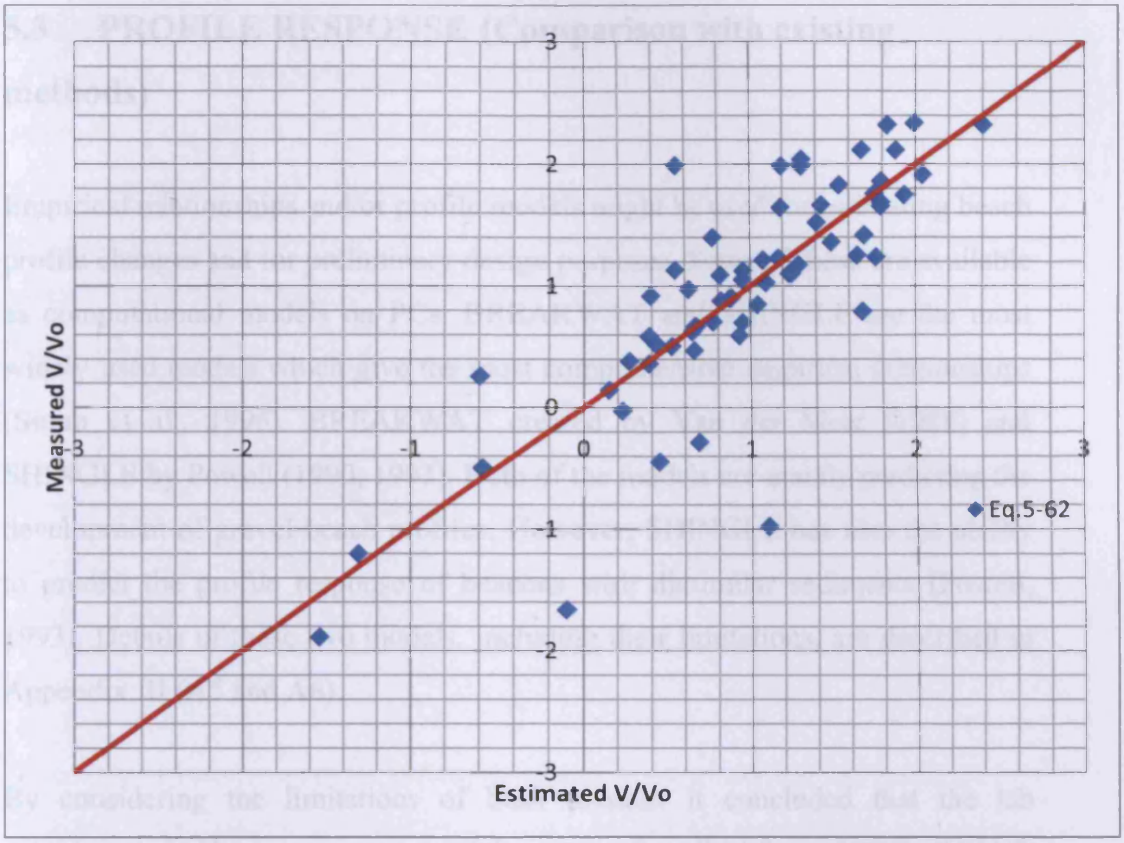

Figure 5-70 Estimated V/V_o vs. Measured V/V_o (Random Beach - Line1)

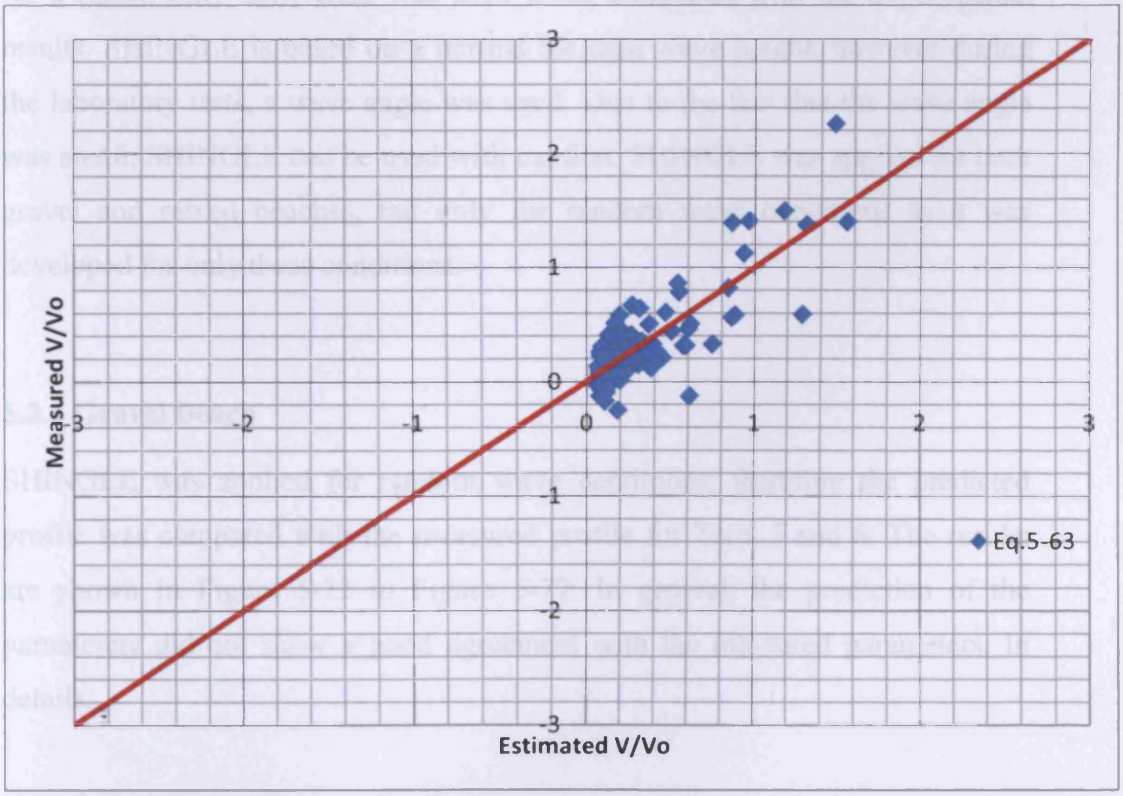

Figure 5-71 Estimated V/V_o vs. Measured V/V_o (Random waves – Lines 2 & 3)

5.3 PROFILE RESPONSE (Comparison with existing methods)

Empirical relationships and/or profile models might be used for estimating beach profile changes and for preliminary design purposes. Some of these are available as computational models on PCs. BREAKWAT and SHINGLE are the most widely used models which give the most comprehensive empirical relationships (Simm et al., 1996). BREAKWAT created by Van der Meer (1988) and SHINGLE by Powell (1990, 1993). Both of the models are mainly predicting the development of gravel beach profiles. However, SHINGLE has also the ability to predict the profile response of beaches with dissimilar sediments (Powell, 1993). Details of these two models, including their limitations, are described in Appendix III (A5 and A6).

By considering the limitations of both models, it concluded that the lab experiments in Hannover were out of the range of applicability of BREAKWAT. As a result, only SHINGLE was used to be compared with the experimental results. SHINGLE is based on a normal incident wave height; however during the laboratory tests, a wave angle was used. Due to the fact that the wave angle was small, SHINGLE can be used with caution. SHINGLE was applied for both gravel and mixed beaches, but only for random wave conditions as it was developed for only these conditions.

5.3.1 Gravel Beach

SHINGLE was applied for random wave conditions; therefore the predicted profile was compared with the measured profile for Tests 5 and 6. The results are shown in Figure 5-72 to Figure 5-77. In general, the prediction of the parameters did not show a good agreement with the measured parameters. In details:

Start of the beach: SHINGLE did not predict accurately the position of the start of the beach; it predicted it more seawards compared with the measured position. At the uniform slopes (Lines 2 and 3), SHINGLE underestimated the elevation of the start of the beach initially, but overestimated for longer wave periods. At the trench (Line 1) there was an opposite pattern; initially SHINGLE overestimated the elevation of the start of the beach base but underestimated for longer wave periods.

Step: SHINGLE gave satisfactory prediction for the position of the step. However, the elevation of the step was initially underestimated but overestimated for longer wave period.

Crest: The position and the elevation of the crest could not be predicted by SHINGLE. The elevation was always overestimated and the position was moved landwards compared with the measured position.

End of active profile: The end of the active profile varied between the Lines and the Tests. SHINGLE could not either predict the location or the variation of the end of active profile as it shown from Figure 5-72 to Figure 5-77.

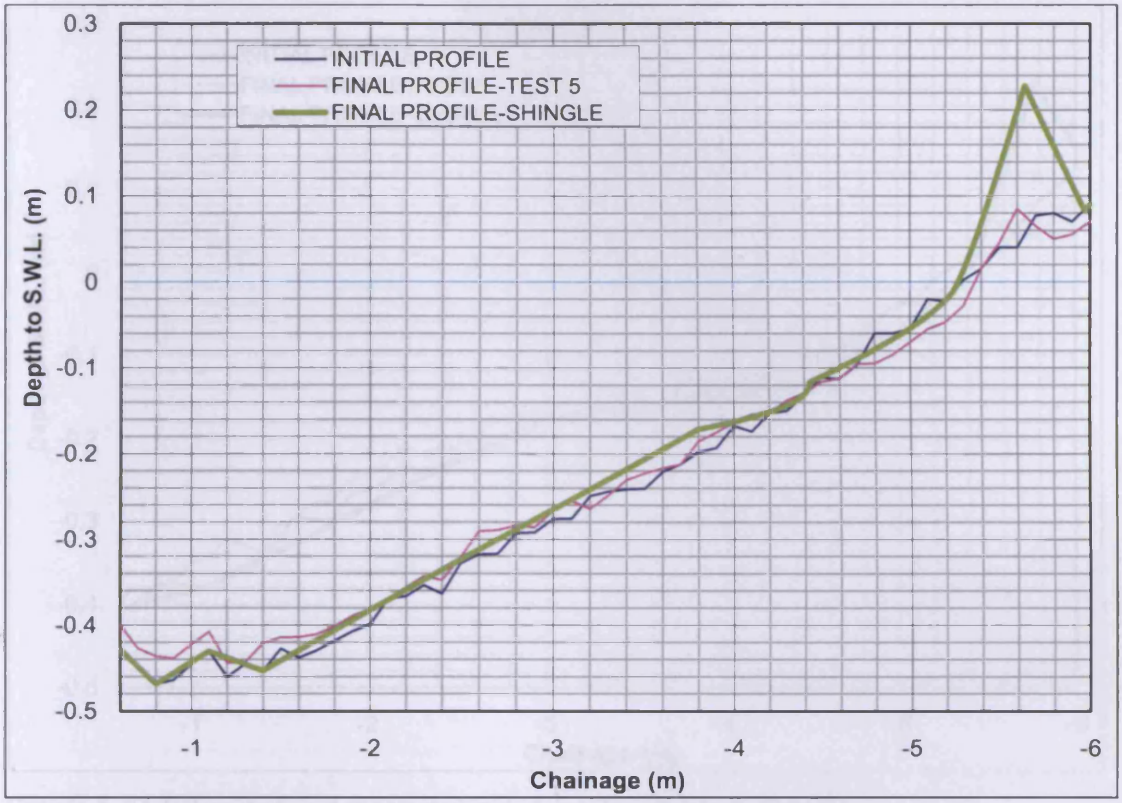

Figure 5-72 Estimated and measured beach profile (Line 1- Test 5)

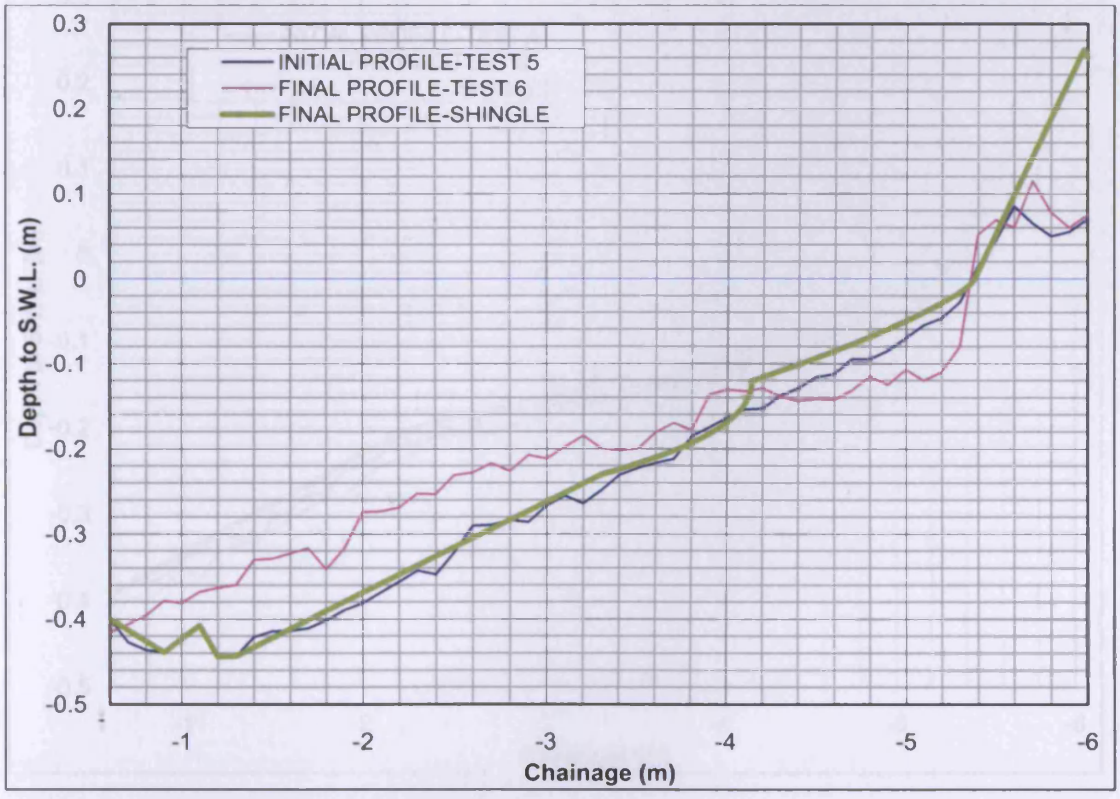

Figure 5-73 Estimated and measured beach profile (Line 1- Test 6)

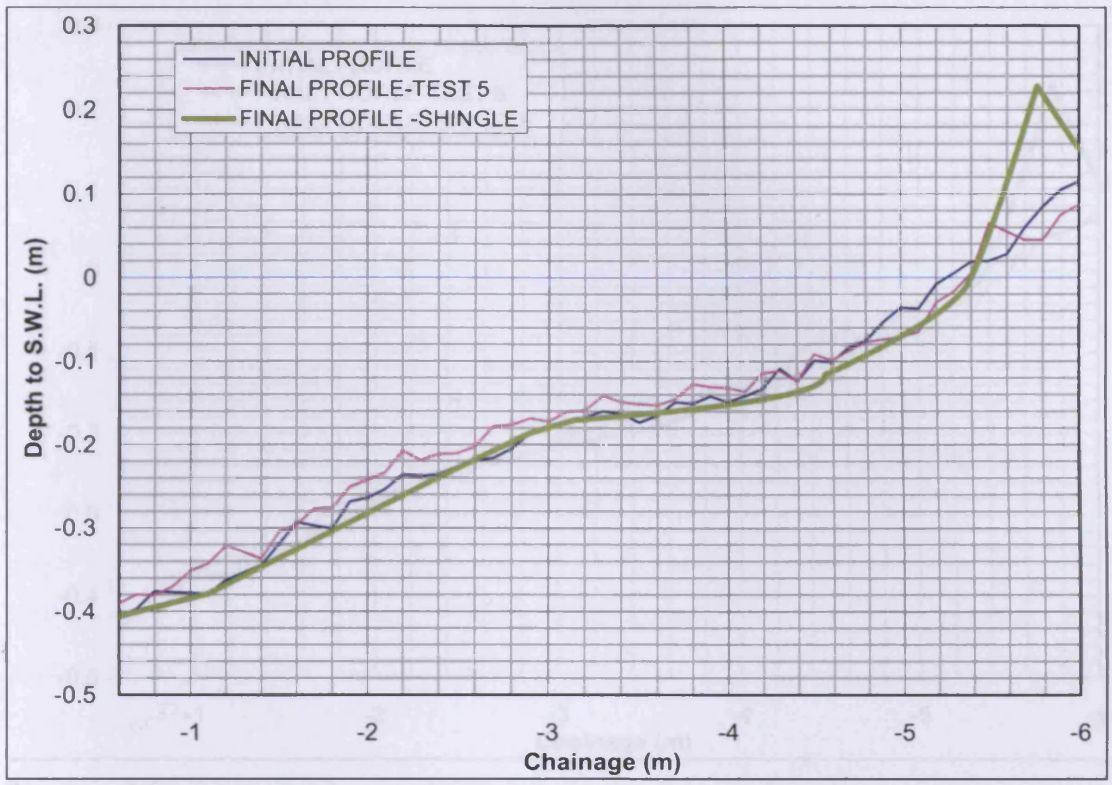

Figure 5-74 Estimated and measured beach profile (Line 2- Test 5)

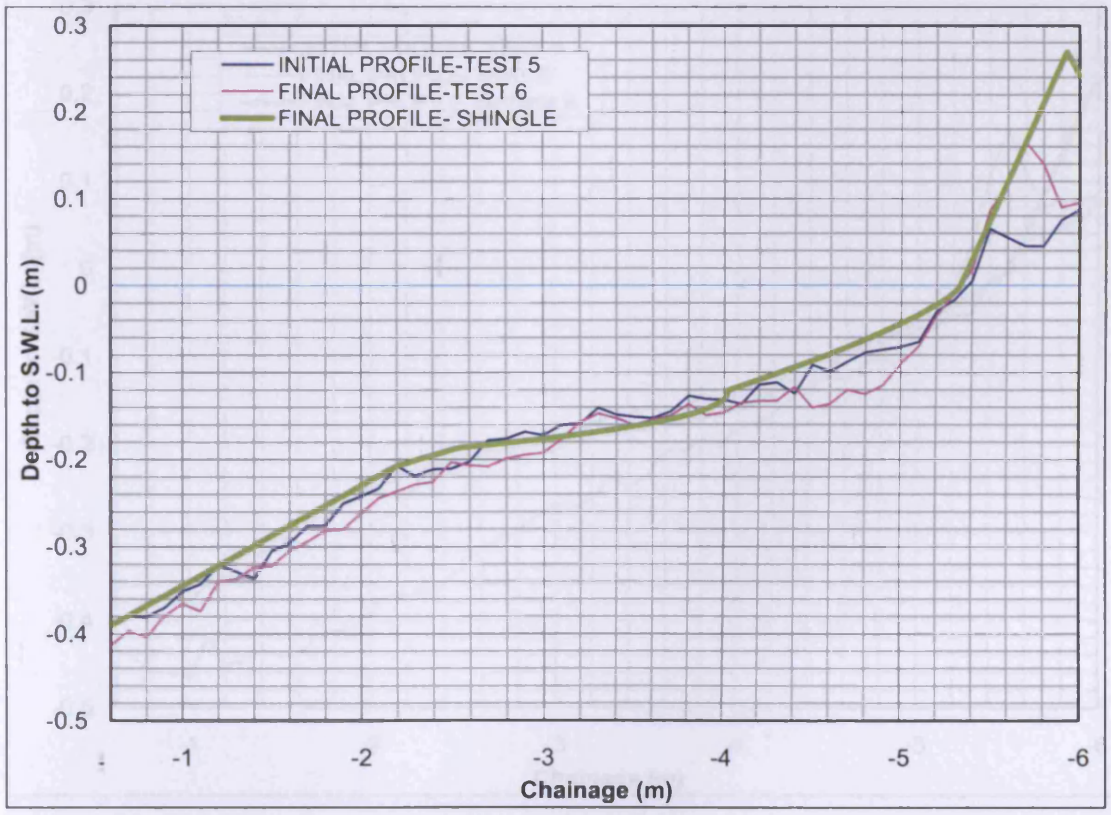

Figure 5-75 Estimated and measured beach profile (Line 2- Test 6)

Figure 5-76 Estimated and measured beach profile (Line 3- Test 5)

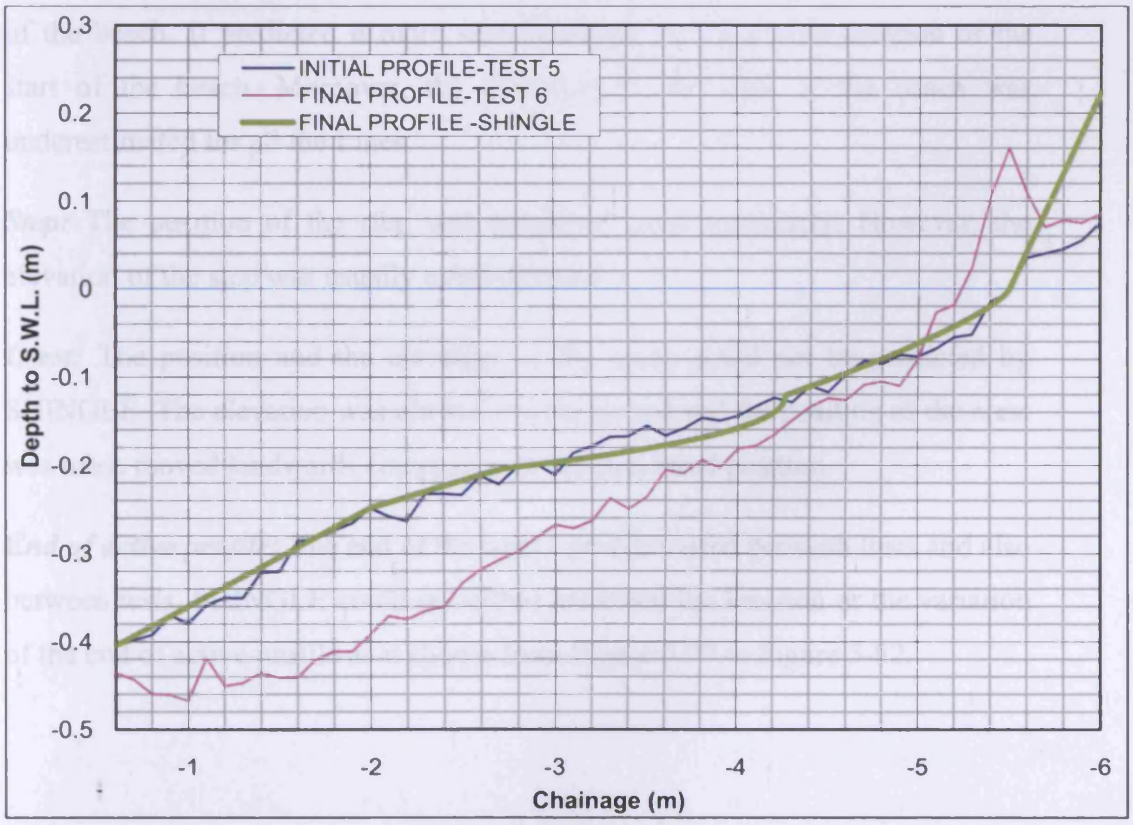

Figure 5-77 Estimated and measured beach profile (Line 3- Test 6)

5.3.2 Mixed Beach

SHINGLE model was not used before for predicting the profile of mixed beach. However, it was used here due to the fact that SHINGLE is a widely used predicting model for gravel beaches and also includes estimation of beach profiles with dissimilar sediments.

The estimated profile was compared with the measured profile for Tests 9 and 10. The results are shown in Figure 5-77 to Figure 5-82. It can be observed that the prediction was not satisfactory. The prediction of the parameters did not show a good agreement with the measured parameters. Interesting was the fact that SHINGLE model compared more accurately with the mixed beach results than with the gravel beach results. In detail:

Start of the beach: SHINGLE did not predict accurately the position of the start of the beach. It predicted it more seawards than the measured position of the start of the beach. Moreover, the elevation of the start of the beach was underestimated for all the Lines.

Step: The position of the step was predicted quite accurately. However, the elevation of the step was usually overestimated.

Crest: The position and the elevation of the crest could not be predicted by SHINGLE. The elevation was always overestimated and the position of the crest was often moved landwards compare with the measured position.

End of active profile: The end of the active profile varied between lines and also between tests. SHINGLE could not either predicted the location or the variation of the end of active profile as it shown from Figure 5-77 to Figure 5-82.

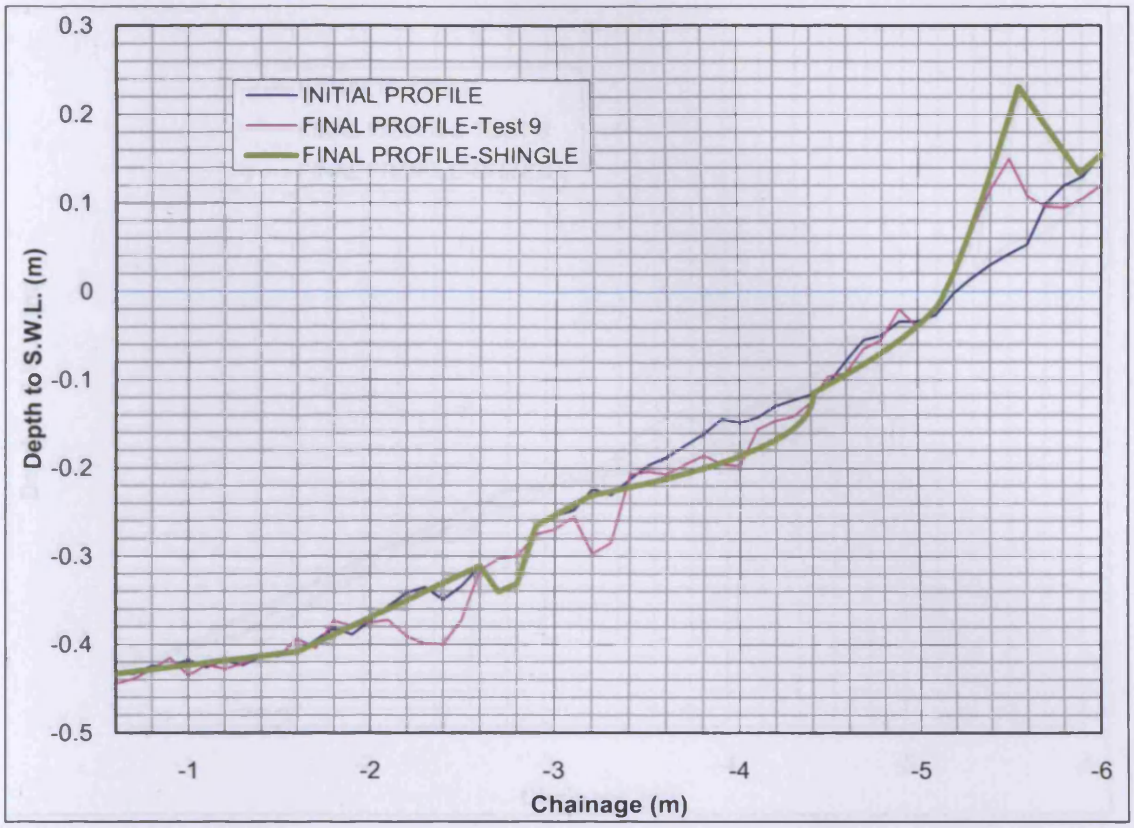

Figure 5-78 Estimated and measured beach profile (Line 1- Test 9)

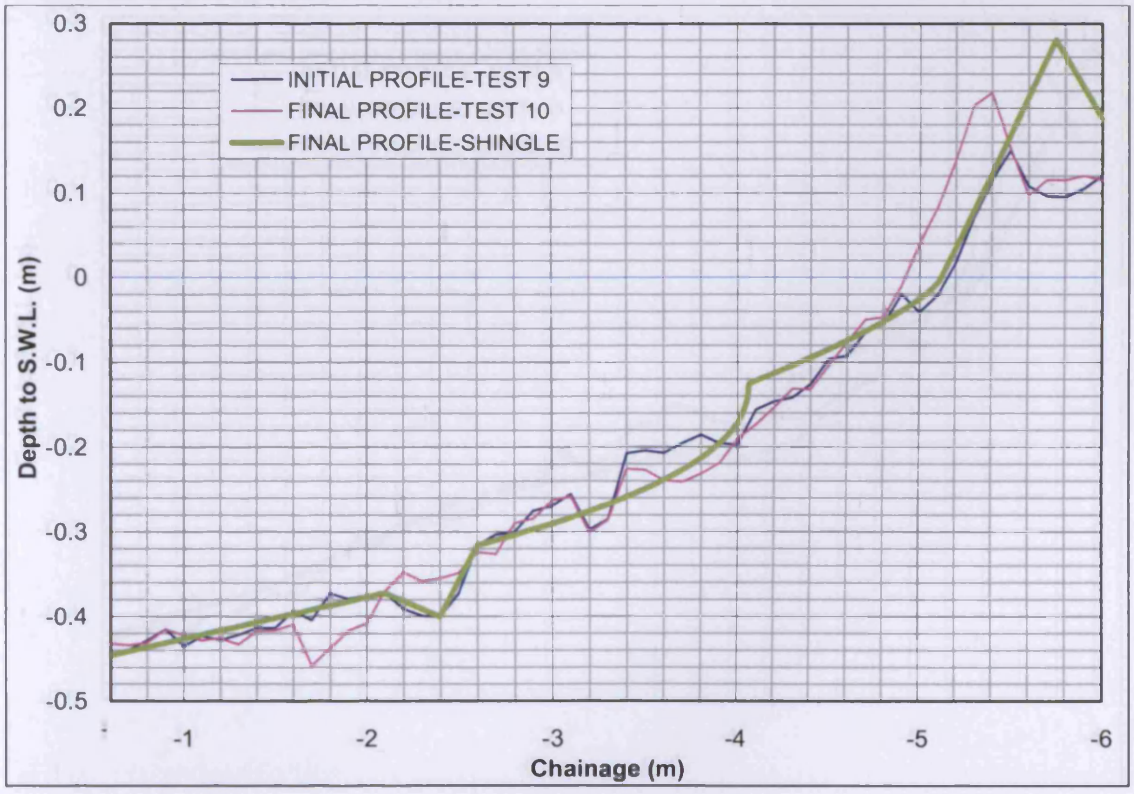

Figure 5-79 Estimated and measured beach profile (Line 1- Test 10)

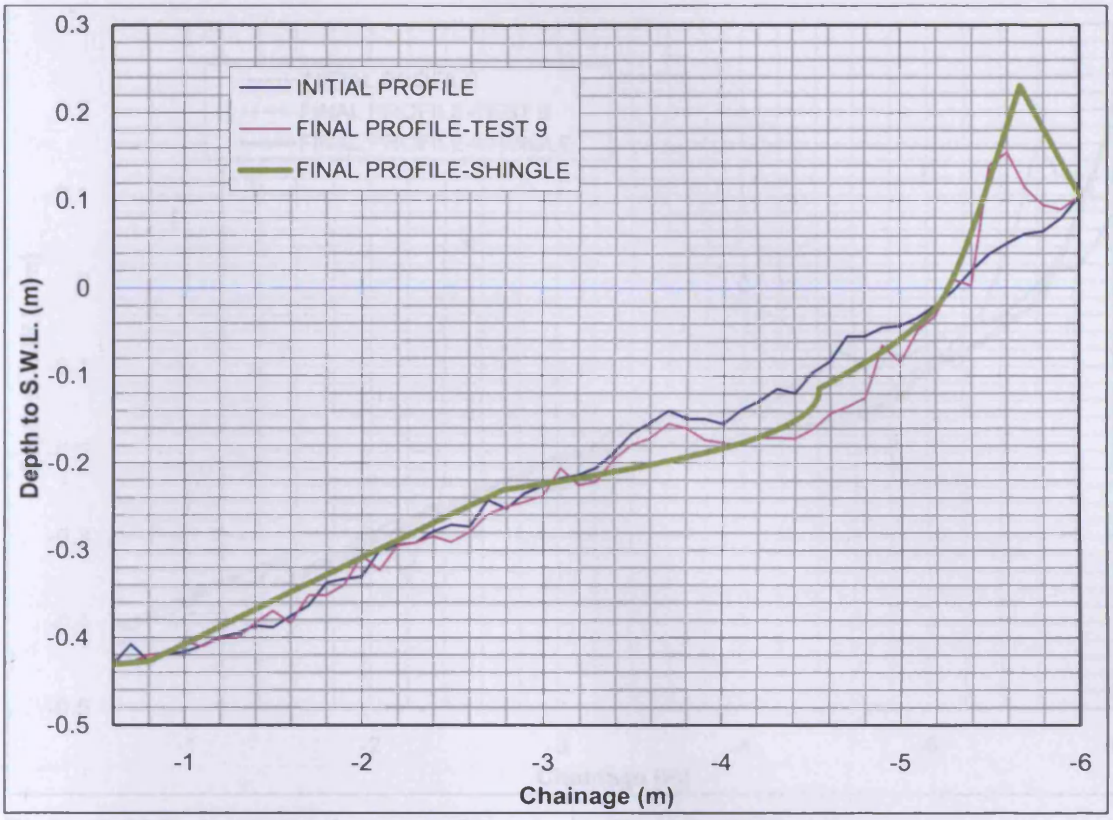

Figure 5-80 Estimated and measured beach profile (Line 2- Test 9)

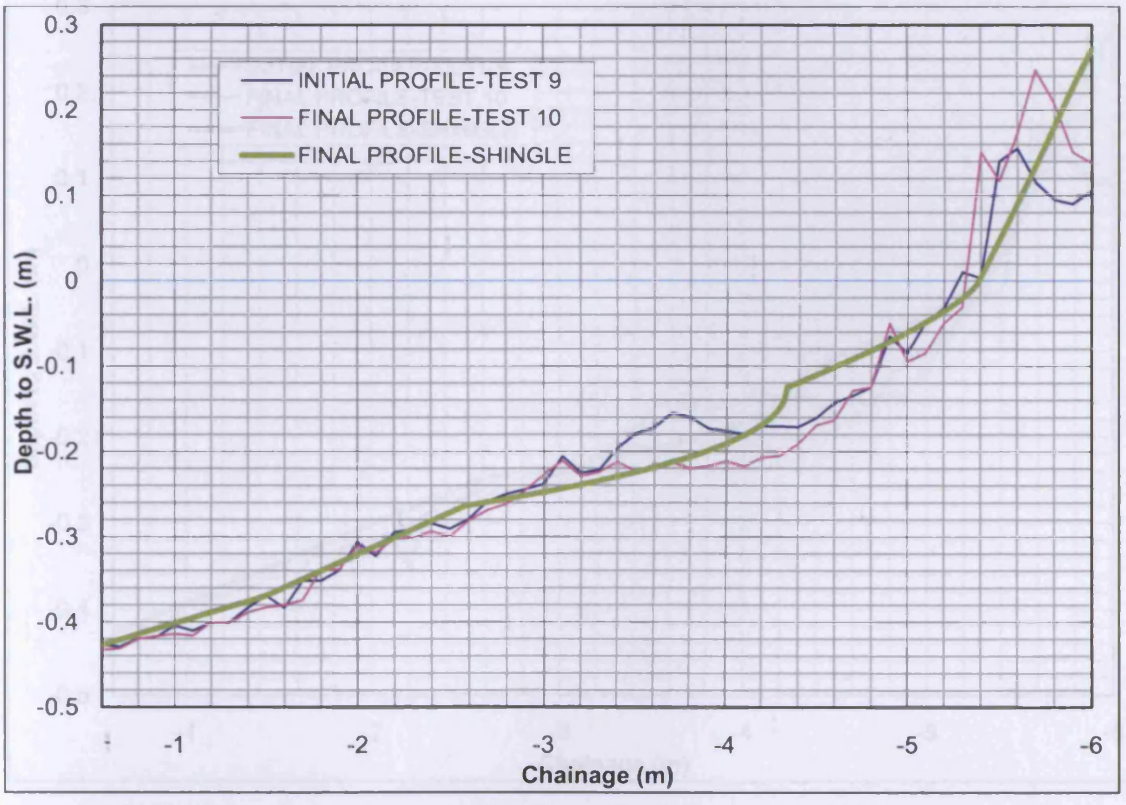

Figure 5-81 Estimated and measured beach profile (Line 2- Test 10)

Figure 5-82 Estimated and measured beach profile (Line 3- Test 9)

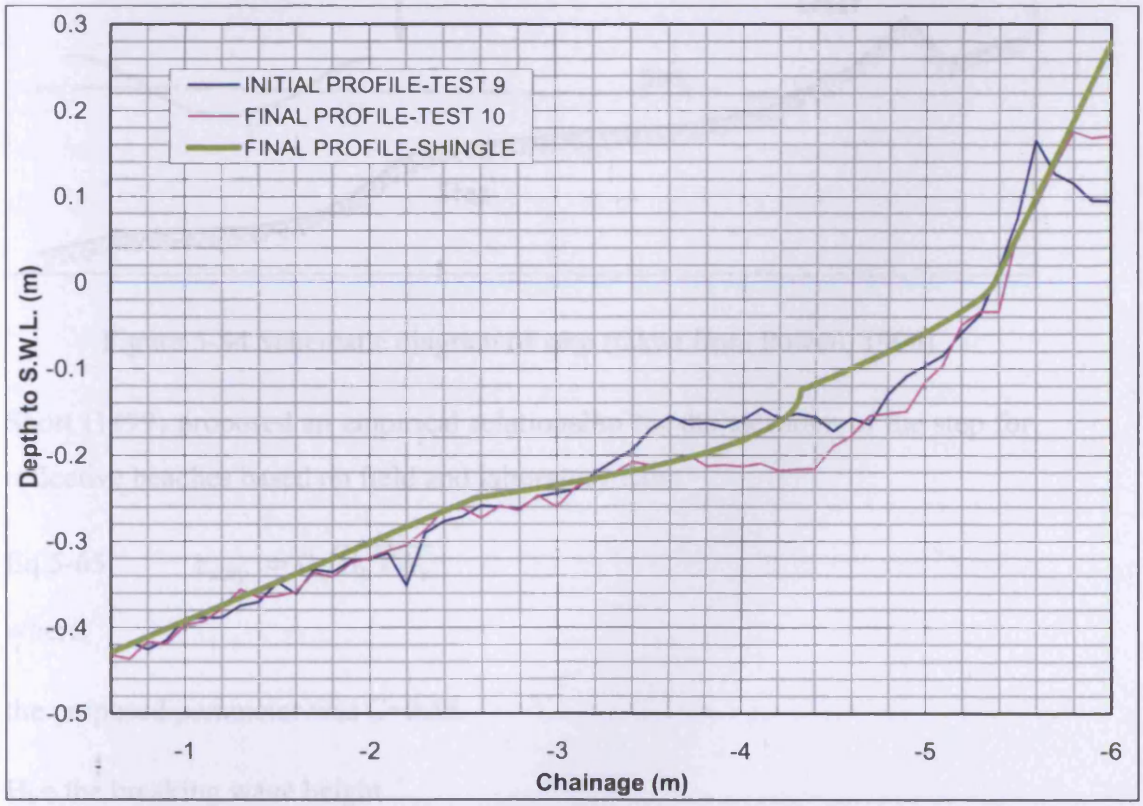

Figure 5-83 Estimated and measured beach profile (Line 3- Test 10)

5.4 Step and Berm elevation

The two empirical methods that were used to compare with the experimental results are based on the prediction of the step and berm elevation. However, these two empirical methods were tested for sandy beaches. Here, their applications on gravel and mixed beaches have been tested.

5.4.1 Step Elevation

A step profile formed by waves of low steepness and associated with beach accretion. The beach step is the final breaking point of waves before they rush up as swash on to the beach face (Figure 5-84). Because this is a high energy environment sediment, along the beach step is typically coarse grained.

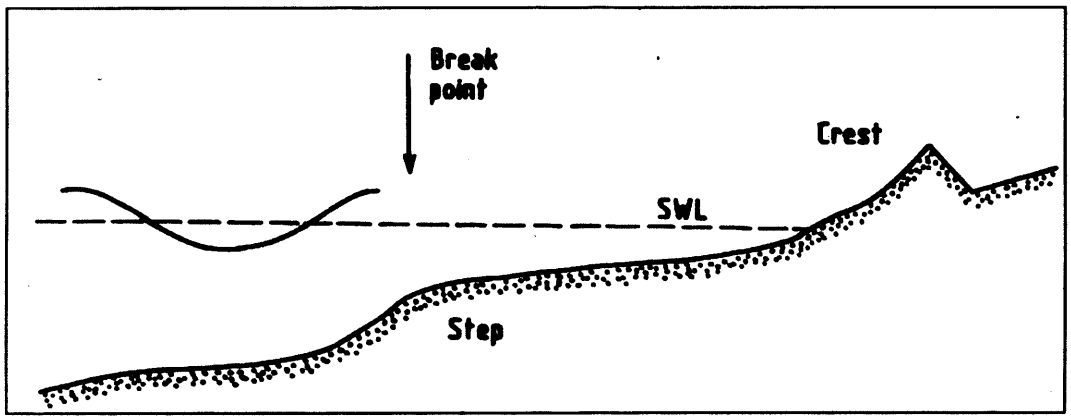

Figure 5-84 Schematic diagram of step (taken from Powell, 1990)

Short (1999) proposed an empirical relationship for the elevation of the step for reflective beaches based on field and laboratory data:

Eq.5-65 $$z_{step} = C\sqrt{H_b TW_s}$$

where,

the proposed parameter was C=0.55

H_b= the breaking wave height

W_s=the fall velocity

Short's measurements are within the following limits, in terms of $\sqrt{H_b T W_s}$:

- 0.04 to 0.2 for laboratory measurements
- 0.25 to 3 for field measurements

With range of applicability $\sqrt{H_b T W_s} = 0.0096$ to 0.023, Lopez de San Roman-Blanco (2003), by investigating the behaviour of mixed and gravel beach with normal incident wave height, proposed the parameter to be:

- C=0.8315 (R^2=0.70) for both sets of data, gravel and mixed beach
- C=0.8457 (R^2=0.70) for the mixed beach data
- C=0.8194 (R^2=0.73) for the gravel beach data

A comparison of the predicted (Eq.5-65) and the measured step elevation (from the experimental results) has been carried out. In contrast with the results of Lopez de San Roman-Blanco (2003), the step elevation was overestimated. The laboratory measurements were within the field limits, in terms of 0.30 to 0.67 which were in the limits of the data used by Short (1999) to derive Eq.5-65.

The fall velocity calculated as recommended by Ahrens (2003), where the breaking wave height, for regular waves, calculated as recommended by Rattanapitikon and Shibayama (2006) and for random waves calculated as recommended by Goda (1985). The proposed coefficients (C) based on the best fit line of step measurements data shown in Figure 5-85 to Figure 5-88. Therefore, the proposed coefficients of the Eq.5-65 for both regular and random waves are:

Regular Waves:

Trench

- C=0.5 (R^2=-4.8) for both sets of data, gravel and mixed beach
- C=0.662 (R^2=0.87) for the mixed beach data
- C=0.465 (R^2=-4.41) for the gravel beach data

Uniform slope

- C=0.364 (R^2=0.41) for both sets of data, gravel and mixed beach
- C=0.472 (R^2=-19.39) for the mixed beach data
- C=0.341 (R^2=0.62) for the gravel beach data

Random Waves:

Trench

- C=0.374 (R^2=-1.91) for both sets of data, gravel and mixed beach
- C=0.473 (R^2=-5.67) for the mixed beach data
- C=0.299 (R^2=-2.93) for the gravel beach data

Uniform slope

- C=0.362 (R^2=0.1) for both sets of data, gravel and mixed beach
- C=0.412 (R^2=0.99) for the mixed beach data
- C=0.322 (R^2=0.17) for the gravel beach data

It can be seen a similarity of the results of the measured step elevation for uniform slope for both regular and random wave conditions. This similarity might be related with the fact that the slopes and the wave energy were similar for both tests of regular and random waves. The results from the trench did not show any similarity between both wave conditions. However, for both trench and uniform slope the step elevation of the mixed beach was higher than the step elevation of the gravel beach, which is more likely due to effect of the present of the sand in the mixed beach.

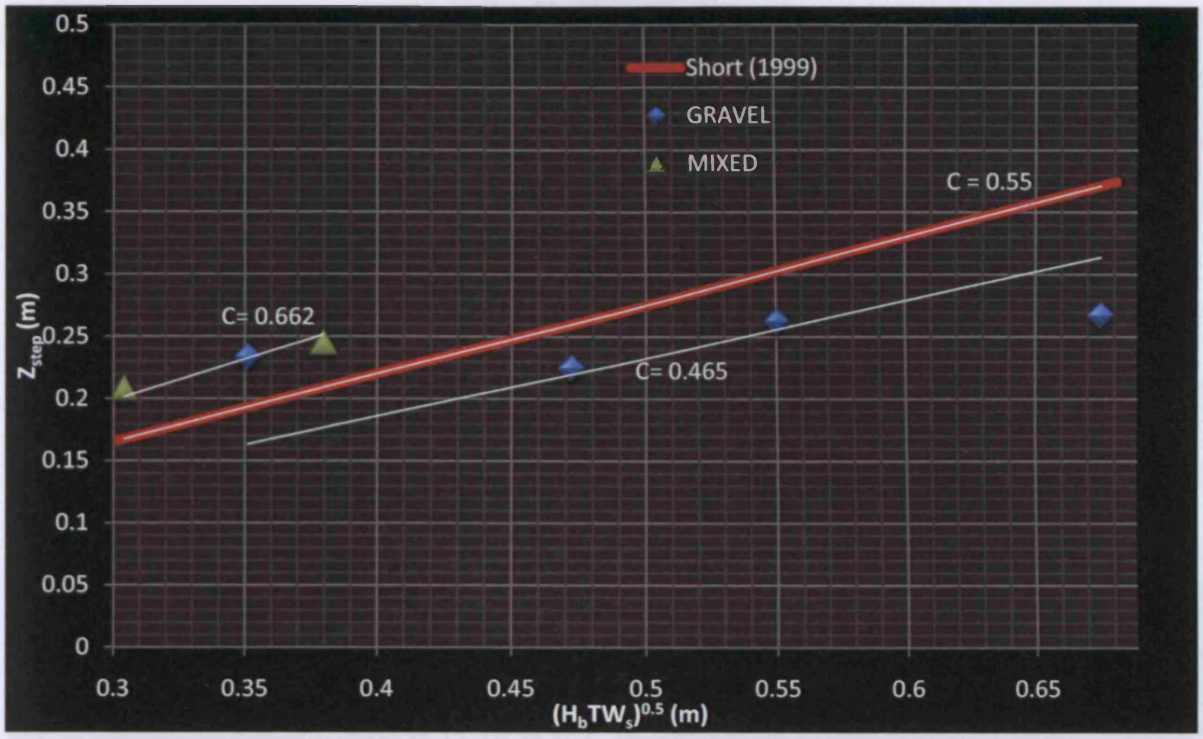

Figure 5-85 Step elevation measurements as a function of wave conditions (Trench-Regular waves)

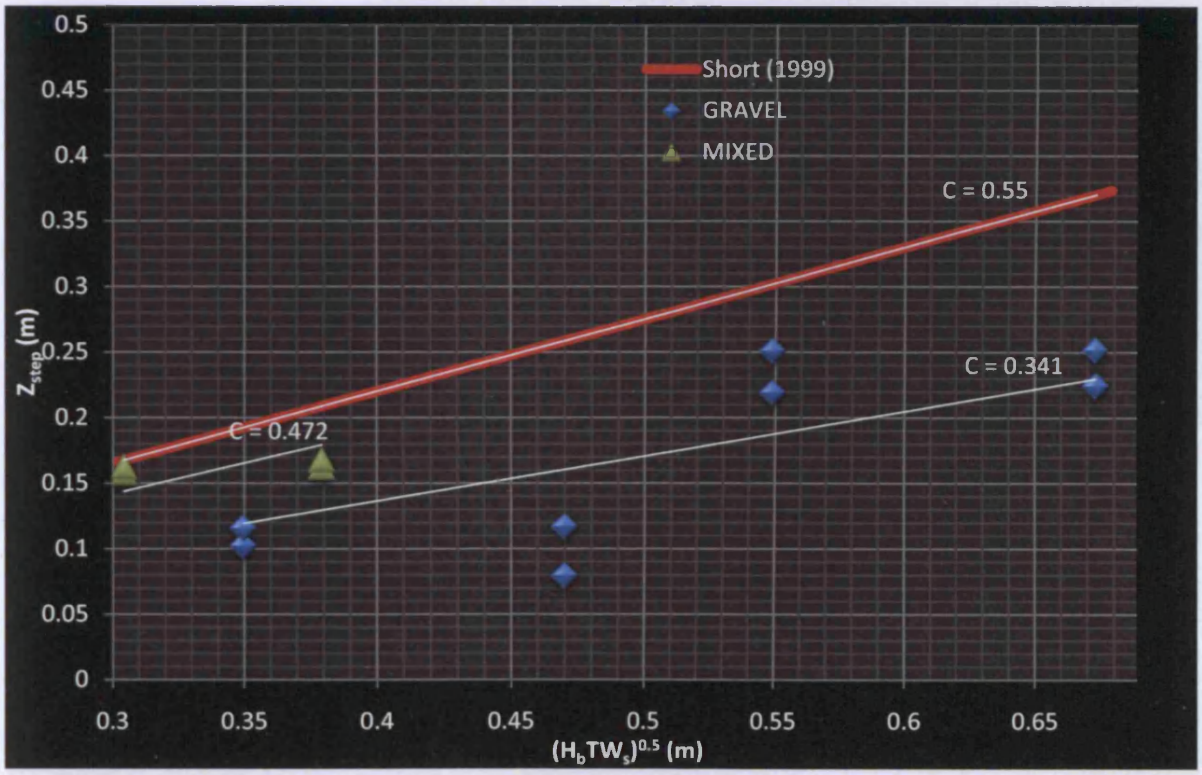

Figure 5-86 Step elevation measurements as a function of wave conditions (Uniform slope-Regular waves)

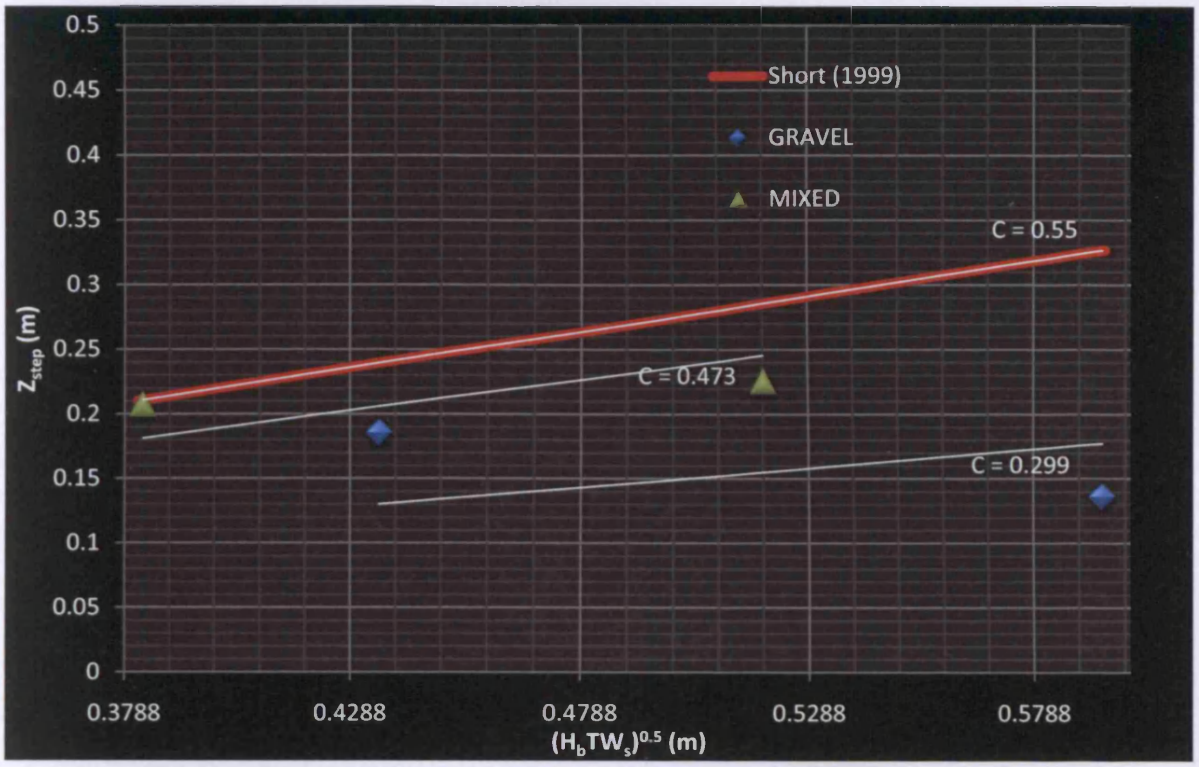

Figure 5-87 Step elevation measurements as a function of wave conditions (Trench-Random waves)

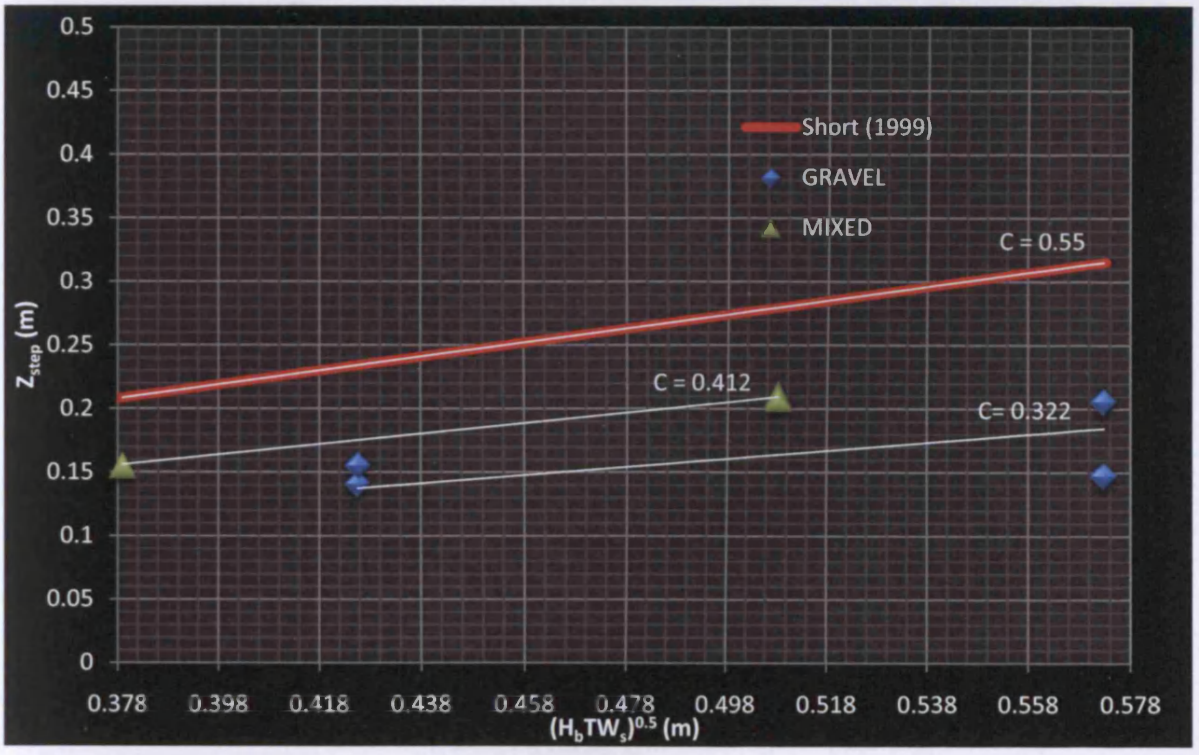

Figure 5-88 Step elevation measurements as a function of wave conditions (Uniform slope-Random waves)

5.4.2 Berm Elevation

Beach berm is defined as a nearly horizontal shore parallel berm formed on the beach due to the landward transport of the coarsest fraction of the beach material by the wave uprush (Figure 5-89). There may be several beach berms and in some cases no berms. Under normal conditions a beach berm is formed on the upper part of the foreshore, and over the backshore during severe events.

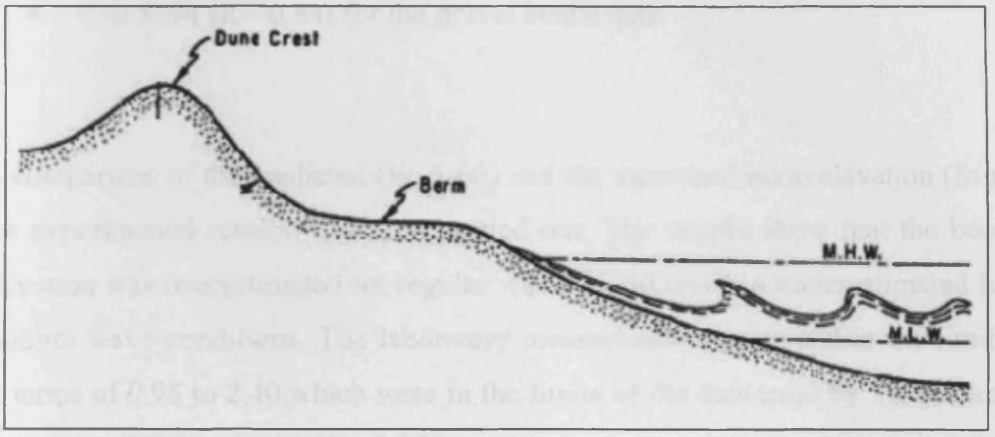

Figure 5-89 Schematic diagram of berm

Takeda and Sunamura (1982) proposed an empirical relationship for the elevation of the berm growth based on field and laboratory data:

Eq.5-66 $$B_h = C(H_b)^{\frac{5}{8}}(gT^2)^{\frac{3}{8}}$$

where,

the proposed parameter was C=0.125

H_b= the breaking wave height

Takeda and Sunamura (1982) measurements are within the following limits, in terms of $(H_b)^{\frac{5}{8}}(gT^2)^{\frac{3}{8}}$:

- 0.3 to 2 for laboratory measurements
- 5 to 25 for field measurements

With range of applicability$(H_b)^{\frac{5}{8}}(gT^2)^{\frac{3}{8}} = 1.6$ to 4.5, Lopez de San Roman-Blanco (2003), by investigating the behaviour of mixed and gravel beach with normal incident wave height, proposed the parameter to be:

- C=0.8315 (R^2=0.76) for both sets of data, gravel and mixed Beach
- C=0.8457 (R^2=0.92) for the mixed beach data
- C=0.8194 (R^2=0.84) for the gravel beach data

A comparison of the predicted (Eq.5-66) and the measured berm elevation (from the experimental results) has been carried out. The results show that the berm elevation was overestimated for regular wave conditions and underestimated for random wave conditions. The laboratory measurements were within the limits, in terms of 0.95 to 2.40 which were in the limits of the data used by Takeda and Sunamura (1982) to derive Eq.5-66.

The breaking wave height for regular waves calculated as recommended by Rattanapitikon and Shibayama (2000, 2006) and for random waves calculated as recommended by Goda (1985). The proposed coefficients (C) based on the best fit line of berm measurements data shown in Figure 5-90 to Figure 5-93. Therefore, the proposed coefficients of the Eq.5-66 for both regular and random waves are:

Regular Waves:

Trench

- C=0.12 (R^2=-0.38) for both sets of data, gravel and mixed Beach
- C=0.658 (R^2=0.76) for the mixed beach data
- C=0.118 (R^2=-0.94) for the gravel beach data

Uniform slope

- C=0.08 (R^2=0.54) for both sets of data, gravel and mixed Beach
- C=0.089 (R^2=0.74) for the mixed beach data
- C=0.078 (R^2=0.53) for the gravel beach data

Random Waves:

Trench

- C=0.107 (R^2=-0.94) for both sets of data, gravel and mixed beach
- C=0.121 (R^2=-3.67) for the mixed beach data
- C=0.093 (R^2=87) for the gravel beach data

Uniform slope

- C=0.144 (R^2=0.26) for both sets of data, gravel and mixed Beach
- C=0.157 (R^2=0.65) for the mixed beach data
- C=0.13 (R^2=-0.05) for the gravel beach data

It can be seen that there is not any similarity of the results of the measured berm elevation either for uniform slope or for trench for both regular and random wave conditions. The results show that for regular waves, the berm elevation for the trench was higher than for uniform slope whether for random waves it was the opposite.

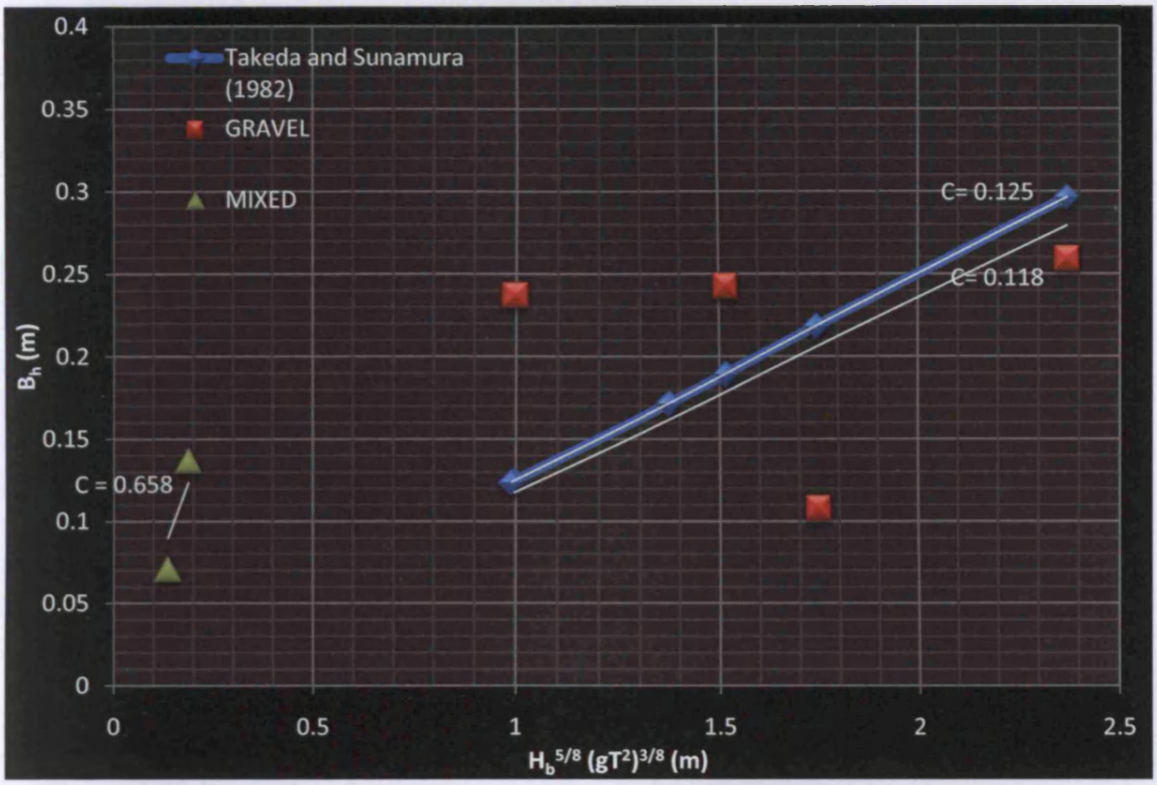

Figure 5-90 Berm elevation measurements as a function of wave conditions (Trench-Regular waves)

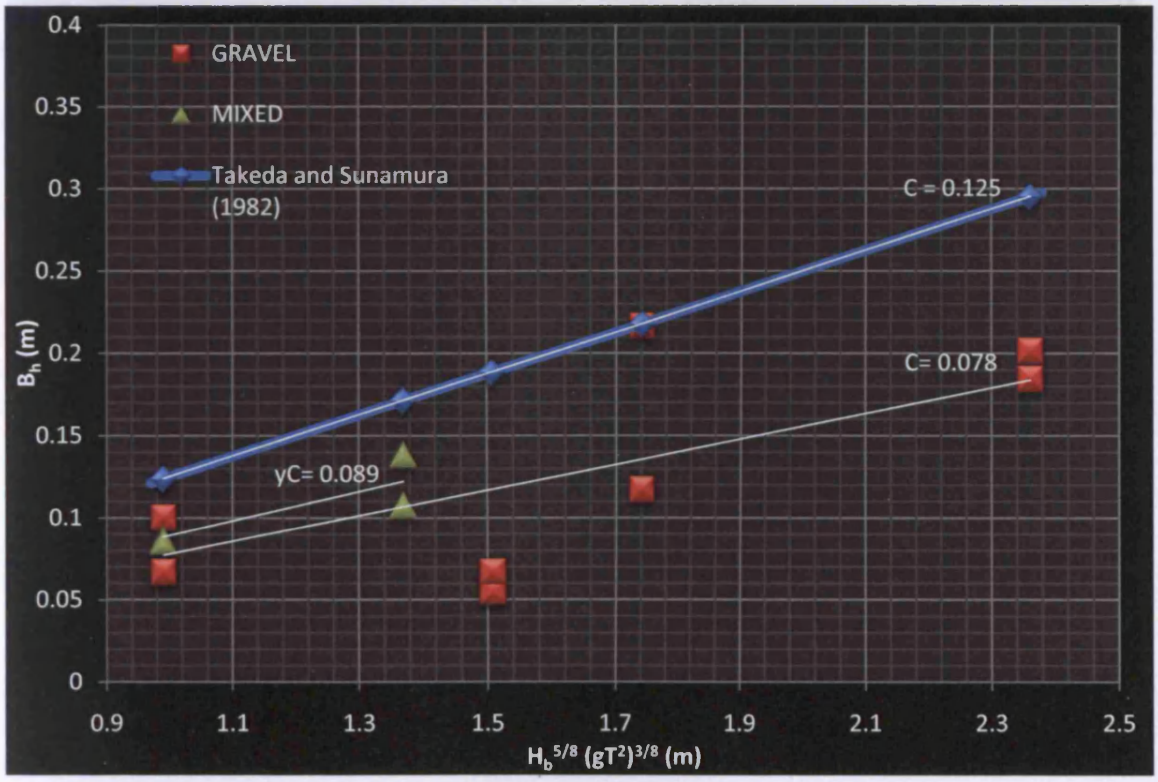

Figure 5-91 Berm elevation measurements as a function of wave conditions (Uniform slope-Regular waves)

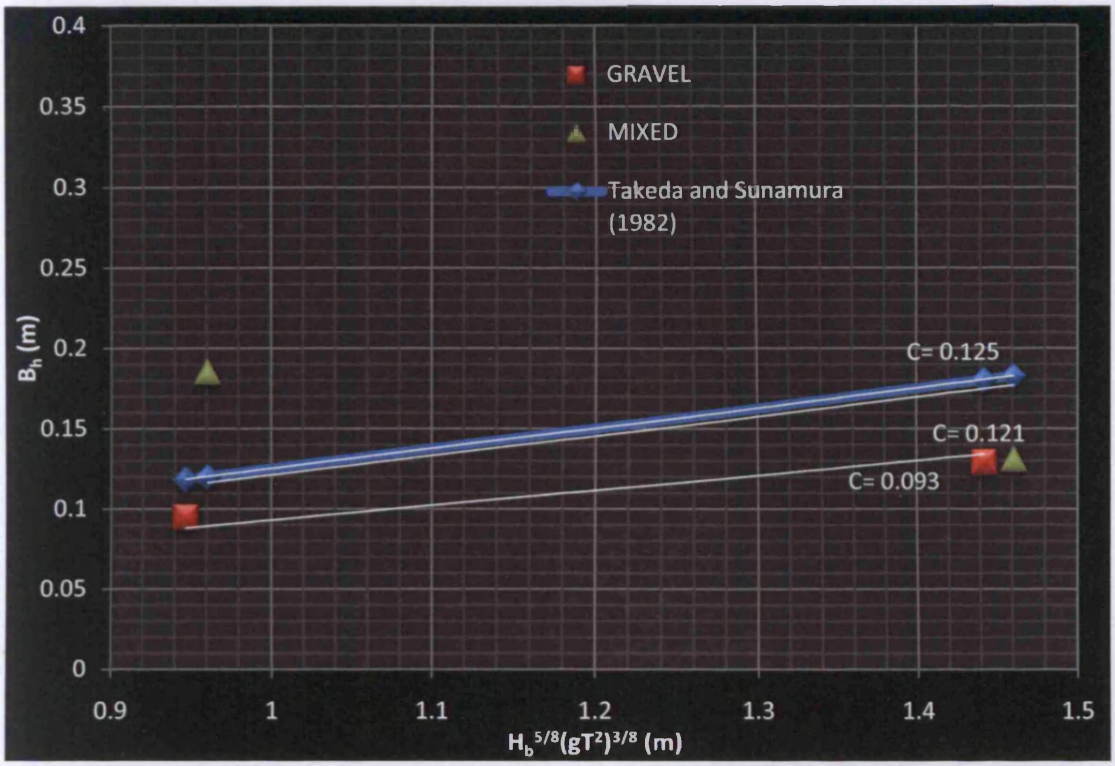

Figure 5-92 Berm elevation measurements as a function of wave conditions (Trench-Random waves)

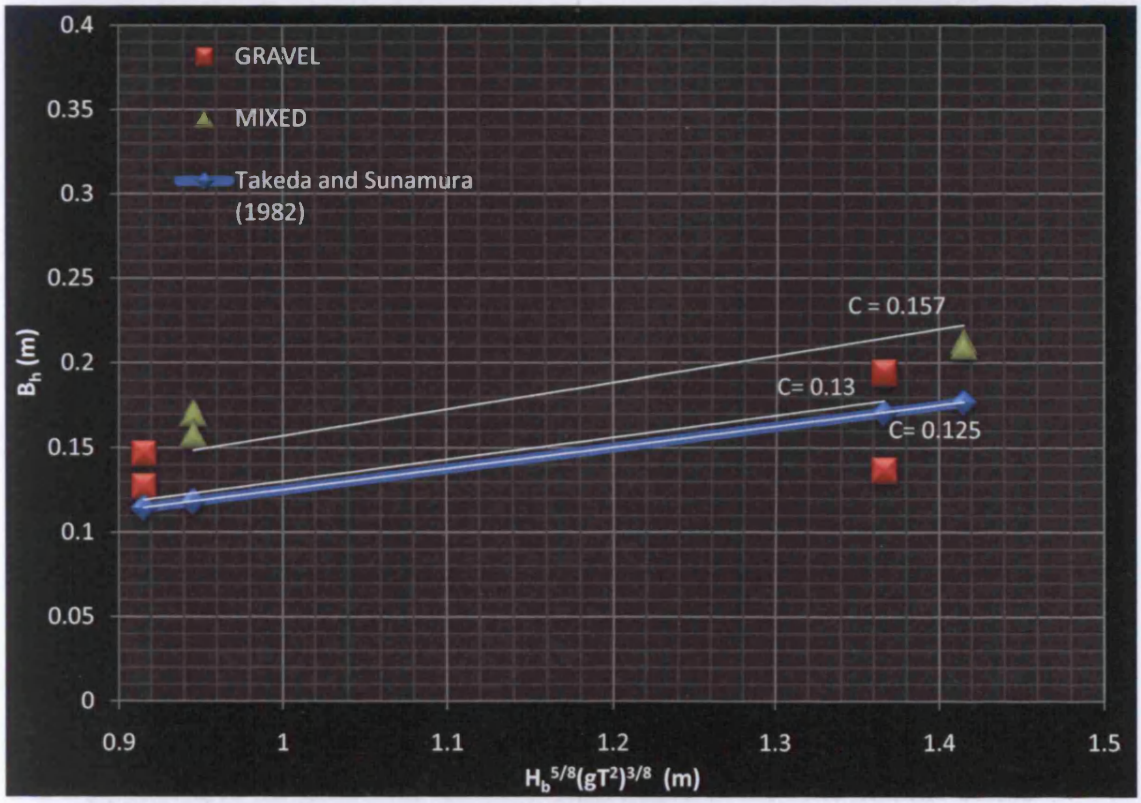

Figure 5-93 Berm elevation measurements as a function of wave conditions (Uniform slope-Random waves)

5.5 SEDIMENT BALANCE

The sediment balance of the three lines is investigated here in two stages:

1. Total Sediment Balance
2. Sediment Balance below and above SWL

In both stages the figures presented the sediment balance along each Line, individually, from the beginning to the end of each Test, for gravel and mixed beach, respectively. The following figures were calculated for each test, and shown in the tables;

- Accretion: indicates total positive volumetric change along each line
- Erosion: indicates total negative volumetric change along each line
- Total: indicates total volumetric change along each line (sum of Accretion and Erosion)
- Difference (%): indicates the relative difference between the accretion and erosion. It also accounts for the conservation of sediment volume and therefore gives an idea of the amount of compaction and settlement that occurred in each line and test. This parameter is calculated by:

$$\text{Eq.5-67} \quad \text{Difference (\%)} = \frac{\text{Accretion} - \text{Erosion}}{\text{Total}} \text{x100}$$

The volumetric change is calculated by the difference, between the area of the line at the beginning of the test and the area of the line at the end of the test, multiple by meter per meter.

It is important to find out if gravel acts like a filter for sand or not. The filter acts like a barrier for the fine material preventing it to pass through the voids of the filter. Based on the soil category "for sand and gravels", the filter criteria by USBR (1994) was $D_{15F} \leq 4D_{85B}$, where D_{15F} indicates the grain size diameter of the filter where 15% by weight of the soil particles are smaller in diameter, and D_{85B} indicates the grain size diameter where 85% of the base or filter soil is

smaller in diameter. For the current experiment D_{15F}=16.66mm > 4*D_{85B}=2.4mm. This shows that gravel did not act as a filter for sand.

5.5.1 Total Sediment Balance

The results for the total sediment balance investigation are listed in Table 5-35 and Table 5-36 and are shown in Figure 5-94 to Figure 5-96. Despite the fact that the number of waves between each test is different, it will not change the trend of the parameters.

Table 5-35 Total Sediment Balance of Line 3 and Line 2

	Line 3				Line 2			
	Accretion (m^3)	Erosion (m^3)	Total (m^3)	Difference (%)	Accretion (m^3)	Erosion (m^3)	Total (m^3)	Difference (%)
Test 1	0.04	0.1775	0.2175	-63.22	0.0001	0.3383	0.3384	-99.94
Test 2	0.1163	0.2348	0.3511	-33.75	0.0627	0.0822	0.1449	-13.46
Test 3	0.0643	0.0063	0.0706	82.15	0.0323	0.0206	0.0529	22.12
Test 4	0.0103	0.0194	0.0297	-30.64	0.0298	0.0189	0.0487	22.38
Test 5	0.0643	0.0312	0.0955	34.66	0.0716	0.0238	0.0954	50.10
Test 6	0.0601	0.3408	0.4009	-70.02	0.0348	0.0742	0.109	-36.15
Test 7	0.1049	0.011	0.1159	81.02	0.013	0.0827	0.0957	-72.83
Test 8	0.0122	0.0712	0.0834	-70.74	0.0479	0.0318	0.0797	20.20
Test 9	0.0634	0.1098	0.1732	-26.79	0.0361	0.0814	0.1175	-38.55
Test 10	0.0297	0.0893	0.119	-50.08	0.0498	0.0676	0.1174	-15.16

Table 5-36 Total Sediment Balance of Line 1

	Line 1			
	Accretion (m^3)	Erosion (m^3)	Total (m^3)	Difference (%)
Test 1	0.0592	0.0327	0.0919	28.84
Test 2	0.1016	0.1122	0.2138	-4.96
Test 3	0.0623	0.0052	0.0675	84.59
Test 4	0.0192	0.0294	0.0486	-20.99
Test 5	0.0584	0.0242	0.0826	41.40
Test 6	0.2307	0.0386	0.2693	71.33
Test 7	0.0304	0.0497	0.0801	-24.09
Test 8	0.069	0.018	0.087	58.62
Test 9	0.0436	0.0742	0.1178	-25.98
Test 10	0.1063	0.0482	0.1545	37.61

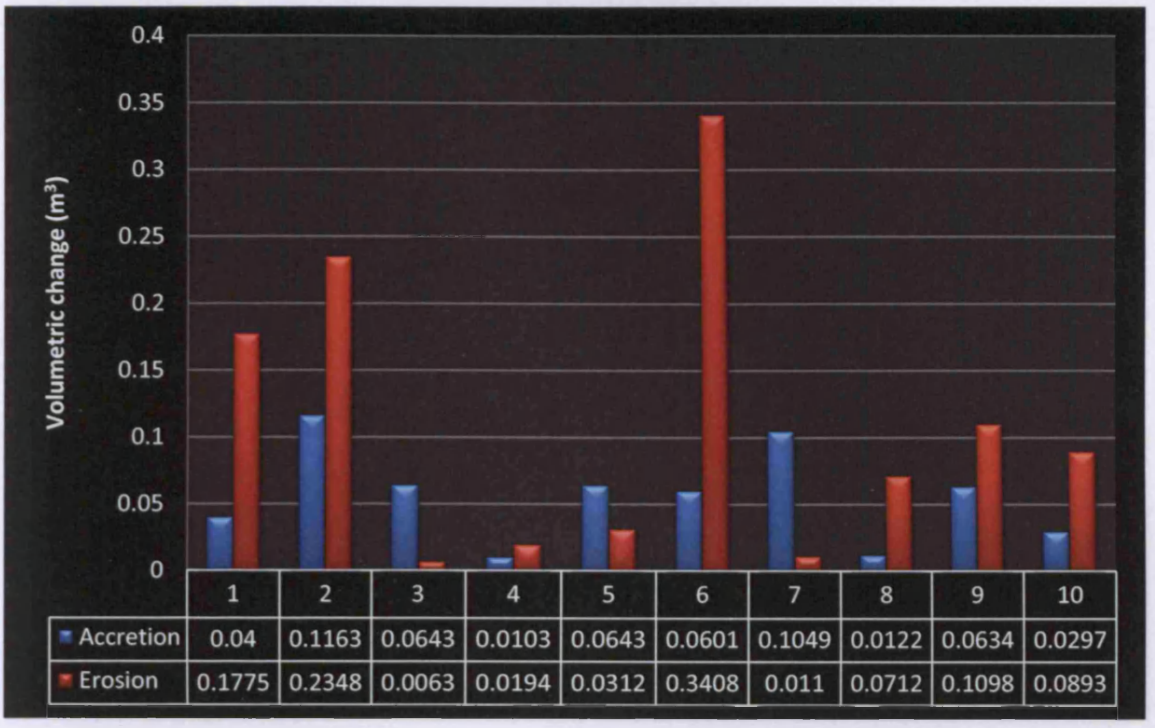

	1	2	3	4	5	6	7	8	9	10
Accretion	0.04	0.1163	0.0643	0.0103	0.0643	0.0601	0.1049	0.0122	0.0634	0.0297
Erosion	0.1775	0.2348	0.0063	0.0194	0.0312	0.3408	0.011	0.0712	0.1098	0.0893

Figure 5-94 Total Sediment Balance of Line 3

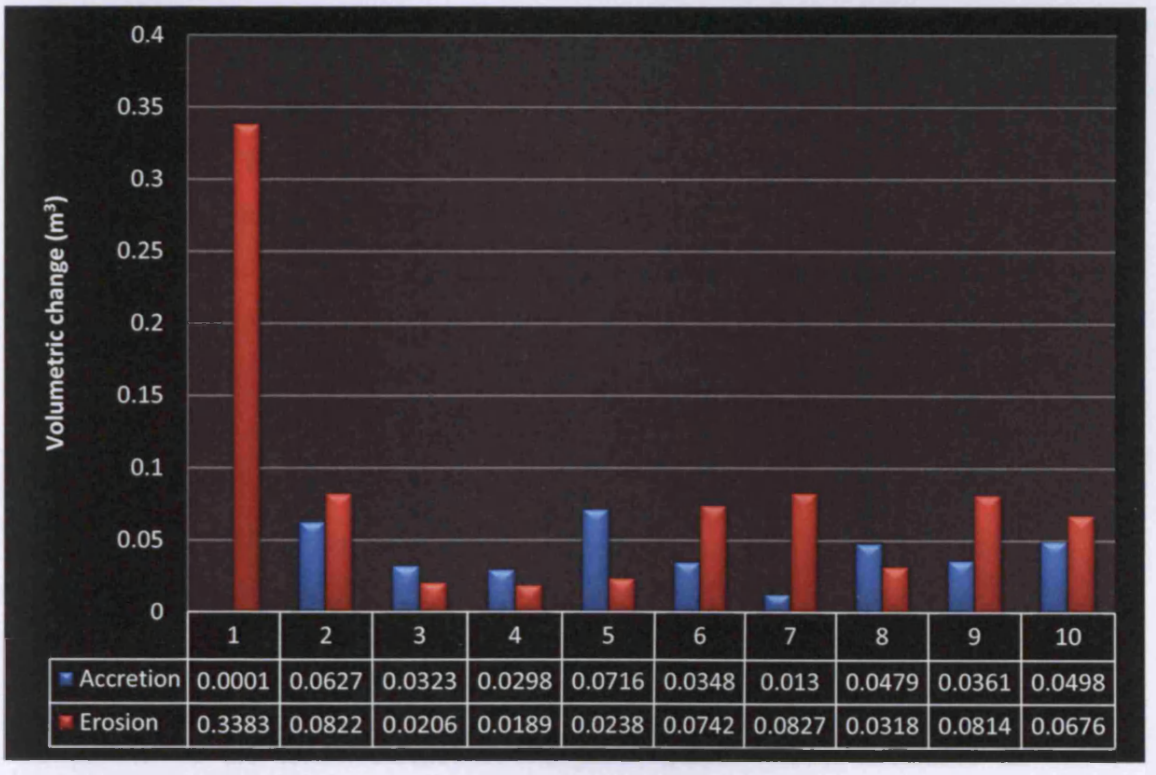

	1	2	3	4	5	6	7	8	9	10
Accretion	0.0001	0.0627	0.0323	0.0298	0.0716	0.0348	0.013	0.0479	0.0361	0.0498
Erosion	0.3383	0.0822	0.0206	0.0189	0.0238	0.0742	0.0827	0.0318	0.0814	0.0676

Figure 5-95 Total Sediment Balance of Line 2

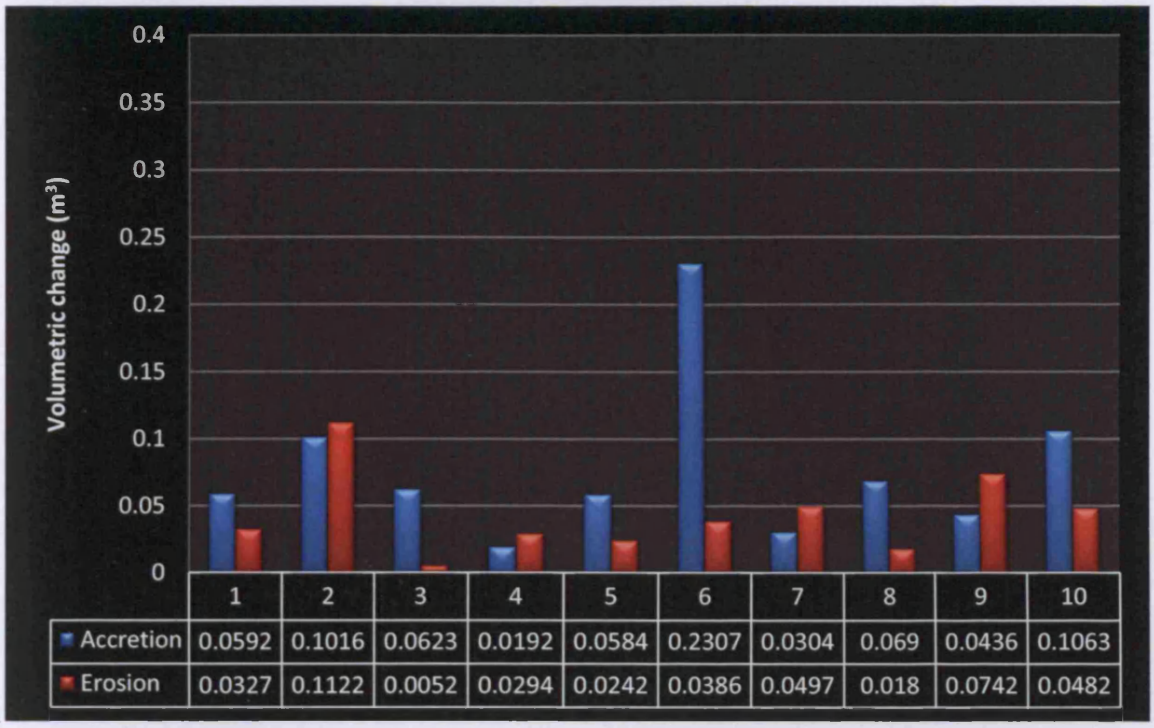

	1	2	3	4	5	6	7	8	9	10
Accretion	0.0592	0.1016	0.0623	0.0192	0.0584	0.2307	0.0304	0.069	0.0436	0.1063
Erosion	0.0327	0.1122	0.0052	0.0294	0.0242	0.0386	0.0497	0.018	0.0742	0.0482

Figure 5-96 Total Sediment Balance of Line 1

Regarding profile change for the gravel beach (Test 1 to Test 6):

Lines 2 and 3

Lines 2 and 3 had the same pattern relating to the accretion and erosion at each test. When Line 3 had more erosion than accretion, Line 2 had the same pattern (except in Test 4). There was not any sign of long-shore sediment transport from Line 3 to Line 2. In general, the pattern of total volumetric change of Line 2 increased in magnitude in relation to the wave steepness where of Line 3 decreased (except at Tests 5 and 6). Line 3 had the highest accretion at Test 2 where Line 2 at Test 5. Line 3 had the highest erosion and total volumetric change at Test 6 where Line 2 at Test 1. Only at Test 5 both Lines had almost the same total volumetric change.

Line 1

The pattern of the total volumetric change of Line 1 often decreased in magnitude in relation to the wave steepness (except Test 3 and 4). The highest accretion of Line 1 was at Test 6 where the highest erosion was at Test 2.By comparing Line 1 with Lines 2 and 3 a pattern of long-shore sediment transport

from Line 3 to Line 1 at Test 4 can be identified. The amount of erosion at Line 3 and Line 2 at Test 4 was almost the same with the amount of the accretion of Line 1 for the same test.

Regarding profile change for the mixed beach (Test 7 to Test 10):

Lines 2 and 3

At Mixed Beach, Line 2 and 3 had different pattern relating to the accretion and erosion only at Tests 7 and 8. There was a sign of long-shore sediment transport between the lines at Test 7 where the amount of erosion at Line 3 was almost the same with the amount of accretion of Line 2 for the same test. Moreover, the pattern of the total volumetric change of both lines increased in magnitude in relation to the wave steepness. The highest accretion at Line 3 was at Test 7 where Line 2 at Test 10. Line 2 had in general low accretion compared to the erosion at each Test (except Test 8). The highest erosion for Line 3 was at Test 9 where for Line 2 was at Test 7. Furthermore, at Test 9 there was the highest total volumetric change for both lines. Both lines had similar total volumetric changes at Test 10.

Line 1

The pattern of total volumetric change of Line 1 for gravel beach was the same in Mixed Beach. It decreased in magnitude in relation to the wave steepness. The highest accretion of Line 1 was at Test 10 where the highest erosion was at Test 9. At Line 1, the amount of erosion was often more than the amount of accretion of each test (except Test 8). The highest total volumetric change of Line 1 was at Test 10. By comparing Line 1 with Lines 2 and 3, a pattern of long-shore sediment transport from the lines to Line 1 could not be identified.

5.5.2 Sediment Balance below and above SWL

The results for the sediment balance below and above Still Water Level (S.W.L.) investigation are listed in Table 5-37 to Table 5-40. Table 5-36 and are shown in Figure 5-97 to Figure 5-102.

Table 5-37 Sediment Balance below S.W.L. of Line 3 and Line 2

	Line 3				Line 2			
	Accretion (m^3)	Erosion (m^3)	Total (m^3)	Difference (%)	Accretion (m^3)	Erosion (m^3)	Total (m^3)	Difference (%)
Test 1	0.0284	0.1507	0.1791	-68.29	0.0001	0.2618	0.2619	-99.92
Test 2	0.1163	0.1695	0.2858	-18.61	0.0414	0.0822	0.1236	-33.01
Test 3	0.0535	0.0063	0.0598	78.93	0.0148	0.0206	0.0354	-16.38
Test 4	0.0066	0.0158	0.0224	-41.07	0.0165	0.0149	0.0314	5.10
Test 5	0.0625	0.0291	0.0916	36.46	0.0654	0.0131	0.0785	66.62
Test 6	0.0146	0.3408	0.3554	-91.78	0.002	0.0742	0.0762	-94.75
Test 7	0.0792	0.011	0.0902	75.61	0.0065	0.0769	0.0834	-84.41
Test 8	0.01	0.0572	0.0672	-70.24	0.0257	0.0317	0.0574	-10.45
Test 9	0.0112	0.1098	0.121	-81.49	0.0066	0.0808	0.0874	-84.90
Test 10	0.0121	0.0788	0.0909	-73.38	0.0037	0.0665	0.0702	-89.46

Table 5-38 Sediment Balance below S.W.L. of Line 1

	Line 1			
	Accretion (m^3)	Erosion (m^3)	Total (m^3)	Difference (%)
Test 1	0.0405	0.0253	0.0658	23.10
Test 2	0.0276	0.1122	0.1398	-60.52
Test 3	0.0508	0.0046	0.0554	83.39
Test 4	0.0169	0.0217	0.0386	-12.44
Test 5	0.0539	0.0174	0.0713	51.19
Test 6	0.2186	0.0375	0.2561	70.71
Test 7	0.0077	0.0497	0.0574	-73.17
Test 8	0.0372	0.0167	0.0539	38.03
Test 9	0.0121	0.0673	0.0794	-69.52
Test 10	0.0525	0.0475	0.1	5.00

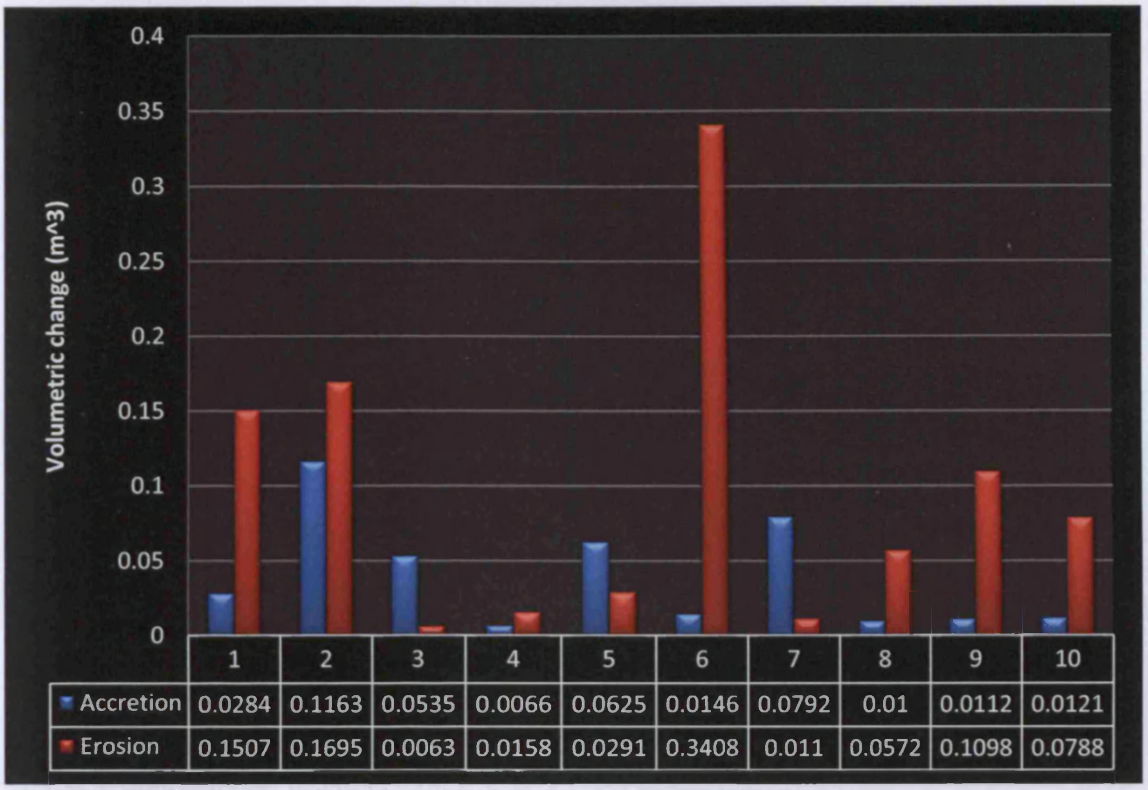

Figure 5-97 Sediment Balance below S.W.L. of Line 3

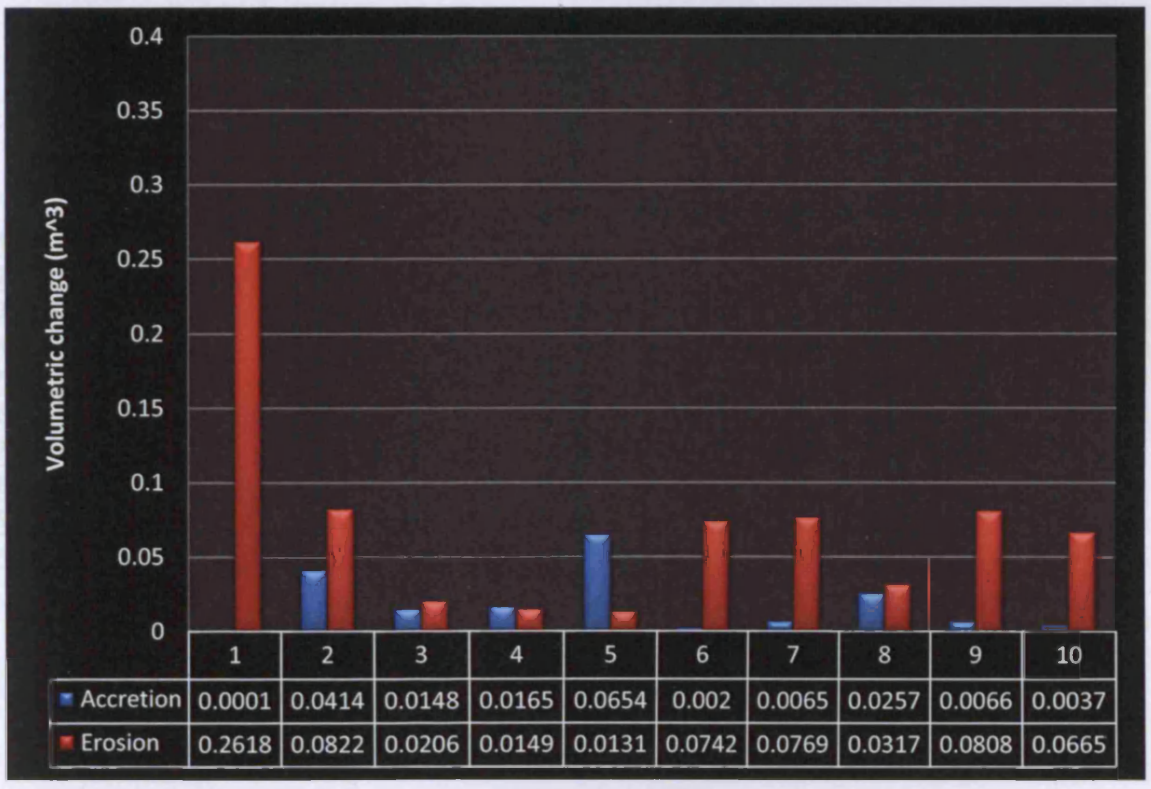

Figure 5-98 Sediment Balance below S.W.L. of Line 2

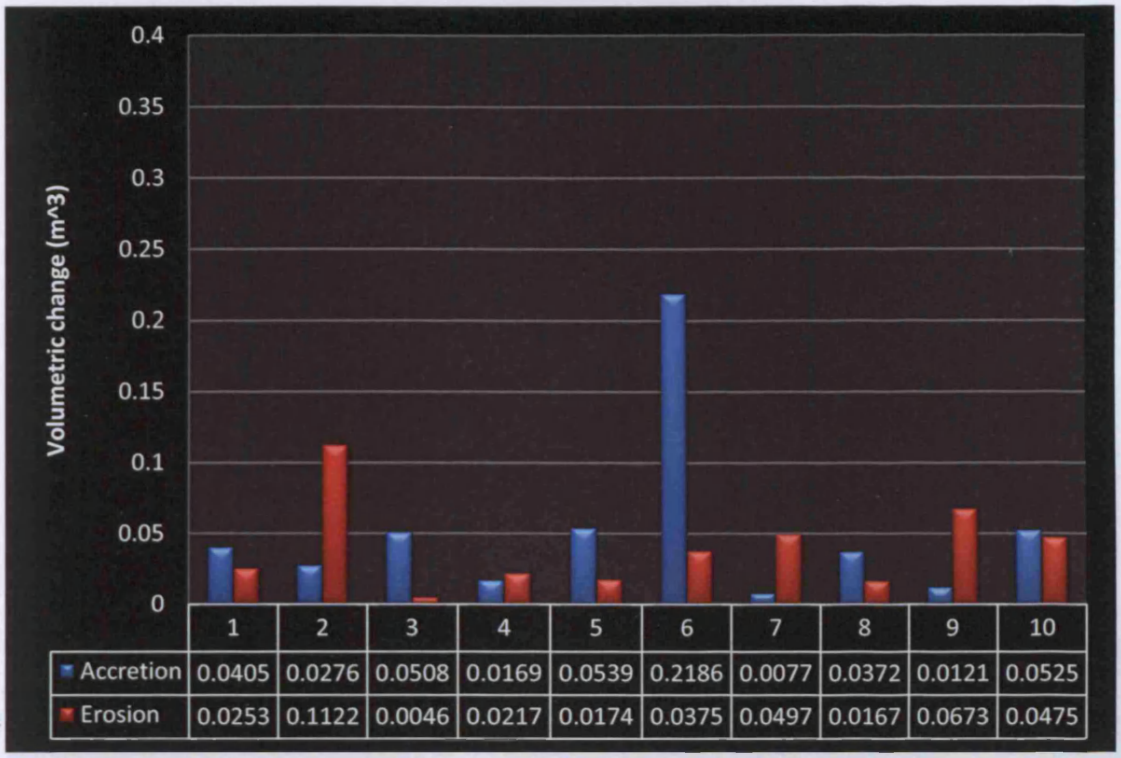

Figure 5-99 Sediment Balance below S.W.L. of Line 1

Table 5-39 Sediment Balance above S.W.L. of Line 3 and Line 2

	Line 3				Line 2			
	Accretion (m^3)	Erosion (m^3)	Total (m^3)	Difference (%)	Accretion (m^3)	Erosion (m^3)	Total (m^3)	Difference (%)
Test 1	0.0116	0.0268	0.0384	-39.58	0	0.0765	0.0765	-100.00
Test 2	0	0.0653	0.0653	-100.00	0.0213	0	0.0213	100.00
Test 3	0.0108	0	0.0108	100.00	0.0175	0	0.0175	100.00
Test 4	0.0037	0.0036	0.0073	1.37	0.0133	0.004	0.0173	53.76
Test 5	0.0018	0.0021	0.0039	-7.69	0.0062	0.0107	0.0169	-26.63
Test 6	0.0455	0	0.0455	100.00	0.0328	0	0.0328	100.00
Test 7	0.0257	0	0.0257	100.00	0.0065	0.0058	0.0123	5.69
Test 8	0.0022	0.014	0.0162	-72.84	0.0222	0.0001	0.0223	99.10
Test 9	0.0522	0	0.0522	100.00	0.0295	0.0006	0.0301	96.01
Test 10	0.0176	0.0105	0.0281	25.27	0.0461	0.0011	0.0472	95.34

Table 5-40 Sediment Balance above S.W.L. of Line 1

	Line 1			
	Accretion (m^3)	Erosion (m^3)	Total (m^3)	Difference (%)
Test 1	0.0187	0.0074	0.0261	43.30
Test 2	0.074	0	0.074	100.00
Test 3	0.0115	0.0006	0.0121	90.08
Test 4	0.0023	0.0077	0.01	-54.00
Test 5	0.0045	0.0068	0.0113	-20.35
Test 6	0.0121	0.0011	0.0132	83.33
Test 7	0.0227	0	0.0227	100.00
Test 8	0.0318	0.0013	0.0331	92.15
Test 9	0.0315	0.0069	0.0384	64.06
Test 10	0.0538	0.0007	0.0545	97.43

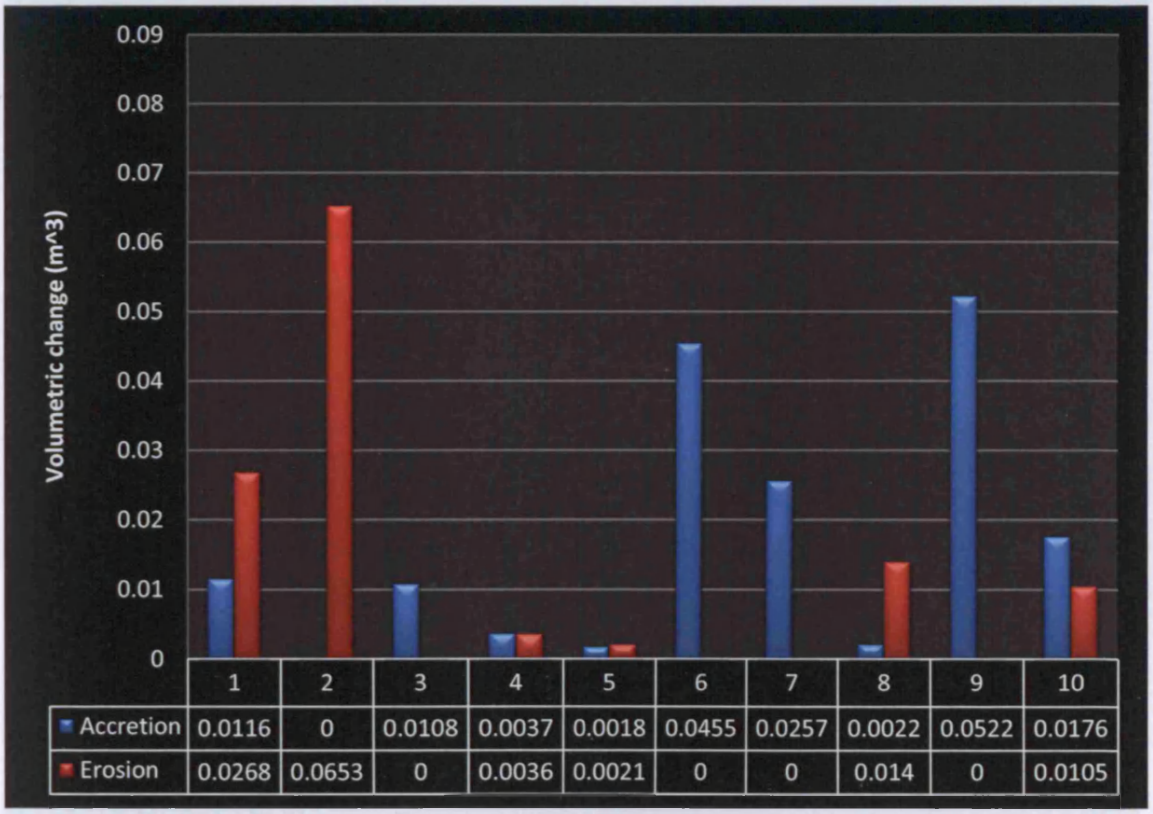

Figure 5-100 Sediment Balance above S.W.L. of Line 3

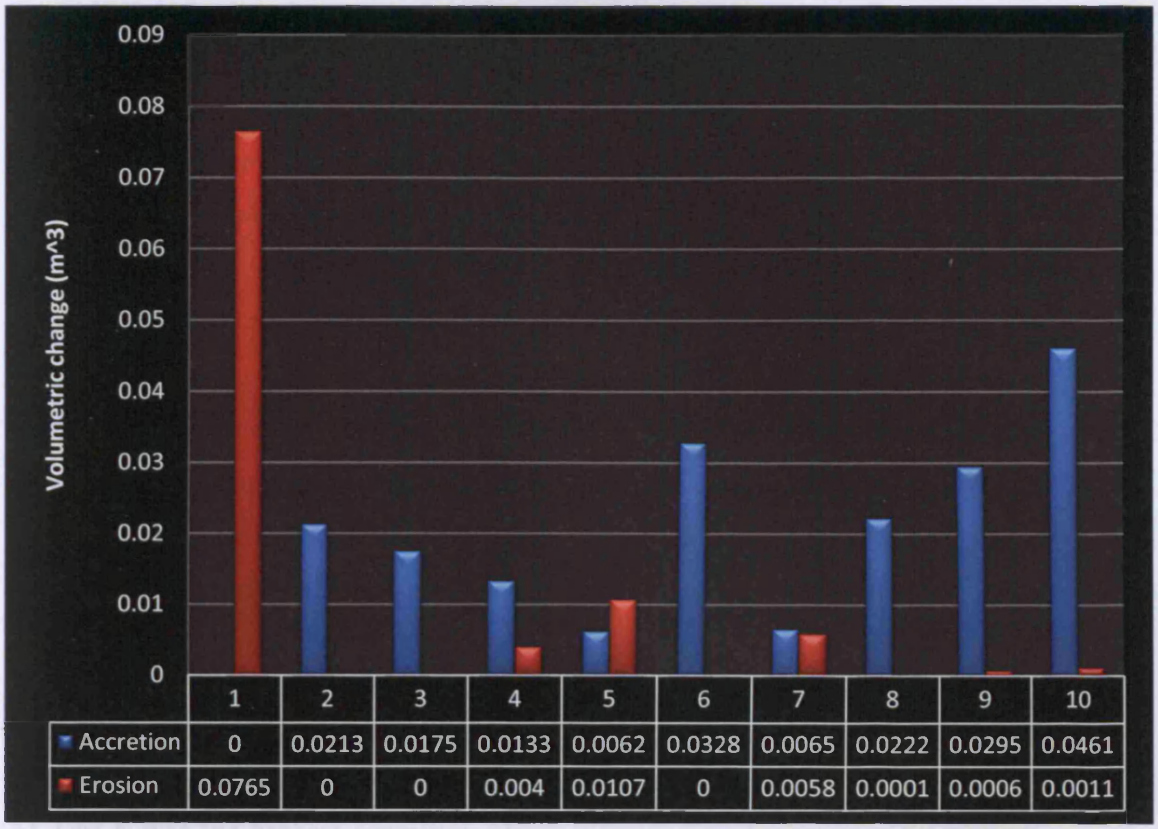

	1	2	3	4	5	6	7	8	9	10
Accretion	0	0.0213	0.0175	0.0133	0.0062	0.0328	0.0065	0.0222	0.0295	0.0461
Erosion	0.0765	0	0	0.004	0.0107	0	0.0058	0.0001	0.0006	0.0011

Figure 5-101 Sediment Balance above S.W.L. of Line 2

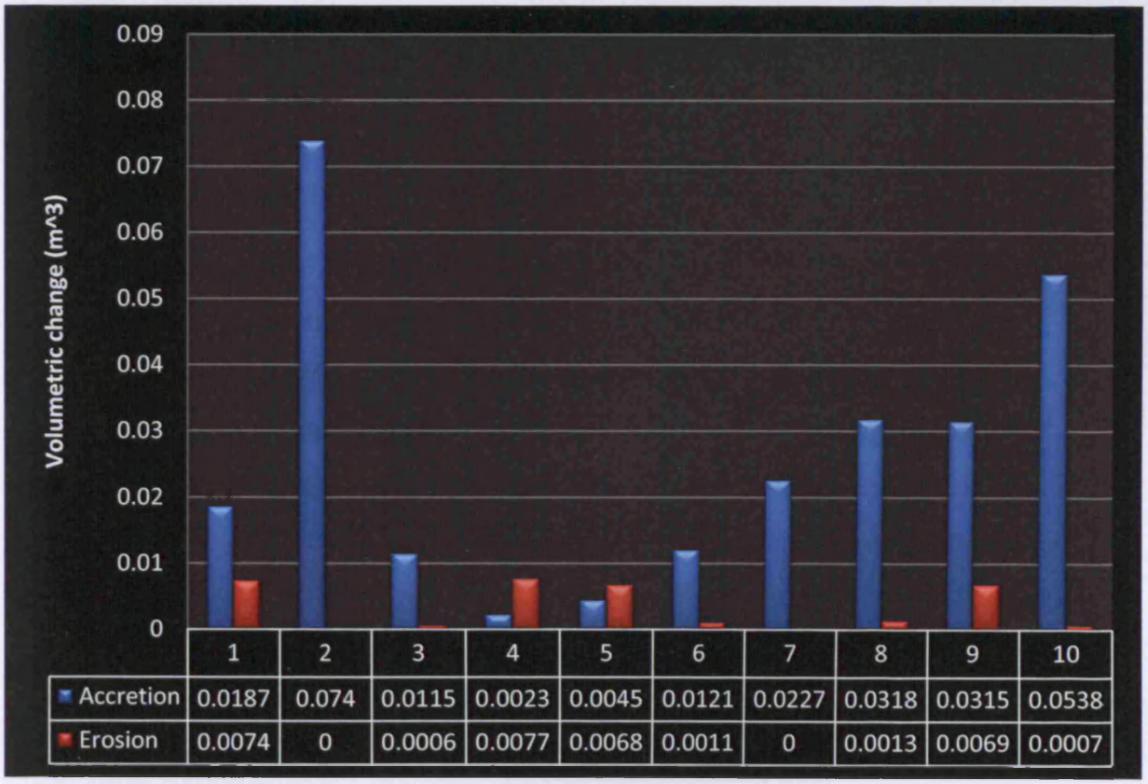

	1	2	3	4	5	6	7	8	9	10
Accretion	0.0187	0.074	0.0115	0.0023	0.0045	0.0121	0.0227	0.0318	0.0315	0.0538
Erosion	0.0074	0	0.0006	0.0077	0.0068	0.0011	0	0.0013	0.0069	0.0007

Figure 5-102 Sediment Balance above S.W.L. of Line 1

Regarding profile change for the gravel beach (Test 1 to Test 6):

Lines 2 and 3

Below the S.W.L. erosion was the major volumetric change for both Lines (except Tests 3 and 5 for Line 3 and Tests 4 and 5 for Line 2). Line 3 had the highest erosion at Test 6 where Line 2 at Test 1. At Test 5, both Lines had similar amount of accretion where at Test 4 had similar amount of erosion. At Test 4 the amount of erosion at Line 3 was similar to the amount of accretion at Line 2 which gives a possible indication of long-shore sediment transport between the two lines below S.W.L. The pattern of total volumetric change of Line 2 below S.W.L. increased in magnitude in relation to the wave steepness where of Line 3 only at Tests 3 and 4.

Above the S.W.L., erosion was the major volumetric change for Line 3 but not for Line 2. At Line 3 only during Tests 3 and 6 accretion was the major and often the only volumetric change where at Line 2 was during Test 2, 3, 4 and 6. At Test 6 was the highest accretion, above S.W.L., for both lines. The highest erosion for Line 3 was at Test 2 where for Line 2 was at Test 1. At Test 1, both below and above S.W.L., Line 2 had the highest erosion. Neither of the two Lines show any sign of long-shore sediment transport above S.W.L. The pattern of total volumetric change of Line 2 above S.W.L. increased in magnitude in relation to the wave steepness where of Line 3 only at Tests 5 and 6.

Line 1

Below the S.W.L., accretion was the major volumetric change for Line 1 (except Tests 2 and 4). The highest erosion was observed at Test 2 and the highest accretion at Test 6. When comparing Line 1 with the other two lines, a possible indication of long-shore sediment transport, below S.W.L., was observed at Test 4 where the amount of erosion of both Lines 2 and 3, was similar to the amount of accretion of Line 1 for the same test. The pattern of total volumetric change of Line 1 below S.W.L. decreased in magnitude in relation to the wave steepness (except Tests 3 and 4).

Above S.W.L., accretion was the major volumetric change of Line 1 (except Tests 4 and 5). The highest accretion has been observed at Test 2 and the highest erosion at Test 4. Comparing Line 1 with the other two lines, a possible indication of long-shore sediment transport, above S.W.L., was observed at Test 4 once more, where the amount of erosion of both Lines 2 and 3, was similar to the amount of accretion of Line 1 for the same test. The same pattern of total volumetric change below S.W.L. was also followed above S.W.L. decreasing in magnitude in relation to the wave steepness (except Tests 3 and 4).

Regarding profile change for the Mixed Beach (Test 7 to Test 10):

Lines 2 and 3

Below the S.W.L., erosion was the major volumetric change for both Lines (except Test 7 for Line 3). Both lines had the highest erosion at Test 9. At Test 7 the amount of accretion of Line 3 was similar to the amount of erosion of Line 2. Line 2 had the highest accretion at Test 7 where Line 3 at Test 7. The pattern of total volumetric change below S.W.L of Line 2 increased in magnitude in relation to the wave steepness whereas in Line 3 only at Tests 9 and 10. Neither of the two lines show any sign of long-shore sediment transport below S.W.L.

Above the S.W.L., accretion was the major volumetric change for both Lines (except Test 8 for Line 3). Line 3 had the highest accretion at Test 9 whereas Line 2 at Test 10. At Line 2 the amount of accretion was increased from Test 7 to Test 10. Line 3 had the highest erosion at Test 8 where Line 2 at Test 7. The pattern of total volumetric change of both lines above S.W.L. decreased in magnitude in relation to the wave steepness. Neither of the two lines show any sign of long-shore sediment transport above S.W.L.

Line 1

Below the S.W.L., neither accretion nor erosion was the major volumetric change for Line 1. The highest accretion has been observed at Test 10 whereas the highest erosion at Test 9. Comparing Line 1 with the other two lines, a possible indication of long-shore sediment transport, below S.W.L., was observed at Test 8 whereas the amount of erosion of Line 2 was similar to the

amount of accretion of Line 1 for the same test. The pattern of erosion of Line 1 below S.W.L. increased in magnitude in relation to the wave steepness (except Tests 3 and 4).

Above S.W.L., accretion was the major volumetric change of Line 1. The highest accretion was observed at Test 10 and the highest erosion at Test 9. Comparing Line 1 with the other two lines, there was no possible indication of long-shore sediment transport, above S.W.L. The pattern of total volumetric change of Line 1, above S.W.L., decreased in magnitude in relation to the wave steepness.

5.5.3 Uniform slope

It can easily be observed that the behaviour of the sediment (gravel and mixed) from Line 3 to Line 2 is not linear. It is likely based on the oblique wave attack and the influence of the cross-shore and long-shore sediment transport. The total volumetric changes for the gravel beach were in the order of 39-65% to those of the mixed beach for the same wave condition. This indicates the greater mobility of the mixed beach in comparison with the gravel beach. This is in contrast with the conclusions of Lopez de San Roman-Blanco (2003). It also shows that this difference in total volumetric change between gravel and mixed beach is inverse proportional to the wave height.

Relative difference between accretion and erosion for the gravel beach vary between -99.94% to +82.15%. These relative differences for the case of mixed beach vary between -72.83% to +81.02% indicating that the sediment volume is conserved well. Comparing the relative difference between tests, it can be observed that it was reduced which might be caused by the fact that only gravel moves on the beach over a stable mixed bed. This is in contrast with the conclusions of Lopez de San Roman-Blanco (2003).

5.5.4 Trench

The total volumetric changes for the gravel beach were in the order of 45% to those of the mixed beach for the same wave condition. This indicates the greater mobility of the Mixed Beach in comparison to the gravel beach. It also shows that this difference in total volumetric change between gravel and Mixed beach is inverse proportional to the wave height.

Relative difference between accretion and erosion for the gravel beach vary between -20.99% to +84.59%. These relative differences in the case of mixed beach are negative in the first test and positive for the following tests. Its relative difference vary between -24.09% to +58.62%.

CHAPTER VI
PREDICTING PROFILE RESPONSE FOR GRAVEL AND MIXED BEACHES

6.0 INTRODUCTION

As aforementioned in Chapter 2, gravel and mixed shingle beaches are two of the most effective natural sea defences and provide an attractive, practical means of coastal protection. They are both relatively permeable to wave action and as a result they can absorb more wave energy. Like any other type of beach, gravel and mixed beaches will suffer erosion under extreme wave conditions or combined storm waves with high water levels. If the erosion is sufficiently severe, the beach will pass the point which it can no longer absorb wave energy. At this point the beach will no longer be considered as a coastal protection system. Therefore, the identification and calculation of the sediment transport and consequently the prediction of the evolution of the gravel and mixed beaches are very important issues.

In order to provide insights into the complexities of beach systems, involving the interrelationships among the many variables and parameters focusing in predicting the evolution of the beaches, the use of models has to be employed. There are various classes of models. The most common are the numerical and the parametric models where the latter will be discussed in this chapter. Parametric models require little or no understanding of the underlying hydrodynamics and attempt to relate directly to the development of various features on the beach to the incident wave conditions and beach material characteristics. At present, the leading model available for predicting profile development of coarse-grained beaches is that of Powell (1990), the SHINGLE model. SHINGLE is also used for predicting the development of dissimilar sediment beaches. In this chapter, a new parametric equilibrium cross-shore model will be developed based on the concept of the development of SHINGLE in order to predict the beach profile evolution of gravel and mixed beaches.

6.1 MODEL DEVELOPMENT

The new parametric model is based on the equilibrium slope ("equilibrium beach profile") concept through which the effects of wave conditions, sediment size, grading and permeability can be taken into account. It is a new approach to predict the equilibrium beach profile of gravel and mixed beaches for trench and uniform slope. Previous parametric models, (BREAKWAT and SHINGLE) that predicting the development of beach profiles, were 2D models. This might be acceptable when waves approaching in a normal wave angle. However, for oblique incident wave angles these 2D parametric models cannot predict accurate the development of beach profile due to the fact that they do not consider the differential longshore transport. The new 3D parameter model has been established by taking into account the differential longshore transport, giving the opportunity to calculate every beach profile of interest along the beach. Furthermore, the model has been validated against the experimental data from the experiment in Hannover.

Based on the literature for gravel and mixed beaches, the variables most influential in the development of their beach profile are:

1. Wave height
2. Wave period
3. Beach material size
4. Permeability
5. Water level
6. Angle of wave attack
7. Initial beach profile

The model uses/calculates all of the variables above and allows the user to predict changes to mixed and gravel beach profiles, with either trench or uniform slope, based upon prescribed input conditions of sea state, water level, sediment size and existing profile. It has to be mentioned that the size of the sediment particle and the permeability assumed to have a constant value for the whole beach.

The model was split in two categories of predicting beach profile, based on the nature of the bed slope:

a) Uniform slope, and
b) Trench

Their profile schematisations are shown in Figure 6-1 to Figure 6- 3. For both of these categories, the profile of the model has been described by four areas. These areas are extending from:

1. The start of the beach to the breaking point,
2. the breaking point to still water level,
3. still water level to crest, and
4. crest to the end of the beach profile.

The position of the predicted beach profile relative to an initial (pre-existing) profile has been established by taking in to account the differential longshore transport. Additionally, the model is attempting to establish the accurate cross-shore distribution of the longshore wave-induced currents.

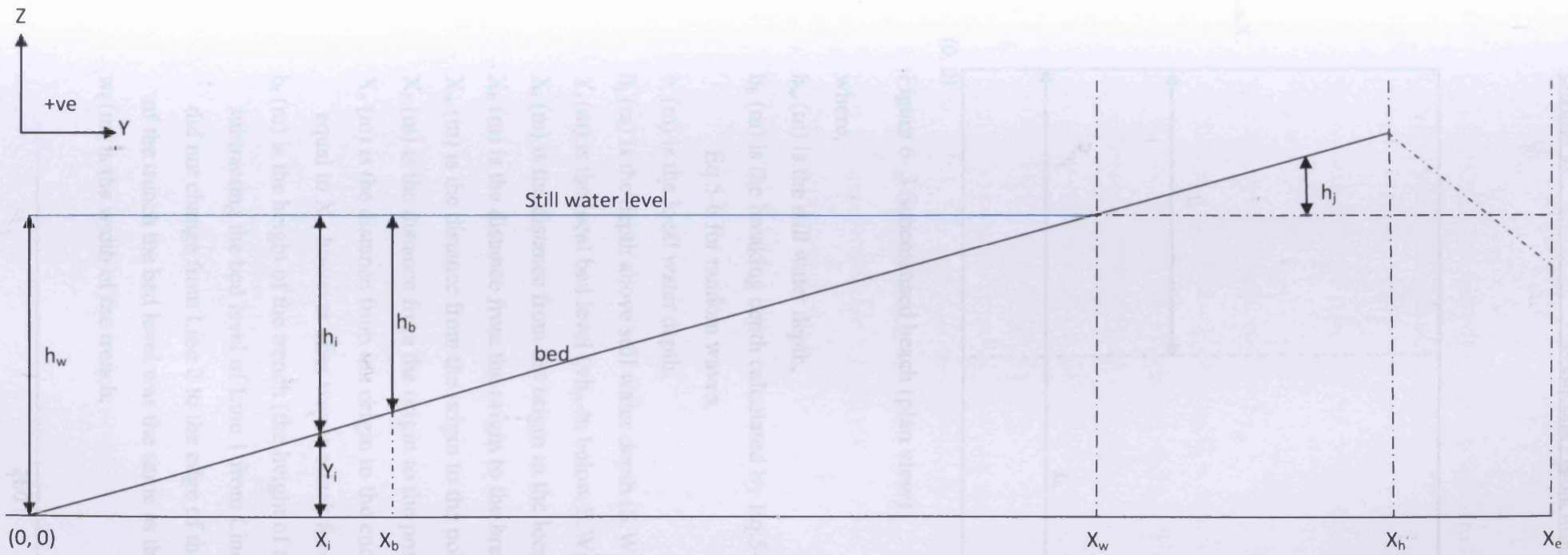

Figure 6-1 Schematised beach profile

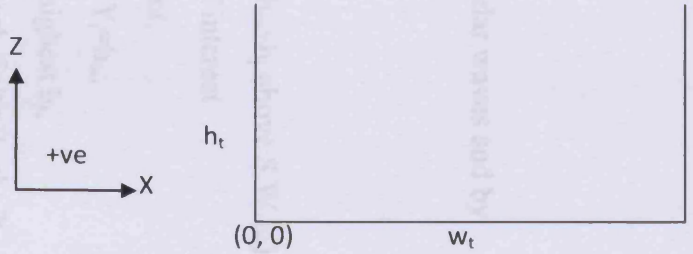

Figure 6-2 Schematised trench (cross-section)

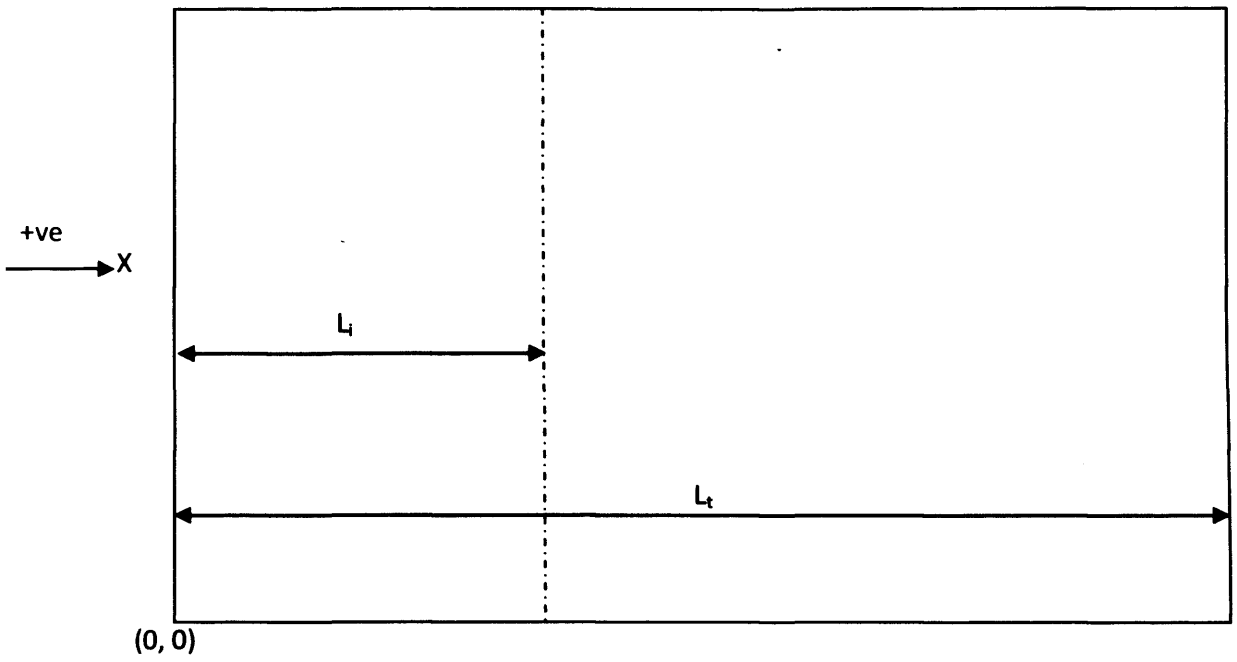

Figure 6- 3 Schematised beach (plan view)

where,

h_w (m) is the still water depth,

h_b (m) is the breaking depth calculated by Eq.5-4 for regular waves and by Eq.5-6 for random waves,

h_i (m) is the local water depth,

h_j (m) is the depth above still water depth (S.W.L.),

Y_i (m) is the local bed level (=h_w-h_i below S.W.L., and =h_w+h_j above S.W.L.),

X_i (m) is the distance from the origin to the local point of interest

X_b (m) is the distance from the origin to the breaking point,

X_w (m) is the distance from the origin to the point where Y_i=h_w,

X_h (m) is the distance from the origin to the point of the highest h_j,

X_e (m) is the distance from the origin to the end of the beach (initially the X_h is equal to X_e, however after waves attack these points are starting to separate),

h_t (m) is the height of the trench (the height of the trench was calculated by subtracting the bed level of Line 1 from Line 2 assuming that the bed level did not change from Line 2 to the edge of the trench and also along the width of the trench the bed level was the same as the bed level of Line 1),

w_t (m) is the width of the trench,

L_i (m) is the length from the origin to the beach profile of interest and,

L_t (m) is the total length of the beach

More parameters are used for the new parametric model. These are listed and described below:

Y_p is the predicted local bed level

c is the wave celerity ($= \sqrt{gh_i}$) (m/s), where h_i is the local water depth and

g is the acceleration due to gravity (=9.81 m/s^2),

H_o is the wave height in deep water (m),

H_{m0} is the estimation of the significant wave height from spectral analysis (m),

T is the wave period (sec),

T_m is the average wave period (sec), for many sites a reasonable estimation is $T_m=0.8T_p$ but can commonly vary from 0.65 to 0.9. The value of T_m used in the parametric model was equal to $0.8T_p$,

L_o is the deep water wave length (m),

L_m is the wave length based on T_m

θ is the incident wave angle (^{0}),

m is the slope of the beach,

D_{50} is the median sediment diameter (mm),

$\frac{H_0}{L_0}, \frac{H_{m0}}{L_m}$ is the wave steepness and,

K is the permeability which was calculated by using the equations of Krumbein and Monk (1943) (Turner, 1993; Kulkarni et al., 2004):

Eq.6-1 $$K = \frac{g}{\nu} 760 d^2 \exp(1.31\sigma) \times 0.987 \times 10^{-12} \text{ (m/s)},$$

where,

d is the median grain size (mm), σ the sorting index (in phi units), g the acceleration due to gravity, and ν the kinematic viscosity of water (m^2/s).

For the calculations based on the gravel beach, the sorting index was calculated according to the following formula (Gordon et al., 1992):

Eq.6-2 $$\sigma = \frac{\phi_{84} - \phi_{16}}{2}$$

where,

phi (φ) units were numerically defined as:

Eq.6-3 $$\phi = -\log_2 \frac{d(mm)}{1.0mm}$$

where,

d(mm) is the particle size in millimetres and the dimensionless aspect of the equation (i.e., d(mm)/1.0 mm) was redefined by McManus (1963) and amplified by Krumbein (1964), (Balsillie and Dabous, 2003).

However, for the calculations based on the mixed beach, the sorting index was calculated differently. It is important to look at the grain-size distribution (GSD) of the mixed sediments in order to get a more accurate estimation of the sorting index. Therefore, the sorting index was applied using the inclusive graphic standard deviation:

Eq.6-4 $$\sigma = \frac{\phi_{84}-\phi_{16}}{4} + \frac{\phi_{95}-\phi_{5}}{6.6}$$

This equation was developed by Folk and Ward (1957) and computes the spread of the distribution in phi units where (for example) φ_{84} is the value of 'phi' corresponding to 84% of the cumulative frequency curve (Batalla and Martin-Vide, 2001; Wittenberg et al., 2007).

6.2 THE MODEL

The parameters that were used in the model were dimensionless in order for the model to be applied independently of the scale. After non-linear regression analysis of the experimental data, equations were derived in order to predict each area of the beach profile, individually. The model took its final forms for the following conditions. The results are shown in Figure 6-4 to Figure 6-31.

6.2.1 Regular Wave Conditions

Gravel Beach-*uniform slope*:

For $0 < X_i < X_b$

Eq.6-5 $$\frac{Y_p}{h_w} = a\frac{Y_i}{h_w} + b\frac{X_i}{X_b} + c\frac{H_0}{L_0} + d\frac{c}{K} + e\frac{m}{\cos\theta} + f\frac{L_i}{L_T} + g \quad (R^2=0.988)$$

where,

a, b, c, d, e, f and g are constants with values of:

a= 1.090258877

b= 0.210100923

c= 2.430548379

d= 0.676947516

e= -8.188104521

f= -0.0784

g= 0.147637943

For $X_b \leq X_i < X_w$

Eq.6-6 $$\frac{Y_p}{h_w} = a\frac{Y_i}{h_w} + b\frac{X_i}{X_W} + c\frac{H_0}{L_0} + d\frac{c}{K} + e\frac{m}{\cos\theta} + f\frac{L_i}{L_T} + g \quad (R^2=0.915)$$

where,

a, b, c, d, e, f and g are constants with values of

a= -0.439969159

b= 0.264469924

c= 1.927826999

d= -0.805932438

e= -11.21244376

f= -0.112785082

g= 2.341769681

For $X_i = X_w$

Eq.6-7 $$\frac{Y_p}{h_w} = a + bA + cB + dB^2 + eB^3 \qquad (R^2=0.999)$$

where,

$$A = \left(\frac{H_o m}{KT \cos\theta}\right)$$

$$B = \left(\frac{X_i L_i}{X_e L_t}\right)$$

a, b, c, d and e are constants with values of

a= 41.22171165

b= 0.650012908

c= -38.29279092

d= 11.70125835

e= -1.162345606

For $X_w < X_i < X_h$

Eq.6-8 $$\frac{Y_p}{h_w} = a + bA + cB + dA^2 + eB^2 + fAB + gA^3 + hB^3 + iAB^2 + jA^2B \qquad (R^2=0.941)$$

where,

$$A = \left(\frac{\cos\theta H_o Y_i}{mKTh_w}\right)$$

$$B = \left(\frac{X_i L_i}{X_e L_t}\right)$$

a, b, c, d, e, f, g, h, i and j are constants with values of

a= -10.56234633

b= 10.18338376

c= 88.17312206

d= -14.89068203

e= -218.786134

f= -36.50120271

g= 27.94114905

h= 165.8126743

i= 87.50198946

j= -40.23801267

For $X_h \leq X_i \leq X_e$

Eq.6- 9 $$\frac{Y_p}{h_w} = a + \frac{b}{A} + \frac{c}{A^2} + dB + eB^2 + fB^3 \qquad (R^2=1)$$

where,

$$A = \left(\frac{\cos\theta H_o X_i}{mKTX_e}\right)$$

$$B = \left(\frac{Y_i L_i}{h_w L_t}\right)$$

a, b, c, d, e and f are constants with values of

a= -141.8895401

b= -11.66055542

c= 0.763929334

d= 927.1770041

e= -1519.31762

f= 824.5338948

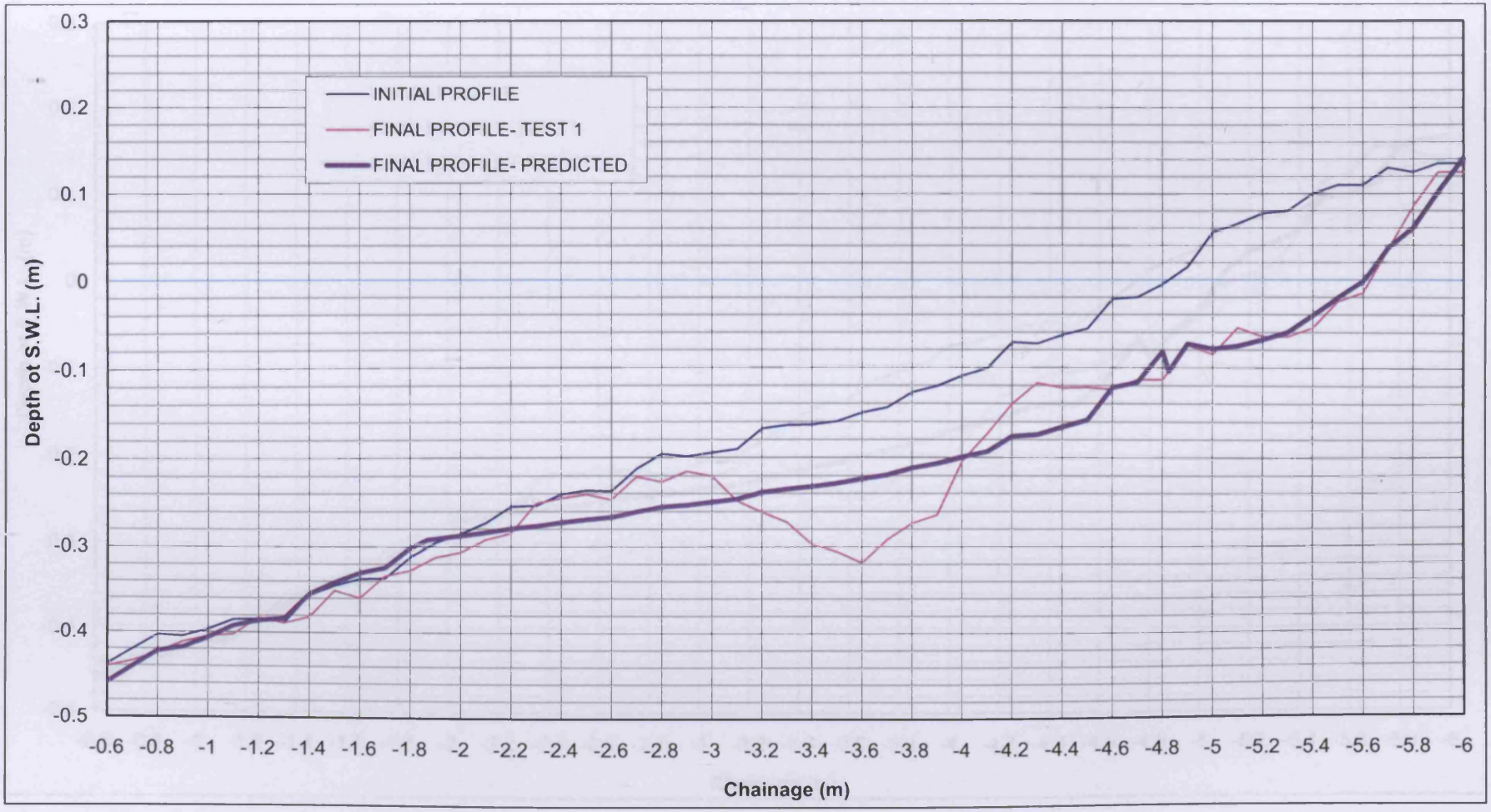

Figure 6-4 Comparison of predicted and measured beach profiles (Line 2-TEST 1)

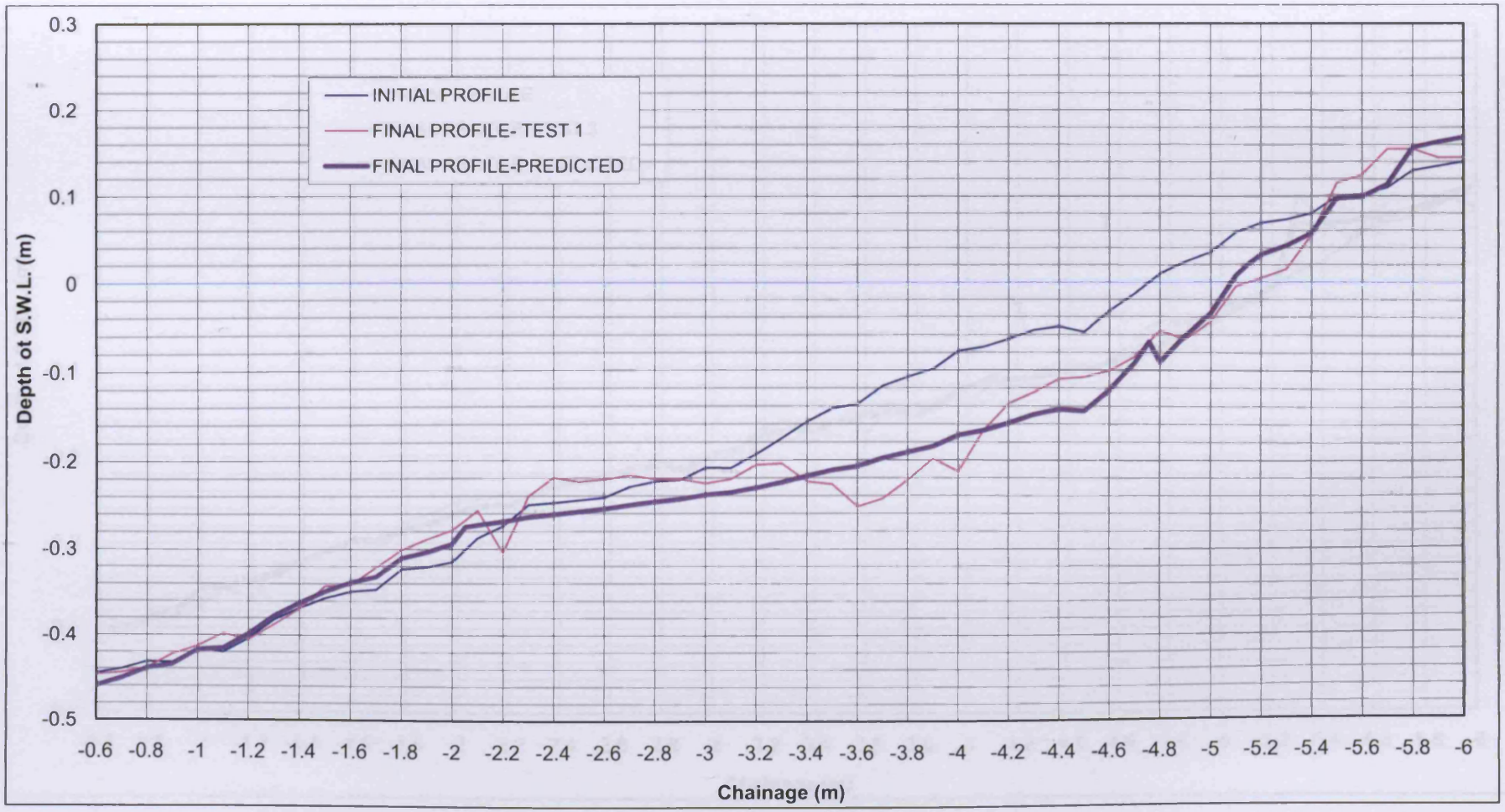

Figure 6-5 Comparison of predicted and measured beach profiles (Line 3-TEST 1)

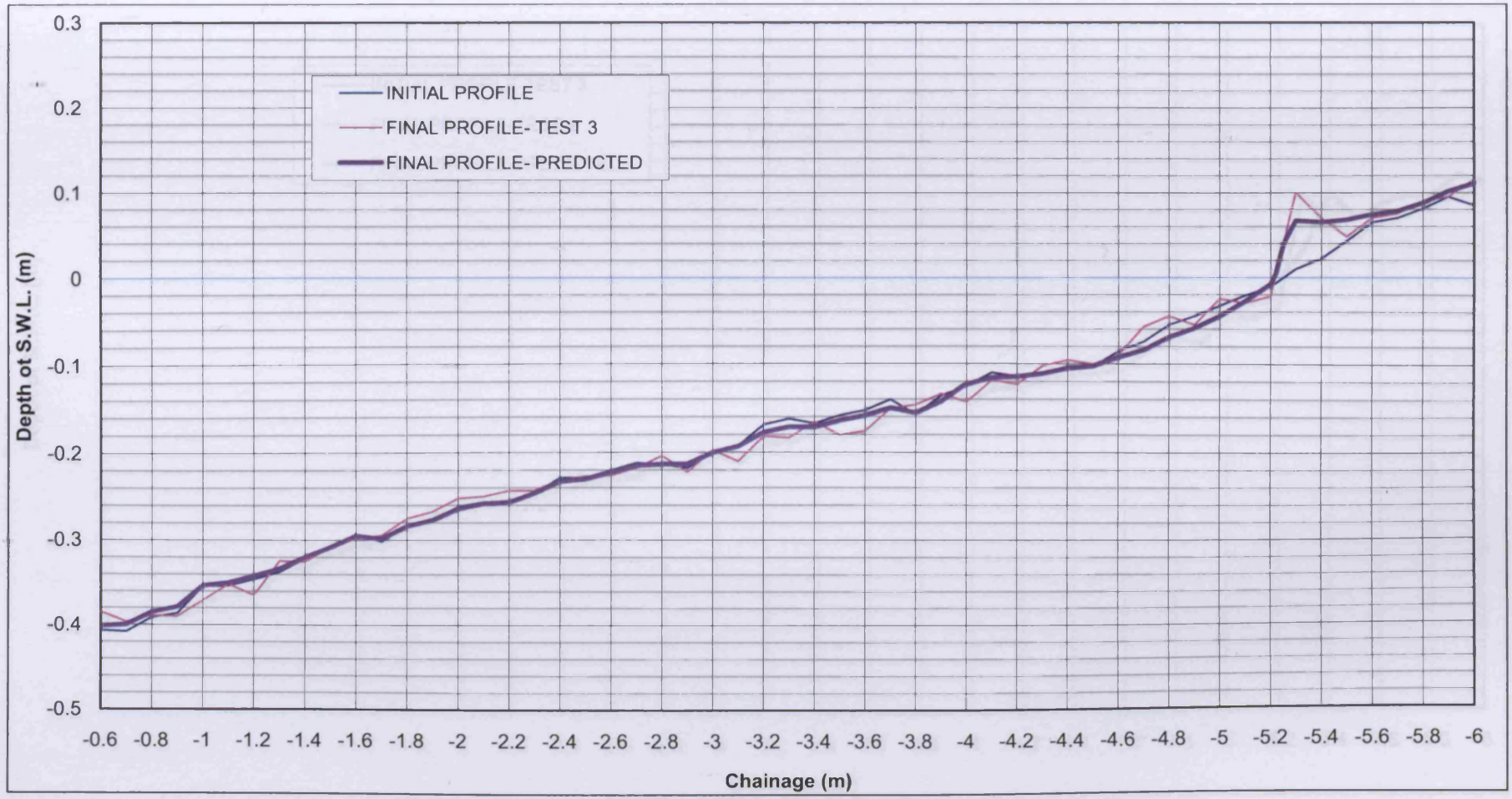

Figure 6-6 Comparison of predicted and measured beach profiles (Line 2-TEST 3)

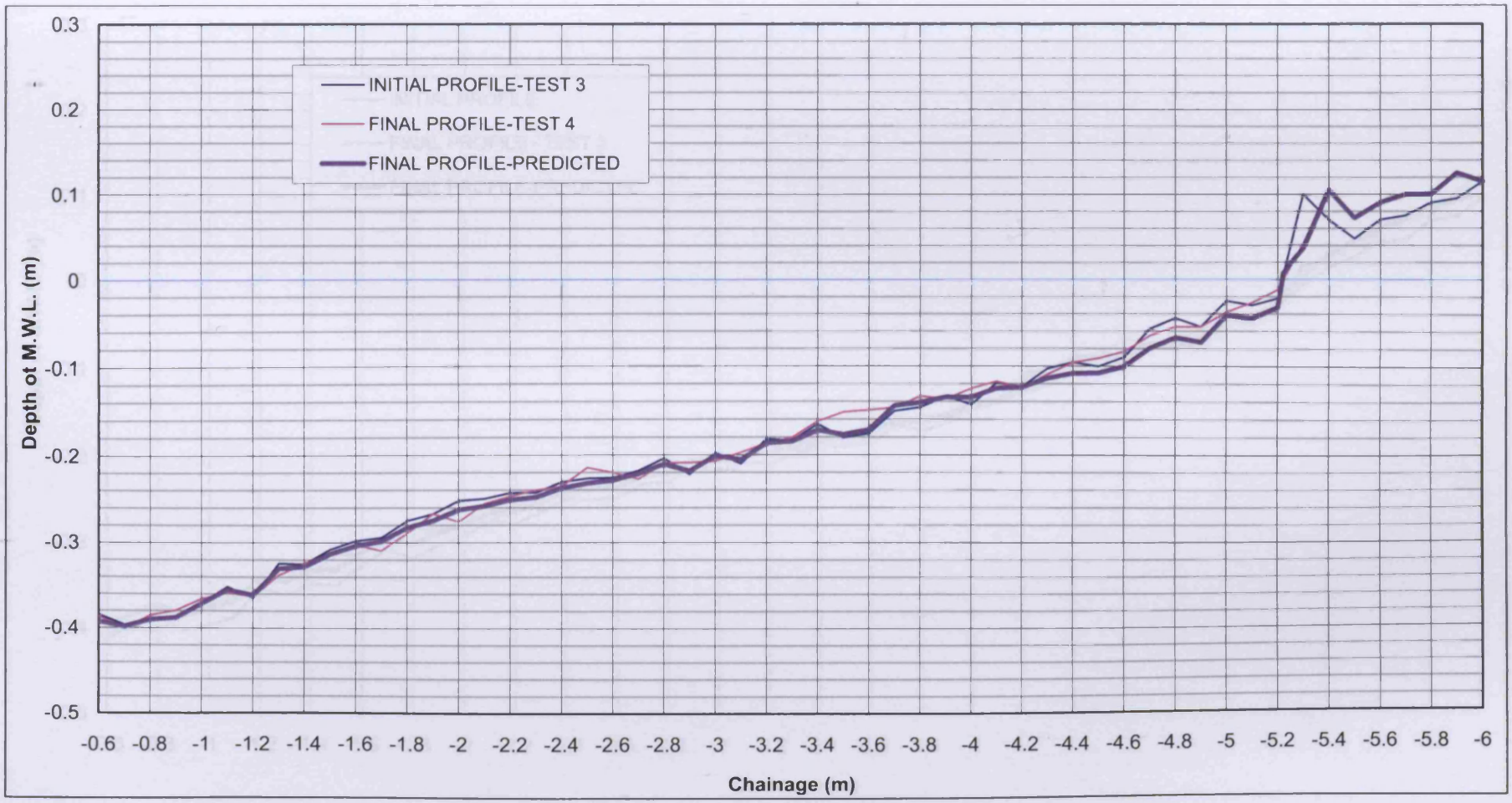

Figure 6-7 Comparison of predicted and measured beach profiles (Line 2-TEST 4)

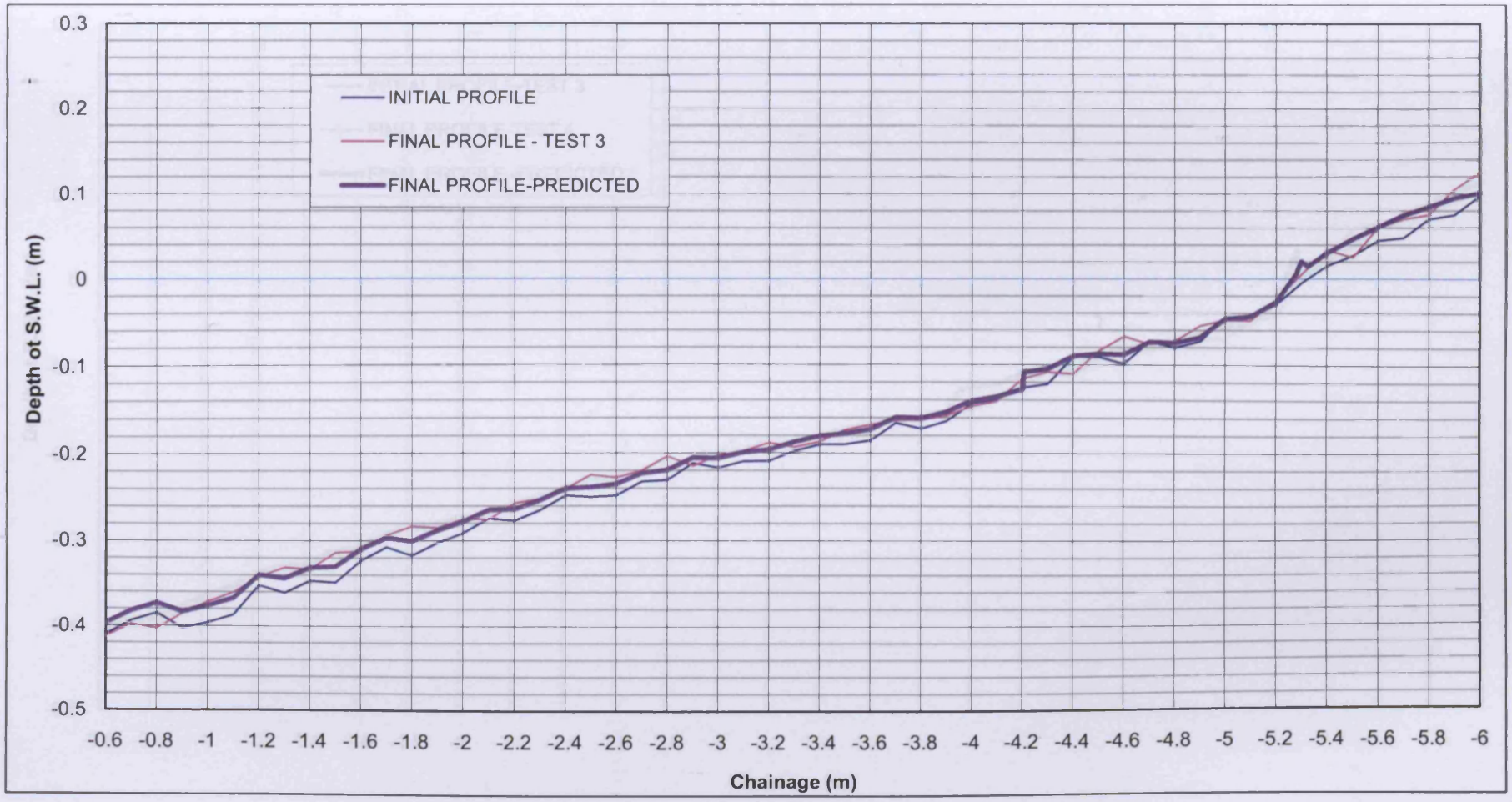

Figure 6-8 Comparison of predicted and measured beach profiles (Line 3-TEST 3)

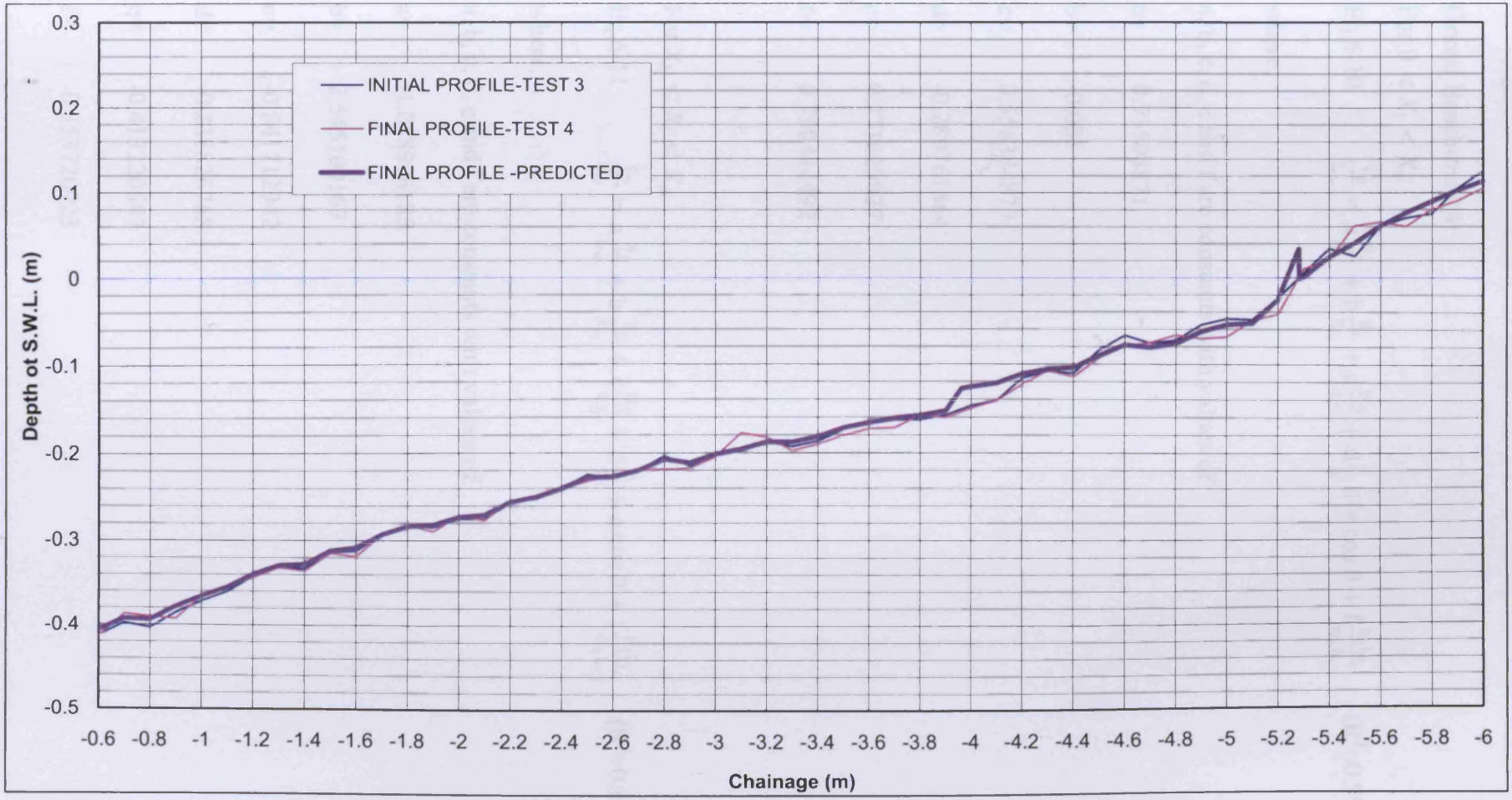

Figure 6-9 Comparison of predicted and measured beach profiles (Line 3-TEST 4)

Gravel Beach-*trench*:

For $0 < X_i < X_b$

Eq.6-10 $$\frac{Y_p}{h_w} = a\frac{Y_i}{h_w} + b\frac{X_i}{X_b} + c\frac{H_0}{L_0} + d\frac{c}{K} + e\cos\theta + f\frac{h_t L_i}{w_t L_t} \qquad (R^2=0.993)$$

where,

a, b, c, d, e and f are constants with values of

a= 0.95508871

b= -0.083

c= 0.556384877

d= -0.289761564

e= 0.271629927

f= 0.790444492

For $X_b \leq X_i < X_w$

Eq.6-11 $$\frac{Y_p}{h_w} = a\frac{Y_i}{h_w} + b\frac{X_i}{X_w} + c\frac{H_0}{L_0} + d\frac{c}{K} + e\cos\theta + f\frac{h_t L_i}{w_t L_t} \qquad (R^2=0.931)$$

where,

a, b, c, d, e and f are constants with values of

a= -1.088996185

b= 2.545100167

c= -0.841712942

d= -0.238826768

e= -0.413220683

f= -0.353720923

For $X_w \leq X_i < X_e$

Eq.6-12 $$\frac{Y_p}{h_w} = a + bA + c\ln(B) + dA^2 + e\ln(B)^2 + fA\ln(B) + gA^3 + $$
$$+h\ln(B)^3 + iA\ln(B)^2 + jA^2\ln(B) \qquad (R^2=0.964)$$

where,

$$A = \left(\frac{H_o \cos\theta w_t}{KTh_t}\right)$$

$$B = \left(\frac{Y_i X_e L_i}{h_w X_i L_t}\right)$$

a, b, c, d, e, f, g, h, i and j are constants with values of

a= 1.253322493

b= 0.0179

c= 1.598499148

d= 0.00292

e= -0.0731

f= -0.0648

g= -0.000165

h= -4.597432492

i= -0.537008503

j= 0.010287216

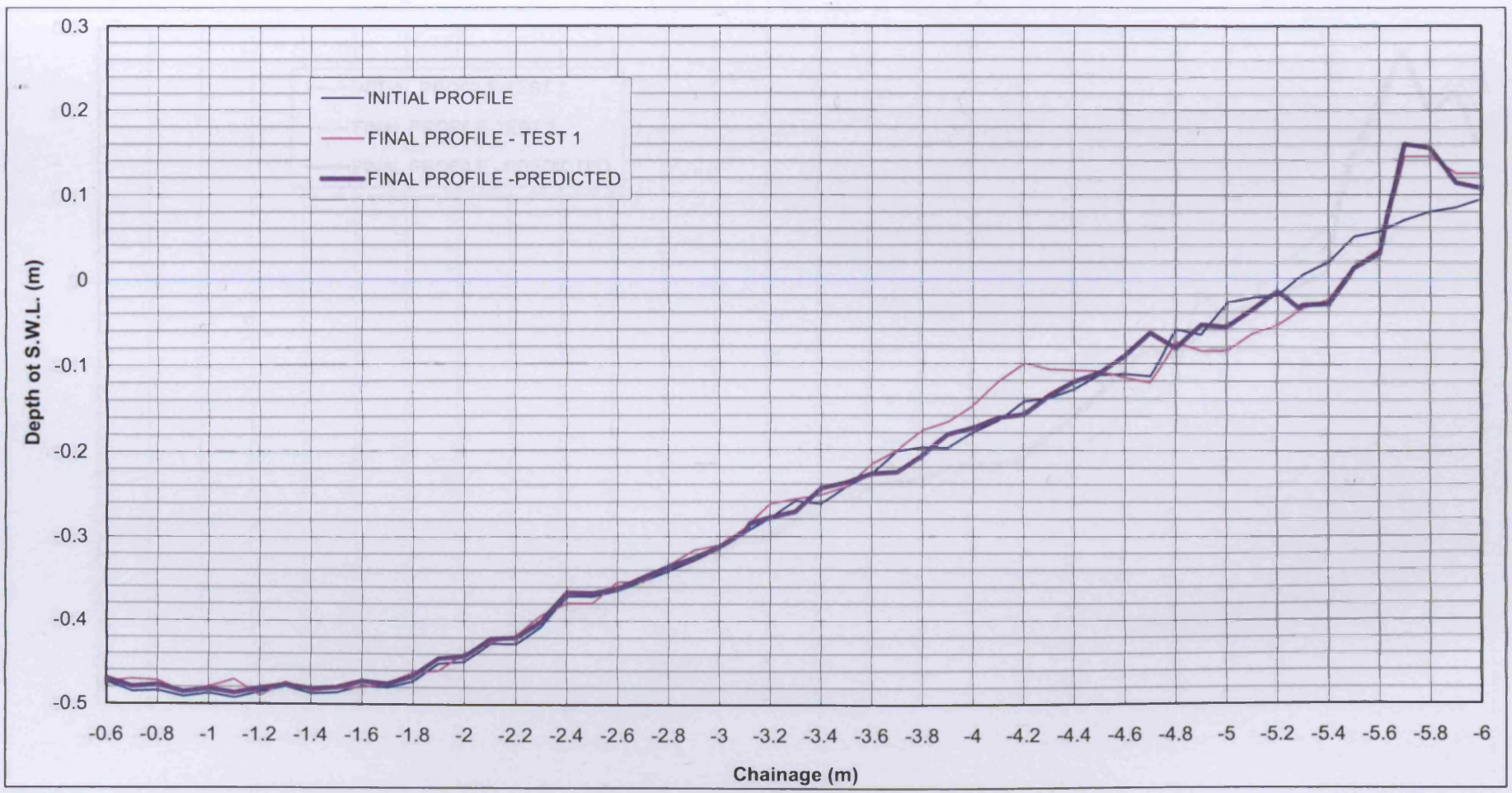

Figure 6-10 Comparison of predicted and measured beach profiles (Line 1-TEST 1)

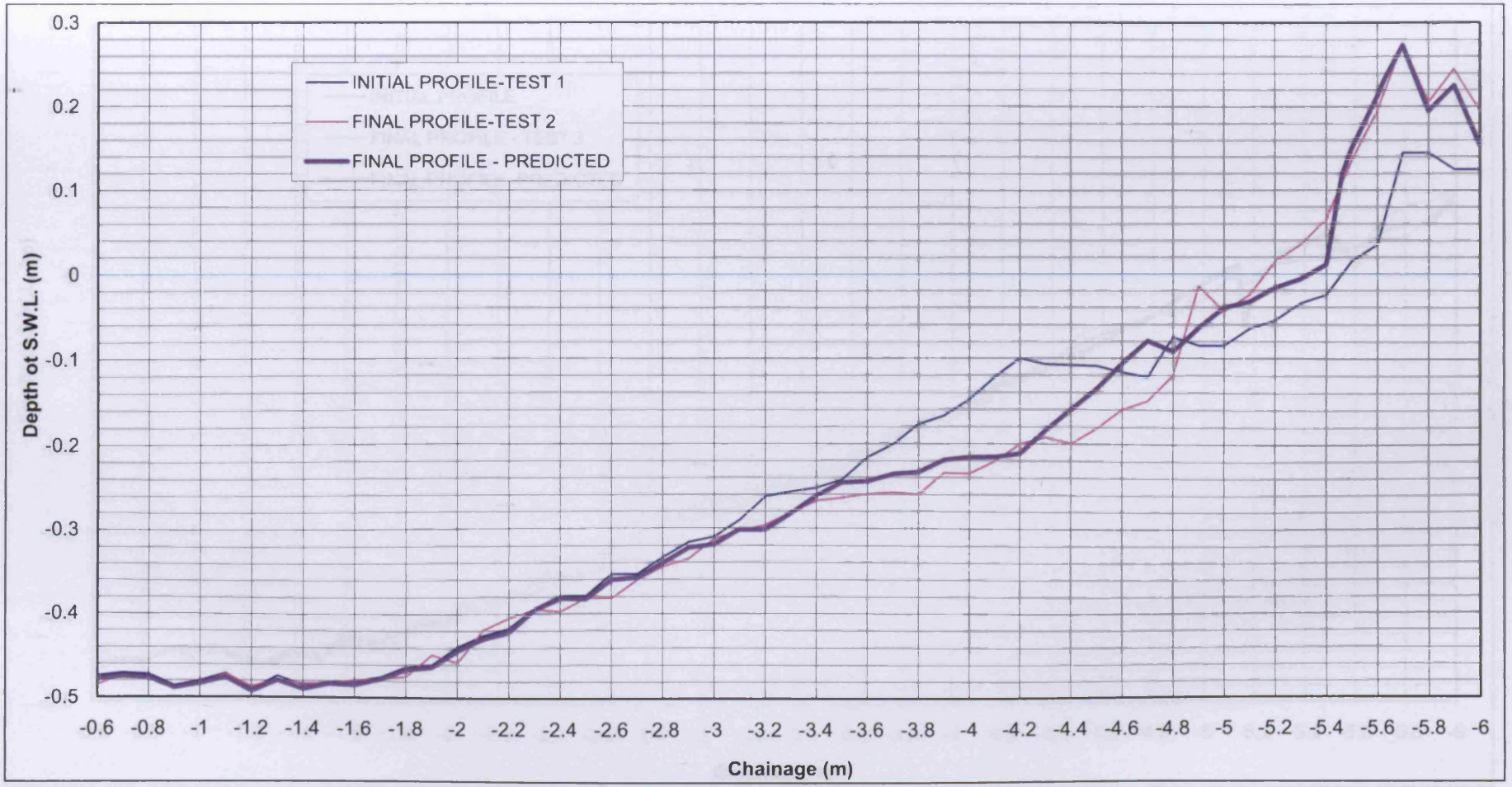

Figure 6-11 Comparison of predicted and measured beach profiles (Line 1-TEST 2)

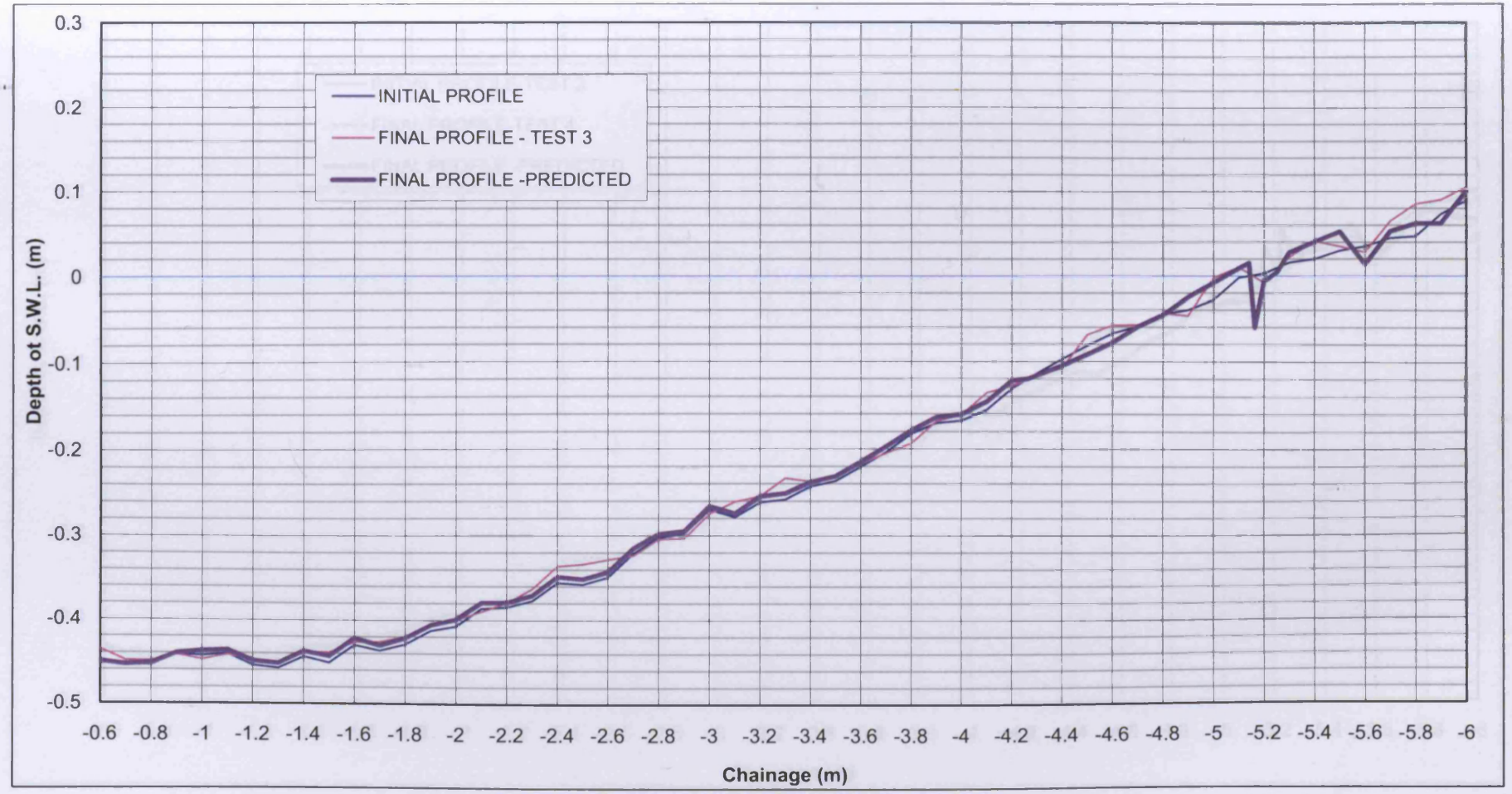

Figure 6-12 Comparison of predicted and measured beach profiles (Line 1-TEST 3)

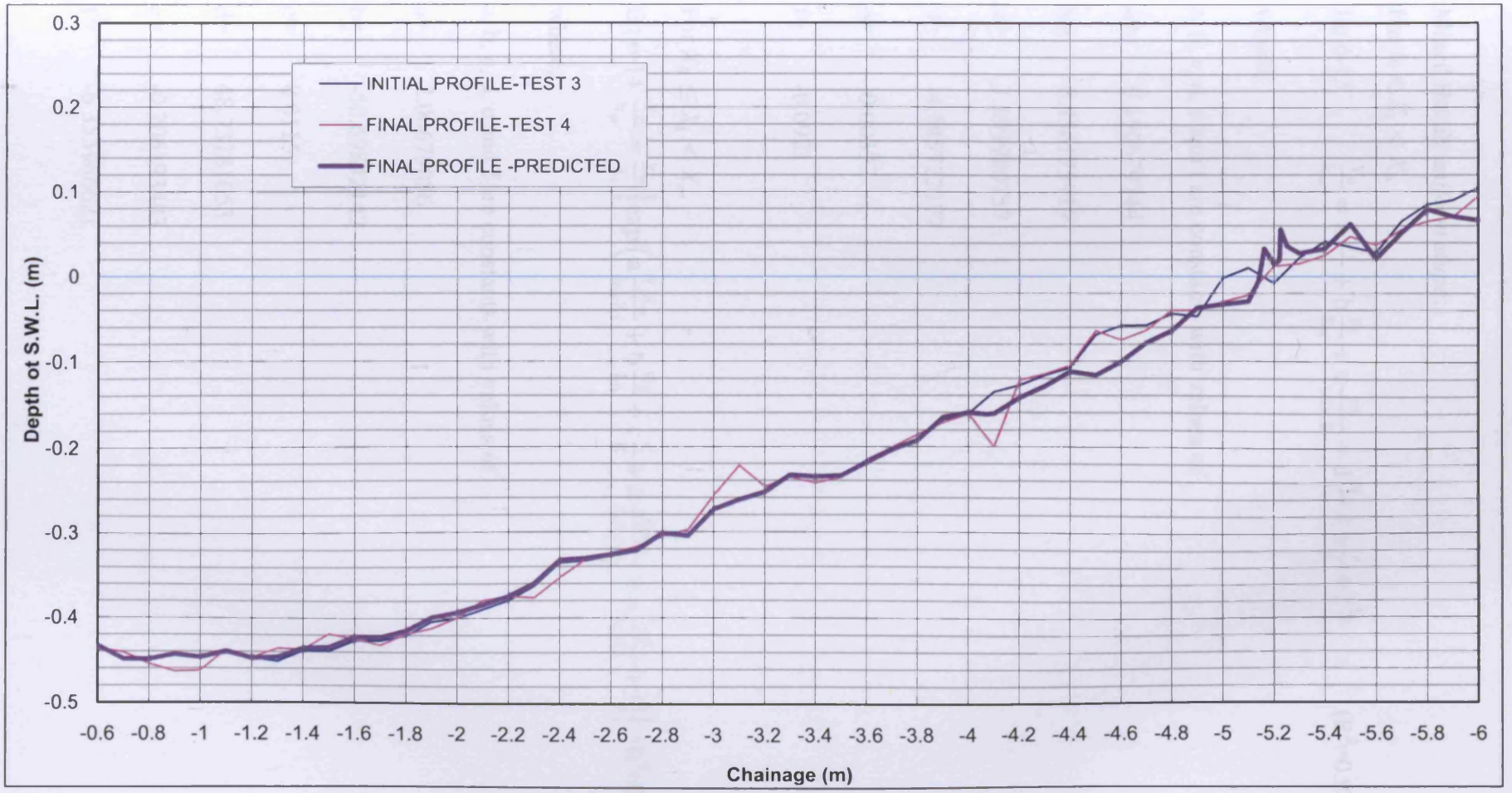

Figure 6- 13 Comparison of predicted and measured beach profiles (Line 1-TEST 4)

Mixed Beach-*uniform slope*:

For $0 < X_i < X_b$

Eq.6-13 $$\frac{Y_p}{h_w} = a\frac{Y_i}{h_w} + b\frac{X_i}{X_b} + c\frac{m}{\cos\theta} + d\frac{H_0}{L_0} + e\frac{c}{K} + f\frac{L_i}{L_t} \qquad (R^2=0.985)$$

where,

a, b, c, d, e and f are constants with values of

a= 0.190679744

b= 0.456175919

c= 3.599980757

d= -4.145722177

e= -0.00397

f= -0.0921

For $X_b \leq X_i < X_w$

Eq.6-14 $$\frac{Y_p}{h_w} = \frac{X_w}{X_i}\left[\exp\left(a\frac{Y_i X_w}{h_w X_i} + b\frac{H_0}{L_0} + c\frac{c}{K} + d\frac{mX_w}{\cos\theta X_i} + e\frac{L_i X_i}{L_t X_w} + f\right)\right] \quad (R^2=0.649)$$

where,

a, b, c, d, e and f are constants with values of

a= 2.00679086

b= -50.69842142

c= 0.0115

d= 48.73181053

e= -0.206193483

f= -6.355966621

For $X_i = X_w$

Eq.6-15 $$\frac{Y_p}{h_w} = a + \frac{b\ln(A)}{A} + c\frac{\ln(A)}{A^2} \qquad (R^2=1)$$

where,

$$A = \left(\frac{H_o \cos\theta X_i L_i}{KTmX_e L_t}\right)$$

a, b, and c are constants with values of

a= 0.259561418

b= -0.01520974

c= 0.000229

For $X_w < X_i < X_h$

Eq.6-16 $$\frac{Y_p}{h_w} = a + \frac{b}{A} + \frac{c}{B} + \frac{d}{A^2} + \frac{e}{B^2} + \frac{f}{AB} + \frac{g}{A^3} + \frac{h}{B^3} + \frac{i}{AB^2} + \frac{j}{A^2B} \qquad (R^2=0.927)$$

where,

$$A = \left(\frac{H_o \cos\theta X_i}{KTmX_e}\right)$$

$$B = \left(\frac{Y_i L_i}{h_w L_t}\right)$$

a, b, c, d, e, f, g, h, i and j are constants with values of

a= 5.573788859

b= -2.007463022

c= 4.668187209

d= 0.182680312

e= -1.753767053

f= -0.173691269

g= -0.00368

h= 0.111750215

i= 0.111215838

j= -0.0172

For $X_h \leq X_i \leq X_e$

Eq.6-17 $$\frac{Y_p}{h_w} = a + bA + \frac{c}{B} + dA^2 + \frac{e}{B^2} + f\frac{A}{B} + gA^3 + \frac{h}{B^3} + i\left(\frac{A}{B^2}\right) + j\left(\frac{A^2}{B}\right)$$

(R^2=0.968)

where,

$$A = \left(\frac{H_o \cos\theta X_i}{KTmX_e}\right)$$

$$B = \left(\frac{Y_i L_i}{h_w L_t}\right)$$

a, b, c, d, e, f, g, h, i and j are constants with values of

a= -89621.66432

b= 2291680.837

c= 37046.75709

d= -19367600.08

e= -5033.041717

f= -638381.0291

g= 54227304.35

h= 223.4255631

i= 44016.07513

j= 2718426.588

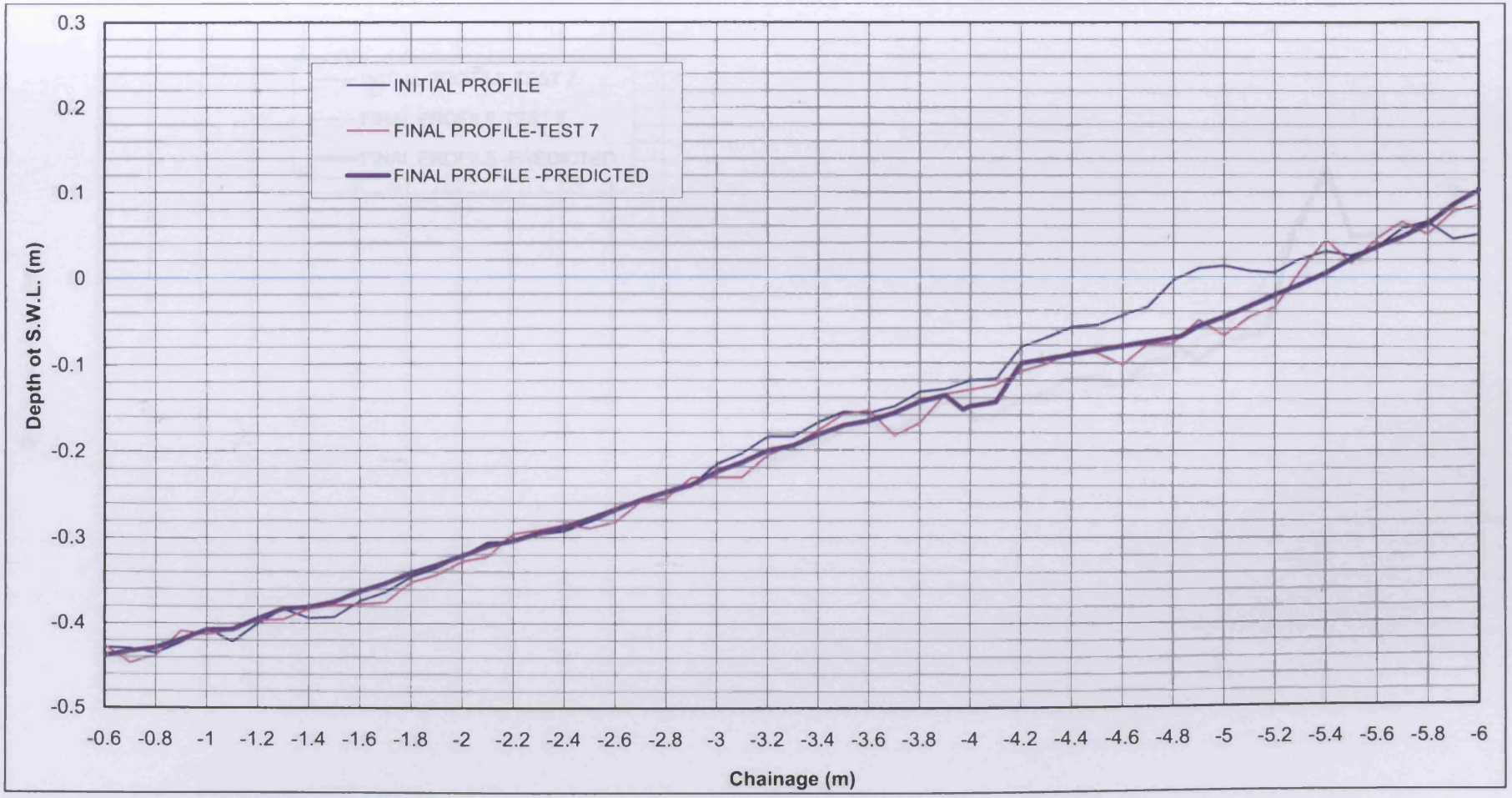

Figure 6-14 Comparison of predicted and measured beach profiles (Line 2-TEST 7)

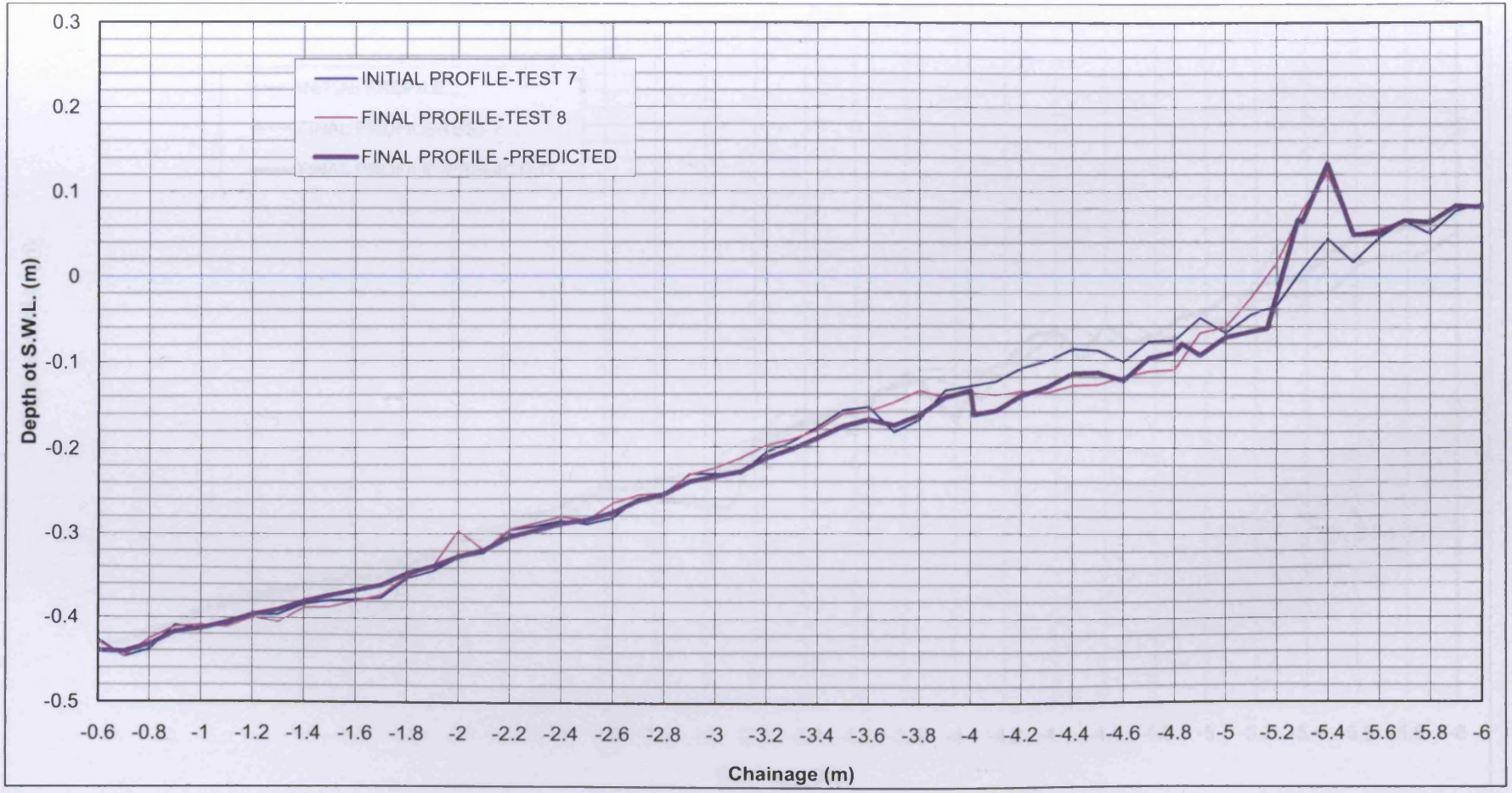

Figure 6-15 Comparison of predicted and measured beach profiles (Line 2-TEST 8)

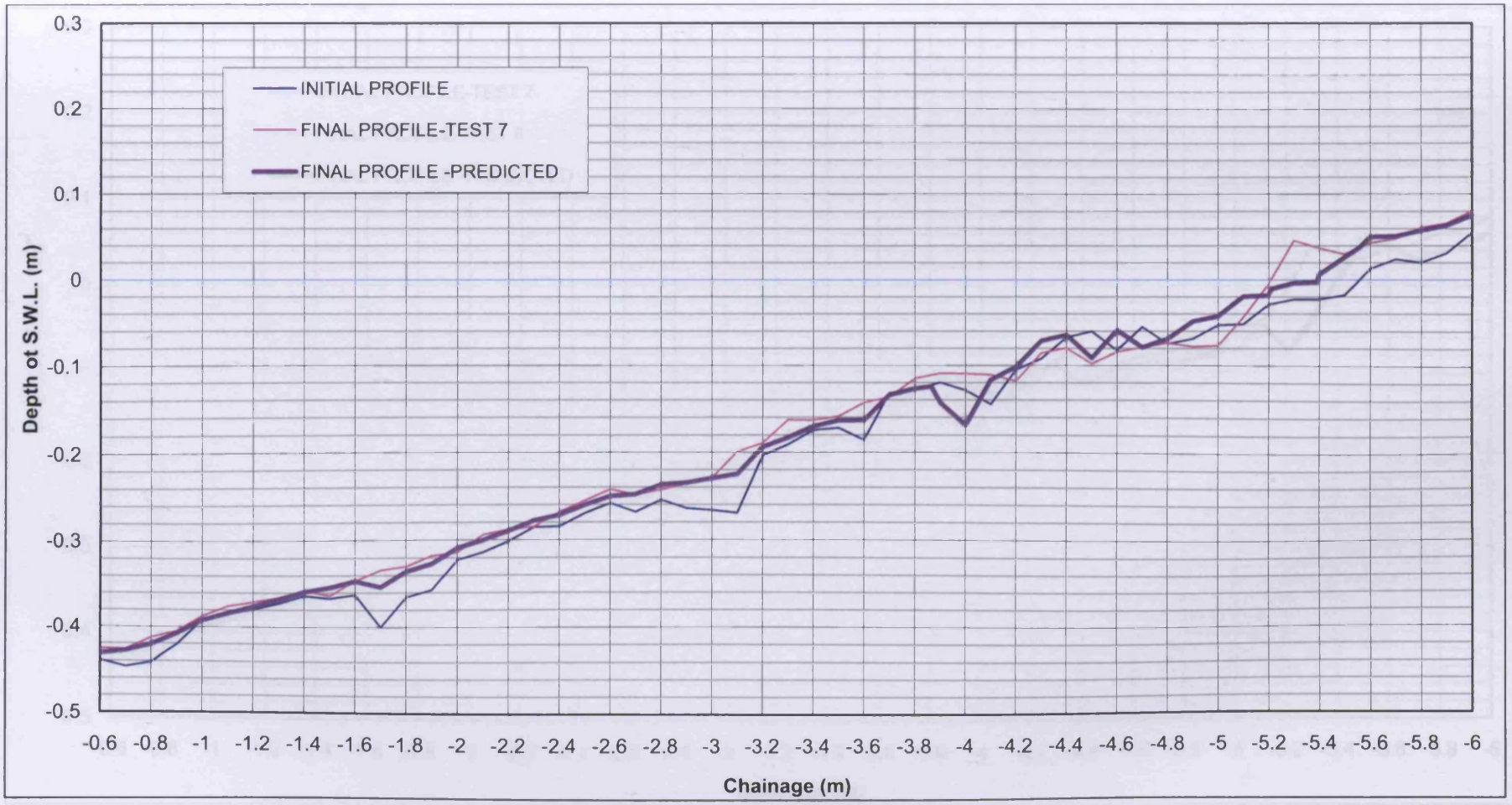

Figure 6-16 Comparison of predicted and measured beach profiles (Line 3-TEST 7)

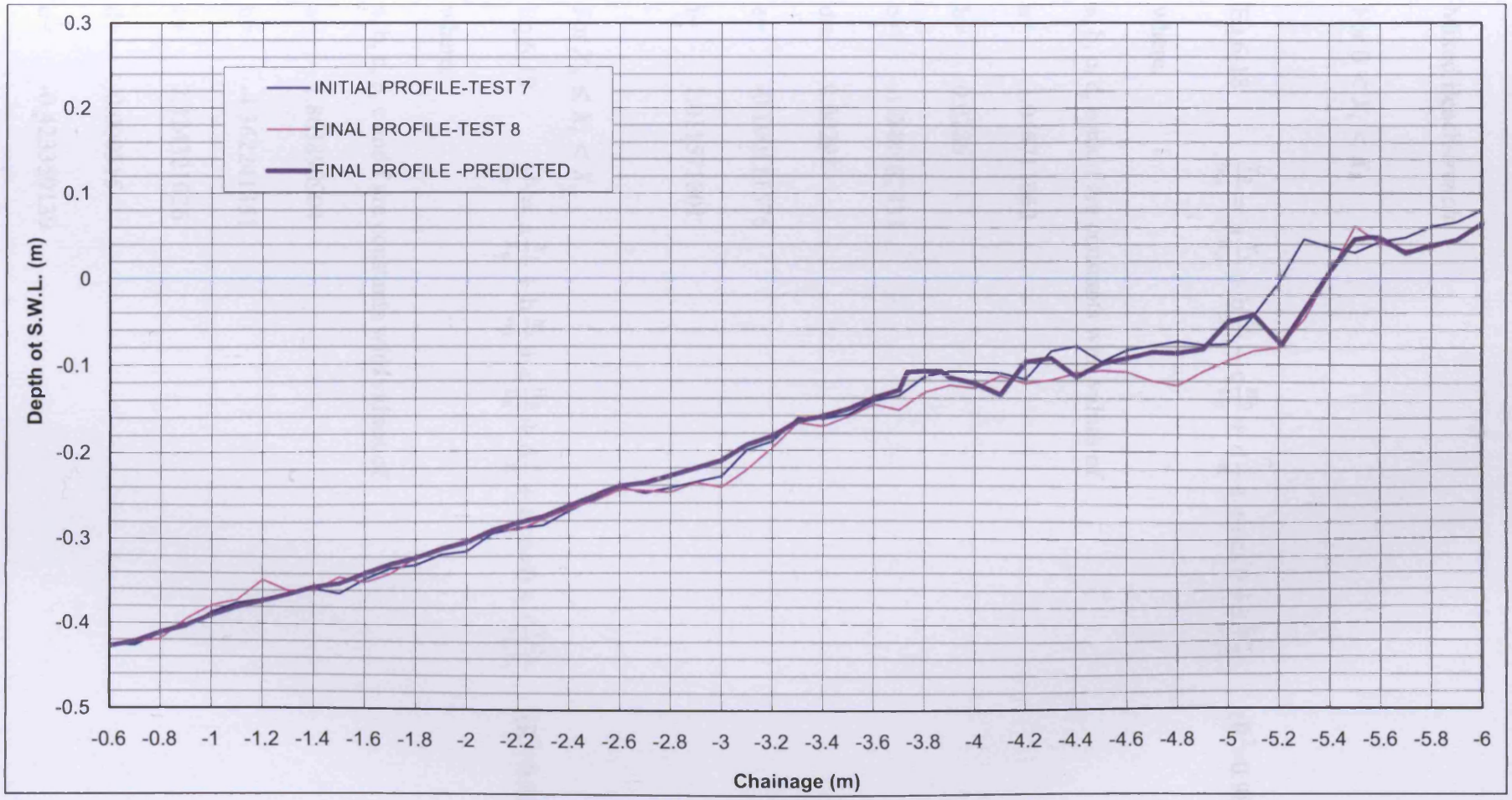

Figure 6-17 Comparison of predicted and measured beach profiles (Line 3-TEST 8)

Mixed Beach-*trench*:

For $0 < X_i < X_b$

Eq.6-18 $$\frac{Y_p}{h_w} = a\frac{Y_i}{h_w} + b\frac{X_i}{X_b} + c\frac{H_0}{L_0} + d\frac{c}{K} + e\cos\theta + f\frac{h_t L_i}{w_t L_t} \quad (R^2=0.982)$$

where,

a, b, c, d, e and f are constants with values of

a= 1.046711962

b= 0.0286

c= -1.948562433

d= 0.00298

e= -0.190111576

f= 1.011571801

For $X_b \leq X_i < X_w$

Eq.6-19 $$\frac{Y_p}{h_w} = a\frac{X_i}{X_w} + b\frac{h_t}{w_t} + c\frac{H_0}{L_0} + d\frac{c}{K} + e\cos\theta + f\frac{Y_i L_i}{h_w L_t} \quad (R^2=0.820)$$

where,

a, b, c, d, e and f are constants with values of

a= 1.863890904

b= -4.362241351

c= 2.324321026

d= -0.000515

e= -0.423359139

f= -0.557716594

For $X_w \leq X_i \leq X_e$

Eq.6-20 $$\frac{Y_p}{h_w} = a + bA + cB + dA^2 + eB^2 + fAB + gA^3 + hB^3 + iAB^2 + jA^2B \qquad (R^2=0.795)$$

where,

$$A = \left(\frac{H_o \cos\theta w_t}{KTh_t}\right)$$

$$B = \left(\frac{Y_i X_e L_i}{h_w X_i L_t}\right)$$

a, b, c, d, e, f, g, h, i and j are constants with values of

a= 2.972510746

b= 0.000226

c= -10.27477712

d= 0.0000675

e= 14.99027003

f= -0.00494

g= 0.00000000981

h= -6.360333755

i= 0.00516

j= -0.0000825

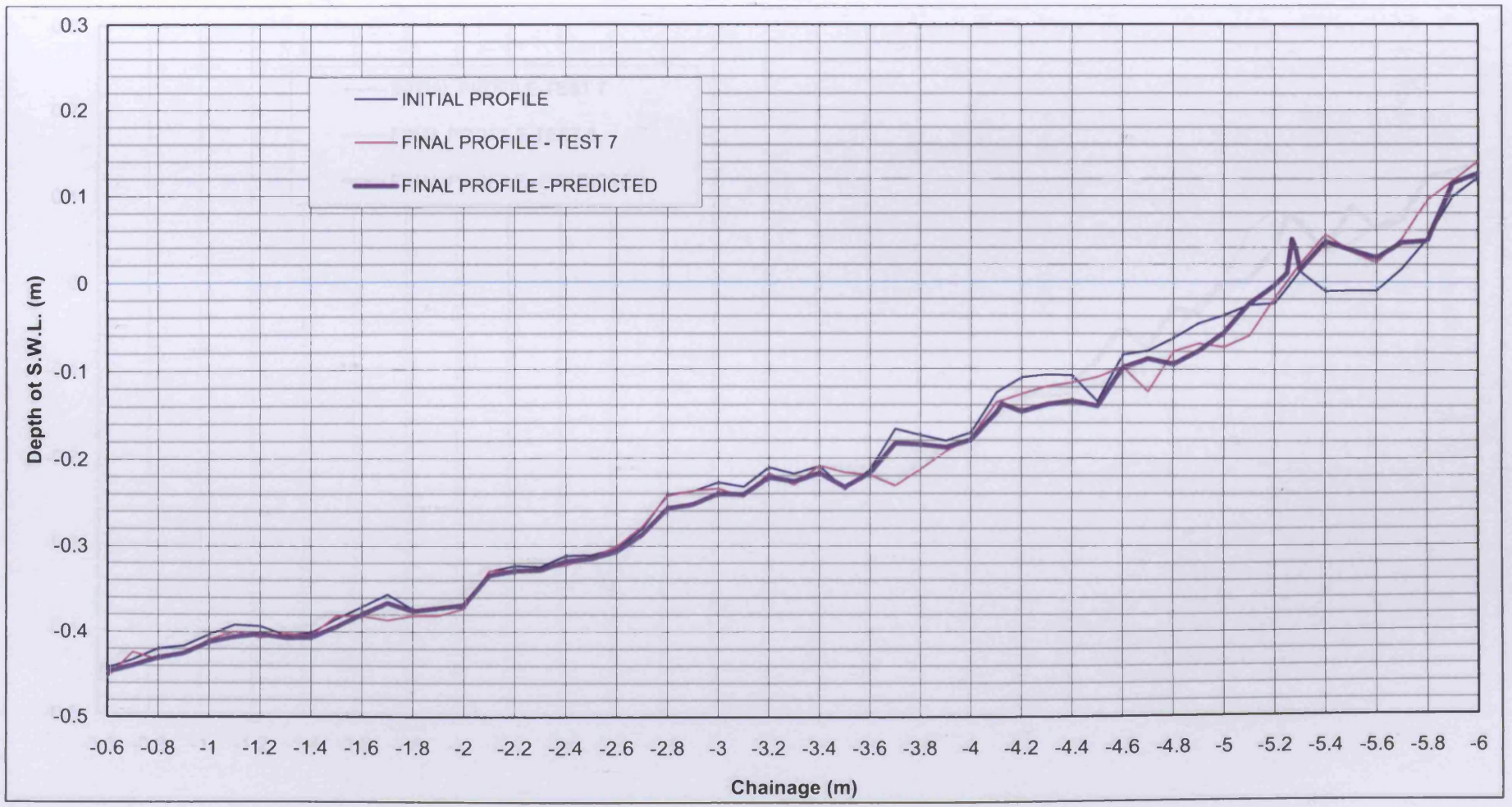

Figure 6-18 Comparison of predicted and measured beach profiles (Line 1-TEST 7)

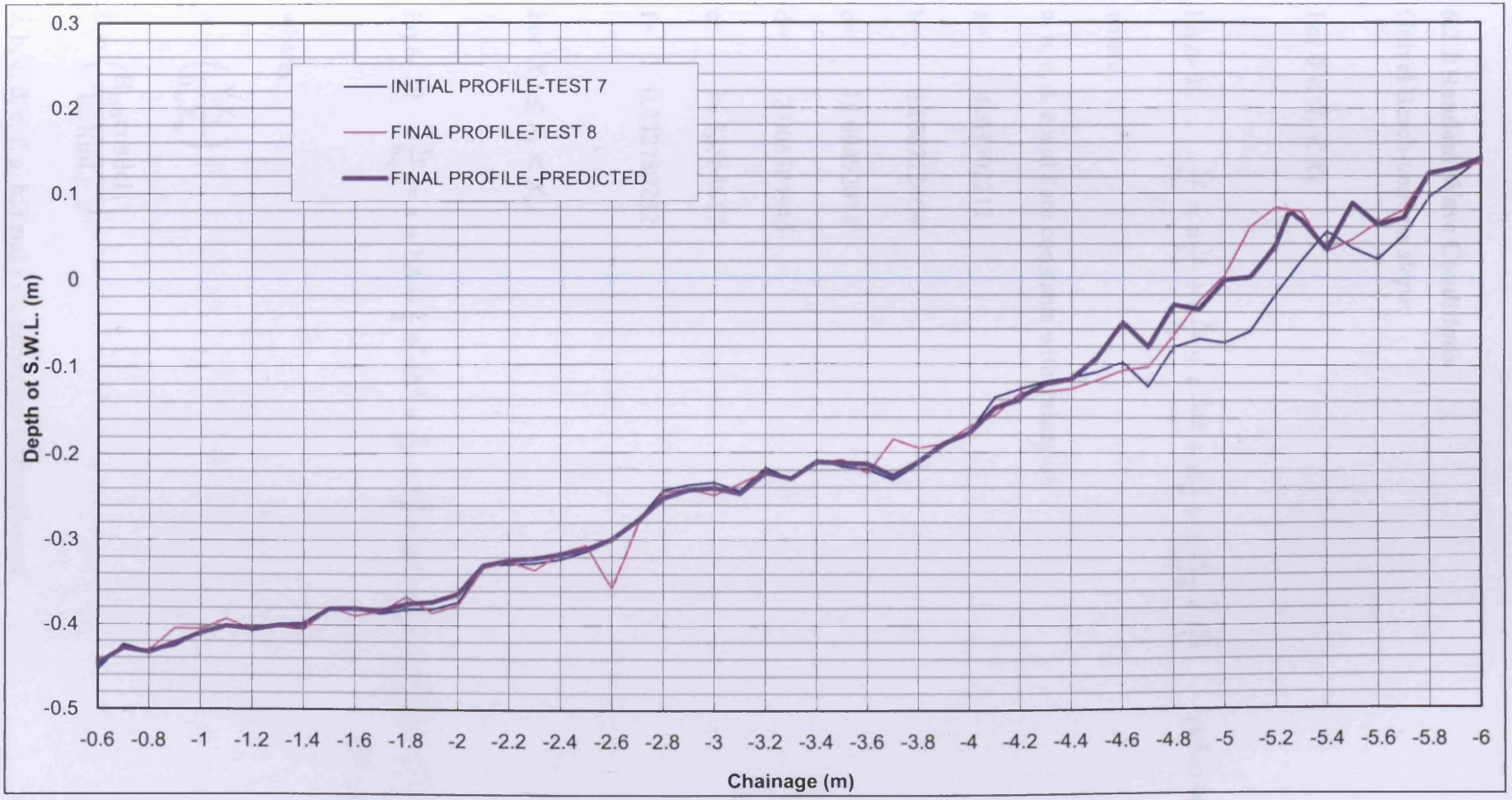

Figure 6-19 Comparison of predicted and measured beach profiles (Line 1-TEST 8)

6.2.2 Random Wave Conditions

Gravel Beach-*uniform slope*:

For $0 < X_i < X_b$

Eq.6- 21 $$\frac{Y_p}{h_w} = a\frac{Y_i}{h_w} + b\frac{X_i}{X_b} + c\frac{H_{m0}}{L_m} + d\frac{c}{K} + e\frac{m}{\cos\theta} + f\frac{L_i}{L_t} \qquad (R^2=0.900)$$

where,

a, b, c, d, e and f are constants with values of

a= -0.635022121

b= 0.180222404

c= 15.69492074

d= -2.006504945

e= 16.83564617

f= 0.332780252

For $X_b \leq X_i < X_w$

Eq.6- 22 $$\frac{Y_p}{h_w} = a + bA + \frac{c}{B} + dA^2 + \frac{e}{B^2} + f\frac{A}{B} + gA^3 + \frac{h}{B^3} + i\left(\frac{A}{B^2}\right) + j\left(\frac{A^2}{B}\right)$$

$(R^2=0.958)$

where,

$$A = \left(\frac{Y_i X_i}{h_w X_w}\right)$$

$$B = \left(\frac{H_{m0}\cos\theta c L_i}{L_m K m L_t}\right)$$

a, b, c, d, e, f, g, h, i and j are constants with values of

a= 0.918153108

b= -0.179624414

c= -0.0252

d= -0.734671258

e= -0.000021

f= 0.067

g= 1.103622082

h= -0.00000014

i= 0.0000871

j= -0.0485

For $X_w \leq X_i \leq X_e$

Eq.6- 23 $$\frac{Y_p}{h_w} = a + bA + \frac{c}{B} + dA^2 + \frac{e}{B^2} + f\frac{A}{B} + gA^3 + \frac{h}{B^3} + i\left(\frac{A}{B^2}\right) + j\left(\frac{A^2}{B}\right)$$

(R^2=0.833)

where,

$$A = \left(\frac{L_i}{L_t}\right)$$

$$B = \left(\frac{Y_i X_i H_{m0} Km}{h_w X_e L_m g T_m \cos\theta}\right)$$

a, b, c, d, e, f, g, h, i and j are constants with values of

a= 22.6470272

b= 529775.1787

c= 39737787.96

d= -2855826.745

e= 0.000000191

f= -214179941.9

g= 3592392.088

h= -6.83×10^{-12}

i= -0.000000107

j= 269408732

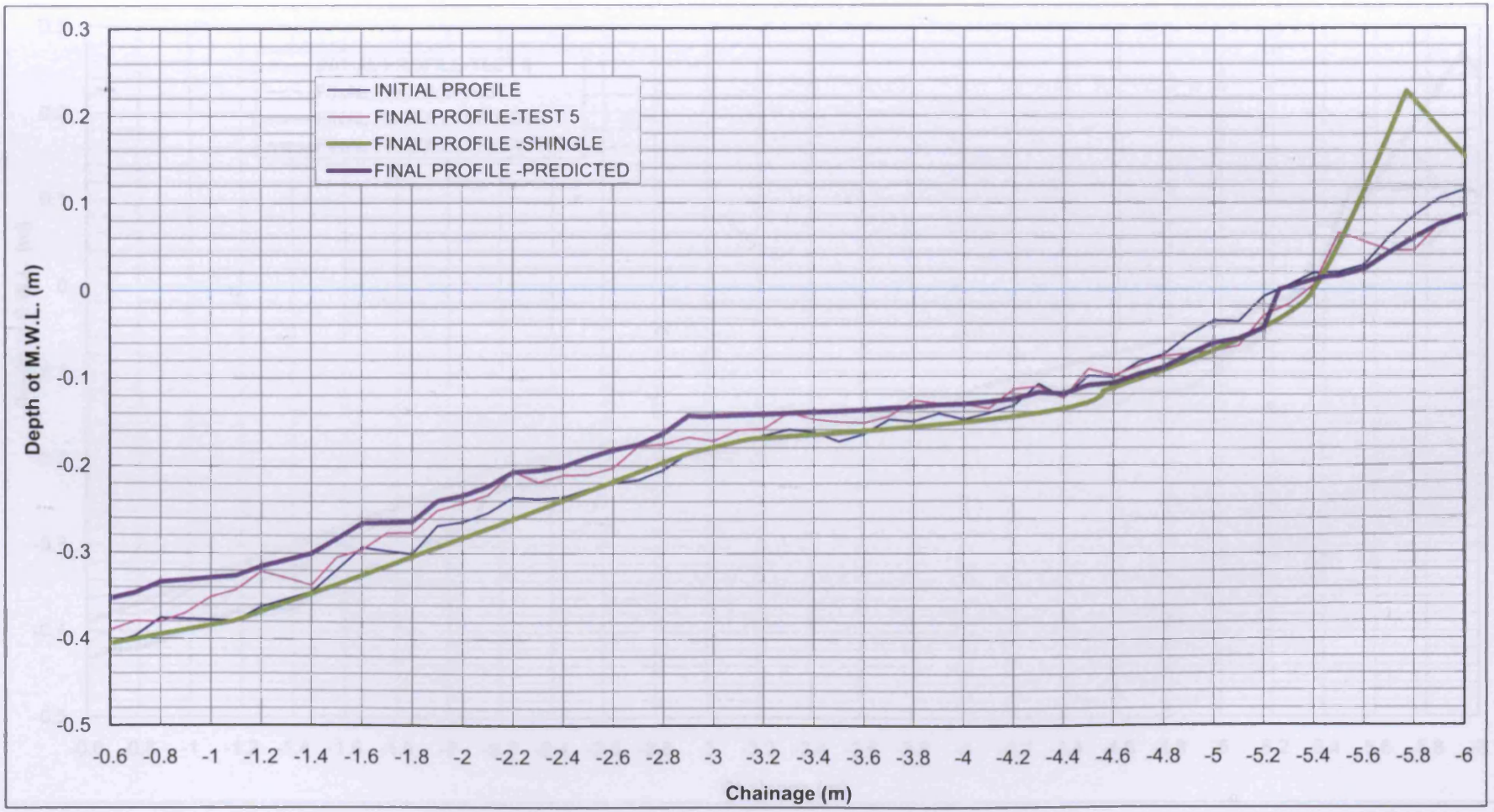

Figure 6- 20 Comparison of predicted and measured beach profiles (Line 2-TEST 5)

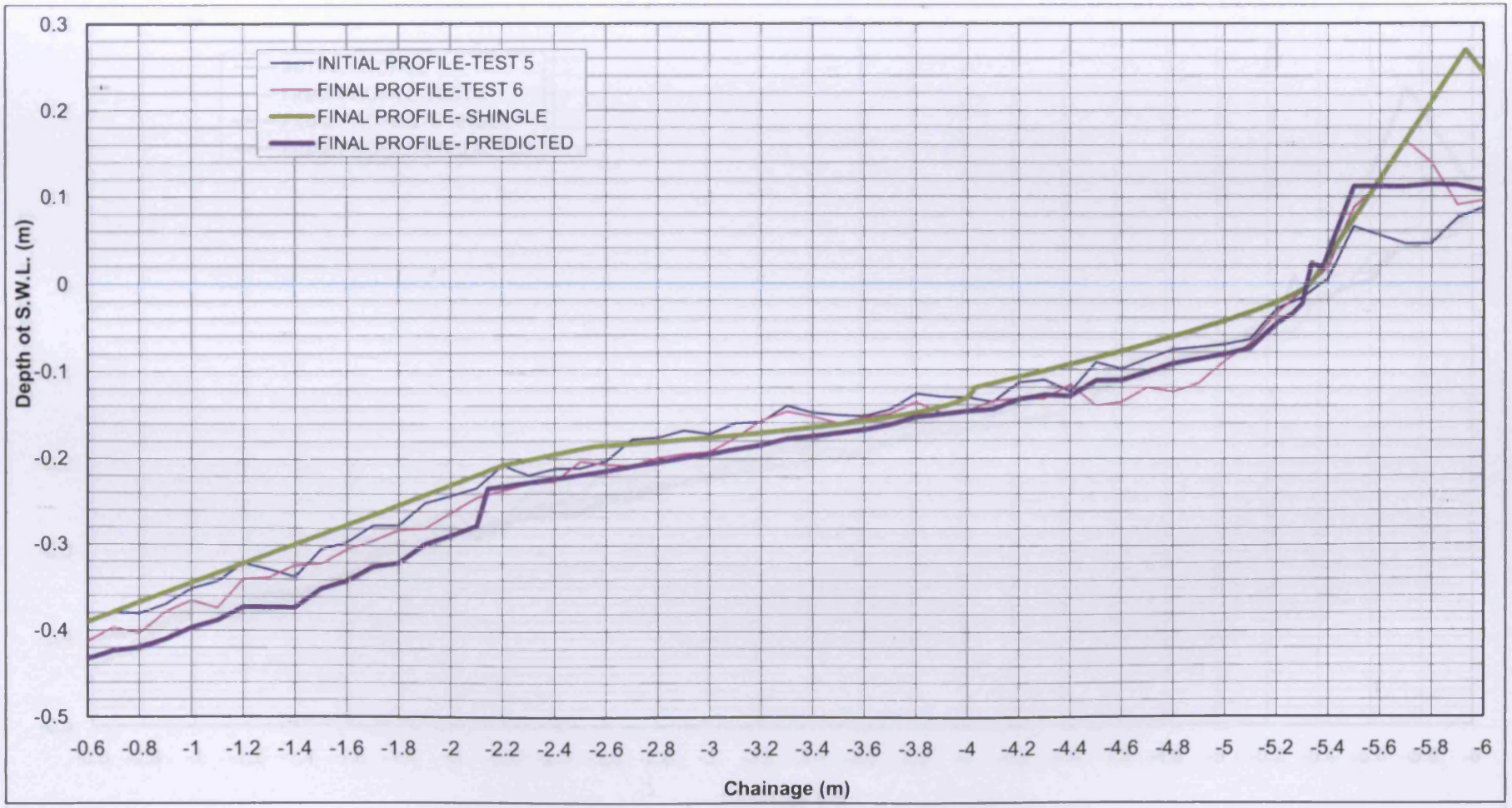

Figure 6- 21 Comparison of predicted and measured beach profiles (Line 2-TEST 6)

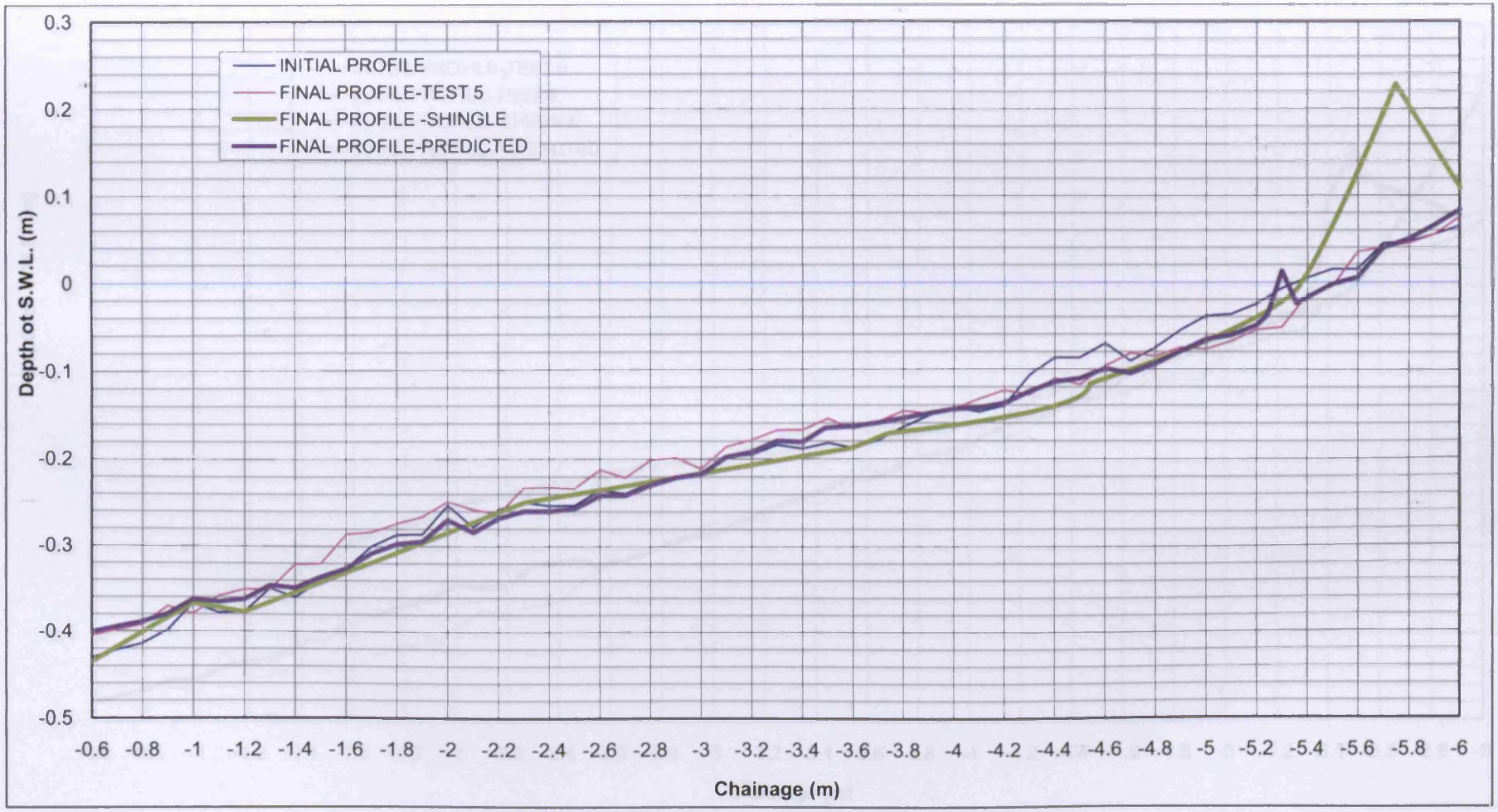

Figure 6- 22 Comparison of predicted and measured beach profiles (Line 3-TEST 5)

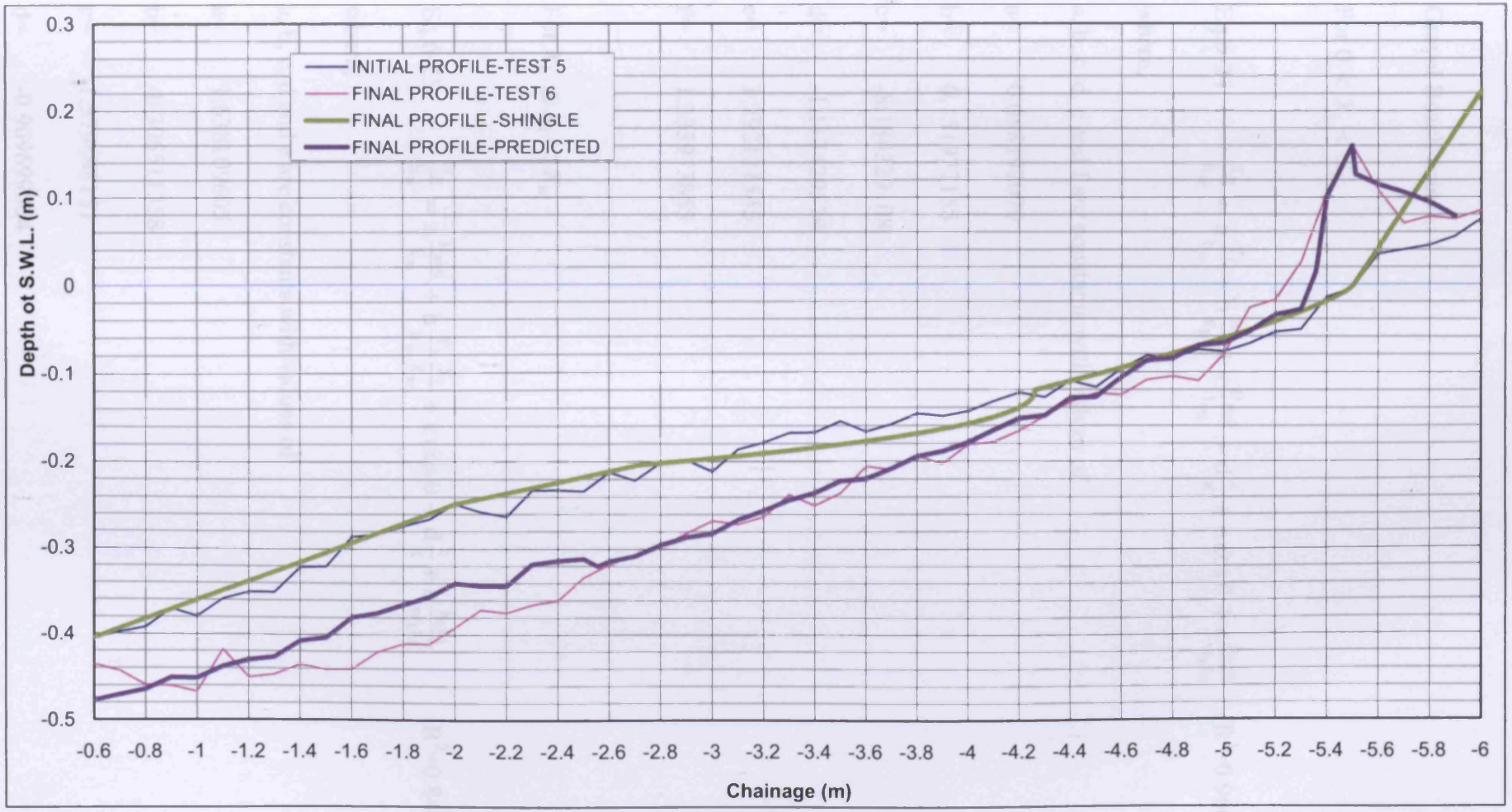

Figure 6- 23 Comparison of predicted and measured beach profiles (Line 3-TEST 6)

Gravel Beach-*trench*:

For $0 < X_i < X_b$

Eq.6-24 $$\frac{Y_p}{h_w} = a\frac{Y_i}{h_w} + b\frac{X_i}{X_b} + c\frac{H_{m0}}{L_m} + d\frac{c}{K} + e\cos\theta + c\frac{h_t L_i}{w_t L_t} \quad (R^2=0.966)$$

where,

a, b, c, d, e and f are constants with values of

a= 0.088192079

b= 0.151977155

c= -8.184329108

d= -1.113429579

e= 1.292121545

f= 1.333973855

For $X_b \leq X_i < X_w$

Eq.6-25 $$\frac{Y_p}{h_w} = a\frac{H_{m0}}{L_m} + b\frac{Y_i}{h_w}\frac{X_i}{X_w} + c\cos\theta + d\frac{c}{K} + e\frac{h_t L_i}{w_t L_t} \quad (R^2=0.844)$$

where,

a, b, c, d and e are constants with values of

a= 1.638109605

b= -0.306511358

c= 1.379698151

d= -0.909699004

e= 0.338331292

For $X_w \leq X_i < X_h$

Eq.6-26 $$\frac{Y_p}{h_w} = a + bA + cA^2 + dA^3 + eA^4 + fA^5 + gB + hB^2 + iB^3 + jB^4 + kB^5 \qquad (R^2=0.963)$$

where,

$$A = \left(\frac{H_{m0}\cos\theta\, w_t}{KTh_t}\right)$$

$$B = \left(\frac{Y_i X_e L_i}{h_w X_i L_t}\right)$$

a, b, c, d, e, f, g, h, i, j and k are constants with values of

a= -589802.5566

b= 0.00041

c= 0.00135

d= -0.000148

e= -0.00000419

f= 0.0000004

g= 3294924.892

h= -7361355.541

i= 8221536.77

j= -4590181.229

k= 1024889.267

For $X_h \leq X_i \leq X_e$

Eq.6-27 $$\frac{Y_p}{h_w} = aA + bB + cC \qquad (R^2=0.986)$$

where,

$$A = \left(\frac{Y_i X_e}{h_w X_i}\right)$$

$$B = \left(\frac{H_{m0} K \cos\theta}{L_m g T_m}\right)$$

$$C = \left(\frac{h_t L_i}{w_t L_t}\right)$$

a, b and c are constants with values of

a= 1.310717393

b= -315.7426255

c= -1.67959865

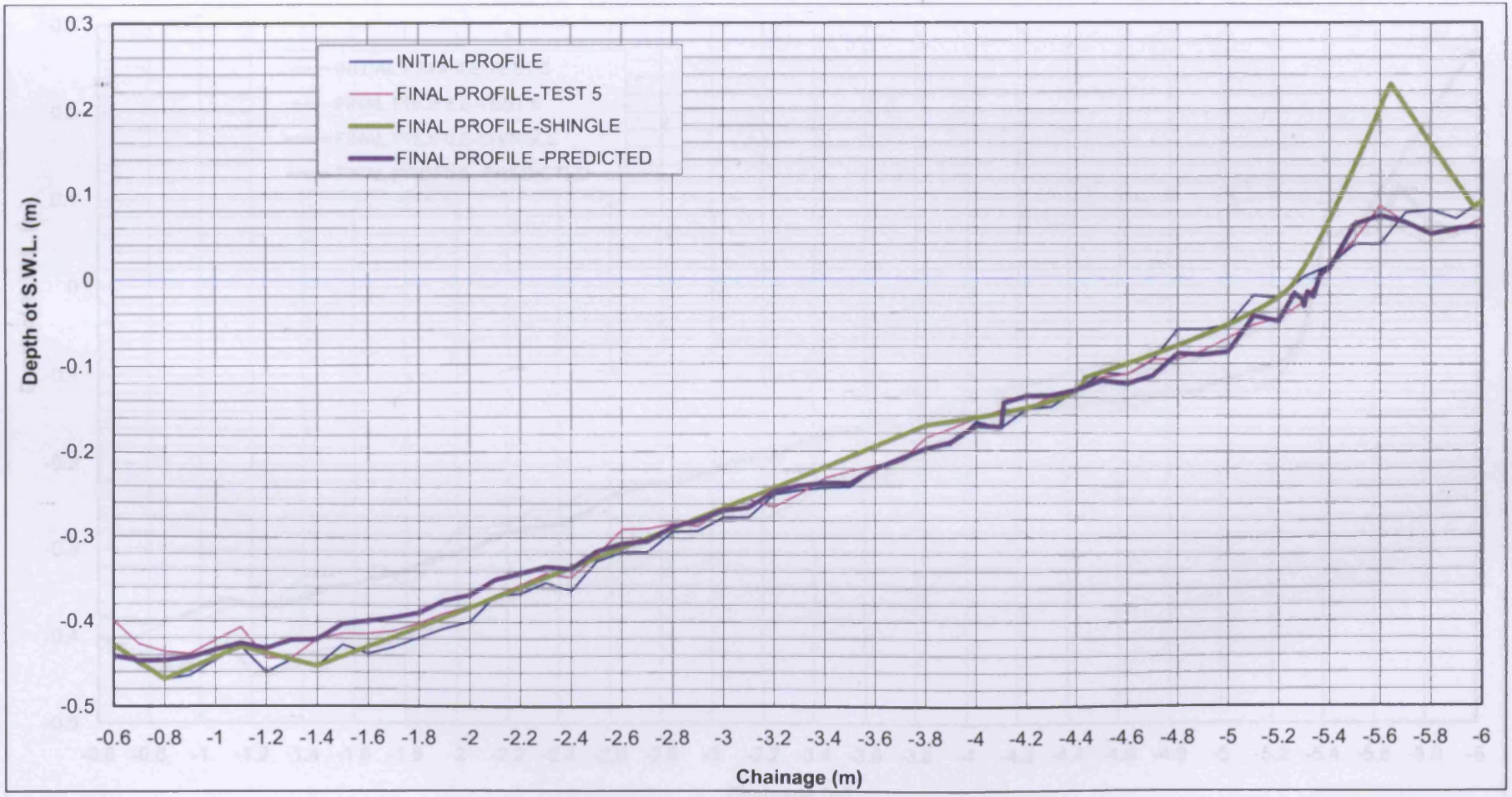

Figure 6-24 Comparison of predicted and measured beach profiles (Line 1-TEST 5)

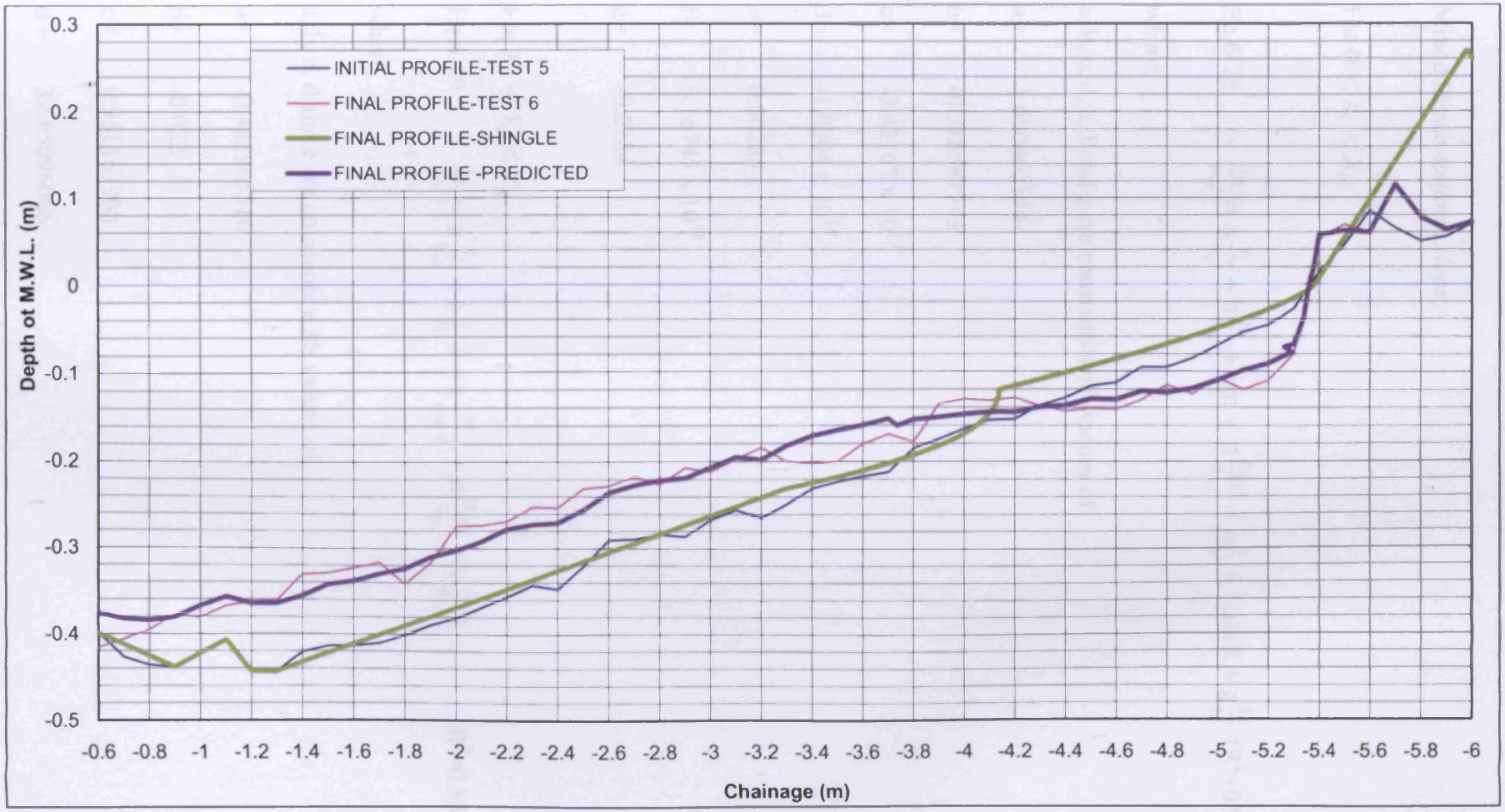

Figure 6-25 Comparison of predicted and measured beach profiles (Line 1-TEST 6)

Mixed Beach-*uniform slope*:

For $0 < X_i < X_b$

Eq.6-28 $$\frac{Y_p}{h_w} = a\frac{Y_i}{h_w} + b\frac{X_i}{X_b} + cm + d\frac{H_{m0}}{L_m} + e\frac{c}{K} + f\cos\theta + g\frac{L_i}{L_t} \quad (R^2=0.981)$$

where,

a, b, c, d, e, f and g are constants with values of

a= 1.690465144

b= -0.316587743

c= -3.42167×10^{13}

d= -1.0804×10^{14}

e= 0.00285

f= 6.16745×10^{12}

g= -0.0184

For $X_b \leq X_i < X_w$

Eq.6-29 $$\frac{Y_p}{h_w} = a\frac{Y_i}{h_w} + b\frac{c}{K} + +c\frac{m}{\cos\theta} + d\frac{H_{m0}}{L_m} + e\frac{X_i L_i}{X_w L_t} \quad (R^2=0.850)$$

where,

a, b, c, d and e are constants with values of

a= -0.445965516

b= -0.022

c= 9.951163908

d= 32.85096066

e= -0.179196367

For $X_i = X_w$

Eq.6-30 $$\frac{Y_p}{h_w} = a + b\frac{X_i}{X_e} + c\frac{L_m L_t}{H_{m0} L_i}$$ (R^2=0.1)

where,

a, b, and c are constants with values of

a= 0.4828152087

b= 6.698564609

c= -0.000966

For $X_w < X_i < X_h$

Eq.6-31 $$\frac{Y_p}{h_w} = a + b\ln(A) + \frac{c}{B} + d\ln(A)^2 + \frac{e}{B^2} + f\frac{\ln(A)}{B} + g\ln(A)^3 + \frac{h}{B^3} + i\frac{\ln(A)}{B^2} + j\frac{\ln(A)^2}{B}$$ (R^2=0.925)

where,

$$A = \left(\frac{Y_i(X_e - X_w)}{h_w(X_i - X_w)}\right)$$

$$B = \left(\frac{H_{m0}\cos\theta L_i}{KT_m m L_t}\right)$$

a, b, c, d, e, f, g, h, i and j are constants with values of

a= -3.555765559

b= 0.387754864

c= 83.21457166

d= -0.359092994

e= -456.3469222

f= 1.194449244

g= 0.0452

h= 767.7741361

i= -4.489845407

j= 0.309546135

For $X_h \leq X_i \leq X_e$

Eq.6-32 $$\frac{Y_p}{h_w} = \frac{X_i}{X_e}(a + bA + cA^2 + dA^3 + eA^4 + fA^5 + gB + hB^2)$$

(R^2=0.999)

where,

$$A = \left(\frac{H_{m0}\cos\theta\, Y_i X_e}{KT_m m h_w X_i}\right)$$

$$B = \left(\frac{X_i L_i}{X_e L_t}\right)$$

a, b, c, d, e, f, g and h are constants with values of

a= -20629.83042

b= 7225.235442

c= -1012.355498

d= 70.90745484

e= -2.48241939

f= 0.0347

g= 33.99008129

h= -43.52337604

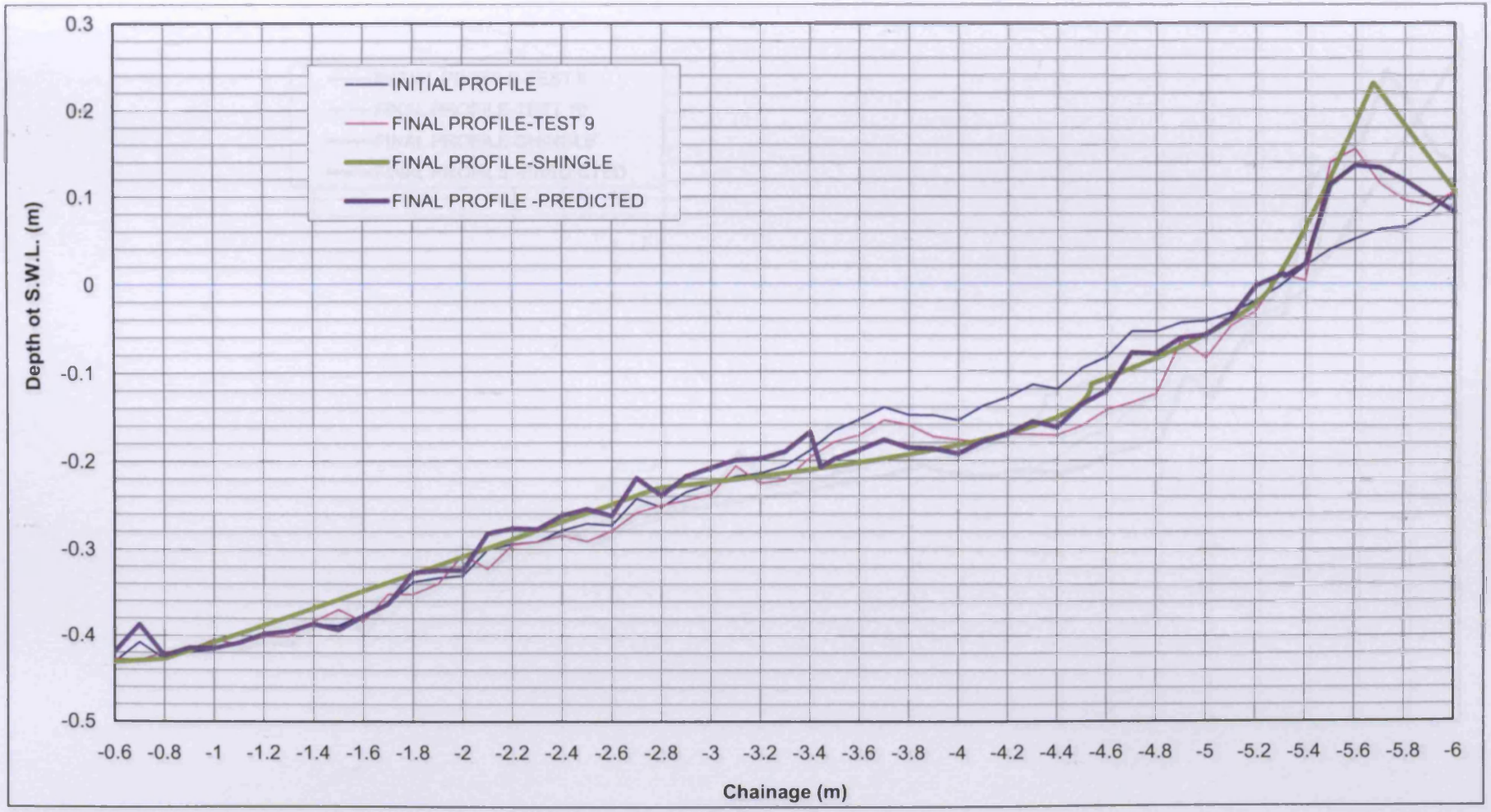

Figure 6-26 Comparison of predicted and measured beach profiles (Line 2-TEST 9)

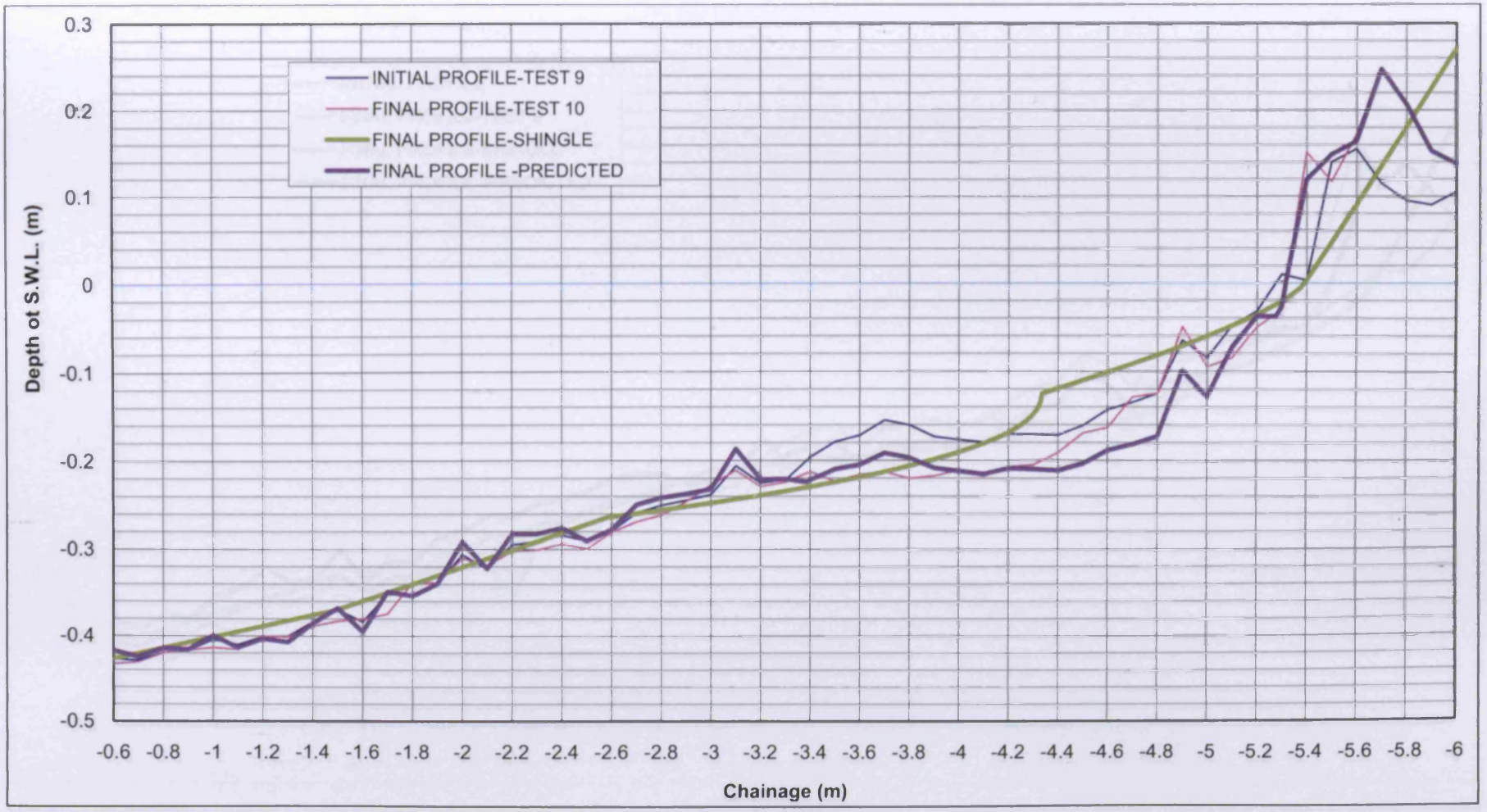

Figure 6-27 Comparison of predicted and measured beach profiles (Line 2-TEST 10)

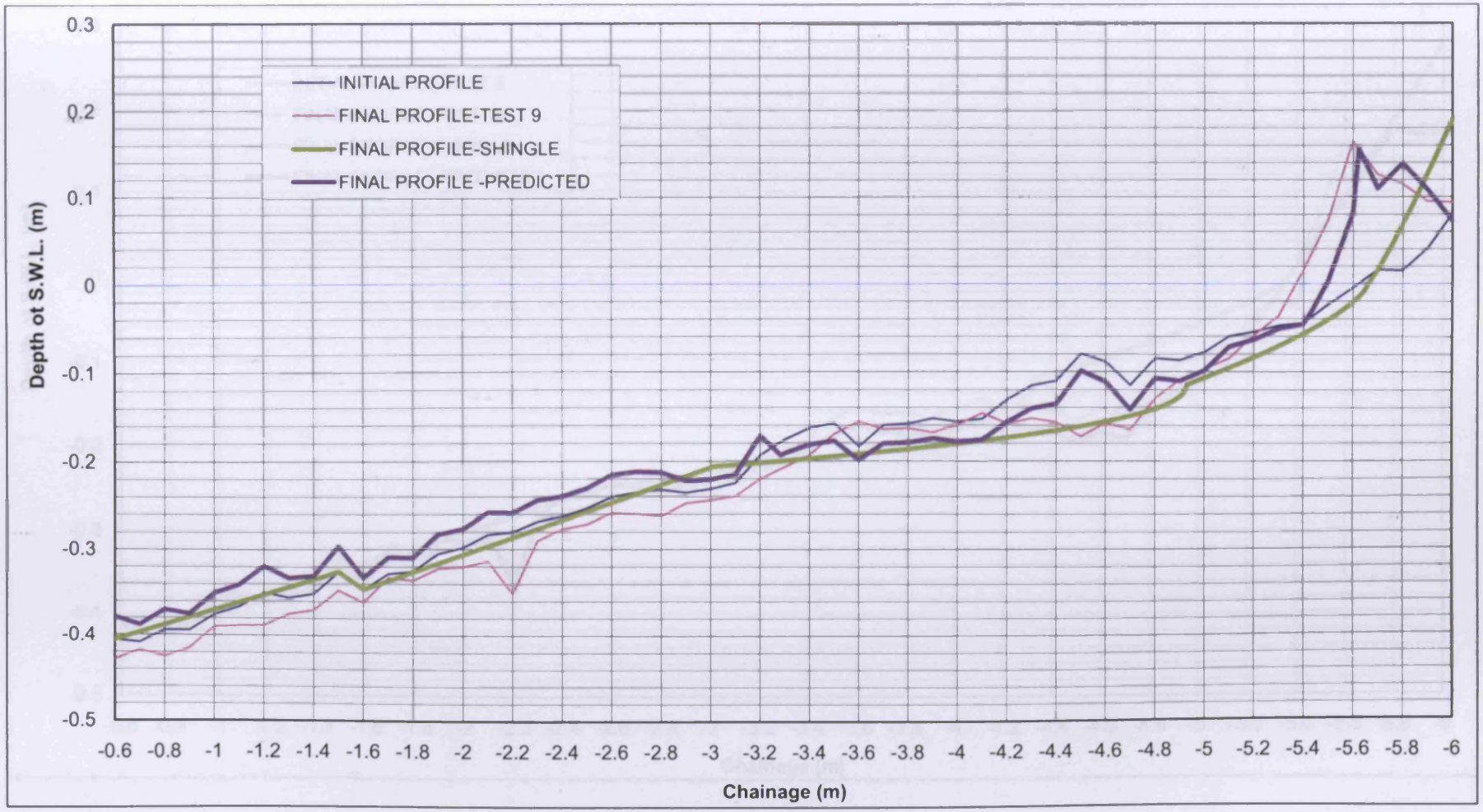

Figure 6-28 Comparison of predicted and measured beach profiles (Line 3-TEST 9)

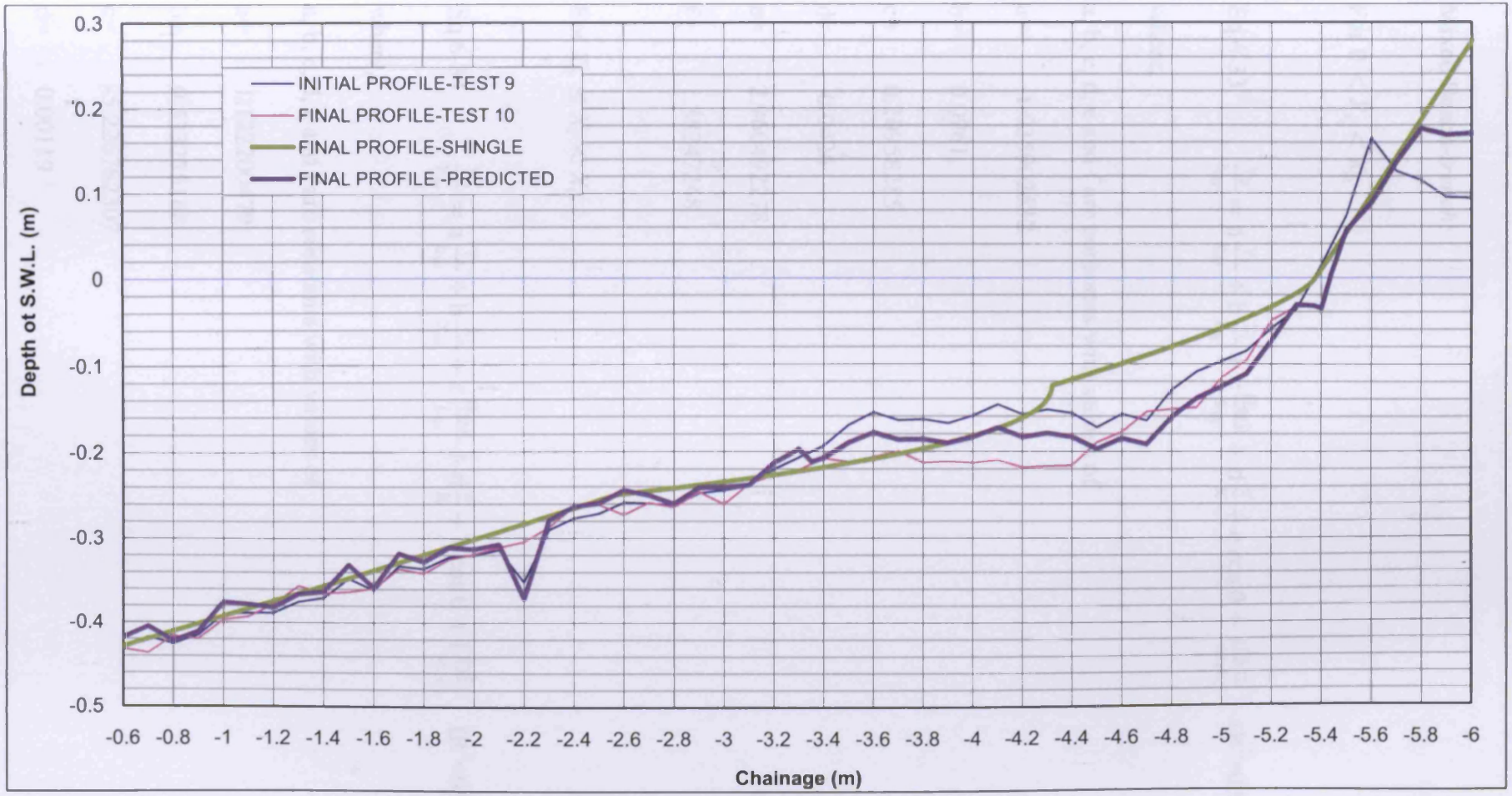

Figure 6-29 Comparison of predicted and measured beach profiles (Line 3-TEST 10)

Mixed Beach-*trench*:

For $0 < X_i < X_b$

Eq.6-33 $$\frac{Y_p}{h_w} = a\frac{Y_i}{h_w} + b\frac{X_i}{X_b} + c\frac{H_{m0}}{L_m} + d\frac{c}{K} + e\cos\theta + f\frac{h_t L_i}{w_t L_t} \quad (R^2=0.927)$$

where,

a, b, c, d, e and f are constants with values of

a= -1.035902532

b= 0.0961

c= 0.20958285

d= -0.0426

e= 2.960492278

f= 1.88247248

For $X_b \leq X_i < X_w$

Eq.6-34 $$\frac{Y_p}{h_w} = a\frac{Y_i}{h_w} + b\frac{X_i}{X_w} + c\frac{H_{m0}}{L_m} + d\frac{c}{K} + e\cos\theta + f\frac{h_t L_i}{w_t L_t} \quad (R^2=0.951)$$

where,

a, b, c, d, e and f are constants with values of

a= 1.122200479

b= 0.533275168

c= -5.226782307

d= 0.00119

e= -0.501373362

f= 1.522847287

For $X_w \leq X_i < X_h$

Eq.6-35 $$\frac{Y_p}{h_w} = a + \frac{b}{A} + \frac{c}{B} + \frac{d}{A^2} + \frac{e}{B^2} + \frac{f}{AB} + \frac{g}{A^3} + \frac{h}{B^3} + \frac{i}{AB^2} + \frac{j}{A^2B} \quad (R^2=0.919)$$

where,

$$A = \left(\frac{H_{m0} \cos\theta\, w_t}{KT_m h_t}\right)$$

$$B = \left(\frac{Y_i X_e L_i}{h_w X_i L_t}\right)$$

a, b, c, d, e, f, g, h, i and j are constants with values of

a= 415.6519499

b= -1066.797369

c= -1188.965857

d= 2223.127864

e= 1133.227714

f= 1894.503176

g= 58643.05915

h= -358.9102695

i= -822.0894337

j= 285.3792091

For $X_h \leq X_i \leq X_e$

Eq.6-36 $$\frac{Y_p}{h_w} = aA + bB + cC \qquad (R^2=0.916)$$

where,

$$A = \left(\frac{Y_i X_e}{h_w X_i}\right)$$

$$B = \left(\frac{H_{m0}}{L_m}\frac{K}{gT_m}\cos\theta\right)$$

$$C = \left(\frac{h_t L_i}{w_t L_t}\right)$$

a, b and c are constants with values of

a= -0.58024258

b= 9860.7249

c= 0.055464052

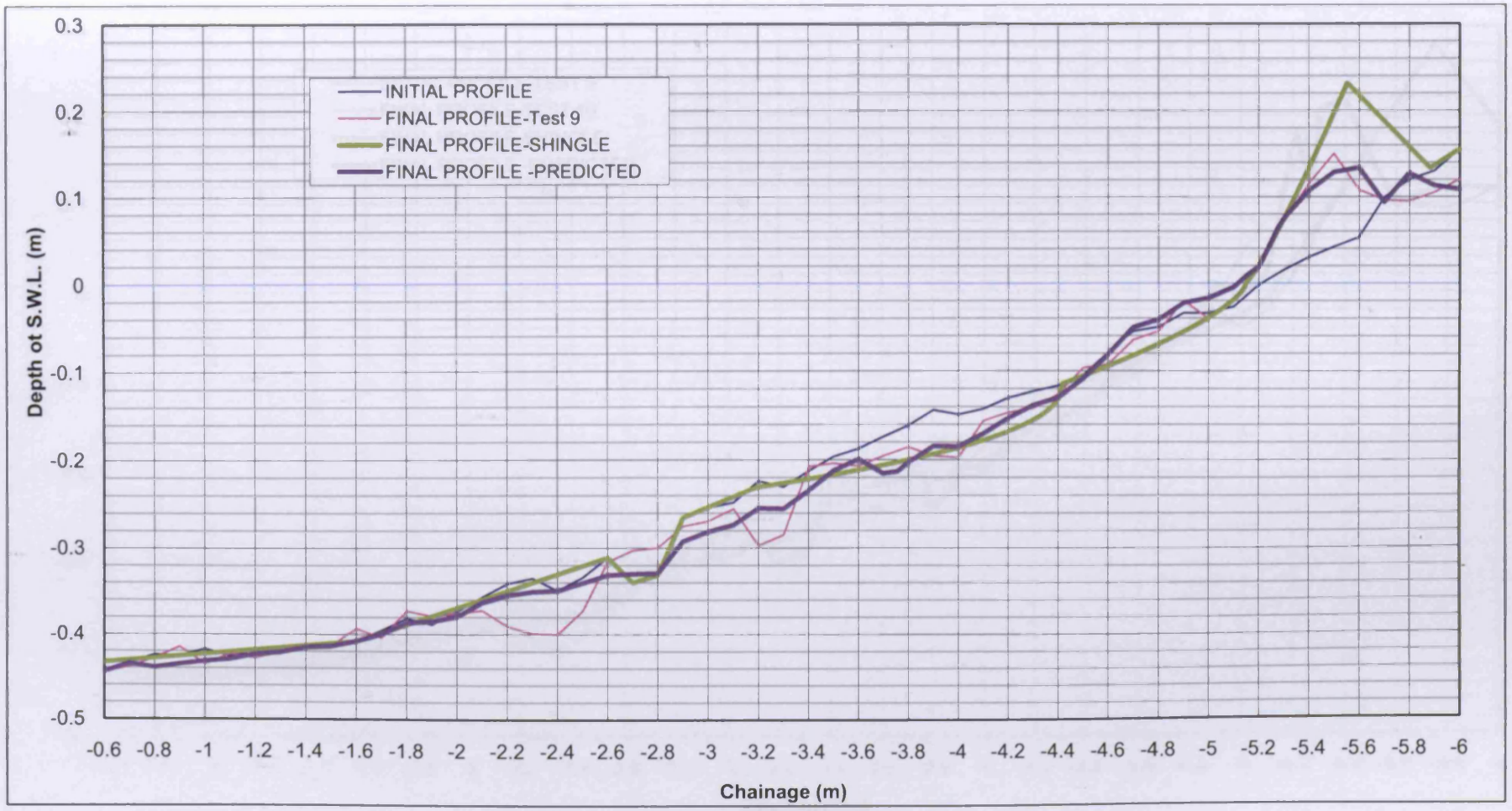

Figure 6-30 Comparison of predicted and measured beach profiles (Line 1-TEST 9)

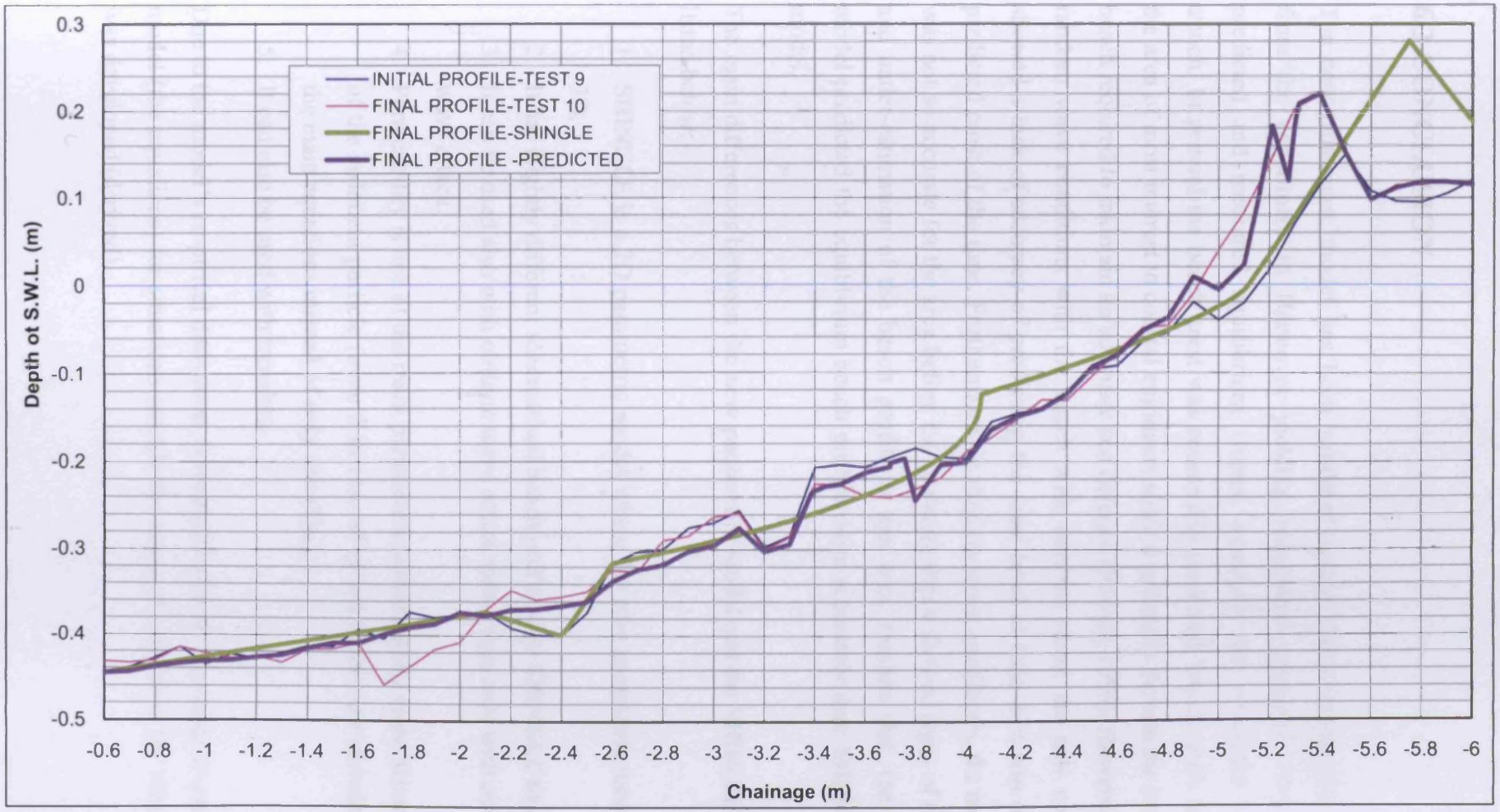

Figure 6-31 Comparison of predicted and measured beach profiles (Line 1-TEST 10)

6.3 CONCLUSION

The new parametric model has been validated against the experimental data from the experiment in Hannover yielding reasonable agreement between predicted and measured equilibrium slopes, especially for conditions with trench. In general the beach crest was reasonably predicted, which tends to be the area of most interest to coastal engineers since it generally defines the size of beach required to maintain an adequate sea defence (Powell, 1990). However, in random wave conditions with the beach with uniform slope, the new model showed a lack of accuracy of predicting the crest level of Line 2; it was over-predicted most of the time. Furthermore, in random wave conditions, the model was not so accurate for the area before the breaking depth showed signs of over- and under-estimation of the beach profile at that area. Despite that, the new model predicted the equilibrium beach profile more accurately than SHINGLE model.

The main differences between the new parametric model and the SHINGLE are listed below:

1. SHINGLE is a 2D parametric model where the new parametric model is 3D.
2. It has slightly different schematised beach profile than SHINGLE has.
3. It can be used also with oblique wave attack rather than only with normal wave attack.
4. Permeability is one of the main parameters, consequently more diameters of the sediment particle (even 5 in case of mixed beach) are included in the main equations instead of only one (D_{50}).
5. It can also be used with trenches.

Due to the model's empirical derivation, it would be unwise to attempt to use the model (the equations) for situations outside the range of conditions for which it was developed (derived).

The model has been validated against an experimental data set. Moreover, the new parametric model has also been validated with a field data of random wave conditions from gravel beach with uniform slope. The results are show in following chapter (Chapter 7).

CHAPTER 7

MODEL APPLICATION (CASE STUDY-CHESIL BEACH)

7.0 INTRODUCTION

The concept of the equilibrium beach profile states that when a beach is exposed to a given water level and wave condition for an extended period of time, the beach will take an equilibrium shape. However, in nature, beaches are exposed to a constantly changing set of wave and water level conditions. Therefore, the equilibrium beach profile concept should be interpreted in order to apply an average profile corresponding to the response of the beach profile to long-term changes in the environment, such as long-term sea level rise (Özkan-Haller and Brundidge, 2007).

The new model, which was described in Chapter 6, was derived to predict the equilibrium beach profile of gravel and mixed beaches with uniform slope and trench. In this chapter, it was used and modified in order to predict the equilibrium average profile of gravel beaches with uniform slope. The modification has been validated against field data taken from 9 profile locations on Chesil beach that were surveyed between 1993 and 1996.

7.1 FIELD DATA

7.1.1 Background

Chesil Beach is known throughout the world as an impressive shingle storm beach. The beach provides a natural barrier to the sea, protecting properties and land against flooding. West Bay, Burton Bradstock, Burton Freshwater and Chiswell have all experienced flooding or potential flooding as a direct result of

sea encroachment over and through the beach and have had studies and works undertaken to alleviate the flooding.

The Chesil Beach is situated on the coast of south west Dorset, between Portland and Abbotsbury (Figure 7-5). From Abbotsbury to Portland Harbour Chesil Beach forms the seaward barrier to the brackish Fleet Lagoon which extends for some 13 km. Along this stretch Chesil Beach is between 150-200m wide, narrowing at the extreme eastern and western ends. The crest of Chesil Beach extends continuously from midway between West Bexington and Abbotsbury to Chesilton. It generally increases in height from west to east, reaching a maximum of around +14m ODN (Babtie Group Ltd, 1997).

Offshore the beach face continues its slope at roughly the same gradient as above the low mark for approximately 70m after which the gradient becomes shallower. The offshore gradient is steepest at the Portland end of the beach and shallower at the West Bay side (Babtie Group Ltd, 1997).

Chesil Beach is frequently termed in the literature as a "fossil feature" in the sense that the material from which the beach is composed are non-renewable and new sources are strictly limited. The material on the shingle bank is well graded longitudinally along the beach, being largest in the east with a D_{50} of approximately 5cm, and smallest in the west with a D_{50} of approximately 0.5cm. The existence of the harbour arms at West Bay has probably arrested the westward movement of material and with Portland Island to the east it seems that Chesil Beach is a closed system (Babtie Group Ltd, 1997).

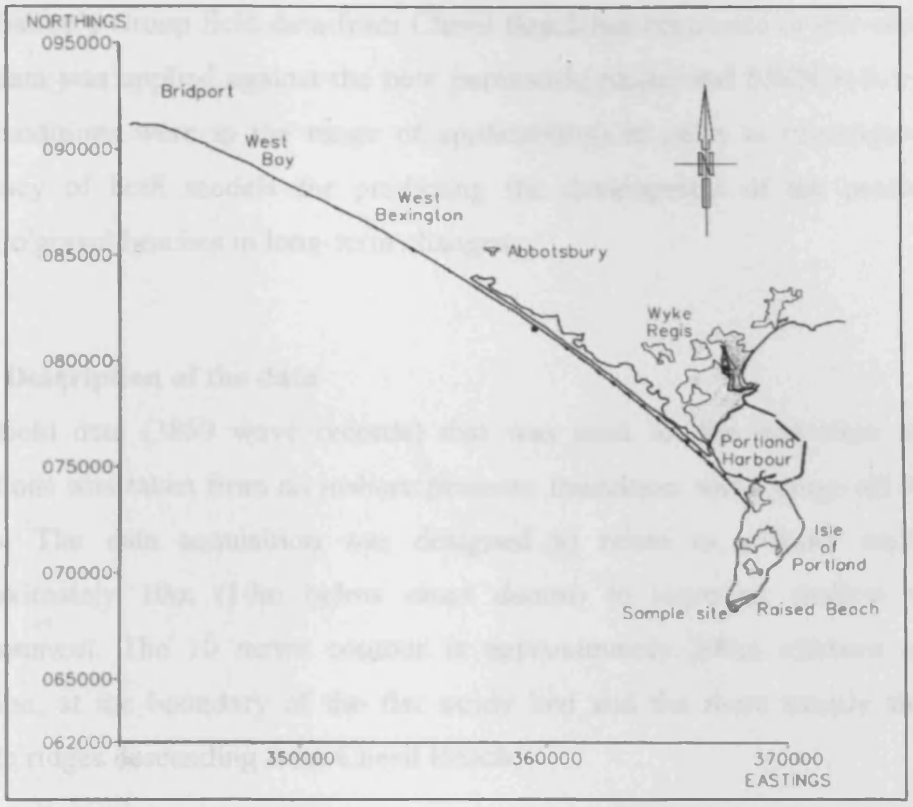

Figure 7-1 The Chesil Beach (taken from Babtie Group, 1997)

Chesil Beach is of importance to the study of coastal geomorphology, both as a classic landform and as a natural laboratory for the study of beach processes. It is also exceptional for its size (both in its length and width), for the linear grading of pebbles, for the variation in the composition of the pebbles and for the historical records of beach changes.

Babtie Group (1997), knowing the importance of the Chesil Beach and wanting to investigate its behaviour further, it managed and monitored the incoming waves and the development of the entire Chesil Beach coastline from West Bay to Portland, collecting in such away a field data for a period of three years. However, due to the adverse hydrodynamic environment at Chesil, the inshore wave monitoring at Wyke Regis was delayed significantly and suffered the most serious problems. All the other operations undertaken to collect data were successful.

The Babtie's Group field data from Chesil Beach has been used in this chapter. The data was applied against the new parametric model and SHINGLE (when the conditions were in the range of applicability) in order to investigate the accuracy of both models for predicting the development of the profile of shingle/gravel beaches in long-term changes.

7.1.2 Description of the data

The field data (3859 wave records) that was used for the derivation of the equations was taken from an inshore pressure transducer wave gauge off Wyke Regis. The data acquisition was designed to relate to a water depth of approximately 10m (10m below chart datum) to represent shallow water environment. The 10 metre contour is approximately 200m offshore at the location, at the boundary of the flat sandy bed and the more steeply sloping pebble ridges descending from Chesil Beach.

A seabed mounted pressure gauge linked to a recording computer ashore was first installed. Nevertheless, as a result of a series of physical environmentally induced problems with the cable, data was lost during the early months. The initial deployment took placed on March 1993 but the delayed starting date was 10th February 1994, and the deployment was completed on 26th May 1996. The average data recovery during this period was 68.5%. (Babtie Group Ltd, 1997)

For the purpose of the current study, only records of the local storms are used from the data. The definition of local storm in this context has been taken if continuous wave heights were recorded for 3 hours or more that were greater than 3m in height. The summary of wave parameters at the biggest local storms that occurred between the surveys and the results of the beach grading analysis are listed in Table 7-1 and Table 7-2.

The data was taken from three different locations. These locations were selected along the study frontage at the west of Burton Bradstock, at Abbotsbury and at Wyke Regis, referenced as side A, B and C respectively (Figure 7-2). Three profiles were surveyed at each location, referenced as n (north), s (south) and m

(middle) respectively. These profiles were approximately 100 metres apart, and extending from the beach crest to low water, typically 50 to 150 metres in length. The beach slope of the three locations varied from 0.14 to 0.29.

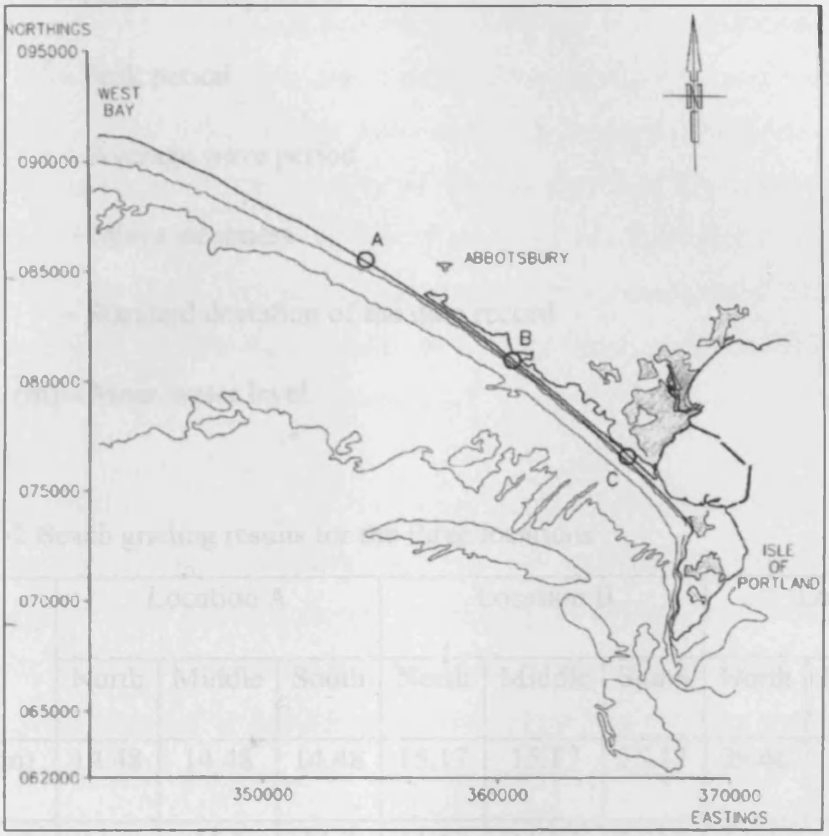

Figure 7-2 Location of the three sides (Babtie Group, 1997)

Table 7-1 Summary of wave parameters at the biggest local storms measured

Period of Tine	H_{m0} (m)	T_z (s)	T_p (s)	T_m (s)	H_s/L_m	SD	M.W.L. (m)
December 1993-April 1994	3.79	9.7	10.2	8.2	0.0365	0.64	18.63
April 1994-October 1994	3.68	7.7	7.8	6.2	0.0605	0.59	13.84
October 1994-December 1994	3.45	7.8	9.5	7.6	0.0383	0.56	13.3
December 1994-March 1995	4.9	8.7	8.8	7.0	0.0633	0.71	21.06
March 1995-May 1996	3.3	7.7	8.3	6.6	0.0479	0.43	18.29

where,

H_{m0} (m) – Estimation of the significant wave height

T_z (m) – Zero-crossing period

T_p (m) – Peak period

T_m (m) – Average wave period

H_{m0}/L_m – Wave steepness

SD (m) – Standard deviation of the data record

M.W.L. (m) – Mean water level

Table 7-2 Beach grading results for the three locations

	Location A			Location B			Location C		
	North	Middle	South	North	Middle	South	North	Middle	South
D_{16} (mm)	14.48	14.48	14.48	15.17	15.17	15.17	29.66	29.66	29.66
D_{50} (mm)	11.3	11.3	11.3	11.52	11.52	11.52	23.04	23.04	23.04
D_{85} (mm)	9.31	9.31	9.31	9.31	9.31	9.31	17.93	17.93	17.93

7.1.3 Model Application

The incoming wave angle for the locations A, B and C was 18^0, 25^0 and 26^0, respectively. The parameters and the schematisation of the new parametric model was developed and applied successfully on the experimental data in Chapter 6. Its range of applicability of slope and incoming wave angle was in the low range of slopes and incoming wave angles in the field data (Chesil beach). Moreover, the range of applicability of D_{50} of gravel of the new parametric model was in the higher range of D_{50} of gravel of the field data (Location C). Despite that, the same parameters and method of schematisation of the new model were used in order the equilibrium average beach profile to be predicted for each of the three locations (A, B and C).

After non-linear regression of the field data, equations were derived in order to predict each beach profile for each location. The equations and the results are shown below. It has to be mentioned that during the derivation of the equations the length of the beach of each locations was assumed to be 300m which , in location A for example, is the distance from a point 50m northern than A-North to a point 50m southern than A-South. The predicted beach profiles were also plotted against the predicted profile of SHINGLE (when the conditions were in the range of applicability). Moreover, the results of the period April 1994 to October 1994 are only shown here due to the fact that it is the only long period that both SHINGLE and the new model can be applied. The rest of the results are shown in Appendix IV (A1).

For $0 < X_i < X_b$

Eq.7-1 $$\frac{Y_p}{h_w} = a\frac{Y_i}{h_w} + b\frac{X_i}{X_b} + c\frac{H_{m0}}{L_m} + d\frac{c}{K} + e\frac{m}{\cos\theta} + f\frac{L_i}{L_t} + g \quad (R^2=0.760)$$

where,

a, b, c, d, e, f and g are constants with values of

a= 0.334544502

b= 0.358845923

c= -4.896054137

d= 0.00214

e= -0.364430734

f= -0.016

g= 0.403954745

For $X_b \leq X_i < X_w$

Eq.7-2 $$\frac{Y_p}{h_w} = a + b\ln(A) + c\ln(A)^2 + d\ln(A)^3 + e\ln(A)^4 + f\ln(A)^5 + \frac{g}{B} + \frac{h}{B^2} + \frac{i}{B^3} + \frac{j}{B^3} + \frac{k}{B^5} \qquad (R^2=0.848)$$

where,

$$A = \left(\frac{Y_i X_i}{h_w X_w}\right)$$

$$B = \left(\frac{cH_{m0}\cos\theta L_i}{KL_m mL_t}\right)$$

a, b, c, d, e, f, g, h, i, j and k are constants with values of

a= 0.99810178

b= 0.600658251

c= 0.300021818

d= 0.084565946

e= 0.01

f= 0.000382

g= 0.0203

h= -0.00155

i= 0.000039

j= -0.000000382

k= 0.00000000127

For $X_w \leq X_i \leq X_e$

Eq.7-3 $$\frac{Y_p}{h_w} = a\frac{Y_i}{h_w} + b\frac{X_i}{X_e} + c\frac{H_{m0}}{L_m} + d\frac{K}{gT_m} + e\frac{m}{\cos\theta} + f\frac{L_i}{L_t} + g \quad (R^2=0.932)$$

where,

a, b, c, d, e, f and g are constants with values of

a= 0.99076347

b= 0.0774

c= 3.001055425

d= 0.542273107

e= 0.372745554

f= 0.0668

g= -0.319404774

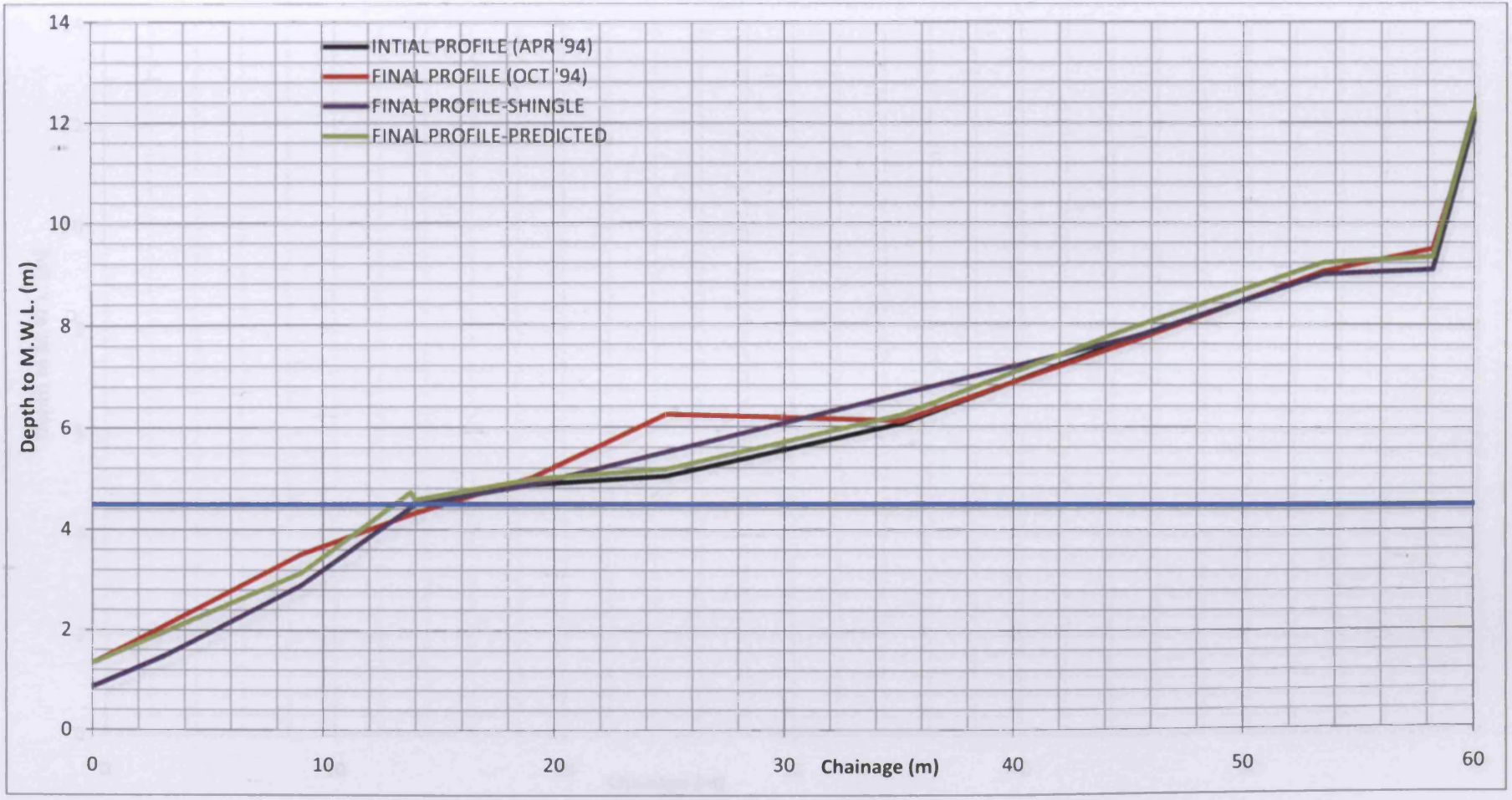

Figure 7-3 Comparison of predicted and measured beach profile for location A-Middle (April '94-October '94)

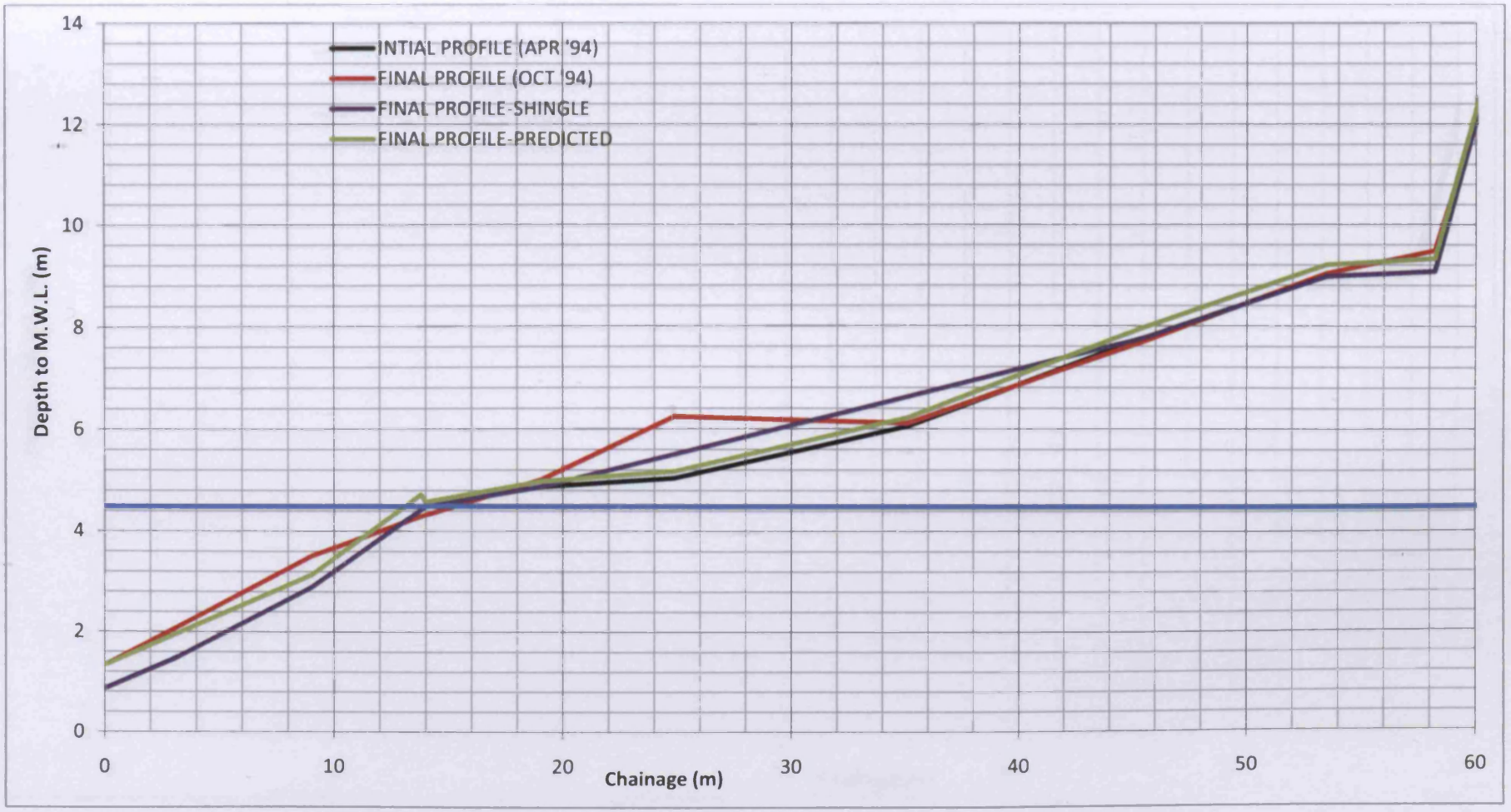

Figure 7-4 Comparison of predicted and measured beach profile for location A-North (April '94-October '94)

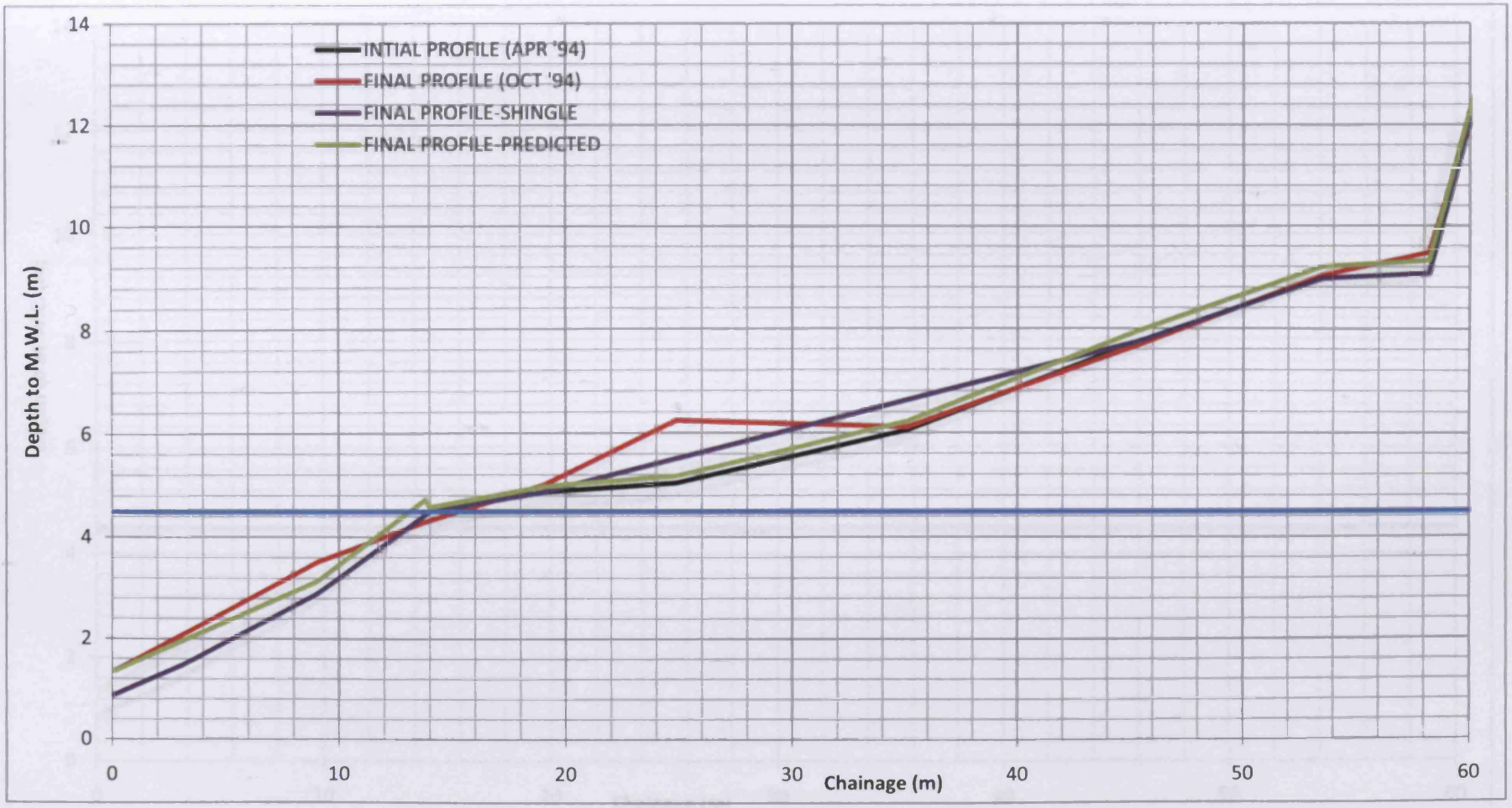

Figure 7-5 Comparison of predicted and measured beach profile for location A-South (April '94-October '94)

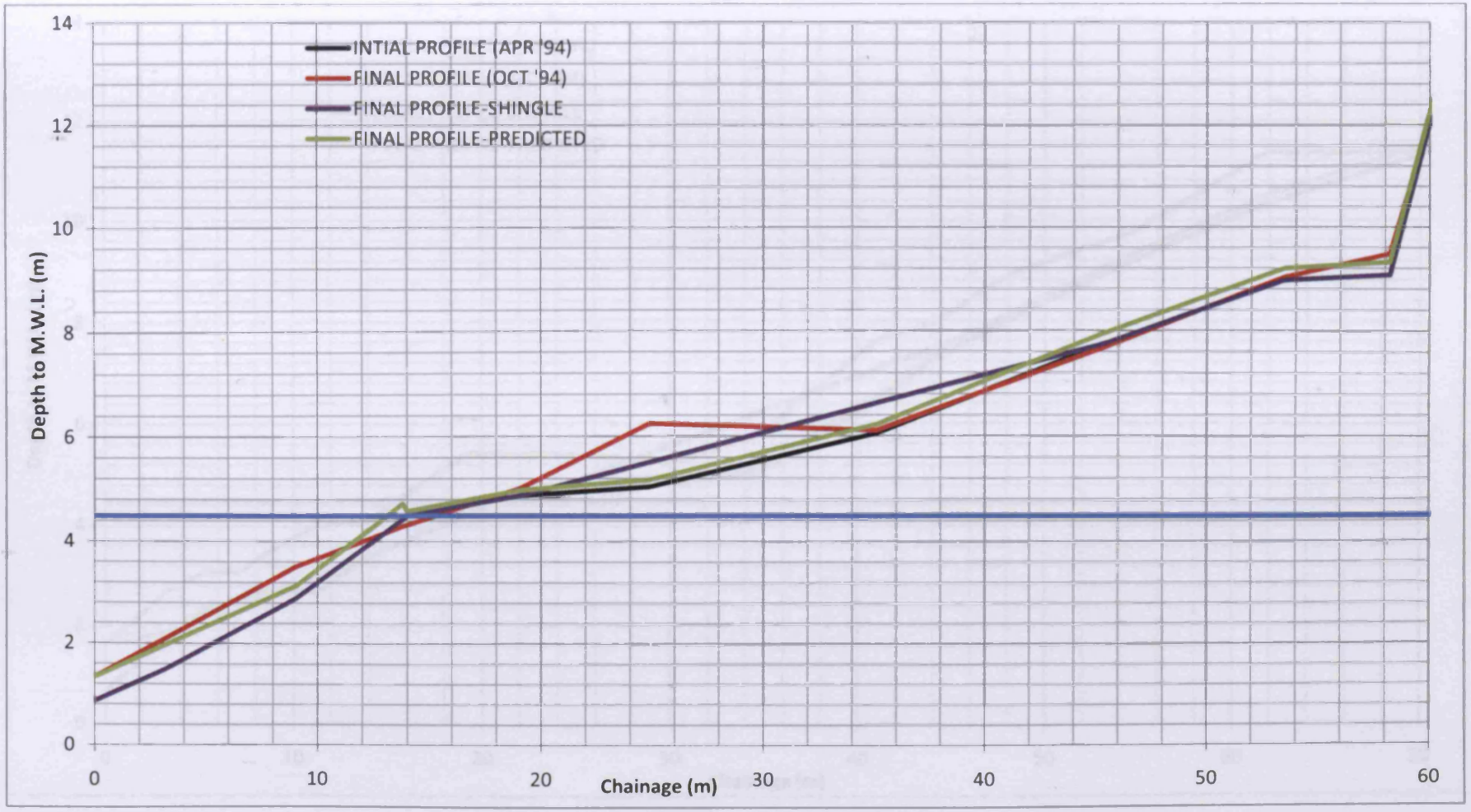

Figure 7-6 Comparison of predicted and measured beach profile for location B-Middle (April '94-October '94)

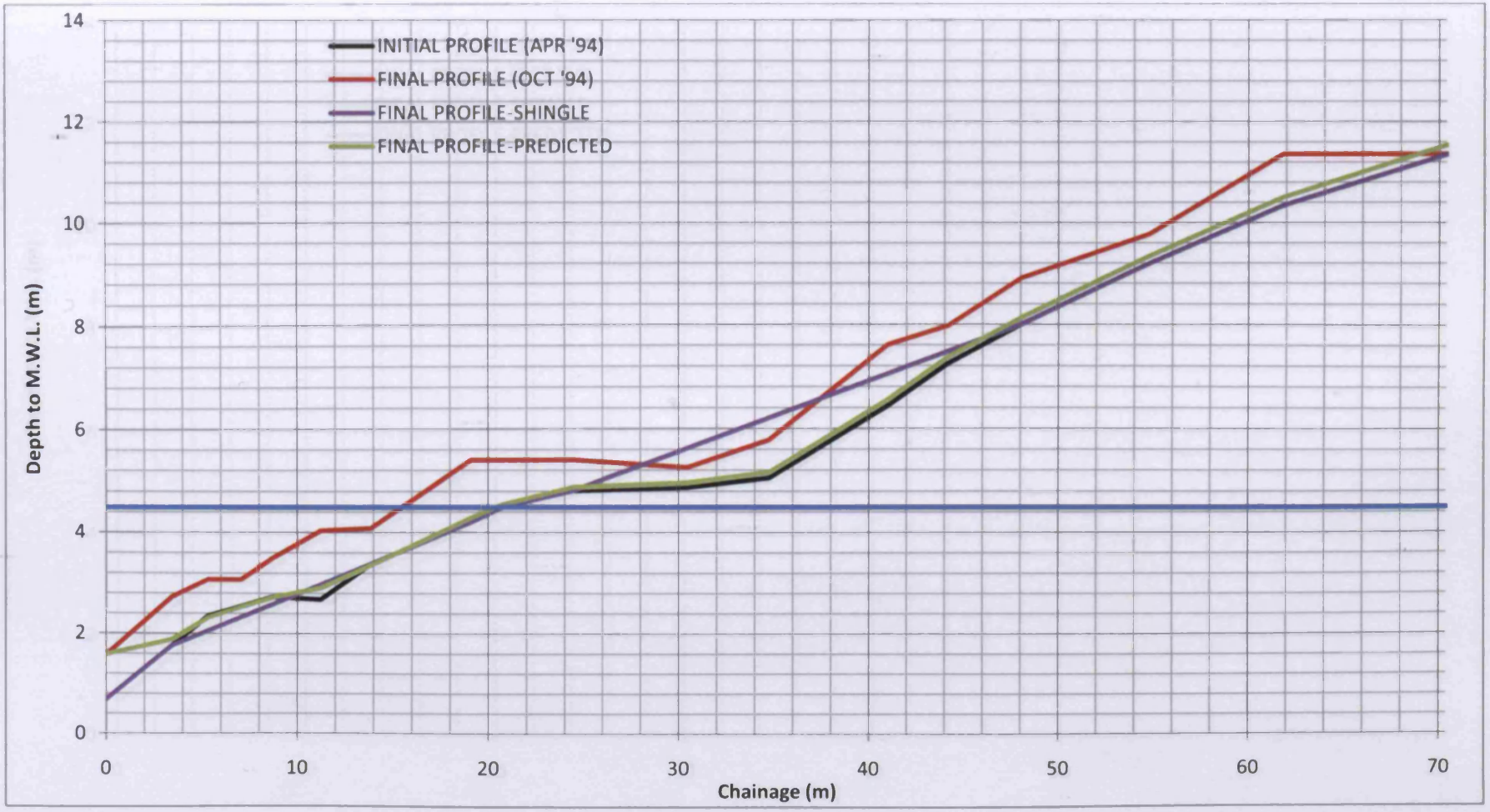

Figure 7-7 Comparison of predicted and measured beach profile for location B-North (April '94-October '94)

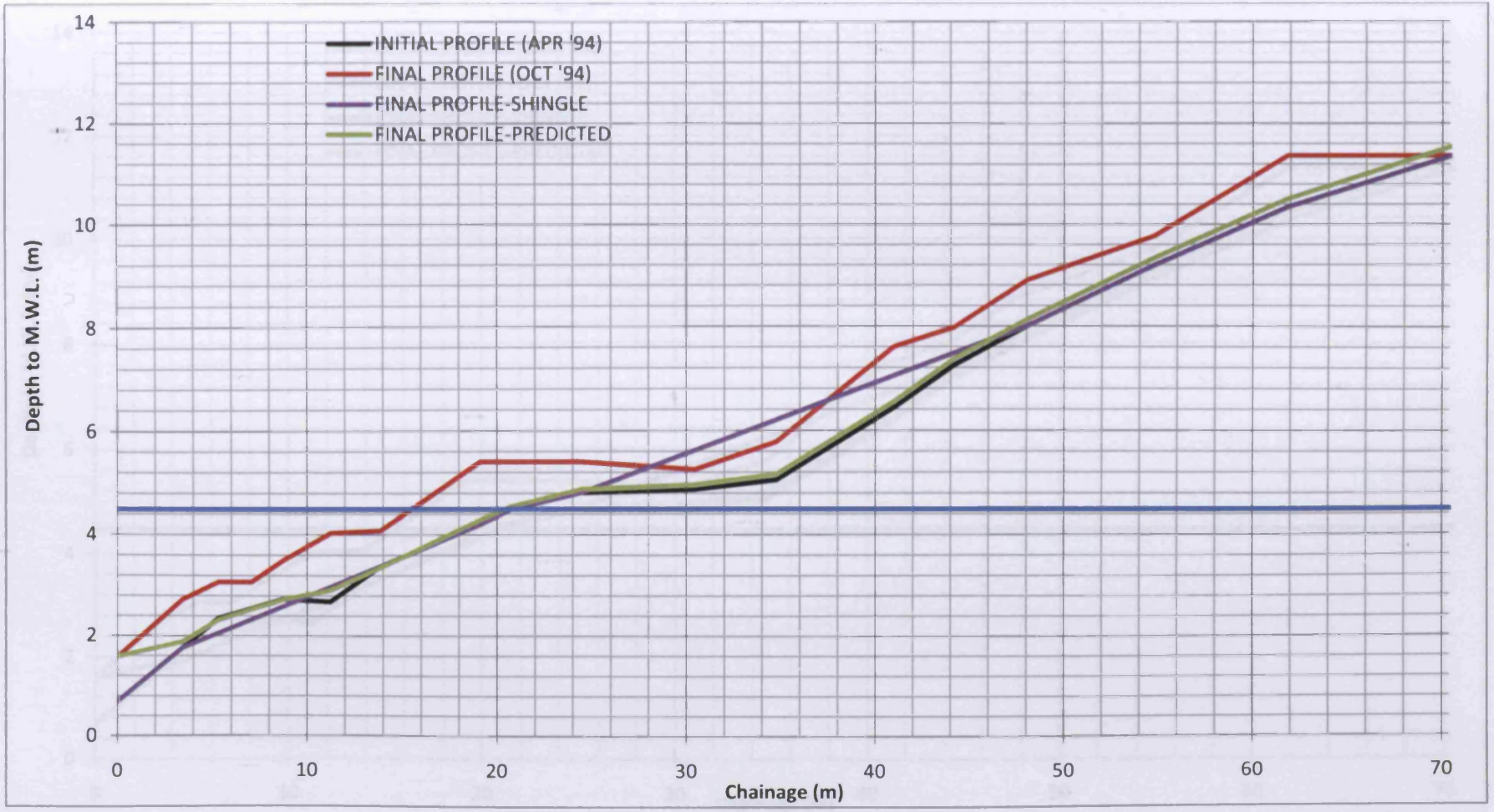

Figure 7-8 Comparison of predicted and measured beach profile for location B-South (April '94-October '94)

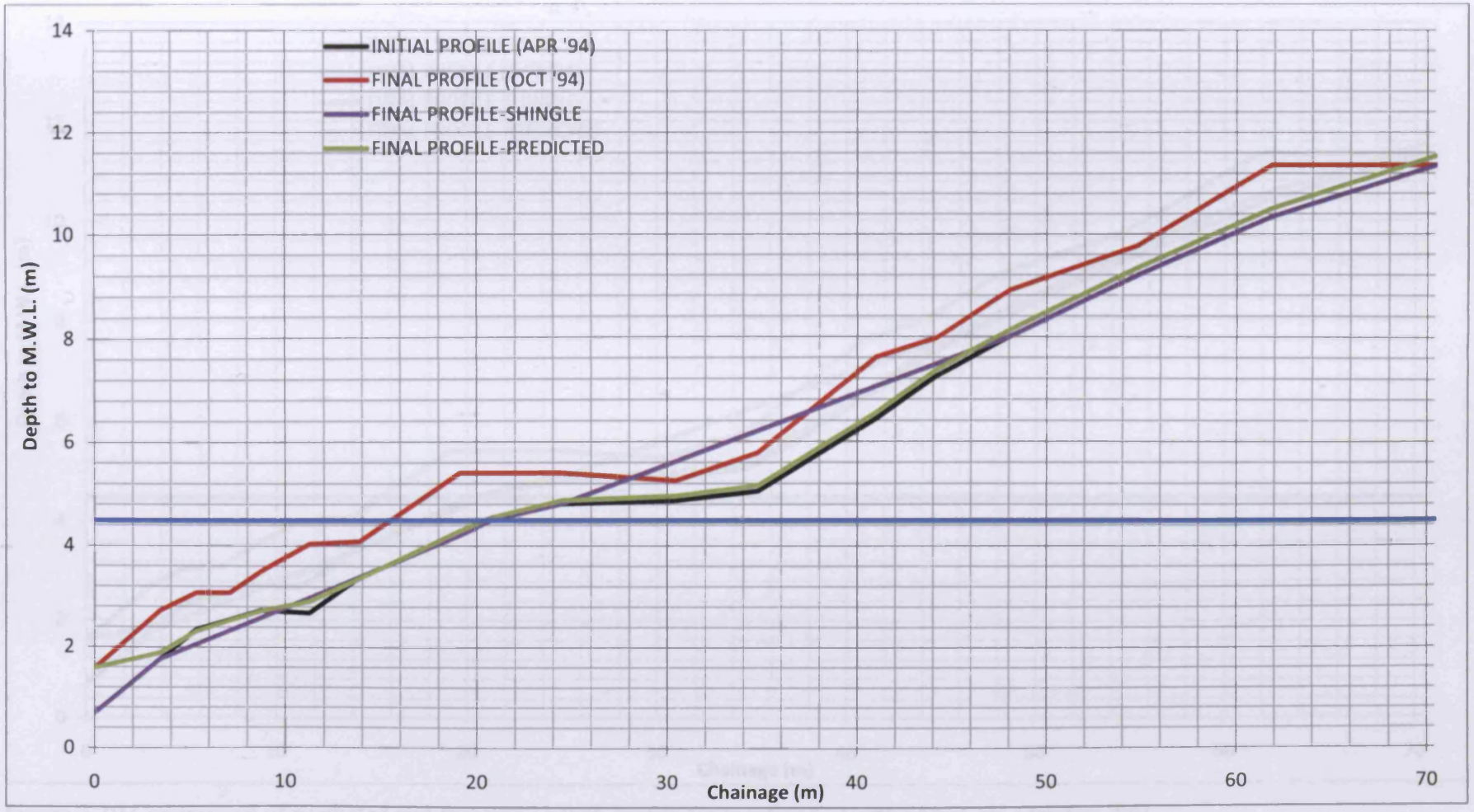

Figure 7-9 Comparison of predicted and measured beach profile for location C-Middle (April '94-October '94)

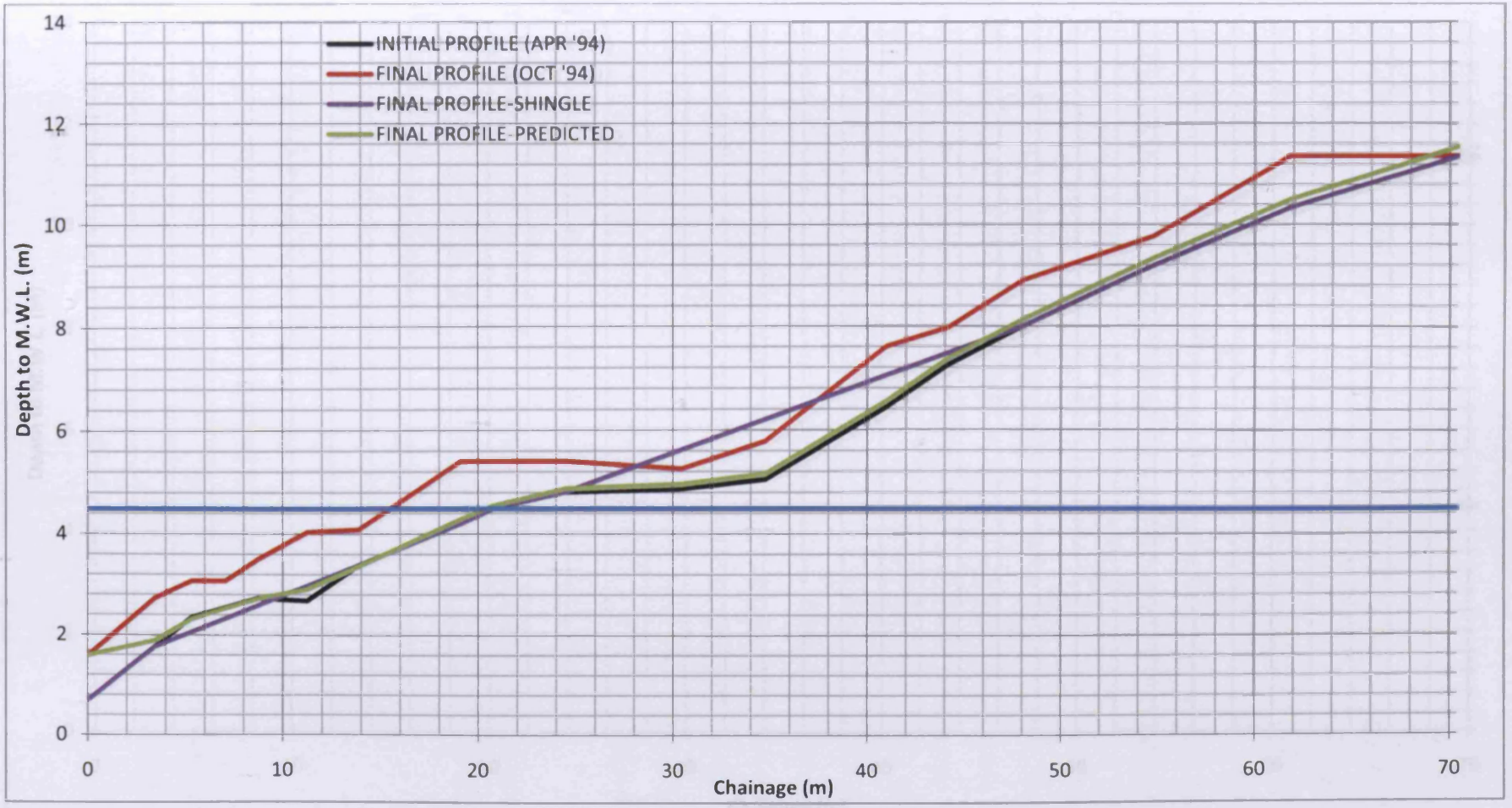

Figure 7-10 Comparison of predicted and measured beach profile for location C-North (April '94-October '94)

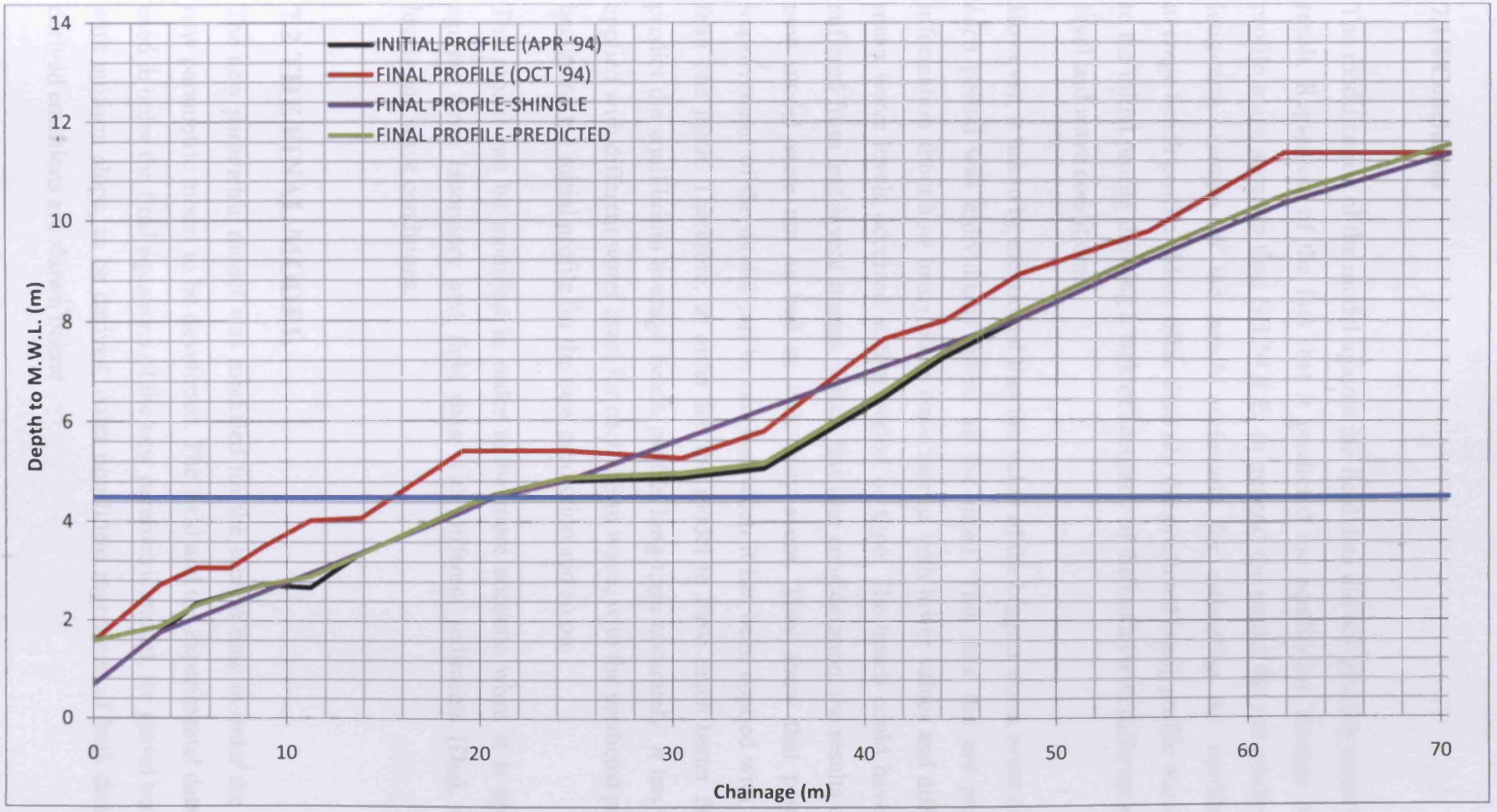

Figure 7-11 Comparison of predicted and measured beach profile for location C-South (April '94-October '94)

7.1.4 Conclusion

The modification of the model against the field data did not give the predictable result. Regardless of the fact that it predicted the equilibrium average beach profile more accurate than SHINGLE, in general the model did not predict the long-term changes of the beach accurately for estimating the equilibrium average beach profile. More often than not the predicted beach profile was close to the initial profile showing a lack of accuracy of the model with different water level and wave conditions.

However, it has to be mentioned that the value of the biggest storm event during each period was individually given as the input. This case did not provide information about how many other wave storms with lower values and different mean water levels occurred at that period of time. The beach could have also suffered from less severe storms. Taken this into consideration, the results of the new model were not as bad as they may seem. They show that potential improvement of the model can be reached when it has been applied with more than one input. Therefore, in order for the model to have much better fit and predict the equilibrium average beach profile long-term accurately, it has to be applied with different water level for each storm wave, with the predicted profile becoming the initial profile for the new prediction and so on.

The model can be modified in order to be more accurate when it is applied against more laboratory and field data with different sediments (D_{50}), water levels and wave conditions.

7.2 THE FINAL MODEL

The new parametric model was modified for the second time in order the final new parametric model to be developed. The field and the experimental data was used in order the final equations of the new parametric model, for gravel beaches with uniform slope, to be derived. After non-linear regression of both data, the derived equations are shown below

For $0 < X_i < X_b$

Eq.7-4 $$\frac{Y_p}{h_w} = a\frac{Y_i}{h_w} + b\frac{X_i}{X_b} + cm + d\frac{H_{m0}}{L_m} + e\frac{c}{K} + f\cos\theta + g\frac{L_i}{L_t} + h$$

(R^2=0.914)

where,

a, b, c, d, e, f, g and h are constants with values of

a= 0.470099039

b= 0.302512333

c= -0.771142109

d= 0.118108097

e= 0.016543001

f= -1.638214251

g= 0.0279

h= 1.628139375

For $X_b \leq X_i < X_w$

Eq.7-5 $$\frac{Y_p}{h_w} = a + b\ln(A) + c\ln(A)^2 + d\ln(A)^3 + e\ln(A)^4 + f\ln(A)^5 + g\ln(B) + h\ln(B)^2 + i\ln(B)^3 + j\ln(B)^4 + k\ln(B)^5$$

(R^2=0.962)

where,

$$A = \left(\frac{Y_i X_i}{h_w X_w}\right)$$

$$B = \left(\frac{cH_{m0}\cos\theta L_i}{KL_m mL_t}\right)$$

a, b, c, d, e, f, g, h, i, j and k are constants with values of

a= 1.030208054

b= 0.642730915

c= 0.32714456

d= 0.0915

e= 0.0108

f= 0.000417

g= 0.0321

h= 0.129519333

i= 0.0716

j= 0.0123

k= 0.00055

For $X_w \leq X_i \leq X_e$

Eq.7-6 $$\frac{Y_p}{h_w} = a\frac{Y_i}{h_w} + b\frac{X_i}{X_e} + c\frac{H_{m0}}{L_m} + d\frac{K}{gT_m} + e\frac{m}{\cos\theta} + f\frac{L_i}{L_t} + g \quad (R^2=0.969)$$

where,

a, b, c, d, e, f and g are constants with values of

a= 0.988884891

b= 0.0753

c= 1.69602196

d= 0.556155128

e= 0.0765

f= 0.047

g= -0.173136352

7.2.1 Model performance

According to Van Rijn et al. (2003), the question of how good a model is should be defined in a more quantitative manner than the usual qualitative ranking (excellent, good, reasonable or poor) that is normally applied. This section defines a number of statistical parameters that can be used to assess the quality of the performance of models. Herein, it is proposed to evaluate the performance of the models on the basis of the Brier Skill Score (BSS) (Murphy and Epstein, 1989; Peet et al., 2002).

For morphology:

Eq.7- 7 $$BSS = 1 - \left[\left\langle \left(\left| z_{b,c} - z_{b,m} \right| - \Delta z_{b,m} \right)^2 \right\rangle / \left\langle \left(z_{b,0} - z_{b,m} \right)^2 \right\rangle \right]$$

in which: z_b = bed level, $\Delta z_{b,m}$ = error of measured bed level, $z_{b,0}$ = initial bed level, index m= measured, index c = computed, <..> = averaging procedure over time series.

It is noted that the statistic parameters of bed level is corrected for the measurement errors (Van Rijn et al., 2000), being $\Delta z_{b,m}$ = 0.1 m for bed level in field conditions and 0.02 m for laboratory conditions. This latter procedure means that the difference between the computed value and the error band envelope of the measured parameter is considered.

According to Van Rijn et al. (2003), the performance of a model relative to a baseline prediction can be judged by calculating the Brier Skill Score. This skill score compares the mean square difference between the prediction and observation with the mean square difference between baseline prediction and observation. Perfect agreement gives a Brier score of 1, whereas modelling the baseline condition gives a score of 0. If the model prediction is further away from the final measured condition than the baseline prediction, the skill score is negative.

The BSS is very suitable for the prediction of bed evolution. The baseline prediction for morphodynamic modelling will usually be that the initial bed remains unaltered. In other words, the initial bathymetry is used as the baseline prediction for the final bathymetry. A limitation of the BSS is that it cannot account for the migration direction of a bar; it just evaluates whether the computed bed level (at time t) is closer to the measured bed level (at time t) than the initial bed level. If the computed bar migration is in the wrong direction, but relatively small; this may result in a higher BSS compared to the situation with bar migration in the right direction, but much too large (Van Rijn et al., 2003).

The BSS will even be negative, if the bed profile in the latter situation is further away from the measured profile than the initial profile. The limitation shown here is that position and amplitude errors are included in the BSS. Telling position errors from amplitude errors, requires a visual inspection of measured and modelled profiles or the calculation of further statistics (Murphy and Epstein, 1989; Peet et al., 2002). The BSS can be extremely sensitive to small changes when the denominator is low, in common with other non-dimensional skill scores derived from the ratio of two numbers (Van Rijn et al., 2003). The qualification of model performance is given in the following Table 7- 3. The value ranges of Table 7- 3 give a tough set of standards for models to achieve.

Table 7- 3 Qualification of the process parameters. (taken from Van Rijn et al., 2003)

Qualification	Morphology; BSS
Excellent	1.0-0.08
Good	0.8-0.6
Reasonable/fair	0.6-0.3
Poor	0.3-0.0
Bad	<0

It was found from the statistical analysis for the final parametric model prediction that the BSS for:

1. $0 < X_i < X_b$ was 0.52
2. $X_b \leq X_i < X_w$ was 0.78
3. $X_w \leq X_i \leq X_e$ was 0.22

According to the standard set here it was found that the present model could be treated as a reasonably good model to predict the bed level changes and consequently the equilibrium beach profiles.

CHAPTER 8

CONCLUIONS AND RECOMMENDATIONS FOR FUTURE RESEARCH

8.1 INTRODUCTION

In this chapter the conclusions drawn throughout the thesis are put together in order to emphasise the knowledge gained within the thesis. A summary of the main findings and proposed relationships arising from the present research as well as some recommendations for future research are presented here.

The main aim of the present research study was to investigate the hydrodynamics and the cross-shore sediment transport of gravel and mixed beaches evolved by oblique wave attack. Also, an examination of the influence of a feature (trench) in their behaviour was carried out. In order to achieve these aims a 1:1 scale 3D physical model was conducted as a central part of this thesis.

The analysis of the experimental data leads to conclusions about the behaviour of gravel and mixed beaches and their inter-relationship. The conclusions were divided into two categories (wave-induced currents and beach profile response) and summarised below.

8.1.1 Wave-induced current

The analysis of the wave-induced currents was divided into the cross-shore and long-shore currents. The gravel and mixed beach had similar cross-shore and long-shore current velocities. However, it has to be mentioned, in case of comparison between the trench and the uniform slope beach, that the trench had higher values of cross-shore current velocities for the mixed beach than the

gravel beach and lower values of long-shore current velocities for the gravel beach than the mixed beach compared to the uniform slope beach.

The analysis of the cross-shore currents in both gravel and mixed beaches focused on the behaviour of the undertow (reverse flow) and especially its behaviour near the bed. The undertow was observed in both trench and uniform slope for both types of beach. However, near the bed, the trench had higher values of undertow flow compared to the uniform slope beach and also had higher values than the mixed beach compared to the gravel beach.

The cross-shore currents near the bed for both gravel and mixed beaches showed no reduction of their values and also showed an oscillated direction, from seaward to shoreward and from shoreward to seaward, along the cross-shore section of the beach. This behaviour including the case where the value of the cross-shore current velocity increased instead of being decreased can be caused from the permeability of the beach and also the mechanism of the bed-generated turbulence. This behaviour influenced the cross-shore sediment transport at the bed and it is more noticeable at the gravel beach due to its higher permeability compared with the mixed beach.

As far as the behaviour of the long-shore currents is concerned, a long-shore flow, in a different direction to the incoming waves, was observed for both gravel and mixed beaches at the trench. This behaviour could be due to the reflected waves generated at the trench and is more likely due to the fact that the irregular beach profile of the trench with the combination of the oblique waves a wave-driven circulation current has been created leading to the this return long-shore current. At the uniform slope beach this return long-shore current was observed before the breaking point during Tests 1 and 2 where there were the highest wave conditions of the experiment. However, in the case of the return flow, that could be explained by the creation of potential rip currents at that location.

8.1.2 Beach profile response

The beach profile response to wave action and especially in storm events is very important because storm events dominate erosion.

Powell (1990) noticed that the profile of gravel beaches steepen during storms due to crest build up. Lopez de San Román Blanco (2003) observed that the bed step is formed inshore at the location of the breaking waves due to erosion where the crest is formed further onshore due to accretion. The size of the active beach profile changing depends on the storm magnitude. This behaviour of the gravel beach profile was observed during Tests 1 and 2 for both trench and uniform slope. However, the beach with the uniform slope shows high erosion below and above S.W.L. and the crest was slightly formed further onshore. On the contrary, at trench, the beach profile was slightly eroded below the S.W.L. and accretion occurred above S.W.L. formed the highest crest along the beach. The behaviour of the beach profile along the beach is explained due to the long-shore sediment transport occurred by the oblique wave action. As a result, the uniform slope eroded and the beach material moved and built-up at the trench. Similar behaviour was observed in Test 4. This behaviour was also observed during tests for the mixed beach.

The response of the initial profile of the mixed beach to the wave action, led to the built-up of material above the SWL and associated erosion below the SWL showing similarities with the behaviour of a gravel beach. However, the mixed beach developed quite differently than the gravel one did. The main morphological differences can be seen at random wave conditions. These were:

- The crest for the mixed beach was of much higher elevation compared to the gravel beach. This behaviour is explained by the fact that mixed beaches dissipate less energy through infiltration (less permeable) than a gravel beach and as a result the run-up will be higher and consequently the crest elevation.

- The extent of the onshore movement is greater than that of gravel beaches. This is in contrast with the conclusions of Lopez de San Roman Blanco (2003)
- The step formation was easier to locate for the mixed beach rather than the gravel beach.
- The erosion below the S.W.L. was larger for the mixed beach compared to the gravel beach. This is the result of the settlement of the sand and also its movement offshore.
- Irregularities in the profile (especially at Line 1) were larger for the mixed beach.
- The mobility of the mixed beach is greater in comparison with gravel beach. This is in contrast with the conclusions of Lopez de San Román Blanco (2003).

8.2 PROPOSED FORMULATIONS

The following formulations and model have been proposed, based on the research presented in this thesis for gravel and mixed beaches. The range of applicability of all the formulas is limited to the wave and beach parameters of the present experiment:

- New formula for the longshore velocity at the breaking point, so that $v_B = C\widehat{u_b}\sin\theta_b\cos\theta_b$ with the coefficient C with the following values:

  For regular wave conditions

  C=0.554 for trench in gravel beaches

  C=2.68 for mixed beaches with uniform slope

  For random wave conditions

  C=0.438 for gravel beaches with uniform slope

  C=0.212 for mixed beaches with uniform slope

  C=0.412 for trench in gravel beaches

- New formula for wave breaking index:

$$\gamma = -14.22 + 0.2242\xi + 0.7682\xi^2 - 0.1143\xi^3 - 0.6504\xi^4 + 0.1423\xi^5 - 21.3294\ln\frac{H_0}{L_0} - 12.3056\left(\ln\frac{H_0}{L_0}\right)^2 - 3.5954\left(\ln\frac{H_0}{L_0}\right)^3 - 0.5309\left(\ln\frac{H_0}{L_0}\right)^4 - 0.0315\left(\ln\frac{H_0}{L_0}\right)^5$$

- New formula for breaking height:

$$H_b = 0.1657\cos\theta_0 - 0.1885m + 1.0284H_0 + 0.00189L_0 - 0.1504$$

- New formula for breaking depth:

$$d_b = -0.0466\cos\theta_0 - 0.5693m + 1.535H_0 - 1.4114\frac{H_0}{L_0} + 0.0853$$

- New formula for undertow velocity:

For trench in gravel beaches (regular wave conditions)

$$\frac{U}{u_{GB}} = -2278.898 + \frac{6828.806}{X} + 775.664A - \frac{6748.670}{X^2} - 87.836A^2 - 1563.506\frac{A}{X} + \frac{2199.256}{X^3} + 3.224A^3 + 89.543\frac{A^2}{X} + 776.899\frac{A}{X^2} + AX$$

For gravel beaches with uniform slope (regular wave conditions)

$$\frac{U}{u_{GB}} = 0.333 + 2.815\ln(X) + 5.709\ln(X)^2 - 19.254\ln(X)^3 + 6.966\ln(X)^4 - 0.906\ln(X)^5 - 1.215A - 0.134A^2 + (4.4x10^{-3})A^3 + (2.86x10^{-4})A^4 - (2.729x10^{-7})A^5 + AX$$

For trench in mixed beaches (regular wave conditions)

$$\frac{U}{u_{GB}} = -160.807 + 19.584X - 11.530X^2 + 2.695X^3 - 0.304X^4 + 0.01268X^5 + \frac{1933.442}{A} - \frac{10066.703}{A^2} + \frac{25203.259}{A^3} - \frac{29766.799}{A^4} + \frac{13102.164}{+A^5} + AX$$

For mixed beaches with uniform slope (regular wave conditions)

$$\frac{U}{u_{GB}} = 0.135 + 1.015\ln(X) - 1.044A + 38.768\ln(X)^2 + 0.686A^2 - 11.093\ln(X)A + 1.734\ln(X)^3 - 0.13A^3 + 1.902\ln(X)A^2 - 8.27\ln(X)^2A + AX$$

For trench in gravel beaches (random wave conditions)

$$\frac{U}{u_{GB}} = -53.142 + 127.971X - 112.891X^2 + 49.620X^3 - 11.038X^4 + 0.977X^5 - 1.873A + 0.0282A^2 - 0.016A^3 - 0.00124A^4 + 0.000155A^5 + AX$$

For gravel beaches with uniform slope (random wave conditions)

$$\frac{U}{u_{GB}} = 592.981 - \frac{1632.502}{X} - 178.205A + \frac{1485.708}{X^2} + 16.502A^2 + 328.302\frac{A}{X} - \frac{445.855}{X^3} - 0.507A^3 - 15.449\frac{A^2}{X} - 150.941\frac{A}{X^2} + AX$$

For trench in mixed beaches (random wave conditions)

$$\frac{U}{u_{GB}} = 33.472 - 64.842X + 47.024X^2 - 18.41X^3 + 3.42X^4 - 0.241X^5 + 4.626A - 2.842A^2 + 0.9A^3 - 0.133A^4 + 0.0068A^5 + AX$$

For mixed beaches with uniform slope (random wave conditions)

$$\frac{U}{u_{GB}} = 0.533 + 3.881\ln(X) - 1.553A - 10.534\ln(X)^2 - 0.382A^2 + 3.182\ln(X)A - 127.824\ln(X)^3 + 0.481A^3 - 9.071\ln(X)A^2 + 57.488\ln(X)^2A + AX$$

- New formula for long-shore current velocity:

For trench in both gravel and mixed beaches (regular wave conditions)

For 0<X<1

$$\frac{V}{V_0} = B_1X^{P1} + AX$$

For X>1

$$\frac{V}{V_0} = -101705.154 + 18.494\ln(X) - 37.546\ln(X)^2 + 35.384\ln(X)^3 - 15.066\ln(X)^4 + 2.341\ln(X)^5 + \frac{665.386}{P} - \frac{1.733}{P^2} + \frac{2.24x10^{-3}}{P^3} - \frac{1.45x10^{-4}}{P^4} + \frac{3.71x10^{-10}}{P^5}$$

For gravel and mixed beaches with uniform slope (regular wave conditions)

For 0<X<1

$$\frac{V}{V_0} = 70174.738Z^3 - 169318.731Z^2 + 135695.725Z - -36105.255$$

For X>1

$$\frac{V}{V_0} = -177.316 - \frac{860.318}{X} + \frac{1.01}{P} - \frac{339.42}{X^2} - \frac{1.66x10^{-3}}{P^2} + \frac{2.196}{XP} - \frac{100.535}{X^3} + \frac{8.42x10^{-7}}{P^3} - \frac{1.43x10^{-3}}{XP^2} + \frac{0.52}{X^2P}$$

For trench in both gravel and mixed beaches (random wave conditions)

For 0<X<1

$$\frac{V}{V_0} = -5152513.157Z^7 + 25185233.7Z^6 - 52369077.84Z^5 + 60030146.93Z^4 - 40955313.23Z^3 + 16624677.17Z^2 - 3716458.238Z + 352848.033$$

For X>1

$$\frac{V}{V_0} = 820.091 - \frac{1047.845}{X} - 1169474.046P + \frac{264.861}{X^2} + 542259155.4P^2 + 1099136.529\frac{P}{X} - \frac{20.06}{X^3} - 81322770544P^3 - 284939904.4\frac{P^2}{X} - 142041.178\frac{P}{X^2}$$

For gravel and mixed beaches with uniform slope (random wave conditions)

For 0<X<1

$$\frac{V}{V_0} = 80196.904 - 1089.686X + 3431.418X^2 - 5304.364X^3 + 4022.446X^4 - 1198.603X^5 - 291109103.436P + (4.21469x10^{11})P^2 - (3.03686x10^{14})P^3 + (1.08894236469046x10^{17})P^4 - (1.55460815105334x10^{19})P^5$$

For X>1

$$\frac{V}{V_0} = -8.869 - \frac{70.557}{X} + \frac{0.109}{P} - \frac{54.862}{X^2} - \frac{3.16x10^{-4}}{P^2} + \frac{0.317}{XP} - \frac{4.202}{X^3} + \frac{2.65x10^{-7}}{P^3} - \frac{3.38x10^{-4}}{XP^2} + \frac{0.102}{X^2P}$$

- New formula of the step elevation, so that $z_{step} = C\sqrt{H_b T W_s}$, with the coefficient C taking the following values:

  For regular wave conditions

  C=0.5 for trench in both gravel and mixed beaches

  C=0.662 for trench in mixed beaches

  C=0.465 for trench in gravel beaches

  C=0.364 for both gravel and mixed beaches with uniform slope

  C=0.472 for mixed beaches with uniform slope

  C=0.341 for gravel beaches with uniform slope

  For random wave conditions

  C=0.374 for trench in both gravel and mixed beaches

  C=0.473 for trench in mixed beaches

  C=0.299 for trench in gravel beaches

  C=0.362 for both gravel and mixed beaches with uniform slope

  C=0.412 for mixed beaches with uniform slope

  C=0.322 for gravel beaches with uniform slope

- New formula of the berm elevation, so that $B_h = C(H_b)^{\frac{5}{8}}(gT^2)^{\frac{3}{8}}$, with the coefficient C taking the following values:

  For regular wave conditions

  C=0.12 for trench in both gravel and mixed beaches

  C=0.658 for trench in mixed beaches

  C=0.118 for trench in gravel beaches

  C=0.08 for both gravel and mixed beaches with uniform slope

  C=0.089 for mixed beaches with uniform slope

  C=0.078 for gravel beaches with uniform slope

  For random wave conditions

  C=0.107 for trench in both gravel and mixed beaches

  C=0.121 for trench in mixed beaches

C=0.093 for trench in gravel beaches

C=0.144 for both gravel and mixed beaches with uniform slope

C=0.157 for mixed beaches with uniform slope

C=0.13 for gravel beaches with uniform slope

- New empirical parametric model for predicting the equilibrium beach profile of both gravel and mixed beaches (uniform slope and trench). It is described in Chapters 6 and 7.

8.3 RECOMMENDATIONS FOR FUTURE RESEARCH

The present research work was a step forward in understanding the hydrodynamics and the cross-shore sediment transport of gravel and mixed beaches evolved by oblique wave attack and their interaction. However, there is a need for more research work in the future. The recommendations for future research, which are generally correlated in further laboratory experiments, are listed below:

- During the present experiment the mixed beach was composed of 40% sand and 60% gravel. The mixed beach with high percentage of sand can behave more like a sand beach and it can behave more like a gravel beach with a high percentage of gravel. An investigation of a wide range of sediment mixtures to determine the influence of the ratio of each component to the whole sediment mix is needed, as well as to determine from which ratio they behave like gravel beaches, from which ratio onwards they behave like sand beaches and what happens in between this situations.
- An investigation into the different sediment sizes of gravel and of sand will give more information about the behaviour of gravel and mixed beaches for varying porosity, permeability and infiltration /exfiltration.

- The profile response of both gravel and mixed beaches has to be examined by changing the factor of influence. Therefore, investigation into the effect of different water levels (tides), various wave angles and various wave heights and periods is needed. The change of water level and the wave heights periods can show the influence of groundwater and different type of wave breaking to the sediment transport of the beach.
- At the present experiment the feature of the trench was investigated. However, this investigation was based on a trench with the same width, height, length and orientation. The influence on sediment transport and furthermore to the beach profile response of various sizes and orientations of the trench in gravel and mixed beach can then be investigated.
- The combination of all the above recommendations in one extensive laboratory experiment will constitute a vast improvement of the knowledge and understanding of how the gravel and mixed beaches behave. The results from this experiment will be used in order to improve the accuracy of the current formulae and also will give the opportunity to derive and develop new ones.

REFERENCES

Ahrens, J.P., 2003. Simple equations to calculate fall velocity and sediment scale parameter. *Journal of Waterway, Port, Coastal, Ocean Eng.*, Vol.129, No.3, pp.146-150.

Babtie Group Ltd., 1997. *Chesil Beach Study (Final Report)*. June 1997, Vol.1, JOB No. BWA 022063.

Baird, A. J., Mason, T., and Horn, D.P., 1996. Mechanisms of beach ground water and swash interaction. In: *Proceedings of the 25th International Conference on Coastal Engineering*, ASCE, pp. 4120-4133.

Baird, A. J., Mason, T., Horn, D.P., and Baldock, T.E., 1997. Monitoring and modelling groundwater behaviour in sandy beaches as a basis for improved models of swash zone sediment transport. *Coastal Dynamics '97*, ASCE, pp. 774-783.

Balsillie, J. H., and Dabous, A. A., 2003. A new type of sieve shaker: the Meinzer II, a comparative study with Rotap technology. *Florida Geological Survey Open File Report No. 87*, 93p.

Basco, D.R., 1985. A qualitative description of wave breaking. *Journal of Waterway, Port, Coastal and Ocean Engineering*, Vol.111, No.2, ASCE, pp.171-188.

Batalla, R.J. and Martin-Vide, J.P., 2001. Threshold for particle entrainment in a poorly sorted sandy gravel-bed river. *Catena*, Vol. 44, pp: 223–243.

Battjes, J.A., 1974. Surf-Similarity. In: *Proceedings of the 14th Coastal Engineering Conference*, ASCE, pp.466-480.

Bluck, B.J., 1967. Sedimentation of beach gravels: examples from South Wales. *Journal of Sedimentary Petrology*, Vol. 37, No.1, pp.128-156.

Bluck, B.J., 1999. Clast assembling, bed-forms and structure in gravel beaches. *Transactions of the Royal Society of Edinburgh: Earth Sciences*, Vol. 89, pp. 291-323.

Bodge, K.R., 1992. Representing equilibrium beach profiles with an exponential expression. *Journal of Coastal Research*, Vol.8, No.1, pp. 47-55.

Briand, M.-H., G., and Kamphuis J.W., 1993. Waves and currents on natural beaches: a quasi 3D numerical model. *Journal of Coastal Engineering*, Vol. 20, pp. 101-134.

Bruun, P., 1954. Coastal erosion and development of beach profiles. *U.S. Army Beach Erosion Board Technical Memorandum No.44*, Beach Erosion Board, U.S. Army Corps of Engineers, Washington, DC.

Bruun, P., 1962. Sea-level rise as a cause of shore erosion. *Journal of Waterways and Harbor Division*, Vol.88, ASCE, pp.117-130.

Buffin-Bélanger, T., Roy, A.G., and Kirkbride, A.D., 2000. On large-scale flow structures in a gravel-bed river. *Geomorphology*, 32 (3-4), pp. 417-435.

Bujalesky, G.G., and Gonzale-Bonorino, G., 1991. Gravel spit stabilized by unusual high-energy wave climate in Bay Side, Tierra del Fuego. In: *Proceedings of Coastal Sediments '91*, ASCE, pp. 960-974.

Caldwell, N.E. and Williams, A.T., 1986. Spatial and seasonal pebble beach profile characteristics. *Geological Journal*, Vol. 21, pp. 127-138.

Carr, A.P., 1969. Size grading along a pebble beach: Chesil Beach, England. *Journal of Sedimentary Petrology*, Vol.39, No.1, pp. 297-311.

Carr, A.P., 1971. Experiments on longshore transport and sorting of pebbles: Chesil Beach, England. *Journal of Sedimentary Petrology*, Vo.41, No.4, pp. 1084-1104.

Carter, R.W.G. and Orford, J.D., 1981. Overwash processes along a gravel beach in southeast Ireland. *Earth Surface Processes and Landforms*, Vol. 6, pp. 413-426.

Carter, R.W.G. and Orford, J.D., 1984. Coarse clastic barrier beaches: a discussion of the distinctive dynamic and morphosedimentary characteristics. *Marine Geology*, Vol. 60, pp. 377-389.

Carter, R.W.G., Orford J.D., Forbes D.L., and Taylor R.B., 1990a. Morpho-sedimentary development of drumlin-frank barriers with rapidly rising sea level, Story Head, Nova Scotia. *Sedimentary Geology*, Vol. 69, pp. 117-138.

Chesnutt, C.B., 1975. Laboratory effects in coastal movable bed models. In: *Proc Sym on Modelling Techniques*, ASCE, San Francisco, pp.945-992.

Chien, N., and Wan, Z., 1999. *Mechanics of Sediment Transport.* ASCE press, 899p.

Chiu, T.Y., and Dean, R.G., 1984, .Methodology on coastal construction control line establishment. *Tech. and Design Memorandum 84-6*, Beaches and Shores Resource Center, Florida State University, Tallahassee, FL.

Chiu, T.Y., and Dean, R.G., 1986. Additional comparisons between computed and measured erosion by hurricanes. *Tech. Report*, Beaches and Shores Resource Center, Florida State University, Tallahassee, FL.

Ciavola, P., 1997. Coastal dynamics and impact of coastal protection works at Spurn Head Spit (UK). *Catena*, Vol.30, No.4, pp. 369-389.

CIRIA, 1996. Beach Management Manual. *CIRIA Report 153*, Construction Industry Research and Information Association, ISBN: 0-86017-438-7,448p.

Coates, T.T. and Damgaard, J.S., 1999. Towards improved management of mixed grain beaches. In: *Proceeding of HYDRALAB workshop in Hannover*, ISBN 3-00-004942-8; pp. 69-73.

Coastal Engineering Manual, 2003. *Surf zone hydrodynamics*. EM 1110-2-100, Part II, Chapter 4, US Army Corps. of Engineers, 40p.

Cokelet, E.D., 1977. Steep gravity waves in water of arbitrary uniform depth. *Philos.Trans.R.Soc.Lond*, Ser. A:Math.Phys.Sci., pp.183-230.

Collins, I.A., 1970. Probability of breaking wave characteristics. In: *Proc.12th Conf.Coastal Engr.*, ASCE, pp.199-414.

Dally, W. R., and Dean, R. G. 1984. Suspended Sediment Transport and Beach Profile Evolution. *Journal of Waterway, Port, Coastal, and Ocean Engineering*, Vol 110, No. 1, pp 15-33.

Dally, W.R., Dean, R.G., and Dalrymple, R.G., 1985. Wave height variation across beaches of arbitrary profile. *Journal of Geophysical Research*, Vo.90, No. C6, pp. 11917-11927.

Dalrymple, R.A. and Thompson, W.W., 1976. Study of equilibrium beach profile. In: *Proc 15th Conf on Coastal Eng*, Honolulu, Hawaii, ASCE, pp. 1277-1296.

Danish Hydraulic Institute (DHI), July 1999. *User Manual, DHI Hydraulic Power Pack Type 302/45, DHI Servo Actuator Type 63/40-710.* Laboratory Technology, Germany, 9p.

Danish Hydraulic Institute (DHI) quotation to the Fanzius-Insitut for the supply of the DHI Basin Wave Generating System for generation of long-crested (2D) irregular waves, 24 February 1998.

Davidson, M.A., Bird, P.A.D., Bullock, G.N., and Huntley, D.A., 1994. Wave reflection: field measurements, analysis and theoretical developments. *Coastal Dynamics '94*, ASCE, pp. 642-655.

Dean, R.G., 1977. Equilibrium beach profiles: U.S. Atlantic and Gulf Coasts. *Department of Civil Engineering, Ocean Engineering Report No. 12*, University of Delaware, Newark.

Dean, R.G., 1987. Coastal sediment processes: Toward engineering solutions. In: *Proceedings, Specialty Conference on Coastal Sediments '87*, ASCE, pp. 1-24.

Dean, R.G., 1991, Equilibrium beach profiles: Characteristics and applications. *Journal of Coastal Research*, Vol.7, No.1, pp. 53-84.

Dean, R.G., 1994. Stream function representation of nonlinear ocean waves. *J.Geophysical Research*, Vol.73, pp. 4561-4572.

Dean, R.G. and Maurmeyer, E.M., 1983. Models for beach profile response. *CRC Handbook on beach erosion and coastal processes, Chapter 7*, P.D. Komar, ed., pp. 151-166.

Dean, R.G., and Dalrymple, R.A., 2002. *Coastal Processes with Engineering Applications.* Cambridge, 475p.

Dean, R.G., Kriebel, D. and Walton, T., 2002. *Chapter III-3: Cross-shore sediment transport processes,* EM 1110-2-1100, Coastal Engineering Research Center, U.S. Army Engineer Waterways Experiment Station, Vicksburg, MS.

DEFRA (Department for Environment, Food and Rural Affairs), 2003. *Project title: Development of predictive tools and design guidance for mixed beaches – Stage 2, Final Project Report,* CSG 15, FD1901, 17p.

Deigaard, R., Justesen, P., and Fredsoe, J., 1991. Modelling of undertow by a one-equation turbulence model. *Coastal Engineering,* Vol.15, pp. 431-458.

Dyhr-Nielsen, M., and Sorensen, T. 1970. Some Sand Transport Phenomena on Coasts with Bars. In: *Proceedings of the 12th Coastal Engineering Conference,* American Society of Civil Engineers, pp. 1993- 2004.

Edelman, T., 1968. Dune erosion during storm conditions, In: *Proc. 11th Int. Conf. on Coastal Eng.*, London, Ch. 46, pp. 719-722.

Edelman, T., 1972. Dune erosion during storm conditions. In: *Proc. 13th Int. Conf. on Coastal Eng.*, Vancouver, vol.2, pp. 1305-1311.

Engeln-Mullges, G., and Reutter, F., 1986. *Formelsammlung zur Numerischen Mathematik mit Standard-FORTRAN77-Programmen.* B.I.-Wissenschaftsverlag, Mannheim, Wien, Zurich, pp. 1-533.

Engelund, 1981. F. Engelund, A simple theory of weak hydraulic jumps. In: *Progress Report No. 54*, Institute of Hydrodynamics and Hydraulic Engineering, ISVA, Technical University Denmark (1981), pp. 29–32.

Fenton, J.D., and Abbott, J.E., 1977. Initial movement of grains on a streambed: the effect of relative protrusion. *Proceedings of the Royal Society of London*, A 352, pp. 523-531.

Fenton, J.D., and McKee, W.D., 1990. On calculating the lengths of water waves. *Coastal Engineering*, vol.14, pp. 499-513.

Finkelstein, K., 1982. Morphological variations and sediment transport in crenulate-bay beaches, Kodiak Island, Alaska. *Marine Geology*, Vol.47, pp. 261-281.

Folk, R.L., Ward, W.C., 1957. Brazos River bar: a study on the significance of grain size parameters. *Journal of Sedimentary Petrology*, vol. 27, pp. 3–26.

Forbes, D.L. Orford, J.D. Carter, R.W.G., Shaw, J. and Jennings, S.C., 1995. Morphodynamic evolution, self-organisation, and instability of coarse clastic barriers on paraglacial coasts. *Marine Geology*, Vol. 126, pp. 63-85.

FRANZIUS-INSTITUT (Universitat Hannover) fur wasserbau und kunsteningenieurwesen, 1993 (February). *Hydraulic Laboratory Software Vol.V, User's Manual (WAVEPC)*. Contractor: Finanzbauamt Munchen II, pp. 1-60.

Fredsoe, J., and Deigaard, R., 1995. *Mechanics of Coastal Sediment Transport*. 3rd edition, Advanced Series on Ocean Engineering, Vol.3, World Scientific, 369p.

Galvin, C.J., and Eagleson, P.S., 1965, Experimental study of longshore currents on a plane beach, *Tech. Mem. 10*, U.S. Army Coastal Eng. Res. Center.

Galvin, C.J., 1968. Breaker Type Classification on Three Laboratory Beaches. *Journal of Geophysical Research*, Vol.73, No.12, pp. 3651-3659.

Galvin, C.J., 1969. Breaker travel and choice of design wave height. *Journal of Waterway Harbors Div.*, ASCE, 95, WW2, pp. 175-200.

Goda, Y., 1964. Wave forces on a vertical circular cylinder: Experiments and a proposed method of wave force computation. *Report of the Port and Harbor Research Institute*, Ministry of Transportation, No.8, pp. 74.

Goda, Y., 1970. A synthesis of breaker indices. *Trans. JSCE*, 2, pp. 227-230.

Goda, Y., 1974. New wave pressure formula for composite breakwater. In: *Proc. 14th Coastal Eng. Conf.*, ASCE, pp. 1702-1720.

Goda, Y., 1983. A unified nonlinearity parameter of water waves. *Report of Port Harbour Res. Inst.*, 22 (3), pp. 3-30.

Goda, Y., 1985. *Random Seas and Design of Maritime Structures*. University of Tokyo Press., ISBN 0-86008-369-1, Tokyo, 464p.

Gordon, N.D., Mac Mahon, T.A., Finlayson, B.L., 1992. *Stream Hydrology, An Introduction for Ecologists*. Wiley, Chichester, 526p.

Gourlay, M.R., 1980. Beaches: Profiles, Processes and Permeability. *Res Report No. CE14*, Dept of Civil Eng Univ of Queensland, Australia.

Grasmeijer, B., 2002. Process-based cross-shore modelling of barred beaches. *Netherlands Geographical Studies 302*, The Royal Dutch Geographical Society/Faculty of Geographical Sciences, Utrecht University, 260p.

Grasmeijer, B.T., and Ruessink, B.G., 2003. Modelling of waves and currents in the nearshore parametric vs. Probabilistic approach. *Journal of Coastal Engineering*, vol.49, pp. 185-207.

Greenwood, B. and Sherman, D. J., 1986. Longshore current profiles and lateral mixing across the surf zone of a barred nearshore. *Coastal Engineering*, 10, pp. 149-167.

Hallermeier, R.J., 1981a. Fall velocity of beach sands. *Coastal Engineering Technical Note, CETN-II-4*, Coastal Engineering Research Center, U.S. Army Engineer Waterways Experiment Station, Vicksburg, MS.

Hansen, J. B., and Svendsen, I. A. 1984. A Theoretical and Experimental Study of Undertow. In: *Proceedings of the 19th Coastal Engineering Conference*, American Society of Civil Engineers, pp. 2246-2262.

Hayden, B., Felder, W., Fisher, J., Resio, D., Vincent, L. and Dolan, R., 1975. Systematic variations in inshore bathymetry. *Department of Environmental Science, Technical Report 10*, University of Virginia, Charlottesville, VA.

Hill, P.R., 1990. Coastal geology of the King Point Area, Yukon Territory, Canada. *Marine Geology*, Vol. 91, pp. 93-111.

Horn, D.P., 1992. A numerical model for shore-normal sediment size variation on a macrotidal beach. *Earth Surface Processes and Landforms*, Vol. 17, pp. 755-773.

HR Wallingford, 1999. *Collaborative Shingle Beach Transport Project: Technical Report TR 29*, HR Wallingford Ltd.

Hughes, S.A., 1994. *Physical models and laboratory techniques in coastal engineering.* World Scientific, River Edge, NJ, 550p.

Hughes, S.A. and Chiu, T.S., 1978. The variations in beach profiles when approximated by a theoretical curve. *Department of Coastal and Oceanographic Engineering, Report No. 78/010.*

Hughes, S.A. and Chiu, T.S., 1981. Beach and dune erosion during severe storms. *Coastal and Oceanographic Engrg. Dept, Univ. of Florida, Report No UFL/COEL/TR/043.*

Inman, D.L. and Bagnold, R.A., 1966. "Nearshore sediment processes", in Hill M.N. (ed.) "*The Sea: Ideas and Observations, Vol. 3*", 2nd Edition, Interscience, New York, pp. 532.

Inman, D.L., Elwany, M.H.S., Jenkins, S.A., 1993. Shorerise and bar–berm profiles on ocean beaches. *J. Geophys. Res.*, 98 (C10), pp:11,181– 18,199.

Isla, F.I., 1993. Overpassing and armouring phenomena on gravel beaches. *Marine Geology*, Vol. 110, pp. 369-376.

Isla, F.I. and Bujalesky, G.G., 1993. Saltation on beach gravels, Tierra del Fuego, Argentina. *Marine Geology*, Vol. 115, pp. 263-270.

Isobe, M., 1985. Calculation and application of first-order cnodial wave theory. *Coastal Engineering Journal*, Vol.9, pp. 309-325.

Isobe, M., 1987. A parabolic equation model for transformation of irregular waves due to refraction, diffraction and breaking. *Coastal Engineering in Japan*, JSCE, Vol. 30, pp. 33-47.

Iversen, H.W., 1952. Laboratory study of breakers, *Symposium on Gravity Waves*, Circular 52, US Bureau of Standards, pp. 9-32.

Kaminsky, G.M., and Kraus, C.N., 1993. Evaluation of depth-limited wave breaking criteria. In: *Proc. of the 2nd International Symposium (Ocean '93)*, W.P.C.O.D., ASCE, pp. 180-193.

Karambas, T.V., and Koutitas, C., 2002. Surf and swash zone morphology evolution induced by nonlinear waves. *Journal of Waterway Port, Coastal and Ocean Engineering*, Vol.128, No.3, ASCE, pp. 102-113.

Kemp, P.H.,1963. A field study of wave action on natural beaches. In: *10th IAHR Congress*, London.

Keulegan, G.H. and Krumbein, W.C., 1949. Stable configuration of beach slope in a shallow sea and its bearing on geological processes. *EOS Transactions, American Geological Union*, Vol. 30, No.6, pp. 855-861.

King, C.A.M., 1972. *Beaches and Coasts*. Edward Arnold Ltd, London, 570p.

Kirk, R.M., 1969. Beach erosion and coastal development in the Canterbury Bight. *New Zealand Geographer*, Vol. 25, pp. 23-35.

Kirk, R.M., 1975. Aspects of surf and runup processes on mixed sand and gravel beaches. *Geogr. Ann.*, 57A, pp. 117–133.

Kirk, R.M., 1980. Mixed sand and gravel beaches: morphology, processes and sediments. *Progress in Physical Geography*, Vol. 4, pp. 189-210.

Kobayashi, N., 1987. Analytical solution for dune erosion by storms. *Journal of Waterway Port, Coastal and Ocean Engineering*, Vol.113, No.4, ASCE, pp. 401-418.

Kobayashi, N., and Karjadi, E.A., 2001. Obliquely incident wave reflection and runup on steep rough slope. *Journal of Coastal Research*, Vol.17, No.4, West Palm Beach (Florida), pp. 919-930.

Kobayashi, N., Karjadi, E.A., and Johnson, B.D., 1997. Dispersion effects on longshore currents in surf zones. *Journal of Waterway Port, Coastal and Ocean Engineering*, Vol.123, No.5, ASCE, pp. 240-248.

Komar, P.D., 1976. *Beach Processes and Sedimentation*. Prentice-Hall, Englewood Cliffs, NJ, 429p.

Komar, P.D., 1998. *Beach Processes and Sedimentation*. Prentice Hall, Upper Saddle River, N.J., 543p.

Komar, P.D., and Gaughan, M.K., 1973. Airy wave theory and breaker height prediction. In: *Proceedings of the 13th Coastal Engineering Conference*, ASCE, pp. 405-418.

Komar, P.D. and Li, Z., 1986. Pivoting analyses of the selective entrainment of sediments by shape and size with application to gravel threshold. *Sedimentology*, Vol. 33, pp. 425-436.

Komar, P.D. and McDougal, W.G., 1994. The analysis of exponential beach profiles. *Journal of Coastal Research*, Vol. 10, pp. 59-69.

Kriebel, D.L., 1982. *Beach and dune response to hurricanes*. M.Sc. Thesis, Department of Civil Engineering, University of Delware, Newark. DE.

Kriebel, D.L., 1986. Verification study of a dune erosion model. *Shore and Beach*, vol.54, no.3, pp. 13-20.

Kriebel, D.L., and Dean, R.G., 1985. Numerical simulation of time-dependent beach and dune erosion. *Coastal Engineering*, vol. 9, pp. 221-245.

Kriebel, D. L. and Dean, R. G., 1993. Convolution method for time-dependent beach-profile response. *Journal of Waterway, Port, Coastal and Ocean Engineering*, Vol. 119, No.2, ASCE Press, pp. 204-226.

Kriebel, D.L., Kraus, N.C. and Larson, M., 1991. Engineering methods for predicting beach profile response. In: *Proceedings of Conference on Coastal Sediments '91*, American Society of Civil Engineers, pp. 557-571.

Krumbein, W.C., 1964. Some remarks on the phi-notation. *Journal of Sedimentary Petrology*, vol. 34, No. 1/Mar., pp. 195–197.

Krumbein, W.C., Monk, G.D., 1943. Permeability as a function of the size parameters of unconsolidated sand, *Transactions of the American Institute of Mining and Metallurgical Engineers*, 151, pp. 153–163.

Kuhnle, R.A., 1994. Incipient motion of sand-gravel sediment mixtures. *Journal of Hydraulic Engineering*, Vol. 119, pp. 1400-1415.

Kulkarni, C.D., Levoy, F., Monfort, O., Miles, J., 2004. Morphological variations of a mixed sediment beachface (Teignmouth, UK). *Continental Shelf Research*, 24, pp. 1203–1218.

Kuriyama, Y., 1996. Models of wave height and fraction of breaking waves on a barred beach. In: *Proc. 25th Coastal Eng. Conf.*, ASCE, pp. 247-260.

Kuriyama, Y., and Ozaki, Y., 1996. Wave height and fraction of breaking waves on a bar-trough beach – field measurements at HORS and modelling. *Report Port Harbour Res. Inst.*, 35 (1), pp. 1-38.

Kuriyama, Y., and Nakatsukasa, T., 2000. A one-dimensional model for undertow and longshore current on a barred beach. *Journal of Coastal Engineering*, Vol.40, pp. 39-58.

Lara, J.L., Losada, I.J., Cowen, E.A., 2002. Large-scale turbulence structures over an immobile gravel-bed inside the surf zone. In: *Proceedings of the 28th International Conference on Coastal Engineering*, ICCE, ed. Smith J.M., World Scientific, London, pp. 1050–1061.

Larson, M., 1988. Quantification of beach profile change. *Report No.1008*, Department of Water Resources and Engineering, University of Lund, Lund, Sweden.

Larson, M. and Kraus, N.C., 1989. SBEACH: Numerical model for simulation storm-induced beach change; Report 1: Empirical foundation and model development. *Technical Report CERC-89-9*, U.S. Army Engineer Waterways Experiment Station, Vicksburg, MS.

Larson, M., Kraus, N.C. and Byrnes, M.R., 1989. SBEACH: Numerical model for simulating storm-induced beach change. Report 2: Numerical formulation and model tests. *Tech. Report CERC 89-9*, Coastal Engineering Research Center, U.S. Army Waterway Experiment Station, Vicksburg, MS.

Larson, M., Kraus, N.C. and Byrnes, M.R., 1996. SBEACH: Numerical model for simulating storm-induced beach change. Report 4: Cross-shore transport under random waves and model validation with SUPERTANK and field data. *Tech. Report CERC 89-9*, Coastal Engineering Research Center, U.S. Army Waterway Experiment Station, Vicksburg, MS.

Larson, M., Kraus, N.C., Wise, R.A., 1999. Equilibrium beach profiles under breaking and non-breaking waves. *Coast. Eng.*, Vol.36, pp. 59– 85.

Lawrence, J., Karunarathna, H., Chadwick, A.J., Fleming, C.A., 2003. Cross-shore sediment transport on mixed coarse grain sized beaches: modeling and measurements. In: *Proceedings of the 28th International Conference on Coastal Engineering*, ICCE, ed. Smith J.M., World Scientific, London, pp. 2565-2577.

Le roux, J.P., 2007. A simple method to determine breaker height and depth for different deepwater wave height/length ratios and sea floor slopes. *Journal of Coastal Engineering*, Vol.54, pp. 271-277.

Lee, C.-E, Kim, M.-H., and Edge, B.L., 1996. Numerical model for on-offshore sediment transport with moving boundaries. *Journal of Waterway Port, Coastal and Ocean Engineering*, Vol.122, No.2, ASCE, pp. 84-92.

Lee, C.-E, Kim, M.-H., and Edge, B.L., 1999. Generation of nearshore bars by multi-domain hybrid numerical model. *Journal of Coastal Research*, Vol.15, No.4, Royal Palm Beach (Florida), pp. 892-90.

Leont'yev, I.O., 1996. Numerical modelling of beach erosion during storm event. *Coastal Engineering*, Vol. 29, pp. 187-200.

Leont'yev, I.O., 1999. Modelling of morphological changes due to coastal structures. *Coastal Engineering*, Vol. 38, pp. 143-166.

Leont'yev, I.O., 2003. Modeling the Morphological Response in a Coastal Zone for Different Temporal Scales. In: *Advances in Coastal Modeling*, by V.C. Lakhan, Elsevier Science Ltd, pp. 299-236.

Liu, P.L.F., 1994. *Advances in coastal and ocean engineering*. Vol.1, World Scientific, River Edge, NJ, 274p.

Lohrmann, A., Cabrera, R. and Klaus, N., 1994. Acoustic-Doppler Velocimeter (ADV) for Laboratory use. In: *Proc. Of Fundamentals and Advancements in Hydraulics Measurements and Experimentation,* Buffalo, New York.

Longuet-Higgins, M.S., 1970a. Longshore Currents by Obliquely Incident Sea Waves,1. *Journal of Geophysical Research*, Vol. 75, No. 33, pp. 6778-6789.

Longuet-Higgins, M.S., 1970b. Longshore Currents by Obliquely Incident Sea Waves,2. *Journal of Geophysical Research*, Vol. 75, No. 33, pp. 6790-6801.

Longuet-Higgins, M.S., 1972. Recent Progress in the Study of Longshore Currents. In: *Waves on Beaches*, ed. R. E. Meyer, New York: Academic Press, pp. 203-248.

Lopez de San Roman-Blanco, B., Damgaard, J.S., Coates, and T.T., Holmes, P., 2000. Management of Mixed Sediment Beaches. In: *Proceedings of the 1st International Conference on Soft Shore Protection*, University of Patras, Greece.

Lopez de San Roman–Blanco, B. and Holmes, P., 2002. Further insight on behaviour of mixed sand and gravel beaches – large scale experiments on profile development. *Coastal Engineering 2002*, J. McKee Smith (ed.), World Scientific, pp. 2651-2663.

Lopez de San Roman-Blanco, B., Coates T.T., and Whitehouse, R.J.S., 2003. Development of Predictive Tools and Design Guidance for Mixed Beaches – Stage 2 (Final Report). *Report SR 628*, HR Wallingford, pp. 310.

Lopez de San Roman-Blanco, B., Coates, T.T., Holmes, P., Chadwick, A.J., Bradbury A., Baldock, T.E., Pedrono-Acuna, A., Lawrence, J., and Grune, J., 2006. Large scale experiments on gravel and mixed beaches: Experimental procedure, data documentation and initial results. *Journal of Coastal Engineering*, vol.53, pp. 349-362.

Madsen, P.A., Sørensen, O.R., and Schaffer, H.A., 1997. Surf zone dynamics simulated by a Boussinesq type model: Part I. Model description and crossshore motion of regular waves. *Coastal Engineering*, Vol.32, pp. 255– 287.

Mason, T., 1997. *Hydrodynamics and Sediment Transport on a Macro-Tidal, Mixed (Sand and Shingle) Beach*, Unpubl. PhD thesis, Department of Oceanography, University of Southampton, 256p.

Mason, T., Voulgaris, G., Simmonds, D.J., and Collins, M.B.,1997. Hydrodynamics and sediment transport on composite (mixed sand/shingle) beaches: a comparison. *Coastal Dynamics '97*, ASCE, pp. 48-57.

Mason, T., and Coates, T.T., 2001. Sediment Transport Processes on Mixed Beaches: a Review for Shoreline Management. *Journal of Coastal Research*, Vol. 17, No. 3, pp. 645-657.

Masselink, G and Li, L., 2001. The role of swash infiltration in determining beachface gradient: a numerical study. *Marine Geology*, Vol. 176, pp. 139-156.

Matthews, E.R., 1983. Measurements of beach pebble attrition in Palliser Bay, southern North Island, New Zealand. *Sedimentology*, Vol.30, pp. 787-799.

McLean, R.F. and Kirk, R.M., 1969. Relationships between grain size, size-sorting, and foreshore slope on mixed sand-shingle beaches. *New Zealand Journal of Geology and Geophysics*, Vol. 12, pp. 138-155.

McManus, D.A., 1963. A criticism of certain usage of the phi notation. *Journal of Sedimentary Petrology*, Vol. 33, pp. 670-674.

Miche, R., 1944. Mouvements ondulatoires des mers en profundeur constante on decroisante. *Annales des Ponts et Chaussees*, Chap.114, pp. 25-78, 131-164, 270-292, 369-406.

Mitsuyasu, H., 1962. Experimental study on wave force against a wall. *Report of the Transportation Technical Research Institute*, No.47, p. 39 (in Japanese).

Moore, B.D., 1982. *Beach profile evolution in response to changes to water level and water height*. M.S. thesis, Department of Civil Engineering, University of Delaware, Newark.

Morfett, J.C., 1990. A "virtual power" function for estimating the alongshore transport of sediment by waves. *Coastal Engineering*, Vol. 14, No. 5, pp. 439-456.

Moutzouris, I.C., 1991. Beach Profiles vs. Cross-shore Distribution of Sediment Grain Sizes. *Coastal Sediments '91*, Vol.1, ASCE, pp. 860-874.

Munk, W.H., 1949. The solitary wave theory and its application to surf problems. *Ann. New York Acad. Sci.*, Vol. 51, pp. 376-423.

Murphy, A.H., and Epstein, E.S., 1989. Skill scores and correlation coefficients in model verification. Monthly Weather Review 117, pp. 572– 581.

Naden, P., 1987. An erosion criterion for gravel-bed rivers. *Earth Surface Processes and Landforms*, Vol. 12, pp. 83-93.

Nicholson, J., 1968. A laboratory study of the relationship between waves and beach profiles. *Inst Engrs Aust Conf on Hydraulics and Fluid Mechanics*.

Nolan, T.J., Kirk R.M., and Shulmeister, J., 1999. Beach cusp morphology on sand and mixed sand and gravel beaches, South Island, New Zealand. *Marine Geology*, 157, pp. 185-198.

NORTEK AS, 1997. *ADV Operation Manual* .Norway, pp. 5 & 18.

Nwogu, O., 1993. Alternative form of Boussinesq equations for nearshore propagation. *Journal of Waterway, Port, Coastal and Ocean Engineering* ,119 (6), pp. 618– 638.

Orford, J.D., 1975. Discrimination of particle zonation on a pebble beach. *Sedimentology*, Vol. 22, pp. 441-463.

Özkan-Haller, H.T., and Brundidge, S., 2007. Equilibrium beach profile concept for Delaware Beaches. *Journal of Waterway, Port, Coastal and Ocean Engineering* ,133 (2), pp. 147– 160.

Parker, G. and Klingeman, P.C., 1982. On why gravel bed streams are paved. *Water Resources Research*, Vol. 18, pp. 1409-1423.

Pedrono-Acuna, A., Simmonds, D.J., Otta, A.K., and Chadwick, A.J., 2006. On the cross-shore profile change of gravel beaches. *Journal of Coastal Engineering*, Vol. 53, pp. 335-347.

Peet, A.H., Sutherland, and J., Soulsby, R.L., 2002. Skill Assessment in Coastal Models. HR Wallingford.

Petrov, V.A., 1989. The differentiation of material on gravel beaches. *Oceanology*, Vol.29, pp. 208-212.

Pontee, N.I., 1996. *The Morphodynamics and Sedimentary Architecture of Mixed Sand and Gravel Beaches*. Suffolk, UK, Unpubl. PhD thesis, Department of Sedimentology, University of Reading.

Powell, K.A., 1986. *The hydraulic behaviour of shingle beaches under regular waves of normal incidence*. PhD Thesis, University of Southampton.

Powell, K.A., 1990. Predicting short term profile response for shingle beaches. *Report SR 219*, Hydraulics Research, Wallingford.

Powell, K.A., 1993. Dissimilar sediments; model tests of replenished beaces using widely graded sediments. *Report SR 350*, HR Wallingford

Pruszak, Z., Rozynski, G., Zeidler, R.B., 1997. Statistical properties of multiple bars. *Coast. Eng.*, Vol. 31, pp. 263–280.

Quick, M.C., 1991. Onshore-offshore sediment transport on beaches. *Journal of Coastal Engineering*, Vol.15, pp.313-332.

Quick, M.C., and Dyksterhuis, P., 1994. Cross-shore transport for beaches of mixed sand and gravel. In: *International Symposium: Waves-Physical and Numerical Modelling*, CSCE, pp. 1443-1452.

Rattanapitikon, W., 1995. *Cross-Shore Sediment Transport and Beach Deformation Model.* Dissertation, Dep. Civil Engineering, Yokohama National University, Yokohama, Japan, 90p.

Rattanapitikon, W., and Shibayama, T., 2000. Verification and modification of breaker height formulas. *Coastal Engineering Journal*, Vol.42, No.4, pp. 389-406.

Rattanapitikon, W., and Shibayama, T., 2006. Breaking wave formulas for breaking depth and orbital to phase velocity ratio. *Coastal Engineering Journal*, Vol.48, No.4, pp. 395-416.

Rector, R.L., 1954. Laboratory study of the equilibrium profiles pf beaches. *US Army BEB Tech Memo 41.*

Romanczyk, W., Boczar-Karakiewiez, B., and Bona, J.L., 2005. Extended equilibrium beach profiles. *Journal of Coastal Engineering*, Vol.52, pp. 727-744.

Sakai, T., and Battjes, J.A., 1980. Wave theory calculated from Cokelet's theory. *Coastal Engineering*, Vol.4, pp.65-84.

Shvidchenko, A.B., Pender, G., and Hoey, T.B., 2001. Critical shear stress for incipient motion of sand/gravel streambeds. *Water Resources Research*, 37, pp. 2273-2284.

Seyama, A., and Kimura, A., 1988. The measured properties of irregular wave breaking and wave height change after breaking on the slope. In: *Proc. 21st Coastal Eng. Conf.*, ASCE, pp. 419-432.

Sherman, D.J., 1991. Gravel Beaches. *National Geographic Research and Exploration*, Vol. 7, No. 4, pp. 442-452.

Sherman, D.J. Orford, J.D. and Carter ,R.W.G., 1993. Development of cusp related, gravel size and shape facies at Malin Head, Ireland. *Sedimentology*, Vol. 40, pp. 1139-1152.

Short, A.D., 1979. Three-dimensional beach stage model. *Journal of Geology*, Vol. 87, pp. 553-571.

Short, A.D., 1999. *Handbook of Beach and Shoreface Morphodynamics*. edited by A.D. Short, John Wiley and sons Ltd. ISBN 0 471 96570 7, 392p.

Shulmeister, J. and Kirk, R.M., 1997. Holocene fluvial-coastal interactions on a mixed sand and gravel beach system, North Canterbury, New Zealand. *Catena*, Vol. 30, No. 4, pp. 337-355.

Shuto, N., 1974. Non-linear long waves in channel of variable section. *Coastal Engineering in Japan*, JSCE, 17, pp. 1-12.

Sievwright, M.J., 1994. *Development and verification of empirical models of profile evolution for dynamically stable rock slopes under wave action.* Oxford Brookes University BEng. Thesis report for HR Wallingford

Simm, J.D, Brampton, A.H., Beech, N.W., and Brooke, J.S., 1996. Beach Management Manual. *Report 153*, CIRIA, pp. 47.

Snyder, W.H., and Castro, I.P., 1999. Acoustic Doppler Velocimeter Evaluation in Stratified Towing Tank. *Journal of Hydraulic Engineering*, Vol.125, No.6, June 1999, ASCE.

Stive, M. J. F., and Wind, H. F. 1986. Cross-shore Mean Flow in the Surf Zone. Coastal Engineering, Vol 10, No. 4, pp 325-340.

Stokes, G.G., 1847. On the theory of oscillatory waves. *Trans. Camb. Phil. Soc.*, 8, pp.411-455.

Svendsen, I.A., 1984a. Mass flux and undertow in a surf zone. *Coastal Engineering*, Vol.8, pp. 347-365.

Svendsen, I.A., 1984b. Wave heights and set-up in a surf zone. *Coastal Engineering*, Vol. 8, pp. 303-329.

Svendsen, I.A. and Buhr Hansen, J., 1988. Cross-shore currents in surf zone modelling. *Coastal Eng.*, 12: 23-42, pp. 11845-11856.

Svendsen, IB. A., and Lorenz, R.S., 1989. Velocities in combined undertow and longshore currents. *Coastal Engineering*, Vol.13, pp. 55-79.

Svendsen, I. A., Schäffer, H. A., and Hansen, J. B. 1987. The Interaction Between the Undertow and the Boundary Layer Flow on a Beach. *Journal of Geophysical Research*, Vol 92, No. C11, pp. 11845-11856.

Sunamura, T. and Horikawa, K., 1974. Two dimensional beach transformation due to waves. In: *Proc 14th Conf on Coastal Eng*, ASCE, pp. 920-938.

Tajima, Y., and Madsen, O. S., 2002. Shoaling, breaking and broken wave characteristics. In: *Proc., 28th Int. Conf. on Coastal Engineering*, ASCE, Reston, Va., pp .222–234.

Tajima, Y., and Madsen, O. S., 2003. Modeling near-shore waves and surface rollers. In: *Proc., 2nd Int. Conf. on Asian and Pacific Coasts* _CD-ROM_, World Scientific, Singapore, ISBN 981-238-558-4.

Tajima, Y., and Madsen, O. S., 2006. Modeling near-shore waves, surface rollers, and undertow velocity profiles. *Journal of Waterway, Port, Coastal, and Ocean Engineering*, Vol. 132, No.6, pp. 429-438.

Takeda, I., and Sunamura, T., 1982. Formation and height of berms. Trans. Japan. Geomorphological Union, Vol.3, pp. 145-157.

Technical Manual for Wave – Height Meter (G.H.M.) dynamic liquid-level measurements, (modifications in circuitry, component values and specifications reserved), page 2, Instrumentation Department Delft Hydraulics Laboratory.

Ting, F.C.K., and Kirby, J.T., 1994. Observation of undertow and turbulence in a laboratory surf zone. *Coastal Engineering*, Vol.24, pp. 51-80.

Torrini, L., and Allsop, N.W.H., 1999. Goda's breaking prediction method- A discussion note on how this should be applied. *HR Report, IT 473*, Wallingford, U.K.

Turner, I.L., 1993. Water table outcropping on macro-tidal beaches: a simulation model. *Marine Geology*, Vol. 115, pp. 227–238.

Ursell, F., Dean, R.G. and YU, S.Y., 1958. Forced small-amplitude water waves: a comparison of theory and experiment. *Techn.Report.Mass.Inst. of Techn, No.29*, Hydrodyn. Lab, pp. 1-33.

U.S. Department of the Interior Bureau of Reclamation, 1994. Design Standards No.13: Embankment Dams. *Chapter 5-Protective Filters*, United States Department of the Interior Bureau of Reclamation, Technical Service Center, Denver, CO.

Van der Graaff, J., 1977. Dune erosion during a storm surge. *Coastal Eng.*, Vol. 1, No.2, pp. 99-134.

Van der Meer, J.W., 1988. *Rock slopes and gravel beaches under wave attack.* Delft Hyd Comm No. 396.

Van der Meer, J.W. and Pilarczyk, K.W., 1986. Dynamic stability of rock slopes and gravel beaches. In: *Proceedings 20th Int. Conf. Coastal Engineering*, Taipei.

Van Hijum, E., 1974. Equilibrium profiles of coarse material under wave attack. In: *Proc 14th Conf on Coastal Eng*, 2.

Van Hijum, E. and Pilarczyk, K.W., 1982. *Equilibrium profile and longshore transport of coarse material under regular and irregular wave attack.* Delft Hyd Lb Pub No. 274.

Van Rijn, L. C. 1993. *Principles of sediment transport in rivers, estuaries and coastal seas*. Aqua Publications, Amsterdam, ISBN 90-800356-2-9.

Van Rijn, L.C., 2000. Hydrodynamics, sediment dynamics and morphodynamics during storm events 1998 in the nearshore zone of Egmond, The Netherlands, Delft Hydraulics. Report Z2897, Delft, The Netherlands.

Van Rijn, L.C., Walstra, D.J.R., Sutherland, J., Pan, S., and Sierra, J.P. 2003. The predictability of cross-shore bed evolution of sandy beaches at the time scale of storms and seasons using process-based Profile models. *Coastal Engineering*, Vol. 47, pp. 295-327.

Van Wellen, E., Chadwick, A.J., Bird, P.A.D., Bray, M., Lee, M., and Morfett, J., 1997. Coastal sediment transport on shingle beaches. In: *Coastal Dynamics '97*, ASCE, pp. 38-47.

Van Wellen, E., Chadwick, A.J. and Mason, T., 2000. A review and assessment of longshore sediment transport equations for coarse-grained beaches. *Coastal Engineering*, Vol. 40, pp. 243-275.

Vellinga, P., 1982. Beach and dune erosion during storm surges. *Coastal Eng.*, vol.6, pp. 361-387.

Vellinga, P., 1983. Predictive computational model for beach and dune erosion during storm surges. In: *Proc. Coastal Structures'83*, ASCE, pp. 806-819.

Vellinga, P., 1984. A Tentative Description of a Universal Erosion Profile for Sandy Beaches and Rock Beaches. *Coastal Engineering*, Vol. 8, N°2, pp. 177-188.

Vellinga P., 1986. *Beach and dune erosion during storm surges*. Dissertation, Delft Technical University, Delft Hydraulics Laboratory Communications No. 372, 185 p.

Visser, P. J., 1991. Laboratory Measurements of Uniform Longshore Currents. *Coastal Engineering*, Vol. 15, No. 5, pp. 563-593.

Walker, J.R., Everts, C.H., Schmelig, S. and Demirel, V., 1991. Observations of a tidal inlet on a shingle beach. In: *Proceedings of Coastal Sediments '91*, ASCE, pp. 975-989.

Watts, G. M. and Dearduff, R.F., 1954. Laboratory study of effects of tidal action on wave formed beach profiles. *BEB Tech memo No. 52.*

Watanabe, A., Hara, T. & Horikawa, K., 1984. Study on breaking condition for compound wave trains. *Coastal Engineering in Japan*, JSCE 27, pp. 71-82.

Weggel, J.R., 1972. Maximum breaker height. *J.Waterw.Harbors Coastal Eng. Div.*, pp. 529-548.

Williams, A.T. and Caldwell, N.E., 1988. Particle size and shape in pebble-beach sedimentation. *Marine Geology*, Vol. 82, pp. 199-215.

Wittenberg, L., Laronne, J.B., and Newson, M.D., 2007. Bed clusters in humid perennial and Mediterranean ephemeral gravel-bed streams: The effect of clast size and bed material sorting. *Journal of Hydrology*, 334, pp. 312-318.

Zheng, J., and Dean, R.G., 1997. Numerical models and intercomparisons of beach profile evolution. *Journal of Coastal Engineering*, Vol.30, pp. 169-201.

Zimmermann, C., Daemrich, F.,Streich, G., and Ohle, N., (June 1999 – February 2000).*Neues Wellenbecken zur Simulation von 3-dimensionalen Seegang.* Universitat Hannover, Franzius-Institut fur Wasserbau und Kusteningenieurwesen.

WAVE-INDUCED CURRENTS AND SEDIMENT TRANSPORT ON GRAVEL AND MIXED BEACHES

APPENDICES

A thesis submitted to the Cardiff University

In candidature for the degree of

Doctor of Philosophy

by

Christos Antoniadis

B.Eng., M.Eng.

Division of Civil Engineering, Cardiff School of Engineering

Cardiff University

September 2008

APPENDIX I

A1. The wave basin and the construction of both beach models

Figure A1- 1. The wave paddles

Figure A1- 2. The location where the model beach was constructed at

Figure A1- 3. First stage of construction

Figure A1- 4. Construction of the uniform slope

Figure A1- 5. The gravel beach

Figure A1- 6. The mixed beach

Figure A1- 7. The reinforcement of the rear side of the model (left side)

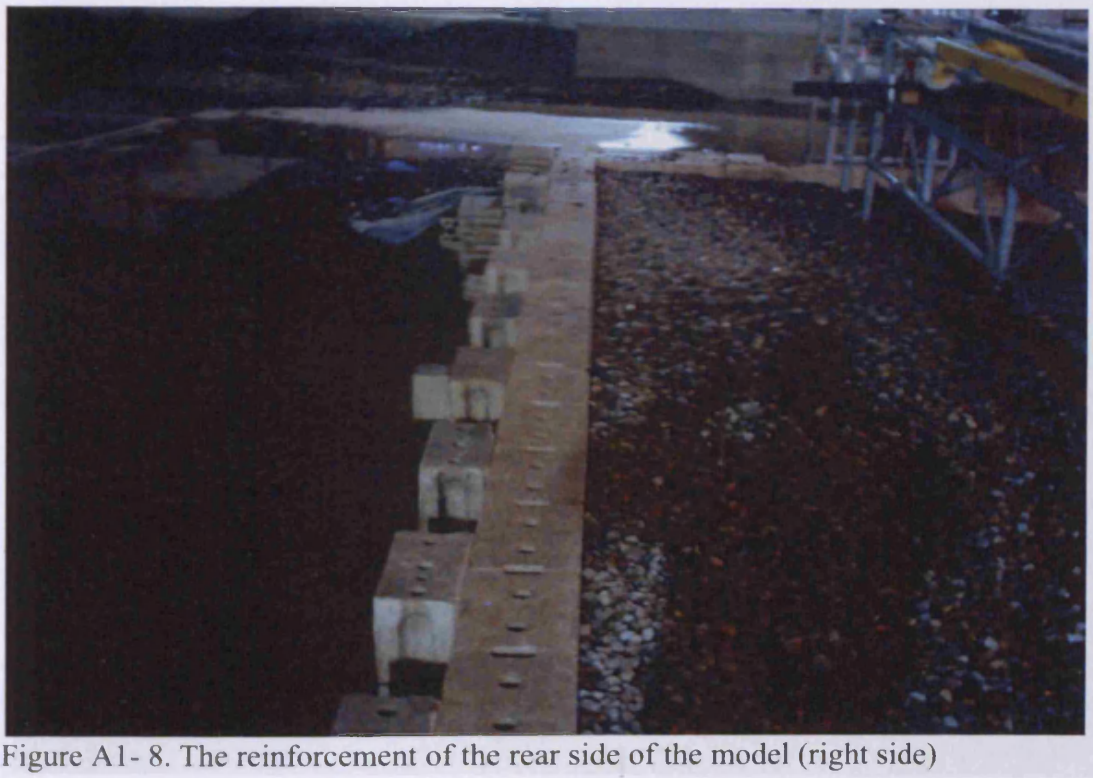

Figure A1- 8. The reinforcement of the rear side of the model (right side)

Figure A1- 9. The reinforcement of the right side of the model

Figure A1- 10. The additional structure

Figure A1- 11. The walkway that connected the model beach with the side of the wave basin

A2. Instrumentation

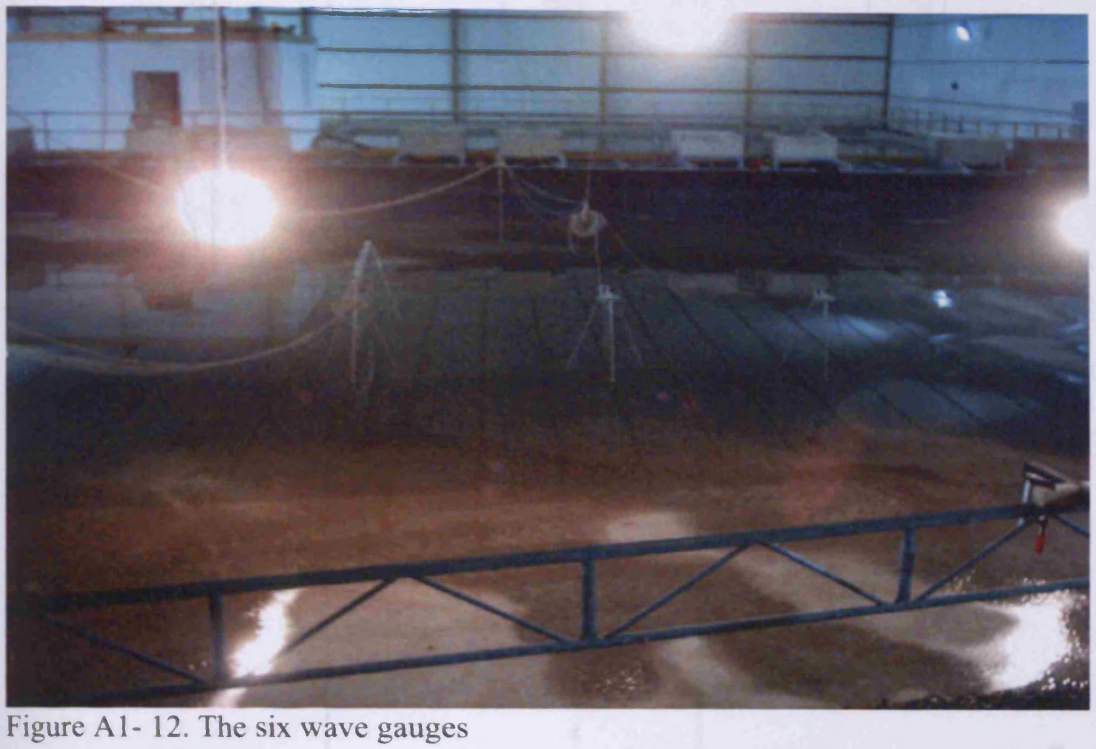

Figure A1- 12. The six wave gauges

Figure A1- 13. The components of the wave gauge

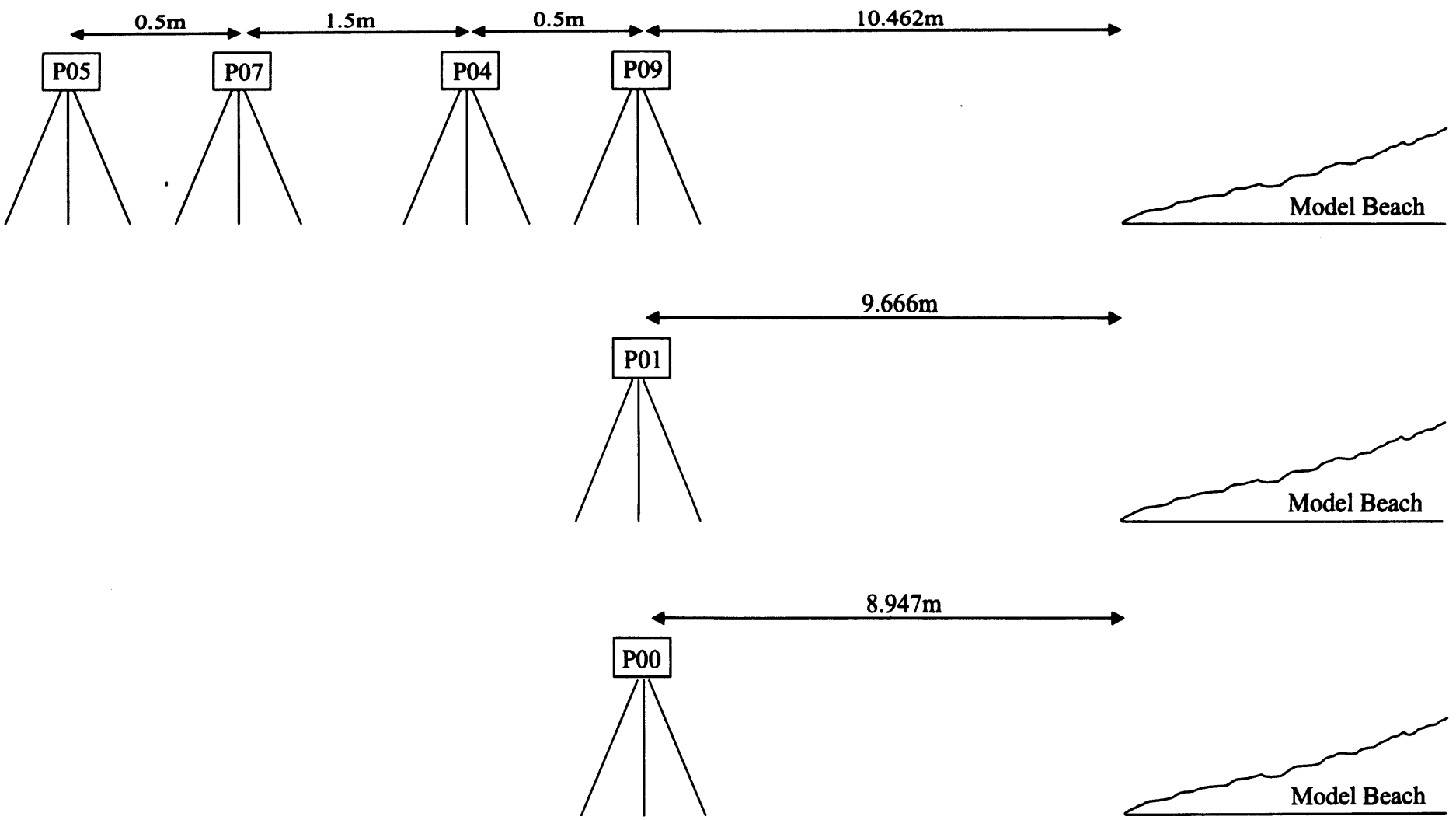

Figure A1- 14. The location of the wave gauges compare to the beach

A3. The components of the wave generation system and the software used

A3.1 The DHI Wave Synthesizer – computer Control

For the computer control of the wave generation process, the Wave Synthesizer (WS) package was used. The WS was a menu-operated software package for PC computers for the generation of wave control signals, for on-line control of the wave paddle, for data logging, and data analysis. The WS had options for the generation of regular as well as random waves. Irregular random waves can be synthesized from a large number of spectrum types.

Noises filtering techniques or iFFT techniques were used together with the appropriate Biesel transfer function to synthesise the wave generator series. The duration of the control signal, which was non-repetitive, was limited only by the PC data storage capacity. The steering frequency could be selected by the operator and was typically between 20 and 40Hz.

The wave generator was controlled in real-time mode from the PC by a quartz clock. The wave generator could be started and stopped at any time from the PC.

Simultaneously with the wave generator on-line control, the WS permitted quartz clock controlled data acquisition from 16 analogue input channels. The sampling frequency was user-defined. Data were stored in standard format on disk for flexible post-processing and display.

The measuring time series could be analysed by a set of time series analysis programmes. The WS could produce graphic output on suitable monitors and printers. Data could be displayed in time series format or in bar diagrams, and spectra in standard format.

A3.2 WAVEPC Software (Franzius-Institut, 1993)

The WAVEPC software package was established on IBM-compatible Micros as a development of the WAVE100-Software. The aim of the software was to enable the user in the field of sea state simulation and analysis and it could be used also for periodic signal analysis. The programs in WAVEPC were developed to work with in hydraulic models in wave tanks. They enclosed

- the definition of wavetrains (time-serials)
- the creation of control-signals for a wave paddle
- the driving of a wave paddle and simultaneously measurement in the model
- the analysis of a measurement and
- a short list of utilities for data monitoring and managing.

An overview of the programs that were available for control signal creation and analysis is shown at the following Figure A3- 15.

The overview was organised like a typical test run in a hydraulic model:

1. creation of a control-signal
2. control and measurement in the model
3. analysis of measurement and definition of new control signal

The routines of WAVEPC were developed for a broad band of application. The user was often asked to enter parameters.

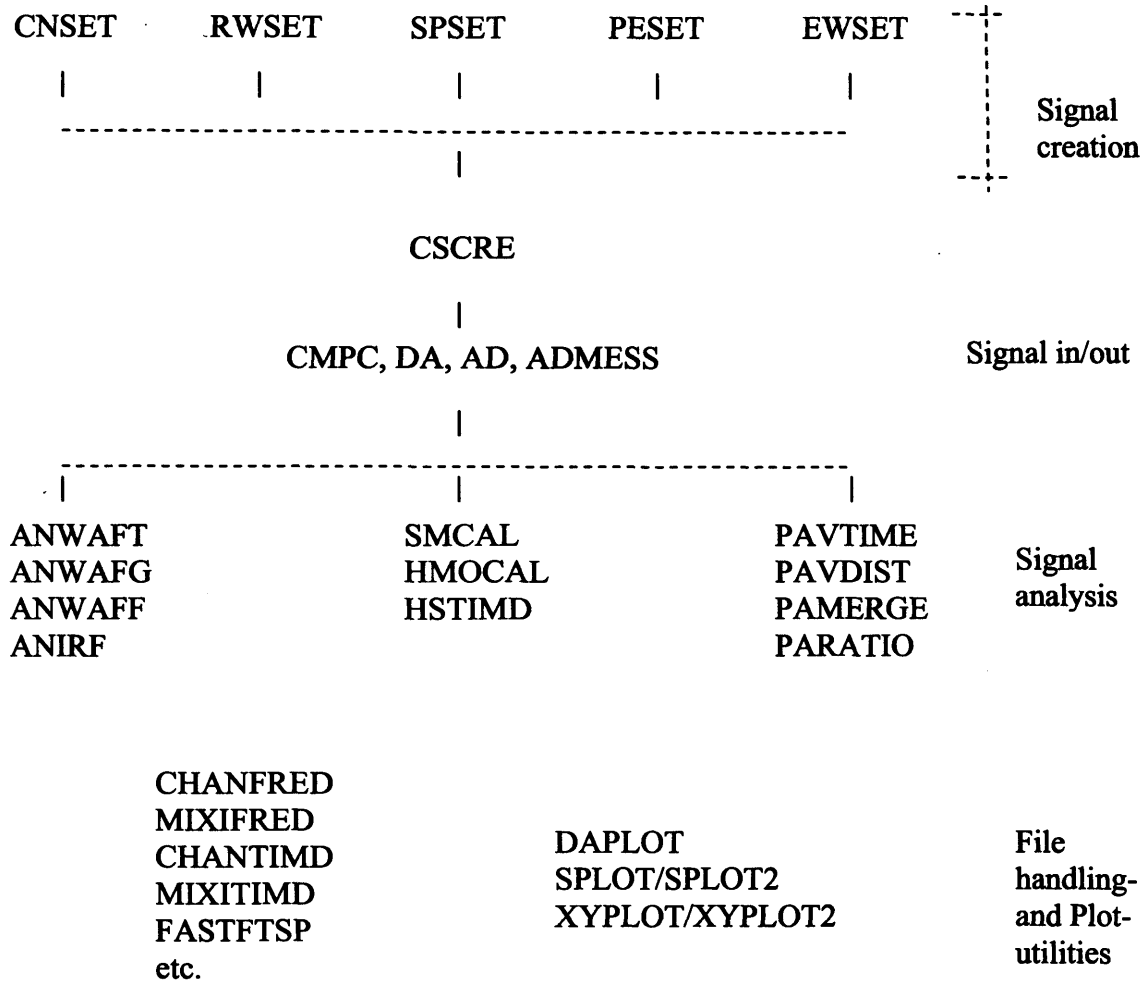

Figure A3- 15. Programs of WAVEPC (Franzius-Institut, 1993)

A3.2.1 *Signal Creation*

The first two steps on the way to the control-signal for a wave paddle were:

1. definition of regular or irregular waves to be produced in a wave-tank and
2. computation of a control-signal on the basis of a time-series or spectrum.

A3.2.1.1 *Defining procedures in Time- and Frequency Domain*

View routines dealt with the definition of regular and irregular waves. During the experiment only the routines RWSET and SPSET were used. The output files contained frequency domain data. Moreover, due to hardware restriction of the analog output card the digitising rate ought to be 10msec or an integer multiplex of 10msec; on this account the user was asked to define the minimum digitising rate. The routines was then fit the chosen wave parameter with the minimum digitising rate and came out with a time increment which was equal or an integer multiplex of the desired one and possible fitted the desired wave parameter.

Example: wave period T = 2sec
minimum rate dt = 10msec
blocksize N = 32
⟶ T/N = 2/32 = 0.0625
RWSET: DT = 0.070 ⟶ T = 2.24sec

If desired DT is 0.06sec, the input wave period T ought to be T = 1.92sec.

The routine RWSET defined a regular wave profile of I., II., III. or V. Stokes Order theory. For purpose of the experiment, RWSET defined a regular wave profile of I. Stokes Order theory.

As far as the routine SPSET is concerned, it defined the frequency domain data of an irregular wave train. Moreover, there were three paths available to follow for the definition of the spectrum:

1. calculation of a theoretical energy distribution (PM, JONSWAP) combined with random phase distribution,
2. calculation of the energy distribution according to wind parameter combined with random phase distribution, and
3. manual design of energy distribution combined either with manual design of phase distribution or random phase angles.

For purpose of the experiment, the first path was followed for the definition of the spectrum.

A3.2.1.2 *CSCRE (Control signal CREation)*

This is the second step on the way to a control signal for a wave paddle. CSCRE asked for a file with frequency domain data of the desired wave train. The routine calculated the control-signal for a specified wave padle with respect to

- machine layout (type of movement, calibration paddle displacement/voltage)
- transferfunction wave paddle
- hydraulic transferfunction (displacement of paddle/water surface elevation)
- transferfunction of distance: phase lag at a certain distance from wave paddle.

The possibility to reduce the digitising rate of the control signal compared to the input file with the wave data was opened by CSCRE. This was occurred by extending the frequency domain with additional frequency components set to zero. Extending the frequency domain with factor 2 meant halving the digitising rate of the time domain data but doubling the number of frequency components.

The hydraulic transferfunction was calculated by the linear wave paddle theory (Ursell et al., 1958). The transferfunction of distance calculated a phase shift of each frequency component to be given to the wave paddle in order to compensate the phase velocity of the frequency component. The amplitude remained uncharged.

CSCRE finished with a protocol written on the screen and a text-file. The protocol was a print put of the header of the control-signal file. The header information of the control-signal was also listened when using CMPC.

A3.2.1.3 *Control and Measurement: CMPC*

CMPC was designed for control and measurement purposes on IBM-compatible PCs under the MS-DOS operating system. CMPC had 3 tasks:

1. Measurement
2. Control Signal Output or
3. Measurement and Control Signal Output

CMPC combined two tasks (control signal output, measurement) in one program. In case of *Measurement* the necessary parameter could be entered directly or read from a file. If the task was only measurement, CMPC would ask for the digitising rate. In case of *control signal output* the digitising rate would be the same as the rate of the output signal.

The operation of measurement was performed IANZ (number of measurements for each channel) times on every input channel and stopped when the IANZ data samples were caught. One file created for each input-channel and another file with all parameter important for analysis of the measured data.

In the Control Signal Output case a file with control signal was needed. CMPC read the stored control-signal time series and wrote the header on the screen.

A3.2.2 *Signal Analysis*

The programs of the Signal Analysis allowed the analysis of a measured or computed time series. The routines would carry out an interactive dialogue with the user. Parameter could partly be read from files. The results of the analysis were written to the screen and a textile. Optional the analysed time series and the

computed data (spectra and zero crossing data) could be stored in files. During the experiment, ANWAFT was the program of the signal analysis which was used.

A3.2.2.1 *Analysis in Time-and Frequency domain: ANWAFT*

ANWAFT calculated characteristic wave heights of a time series according to different analysis techniques in time and frequency domain. The characteristic wave heights were:

- $H_{m_o} = 4\sqrt{m_o}$ (Eq.5)
- $H_{1/3}$ medium of 33% highest waves of a record,
- $H_{1/10}$ medium of 10% highest waves of a record,
- H_{max} maximum wave height of a record.

$H_{1/3}$, $H_{1/10}$ and H_{max} were calculated with a zero-downcrossing routine, using a threshold level of 0.01 x $H_{1/3}$. The analysed wave train, the resulting frequency domain data as well as the parameters of individual waves were stored optionally in files.

A3.2.2.1.1 Data input

During the experiment, the measurement with PC was used as the time series to be analysed in ANWAFT. In this case, the several channels (analog input channels) could be analysed in one program run. If the time series to be analysed contented more than 20,000 samples, then only the samples 1 to 20,000 could be analysed. The parameter necessary for the analysis could be divided into two groups:

- wave gauge parameter, they were individual for each channel
- analysis parameter, they were global for all channels.

The wave gauge parameter and the analysis parameter could be put into two files for easy cal of ANWAFT. The parameter list read from files had to be confirmed by the user.

A3.2.2.1.2 Calculation method

The program analysed data with increasing order of channel number. If the calculation with the actual file was terminated, the output files were closed and the next data file was opened for calculation.
The wave gauge parameter and the analysis parameter were read firstly and then the loop over all files was opened. Each time series was analysed record wise in the above mentioned way, according to the analysis parameter. The wave height H_{mo} was calculated from the power spectrum density. ANWAFT tried to extend the spectrum with zero values to provide a smaller digitising rate before calling the zero-down crossing routine.

The maximum number of samples in a time series (N-blocksize) was 4096 and if N was less than 4096 then the spectrum would be extended in the frequency domain up to factor "4". The zero-down crossing routine came out with $H_{1/3}$, $H_{1/10}$ and H_{max}.

Moreover, if sufficient data samples were available, then the computation in one time series was repeated NBLOCK (number of records) times. Nevertheless, if there were not sufficient data samples available, then ANWAFT would finish the analysis and continued with the next data file.

The average of $H_{1/3}$ and $H_{1/10}$ was calculated and printed out when NBLOCK was less than one. The average values for the power spectrum density were also calculated.

A3.2.2.1.3 Output

The input parameter and the calculated characteristic wave parameter were written to the screen. Additionally at least one, optional up to five files were created.

1. The text file
2. The wave file
3. The spectrum file
4. The zero crossing file and
5. The parameter file.

The text file was created automatically but the other files were generated optionally. The text file contained the same parameter list as the text written to the screen with the results of the calculation.

The analysed time series from the beginning of the first to the end of the last analysed record was stored (no calibration applied and only measured data with dimension mV) in the wave file.

In the spectrum file the frequency domain data were stored, The phase angle information was available only if NBLOCK is equal to 1 and if NBLOCK > 1 average values of the power spectrum density were calculated and written to this file, the frequency domain data in rectangular and polar coordinates were set to zero.

The results of the zero-down crossing analysis were contained in the zero crossing file. If NBLOCK >1, only the zero crossing data of the last analysed record were stored here.

The parameter file contained the same header as the text file. The header was followed by a dataset for every analysis round with wave heights (same parameter as in the text file) and a number of frequency components (power spectrum and phase angle).

APPENDIX II

A1. The wave measured parameters

The wave measured parameters are listed below:

- H_{m0} : zeroth-moment wave height equal to four times standard deviation of sea- surface elevations
- $H_{1/3}$: mean height of 33% highest waves of the record,
- $H_{1/10}$: mean height of 10% highest waves of a record,
- H_{max} : maximum wave height of a record,
- H_{rms} : root-mean-square wave height,
- H_{mean} : mean wave height,
- mean H_{m0},
- $TH_{1/3}$: mean period of mean wave height of 33% highest waves of a record,
- $TH_{1/10}$: mean period of mean wave height of 10% highest waves of a record, and
- TH_{max} : mean period of maximum wave height of a record.

Table A2- 1.Wave measured parameters at Test 1

Parameters	Wave probes numbers					
	P00	P01	P04	P05	P07	P09
H_{mo} (cm)	35.774	30.557	30.978	31.606	33.456	32.715
$H_{1/3}$ (cm)	27.945	24.382	25.137	26.806	26.733	25.338
$H_{1/10}$ (cm)	28.436	25.589	25.660	27.185	27.060	25.675
H_{max} (cm)	28.912	27.086	26.208	27.667	27.552	26.052
H_{rms} (cm)	26.916	23.007	24.177	25.855	25.929	24.474
H_{mean} (cm)	26.889	22.968	24.155	25.766	25.849	24.454
$TH_{1/3}$ (sec)	2.011	2.013	2.016	2.016	2.017	2.016
$TH_{1/10}$ (sec)	2.013	1.997	2.015	2.015	2.013	2.017
TH_{max} (sec)	2.009	1.994	2.035	2.053	2.015	2.012

Table A2- 2. Wave measured parameters at Test 2

Parameters	Wave probes numbers					
	P00	P01	P04	P05	P07	P09
H_{mo} (cm)	29.724	29.144	21.409	27.453	27.214	20.784
$H_{1/3}$ (cm)	26.054	26.458	22.287	26.143	25.349	21.761
$H_{1/10}$ (cm)	26.676	27.187	22.843	26.591	25.786	22.319
H_{max} (cm)	27.607	28.216	23.213	27.179	26.154	23.027
H_{rms} (cm)	21.177	22.017	19.466	25.130	24.459	20.117
H_{mean} (cm)	20.093	20.920	18.773	25.077	24.412	19.870
$TH_{1/3}$ (sec)	3.007	3.009	3.001	3.006	3.007	3.003
$TH_{1/10}$ (sec)	2.999	3.004	2.984	3.002	2.991	2.997
TH_{max} (sec)	3.046	3.009	3.011	2.973	3.017	3.019

Table A2- 3. Wave measured parameters at Test 3

Parameters	Wave probes numbers					
	P00	P01	P04	P05	P07	P09
H_{m0} (cm)	11.549	9.283	11.265	10.856	11.088	10.982
$H_{1/3}$ (cm)	8.923	7.352	8.492	8.330	8.685	8.610
$H_{1/10}$ (cm)	9.330	7.646	8.674	8.575	8.938	8.774
H_{max} (cm)	10.312	8.957	9.242	8.945	9.104	9.078
H_{rms} (cm)	8.494	6.871	8.111	7.939	8.206	8.242
H_{mean} (cm)	8.463	6.841	8.052	7.912	8.176	8.212
$TH_{1/3}$ (sec)	2.016	2.016	2.013	2.014	2.014	2.016
$TH_{1/10}$ (sec)	2.010	2.015	2.007	2.010	2.012	2.008
TH_{max} (sec)	1.900	1.881	1.882	2.019	2.011	1.879

Table A2- 4. Wave measured parameters at Test 4

Parameters	Wave probes numbers					
	P00	P01	P04	P05	P07	P09
H_{m0} (cm)	10.566	8.752	10.835	10.785	11.847	11.079
$H_{1/3}$ (cm)	8.773	7.248	8.832	8.389	9.221	9.206
$H_{1/10}$ (cm)	9.253	7.591	8.972	8.550	9.383	9.350
H_{max} (cm)	9.829	8.312	9.134	8.749	9.496	9.425
H_{rms} (cm)	8.258	6.913	8.363	8.063	8.874	8.797
H_{mean} (cm)	8.218	6.897	8.298	8.049	8.866	8.775
$TH_{1/3}$ (sec)	3.002	3.005	3.009	3.002	3.010	3.009
$TH_{1/10}$ (sec)	2.984	2.989	3.009	3.009	3.011	3.009
TH_{max} (sec)	3.005	2.762	3.014	2.994	3.020	3.008

Table A2- 5. Wave measured parameters at Test 5

Parameters	Wave probes numbers					
	P00	P01	P04	P05	P07	P09
H_{m0} (cm)	12.603	10.585	10.848	10.897	10.749	10.841
$H_{1/3}$ (cm)	11.805	10.140	10.383	10.705	10.450	10.485
$H_{1/10}$ (cm)	15.686	12.886	12.838	13.380	13.311	13.177
H_{max} (cm)	21.245	17.562	19.024	17.103	17.692	17.520
H_{rms} (cm)	8.253	7.077	7.319	7.523	7.378	7.369
H_{mean} (cm)	7.058	6.153	6.446	6.587	6.417	6.470
$TH_{1/3}$ (sec)	2.236	2.265	2.258	2.206	2.247	2.264
$TH_{1/10}$ (sec)	2.240	2.239	2.247	2.288	2.303	2.270
TH_{max} (sec)	2.103	2.104	2.116	2.127	2.235	2.080

Table A2- 6. Wave measured parameters at Test 6

Parameters	Wave probes numbers					
	P00	P01	P04	P05	P07	P09
H_{m0} (cm)	12.401	10.819	11.057	10.957	11.036	11.049
$H_{1/3}$ (cm)	12.689	11.062	11.384	11.171	11.378	11.282
$H_{1/10}$ (cm)	16.693	14.652	15.310	15.319	15.889	15.099
H_{max} (cm)	21.256	19.316	19.037	20.332	21.648	20.653
H_{rms} (cm)	8.866	7.607	7.872	7.686	7.864	7.725
H_{mean} (cm)	7.642	6.424	6.668	6.418	6.537	6.479
$TH_{1/3}$ (sec)	3.206	3.284	3.217	3.108	3.158	3.244
$TH_{1/10}$ (sec)	3.156	3.274	3.094	3.181	3.212	3.184
TH_{max} (sec)	3.259	3.269	3.210	3.117	3.194	3.266

Table A2- 7. Wave measured parameters at Test 7

Parameters	Wave probes numbers					
	P00	P01	P04	P05	P07	P09
H_{m0} (cm)	11.536	9.526	12.043	11.214	9.823	11.041
$H_{1/3}$ (cm)	8.531	7.407	8.796	8.685	7.603	8.570
$H_{1/10}$ (cm)	8.619	7.768	8.935	8.839	7.978	8.729
H_{max} (cm)	8.910	8.946	9.184	9.036	8.770	8.997
H_{rms} (cm)	8.311	7.030	8.455	8.284	7.147	8.226
H_{mean} (cm)	8.282	7.002	8.422	8.253	7.118	8.196
$TH_{1/3}$ (sec)	2.014	2.017	2.013	2.014	2.015	2.015
$TH_{1/10}$ (sec)	2.006	2.015	2.011	2.016	2.016	2.005
TH_{max} (sec)	1.894	1.886	2.024	2.020	1.946	1.882

Table A2- 8. Wave measured parameters at Test 8

Parameters	Wave probes numbers					
	P00	P01	P04	P05	P07	P09
H_{m0} (cm)	9.060	6.581	8.402	10.740	11.006	9.021
$H_{1/3}$ (cm)	7.783	5.874	7.363	9.234	8.656	7.673
$H_{1/10}$ (cm)	8.445	6.541	7.686	9.639	8.833	8.075
H_{max} (cm)	9.567	8.099	8.179	9.920	9.260	8.325
H_{rms} (cm)	7.099	4.518	6.610	8.545	8.285	5.818
H_{mean} (cm)	7.064	4.246	6.466	8.514	8.268	5.519
$TH_{1/3}$ (sec)	3.003	3.004	2.998	3.010	3.008	3.005
$TH_{1/10}$ (sec)	2.992	2.997	2.970	3.007	3.012	2.995
TH_{max} (sec)	2.745	2.762	2.774	3.024	3.032	2.997

Table A2- 9. Wave measured parameters at Test 9

Parameters	Wave probes numbers					
	P00	P01	P04	P05	P07	P09
H_{m0} (cm)	12.748	10.887	11.102	11.067	11.028	10.983
$H_{1/3}$ (cm)	12.342	10.483	10.497	10.707	10.737	10.540
$H_{1/10}$ (cm)	15.978	13.333	13.272	13.514	13.782	13.390
H_{max} (cm)	23.092	16.733	18.965	17.399	17.772	18.163
H_{rms} (cm)	8.726	7.471	7.334	7.613	7.590	7.427
H_{mean} (cm)	7.643	6.648	6.375	6.686	6.639	6.506
$TH_{1/3}$ (sec)	2.256	2.290	2.227	2.240	2.233	2.278
$TH_{1/10}$ (sec)	2.280	2.240	2.193	2.334	2.305	2.254
TH_{max} (sec)	2.076	2.348	2.161	2.260	2.170	2.147

Table A2- 10. Wave measured parameters at Test 10

Parameters	Wave probes numbers					
	P00	P01	P04	P05	P07	P09
H_{m0} (cm)	13.809	11.923	11.673	11.793	11.733	11.741
$H_{1/3}$ (cm)	13.517	11.646	11.665	11.831	11.604	11.785
$H_{1/10}$ (cm)	17.764	15.765	15.583	16.240	16.282	15.613
H_{max} (cm)	23.702	21.918	22.635	21.991	22.882	22.724
H_{rms} (cm)	9.179	7.841	8.005	7.974	7.891	8.063
H_{mean} (cm)	7.598	6.390	6.779	6.485	6.436	6.726
$TH_{1/3}$ (sec)	3.062	2.988	3.033	3.184	3.065	3.053
$TH_{1/10}$ (sec)	3.062	3.191	3.167	3.135	3.124	3.187
TH_{max} (sec)	3.276	3.344	3.319	3.000	3.020	3.292

A2. Wave-induced current velocities

Table A2- 11. Line 1-Test 1

Long-shore Distance (m)	Cross-shore Distance (m)	Depth relating to S.W.L. (m)	Vy (cm/s)	Vx (cm/s)	Vz (cm/s)
2	-0.6	-0.15	11.81	4.22	
2	-0.6	-0.20		3.24	0.42
2	-0.6	-0.25	4.71	2.50	1.08
2	-0.6	-0.30	2.76	1.33	0.69
2	-0.6	-0.35	3.17	0.00	0.35
2	-0.6	-0.40	0.46	-2.41	0.05
2	-0.7	-0.15	14.90	3.94	
2	-0.7	-0.20	7.42	2.93	1.40
2	-0.7	-0.25	6.69	2.22	1.39
2	-0.7	-0.30	6.28	2.47	0.14
2	-0.7	-0.35	3.86	2.38	-0.15
2	-0.7	-0.40	3.26	0.89	-0.18
2	-0.7	-0.45	1.75	-0.24	-0.37
2	-0.8	-0.15	14.76	2.87	

2	-0.8	-0.20	7.98	2.72	1.12
2	-0.8	-0.25	4.75	2.67	0.76
2	-0.8	-0.30	4.85	0.75	0.57
2	-0.8	-0.35	3.22	0.45	0.21
2	-0.8	-0.40	0.99	0.58	0.09
2	-0.8	-0.45	-1.28	0.00	0.04
2	-0.9	-0.15	12.54	5.20	
2	-0.9	-0.20	6.98	1.60	1.13
2	-0.9	-0.25	6.66	2.25	0.07
2	-0.9	-0.30	3.02	0.50	0.51
2	-0.9	-0.35	2.26	-0.78	0.30
2	-0.9	-0.40	1.15	-0.05	0.01
2	-0.9	-0.45	-0.21	-0.24	-0.40
2	-1	-0.15	10.09	1.02	
2	-1	-0.20	9.00	0.34	0.86
2	-1	-0.25	4.40	0.08	0.82
2	-1	-0.30	5.00	-0.21	-0.02
2	-1	-0.35	2.84	-0.52	0.38
2	-1	-0.40	1.43	0.29	0.27
2	-1	-0.45	2.39	-0.93	-0.67
2	-1.1	-0.15	12.33	4.27	0.43
2	-1.1	-0.20	9.21	2.33	0.12
2	-1.1	-0.25	4.29	1.46	0.80
2	-1.1	-0.30	2.83	0.91	0.33
2	-1.1	-0.35	1.71	0.39	0.12
2	-1.1	-0.40	1.78	0.25	-0.23
2	-1.2	-0.15	12.81	3.58	
2	-1.2	-0.20	7.78	0.58	0.26
2	-1.2	-0.25	5.69	1.70	0.55
2	-1.2	-0.30	3.87	0.34	0.25
2	-1.2	-0.35	5.29	0.65	0.02
2	-1.2	-0.40	1.25	0.08	-0.29
2	-1.3	-0.15	10.97	0.33	-0.45
2	-1.3	-0.20	8.52	0.52	0.50
2	-1.3	-0.25	6.87	-0.96	0.15
2	-1.3	-0.30	7.66	-1.22	0.02
2	-1.3	-0.35	5.83	-1.59	-0.03
2	-1.3	-0.40	2.54	0.35	-0.18
2	-1.4	-0.15	10.69	0.72	-0.11
2	-1.4	-0.20	8.03	1.08	0.54

2	-1.4	-0.25	5.05	0.28	0.48
2	-1.4	-0.30	4.08	-0.56	0.09
2	-1.4	-0.35	2.74	-0.34	0.03
2	-1.4	-0.40	2.35	-0.37	0.17
2	-1.5	-0.15	11.74	0.12	-1.11
2	-1.5	-0.20	8.33	-0.84	-0.22
2	-1.5	-0.25	6.73	-1.40	-0.35
2	-1.5	-0.30	4.09	-0.70	-0.15
2	-1.5	-0.35	3.02	-0.98	0.15
2	-1.5	-0.40	2.90	-0.32	0.08
2	-1.6	-0.15	11.46	0.54	-0.24
2	-1.6	-0.20	8.20	-1.73	0.29
2	-1.6	-0.25	8.39	-1.83	0.49
2	-1.6	-0.30	6.72	-3.40	0.04
2	-1.6	-0.35	3.80	-2.19	0.17
2	-1.6	-0.40	2.25	-2.62	-0.04
2	-1.7	-0.15	13.45	-0.40	-1.46
2	-1.7	-0.20	9.75	-2.38	-1.09
2	-1.7	-0.25	8.24	-4.03	-0.28
2	-1.7	-0.30	9.10	-3.39	-0.59
2	-1.7	-0.35	5.93	-2.26	0.13
2	-1.7	-0.40	4.60	-2.84	0.06
2	-1.8	-0.15	10.60	-1.59	-0.65
2	-1.8	-0.20	8.39	-5.50	-0.43
2	-1.8	-0.25	6.70	-7.10	-0.66
2	-1.8	-0.30	6.24	-6.03	-0.43
2	-1.8	-0.35	3.97	-6.27	-0.21
2	-1.8	-0.40	4.79	-4.14	-0.80
2	-1.9	-0.15	10.85	-1.43	0.02
2	-1.9	-0.20	7.59	-5.24	-0.47
2	-1.9	-0.25	6.72	-4.37	-0.41
2	-1.9	-0.30	6.09	-6.03	-0.40
2	-1.9	-0.35	4.03	-5.15	-0.39
2	-1.9	-0.40	5.23	-2.58	-1.24
2	-2	-0.15	10.26	-2.33	-0.43
2	-2	-0.20	9.85	-5.44	-1.36
2	-2	-0.25	7.78	-7.04	-0.69
2	-2	-0.30	7.29	-8.48	-1.28
2	-2	-0.35	6.15	-7.22	-1.00
2	-2	-0.40	2.51	-2.12	0.07

2	-2.1	-0.15	10.96	-5.82	0.09
2	-2.1	-0.20	9.36	-2.56	-0.51
2	-2.1	-0.25	8.56	-6.47	-0.89
2	-2.1	-0.30	10.40	-5.66	-2.01
2	-2.1	-0.35	6.97	-4.02	-2.16
2	-2.1	-0.40	-2.87	-4.64	
2	-2.2	-0.15	10.47	-2.68	-1.17
2	-2.2	-0.20	9.25	-3.08	0.00
2	-2.2	-0.25	9.63	-5.88	-2.34
2	-2.2	-0.30	9.12	-8.46	-1.42
2	-2.2	-0.35	4.60	-2.65	-0.63
2	-2.3	-0.15	9.64	-1.11	-0.82
2	-2.3	-0.20	8.79	-1.12	-0.99
2	-2.3	-0.25	8.63	-4.05	-0.76
2	-2.3	-0.30	7.18	-3.77	-0.22
2	-2.3	-0.35	1.77	-4.06	
2	-2.4	-0.15	16.53	-11.95	
2	-2.4	-0.20	10.87	-10.65	-0.51
2	-2.4	-0.25	7.98	-6.29	-0.46
2	-2.4	-0.30	7.37	-5.49	-1.09
2	-2.4	-0.35	1.86	-7.11	-0.53
2	-2.5	-0.15	11.14	-0.19	-0.54
2	-2.5	-0.20	10.73	-4.20	0.25
2	-2.5	-0.25	9.48	-5.92	-0.58
2	-2.5	-0.30	7.04	-0.82	-0.68
2	-2.5	-0.35	-4.30	-0.55	
2	-2.6	-0.15		-6.58	
2	-2.6	-0.20	12.58	-10.03	-0.07
2	-2.6	-0.25	10.87	-5.30	-0.48
2	-2.6	-0.30	8.13	-3.90	-0.52
2	-2.7	-0.15	12.18	-1.11	
2	-2.7	-0.20	10.70	-6.68	0.68
2	-2.7	-0.25	9.59	-7.56	-0.49
2	-2.7	-0.30	5.96	-4.88	-0.67
2	-2.8	-0.15	11.64	-8.12	-1.31
2	-2.8	-0.20	11.60	-3.53	-1.12
2	-2.8	-0.25	7.98	-1.79	-0.87
2	-2.8	-0.30	7.07	-0.03	-1.34
2	-2.9	-0.15	12.37	-6.34	
2	-2.9	-0.20	12.25	-6.72	-1.15

2	-2.9	-0.25	11.60	-12.08	-1.03
2	-2.9	-0.30	4.54	-4.25	
2	-3	-0.15	12.40	-6.26	-1.14
2	-3	-0.20	10.40	-7.97	-1.76
2	-3	-0.25	12.48	-11.32	-1.83
2	-3.1	-0.15	12.46	-10.72	-1.92
2	-3.1	-0.20	12.50	-7.72	-2.11
2	-3.1	-0.25	12.05	-12.44	
2	-3.2	-0.20	9.91	-7.68	
2	-3.2	-0.25	5.49		
2	-3.3	-0.20	12.43	-12.95	

Table A2- 12. Line 2-Test 1

Long-shore Distance (m)	**Cross-shore Distance (m)**	**Depth relating to S.W.L. (m)**	**Vy (cm/s)**	**Vx (cm/s)**	**Vz (cm/s)**
4	-0.6	-0.15	22.87	13.85	-3.04
4	-0.6	-0.20	8.33	5.65	-0.37
4	-0.6	-0.25	8.42	5.37	0.06
4	-0.6	-0.30	5.40	4.82	-0.27
4	-0.6	-0.35	3.36	3.73	-0.29
4	-0.6	-0.40	1.77	1.31	
4	-0.7	-0.15	17.08	15.36	-2.71
4	-0.7	-0.20	6.90	7.64	-0.62
4	-0.7	-0.25	4.95	5.77	0.02
4	-0.7	-0.30	5.99	3.89	-0.05
4	-0.7	-0.35	2.83	3.63	-0.65
4	-0.7	-0.40	0.43	0.73	
4	-0.8	-0.15	16.59	13.38	-2.18
4	-0.8	-0.20	7.54	6.98	-0.66
4	-0.8	-0.25	4.91	5.94	-0.67
4	-0.8	-0.30	3.98	3.39	-0.06
4	-0.8	-0.35	3.45	2.76	-0.38
4	-0.9	-0.15	18.80	11.87	-2.76
4	-0.9	-0.20	8.86	5.99	-1.12
4	-0.9	-0.25	6.11	4.39	-0.37
4	-0.9	-0.30	3.56	3.93	-0.31
4	-0.9	-0.35	3.73	1.89	-0.03
4	-1	-0.15	11.74	10.46	-1.92

4	-1	-0.20	7.02	6.65	-1.41
4	-1	-0.25	4.01	5.97	-1.04
4	-1	-0.30	3.84	4.04	-0.45
4	-1	-0.35	2.78	1.56	-0.46
4	-1.1	-0.15	16.71	11.73	-2.55
4	-1.1	-0.20	7.80	6.44	-1.08
4	-1.1	-0.25	4.73	6.11	-0.87
4	-1.1	-0.30	3.74	4.14	-0.62
4	-1.1	-0.35	2.07	0.25	-0.53
4	-1.2	-0.15	14.87	5.68	-1.64
4	-1.2	-0.20	9.68	3.94	-0.66
4	-1.2	-0.25	5.99	2.90	-0.65
4	-1.2	-0.30	2.00	2.11	-0.05
4	-1.2	-0.35	-0.24	-1.06	
4	-1.3	-0.15	16.65	10.91	-2.60
4	-1.3	-0.20	6.77	6.55	-1.74
4	-1.3	-0.25	6.25	4.45	-1.23
4	-1.3	-0.30	3.07	3.51	-0.02
4	-1.3	-0.35	-3.43	-0.07	
4	-1.4	-0.15	20.07	11.45	-2.35
4	-1.4	-0.20	11.77	3.95	
4	-1.4	-0.25	5.45	2.90	-0.27
4	-1.4	-0.30	3.80	2.65	-0.36
4	-1.4	-0.35	0.80	1.28	
4	-1.5	-0.15	21.76	10.62	-1.78
4	-1.5	-0.20	9.16	4.66	-1.27
4	-1.5	-0.25	6.74	3.46	-0.72
4	-1.5	-0.30	4.83	1.50	-0.76
4	-1.6	-0.15	21.69	10.59	-2.30
4	-1.6	-0.20	11.04	5.53	-1.00
4	-1.6	-0.25	6.32	3.47	-0.95
4	-1.6	-0.30	3.93	1.45	
4	-1.7	-0.15	20.90	2.86	
4	-1.7	-0.20	9.44	1.09	-0.78
4	-1.7	-0.25	7.55	0.95	-1.05
4	-1.7	-0.30	3.75	1.60	
4	-1.8	-0.15	22.85	7.45	
4	-1.8	-0.20	11.79	0.74	-1.67
4	-1.8	-0.25	4.39	-0.80	-1.40
4	-1.8	-0.30	1.17	-0.36	

4	-1.9	-0.15	21.56	2.78	-2.31
4	-1.9	-0.20	10.81	-4.19	-1.32
4	-1.9	-0.25	6.87	0.11	-1.15
4	-2	-0.15	20.72		
4	-2	-0.20	7.62	-0.10	-0.84
4	-2	-0.25	5.11	0.90	-0.16
4	-2.1	-0.15	20.33	0.35	
4	-2.1	-0.20	10.23	-4.90	-1.62
4	-2.1	-0.25	5.98	-4.45	
4	-2.2	-0.15	24.39		
4	-2.2	-0.20	10.56		
4	-2.2	-0.25	9.07		
4	-2.3	-0.15	20.73		
4	-2.3	-0.20	11.84	-5.72	
4	-2.4	-0.15	16.09		
4	-2.4	-0.20	10.27		

Table A2- 13. Line 3-Test 1

5.64	-0.6	-0.15	13.53	5.24	0.09
5.64	-0.6	-0.20	10.17	5.13	-0.15
5.64	-0.6	-0.25	6.07	5.02	-0.02
5.64	-0.6	-0.30	3.60	4.22	0.53
5.64	-0.6	-0.35	7.71	3.55	-0.11
5.64	-0.6	-0.40	3.87	2.95	
5.64	-0.7	-0.15	12.02	7.51	-1.47
5.64	-0.7	-0.20	9.36	4.93	-1.56
5.64	-0.7	-0.25	6.77	5.19	-0.95
5.64	-0.7	-0.30	7.32	4.34	-1.04
5.64	-0.7	-0.35	7.13	2.44	-0.94
5.64	-0.7	-0.40	4.60	0.30	
5.64	-0.8	-0.15	17.26	6.64	
5.64	-0.8	-0.20	9.53	4.79	-1.72
5.64	-0.8	-0.25	9.09	3.03	-0.58
5.64	-0.8	-0.30	8.69	3.51	-0.94
5.64	-0.8	-0.35	7.49	1.99	-1.21
5.64	-0.8	-0.40	1.72	-0.02	
5.64	-0.9	-0.15	11.72	6.59	-1.58
5.64	-0.9	-0.20	10.17	6.29	-0.99

5.64	-0.9	-0.25	8.00	3.41	-0.72
5.64	-0.9	-0.30	6.10	3.26	-0.96
5.64	-0.9	-0.35	7.11	2.05	-1.25
5.64	-1	-0.15	14.64	7.59	-2.61
5.64	-1	-0.20	10.93	6.12	-2.03
5.64	-1	-0.25	8.12	5.43	-1.80
5.64	-1	-0.30	7.59	4.43	-1.49
5.64	-1	-0.35	5.28	2.57	-0.90
5.64	-1	-0.40	-4.60	-1.33	
5.64	-1.1	-0.15	17.65	10.73	-3.35
5.64	-1.1	-0.20	9.18	6.52	-1.80
5.64	-1.1	-0.25	7.96	6.36	-1.68
5.64	-1.1	-0.30	7.13	5.39	-1.42
5.64	-1.1	-0.35	4.16	4.08	-1.40
5.64	-1.2	-0.15	10.08	2.08	0.26
5.64	-1.2	-0.20	8.65	1.70	0.57
5.64	-1.2	-0.25	7.55	0.38	0.23
5.64	-1.2	-0.30	6.00	2.04	-0.33
5.64	-1.2	-0.35	-0.14	-0.12	0.01
5.64	-1.3	-0.15	21.27	10.80	-3.21
5.64	-1.3	-0.20	9.80	5.25	-1.59
5.64	-1.3	-0.25	8.27	3.04	-0.60
5.64	-1.3	-0.30	5.91	3.95	-0.96
5.64	-1.4	-0.15	22.32	9.41	-2.31
5.64	-1.4	-0.20	11.30	5.36	-1.04
5.64	-1.4	-0.25	8.72	3.17	-0.85
5.64	-1.4	-0.30	4.83	2.19	-0.61
5.64	-1.5	-0.15	12.50	2.98	0.03
5.64	-1.5	-0.20	8.95	1.23	0.48
5.64	-1.5	-0.25	7.09	0.09	-0.29
5.64	-1.5	-0.30	2.43	-1.70	0.04
5.64	-1.6	-0.15	19.59	9.58	-1.25
5.64	-1.6	-0.20	8.79	2.35	0.12
5.64	-1.6	-0.25	7.65	3.51	-0.24
5.64	-1.6	-0.30	2.56	2.34	
5.64	-1.7	-0.15	21.54	10.07	-2.18
5.64	-1.7	-0.20	10.17	4.96	-1.15
5.64	-1.7	-0.25	4.86	2.81	-0.55
5.64	-1.7	-0.30	-2.14	-0.58	
5.64	-1.8	-0.15	22.12	8.52	-1.79

5.64	-1.8	-0.20	10.99	4.75	-1.17
5.64	-1.8	-0.25	5.98	1.96	-0.94
5.64	-1.8	-0.30	-1.03	1.82	
5.64	-1.9	-0.15	17.42	5.18	-1.47
5.64	-1.9	-0.20	7.16	2.99	-0.41
5.64	-1.9	-0.25	6.73		
5.64	-2	-0.15	21.35	4.88	-1.51
5.64	-2	-0.20	10.08	1.04	-0.50
5.64	-2	-0.25	13.66	10.69	
5.64	-2.1	-0.15	18.40	4.85	-1.68
5.64	-2.1	-0.20	6.95	0.27	-0.68
5.64	-2.1	-0.25	-3.96	0.92	
5.64	-2.2	-0.15	12.01	-2.84	-1.26
5.64	-2.2	-0.20	3.70	-2.53	
5.64	-2.3	-0.15	10.62	-5.45	-0.71
5.64	-2.3	-0.20	0.44	-1.72	
5.64	-2.4	-0.15	7.55	-6.75	-0.28
5.64	-2.4	-0.20	-0.70	1.20	
5.64	-2.5	-0.15	7.45	-7.92	-0.44
5.64	-2.6	-0.15	7.35	-9.46	
5.64	-2.7	-0.15	3.85	-8.91	0.70

Table A2- 14. Line 1-Test 2

Long-shore Distance (m)	**Cross-shore Distance (m)**	**Depth relating to S.W.L. (m)**	**Vy (cm/s)**	**Vx (cm/s)**	**Vz (cm/s)**
2	-0.6	-0.10	6.68	3.57	-1.08
2	-0.6	-0.15	-1.54	5.26	-1.18
2	-0.6	-0.20	-3.32	1.50	-0.56
2	-0.6	-0.25	-4.69	-0.36	1.16
2	-0.6	-0.30	-3.75	-0.31	-0.64
2	-0.6	-0.35	-2.36	5.63	-0.64
2	-0.6	-0.40	-2.48	8.65	-0.57
2	-0.6	-0.45	-0.01	7.18	-0.93
2	-0.7	-0.10	7.56	2.01	-0.82
2	-0.7	-0.15	8.42	2.14	-1.35
2	-0.7	-0.20	4.77	6.19	-1.08
2	-0.7	-0.25	3.41	4.68	-0.64
2	-0.7	-0.30	7.64	3.96	-0.50

2	-0.7	-0.35	5.54	2.93	-0.14
2	-0.7	-0.40	6.07	3.78	-0.30
2	-0.7	-0.45	4.17	5.18	-0.90
2	-0.8	-0.15	16.85	4.61	-1.90
2	-0.8	-0.20	13.15	1.99	-0.87
2	-0.8	-0.25	16.96	1.57	-0.06
2	-0.8	-0.30	18.10	12.41	-1.67
2	-0.8	-0.35	3.13	12.17	-0.08
2	-0.8	-0.40	6.11	7.73	-0.65
2	-0.8	-0.45	3.12	9.40	
2	-0.9	-0.10	18.20	-2.58	-0.21
2	-0.9	-0.15	20.95	4.05	-0.72
2	-0.9	-0.20	6.13	9.53	-0.77
2	-0.9	-0.25	7.02	7.98	-1.32
2	-0.9	-0.30	8.23	13.74	-0.67
2	-0.9	-0.35	3.84	13.21	-0.56
2	-0.9	-0.40	8.54	13.41	-0.87
2	-0.9	-0.45	1.89	10.37	-1.44
2	-1	-0.10	18.86	7.82	-1.72
2	-1	-0.15	16.80	1.95	-1.15
2	-1	-0.20	13.11	9.25	-0.27
2	-1	-0.25	5.77	8.46	-0.45
2	-1	-0.30	2.66	7.05	-0.27
2	-1	-0.35	5.69	8.86	-0.37
2	-1	-0.40	6.96	11.15	-0.72
2	-1	-0.45	5.05	10.41	-1.32
2	-1.1	-0.10	21.04	2.92	-0.54
2	-1.1	-0.15	14.90	4.78	-1.44
2	-1.1	-0.20	6.10	7.07	-1.53
2	-1.1	-0.25	7.98	10.18	-0.87
2	-1.1	-0.30	1.89	10.54	0.04
2	-1.1	-0.35	6.42	11.96	-0.72
2	-1.1	-0.40	2.64	11.48	-1.02
2	-1.1	-0.45	-0.03	5.20	0.12
2	-1.2	-0.10	20.00	-1.46	-0.92
2	-1.2	-0.15	15.15	4.04	-0.62
2	-1.2	-0.20	12.28	4.32	-1.10
2	-1.2	-0.25	4.91	12.89	-0.13
2	-1.2	-0.30	4.26	8.60	-1.07
2	-1.2	-0.35	12.37	8.85	-1.17

2	-1.2	-0.40	9.20	15.45	-1.70
2	-1.2	-0.45	3.83	12.04	
2	-1.3	-0.10	13.51	0.24	-0.62
2	-1.3	-0.15	13.17	3.31	-1.43
2	-1.3	-0.20	14.08	4.66	-0.75
2	-1.3	-0.25	12.78	5.36	-0.89
2	-1.3	-0.30	9.29	5.12	-0.81
2	-1.3	-0.35	5.29	9.59	-0.56
2	-1.3	-0.40	0.26	10.35	-0.25
2	-1.3	-0.45	3.54	6.65	-0.84
2	-1.4	-0.10	17.83	2.19	-1.91
2	-1.4	-0.15	18.83	3.06	-0.66
2	-1.4	-0.20	14.96	2.60	-0.62
2	-1.4	-0.25	8.45	7.95	0.10
2	-1.4	-0.30	7.20	11.26	-0.31
2	-1.4	-0.35	7.45	14.09	-1.06
2	-1.4	-0.40	4.59	13.99	-1.16
2	-1.4	-0.45	2.58	7.78	-0.58
2	-1.5	-0.10	19.05		-0.37
2	-1.5	-0.15	20.62	-0.08	-0.79
2	-1.5	-0.20	16.12	4.05	-0.28
2	-1.5	-0.25	6.72	2.31	-0.32
2	-1.5	-0.30	7.11	4.13	-0.34
2	-1.5	-0.35	8.65	5.58	-0.80
2	-1.5	-0.40	6.41	5.09	-1.13
2	-1.5	-0.45	3.38	8.82	
2	-1.6	-0.10	8.57	-1.39	-0.43
2	-1.6	-0.15	2.29	1.22	-0.07
2	-1.6	-0.20	8.93	-0.44	-1.42
2	-1.6	-0.25	10.90	-1.52	-1.33
2	-1.6	-0.30	7.93	3.46	-0.99
2	-1.6	-0.35	1.09	12.51	-0.70
2	-1.6	-0.40	2.17	4.88	-0.61
2	-1.6	-0.45	1.90	4.17	
2	-1.7	-0.10		0.23	-1.56
2	-1.7	-0.15	20.68	1.42	-1.26
2	-1.7	-0.20	19.88	3.26	-0.10
2	-1.7	-0.25	1.36	4.40	-0.43
2	-1.7	-0.30	14.25	5.32	-1.05
2	-1.7	-0.35	10.09	11.10	-1.48

2	-1.7	-0.40	-0.94	4.96	-0.34
2	-1.7	-0.45	0.84	2.83	
2	-1.8	-0.15	8.33	-1.06	-1.26
2	-1.8	-0.20	10.04	0.73	-0.97
2	-1.8	-0.25	9.95	4.12	-0.79
2	-1.8	-0.30	5.87	8.12	-0.70
2	-1.8	-0.35	-3.00	10.50	0.92
2	-1.8	-0.40	-0.86	3.49	-0.04
2	-1.8	-0.45	1.89	1.25	
2	-1.9	-0.15	18.79	1.28	-0.99
2	-1.9	-0.20	9.83	0.25	-0.30
2	-1.9	-0.25	9.87	-1.50	-1.00
2	-1.9	-0.30	16.30	-0.55	-1.48
2	-1.9	-0.35	17.66	4.94	-3.44
2	-1.9	-0.40	7.04	7.51	
2	-1.9	-0.45	2.78	3.23	
2	-2	-0.15	10.86	-8.79	-1.05
2	-2	-0.20	14.20	-10.32	-1.22
2	-2	-0.25	12.16	-3.45	-0.97
2	-2	-0.30	14.84	-1.42	-2.09
2	-2	-0.35	11.89	5.79	-1.57
2	-2	-0.40	6.77	1.49	-0.71
2	-2.1	-0.15	21.73	-1.65	-0.52
2	-2.1	-0.20	19.53	-0.34	-1.67
2	-2.1	-0.25	15.89	0.25	-0.81
2	-2.1	-0.30	13.25	-1.03	-1.75
2	-2.1	-0.35	11.05	-2.57	-2.14
2	-2.1	-0.40	2.53	3.75	
2	-2.2	-0.15	10.67	-7.70	-0.92
2	-2.2	-0.20	15.86	-10.81	-1.21
2	-2.2	-0.25	16.75	-4.04	-1.35
2	-2.2	-0.30	6.44	4.42	-0.53
2	-2.2	-0.35	11.78	-1.30	-1.18
2	-2.2	-0.40		-3.35	
2	-2.3	-0.10	11.54	-7.66	-3.28
2	-2.3	-0.15	10.33	-12.65	-1.30
2	-2.3	-0.20	8.82	-8.00	-0.41
2	-2.3	-0.25	16.18	-8.34	-1.69
2	-2.3	-0.30	8.83	-4.56	-0.86
2	-2.3	-0.35	0.61	3.30	-0.63

2	-2.4	-0.10	2.43	-8.68	-0.82
2	-2.4	-0.15	11.63	-15.43	-1.08
2	-2.4	-0.20	11.01	-11.42	-0.36
2	-2.4	-0.25	13.11	-12.32	-0.74
2	-2.4	-0.30	6.03	-6.21	-0.15
2	-2.4	-0.35	4.08	-3.30	0.07
2	-2.5	-0.10	4.44	-7.13	-2.37
2	-2.5	-0.15	10.11	-13.12	-0.10
2	-2.5	-0.20	9.54	-12.38	-0.53
2	-2.5	-0.25	14.72	-13.11	-1.51
2	-2.5	-0.30	7.62	-10.06	-1.12
2	-2.5	-0.35	4.13	-4.93	-1.30
2	-2.6	-0.10	10.96	-13.99	-0.70
2	-2.6	-0.15	14.00	-16.50	-0.39
2	-2.6	-0.20	11.41	-13.90	-0.70
2	-2.6	-0.25	13.08	-11.83	-0.85
2	-2.6	-0.30	13.29	-11.88	-1.00
2	-2.7	-0.10	5.11	-15.63	-1.21
2	-2.7	-0.15	15.41	-23.64	-0.85
2	-2.7	-0.20	11.91	-20.76	-0.27
2	-2.7	-0.25	7.11	-12.31	-0.71
2	-2.7	-0.30	9.57	-10.67	-1.46
2	-2.8	-0.10	6.24	-0.70	-0.12
2	-2.8	-0.15	9.18	0.01	-0.48
2	-2.8	-0.20	13.51	-18.52	-1.40
2	-2.8	-0.25	13.99	-17.67	-1.74
2	-2.8	-0.30	8.04	-8.98	-1.12
2	-2.9	-0.10	14.51	-20.11	-0.74
2	-2.9	-0.15	16.00	-14.02	0.08
2	-2.9	-0.20	12.05	-14.52	-0.87
2	-2.9	-0.25	4.49	-1.38	-0.44
2	-3	-0.10	0.68	-10.80	-1.76
2	-3	-0.15	13.66	-16.45	-0.58
2	-3	-0.20	10.29	-6.36	-0.47
2	-3	-0.25	7.87	-10.24	-1.64
2	-3	-0.30		0.36	-0.24
2	-3.1	-0.10	19.05	-25.06	-0.48
2	-3.1	-0.15	12.97	-17.54	-0.72
2	-3.1	-0.20	11.35	-9.65	-1.06
2	-3.1	-0.25	3.33	-5.86	-0.46

2	-3.2	-0.10	14.46	-13.23	-1.31
2	-3.2	-0.15	12.36	-15.27	-0.51
2	-3.2	-0.20	10.55	-7.47	-0.59
2	-3.3	-0.10	10.77	-11.08	-0.36
2	-3.3	-0.15	8.61	-5.48	-0.96
2	-3.3	-0.20	8.46	0.44	
2	-3.4	-0.10	6.15	-3.05	-0.22
2	-3.4	-0.15	10.00	-0.17	-1.18
2	-3.4	-0.20	9.51	1.30	-0.94
2	-3.5	-0.10	9.37	-0.48	-2.32
2	-3.5	-0.15	8.47	-0.55	-1.33
2	-3.5	-0.20	5.38	-0.39	-1.53
2	-3.6	-0.10	9.09	-4.49	-1.11
2	-3.6	-0.15	5.66	1.92	-0.36
2	-3.6	-0.20	0.39	2.55	0.97
2	-3.7	-0.10	5.69	1.28	-0.82
2	-3.7	-0.15	4.96	3.03	-0.67
2	-3.7	-0.20	1.49	0.68	-0.04
2	-3.8	-0.10	4.17	1.55	-1.14
2	-3.8	-0.15	4.81	2.64	-0.92
2	-3.9	-0.10	2.99	3.27	-1.20
2	-3.9	-0.15	2.55	1.57	-0.44
2	-4	-0.10	2.72	-0.33	-2.54
2	-4.1	-0.10	15.90		
2	-4.2	-0.10			-0.27

Table A2- 15. Line 2-Test 2

Long-shore Distance (m)	**Cross-shore Distance (m)**	**Depth relating to S.W.L. (m)**	**Vy (cm/s)**	**Vx (cm/s)**	**Vz (cm/s)**
4	-0.6	-0.15	4.18	9.33	-0.22
4	-0.6	-0.20	4.73	13.04	0.49
4	-0.6	-0.25	2.01	14.51	-0.77
4	-0.6	-0.30	0.65	16.37	-1.09
4	-0.6	-0.35	-1.98	12.23	-0.57
4	-0.6	-0.40	2.59	9.35	-0.46
4	-0.7	-0.10	-3.85	6.02	-0.13
4	-0.7	-0.15	4.05	10.22	-0.09
4	-0.7	-0.20	-2.02	11.17	0.00

4	-0.7	-0.25	-4.81	10.70	-0.13
4	-0.7	-0.30	-2.73	12.49	-0.74
4	-0.7	-0.35	-0.18	9.48	-0.37
4	-0.7	-0.40	3.02	6.52	-1.55
4	-0.8	-0.10	-0.50	7.80	0.11
4	-0.8	-0.15	1.87	11.79	-0.41
4	-0.8	-0.20	0.55	9.96	-0.06
4	-0.8	-0.25	-2.37	11.91	-0.33
4	-0.8	-0.30	-4.12	10.11	0.18
4	-0.8	-0.35	0.78	9.58	-0.28
4	-0.8	-0.40	2.66	3.90	
4	-0.9	-0.10	-0.41		-0.14
4	-0.9	-0.15	-0.15	12.72	-0.69
4	-0.9	-0.20	-2.99	7.80	-0.05
4	-0.9	-0.25	-2.06	8.49	0.02
4	-0.9	-0.30	-2.09	8.33	-0.23
4	-0.9	-0.35	0.25	9.34	-0.35
4	-0.9	-0.40		1.88	1.20
4	-1	-0.10	7.39	10.81	-0.58
4	-1	-0.15	-1.18	12.49	-0.40
4	-1	-0.20	-2.21	11.64	-0.30
4	-1	-0.25	-1.89	8.44	-0.47
4	-1	-0.30	-1.75	9.87	-0.33
4	-1	-0.35	2.14	7.90	-0.93
4	-1.1	-0.10	2.90	-1.77	-0.62
4	-1.1	-0.15	7.07	4.49	-0.68
4	-1.1	-0.20	0.35	2.16	0.12
4	-1.1	-0.25	-0.68	-8.75	0.15
4	-1.1	-0.30	1.35	-9.20	-0.02
4	-1.1	-0.35	3.57	-1.09	-0.53
4	-1.2	-0.10	3.60	-3.26	-1.05
4	-1.2	-0.15	6.85	-2.22	-1.14
4	-1.2	-0.20	4.53	-3.94	-1.03
4	-1.2	-0.25	4.11	-5.06	-0.86
4	-1.2	-0.30	3.96	-1.77	-1.21
4	-1.2	-0.35	0.54	-0.81	-1.50
4	-1.3	-0.15	9.83	-1.98	-1.43
4	-1.3	-0.20	6.45	-4.06	-1.16
4	-1.3	-0.25	4.87	-3.56	-1.50
4	-1.3	-0.30	6.36	-1.65	-1.64

4	-1.3	-0.35	3.14	-0.44	
4	-1.4	-0.10	4.36	-4.92	-0.99
4	-1.4	-0.15	6.96	-4.38	-1.07
4	-1.4	-0.20	5.96	-4.00	-0.78
4	-1.4	-0.25	6.71	-3.78	-0.88
4	-1.4	-0.30	4.74	-0.95	-0.54
4	-1.5	-0.10	4.75	-3.52	-0.72
4	-1.5	-0.15	7.69	-6.68	-1.33
4	-1.5	-0.20	4.99	-4.38	-1.02
4	-1.5	-0.25	5.58	-3.80	-1.19
4	-1.5	-0.30	5.53	-2.80	-1.27
4	-1.6	-0.10	11.34	-4.98	-1.53
4	-1.6	-0.15	5.80	0.40	-1.00
4	-1.6	-0.20	4.46	-4.66	-0.92
4	-1.6	-0.25	5.03	-7.84	-1.55
4	-1.6	-0.30	4.08	-3.38	-1.41
4	-1.7	-0.10	10.39	-4.32	-1.79
4	-1.7	-0.15	5.10	-8.79	-1.01
4	-1.7	-0.20	5.45	-6.20	-1.24
4	-1.7	-0.25	7.85	-4.52	-1.54
4	-1.7	-0.30	5.19	-0.56	
4	-1.8	-0.10	7.82	-4.56	-1.48
4	-1.8	-0.15	5.95	-5.17	-1.06
4	-1.8	-0.20	7.27	-9.46	-1.64
4	-1.8	-0.25	6.71	-4.58	-1.47
4	-1.9	-0.10	-4.36	-11.87	-0.20
4	-1.9	-0.15	7.77	-6.98	-1.34
4	-1.9	-0.20	7.15	-8.67	-1.38
4	-1.9	-0.25	5.52	-3.55	
4	-2	-0.10	1.59	-8.94	-0.89
4	-2	-0.15	7.32	-11.28	-1.14
4	-2	-0.20	7.56	-7.71	-1.35
4	-2.1	-0.10	2.31	-8.42	-0.82
4	-2.1	-0.15	9.14	-10.64	-1.04
4	-2.1	-0.20	8.50	-9.82	-0.64
4	-2.2	-0.10	10.27	-9.69	-1.33
4	-2.2	-0.15	11.32	-11.49	-1.64
4	-2.2	-0.20	8.05	-10.02	-1.99
4	-2.3	-0.10	4.01		
4	-2.3	-0.15	13.26	-5.77	-1.66

4	-2.3	-0.20	6.46	-7.83	-1.00
4	-2.4	-0.10	1.58		
4	-2.4	-0.15	9.81	-15.40	-1.11
4	-2.4	-0.20	18.06	-1.65	
4	-2.5	-0.10	9.76	-5.80	
4	-2.5	-0.15	10.18	-14.02	-1.11
4	-2.6	-0.10	13.61	-7.47	-2.59
4	-2.6	-0.15	13.66	-12.47	-1.31
4	-2.6	-0.20		-11.23	
4	-2.7	-0.10	11.96		
4	-2.7	-0.15	10.28	-15.83	-1.13
4	-2.7	-0.20	-1.69	-13.67	-1.21
4	-2.9	-0.10	10.43		
4	-2.9	-0.15	13.11	-14.65	-1.30
4	-2.9	-0.20	0.57	-11.55	-1.03
4	-3	-0.15	12.74	-12.36	-1.25
4	-3	-0.20	-1.81	-13.81	0.32
4	-3.1	-0.15	11.89	-10.46	0.91
4	-3.1	-0.20	5.53	-11.53	0.34
4	-3.2	-0.10	8.81		
4	-3.2	-0.15	12.03	-6.90	0.88
4	-3.2	-0.20	5.16	-6.04	0.83
4	-3.3	-0.10		-3.86	0.46
4	-3.3	-0.15	7.58	-5.35	2.23
4	-3.3	-0.20	2.06	-6.48	1.28
4	-3.4	-0.10			0.84
4	-3.4	-0.15	10.02	-9.41	-0.07
4	-3.4	-0.20	3.99	-3.48	-0.40
4	-3.6	-0.10	14.72	-17.16	0.09
4	-3.6	-0.15	4.55	-4.96	-0.18
4	-3.6	-0.20	0.88	-1.20	-0.21
4	-3.7	-0.10	8.87	-10.96	0.07
4	-3.7	-0.15	9.58	-7.55	-1.05
4	-3.7	-0.20	3.54		
4	-3.8	-0.10	14.82	-14.74	-0.31
4	-3.8	-0.15	7.98	-9.29	-0.06

Table A2- 16. Line 3-Test 2

Long-shore Distance (m)	Cross-shore Distance (m)	Depth relating to S.W.L. (m)	Vy (cm/s)	Vx (cm/s)	Vz (cm/s)
5.64	-0.6	-0.15	1.22	12.38	0.18
5.64	-0.6	-0.20	-0.13	2.31	0.13
5.64	-0.6	-0.25	0.59	-4.78	0.82
5.64	-0.6	-0.30	-1.77	-8.57	0.34
5.64	-0.6	-0.35	-1.42	-5.68	-0.18
5.64	-0.6	-0.40	-3.63	-3.80	-0.04
5.64	-0.7	-0.15	-0.14	1.96	-0.87
5.64	-0.7	-0.20	1.35	-4.16	0.27
5.64	-0.7	-0.25	1.76	-4.09	0.13
5.64	-0.7	-0.30	1.93	-4.74	0.10
5.64	-0.7	-0.35	-0.43	-5.63	-0.27
5.64	-0.7	-0.40	-4.12	-3.77	0.04
5.64	-0.8	-0.15	3.41	-5.00	0.80
5.64	-0.8	-0.20	0.84	-7.27	1.08
5.64	-0.8	-0.25	0.86	-5.38	0.72
5.64	-0.8	-0.30	-1.34	-5.43	0.11
5.64	-0.8	-0.35	-5.81	-4.87	0.55
5.64	-0.8	-0.40	-3.78	-3.89	0.09
5.64	-0.9	-0.15	1.16	-2.85	1.26
5.64	-0.9	-0.20	0.76	-3.63	1.63
5.64	-0.9	-0.25	-0.58	-4.98	0.89
5.64	-0.9	-0.30	-0.96	-4.56	0.67
5.64	-0.9	-0.35	-0.59	-4.07	0.05
5.64	-0.9	-0.40	-2.86	-2.86	
5.64	-1	-0.20	4.84	-1.67	0.90
5.64	-1	-0.25	-0.03	-10.75	0.16
5.64	-1	-0.30	0.62	-11.74	-0.44
5.64	-1	-0.35	1.25	-5.66	-0.04
5.64	-1.1	-0.15	-0.17	-2.89	0.41
5.64	-1.1	-0.20	-1.25	-6.79	0.22
5.64	-1.1	-0.25	-1.50	-5.74	0.33
5.64	-1.1	-0.30	0.29	-5.42	0.31
5.64	-1.1	-0.35	-2.37	-1.00	0.29
5.64	-1.1	-0.40	0.40	-2.35	-0.20
5.64	-1.2	-0.15	1.04	-5.23	0.36

5.64	-1.2	-0.20	-1.82	-7.55	0.45
5.64	-1.2	-0.25	-2.19	-6.92	0.95
5.64	-1.2	-0.30	-0.32	-5.45	0.42
5.64	-1.2	-0.35	2.55	-0.78	-0.08
5.64	-1.3	-0.15	-0.07	1.19	1.25
5.64	-1.3	-0.20	0.05	2.42	1.68
5.64	-1.3	-0.25	1.01	1.30	1.03
5.64	-1.3	-0.30	2.93	-2.54	-0.02
5.64	-1.3	-0.35	1.17	-3.23	-0.70
5.64	-1.4	-0.15	-1.45	-10.27	-0.05
5.64	-1.4	-0.20	0.14	-7.34	0.05
5.64	-1.4	-0.25	0.32	-6.55	0.26
5.64	-1.4	-0.30	0.84	-5.89	0.24
5.64	-1.4	-0.35	0.85	-0.72	0.06
5.64	-1.5	-0.15	-2.12	-8.69	0.03
5.64	-1.5	-0.20	-3.45	-8.34	0.18
5.64	-1.5	-0.25	1.64	-2.68	0.13
5.64	-1.5	-0.30	4.33	-0.35	-0.11
5.64	-1.6	-0.15	0.09	-5.49	-0.14
5.64	-1.6	-0.20	-2.33	-8.21	0.18
5.64	-1.6	-0.25	0.73	-8.41	-0.30
5.64	-1.6	-0.30	-0.04	-3.24	-0.78
5.64	-1.7	-0.10			1.12
5.64	-1.7	-0.15	-0.80	-6.49	0.45
5.64	-1.7	-0.20	-1.86	-5.22	0.37
5.64	-1.7	-0.25	0.22	-4.52	-0.20
5.64	-1.7	-0.30	2.92	-0.03	-0.33
5.64	-1.8	-0.10	-0.89	0.72	0.34
5.64	-1.8	-0.15	1.66	3.76	-0.14
5.64	-1.8	-0.20	1.71	5.22	0.05
5.64	-1.8	-0.25	5.09	3.87	-0.28
5.64	-1.9	-0.10	2.99	-8.17	-0.26
5.64	-1.9	-0.15	2.02	-9.06	-0.40
5.64	-1.9	-0.20	-0.89	-10.13	-0.22
5.64	-1.9	-0.25	2.84	-5.00	-0.37
5.64	-2	-0.10	-0.15	-5.27	-0.13
5.64	-2	-0.15	-0.88	-5.60	-0.55
5.64	-2	-0.20	-0.15	-4.86	-0.62
5.64	-2	-0.25	6.34	-0.44	-1.30
5.64	-2.1	-0.10	2.12	4.43	-0.17

5.64	-2.1	-0.15	5.01	3.43	0.24
5.64	-2.1	-0.20	3.69	0.45	0.13
5.64	-2.2	-0.10	1.07	2.44	-0.81
5.64	-2.2	-0.15	1.62	4.13	-0.95
5.64	-2.2	-0.20	1.54	2.84	-0.49
5.64	-2.3	-0.10	1.02	-0.75	-0.62
5.64	-2.3	-0.15	5.84	2.26	-0.86
5.64	-2.3	-0.20	4.13	1.25	-1.10
5.64	-2.4	-0.10	5.37	-0.69	-2.10
5.64	-2.4	-0.15	3.47	-3.85	-0.98
5.64	-2.4	-0.20	2.36	-1.90	-0.73
5.64	-2.5	-0.10	2.94	-2.76	-1.94
5.64	-2.5	-0.15	2.37	-5.00	-1.05
5.64	-2.5	-0.20	3.85	-1.37	-0.37
5.64	-2.6	-0.10	8.27	-2.04	-1.60
5.64	-2.6	-0.15	3.31	-4.38	-1.32
5.64	-2.6	-0.20	-2.73	-4.17	-0.81
5.64	-2.7	-0.10	6.89	-3.78	-2.50
5.64	-2.7	-0.15	2.36	-6.76	-1.62
5.64	-2.7	-0.20	1.98	-4.15	-1.34
5.64	-2.8	-0.10	15.24	-2.79	
5.64	-2.8	-0.15	2.35	-8.11	-0.96
5.64	-2.8	-0.20	0.96	-2.21	-0.69
5.64	-2.9	-0.10	9.18	-5.25	-2.48
5.64	-2.9	-0.15	1.10	-8.39	-1.32
5.64	-2.9	-0.20	-2.59	-4.96	-0.62
5.64	-3	-0.10	7.18	-2.43	-2.56
5.64	-3	-0.15	1.25	-5.67	-1.80
5.64	-3	-0.20	-5.11	-4.42	-1.59
5.64	-3.1	-0.10	4.70	-3.31	-1.31
5.64	-3.1	-0.15	2.92	-1.89	-0.99
5.64	-3.1	-0.20	-6.57	-0.44	-0.31
5.64	-3.2	-0.15	6.08	0.89	-0.74
5.64	-3.2	-0.20	-8.13	-4.82	-0.32
5.64	-3.3	-0.15	4.51	-0.61	-0.30
5.64	-3.3	-0.20	-9.40	-0.39	0.40
5.64	-3.4	-0.15	6.11	0.77	0.71
5.64	-3.4	-0.20	-4.47	0.23	0.10
5.64	-3.5	-0.10	4.65	-2.60	-1.38
5.64	-3.5	-0.15	15.35	-9.28	1.39

5.64	-3.5	-0.20	-3.81		

Table A2- 17. Line 1-Test 3

Long-shore Distance (m)	Cross-shore Distance (m)	Depth relating to S.W.L. (m)	Vy (cm/s)	Vx (cm/s)	Vz (cm/s)
2	-0.6	-0.10	13.51	-8.17	-0.23
2	-0.6	-0.15	6.78	-5.14	0.54
2	-0.6	-0.20	3.67	-3.85	0.64
2	-0.6	-0.25	1.50	-3.28	0.50
2	-0.6	-0.30	0.40	-3.41	0.02
2	-0.6	-0.35	-0.80	-2.35	-0.11
2	-0.6	-0.40	0.59	-0.97	
2	-0.8	-0.10	4.98	-4.89	-0.54
2	-0.8	-0.15	3.86	-5.13	-0.91
2	-0.8	-0.20	2.68	-5.06	-0.74
2	-0.8	-0.25	0.46	-2.31	-0.50
2	-0.8	-0.30	-0.17	-2.56	0.27
2	-0.8	-0.35	-1.15	-2.57	-0.14
2	-0.8	-0.40	-1.61	-1.74	0.30
2	-1	-0.10	6.37	-5.76	0.09
2	-1	-0.15	4.23	-6.02	0.31
2	-1	-0.20	2.50	-4.75	0.17
2	-1	-0.25	1.12	-4.10	0.35
2	-1	-0.30	-0.36	-3.31	0.30
2	-1	-0.35	-0.97	-2.49	0.39
2	-1	-0.40	-0.67	-2.14	
2	-1.2	-0.10	9.31	-11.69	-0.24
2	-1.2	-0.15	5.55	-6.74	0.66
2	-1.2	-0.20	2.84	-4.17	1.49
2	-1.2	-0.25	2.05	-4.06	0.70
2	-1.2	-0.30	0.63	-3.59	0.52
2	-1.2	-0.35	0.68	-3.19	0.58
2	-1.2	-0.40	1.54	-2.29	-0.02
2	-1.4	-0.10	10.32	-12.71	0.03
2	-1.4	-0.15	8.51	-11.31	0.28
2	-1.4	-0.20	4.43	-7.76	0.39
2	-1.4	-0.25	2.89	-6.20	0.57
2	-1.4	-0.30	2.73	-5.10	0.81

2	-1.4	-0.35	2.05	-4.96	0.77
2	-1.4	-0.40	1.55	-4.58	0.18
2	-1.6	-0.10	9.89	-12.30	0.60
2	-1.6	-0.15	8.98	-12.88	0.04
2	-1.6	-0.20	7.12	-10.83	-0.42
2	-1.6	-0.25	5.64	-10.31	-0.04
2	-1.6	-0.30	4.66	-9.92	-0.02
2	-1.6	-0.35	5.02	-9.12	-0.30
2	-1.6	-0.40	4.20	-6.49	-0.13
2	-1.8	-0.10	7.99	-9.75	0.12
2	-1.8	-0.15	8.80	-9.71	-0.45
2	-1.8	-0.20	6.80	-9.34	-0.08
2	-1.8	-0.25	6.47	-10.51	-0.78
2	-1.8	-0.30	5.61	-10.65	0.12
2	-1.8	-0.35	5.41	-10.84	-0.37
2	-1.8	-0.40	2.88	-5.96	-0.19
2	-2	-0.10	7.12	-5.20	-0.11
2	-2	-0.15	6.54	-6.37	-0.57
2	-2	-0.20	6.44	-7.27	-0.48
2	-2	-0.25	5.67	-10.71	-0.24
2	-2	-0.30	5.00	-9.97	-0.03
2	-2	-0.35	4.83	-11.33	-0.27
2	-2.2	-0.10	8.19	-4.59	0.13
2	-2.2	-0.15	7.63	-5.55	0.73
2	-2.2	-0.20	7.14	-7.09	0.55
2	-2.2	-0.25	5.66	-8.42	1.07
2	-2.2	-0.30	4.17	-7.49	0.18
2	-2.2	-0.35	0.60	-6.38	0.34
2	-2.4	-0.10	6.80	-2.86	0.32
2	-2.4	-0.15	7.50	-5.07	0.93
2	-2.4	-0.20	6.77	-5.61	0.60
2	-2.4	-0.25	5.48	-6.09	0.52
2	-2.4	-0.30	3.29	-6.07	
2	-2.6	-0.10	6.08	-1.51	0.03
2	-2.6	-0.15	7.18	-2.86	0.29
2	-2.6	-0.20	7.21	-4.64	0.23
2	-2.6	-0.25	6.17		0.16
2	-2.8	-0.10	5.00	0.29	0.03
2	-2.8	-0.15	5.79	-0.37	-0.09
2	-2.8	-0.20	6.55	-3.01	-0.23

2	-2.8	-0.25	6.11	-4.33	-0.35
2	-3	-0.10	5.85	2.19	0.03
2	-3	-0.15	6.77	1.17	0.04
2	-3	-0.20	6.39		0.21
2	-3	-0.25	0.38	-2.37	0.09
2	-3.2	-0.10	6.92	3.89	-0.01
2	-3.2	-0.15	10.13	3.41	-0.93
2	-3.2	-0.20	5.64	0.55	
2	-3.2	-0.25	3.00	-1.24	-0.26
2	-3.4	-0.10	9.12	7.10	-0.80
2	-3.4	-0.15	7.93	4.85	-0.53
2	-3.4	-0.20	5.61	0.77	-0.16
2	-3.6	-0.10	12.01	10.32	-2.09
2	-3.6	-0.15	4.28	2.61	
2	-3.6	-0.20	3.86	1.19	-1.16
2	-3.8	-0.10	11.27	9.59	-1.98
2	-3.8	-0.15	5.15	4.57	-0.79
2	-4	-0.10	8.24	7.10	-1.52
2	-4	-0.15	-2.71	0.84	0.11
2	-4.2	-0.10	2.47	1.86	0.24

Table A2- 18. Line 2-Test 3

Long-shore Distance (m)	**Cross-shore Distance (m)**	**Depth relating to S.W.L. (m)**	**Vy (cm/s)**	**Vx (cm/s)**	**Vz (cm/s)**
4	-0.6	-0.10	-1.74	-1.28	0.31
4	-0.6	-0.15	-0.60	-1.16	0.39
4	-0.6	-0.20	-0.49	-0.62	0.58
4	-0.6	-0.25	-0.26	-0.54	0.29
4	-0.6	-0.30	0.04	-0.33	0.18
4	-0.6	-0.35	-0.02	-1.04	
4	-0.8	-0.10	0.35	-1.27	0.33
4	-0.8	-0.15	0.27	-1.06	0.24
4	-0.8	-0.20	0.02	-0.92	0.23
4	-0.8	-0.25	0.19	-0.80	0.16
4	-0.8	-0.30	-0.23	-0.55	0.44
4	-0.8	-0.35	-0.21	-0.25	0.53
4	-1	-0.10	-0.38	-1.90	0.16

4	-1	-0.15	0.65	-1.62	0.16
4	-1	-0.20	0.37	-1.31	0.31
4	-1	-0.25	0.20	-1.19	0.38
4	-1	-0.30	0.53	-0.44	0.25
4	-1.2	-0.10	0.31	-1.81	0.26
4	-1.2	-0.15	0.63	-1.69	0.12
4	-1.2	-0.20	0.23	-1.59	0.09
4	-1.2	-0.25	0.26	-0.82	0.27
4	-1.2	-0.30	0.23	0.06	
4	-1.4	-0.10	1.31	-1.87	0.09
4	-1.4	-0.15	1.27	-1.26	0.39
4	-1.4	-0.20	0.36	-1.10	0.28
4	-1.4	-0.25		-0.10	0.36
4	-1.4	-0.30	0.24	0.93	0.27
4	-1.6	-0.10	1.30	-1.77	0.24
4	-1.6	-0.15	1.31	-1.37	0.28
4	-1.6	-0.20	1.00	-1.27	0.17
4	-1.6	-0.25	1.32	-0.37	-0.29
4	-1.8	-0.10	1.63	-1.34	0.23
4	-1.8	-0.15	2.40	-1.44	-0.50
4	-1.8	-0.20	0.72	-0.79	-0.17
4	-1.8	-0.25	-0.48	-1.51	-0.05
4	-2	-0.10	1.31	-1.88	-0.06
4	-2	-0.15	1.68	-1.26	-0.16
4	-2	-0.20	-0.41	-2.35	
4	-2.2	-0.10	3.13	-3.15	-0.61
4	-2.2	-0.15	2.02	-3.18	-0.59
4	-2.2	-0.20	-0.11	-2.32	
4	-2.4	-0.10	4.62	-4.29	-0.18
4	-2.4	-0.15	2.70	-3.72	0.19
4	-2.4	-0.20	-1.19	-2.50	
4	-2.6	-0.10	5.59	-6.71	-0.15
4	-2.6	-0.15	3.18	-4.38	-0.15
4	-2.6	-0.20	-0.24	-3.45	-0.20
4	-2.8	-0.10	7.41	-9.97	-0.14
4	-2.8	-0.15	4.35	-5.77	-0.05
4	-2.8	-0.20	-1.32	-2.10	0.25
4	-3	-0.10	10.21	-15.92	-0.49
4	-3	-0.15	5.41	-10.10	
4	-3.2	-0.10	11.33	-17.55	-0.89

4	-3.2	-0.15	4.27	-11.52	-0.50
4	-3.4	-0.10	10.19	-15.65	-0.32
4	-3.4	-0.15	-3.93		
4	-3.6	-0.10	9.62	-11.29	
4	-3.8	-0.10	7.01	-10.05	-0.94
4	-4	-0.10	3.25	-7.45	
4	-4.2	-0.10	-2.60	-4.31	-0.18

Table A2- 19. Line 3-Test 3

Long-shore Distance (m)	Cross-shore Distance (m)	Depth relating to S.W.L. (m)	Vy (cm/s)	Vx (cm/s)	Vz (cm/s)
5.64	-0.6	-0.10	1.49	-0.27	0.05
5.64	-0.6	-0.15	0.68	-1.29	0.39
5.64	-0.6	-0.20	0.29	-1.20	0.18
5.64	-0.6	-0.25	0.21	-1.63	0.22
5.64	-0.6	-0.30	-0.03	-1.52	0.16
5.64	-0.6	-0.35	0.35	-0.86	0.11
5.64	-0.8	-0.10	0.58	-1.25	-0.21
5.64	-0.8	-0.15	0.83	-0.79	-0.04
5.64	-0.8	-0.20	1.08	-0.55	0.14
5.64	-0.8	-0.25	1.32	-0.82	0.18
5.64	-0.8	-0.30	0.24	-0.77	0.02
5.64	-0.8	-0.35		-0.70	-0.27
5.64	-1	-0.10	1.48	-0.59	0.16
5.64	-1	-0.15	1.15	-0.51	0.40
5.64	-1	-0.20	0.57	-0.53	0.30
5.64	-1	-0.25	-0.24	-0.27	0.28
5.64	-1	-0.30	0.23	-0.66	-0.01
5.64	-1	-0.35	-0.06	0.15	-0.12
5.64	-1.2	-0.10	1.56	-0.45	-0.01
5.64	-1.2	-0.15	1.00	-0.69	-0.06
5.64	-1.2	-0.20	0.93	-0.92	0.07
5.64	-1.2	-0.25	0.96	-0.28	0.13
5.64	-1.2	-0.30	1.27	1.02	
5.64	-1.4	-0.10	1.81	-0.55	0.16
5.64	-1.4	-0.15	1.70	-0.42	-0.09
5.64	-1.4	-0.20	0.47	-0.56	0.02
5.64	-1.4	-0.25	0.17	-0.05	0.05

5.64	-1.4	-0.30	-0.92	0.20	0.25
5.64	-1.6	-0.10	1.33	-0.39	0.29
5.64	-1.6	-0.15	1.13	-0.42	-0.02
5.64	-1.6	-0.20	1.00	-0.43	0.27
5.64	-1.6	-0.25	0.93	0.16	0.19
5.64	-1.6	-0.30	-1.07	-0.28	0.10
5.64	-1.8	-0.10	1.95	-0.37	0.30
5.64	-1.8	-0.15	1.18	-0.60	0.26
5.64	-1.8	-0.20	0.41	-1.03	0.20
5.64	-1.8	-0.25	0.47	-0.93	-0.08
5.64	-2	-0.10	2.08	-0.46	0.23
5.64	-2	-0.15	0.71	-1.11	0.22
5.64	-2	-0.20	1.01		0.33
5.64	-2	-0.25	-0.43	0.27	0.15
5.64	-2.2	-0.10	1.92	-1.11	0.12
5.64	-2.2	-0.15	1.48	-0.90	0.06
5.64	-2.2	-0.20	-0.58		
5.64	-2.2	-0.25	-0.19	-1.03	1.22
5.64	-2.4	-0.10	3.46	-2.16	-0.18
5.64	-2.4	-0.15	1.89	-1.03	0.15
5.64	-2.4	-0.20	0.35	-0.78	0.18
5.64	-2.6	-0.10	2.89	-2.17	-0.27
5.64	-2.6	-0.15			0.22
5.64	-2.6	-0.20	-0.02	-1.56	0.21
5.64	-2.8	-0.10	2.50	-2.05	0.06
5.64	-2.8	-0.15	1.33	-1.58	-0.12
5.64	-2.8	-0.20		0.35	
5.64	-3	-0.10	6.80	-4.93	-0.23
5.64	-3	-0.15	3.72	-4.13	0.14
5.64	-3.2	-0.10	7.09	-9.98	-0.32
5.64	-3.2	-0.15	6.00	-5.77	
5.64	-3.4	-0.10	9.69	-15.79	-0.44
5.64	-3.4	-0.15	6.56	-9.89	
5.64	-3.6	-0.10	9.51	-17.16	-0.82
5.64	-3.6	-0.15	4.41	-10.45	-0.98
5.64	-3.8	-0.10	9.58	-16.07	
5.64	-3.8	-0.15	2.38	-2.92	-0.29
5.64	-4	-0.10	8.97	-13.88	-0.07
5.64	-4.2	-0.10	9.25	-12.65	-1.21

Table A2- 20. Line 1-Test 4

Long-shore Distance (m)	Cross-shore Distance (m)	Depth relating to S.W.L. (m)	Vy (cm/s)	Vx (cm/s)	Vz (cm/s)
2	-0.6	-0.10	10.85	-6.61	-0.08
2	-0.6	-0.15	5.19	-4.22	0.08
2	-0.6	-0.20	3.73	-3.69	0.07
2	-0.6	-0.25	1.29	-2.37	0.43
2	-0.6	-0.30	1.35	-2.42	0.03
2	-0.6	-0.35	-0.37	-1.27	0.25
2	-0.6	-0.40	-0.23	-1.56	-0.01
2	-0.8	-0.10	6.11	-4.37	0.05
2	-0.8	-0.15	4.77	-3.78	0.19
2	-0.8	-0.20	2.86	-2.72	0.69
2	-0.8	-0.25	1.98	-2.97	0.21
2	-0.8	-0.30	0.15	-1.57	0.09
2	-0.8	-0.35	-0.66	-1.03	0.24
2	-0.8	-0.40	-0.22	-1.22	
2	-1	-0.10	5.82	-5.39	0.23
2	-1	-0.15	6.12	-5.45	0.13
2	-1	-0.20	2.97	-3.42	0.05
2	-1	-0.25	2.39	-1.71	0.64
2	-1	-0.30	2.00	-2.68	-0.10
2	-1	-0.35	1.70	-1.58	-0.01
2	-1	-0.40	0.72	-1.30	
2	-1.2	-0.10	8.52	-9.19	-0.21
2	-1.2	-0.15	8.22	-7.64	-0.05
2	-1.2	-0.20	6.22	-6.53	-0.27
2	-1.2	-0.25	5.96	-6.13	0.34
2	-1.2	-0.30	5.04	-5.07	-0.07
2	-1.2	-0.35	3.21	-4.11	-0.19
2	-1.2	-0.40	2.82	-2.85	
2	-1.4	-0.10	11.33	-11.69	-0.44
2	-1.4	-0.15	9.83	-10.56	-0.93
2	-1.4	-0.20	8.80	-9.00	-1.01
2	-1.4	-0.25	7.25	-8.49	-0.33
2	-1.4	-0.30	6.56	-8.16	-0.68
2	-1.4	-0.35	5.67	-6.88	-0.45
2	-1.4	-0.40	1.65	-3.57	

2	-1.6	-0.10	10.49	-8.39	-0.44
2	-1.6	-0.15	9.56	-9.22	-0.61
2	-1.6	-0.20	8.76	-8.79	-0.28
2	-1.6	-0.25	7.91	-8.57	-0.16
2	-1.6	-0.30	6.15	-8.54	-0.27
2	-1.6	-0.35	5.87	-7.50	-0.08
2	-1.6	-0.40	3.43	-4.55	0.18
2	-1.8	-0.10	6.99	-5.37	-0.37
2	-1.8	-0.15	7.44	-6.69	-0.13
2	-1.8	-0.20	6.38	-7.45	-0.22
2	-1.8	-0.25	6.56	-7.86	-0.22
2	-1.8	-0.30	5.83	-7.72	
2	-1.8	-0.35	5.68	-7.48	-0.06
2	-2	-0.10	5.40	-1.97	-0.80
2	-2	-0.15	4.16	-3.88	-0.82
2	-2	-0.20	5.37	-5.45	0.03
2	-2	-0.25	5.09	-6.51	-0.39
2	-2	-0.30	5.18	-7.81	-0.31
2	-2	-0.35	4.37	-5.44	-0.12
2	-2.2	-0.10	4.80	-1.14	-0.21
2	-2.2	-0.15	4.10	-2.99	-0.47
2	-2.2	-0.20	3.96	-3.93	-0.23
2	-2.2	-0.25	4.62	-6.16	-0.37
2	-2.2	-0.35	1.32	-4.09	0.16
2	-2.4	-0.10	5.41	-0.44	-0.13
2	-2.4	-0.15	4.41	-2.96	0.05
2	-2.4	-0.20	5.26	-4.51	0.18
2	-2.4	-0.25	4.66	-6.31	0.05
2	-2.4	-0.30		-5.18	0.69
2	-2.6	-0.10	4.35	0.35	0.07
2	-2.6	-0.15	4.49	-2.80	-0.20
2	-2.6	-0.20	4.20	-4.30	0.73
2	-2.6	-0.25	2.52	-4.11	0.31
2	-2.6	-0.30	0.12	-1.07	0.63
2	-2.8	-0.10	4.78	0.74	0.06
2	-2.8	-0.15	3.24	-1.70	0.72
2	-2.8	-0.20	3.66	-3.67	0.29
2	-2.8	-0.25	1.93	-3.04	
2	-3	-0.10	3.05	0.23	0.19
2	-3	-0.15	2.88	-0.49	0.14

2	-3	-0.20		-1.37	
2	-3	-0.25	-1.17	-2.80	-0.67
2	-3.2	-0.10	2.51	0.35	-0.13
2	-3.2	-0.15	2.89	0.34	-0.05
2	-3.2	-0.20	2.01	-0.56	0.14
2	-3.4	-0.10	2.13	0.41	-0.02
2	-3.4	-0.15	1.74	-0.11	-0.25
2	-3.4	-0.20	0.04	-0.16	-0.28
2	-3.6	-0.10	1.75	-0.12	-0.07
2	-3.6	-0.15	1.09	0.18	-0.32
2	-3.6	-0.20	-1.70	0.00	-0.76
2	-3.8	-0.10	2.48	0.13	-0.12
2	-3.8	-0.15	-1.98	-1.05	0.13
2	-4	-0.10		0.04	-0.15
2	-4	-0.15	0.60	3.59	0.60
2	-4.2	-0.10	-0.10		
2	-4.4	-0.10	-0.05	-0.05	

Table A2- 21. Line 2-Test 4

Long-shore Distance (m)	**Cross-shore Distance (m)**	**Depth relating to S.W.L. (m)**	**Vy (cm/s)**	**Vx (cm/s)**	**Vz (cm/s)**
4	-0.6	-0.10	-0.59	-3.57	0.03
4	-0.6	-0.15	0.28	-2.78	-0.27
4	-0.6	-0.20	0.00	-1.81	0.24
4	-0.6	-0.25	0.45	-1.44	0.02
4	-0.6	-0.30	0.24	-0.44	0.11
4	-0.6	-0.35	1.09	0.19	
4	-0.8	-0.10	1.74	-1.43	-0.04
4	-0.8	-0.15	1.58	-0.98	0.18
4	-0.8	-0.20	1.29	-1.36	-0.02
4	-0.8	-0.25	0.88	-1.01	0.03
4	-0.8	-0.30	0.20	-0.61	0.50
4	-0.8	-0.35		0.52	1.38
4	-1	-0.10	1.85	-0.90	-0.03
4	-1	-0.15	1.62	-0.99	-0.05
4	-1	-0.20	1.19	-0.96	-0.04
4	-1	-0.25	0.75	-0.90	0.17
4	-1	-0.30	0.18	-0.24	0.17

4	-1	-0.35	-1.06	0.85	0.25
4	-1.2	-0.10	1.73	-1.48	0.06
4	-1.2	-0.15	1.10	-1.63	-0.05
4	-1.2	-0.20	1.55	-1.07	-0.05
4	-1.2	-0.25	1.35	-1.12	-0.02
4	-1.2	-0.30	0.92	0.11	-0.12
4	-1.2	-0.35	0.37	-0.55	-0.08
4	-1.4	-0.10	1.94	-1.01	0.04
4	-1.4	-0.15	1.10	-1.02	0.02
4	-1.4	-0.20	1.44	-0.50	
4	-1.4	-0.25	1.63	-0.30	-0.22
4	-1.4	-0.30	-1.65	0.18	0.55
4	-1.6	-0.10	2.05	-1.46	-0.18
4	-1.6	-0.15	1.22		-0.28
4	-1.6	-0.20	1.22	-0.43	-0.37
4	-1.6	-0.25	2.40	-0.64	
4	-1.8	-0.10	2.18	-1.74	-0.07
4	-1.8	-0.15	1.94	-1.52	-0.06
4	-1.8	-0.20	1.36	-1.46	0.03
4	-1.8	-0.25	-1.56	-2.54	0.68
4	-2	-0.10	2.57	-2.41	-0.25
4	-2	-0.15	2.47	-2.09	-0.39
4	-2	-0.20	1.88	-1.63	-0.47
4	-2.2	-0.10	3.57	-3.73	
4	-2.2	-0.15	2.60	-2.87	-0.54
4	-2.2	-0.20	1.56	-1.70	
4	-2.4	-0.10	6.11	-6.57	-0.52
4	-2.4	-0.15	2.48	-5.79	
4	-2.4	-0.20	-0.75	-3.50	-0.47
4	-2.6	-0.10	9.24	-9.66	
4	-2.6	-0.15	4.09		-0.24
4	-2.6	-0.20	-2.64	-3.90	1.06
4	-2.8	-0.10	10.25	-11.56	-0.13
4	-2.8	-0.15	5.35		
4	-3	-0.10	11.29	-12.50	-0.34
4	-3	-0.15	4.14		
4	-3.2	-0.10	10.38	-13.03	
4	-3.2	-0.15	1.43	-7.80	
4	-3.4	-0.10	12.10		0.58
4	-3.4	-0.15	-0.42	-0.26	0.08

4	-3.6	-0.15	0.89	-0.59	0.12
4	-3.8	-0.10	6.54	-9.04	
4	-4	-0.10	5.72	-6.31	

Table A2- 22. Line 3-Test 4

Long-shore Distance (m)	Cross-shore Distance (m)	Depth relating to S.W.L. (m)	Vy (cm/s)	Vx (cm/s)	Vz (cm/s)
5.64	-0.6	-0.10	-1.64	-0.89	0.32
5.64	-0.6	-0.15	-0.70	0.24	0.03
5.64	-0.6	-0.20	0.37	-0.51	0.02
5.64	-0.6	-0.25	-0.31	-0.36	0.60
5.64	-0.6	-0.30	0.05	-0.25	0.30
5.64	-0.6	-0.35		-0.81	
5.64	-0.6	-0.40	-0.53	0.79	0.05
5.64	-0.8	-0.10	1.05	-1.04	0.02
5.64	-0.8	-0.15	0.96	-0.87	0.28
5.64	-0.8	-0.20	0.83	-0.89	0.18
5.64	-0.8	-0.25	0.93	-0.43	0.11
5.64	-0.8	-0.30	0.42	-0.13	0.13
5.64	-0.8	-0.35	-0.39	-0.12	0.32
5.64	-1	-0.10	1.61	-0.97	0.09
5.64	-1	-0.15	1.69	-1.17	0.12
5.64	-1	-0.20	1.25	-1.12	0.39
5.64	-1	-0.25	0.12	-0.53	0.90
5.64	-1	-0.35	-0.29	-0.33	0.56
5.64	-1.2	-0.10	0.96	-1.26	0.01
5.64	-1.2	-0.15	1.96	-0.33	0.19
5.64	-1.2	-0.20	1.60	-0.75	-0.16
5.64	-1.2	-0.25	1.52	-0.70	-0.40
5.64	-1.2	-0.30	1.43	0.09	-0.29
5.64	-1.4	-0.10	1.99	-1.06	0.64
5.64	-1.4	-0.15	1.29	-1.36	0.49
5.64	-1.4	-0.20	0.83	-1.26	0.29
5.64	-1.4	-0.25	0.67	-0.22	0.24
5.64	-1.4	-0.30	0.99	-0.31	0.53
5.64	-1.6	-0.10	1.61	-0.97	0.51
5.64	-1.6	-0.15	1.25	-1.27	0.23
5.64	-1.6	-0.20	1.34	-0.92	0.13

5.64	-1.6	-0.25	-1.27	-1.68	
5.64	-1.8	-0.10	1.74	-0.78	0.24
5.64	-1.8	-0.15	1.43	-0.89	0.27
5.64	-1.8	-0.20	1.13	-1.08	0.15
5.64	-1.8	-0.25	2.74	-0.43	
5.64	-2	-0.10	2.19	-1.12	0.22
5.64	-2	-0.15	2.20	-1.06	0.09
5.64	-2	-0.20	1.20	-0.42	0.03
5.64	-2	-0.25	0.14	-0.20	-0.23
5.64	-2.2	-0.10	2.52	-1.86	-0.05
5.64	-2.2	-0.15	2.58	-1.67	
5.64	-2.2	-0.20	2.80	-1.02	
5.64	-2.4	-0.10	3.76	-2.27	-0.15
5.64	-2.4	-0.15	2.92	-2.43	-0.16
5.64	-2.4	-0.20	1.54	-2.35	-0.01
5.64	-2.6	-0.10	4.04	-3.67	
5.64	-2.6	-0.15	2.78	-2.37	-0.46
5.64	-2.6	-0.20	-0.31	-1.76	
5.64	-2.8	-0.10	5.35	-5.87	-0.45
5.64	-2.8	-0.15		-3.96	
5.64	-3	-0.10	7.32	-9.12	-0.70
5.64	-3	-0.15	2.80	-7.00	
5.64	-3.2	-0.10	10.21	-12.80	-0.73
5.64	-3.2	-0.15	6.48	-7.79	
5.64	-3.4	-0.10	10.83	-14.32	-0.80
5.64	-3.4	-0.15	4.07	-8.55	
5.64	-3.6	-0.15	-2.35	-7.10	
5.64	-3.8	-0.10	11.69		
5.64	-3.8	-0.15		-2.02	-0.03
5.64	-4	-0.10		-11.46	

Table A2- 23. Line 1-Test 5

Long-shore Distance (m)	Cross-shore Distance (m)	Depth relating to S.W.L. (m)	Vy (cm/s)	Vx (cm/s)	Vz (cm/s)
2	-0.6	-0.15	3.36	-1.79	-0.12
2	-0.6	-0.25	1.66	-1.50	0.15
2	-0.6	-0.35	-0.01	-1.10	0.12
2	-0.6	-0.45	-2.56	-0.34	-0.36
2	-0.8	-0.15	2.55	-1.93	-0.16
2	-0.8	-0.25	2.00	-1.76	-0.08
2	-0.8	-0.35	1.31	-1.26	-0.25
2	-0.8	-0.45	-0.41	-0.05	-0.14
2	-1	-0.15	3.49	-2.52	-0.04
2	-1	-0.25	2.35	-1.88	-0.19
2	-1	-0.35	0.11	-1.20	-0.06
2	-1	-0.45	-0.87	-0.55	-0.03
2	-1.2	-0.15	3.86	-2.59	-0.17
2	-1.2	-0.25	2.25	-2.02	-0.04
2	-1.2	-0.35	1.07	-1.73	-0.10
2	-1.2	-0.45	-0.13	-0.67	0.23
2	-1.4	-0.15	4.07	-2.62	-0.04
2	-1.4	-0.25	2.41	-3.08	-0.48
2	-1.4	-0.35	0.09	-1.95	-0.04
2	-1.4	-0.45	-1.07	-0.83	-1.19
2	-1.8	-0.05			-0.10
2	-1.8	-0.15	4.75	-4.28	-0.43
2	-1.8	-0.25	2.33	-2.80	-0.06
2	-1.8	-0.35	1.03	-1.37	-0.01
2	-2	-0.15	5.21	-4.32	-0.15
2	-2	-0.25	3.08	-2.87	-0.20
2	-2	-0.35	1.57	-1.98	-0.29
2	-2.2	-0.05	1.84		-0.22
2	-2.2	-0.15	6.13	-5.26	-0.36
2	-2.2	-0.25	3.87	-4.35	-0.33
2	-2.2	-0.35	0.84	-1.94	-0.37
2	-2.4	-0.05	1.69	-6.47	-0.12
2	-2.4	-0.15	7.22	-6.00	-0.42
-2	-2.4	-0.25	4.78	-4.24	-0.36
2	-2.4	-0.35	1.19	-1.52	-1.09
2	-2.6	-0.05	2.27		0.10

2	-2.6	-0.15	7.87	-5.78	-0.35
2	-2.6	-0.25	5.81		
2	-2.8	-0.05	1.56		0.01
2	-2.8	-0.05	1.56		0.01
2	-2.8	-0.15	7.75	-5.35	-0.35
2	-2.8	-0.25	6.47	-3.72	-0.40
2	-3	-0.05	2.19		-0.18
2	-3	-0.15	7.74	-5.14	-0.49
2	-3	-0.25	4.04	-3.55	-0.06
2	-3.2	-0.15	7.69	-4.78	-0.34
2	-3.4	-0.15	7.72	-3.87	-0.56
2	-3.6	-0.15	9.57	-3.42	-0.77
2	-3.8	-0.15	8.61	-1.62	-1.06
2	-4	-0.15	5.54	-2.58	-0.20
2	-4.2	-0.15	1.92	-2.33	0.48

Table A2- 24. Line 2-Test 5

Long-shore Distance (m)	**Cross-shore Distance (m)**	**Depth relating to S.W.L. (m)**	**Vy (cm/s)**	**Vx (cm/s)**	**Vz (cm/s)**
4	-0.6	-0.15	0.58	0.45	0.23
4	-0.6	-0.25	-0.35	0.12	0.18
4	-0.6	-0.35	-0.18	0.09	0.03
4	-0.8	-0.15	0.48	-0.39	0.27
4	-0.8	-0.25	-0.49	-0.59	0.15
4	-0.8	-0.35	-0.47	-0.62	-0.02
4	-1	-0.15	0.38	-0.37	0.25
4	-1	-0.25	-0.74	-0.40	0.10
4	-1	-0.35	-0.35	-0.19	0.03
4	-1.2	-0.05			-0.01
4	-1.2	-0.15	0.91	-1.13	0.09
4	-1.2	-0.25	0.31	-1.07	0.11
4	-1.2	-0.35	-1.21	-0.92	0.42
4	-1.4	-0.05		-2.26	0.15
4	-1.4	-0.15	0.39	-0.40	0.19
4	-1.4	-0.25	-0.33	-0.69	0.10
4	-1.6	-0.05	-2.98	-1.58	0.20
4	-1.6	-0.15	0.94	-0.72	0.09

4	-1.6	-0.25	-0.13	-0.60	-0.10
4	-1.8	-0.05	-3.03	-0.90	-0.06
4	-1.8	-0.15	1.06	-0.56	0.11
4	-1.8	-0.25	0.76	-0.56	0.04
4	-2	-0.05	-3.09	-2.02	0.09
4	-2	-0.15	0.28	-1.04	0.05
4	-2	-0.25	1.38	-0.36	0.10
4	-2.2	-0.05	-1.83	-1.90	-0.10
4	-2.2	-0.15	0.44	-1.74	-0.14
4	-2.4	-0.05	-0.59	-3.20	-0.01
4	-2.4	-0.15	0.06	-2.13	-0.19
4	-2.6	-0.05	-0.86	-3.99	-0.06
4	-2.6	-0.15	0.07	-2.22	-0.18
4	-2.8	-0.05	-1.20	-4.68	0.01
4	-2.8	-0.15	-0.86	-2.74	0.17
4	-3	-0.05	-0.37	-6.26	-0.41
4	-3	-0.15	-2.38	-2.94	0.08
4	-3.2	-0.05	0.36	-7.60	-0.21
4	-3.2	-0.15	-2.61	-3.25	-0.36
4	-3.4	-0.05	2.02	-8.61	-0.58
4	-3.4	-0.15	0.48	-0.15	0.08
4	-3.6	-0.05	2.95	-8.83	-0.32
4	-3.6	-0.15	-2.66	-1.04	0.19
4	-3.8	-0.05	1.89		-0.01

Table A2- 25. Line 3-Test 5

Long-shore Distance (m)	**Cross-shore Distance (m)**	**Depth relating to S.W.L. (m)**	**Vy (cm/s)**	**Vx (cm/s)**	**Vz (cm/s)**
5.64	-0.6	-0.15	0.71	0.44	0.29
5.64	-0.6	-0.25	0.54	0.39	0.25
5.64	-0.6	-0.35	-0.53	-0.04	0.17
5.64	-0.8	-0.15	0.35	-0.09	0.32
5.64	-0.8	-0.25	-0.49	-0.26	0.14
5.64	-0.8	-0.35	-0.23	0.01	-0.23
5.64	-1	-0.15	0.52	0.07	0.26
5.64	-1	-0.25	-0.19	-0.11	0.10
5.64	-1	-0.35	-2.14	-0.24	-0.44
5.64	-1.2	-0.15	0.30	-0.19	0.04
5.64	-1.2	-0.25	-0.46	-0.07	0.04

5.64	-1.4	-0.15	0.25	-0.22	0.23
5.64	-1.4	-0.25	-0.15	-0.48	0.21
5.64	-1.6	-0.15	0.25	-0.58	0.19
5.64	-1.6	-0.25	0.34	-0.30	0.24
5.64	-1.8	-0.15	-0.08	-0.81	0.00
5.64	-1.8	-0.25	-0.60	-0.48	0.18
5.64	-2	-0.15	0.54	-0.29	-0.09
5.64	-2	-0.25	0.03	0.01	-0.01
5.64	-2.2	-0.15	0.73	-0.59	-0.08
5.64	-2.4	-0.15	-0.35	-0.94	0.20
5.64	-2.6	-0.15	0.22	-0.85	0.00
5.64	-2.8	-0.15		-0.56	0.06
5.64	-3	-0.05	-0.82	-2.47	0.04
5.64	-3	-0.15	0.09	-1.58	-0.31
5.64	-3.2	-0.05	-0.66	-3.75	-0.01
5.64	-3.2	-0.15	0.60	-1.19	-0.24
5.64	-3.4	-0.05	0.19	-5.56	-0.17
5.64	-3.4	-0.15	0.31	-3.11	-0.21
5.64	-3.6	-0.05	-0.89	-7.63	-0.21
5.64	-3.6	-0.15	0.50	-3.56	0.01
5.64	-3.8	-0.05	-0.50	-9.32	0.01

Table A2- 26. Line 1-Test 6

Long-shore Distance (m)	**Cross-shore Distance (m)**	**Depth relating to S.W.L. (m)**	**Vy (cm/s)**	**Vx (cm/s)**	**Vz (cm/s)**
2	-0.6	-0.15	1.25	-2.27	-0.07
2	-0.6	-0.25	2.37	-2.26	-0.17
2	-0.6	-0.35	0.87	-1.20	-0.03
2	-0.8	-0.05	-1.05	-2.72	-0.04
2	-0.8	-0.15	3.59	-2.51	-0.21
2	-0.8	-0.25	1.53	-2.12	-0.22
2	-0.8	-0.35	0.94	-1.40	-0.27
2	-1	-0.15	2.06	-2.74	-0.14
2	-1	-0.25	2.19	-2.19	0.02
2	-1	-0.35	1.12	-1.36	-0.09
2	-1.2	-0.05	-0.36	-4.08	0.09
2	-1.2	-0.15	4.38	-3.34	-0.13
2	-1.2	-0.25	2.68	-3.20	-0.37
2	-1.2	-0.35	1.38	-1.44	-0.12

2	-1.4	-0.05	0.51	-3.76	-0.13
2	-1.4	-0.15	4.20	-4.01	-0.05
2	-1.4	-0.25	2.95	-3.39	-0.22
2	-1.4	-0.35	2.10	-2.56	-0.28
2	-1.6	-0.05	1.33	-4.30	-0.03
2	-1.6	-0.15	4.53	-4.99	-0.20
2	-1.6	-0.25	3.20	-3.41	-0.15
2	-1.6	-0.35	1.91	-3.03	-0.09
2	-1.8	-0.05	1.26	-5.00	-0.20
2	-1.8	-0.15	4.53	-4.84	-0.30
2	-1.8	-0.25	3.57	-4.16	-0.41
2	-1.8	-0.35	1.63	-2.68	-0.09
2	-2	-0.05	2.90	-5.52	-0.27
2	-2	-0.15	5.76	-5.37	-0.41
2	-2	-0.25	3.64	-4.74	-0.29
2	-2	-0.35		-2.20	-0.18
2	-2.2	-0.05	2.90	-5.16	0.13
2	-2.2	-0.15	6.94	-5.12	-0.30
2	-2.2	-0.25	3.44	-4.86	-0.53
2	-2.4	-0.05	2.93	-5.63	-0.11
2	-2.4	-0.15	6.03	-4.74	-0.28
2	-2.4	-0.25	4.87	-5.28	-0.66
2	-2.6	-0.05	2.69	-4.79	-0.11
2	-2.6	-0.15	7.06	-5.60	-0.59
2	-2.6	-0.25	5.29	-4.29	-0.57
2	-2.8	-0.05	2.86	-3.38	-0.35
2	-2.8	-0.15	8.62	-5.02	-0.68
2	-2.8	-0.25	4.09	-3.26	0.11
2	-3	-0.05	2.03	-3.41	-0.35
2	-3	-0.15	7.94	-3.06	-0.65
2	-3	-0.25	2.99	-3.48	-1.02
2	-3.2	-0.05	1.43	-2.99	-0.22
2	-3.2	-0.15	7.29	-2.74	-0.70
2	-3.2	-0.25	1.56	-1.82	-0.94
2	-3.4	-0.05	1.19	-1.31	-0.42
2	-3.4	-0.15	8.94	-2.35	-0.94
2	-3.6	-0.15	6.57	-0.98	-0.78
2	-3.8	-0.15	5.62	0.01	-0.65
2	-4	-0.15	2.68	1.07	-0.73
2	-4.2	-0.15	-1.98	-0.73	

Table A2- 27. Line 2-Test 6

Long-shore Distance (m)	Cross-shore Distance (m)	Depth relating to S.W.L. (m)	Vy (cm/s)	Vx (cm/s)	Vz (cm/s)
4	-0.6	-0.15	-0.41	-0.69	0.17
4	-0.6	-0.25	-0.46	-0.46	0.20
4	-0.6	-0.35	1.04	-0.27	-0.11
4	-0.8	-0.15	-0.09	-0.44	0.35
4	-0.8	-0.25	-0.58	-0.53	0.16
4	-0.8	-0.35	0.80	-0.26	-0.33
4	-1	-0.15	-0.27	-0.62	0.15
4	-1	-0.25	-0.12	0.00	0.12
4	-1.2	-0.05	-4.11	-0.71	-0.01
4	-1.2	-0.15	-0.15	-0.39	0.04
4	-1.2	-0.25	-0.40		
4	-1.4	-0.05			0.06
4	-1.4	-0.15	-0.30	-0.95	-0.01
4	-1.4	-0.25	0.55		-0.27
4	-1.6	-0.05	-3.78	-1.47	0.05
4	-1.6	-0.15	0.25	-1.11	-0.13
4	-1.6	-0.25	-0.53	0.28	-0.11
4	-1.8	-0.05	-3.00	-2.38	0.00
4	-1.8	-0.15	0.96	-1.34	
4	-1.8	-0.25		-0.08	-0.43
4	-2	-0.05	-2.19	-3.33	-0.15
4	-2	-0.15	2.49	-2.43	-0.31
4	-2.2	-0.05	-1.05	-3.10	-0.25
4	-2.2	-0.15	1.03	-3.24	-0.30
4	-2.4	-0.15	0.08	-3.03	-0.33
4	-2.6	-0.05	-0.75	-5.80	-0.08
4	-2.6	-0.15	0.15	-3.68	0.02
4	-2.8	-0.05	0.46	-6.38	-0.14
4	-2.8	-0.15	-1.21	-4.42	-0.08
4	-3	-0.05	0.59	-6.95	-0.44
4	-3	-0.15	-2.49	-3.74	-0.50
4	-3.2	-0.05	0.54	-6.74	-0.42

Table A2- 28. Line 3-Test 6

Long-shore Distance (m)	Cross-shore Distance (m)	Depth relating to S.W.L. (m)	Vy (cm/s)	Vx (cm/s)	Vz (cm/s)
5.64	-0.6	-0.15	-0.23	-0.54	0.28
5.64	-0.6	-0.25	-0.35	0.30	0.20
5.64	-0.6	-0.35	-0.27		
5.64	-0.8	-0.15	0.15	-0.05	0.27
5.64	-0.8	-0.25	0.22	-0.29	0.08
5.64	-0.8	-0.35	1.52	0.17	-0.33
5.64	-1	-0.15	-0.09	0.15	0.19
5.64	-1	-0.25	-0.27	-0.28	0.10
5.64	-1	-0.35	0.85	0.34	-0.61
5.64	-1.2	-0.15	0.01	-0.41	0.18
5.64	-1.2	-0.25	0.47	-0.18	0.06
5.64	-1.4	-0.15	0.02	0.03	0.14
5.64	-1.4	-0.25	0.57	-0.49	0.07
5.64	-1.6	-0.15	-0.24	-1.13	0.07
5.64	-1.6	-0.25	2.05	-0.19	0.48
5.64	-1.8	-0.15	2.19	-0.27	-0.13
5.64	-1.8	-0.25	0.87	-0.36	0.06
5.64	-2	-0.15	1.04	0.16	-0.07
5.64	-2	-0.25	-0.79	0.58	0.89
5.64	-2.2	-0.15	0.65	-0.88	-0.08
5.64	-2.2	-0.25	-2.56	-0.91	-0.48
5.64	-2.4	-0.15	1.52	-1.11	-0.16
5.64	-2.6	-0.15	1.12	-1.25	-0.06
5.64	-2.8	-0.15	1.29	-1.45	0.18
5.64	-3	-0.15	0.94	-1.09	-0.22
5.64	-3.2	-0.15	2.59	-1.00	0.14
5.64	-3.4	-0.15	3.19	-3.05	-0.45
5.64	-3.6	-0.15	2.49	-4.89	-0.19
5.64	-3.8	-0.15	4.29	-4.51	-0.07

Table A2- 29. Line 1-Test 7

Long-shore Distance (m)	Cross-shore Distance (m)	Depth relating to S.W.L. (m)	Vy (cm/s)	Vx (cm/s)	Vz (cm/s)
2	-0.6	-0.10	4.84	-0.30	-0.34
2	-0.6	-0.15	-0.23	-2.13	0.02
2	-0.6	-0.20	-0.55	-2.16	0.23
2	-0.6	-0.25	0.46	-1.21	0.23
2	-0.6	-0.30	0.57	-0.90	0.26
2	-0.6	-0.35	0.32	-0.32	0.07
2	-0.6	-0.40	0.24	-0.49	-0.19
2	-0.8	-0.05		-0.25	0.19
2	-0.8	-0.10	0.31	0.43	0.37
2	-0.8	-0.15	0.31	-0.59	0.13
2	-0.8	-0.20	0.04	-0.79	0.21
2	-0.8	-0.25	-0.03	-0.52	0.21
2	-0.8	-0.30	-0.31	-0.73	0.23
2	-0.8	-0.35	-0.71	-0.37	0.20
2	-1	-0.10	2.04	-0.47	-0.34
2	-1	-0.15	1.91	-0.57	-0.49
2	-1	-0.20	0.02	-1.12	0.37
2	-1	-0.25	-0.39	-0.72	0.20
2	-1	-0.30	0.34	-1.06	-0.05
2	-1	-0.35	0.61	-0.49	0.21
2	-1.2	-0.10	1.34	-1.69	0.12
2	-1.2	-0.15	0.83	-1.50	0.10
2	-1.2	-0.20	0.47	-0.75	0.18
2	-1.2	-0.25	0.40	-0.94	0.22
2	-1.2	-0.30	0.31	-0.85	-0.07
2	-1.2	-0.35	2.94	-0.86	-0.29
2	-1.4	-0.10	4.20	-2.51	-0.55
2	-1.4	-0.15	1.12	-1.96	0.10
2	-1.4	-0.20	1.20	-2.26	-0.28
2	-1.4	-0.25	-0.11	-1.56	0.08
2	-1.4	-0.30	0.36	-1.65	-0.03
2	-1.4	-0.35	-0.38	-0.88	0.24
2	-1.6	-0.10	4.21	-3.02	-0.07
2	-1.6	-0.15	2.18	-2.19	0.45
2	-1.6	-0.20	0.66	-1.75	0.07

2	-1.6	-0.25	0.50	-2.32	0.38
2	-1.6	-0.30	1.11	-1.32	-0.03
2	-1.6	-0.35	0.38	-1.29	-0.06
2	-1.8	-0.10	3.68	-3.21	0.28
2	-1.8	-0.15	2.15	-2.21	0.73
2	-1.8	-0.20	2.79	-3.97	-0.06
2	-1.8	-0.25	2.26	-2.62	0.41
2	-1.8	-0.30	1.05	-1.65	0.13
2	-1.8	-0.35	-2.64	-1.42	0.04
2	-2	-0.10	5.54	-6.40	-0.22
2	-2	-0.15	5.42	-6.33	-0.53
2	-2	-0.20	4.57	-5.94	-0.29
2	-2	-0.25	0.68	-2.93	-0.01
2	-2	-0.30	4.98	-7.54	-0.68
2	-2	-0.35	-0.53	-2.71	-0.32
2	-2.2	-0.10	8.10	-8.62	-1.03
2	-2.2	-0.15	7.94	-8.67	-0.71
2	-2.2	-0.20	6.90	-8.24	-1.01
2	-2.2	-0.25	6.79	-8.21	-0.73
2	-2.2	-0.30	3.21	-3.63	0.73
2	-2.4	-0.10	8.40	-7.34	-3.18
2	-2.4	-0.15	6.10	-9.19	-1.87
2	-2.4	-0.20	5.90	-10.16	-1.71
2	-2.4	-0.25	4.43	-9.33	-0.90
2	-2.4	-0.30	1.56	-6.98	-1.24
2	-2.6	-0.10	8.89	-5.72	-0.47
2	-2.6	-0.15	5.06	-9.58	-0.23
2	-2.6	-0.20	4.36	-10.22	0.03
2	-2.6	-0.25	3.93	-8.03	-0.02
2	-2.8	-0.10	8.64	-5.31	-0.43
2	-2.8	-0.15	6.36	-7.77	-0.16
2	-2.8	-0.20	4.33	-8.31	-0.79
2	-3	-0.05		-1.05	0.90
2	-3	-0.10	7.86	-2.80	0.80
2	-3	-0.15	5.92	-5.26	0.41
2	-3	-0.20	3.64	-2.81	0.99
2	-3.2	-0.10	14.90	3.76	-1.43
2	-3.2	-0.15	11.02	-1.08	-1.50
2	-3.2	-0.20	5.12	-2.41	-0.73
2	-3.4	-0.10	12.46	2.27	-0.70

2	-3.4	-0.15	8.71	0.36	-1.11
2	-3.6	-0.10	9.30	1.81	-0.81
2	-3.6	-0.15	6.67	1.10	-1.55
2	-3.8	-0.10	9.61	2.85	-0.28
2	-3.8	-0.15	4.47	0.48	-1.34
2	-4	-0.10	5.18	1.59	-0.78
2	-4	-0.15	0.17	0.89	-0.18
2	-4.2	-0.10	3.09	-2.25	0.11
2	-4.4	-0.010	0.16	-0.77	-0.45

Table A2- 30. Line 2-Test 7

Long-shore Distance (m)	**Cross-shore Distance (m)**	**Depth relating to S.W.L. (m)**	**Vy (cm/s)**	**Vx (cm/s)**	**Vz (cm/s)**
4	-0.6	-0.10	1.11	0.84	-0.22
4	-0.6	-0.15	0.76	-2.29	0.46
4	-0.6	-0.20	1.46	-2.51	0.40
4	-0.6	-0.25	1.01	-1.96	0.55
4	-0.6	-0.30	0.45	-1.91	0.19
4	-0.6	-0.35	0.91	-0.95	0.20
4	-0.6	-0.40	0.78	-0.69	0.15
4	-0.8	-0.10	2.29	-1.06	0.12
4	-0.8	-0.15	1.87	-1.24	0.11
4	-0.8	-0.20	1.64	-0.98	0.09
4	-0.8	-0.25	1.42	-0.88	-0.08
4	-0.8	-0.30	0.75	-0.93	-0.03
4	-0.8	-0.35	0.42	-0.39	0.30
4	-0.8	-0.40	0.72	-0.25	0.11
4	-1	-0.10	1.15	-1.21	0.58
4	-1	-0.15	0.90	-0.89	0.33
4	-1	-0.20	0.90	-0.53	-0.06
4	-1	-0.25	0.64	-0.31	-0.09
4	-1	-0.30	0.66	-0.04	-0.11
4	-1	-0.35	0.38	0.11	-0.05
4	-1.2	-0.10	0.97	0.26	0.33
4	-1.2	-0.15	0.76	0.24	0.46
4	-1.2	-0.20	0.50	0.09	0.18
4	-1.2	-0.25	0.61	0.33	0.29
4	-1.2	-0.30	1.73	0.35	0.31
4	-1.2	-0.35	1.90	-0.06	0.02

4	-1.4	-0.10	-0.41	-1.32	0.39
4	-1.4	-0.15	-0.58	-0.63	0.23
4	-1.4	-0.20	-0.01	-0.68	0.54
4	-1.4	-0.25	0.43	-0.95	0.47
4	-1.4	-0.30	0.91	-0.64	0.41
4	-1.4	-0.35	1.78	0.06	0.14
4	-1.6	-0.10	0.11	0.23	0.47
4	-1.6	-0.15	-0.52	-0.06	0.27
4	-1.6	-0.20	0.83	0.30	0.26
4	-1.6	-0.25	0.87	-0.66	0.36
4	-1.6	-0.30	1.96	0.12	0.06
4	-1.6	-0.35	3.09	0.57	0.02
4	-1.8	-0.10	0.94	0.38	0.16
4	-1.8	-0.15	0.18	0.47	0.05
4	-1.8	-0.20	0.09	0.45	-0.04
4	-1.8	-0.25	0.54	0.32	0.03
4	-1.8	-0.30	0.29	0.18	-0.10
4	-2	-0.05	-2.13	-0.14	-0.08
4	-2	-0.10	1.40	0.60	0.12
4	-2	-0.15	-0.34	-0.59	-0.01
4	-2	-0.20	0.07	-0.58	0.08
4	-2	-0.25	0.15	-0.32	0.19
4	-2	-0.30	0.09	-0.94	0.65
4	-2.2	-0.05	-2.17	-0.41	
4	-2.2	-0.10	1.54	0.37	-0.34
4	-2.2	-0.15	-0.09	-0.11	0.31
4	-2.2	-0.20	0.24	0.64	0.13
4	-2.2	-0.25	-0.38	0.84	-0.12
4	-2.4	-0.05	-2.10	0.29	
4	-2.4	-0.10	1.07	0.24	0.59
4	-2.4	-0.15	0.60	0.40	0.55
4	-2.4	-0.20	-0.04	0.11	0.42
4	-2.4	-0.25	0.45	0.21	0.44
4	-2.6	-0.10	0.45	-0.53	0.33
4	-2.6	-0.15	0.83	-0.33	0.07
4	-2.6	-0.20	1.24	-0.17	-0.22
4	-2.8	-0.10	2.71	-1.38	0.43
4	-2.8	-0.15	2.36	-0.74	0.26
4	-2.8	-0.20	0.40	-0.56	0.04
4	-3	-0.10	5.34	-6.25	-0.29

4	-3	-0.15	3.73	-4.83	-0.04
4	-3	-0.20	3.02	-2.27	-0.41
4	-3.2	-0.10	5.57	-10.45	-0.65
4	-3.2	-0.15	5.10	-9.09	-0.84
4	-3.4	-0.10	7.57	-14.15	-0.83
4	-3.4	-0.15	1.59	-7.82	
4	-3.6	-0.10	8.83	-15.80	-1.63
4	-3.8	-0.10	5.10	-13.14	0.10
4	-4	-0.10	2.52	-9.19	-0.55

Table A2- 31. Line 3-Test 7

Long-shore Distance (m)	**Cross-shore Distance (m)**	**Depth relating to S.W.L. (m)**	**Vy (cm/s)**	**Vx (cm/s)**	**Vz (cm/s)**
5.64	-0.6	-0.10	-1.49	1.04	0.04
5.64	-0.6	-0.15	-1.55	-0.44	-0.38
5.64	-0.6	-0.20	0.28	-0.52	0.13
5.64	-0.6	-0.25	0.34	-1.74	0.07
5.64	-0.6	-0.30	0.62	-1.89	0.01
5.64	-0.6	-0.35	0.82	-1.48	-0.09
5.64	-0.6	-0.40	1.00	-1.19	-0.10
5.64	-0.8	-0.10	0.99	-0.91	-0.11
5.64	-0.8	-0.15	0.72	-1.27	-0.03
5.64	-0.8	-0.20	0.92	-1.10	0.01
5.64	-0.8	-0.25	1.10	-0.08	0.09
5.64	-0.8	-0.30	-0.10	-0.50	0.24
5.64	-0.8	-0.35	-0.23	-0.44	0.21
5.64	-0.8	-0.40	-0.25	-1.00	-0.16
5.64	-1	-0.10	1.20	-0.56	-0.12
5.64	-1	-0.15	1.30	-0.43	0.21
5.64	-1	-0.20	0.98	-0.63	0.19
5.64	-1	-0.25	0.86	-0.34	0.16
5.64	-1	-0.30	0.47	-0.38	0.15
5.64	-1	-0.35	0.29	-0.23	-0.32
5.64	-1.2	-0.10	1.56	0.16	0.28
5.64	-1.2	-0.15	1.33	-0.09	0.28
5.64	-1.2	-0.20	0.45	-0.02	0.35
5.64	-1.2	-0.25	0.82	0.46	0.11

5.64	-1.2	-0.30	0.08	-0.34	0.02
5.64	-1.2	-0.35	2.33	0.56	-0.17
5.64	-1.4	-0.05	-3.46	0.09	-0.08
5.64	-1.4	-0.10	0.44	0.13	0.08
5.64	-1.4	-0.15	0.42	0.07	0.24
5.64	-1.4	-0.20	-0.13	-0.05	0.23
5.64	-1.4	-0.25	0.58	-0.45	0.19
5.64	-1.4	-0.30	0.55	0.22	0.09
5.64	-1.4	-0.35	-2.03	-2.46	0.03
5.64	-1.6	-0.05	-4.30	0.22	-0.17
5.64	-1.6	-0.10	0.64	0.10	0.10
5.64	-1.6	-0.15	0.00	0.03	-0.01
5.64	-1.6	-0.20	0.58	-0.05	0.07
5.64	-1.6	-0.25	0.40	-0.34	-0.01
5.64	-1.6	-0.30	1.64	-0.52	-0.09
5.64	-1.8	-0.05	-2.04	1.56	0.06
5.64	-1.8	-0.10	0.82	-0.13	0.25
5.64	-1.8	-0.15	0.85	-0.07	0.09
5.64	-1.8	-0.20	0.72	-0.14	0.07
5.64	-1.8	-0.25	1.25	-0.10	-0.24
5.64	-1.8	-0.30	3.32	0.01	-0.75
5.64	-2	-0.05	0.87	-0.13	0.27
5.64	-2	-0.10	1.18	0.12	0.38
5.64	-2	-0.15	0.96	0.23	0.13
5.64	-2	-0.20	1.14	0.20	0.02
5.64	-2	-0.25	0.25	0.11	0.06
5.64	-2	-0.30	-0.19	-0.09	-0.03
5.64	-2.2	-0.05	0.66	0.11	0.10
5.64	-2.2	-0.10	0.86	-0.66	0.61
5.64	-2.2	-0.15	0.83	-0.48	0.54
5.64	-2.2	-0.20	1.35	0.16	0.21
5.64	-2.2	-0.25	1.72	0.15	-0.59
5.64	-2.4	-0.05	-0.32	-0.51	0.23
5.64	-2.4	-0.10	1.08	-0.69	0.38
5.64	-2.4	-0.15	1.48	-0.55	0.23
5.64	-2.4	-0.20	1.14	-0.57	0.12
5.64	-2.4	-0.25	-0.04	1.67	-0.95
5.64	-2.6	-0.05	-0.56	-0.84	0.11
5.64	-2.6	-0.10	2.76	-0.73	-0.14
5.64	-2.6	-0.15	2.48	-0.58	-0.27

5.64	-2.6	-0.20	-0.03	-0.97	-0.09
5.64	-2.8	-0.10	3.00	-0.78	0.21
5.64	-2.8	-0.15	1.76	-0.97	0.38
5.64	-2.8	-0.20	0.85	-0.50	0.36
5.64	-3	-0.05	-2.15	-0.40	0.38
5.64	-3	-0.10	2.44	-0.84	0.66
5.64	-3	-0.15	1.69	-1.22	0.53
5.64	-3	-0.20	1.18	-1.21	-0.15
5.64	-3.2	-0.05	-2.16	-3.61	0.19
5.64	-3.2	-0.10	3.88	-4.13	-0.43
5.64	-3.2	-0.15	4.62	-4.01	-0.63
5.64	-3.4	-0.05	-1.10	-4.41	-0.93
5.64	-3.4	-0.10	6.03	-9.67	-0.64
5.64	-3.4	-0.15	2.96	-4.29	-0.22
5.64	-3.6	-0.05	-0.49		-0.39
5.64	-3.6	-0.10	6.00	-12.56	-0.62
5.64	-3.8	-0.10	3.13	-11.86	-0.41

Table A2- 32. Line 1-Test 8

Long-shore Distance (m)	**Cross-shore Distance (m)**	**Depth relating to S.W.L. (m)**	**Vy (cm/s)**	**Vx (cm/s)**	**Vz (cm/s)**
2	-0.6	-0.10	8.43	-1.72	-0.41
2	-0.6	-0.15	3.02	-2.40	-0.25
2	-0.6	-0.20	2.24	-1.92	0.14
2	-0.6	-0.25	1.72	-1.45	0.06
2	-0.6	-0.30	1.18	-1.70	0.09
2	-0.6	-0.35	0.73	-1.10	0.07
2	-0.6	-0.40	0.54	-0.35	0.05
2	-0.8	-0.10	1.56	-1.04	0.47
2	-0.8	-0.15	1.20	-0.59	0.43
2	-0.8	-0.20	1.21	-0.81	0.50
2	-0.8	-0.25	0.88	-0.69	0.56
2	-0.8	-0.30	0.76	-0.68	0.32
2	-0.8	-0.35	0.84	-0.34	0.26
2	-0.8	-0.40	1.70	0.24	-0.24
2	-1	-0.10	2.13	-1.54	0.22
2	-1	-0.15	0.03	-0.88	0.12
2	-1	-0.20	0.68	-0.75	-0.08

2	-1	-0.25	0.21	-0.59	-0.06
2	-1	-0.30	0.36	-0.29	-0.03
2	-1	-0.35	1.60	-0.34	-0.37
2	-1.2	-0.10	2.18	-1.60	0.04
2	-1.2	-0.15	2.25	-2.21	-0.64
2	-1.2	-0.20	0.92	-0.98	-0.37
2	-1.2	-0.25	1.21	-0.65	-0.48
2	-1.2	-0.30	0.64	-0.64	-0.17
2	-1.2	-0.35	-0.41	-0.12	-0.13
2	-1.4	-0.05	-1.26	-3.38	-0.33
2	-1.4	-0.10	4.19	-3.46	-0.28
2	-1.4	-0.15	3.36	-2.93	-0.15
2	-1.4	-0.20	2.42	-2.99	-0.79
2	-1.4	-0.25	1.78	-1.81	0.17
2	-1.4	-0.30	1.02	-2.11	-0.46
2	-1.4	-0.35	1.26	-1.50	-0.18
2	-1.6	-0.10	5.13	-3.93	-0.10
2	-1.6	-0.15	4.54	-3.22	-0.32
2	-1.6	-0.20	3.01	-3.13	-0.21
2	-1.6	-0.25	2.96	-2.79	-0.41
2	-1.6	-0.30	4.58	-4.08	-0.38
2	-1.6	-0.35	0.36	-1.02	-0.17
2	-1.8	-0.05	3.78	-4.70	-0.10
2	-1.8	-0.10	7.76	-5.57	0.06
2	-1.8	-0.15	7.85	-5.65	-0.02
2	-1.8	-0.20	5.66	-4.19	-0.16
2	-1.8	-0.25	5.30	-3.79	0.02
2	-1.8	-0.30	2.74	-2.63	-0.08
2	-1.8	-0.35	-0.67	-2.29	-0.55
2	-2	-0.05	5.58	-6.35	-0.39
2	-2	-0.10	11.80	-9.43	-0.58
2	-2	-0.15	6.00	-5.70	-0.83
2	-2	-0.20	8.81	-7.06	-0.55
2	-2	-0.25	6.55	-4.80	-0.53
2	-2	-0.30	4.09	-4.79	-1.17
2	-2	-0.35	0.30	-3.73	-1.37
2	-2.2	-0.05	4.85	-8.12	
2	-2.2	-0.10	13.05	-10.67	-0.82
2	-2.2	-0.15	13.01	-9.84	-1.09
2	-2.2	-0.20	11.18	-8.55	-0.72

2	-2.2	-0.25	9.80	-6.79	-0.52
2	-2.2	-0.30	4.97	-3.38	-0.26
2	-2.4	-0.05	1.79	-7.58	
2	-2.4	-0.10	11.31	-8.02	-0.80
2	-2.4	-0.15	12.10	-8.87	-0.99
2	-2.4	-0.20	10.05	-8.40	-0.69
2	-2.4	-0.25	7.79	-7.11	-0.55
2	-2.4	-0.30	2.91	-2.35	-1.03
2	-2.6	-0.05	0.76	-5.00	
2	-2.6	-0.10	9.26	-5.51	-0.57
2	-2.6	-0.15	8.74	-4.78	-0.87
2	-2.6	-0.20	7.73	-6.04	-0.97
2	-2.6	-0.25	4.93	-5.11	-0.52
2	-2.8	-0.05	2.08		
2	-2.8	-0.10	10.11	-3.69	-1.38
2	-2.8	-0.15	9.44	-4.50	-1.82
2	-2.8	-0.20	7.21	-4.74	-1.53
2	-3	-0.10	11.50	-2.89	-1.38
2	-3	-0.15	10.30	-3.48	-0.82
2	-3	-0.20	3.51	-5.19	0.43
2	-3.2	-0.10	9.73	1.41	0.05
2	-3.2	-0.15	9.75	-2.38	-0.32
2	-3.2	-0.20	5.51	-5.43	-0.40
2	-3.4	-0.10	10.60	0.75	-0.62
2	-3.4	-0.15	9.37	-1.79	-0.58
2	-3.4	-0.20	5.78	-2.71	-1.59
2	-3.6	-0.10	8.96	2.24	-1.48
2	-3.6	-0.15	7.99	1.45	-1.86
2	-3.8	-0.10	11.06	3.74	-1.32
2	-3.8	-0.15	4.33	1.66	-1.70
2	-4	-0.10	10.09	4.10	-2.25
2	-4	-0.15	1.21		
2	-4.2	-0.10	12.35	4.76	

Table A2- 33. Line 2-Test 8

Long-shore Distance (m)	Cross-shore Distance (m)	Depth relating to S.W.L. (m)	Vy (cm/s)	Vx (cm/s)	Vz (cm/s)
4	-0.6	-0.10	-1.69	-0.01	0.13
4	-0.6	-0.15	-1.09	-1.57	0.28
4	-0.6	-0.20	-0.57	-1.77	-0.23
4	-0.6	-0.25	0.80	-1.42	-0.03
4	-0.6	-0.30	0.01	-1.81	0.26
4	-0.6	-0.35	0.32	-1.33	-0.03
4	-0.6	-0.40	0.23	-0.93	-0.02
4	-0.8	-0.10	0.51	-1.26	0.41
4	-0.8	-0.15	0.42	-0.98	0.30
4	-0.8	-0.20	0.76	-0.37	0.51
4	-0.8	-0.25	0.23	-0.73	0.39
4	-0.8	-0.30	0.14	-0.24	0.52
4	-0.8	-0.35	0.48	0.09	0.52
4	-0.8	-0.40	0.67	0.08	0.18
4	-1	-0.10	0.32	-0.49	0.33
4	-1	-0.15	-0.16	-0.40	0.41
4	-1	-0.20	-0.09	0.54	0.49
4	-1	-0.25	0.71	0.57	0.42
4	-1	-0.30	1.66	0.70	0.17
4	-1	-0.35	2.21	0.32	0.08
4	-1.2	-0.10	0.97	0.26	0.33
4	-1.2	-0.15	0.76	0.24	0.46
4	-1.2	-0.20	0.50	0.09	0.18
4	-1.2	-0.25	0.61	0.33	0.29
4	-1.2	-0.30	1.73	0.35	0.31
4	-1.2	-0.35	1.90	-0.06	0.02
4	-1.4	-0.10	0.57	-0.87	-0.13
4	-1.4	-0.15	0.26	-0.67	-0.14
4	-1.4	-0.20	0.43	-0.03	0.21
4	-1.4	-0.25	0.60	0.09	0.10
4	-1.4	-0.30	0.59	-0.07	-0.12
4	-1.4	-0.35	1.64	0.10	0.05
4	-1.6	-0.05	-3.78	-1.64	0.22
4	-1.6	-0.10	1.30	0.25	0.21
4	-1.6	-0.15	1.24	0.31	0.08

4	-1.6	-0.20	0.11	-0.80	0.03
4	-1.6	-0.25	0.18	-0.26	-0.10
4	-1.6	-0.30	0.97	0.30	0.01
4	-1.6	-0.35	1.14	0.69	-0.33
4	-1.8	-0.10	1.27	0.02	0.25
4	-1.8	-0.15	1.43	0.01	0.15
4	-1.8	-0.20	1.02	0.15	0.12
4	-1.8	-0.25	1.25	0.22	-0.36
4	-1.8	-0.30	0.62	-0.35	-0.12
4	-2	-0.10	1.58	-0.36	0.17
4	-2	-0.15	0.85	-0.64	-0.02
4	-2	-0.20	1.13	-0.23	-0.10
4	-2	-0.25	0.57	-0.25	-0.16
4	-2.2	-0.05	-3.47	-1.89	0.00
4	-2.2	-0.10	2.29	-1.02	-0.21
4	-2.2	-0.15	1.22	-0.99	-0.09
4	-2.2	-0.20	1.89	-0.43	-0.20
4	-2.2	-0.25	0.82	-0.94	-0.42
4	-2.4	-0.05	-2.64	-2.98	
4	-2.4	-0.10	2.97	-1.65	-0.45
4	-2.4	-0.15	1.64	-1.50	-0.25
4	-2.4	-0.20	0.45	-1.49	-0.20
4	-2.4	-0.25	-2.35	-1.86	0.30
4	-2.6	-0.10	2.73	-2.58	-0.29
4	-2.6	-0.15	1.83	-1.80	-0.08
4	-2.6	-0.20	-0.61	-1.78	0.08
4	-2.6	-0.25	-1.36	-0.83	-0.09
4	-2.8	-0.10	1.94	-3.45	0.17
4	-2.8	-0.15	0.85	-2.26	0.09
4	-2.8	-0.20	-0.72	-1.56	-0.29
4	-3	-0.10	4.60	-6.70	-0.02
4	-3	-0.15	3.37	-4.24	0.20
4	-3	-0.20	-0.40	-2.93	0.07
4	-3.2	-0.10	7.76	-9.62	-0.46
4	-3.2	-0.15	5.34	-7.74	-0.71
4	-3.4	-0.10	10.27	-11.08	-0.42
4	-3.4	-0.15	4.74	-6.78	-0.42
4	-3.6	-0.10	11.93	-12.76	-0.66
4	-3.8	-0.10	15.07	-14.54	-1.11
4	-4	-0.10	11.45	-13.39	-1.33

Table A2- 34. Line 3-Test 8

Long-shore Distance (m)	Cross-shore Distance (m)	Depth relating to S.W.L. (m)	Vy (cm/s)	Vx (cm/s)	Vz (cm/s)
5.64	-0.6	-0.10	-0.60	0.51	0.23
5.64	-0.6	-0.15	0.88	0.03	0.21
5.64	-0.6	-0.20	1.02	0.01	-0.12
5.64	-0.6	-0.25	1.30	0.18	-0.05
5.64	-0.6	-0.30	-0.37	0.06	-0.02
5.64	-0.6	-0.35	-0.12	-0.47	-0.07
5.64	-0.6	-0.40	-0.79	-0.32	-0.43
5.64	-0.8	-0.10	1.21	-0.44	0.13
5.64	-0.8	-0.15	1.02	-0.59	-0.23
5.64	-0.8	-0.20	0.64	-0.58	0.43
5.64	-0.8	-0.25	0.98	0.05	-0.11
5.64	-0.8	-0.30	0.31	-0.41	-0.02
5.64	-0.8	-0.35	0.14	-0.50	-0.04
5.64	-0.8	-0.40	-1.99	-1.09	0.14
5.64	-1	-0.10	1.77	-0.17	-0.29
5.64	-1	-0.15	2.00	-0.02	-0.14
5.64	-1	-0.20	1.87	-0.42	0.04
5.64	-1	-0.25	2.00	-0.36	0.23
5.64	-1	-0.30	0.97	-0.69	0.36
5.64	-1	-0.35	-0.12	-0.44	0.07
5.64	-1.2	-0.10	0.71	0.04	0.60
5.64	-1.2	-0.15	0.95	0.51	0.41
5.64	-1.2	-0.20	0.69	0.61	0.35
5.64	-1.2	-0.25	0.65	0.38	0.48
5.64	-1.2	-0.30	1.16	0.22	0.22
5.64	-1.2	-0.35	2.08	0.11	1.34
5.64	-1.4	-0.10	0.83	0.73	0.31
5.64	-1.4	-0.15	1.02	0.83	0.41
5.64	-1.4	-0.20	1.18	0.42	0.29
5.64	-1.4	-0.25	1.48	0.55	0.22
5.64	-1.4	-0.30	2.36	0.23	-0.28
5.64	-1.6	-0.05			0.10
5.64	-1.6	-0.10	0.63	0.04	0.30
5.64	-1.6	-0.15	0.45	-0.20	0.01
5.64	-1.6	-0.20	1.09	0.47	0.20

5.64	-1.6	-0.25	2.06	0.50	0.16
5.64	-1.6	-0.30	2.67	0.28	-0.31
5.64	-1.8	-0.05	-3.82	-1.25	0.00
5.64	-1.8	-0.10	-0.06	-0.76	0.15
5.64	-1.8	-0.15	-0.02	-0.76	0.04
5.64	-1.8	-0.20	0.58	-0.53	-0.01
5.64	-1.8	-0.25	0.44	-0.45	-0.24
5.64	-1.8	-0.30	-2.84	-1.92	-0.36
5.64	-2	-0.05	-2.78	-1.56	0.19
5.64	-2	-0.10	0.67	-0.38	0.10
5.64	-2	-0.15	0.01	-0.50	0.16
5.64	-2	-0.20	0.86	-0.54	-0.11
5.64	-2	-0.25	0.50	0.14	-0.03
5.64	-2	-0.30	0.41	-0.16	-0.01
5.64	-2.2	-0.05	0.71	0.15	-0.23
5.64	-2.2	-0.10	1.33	-0.32	0.11
5.64	-2.2	-0.15	1.14	-0.30	0.00
5.64	-2.2	-0.20	1.02	-0.32	-0.10
5.64	-2.2	-0.25	2.30	0.16	-0.58
5.64	-2.4	-0.05	-0.15	-0.36	-0.19
5.64	-2.4	-0.10	2.12	-0.56	-0.08
5.64	-2.4	-0.15	1.54	-0.50	-0.14
5.64	-2.4	-0.20	1.71	-0.17	-0.10
5.64	-2.4	-0.25	-5.19	0.02	0.69
5.64	-2.6	-0.05	-0.69	-1.84	-0.46
5.64	-2.6	-0.10	3.13	-1.31	-0.45
5.64	-2.6	-0.15	1.35	-1.54	-0.21
5.64	-2.6	-0.20	0.50	-1.38	-0.46
5.64	-2.8	-0.05	-1.07	-1.27	-0.45
5.64	-2.8	-0.10	2.49	-1.63	-0.25
5.64	-2.8	-0.15	1.70	-1.66	0.08
5.64	-2.8	-0.20	-2.18	-1.88	0.90
5.64	-3	-0.05	-2.45	-2.07	
5.64	-3	-0.10	2.39	-1.63	0.10
5.64	-3	-0.15	0.32	-1.62	0.22
5.64	-3	-0.20	-1.15	-1.32	-0.23
5.64	-3.2	-0.05	-4.11		
5.64	-3.2	-0.10	1.93	-3.76	0.02
5.64	-3.2	-0.15	2.46	-1.92	
5.64	-3.4	-0.10	4.00	-7.97	-0.64

5.64	-3.4	-0.15	-0.30	-4.16	0.18
5.64	-3.6	-0.10	5.45	-10.68	-0.66
5.64	-3.8	-0.10	2.98	-10.13	0.20
5.64	-4	-0.10	3.15	-9.74	
5.64	-4.2	-0.10	5.55	-9.46	

Table A2- 35. Line 1-Test 9

Long-shore Distance (m)	Cross-shore Distance (m)	Depth relating to S.W.L. (m)	Vy (cm/s)	Vx (cm/s)	Vz (cm/s)
2	-0.6	-0.15	3.92	-2.16	-0.32
2	-0.6	-0.25	1.86	-1.89	-0.16
2	-0.6	-0.35	0.23	-1.81	0.13
2	-0.8	-0.05	-0.85		-0.21
2	-0.8	-0.15	3.41	-2.34	0.08
2	-0.8	-0.25	1.63	-2.16	-0.17
2	-0.8	-0.35	0.05	-1.46	0.00
2	-1	-0.05	0.57	-2.75	-0.09
2	-1	-0.15	4.26	-2.88	-0.28
2	-1	-0.25	1.52	-2.64	-0.10
2	-1	-0.35	-0.61	-1.86	0.13
2	-1.2	-0.15	5.58	-3.30	-0.12
2	-1.2	-0.25	2.08	-3.11	-0.33
2	-1.2	-0.35	-0.87	-2.07	0.07
2	-1.4	-0.05	1.86	-3.34	0.11
2	-1.4	-0.15	5.05	-4.03	-0.21
2	-1.4	-0.25	1.56	-2.97	0.02
2	-1.4	-0.35	-0.68	-2.02	0.05
2	-1.6	-0.05	3.70	-4.15	-0.22
2	-1.6	-0.15	5.73	-4.03	0.09
2	-1.6	-0.25	3.10	-3.35	0.04
2	-1.6	-0.35	0.34	-2.05	-0.12
2	-1.8	-0.05	3.46	-4.32	-0.08
2	-1.8	-0.15	5.57	-4.70	-0.21
2	-1.8	-0.25	3.25	-4.18	-0.20
2	-1.8	-0.35	0.30	-2.29	-0.10
2	-2	-0.05	4.61	-4.64	-0.23
2	-2	-0.15	7.65	-5.48	-0.34
2	-2	-0.25	4.02	-5.34	-0.33
2	-2	-0.35	1.06	-3.01	-0.20

2	-2.2	-0.05	5.11	-4.09	-0.14
2	-2.2	-0.15	8.95	-6.02	-0.50
2	-2.2	-0.25	5.66	-6.30	-0.52
2	-2.4	-0.05	4.97	-4.16	-0.19
2	-2.4	-0.15	9.06	-5.60	-0.58
2	-2.4	-0.25	5.47	-6.46	-0.36
2	-2.6	-0.05	5.54	-3.39	-0.28
2	-2.6	-0.15	10.15	-5.45	-0.60
2	-2.6	-0.25	5.95	-6.19	-0.48
2	-2.8	-0.05	5.59	-2.24	-0.32
2	-2.8	-0.15	8.97	-4.93	-0.68
2	-2.8	-0.25	6.12	-6.12	-0.88
2	-3	-0.05	6.76	-2.19	-0.83
2	-3	-0.15	11.83	-3.65	-1.47
2	-3	-0.25	1.84	-4.13	-0.23
2	-3.2	-0.05	5.25	-1.27	-0.55
2	-3.2	-0.15	9.63	-2.63	-1.17
2	-3.4	-0.15	11.40	-2.49	-1.45
2	-3.6	-0.15	10.43	-1.43	-1.85
2	-3.8	-0.15	9.95	-0.70	-0.63

Table A2- 36. Line 2-Test 9

Long-shore Distance (m)	**Cross-shore Distance (m)**	**Depth relating to S.W.L. (m)**	**Vy (cm/s)**	**Vx (cm/s)**	**Vz (cm/s)**
4	-0.6	-0.15	0.61	-0.46	0.31
4	-0.6	-0.25	0.21	-0.79	0.21
4	-0.6	-0.35	0.41	-0.73	-0.01
4	-0.8	-0.15	0.73	-0.60	0.18
4	-0.8	-0.25	-0.26	-0.82	0.15
4	-0.8	-0.35	-0.56	-0.72	-0.05
4	-1	-0.15	0.93	-0.82	0.26
4	-1	-0.25	0.50	-0.69	0.10
4	-1	-0.35	-0.34	-0.69	0.17
4	-1.2	-0.15	0.54	-0.89	0.25
4	-1.2	-0.25	-0.40	-0.65	0.13
4	-1.2	-0.35	-0.54	-0.33	-0.02
4	-1.4	-0.15	0.79	-0.18	0.16
4	-1.4	-0.25	-0.09	-0.42	0.16
4	-1.4	-0.35	-0.55	-0.65	-0.03

4	-1.6	-0.05	-2.05	-0.87	-0.01
4	-1.6	-0.15	1.36	-0.22	0.03
4	-1.6	-0.25	-0.18	-0.22	0.11
4	-1.6	-0.35	-1.21	-0.40	-0.33
4	-1.8	-0.05	-2.42	-1.10	0.02
4	-1.8	-0.15	1.23	-0.48	0.12
4	-1.8	-0.25	-0.68	-0.52	0.07
4	-2	-0.15	1.32	-0.75	0.15
4	-2	-0.25	-0.06	-0.65	0.04
4	-2.2	-0.05	-1.69	-1.64	-0.03
4	-2.2	-0.15	1.23	-1.21	0.01
4	-2.2	-0.25	0.22	-0.95	-0.09
4	-2.4	-0.05	-1.86	-1.64	-0.13
4	-2.4	-0.15	1.26	-1.14	-0.03
4	-2.4	-0.25	0.63	-0.75	-0.11
4	-2.6	-0.05	-3.18	-2.26	0.10
4	-2.6	-0.15	1.38	-1.26	0.12
4	-2.6	-0.25	-0.16	-0.25	0.29
4	-2.8	-0.05	-2.00	-3.30	-0.01
4	-2.8	-0.15	0.85	-1.74	-0.01
4	-2.8	-0.25	0.80	-0.02	-0.45
4	-3	-0.05	-1.14	-4.40	-0.11
4	-3	-0.15	2.28	-2.36	-0.23
4	-3.2	-0.05	-0.72	-3.85	
4	-3.2	-0.15	2.53	-3.78	-0.42
4	-3.4	-0.05	-0.50		
4	-3.4	-0.15	1.69	-3.77	-0.17

Table A2- 37. Line 3-Test 9

Long-shore Distance (m)	**Cross-shore Distance (m)**	**Depth relating to S.W.L. (m)**	**Vy (cm/s)**	**Vx (cm/s)**	**Vz (cm/s)**
5.64	-0.6	-0.15	0.57	0.40	0.53
5.64	-0.6	-0.25	-0.16	0.73	0.23
5.64	-0.6	-0.35	-0.56	-0.10	-0.14
5.64	-0.8	-0.15	-0.27	-0.51	0.23
5.64	-0.8	-0.25	0.26	0.11	0.18
5.64	-0.8	-0.35	-0.55	-0.27	0.05
5.64	-1	-0.15	0.46	0.07	0.22
5.64	-1	-0.25	-0.38	0.13	0.18

5.64	-1	-0.35	0.31	0.26	0.21
5.64	-1.2	-0.05	-3.80	-0.85	0.01
5.64	-1.2	-0.15	0.06	-0.16	0.12
5.64	-1.2	-0.25	-0.21	0.39	0.11
5.64	-1.2	-0.35	-0.89	0.34	-0.07
5.64	-1.4	-0.05	-3.37	-1.53	0.07
5.64	-1.4	-0.15	0.25	0.21	0.12
5.64	-1.4	-0.25	-0.05	0.15	0.06
5.64	-1.4	-0.35	-2.07	0.01	-0.05
5.64	-1.6	-0.05	-3.13	-0.11	0.17
5.64	-1.6	-0.15	0.58	0.53	0.10
5.64	-1.6	-0.25	-0.03	-0.02	0.05
5.64	-1.8	-0.05	-3.61	-0.21	0.06
5.64	-1.8	-0.15	0.31	0.25	0.10
5.64	-1.8	-0.25	-0.37	-0.06	0.12
5.64	-2	-0.05	-2.43	-0.50	0.05
5.64	-2	-0.15	0.48	0.31	0.03
5.64	-2	-0.25	-0.41	-0.06	0.18
5.64	-2.2	-0.05	-2.26	-0.50	0.03
5.64	-2.2	-0.15	0.59	0.23	-0.04
5.64	-2.2	-0.25	-0.31	-0.27	-0.02
5.64	-2.4	-0.05	-2.49	-1.14	0.14
5.64	-2.4	-0.15	0.83	0.04	-0.09
5.64	-2.4	-0.25	0.13	1.35	0.81
5.64	-2.6	-0.05	-0.86	-1.00	-0.04
5.64	-2.6	-0.15	0.74	-0.28	-0.16
5.64	-2.8	-0.05	-0.79	-1.73	-0.07
5.64	-2.8	-0.15	1.00	-0.53	-0.09
5.64	-3	-0.05	-0.37	-2.25	-0.16
5.64	-3	-0.15	1.00	-0.86	0.00
5.64	-3.2	-0.05	-0.15	-2.51	-0.09
5.64	-3.2	-0.15	1.09	-1.54	-0.18
5.64	-3.4	-0.05	-0.80	-3.46	-0.24
5.64	-3.4	-0.15	1.95	-1.61	-0.31
5.64	-3.6	-0.05	0.01	-5.24	-0.70
5.64	-3.6	-0.15	2.75		2.42
5.64	-3.8	-0.15	-1.30	-3.56	-0.44

Table A2- 38. Line 1-Test 10

Long-shore Distance (m)	Cross-shore Distance (m)	Depth relating to S.W.L. (m)	Vy (cm/s)	Vx (cm/s)	Vz (cm/s)
2	-0.6	-0.15	4.91	-2.64	-0.16
2	-0.6	-0.25	4.13	-2.34	-0.15
2	-0.6	-0.35	3.28	-3.29	-0.20
2	-0.8	-0.05	1.18	-2.77	-0.17
2	-0.8	-0.15	5.52	-1.54	-0.35
2	-0.8	-0.25	4.20	-3.21	-0.25
2	-0.8	-0.35	2.53	-2.67	-0.34
2	-1	-0.05	-0.46	-1.74	-0.20
2	-1	-0.15	4.48	-1.94	-0.22
2	-1	-0.25	3.85	-1.88	-0.08
2	-1	-0.35	0.90	-2.66	0.02
2	-1.2	-0.05	0.44		
2	-1.2	-0.15	4.44	-2.04	-0.16
2	-1.2	-0.25	3.60	-2.74	-0.08
2	-1.2	-0.35	1.79	-2.65	-0.19
2	-1.4	-0.05	1.26	-2.18	-0.10
2	-1.4	-0.15	4.76	-1.83	0.07
2	-1.4	-0.25	3.11	-3.32	0.02
2	-1.4	-0.35	0.78	-1.67	-0.11
2	-1.6	-0.05	-0.42	-1.11	-0.06
2	-1.6	-0.15	5.02	-2.15	-0.09
2	-1.6	-0.25	2.66	-1.89	-0.02
2	-1.6	-0.35	0.55	-1.53	-0.24
2	-1.8	-0.05	0.00	-1.52	-0.14
2	-1.8	-0.15	4.40	-2.24	-0.05
2	-1.8	-0.25	1.70	-1.29	-0.07
2	-1.8	-0.35	-0.49	-1.55	-0.04
2	-2	-0.05	-0.06	-0.83	-0.04
2	-2	-0.15	2.73	-1.29	0.11
2	-2	-0.25	1.74	-0.93	0.14
2	-2	-0.35	-0.27	-0.98	-0.16
2	-2.2	-0.05	-0.68	-1.39	-0.07
2	-2.2	-0.15	2.34	-0.49	-0.04
2	-2.2	-0.25	1.62	-1.08	-0.09
2	-2.2	-0.35	-1.14	0.08	0.08

2	-2.4	-0.05	-0.96	-1.40	-0.03
2	-2.4	-0.15	1.70	0.32	-0.04
2	-2.4	-0.25	0.97	0.20	-0.12
2	-2.4	-0.35	0.06	-0.36	-0.36
2	-2.6	-0.05	-1.74		
2	-2.6	-0.15	1.77	-0.11	0.10
2	-2.6	-0.25	1.64	0.43	-0.14
2	-2.8	-0.05			-0.01
2	-2.8	-0.15	0.87	0.91	-0.02
2	-2.8	-0.25	2.68	1.41	-0.44
2	-3	-0.05	-2.04	-0.58	-0.04
2	-3	-0.15	1.35	1.02	-0.24
2	-3	-0.25	2.86	1.30	-0.17
2	-3.2	-0.05	-1.64	0.44	-0.04
2	-3.2	-0.15	3.39	2.04	-0.83
2	-3.2	-0.25	-0.52	0.27	-0.65
2	-3.4	-0.15	3.65	2.36	-0.54
2	-3.6	-0.15	4.55	4.01	-0.56
2	-3.8	-0.15	4.50	4.55	-1.19
2	-4	-0.15	2.36	2.90	-1.10

Table A2- 39. Line 2-Test 10

Long-shore Distance (m)	**Cross-shore Distance (m)**	**Depth relating to S.W.L. (m)**	**Vy (cm/s)**	**Vx (cm/s)**	**Vz (cm/s)**
4	-0.6	-0.15	1.90	-0.78	0.09
4	-0.6	-0.25	1.93	-0.43	-0.18
4	-0.6	-0.35	2.20	-1.17	-0.20
4	-0.8	-0.05	0.27	-0.89	-0.18
4	-0.8	-0.15	2.89	-0.37	-0.20
4	-0.8	-0.25	2.05	-1.20	-0.09
4	-0.8	-0.35	1.03	-0.50	-0.14
4	-1	-0.05	0.07	-0.96	-0.14
4	-1	-0.15	3.07	-0.09	-0.25
4	-1	-0.25	1.74	-1.22	-0.23
4	-1	-0.35	1.19	-0.96	0.03
4	-1.2	-0.05	-1.02	-1.09	-0.18
4	-1.2	-0.15	3.07	-0.29	-0.16
4	-1.2	-0.25	1.83	-0.63	-0.20
4	-1.2	-0.35	0.94	-1.06	-0.12

4	-1.4	-0.05	-0.33	-0.41	-0.19
4	-1.4	-0.15	2.93	-1.01	-0.24
4	-1.4	-0.25	1.88	-0.43	-0.17
4	-1.4	-0.35	0.25	-1.04	0.07
4	-1.6	-0.05	0.55	-0.26	-0.41
4	-1.6	-0.15	3.57	-0.30	-0.37
4	-1.6	-0.25	1.80	-1.12	-0.22
4	-1.6	-0.35	-1.10	-0.53	-0.12
4	-1.8	-0.05	1.44	-0.80	-0.23
4	-1.8	-0.15	3.52	0.06	-0.23
4	-1.8	-0.25	1.60	-0.93	-0.18
4	-1.8	-0.35	0.31	0.12	0.06
4	-2	-0.05	1.68	0.19	-0.44
4	-2	-0.15	3.34	-0.61	-0.43
4	-2	-0.25	1.62	-0.48	-0.23
4	-2.2	-0.05	0.84	-0.47	-0.33
4	-2.2	-0.15	3.44	-0.09	-0.16
4	-2.2	-0.25	0.38	-0.63	0.62
4	-2.4	-0.05	1.68	-0.66	-0.30
4	-2.4	-0.15	3.59	-0.07	-0.12
4	-2.4	-0.25	-0.18	-0.71	0.12
4	-2.6	-0.05	1.49	-0.98	-0.02
4	-2.6	-0.15	3.53	-0.63	-0.21
4	-2.6	-0.25	0.78	-0.45	-0.42
4	-2.8	-0.05	1.31	-1.07	-0.05
4	-2.8	-0.15	3.96	-0.69	-0.29
4	-3	-0.05	0.59	-1.12	-0.18
4	-3	-0.15	3.65	-0.98	-0.25
4	-3.2	-0.05	-1.07	-0.83	
4	-3.2	-0.15	2.91	-0.98	-0.33
4	-3.4	-0.05	0.24	-2.03	-0.21
4	-3.4	-0.15	3.80	-0.36	-0.15
4	-3.6	-0.05	-0.22	-1.96	-0.24
4	-3.6	-0.15	3.71	-0.78	-0.79
4	-3.8	-0.05	0.32	-1.76	-0.26
4	-3.8	-0.15	3.61	-1.45	-1.12
4	-4	-0.05	-0.31	-1.47	-0.27
4	-4	-0.15	4.50	-0.76	-0.54
4	-4.2	-0.15	3.87	-1.21	-0.69
4	-4.4	-0.15	3.74	-1.11	-1.50

Table A2- 40. Line 3-Test 10

Long-shore Distance (m)	Cross-shore Distance (m)	Depth relating to S.W.L. (m)	Vy (cm/s)	Vx (cm/s)	Vz (cm/s)
5.64	-0.6	-0.15	1.24	-0.25	0.05
5.64	-0.6	-0.25	0.87	0.01	-0.01
5.64	-0.6	-0.35	0.83	-0.62	-0.10
5.64	-0.8	-0.15	0.63	-0.91	0.11
5.64	-0.8	-0.25	1.21	-0.67	0.06
5.64	-0.8	-0.35	1.27	-0.24	-0.12
5.64	-1	-0.15	0.83	-0.81	0.05
5.64	-1	-0.25	0.66	-1.37	0.02
5.64	-1	-0.35	1.73	0.10	-0.25
5.64	-1.2	-0.15	1.26	-0.74	-0.07
5.64	-1.2	-0.25	0.65	-1.31	-0.08
5.64	-1.2	-0.35	-0.27	0.11	0.22
5.64	-1.4	-0.15	1.36	-0.91	-0.04
5.64	-1.4	-0.25	1.01	-0.75	-0.10
5.64	-1.4	-0.35	-0.13	-0.87	-0.03
5.64	-1.6	-0.15	0.64	-1.33	0.01
5.64	-1.6	-0.25	0.90	-1.02	-0.27
5.64	-1.6	-0.35	-4.10	-0.60	0.21
5.64	-1.8	-0.05	-1.31	-0.57	-0.20
5.64	-1.8	-0.15	2.02	-1.19	-0.37
5.64	-1.8	-0.25	0.82	-1.20	0.07
5.64	-2	-0.05	-0.84	-1.00	-0.20
5.64	-2	-0.15	2.51	-0.44	-0.20
5.64	-2	-0.25	0.04	-1.41	0.05
5.64	-2.2	-0.05	-0.65	-0.30	-0.23
5.64	-2.2	-0.15	2.10	-0.77	-0.14
5.64	-2.2	-0.25	0.64	-1.08	0.04
5.64	-2.4	-0.05	-0.54	0.20	-0.18
5.64	-2.4	-0.15	1.12	-1.12	-0.07
5.64	-2.4	-0.25	0.46	-0.11	0.01
5.64	-2.6	-0.05	-0.86	0.05	-0.28
5.64	-2.6	-0.15	1.93	-0.91	-0.16
5.64	-2.6	-0.25	-0.65	-0.53	-0.36
5.64	-2.8	-0.05	-1.32	-0.57	-0.42
5.64	-2.8	-0.15	1.89	-0.68	-0.06
5.64	-2.8	-0.25	2.63	-0.50	-0.04

5.64	-3	-0.05	-1.32	-0.73	-0.18
5.64	-3	-0.15	2.81	-0.92	-0.16
5.64	-3.2	-0.05	-0.40	-0.82	-0.02
5.64	-3.2	-0.15	2.52	-1.30	-0.20
5.64	-3.4	-0.05	-2.23	-1.77	-0.26
5.64	-3.4	-0.15	3.56	-1.32	-0.41
5.64	-3.6	-0.15	3.53	-1.95	-0.35
5.64	-3.8	-0.15	3.60	-1.96	-0.63
5.64	-4	-0.15	2.47	-2.03	-0.25
5.64	-4.2	-0.15	2.58	-2.14	-0.21
5.64	-4.4	-0.15	4.65	-2.88	-1.34
5.64	-4.6	-0.15	4.09	-1.51	

A3. Measured cross-shore beach profile

Table A2- 41. Line 1 (Test 1 and Test 2)

ORIGINAL PROFILE			AFTER TEST 1			AFTER TEST 2		
Long-shore distance (m)	**Cross-shore distance (m)**	**Depth relating to S.W.L. (m)**	**Long-shore distance (m)**	**Cross-shore distance (m)**	**Depth relating to S.W.L. (m)**	**Long-shore distance (m)**	**Cross-shore distance (m)**	**Depth relating to S.W.L. (m)**
2	-0.6	-0.474	2	-0.6	-0.474	2	-0.6	-0.485
2	-0.7	-0.486	2	-0.7	-0.471	2	-0.7	-0.474
2	-0.8	-0.485	2	-0.8	-0.473	2	-0.8	-0.479
2	-0.9	-0.492	2	-0.9	-0.486	2	-0.9	-0.488
2	-1	-0.488	2	-1	-0.480	2	-1	-0.483
2	-1.1	-0.493	2	-1.1	-0.471	2	-1.1	-0.472
2	-1.2	-0.486	2	-1.2	-0.491	2	-1.2	-0.488
2	-1.3	-0.480	2	-1.3	-0.474	2	-1.3	-0.479
2	-1.4	-0.488	2	-1.4	-0.485	2	-1.4	-0.484
2	-1.5	-0.486	2	-1.5	-0.482	2	-1.5	-0.483
2	-1.6	-0.479	2	-1.6	-0.480	2	-1.6	-0.479
2	-1.7	-0.480	2	-1.7	-0.475	2	-1.7	-0.477
2	-1.8	-0.473	2	-1.8	-0.463	2	-1.8	-0.475
2	-1.9	-0.452	2	-1.9	-0.461	2	-1.9	-0.449
2	-2	-0.449	2	-2	-0.440	2	-2	-0.458
2	-2.1	-0.427	2	-2.1	-0.426	2	-2.1	-0.419
2	-2.2	-0.427	2	-2.2	-0.418	2	-2.2	-0.405
2	-2.3	-0.406	2	-2.3	-0.394	2	-2.3	-0.395
2	-2.4	-0.371	2	-2.4	-0.379	2	-2.4	-0.398
2	-2.5	-0.371	2	-2.5	-0.379	2	-2.5	-0.382
2	-2.6	-0.364	2	-2.6	-0.354	2	-2.6	-0.382
2	-2.7	-0.353	2	-2.7	-0.354	2	-2.7	-0.361
2	-2.8	-0.341	2	-2.8	-0.335	2	-2.8	-0.346
2	-2.9	-0.329	2	-2.9	-0.316	2	-2.9	-0.336

2	-3	-0.314	2	-3	-0.310	2	-3	-0.313
2	-3.1	-0.295	2	-3.1	-0.291	2	-3.1	-0.303
2	-3.2	-0.279	2	-3.2	-0.263	2	-3.2	-0.297
2	-3.3	-0.259	2	-3.3	-0.257	2	-3.3	-0.282
2	-3.4	-0.263	2	-3.4	-0.253	2	-3.4	-0.268
2	-3.5	-0.243	2	-3.5	-0.243	2	-3.5	-0.264
2	-3.6	-0.228	2	-3.6	-0.216	2	-3.6	-0.260
2	-3.7	-0.202	2	-3.7	-0.201	2	-3.7	-0.257
2	-3.8	-0.197	2	-3.8	-0.177	2	-3.8	-0.260
2	-3.9	-0.198	2	-3.9	-0.167	2	-3.9	-0.235
2	-4	-0.180	2	-4	-0.148	2	-4	-0.235
2	-4.1	-0.166	2	-4.1	-0.122	2	-4.1	-0.221
2	-4.2	-0.143	2	-4.2	-0.100	2	-4.2	-0.201
2	-4.3	-0.140	2	-4.3	-0.107	2	-4.3	-0.193
2	-4.4	-0.130	2	-4.4	-0.108	2	-4.4	-0.200
2	-4.5	-0.114	2	-4.5	-0.109	2	-4.5	-0.182
2	-4.6	-0.112	2	-4.6	-0.117	2	-4.6	-0.160
2	-4.7	-0.115	2	-4.7	-0.122	2	-4.7	-0.150
2	-4.8	-0.060	2	-4.8	-0.075	2	-4.8	-0.120
2	-4.9	-0.066	2	-4.9	-0.085	2	-4.9	-0.015
2	-5	-0.029	2	-5	-0.085	2	-5	-0.045
2	-5.1	-0.023	2	-5.1	-0.065	2	-5.1	-0.025
2	-5.2	-0.020	2	-5.2	-0.055	2	-5.2	0.015
2	-5.3	0.005	2	-5.3	-0.035	2	-5.3	0.035
2	-5.4	0.020	2	-5.4	-0.025	2	-5.4	0.065
2	-5.5	0.050	2	-5.5	0.015	2	-5.5	0.135
2	-5.6	0.056	2	-5.6	0.035	2	-5.6	0.195
2	-5.7	0.070	2	-5.7	0.145	2	-5.7	0.275
2	-5.8	0.080	2	-5.8	0.145	2	-5.8	0.205
2	-5.9	0.085	2	-5.9	0.125	2	-5.9	0.245

2	-6	0.095	2	-6	0.125	2	-6	0.195

Table A2- 42. Line 2 (Test 1 and Test 2)

ORIGINAL PROFILE			AFTER TEST 1			AFTER TEST 2		
Long-shore distance (m)	**Cross-shore distance (m)**	**Depth relating to S.W.L. (m)**	**Long-shore distance (m)**	**Cross-shore distance (m)**	**Depth relating to S.W.L. (m)**	**Long-shore distance (m)**	**Cross-shore distance (m)**	**Depth relating to S.W.L. (m)**
4	-0.6	-0.438	4	-0.6	-0.441	4	-0.6	-0.436
4	-0.7	-0.421	4	-0.7	-0.435	4	-0.7	-0.440
4	-0.8	-0.404	4	-0.8	-0.425	4	-0.8	-0.420
4	-0.9	-0.405	4	-0.9	-0.412	4	-0.9	-0.403
4	-1	-0.397	4	-1	-0.405	4	-1	-0.404
4	-1.1	-0.385	4	-1.1	-0.403	4	-1.1	-0.397
4	-1.2	-0.384	4	-1.2	-0.383	4	-1.2	-0.383
4	-1.3	-0.389	4	-1.3	-0.389	4	-1.3	-0.381
4	-1.4	-0.356	4	-1.4	-0.382	4	-1.4	-0.374
4	-1.5	-0.345	4	-1.5	-0.351	4	-1.5	-0.349
4	-1.6	-0.337	4	-1.6	-0.360	4	-1.6	-0.346
4	-1.7	-0.337	4	-1.7	-0.334	4	-1.7	-0.334
4	-1.8	-0.312	4	-1.8	-0.328	4	-1.8	-0.311
4	-1.9	-0.296	4	-1.9	-0.313	4	-1.9	-0.303
4	-2	-0.286	4	-2	-0.307	4	-2	-0.290
4	-2.1	-0.273	4	-2.1	-0.292	4	-2.1	-0.267
4	-2.2	-0.255	4	-2.2	-0.285	4	-2.2	-0.252
4	-2.3	-0.254	4	-2.3	-0.251	4	-2.3	-0.255
4	-2.4	-0.241	4	-2.4	-0.245	4	-2.4	-0.265
4	-2.5	-0.237	4	-2.5	-0.241	4	-2.5	-0.244
4	-2.6	-0.237	4	-2.6	-0.247	4	-2.6	-0.243

4	-2.7	-0.212	4	-2.7	-0.221	4	-2.7	-0.241
4	-2.8	-0.196	4	-2.8	-0.227	4	-2.8	-0.237
4	-2.9	-0.199	4	-2.9	-0.215	4	-2.9	-0.237
4	-3	-0.195	4	-3	-0.221	4	-3	-0.230
4	-3.1	-0.191	4	-3.1	-0.248	4	-3.1	-0.247
4	-3.2	-0.168	4	-3.2	-0.261	4	-3.2	-0.254
4	-3.3	-0.164	4	-3.3	-0.272	4	-3.3	-0.286
4	-3.4	-0.163	4	-3.4	-0.297	4	-3.4	-0.302
4	-3.5	-0.160	4	-3.5	-0.306	4	-3.5	-0.298
4	-3.6	-0.150	4	-3.6	-0.319	4	-3.6	-0.264
4	-3.7	-0.144	4	-3.7	-0.292	4	-3.7	-0.238
4	-3.8	-0.128	4	-3.8	-0.274	4	-3.8	-0.249
4	-3.9	-0.121	4	-3.9	-0.264	4	-3.9	-0.230
4	-4	-0.109	4	-4	-0.204	4	-4	-0.185
4	-4.1	-0.101	4	-4.1	-0.174	4	-4.1	-0.206
4	-4.2	-0.072	4	-4.2	-0.140	4	-4.2	-0.199
4	-4.3	-0.073	4	-4.3	-0.117	4	-4.3	-0.200
4	-4.4	-0.063	4	-4.4	-0.123	4	-4.4	-0.199
4	-4.5	-0.056	4	-4.5	-0.122	4	-4.5	-0.185
4	-4.6	-0.022	4	-4.6	-0.124	4	-4.6	-0.185
4	-4.7	-0.020	4	-4.7	-0.113	4	-4.7	-0.177
4	-4.8	-0.005	4	-4.8	-0.114	4	-4.8	-0.145
4	-4.9	0.015	4	-4.9	-0.075	4	-4.9	-0.145
4	-5	0.055	4	-5	-0.085	4	-5	-0.145
4	-5.1	0.065	4	-5.1	-0.055	4	-5.1	-0.135
4	-5.2	0.077	4	-5.2	-0.065	4	-5.2	-0.115
4	-5.3	0.080	4	-5.3	-0.065	4	-5.3	-0.065
4	-5.4	0.100	4	-5.4	-0.055	4	-5.4	-0.025
4	-5.5	0.110	4	-5.5	-0.025	4	-5.5	0.005
4	-5.6	0.110	4	-5.6	-0.015	4	-5.6	0.045

4	-5.7	0.130	4	-5.7	0.035	4	-5.7	0.055
4	-5.8	0.125	4	-5.8	0.085	4	-5.8	0.135
4	-5.9	0.135	4	-5.9	0.125	4	-5.9	0.165
4	-6	0.135	4	-6	0.125	4	-6	0.225

Table A2- 43. Line 3 (Test 1 and Test 2)

ORIGINAL PROFILE			AFTER TEST 1			AFTER TEST 2		
Long-shore distance (m)	**Cross-shore distance (m)**	**Depth relating to S.W.L. (m)**	**Long-shore distance (m)**	**Cross-shore distance (m)**	**Depth relating to S.W.L. (m)**	**Long-shore distance (m)**	**Cross-shore distance (m)**	**Depth relating to S.W.L. (m)**
5.64	-0.6	-0.445	5.64	-0.6	-0.447	5.64	-0.6	-0.432
5.64	-0.7	-0.440	5.64	-0.7	-0.445	5.64	-0.7	-0.431
5.64	-0.8	-0.432	5.64	-0.8	-0.439	5.64	-0.8	-0.425
5.64	-0.9	-0.433	5.64	-0.9	-0.423	5.64	-0.9	-0.417
5.64	-1	-0.416	5.64	-1	-0.413	5.64	-1	-0.409
5.64	-1.1	-0.420	5.64	-1.1	-0.398	5.64	-1.1	-0.401
5.64	-1.2	-0.404	5.64	-1.2	-0.405	5.64	-1.2	-0.398
5.64	-1.3	-0.382	5.64	-1.3	-0.387	5.64	-1.3	-0.392
5.64	-1.4	-0.368	5.64	-1.4	-0.369	5.64	-1.4	-0.372
5.64	-1.5	-0.357	5.64	-1.5	-0.343	5.64	-1.5	-0.337
5.64	-1.6	-0.349	5.64	-1.6	-0.342	5.64	-1.6	-0.332
5.64	-1.7	-0.347	5.64	-1.7	-0.321	5.64	-1.7	-0.325
5.64	-1.8	-0.324	5.64	-1.8	-0.301	5.64	-1.8	-0.304
5.64	-1.9	-0.321	5.64	-1.9	-0.289	5.64	-1.9	-0.295
5.64	-2	-0.315	5.64	-2	-0.279	5.64	-2	-0.278
5.64	-2.1	-0.288	5.64	-2.1	-0.257	5.64	-2.1	-0.290
5.64	-2.2	-0.274	5.64	-2.2	-0.305	5.64	-2.2	-0.265
5.64	-2.3	-0.250	5.64	-2.3	-0.241	5.64	-2.3	-0.261

5.64	-2.4	-0.248	5.64	-2.4	-0.219	5.64	-2.4	-0.239
5.64	-2.5	-0.245	5.64	-2.5	-0.225	5.64	-2.5	-0.239
5.64	-2.6	-0.243	5.64	-2.6	-0.222	5.64	-2.6	-0.225
5.64	-2.7	-0.230	5.64	-2.7	-0.217	5.64	-2.7	-0.228
5.64	-2.8	-0.224	5.64	-2.8	-0.221	5.64	-2.8	-0.232
5.64	-2.9	-0.222	5.64	-2.9	-0.222	5.64	-2.9	-0.223
5.64	-3	-0.209	5.64	-3	-0.226	5.64	-3	-0.217
5.64	-3.1	-0.209	5.64	-3.1	-0.222	5.64	-3.1	-0.212
5.64	-3.2	-0.194	5.64	-3.2	-0.206	5.64	-3.2	-0.220
5.64	-3.3	-0.176	5.64	-3.3	-0.204	5.64	-3.3	-0.218
5.64	-3.4	-0.157	5.64	-3.4	-0.224	5.64	-3.4	-0.216
5.64	-3.5	-0.143	5.64	-3.5	-0.227	5.64	-3.5	-0.217
5.64	-3.6	-0.138	5.64	-3.6	-0.253	5.64	-3.6	-0.210
5.64	-3.7	-0.118	5.64	-3.7	-0.244	5.64	-3.7	-0.202
5.64	-3.8	-0.108	5.64	-3.8	-0.222	5.64	-3.8	-0.214
5.64	-3.9	-0.099	5.64	-3.9	-0.199	5.64	-3.9	-0.227
5.64	-4	-0.078	5.64	-4	-0.213	5.64	-4	-0.229
5.64	-4.1	-0.074	5.64	-4.1	-0.167	5.64	-4.1	-0.229
5.64	-4.2	-0.065	5.64	-4.2	-0.137	5.64	-4.2	-0.235
5.64	-4.3	-0.054	5.64	-4.3	-0.125	5.64	-4.3	-0.239
5.64	-4.4	-0.050	5.64	-4.4	-0.110	5.64	-4.4	-0.227
5.64	-4.5	-0.057	5.64	-4.5	-0.108	5.64	-4.5	-0.212
5.64	-4.6	-0.033	5.64	-4.6	-0.101	5.64	-4.6	-0.193
5.64	-4.7	-0.013	5.64	-4.7	-0.085	5.64	-4.7	-0.203
5.64	-4.8	0.010	5.64	-4.8	-0.055	5.64	-4.8	-0.165
5.64	-4.9	0.024	5.64	-4.9	-0.065	5.64	-4.9	-0.145
5.64	-5	0.035	5.64	-5	-0.045	5.64	-5	-0.155
5.64	-5.1	0.058	5.64	-5.1	-0.005	5.64	-5.1	-0.145
5.64	-5.2	0.069	5.64	-5.2	0.005	5.64	-5.2	-0.125
5.64	-5.3	0.073	5.64	-5.3	0.015	5.64	-5.3	-0.115

5.64	-5.4	0.080	5.64	-5.4	0.055	5.64	-5.4	-0.075
5.64	-5.5	0.100	5.64	-5.5	0.115	5.64	-5.5	-0.045
5.64	-5.6	0.102	5.64	-5.6	0.125	5.64	-5.6	-0.015
5.64	-5.7	0.110	5.64	-5.7	0.155	5.64	-5.7	0.025
5.64	-5.8	0.130	5.64	-5.8	0.155	5.64	-5.8	0.035
5.64	-5.9	0.135	5.64	-5.9	0.145	5.64	-5.9	0.065
5.64	-6	0.140	5.64	-6	0.145	5.64	-6	0.135

Table A2- 44. Line 1 (Test 3 and Test 4)

ORIGINAL PROFILE			AFTER TEST 3			AFTER TEST 4		
Long-shore distance (m)	**Cross-shore distance (m)**	**Depth relating to S.W.L. (m)**	**Long-shore distance (m)**	**Cross-shore distance (m)**	**Depth relating to S.W.L. (m)**	**Long-shore distance (m)**	**Cross-shore distance (m)**	**Depth relating to S.W.L. (m)**
2	-0.6	-0.452	2	-0.6	-0.436	2	-0.6	-0.437
2	-0.7	-0.455	2	-0.7	-0.449	2	-0.7	-0.441
2	-0.8	-0.455	2	-0.8	-0.450	2	-0.8	-0.455
2	-0.9	-0.442	2	-0.9	-0.442	2	-0.9	-0.464
2	-1	-0.443	2	-1	-0.448	2	-1	-0.463
2	-1.1	-0.441	2	-1.1	-0.442	2	-1.1	-0.438
2	-1.2	-0.455	2	-1.2	-0.448	2	-1.2	-0.448
2	-1.3	-0.458	2	-1.3	-0.452	2	-1.3	-0.436
2	-1.4	-0.444	2	-1.4	-0.439	2	-1.4	-0.437
2	-1.5	-0.451	2	-1.5	-0.439	2	-1.5	-0.419
2	-1.6	-0.430	2	-1.6	-0.426	2	-1.6	-0.425
2	-1.7	-0.437	2	-1.7	-0.426	2	-1.7	-0.432
2	-1.8	-0.429	2	-1.8	-0.420	2	-1.8	-0.418
2	-1.9	-0.413	2	-1.9	-0.404	2	-1.9	-0.412
2	-2	-0.407	2	-2	-0.400	2	-2	-0.400
2	-2.1	-0.386	2	-2.1	-0.390	2	-2.1	-0.380

2	-2.2	-0.385	2	-2.2	-0.380	2	-2.2	-0.375
2	-2.3	-0.377	2	-2.3	-0.363	2	-2.3	-0.377
2	-2.4	-0.356	2	-2.4	-0.336	2	-2.4	-0.353
2	-2.5	-0.358	2	-2.5	-0.334	2	-2.5	-0.332
2	-2.6	-0.349	2	-2.6	-0.328	2	-2.6	-0.325
2	-2.7	-0.321	2	-2.7	-0.323	2	-2.7	-0.318
2	-2.8	-0.303	2	-2.8	-0.304	2	-2.8	-0.305
2	-2.9	-0.298	2	-2.9	-0.304	2	-2.9	-0.298
2	-3	-0.270	2	-3	-0.275	2	-3	-0.258
2	-3.1	-0.279	2	-3.1	-0.261	2	-3.1	-0.223
2	-3.2	-0.261	2	-3.2	-0.255	2	-3.2	-0.247
2	-3.3	-0.258	2	-3.3	-0.234	2	-3.3	-0.237
2	-3.4	-0.243	2	-3.4	-0.237	2	-3.4	-0.243
2	-3.5	-0.237	2	-3.5	-0.233	2	-3.5	-0.237
2	-3.6	-0.220	2	-3.6	-0.217	2	-3.6	-0.216
2	-3.7	-0.204	2	-3.7	-0.205	2	-3.7	-0.201
2	-3.8	-0.183	2	-3.8	-0.194	2	-3.8	-0.186
2	-3.9	-0.170	2	-3.9	-0.168	2	-3.9	-0.172
2	-4	-0.168	2	-4	-0.161	2	-4	-0.162
2	-4.1	-0.155	2	-4.1	-0.136	2	-4.1	-0.200
2	-4.2	-0.131	2	-4.2	-0.128	2	-4.2	-0.122
2	-4.3	-0.114	2	-4.3	-0.116	2	-4.3	-0.115
2	-4.4	-0.097	2	-4.4	-0.108	2	-4.4	-0.105
2	-4.5	-0.081	2	-4.5	-0.069	2	-4.5	-0.064
2	-4.6	-0.067	2	-4.6	-0.058	2	-4.6	-0.075
2	-4.7	-0.059	2	-4.7	-0.058	2	-4.7	-0.064
2	-4.8	-0.045	2	-4.8	-0.044	2	-4.8	-0.040
2	-4.9	-0.040	2	-4.9	-0.047	2	-4.9	-0.040
2	-5	-0.028	2	-5	-0.002	2	-5	-0.030
2	-5.1	-0.002	2	-5.1	0.010	2	-5.1	-0.022

2	-5.2	0.003	2	-5.2	-0.008	2	-5.2	0.012
2	-5.3	0.016	2	-5.3	0.022	2	-5.3	0.015
2	-5.4	0.020	2	-5.4	0.041	2	-5.4	0.025
2	-5.5	0.030	2	-5.5	0.035	2	-5.5	0.047
2	-5.6	0.035	2	-5.6	0.028	2	-5.6	0.037
2	-5.7	0.045	2	-5.7	0.065	2	-5.7	0.055
2	-5.8	0.047	2	-5.8	0.085	2	-5.8	0.065
2	-5.9	0.073	2	-5.9	0.090	2	-5.9	0.070
2	-6	0.089	2	-6	0.105	2	-6	0.095

Table A2- 45. Line 2 (Test 3 and Test 4)

ORIGINAL PROFILE			AFTER TEST 3			AFTER TEST 4		
Long-shore distance (m)	**Cross-shore distance (m)**	**Depth relating to S.W.L. (m)**	**Long-shore distance (m)**	**Cross-shore distance (m)**	**Depth relating to S.W.L. (m)**	**Long-shore distance (m)**	**Cross-shore distance (m)**	**Depth relating to S.W.L. (m)**
4	-0.6	-0.407	4	-0.6	-0.385	4	-0.6	-0.387
4	-0.7	-0.408	4	-0.7	-0.397	4	-0.7	-0.401
4	-0.8	-0.391	4	-0.8	-0.389	4	-0.8	-0.386
4	-0.9	-0.387	4	-0.9	-0.390	4	-0.9	-0.380
4	-1	-0.355	4	-1	-0.371	4	-1	-0.366
4	-1.1	-0.354	4	-1.1	-0.352	4	-1.1	-0.359
4	-1.2	-0.346	4	-1.2	-0.365	4	-1.2	-0.363
4	-1.3	-0.338	4	-1.3	-0.324	4	-1.3	-0.338
4	-1.4	-0.322	4	-1.4	-0.325	4	-1.4	-0.325
4	-1.5	-0.309	4	-1.5	-0.308	4	-1.5	-0.313
4	-1.6	-0.293	4	-1.6	-0.298	4	-1.6	-0.303
4	-1.7	-0.302	4	-1.7	-0.295	4	-1.7	-0.310
4	-1.8	-0.284	4	-1.8	-0.275	4	-1.8	-0.290

4	-1.9	-0.277	4	-1.9	-0.267	4	-1.9	-0.267
4	-2	-0.262	4	-2	-0.252	4	-2	-0.276
4	-2.1	-0.256	4	-2.1	-0.250	4	-2.1	-0.256
4	-2.2	-0.258	4	-2.2	-0.243	4	-2.2	-0.248
4	-2.3	-0.246	4	-2.3	-0.243	4	-2.3	-0.240
4	-2.4	-0.229	4	-2.4	-0.231	4	-2.4	-0.236
4	-2.5	-0.229	4	-2.5	-0.227	4	-2.5	-0.214
4	-2.6	-0.220	4	-2.6	-0.226	4	-2.6	-0.220
4	-2.7	-0.212	4	-2.7	-0.218	4	-2.7	-0.228
4	-2.8	-0.214	4	-2.8	-0.204	4	-2.8	-0.209
4	-2.9	-0.218	4	-2.9	-0.222	4	-2.9	-0.209
4	-3	-0.200	4	-3	-0.198	4	-3	-0.207
4	-3.1	-0.193	4	-3.1	-0.210	4	-3.1	-0.197
4	-3.2	-0.169	4	-3.2	-0.182	4	-3.2	-0.187
4	-3.3	-0.162	4	-3.3	-0.184	4	-3.3	-0.180
4	-3.4	-0.167	4	-3.4	-0.166	4	-3.4	-0.162
4	-3.5	-0.158	4	-3.5	-0.181	4	-3.5	-0.152
4	-3.6	-0.153	4	-3.6	-0.176	4	-3.6	-0.150
4	-3.7	-0.141	4	-3.7	-0.151	4	-3.7	-0.147
4	-3.8	-0.157	4	-3.8	-0.147	4	-3.8	-0.134
4	-3.9	-0.136	4	-3.9	-0.134	4	-3.9	-0.137
4	-4	-0.125	4	-4	-0.143	4	-4	-0.125
4	-4.1	-0.110	4	-4.1	-0.119	4	-4.1	-0.117
4	-4.2	-0.114	4	-4.2	-0.123	4	-4.2	-0.125
4	-4.3	-0.112	4	-4.3	-0.103	4	-4.3	-0.109
4	-4.4	-0.103	4	-4.4	-0.096	4	-4.4	-0.096
4	-4.5	-0.103	4	-4.5	-0.100	4	-4.5	-0.091
4	-4.6	-0.086	4	-4.6	-0.090	4	-4.6	-0.083
4	-4.7	-0.074	4	-4.7	-0.057	4	-4.7	-0.065
4	-4.8	-0.055	4	-4.8	-0.045	4	-4.8	-0.055

4	-4.9	-0.045	4	-4.9	-0.055	4	-4.9	-0.055
4	-5	-0.033	4	-5	-0.025	4	-5	-0.038
4	-5.1	-0.021	4	-5.1	-0.030	4	-5.1	-0.027
4	-5.2	-0.011	4	-5.2	-0.022	4	-5.2	-0.012
4	-5.3	0.010	4	-5.3	0.100	4	-5.3	0.042
4	-5.4	0.022	4	-5.4	0.070	4	-5.4	0.105
4	-5.5	0.043	4	-5.5	0.048	4	-5.5	0.072
4	-5.6	0.065	4	-5.6	0.070	4	-5.6	0.090
4	-5.7	0.070	4	-5.7	0.075	4	-5.7	0.100
4	-5.8	0.081	4	-5.8	0.090	4	-5.8	0.100
4	-5.9	0.095	4	-5.9	0.095	4	-5.9	0.125
4	-6	0.085	4	-6	0.115	4	-6	0.115

Table A2- 46. Line 3 (Test 3 and Test 4)

ORIGINAL PROFILE			AFTER TEST 3			AFTER TEST 4		
Long-shore distance (m)	**Cross-shore distance (m)**	**Depth relating to S.W.L. (m)**	**Long-shore distance (m)**	**Cross-shore distance (m)**	**Depth relating to S.W.L. (m)**	**Long-shore distance (m)**	**Cross-shore distance (m)**	**Depth relating to S.W.L. (m)**
5.64	-0.6	-0.411	5.64	-0.6	-0.413	5.64	-0.6	-0.414
5.64	-0.7	-0.394	5.64	-0.7	-0.398	5.64	-0.7	-0.387
5.64	-0.8	-0.385	5.64	-0.8	-0.404	5.64	-0.8	-0.391
5.64	-0.9	-0.403	5.64	-0.9	-0.386	5.64	-0.9	-0.393
5.64	-1	-0.396	5.64	-1	-0.372	5.64	-1	-0.366
5.64	-1.1	-0.387	5.64	-1.1	-0.361	5.64	-1.1	-0.355
5.64	-1.2	-0.352	5.64	-1.2	-0.343	5.64	-1.2	-0.344
5.64	-1.3	-0.361	5.64	-1.3	-0.331	5.64	-1.3	-0.332
5.64	-1.4	-0.347	5.64	-1.4	-0.333	5.64	-1.4	-0.336
5.64	-1.5	-0.349	5.64	-1.5	-0.314	5.64	-1.5	-0.315

5.64	-1.6	-0.323	5.64	-1.6	-0.313	5.64	-1.6	-0.319
5.64	-1.7	-0.308	5.64	-1.7	-0.294	5.64	-1.7	-0.294
5.64	-1.8	-0.317	5.64	-1.8	-0.284	5.64	-1.8	-0.283
5.64	-1.9	-0.303	5.64	-1.9	-0.286	5.64	-1.9	-0.290
5.64	-2	-0.292	5.64	-2	-0.276	5.64	-2	-0.272
5.64	-2.1	-0.275	5.64	-2.1	-0.276	5.64	-2.1	-0.277
5.64	-2.2	-0.277	5.64	-2.2	-0.257	5.64	-2.2	-0.255
5.64	-2.3	-0.265	5.64	-2.3	-0.252	5.64	-2.3	-0.253
5.64	-2.4	-0.248	5.64	-2.4	-0.241	5.64	-2.4	-0.241
5.64	-2.5	-0.250	5.64	-2.5	-0.225	5.64	-2.5	-0.232
5.64	-2.6	-0.248	5.64	-2.6	-0.228	5.64	-2.6	-0.225
5.64	-2.7	-0.233	5.64	-2.7	-0.220	5.64	-2.7	-0.220
5.64	-2.8	-0.231	5.64	-2.8	-0.204	5.64	-2.8	-0.219
5.64	-2.9	-0.212	5.64	-2.9	-0.215	5.64	-2.9	-0.218
5.64	-3	-0.217	5.64	-3	-0.203	5.64	-3	-0.205
5.64	-3.1	-0.210	5.64	-3.1	-0.198	5.64	-3.1	-0.178
5.64	-3.2	-0.209	5.64	-3.2	-0.188	5.64	-3.2	-0.183
5.64	-3.3	-0.198	5.64	-3.3	-0.193	5.64	-3.3	-0.198
5.64	-3.4	-0.190	5.64	-3.4	-0.187	5.64	-3.4	-0.191
5.64	-3.5	-0.190	5.64	-3.5	-0.174	5.64	-3.5	-0.181
5.64	-3.6	-0.186	5.64	-3.6	-0.168	5.64	-3.6	-0.173
5.64	-3.7	-0.166	5.64	-3.7	-0.163	5.64	-3.7	-0.172
5.64	-3.8	-0.172	5.64	-3.8	-0.163	5.64	-3.8	-0.158
5.64	-3.9	-0.164	5.64	-3.9	-0.158	5.64	-3.9	-0.161
5.64	-4	-0.144	5.64	-4	-0.147	5.64	-4	-0.150
5.64	-4.1	-0.139	5.64	-4.1	-0.141	5.64	-4.1	-0.142
5.64	-4.2	-0.126	5.64	-4.2	-0.116	5.64	-4.2	-0.123
5.64	-4.3	-0.122	5.64	-4.3	-0.108	5.64	-4.3	-0.108
5.64	-4.4	-0.091	5.64	-4.4	-0.111	5.64	-4.4	-0.114
5.64	-4.5	-0.091	5.64	-4.5	-0.084	5.64	-4.5	-0.093

5.64	-4.6	-0.099	5.64	-4.6	-0.067	5.64	-4.6	-0.080
5.64	-4.7	-0.074	5.64	-4.7	-0.076	5.64	-4.7	-0.076
5.64	-4.8	-0.080	5.64	-4.8	-0.073	5.64	-4.8	-0.067
5.64	-4.9	-0.073	5.64	-4.9	-0.055	5.64	-4.9	-0.071
5.64	-5	-0.045	5.64	-5	-0.048	5.64	-5	-0.069
5.64	-5.1	-0.045	5.64	-5.1	-0.049	5.64	-5.1	-0.050
5.64	-5.2	-0.030	5.64	-5.2	-0.024	5.64	-5.2	-0.043
5.64	-5.3	-0.005	5.64	-5.3	0.005	5.64	-5.3	0.010
5.64	-5.4	0.015	5.64	-5.4	0.034	5.64	-5.4	0.021
5.64	-5.5	0.027	5.64	-5.5	0.025	5.64	-5.5	0.061
5.64	-5.6	0.045	5.64	-5.6	0.060	5.64	-5.6	0.065
5.64	-5.7	0.048	5.64	-5.7	0.070	5.64	-5.7	0.060
5.64	-5.8	0.070	5.64	-5.8	0.075	5.64	-5.8	0.080
5.64	-5.9	0.075	5.64	-5.9	0.105	5.64	-5.9	0.090
5.64	-6	0.097	5.64	-6	0.125	5.64	-6	0.105

Table A2- 47. Line 1 (Test 5 and Test 6)

ORIGINAL PROFILE			AFTER TEST 5			AFTER TEST 6		
Long-shore distance (m)	**Cross-shore distance (m)**	**Depth relating to S.W.L. (m)**	**Long-shore distance (m)**	**Cross-shore distance (m)**	**Depth relating to S.W.L. (m)**	**Long-shore distance (m)**	**Cross-shore distance (m)**	**Depth relating to S.W.L. (m)**
2	-0.6	-0.428	2	-0.6	-0.400	2	-0.6	-0.416
2	-0.7	-0.451	2	-0.7	-0.427	2	-0.7	-0.406
2	-0.8	-0.469	2	-0.8	-0.436	2	-0.8	-0.396
2	-0.9	-0.464	2	-0.9	-0.439	2	-0.9	-0.378
2	-1	-0.446	2	-1	-0.423	2	-1	-0.381
2	-1.1	-0.430	2	-1.1	-0.408	2	-1.1	-0.368

2	-1.2	-0.460	2	-1.2	-0.444	2	-1.2	-0.363
2	-1.3	-0.446	2	-1.3	-0.444	2	-1.3	-0.360
2	-1.4	-0.453	2	-1.4	-0.421	2	-1.4	-0.330
2	-1.5	-0.427	2	-1.5	-0.414	2	-1.5	-0.329
2	-1.6	-0.438	2	-1.6	-0.414	2	-1.6	-0.323
2	-1.7	-0.430	2	-1.7	-0.411	2	-1.7	-0.317
2	-1.8	-0.418	2	-1.8	-0.401	2	-1.8	-0.342
2	-1.9	-0.407	2	-1.9	-0.389	2	-1.9	-0.317
2	-2	-0.399	2	-2	-0.381	2	-2	-0.274
2	-2.1	-0.369	2	-2.1	-0.369	2	-2.1	-0.273
2	-2.2	-0.366	2	-2.2	-0.356	2	-2.2	-0.269
2	-2.3	-0.354	2	-2.3	-0.343	2	-2.3	-0.253
2	-2.4	-0.363	2	-2.4	-0.348	2	-2.4	-0.253
2	-2.5	-0.328	2	-2.5	-0.321	2	-2.5	-0.231
2	-2.6	-0.318	2	-2.6	-0.291	2	-2.6	-0.228
2	-2.7	-0.317	2	-2.7	-0.289	2	-2.7	-0.217
2	-2.8	-0.293	2	-2.8	-0.284	2	-2.8	-0.226
2	-2.9	-0.292	2	-2.9	-0.286	2	-2.9	-0.207
2	-3	-0.276	2	-3	-0.267	2	-3	-0.212
2	-3.1	-0.276	2	-3.1	-0.255	2	-3.1	-0.198
2	-3.2	-0.249	2	-3.2	-0.264	2	-3.2	-0.185
2	-3.3	-0.244	2	-3.3	-0.249	2	-3.3	-0.200
2	-3.4	-0.242	2	-3.4	-0.231	2	-3.4	-0.202
2	-3.5	-0.241	2	-3.5	-0.223	2	-3.5	-0.200
2	-3.6	-0.221	2	-3.6	-0.217	2	-3.6	-0.181
2	-3.7	-0.212	2	-3.7	-0.212	2	-3.7	-0.170
2	-3.8	-0.198	2	-3.8	-0.186	2	-3.8	-0.178
2	-3.9	-0.193	2	-3.9	-0.175	2	-3.9	-0.136
2	-4	-0.167	2	-4	-0.164	2	-4	-0.131
2	-4.1	-0.174	2	-4.1	-0.154	2	-4.1	-0.133

2	-4.2	-0.153	2	-4.2	-0.153	2	-4.2	-0.129
2	-4.3	-0.150	2	-4.3	-0.138	2	-4.3	-0.139
2	-4.4	-0.131	2	-4.4	-0.129	2	-4.4	-0.144
2	-4.5	-0.111	2	-4.5	-0.116	2	-4.5	-0.141
2	-4.6	-0.113	2	-4.6	-0.112	2	-4.6	-0.142
2	-4.7	-0.096	2	-4.7	-0.095	2	-4.7	-0.132
2	-4.8	-0.060	2	-4.8	-0.095	2	-4.8	-0.115
2	-4.9	-0.060	2	-4.9	-0.085	2	-4.9	-0.125
2	-5	-0.055	2	-5	-0.070	2	-5	-0.107
2	-5.1	-0.020	2	-5.1	-0.055	2	-5.1	-0.120
2	-5.2	-0.023	2	-5.2	-0.047	2	-5.2	-0.110
2	-5.3	0.002	2	-5.3	-0.028	2	-5.3	-0.080
2	-5.4	0.015	2	-5.4	0.015	2	-5.4	0.052
2	-5.5	0.040	2	-5.5	0.045	2	-5.5	0.069
2	-5.6	0.040	2	-5.6	0.085	2	-5.6	0.060
2	-5.7	0.077	2	-5.7	0.065	2	-5.7	0.115
2	-5.8	0.080	2	-5.8	0.050	2	-5.8	0.078
2	-5.9	0.070	2	-5.9	0.055	2	-5.9	0.060
2	-6	0.090	2	-6	0.070	2	-6	0.075

Table A2- 48. Line 2 (Test 5 and Test 6)

ORIGINAL PROFILE			AFTER TEST 5			AFTER TEST 6		
Long-shore distance (m)	**Cross-shore distance (m)**	**Depth relating to S.W.L. (m)**	**Long-shore distance (m)**	**Cross-shore distance (m)**	**Depth relating to S.W.L. (m)**	**Long-shore distance (m)**	**Cross-shore distance (m)**	**Depth relating to S.W.L. (m)**
4	-0.6	-0.406	4	-0.6	-0.391	4	-0.6	-0.414
4	-0.7	-0.397	4	-0.7	-0.380	4	-0.7	-0.397
4	-0.8	-0.376	4	-0.8	-0.381	4	-0.8	-0.404

4	-0.9	-0.377	4	-0.9	-0.370	4	-0.9	-0.379
4	-1	-0.378	4	-1	-0.351	4	-1	-0.366
4	-1.1	-0.379	4	-1.1	-0.343	4	-1.1	-0.374
4	-1.2	-0.363	4	-1.2	-0.321	4	-1.2	-0.340
4	-1.3	-0.354	4	-1.3	-0.329	4	-1.3	-0.338
4	-1.4	-0.345	4	-1.4	-0.337	4	-1.4	-0.323
4	-1.5	-0.319	4	-1.5	-0.305	4	-1.5	-0.322
4	-1.6	-0.293	4	-1.6	-0.296	4	-1.6	-0.304
4	-1.7	-0.297	4	-1.7	-0.277	4	-1.7	-0.294
4	-1.8	-0.301	4	-1.8	-0.276	4	-1.8	-0.282
4	-1.9	-0.268	4	-1.9	-0.251	4	-1.9	-0.280
4	-2	-0.264	4	-2	-0.242	4	-2	-0.262
4	-2.1	-0.254	4	-2.1	-0.233	4	-2.1	-0.245
4	-2.2	-0.236	4	-2.2	-0.207	4	-2.2	-0.237
4	-2.3	-0.238	4	-2.3	-0.219	4	-2.3	-0.229
4	-2.4	-0.236	4	-2.4	-0.211	4	-2.4	-0.226
4	-2.5	-0.227	4	-2.5	-0.211	4	-2.5	-0.203
4	-2.6	-0.220	4	-2.6	-0.203	4	-2.6	-0.207
4	-2.7	-0.216	4	-2.7	-0.178	4	-2.7	-0.208
4	-2.8	-0.205	4	-2.8	-0.176	4	-2.8	-0.199
4	-2.9	-0.186	4	-2.9	-0.168	4	-2.9	-0.195
4	-3	-0.179	4	-3	-0.172	4	-3	-0.193
4	-3.1	-0.175	4	-3.1	-0.161	4	-3.1	-0.177
4	-3.2	-0.167	4	-3.2	-0.159	4	-3.2	-0.158
4	-3.3	-0.160	4	-3.3	-0.141	4	-3.3	-0.147
4	-3.4	-0.163	4	-3.4	-0.149	4	-3.4	-0.153
4	-3.5	-0.173	4	-3.5	-0.151	4	-3.5	-0.161
4	-3.6	-0.165	4	-3.6	-0.153	4	-3.6	-0.154
4	-3.7	-0.149	4	-3.7	-0.145	4	-3.7	-0.150
4	-3.8	-0.151	4	-3.8	-0.127	4	-3.8	-0.137

4	-3.9	-0.142	4	-3.9	-0.131	4	-3.9	-0.150
4	-4	-0.149	4	-4	-0.132	4	-4	-0.147
4	-4.1	-0.142	4	-4.1	-0.137	4	-4.1	-0.135
4	-4.2	-0.133	4	-4.2	-0.115	4	-4.2	-0.133
4	-4.3	-0.109	4	-4.3	-0.112	4	-4.3	-0.133
4	-4.4	-0.124	4	-4.4	-0.125	4	-4.4	-0.117
4	-4.5	-0.099	4	-4.5	-0.092	4	-4.5	-0.141
4	-4.6	-0.101	4	-4.6	-0.099	4	-4.6	-0.137
4	-4.7	-0.084	4	-4.7	-0.088	4	-4.7	-0.120
4	-4.8	-0.075	4	-4.8	-0.077	4	-4.8	-0.125
4	-4.9	-0.053	4	-4.9	-0.074	4	-4.9	-0.115
4	-5	-0.036	4	-5	-0.071	4	-5	-0.090
4	-5.1	-0.037	4	-5.1	-0.065	4	-5.1	-0.070
4	-5.2	-0.008	4	-5.2	-0.030	4	-5.2	-0.035
4	-5.3	0.005	4	-5.3	-0.017	4	-5.3	-0.010
4	-5.4	0.019	4	-5.4	0.005	4	-5.4	0.018
4	-5.5	0.020	4	-5.5	0.065	4	-5.5	0.087
4	-5.6	0.028	4	-5.6	0.055	4	-5.6	0.115
4	-5.7	0.060	4	-5.7	0.045	4	-5.7	0.165
4	-5.8	0.085	4	-5.8	0.045	4	-5.8	0.140
4	-5.9	0.105	4	-5.9	0.075	4	-5.9	0.090
4	-6	0.115	4	-6	0.087	4	-6	0.095

Table A2- 49. Line 3 (Test 5 and Test 6)

ORIGINAL PROFILE			AFTER TEST 5			AFTER TEST 6		
Long-shore distance (m)	**Cross-shore distance (m)**	**Depth relating to S.W.L. (m)**	**Long-shore distance (m)**	**Cross-shore distance (m)**	**Depth relating to S.W.L. (m)**	**Long-shore distance (m)**	**Cross-shore distance (m)**	**Depth relating to S.W.L. (m)**
5.64	-0.6	-0.431	5.64	-0.6	-0.405	5.64	-0.6	-0.436
5.64	-0.7	-0.422	5.64	-0.7	-0.398	5.64	-0.7	-0.443
5.64	-0.8	-0.414	5.64	-0.8	-0.393	5.64	-0.8	-0.460
5.64	-0.9	-0.398	5.64	-0.9	-0.371	5.64	-0.9	-0.461
5.64	-1	-0.367	5.64	-1	-0.379	5.64	-1	-0.467
5.64	-1.1	-0.378	5.64	-1.1	-0.359	5.64	-1.1	-0.419
5.64	-1.2	-0.377	5.64	-1.2	-0.351	5.64	-1.2	-0.451
5.64	-1.3	-0.349	5.64	-1.3	-0.351	5.64	-1.3	-0.447
5.64	-1.4	-0.360	5.64	-1.4	-0.321	5.64	-1.4	-0.435
5.64	-1.5	-0.340	5.64	-1.5	-0.321	5.64	-1.5	-0.441
5.64	-1.6	-0.326	5.64	-1.6	-0.286	5.64	-1.6	-0.441
5.64	-1.7	-0.300	5.64	-1.7	-0.284	5.64	-1.7	-0.421
5.64	-1.8	-0.287	5.64	-1.8	-0.274	5.64	-1.8	-0.411
5.64	-1.9	-0.286	5.64	-1.9	-0.266	5.64	-1.9	-0.411
5.64	-2	-0.253	5.64	-2	-0.249	5.64	-2	-0.392
5.64	-2.1	-0.278	5.64	-2.1	-0.258	5.64	-2.1	-0.371
5.64	-2.2	-0.258	5.64	-2.2	-0.263	5.64	-2.2	-0.375
5.64	-2.3	-0.250	5.64	-2.3	-0.233	5.64	-2.3	-0.365
5.64	-2.4	-0.253	5.64	-2.4	-0.232	5.64	-2.4	-0.360
5.64	-2.5	-0.253	5.64	-2.5	-0.234	5.64	-2.5	-0.334
5.64	-2.6	-0.236	5.64	-2.6	-0.212	5.64	-2.6	-0.318
5.64	-2.7	-0.239	5.64	-2.7	-0.221	5.64	-2.7	-0.307
5.64	-2.8	-0.227	5.64	-2.8	-0.202	5.64	-2.8	-0.298
5.64	-2.9	-0.220	5.64	-2.9	-0.199	5.64	-2.9	-0.282
5.64	-3	-0.218	5.64	-3	-0.211	5.64	-3	-0.268

5.64	-3.1	-0.198	5.64	-3.1	-0.186	5.64	-3.1	-0.272
5.64	-3.2	-0.195	5.64	-3.2	-0.179	5.64	-3.2	-0.263
5.64	-3.3	-0.185	5.64	-3.3	-0.168	5.64	-3.3	-0.237
5.64	-3.4	-0.189	5.64	-3.4	-0.168	5.64	-3.4	-0.250
5.64	-3.5	-0.182	5.64	-3.5	-0.155	5.64	-3.5	-0.236
5.64	-3.6	-0.188	5.64	-3.6	-0.167	5.64	-3.6	-0.206
5.64	-3.7	-0.179	5.64	-3.7	-0.159	5.64	-3.7	-0.209
5.64	-3.8	-0.164	5.64	-3.8	-0.147	5.64	-3.8	-0.194
5.64	-3.9	-0.152	5.64	-3.9	-0.150	5.64	-3.9	-0.203
5.64	-4	-0.143	5.64	-4	-0.144	5.64	-4	-0.181
5.64	-4.1	-0.148	5.64	-4.1	-0.133	5.64	-4.1	-0.178
5.64	-4.2	-0.141	5.64	-4.2	-0.124	5.64	-4.2	-0.166
5.64	-4.3	-0.107	5.64	-4.3	-0.129	5.64	-4.3	-0.150
5.64	-4.4	-0.087	5.64	-4.4	-0.110	5.64	-4.4	-0.134
5.64	-4.5	-0.087	5.64	-4.5	-0.117	5.64	-4.5	-0.124
5.64	-4.6	-0.070	5.64	-4.6	-0.096	5.64	-4.6	-0.126
5.64	-4.7	-0.090	5.64	-4.7	-0.082	5.64	-4.7	-0.109
5.64	-4.8	-0.075	5.64	-4.8	-0.085	5.64	-4.8	-0.105
5.64	-4.9	-0.055	5.64	-4.9	-0.075	5.64	-4.9	-0.110
5.64	-5	-0.039	5.64	-5	-0.077	5.64	-5	-0.080
5.64	-5.1	-0.037	5.64	-5.1	-0.068	5.64	-5.1	-0.027
5.64	-5.2	-0.025	5.64	-5.2	-0.055	5.64	-5.2	-0.018
5.64	-5.3	-0.007	5.64	-5.3	-0.052	5.64	-5.3	0.025
5.64	-5.4	0.005	5.64	-5.4	-0.015	5.64	-5.4	0.105
5.64	-5.5	0.015	5.64	-5.5	-0.005	5.64	-5.5	0.160
5.64	-5.6	0.015	5.64	-5.6	0.035	5.64	-5.6	0.109
5.64	-5.7	0.045	5.64	-5.7	0.040	5.64	-5.7	0.070
5.64	-5.8	0.047	5.64	-5.8	0.045	5.64	-5.8	0.078
5.64	-5.9	0.055	5.64	-5.9	0.055	5.64	-5.9	0.075
5.64	-6	0.065	5.64	-6	0.075	5.64	-6	0.085

Table A2- 50. Line 1 (Test 7 and Test 8)

' ORIGINAL PROFILE			AFTER TEST 7			AFTER TEST 8		
Long-shore distance (m)	**Cross-shore distance (m)**	**Depth relating to S.W.L. (m)**	**Long-shore distance (m)**	**Cross-shore distance (m)**	**Depth relating to S.W.L. (m)**	**Long-shore distance (m)**	**Cross-shore distance (m)**	**Depth relating to S.W.L. (m)**
2	-0.6	-0.443	2	-0.6	-0.454	2	-0.6	-0.445
2	-0.7	-0.433	2	-0.7	-0.424	2	-0.7	-0.427
2	-0.8	-0.420	2	-0.8	-0.433	2	-0.8	-0.431
2	-0.9	-0.417	2	-0.9	-0.426	2	-0.9	-0.405
2	-1	-0.403	2	-1	-0.409	2	-1	-0.405
2	-1.1	-0.392	2	-1.1	-0.400	2	-1.1	-0.393
2	-1.2	-0.393	2	-1.2	-0.407	2	-1.2	-0.405
2	-1.3	-0.404	2	-1.3	-0.402	2	-1.3	-0.402
2	-1.4	-0.401	2	-1.4	-0.405	2	-1.4	-0.406
2	-1.5	-0.385	2	-1.5	-0.381	2	-1.5	-0.380
2	-1.6	-0.371	2	-1.6	-0.382	2	-1.6	-0.389
2	-1.7	-0.356	2	-1.7	-0.387	2	-1.7	-0.384
2	-1.8	-0.374	2	-1.8	-0.382	2	-1.8	-0.367
2	-1.9	-0.373	2	-1.9	-0.382	2	-1.9	-0.386
2	-2	-0.372	2	-2	-0.373	2	-2	-0.377
2	-2.1	-0.330	2	-2.1	-0.329	2	-2.1	-0.333
2	-2.2	-0.323	2	-2.2	-0.329	2	-2.2	-0.325
2	-2.3	-0.324	2	-2.3	-0.327	2	-2.3	-0.335
2	-2.4	-0.312	2	-2.4	-0.323	2	-2.4	-0.315
2	-2.5	-0.311	2	-2.5	-0.314	2	-2.5	-0.306
2	-2.6	-0.303	2	-2.6	-0.301	2	-2.6	-0.357
2	-2.7	-0.281	2	-2.7	-0.278	2	-2.7	-0.283
2	-2.8	-0.241	2	-2.8	-0.243	2	-2.8	-0.245
2	-2.9	-0.238	2	-2.9	-0.237	2	-2.9	-0.242

2	-3	-0.227	2	-3	-0.234	2	-3	-0.249
2	-3.1	-0.232	2	-3.1	-0.244	2	-3.1	-0.236
2	-3.2	-0.210	2	-3.2	-0.217	2	-3.2	-0.221
2	-3.3	-0.218	2	-3.3	-0.230	2	-3.3	-0.231
2	-3.4	-0.209	2	-3.4	-0.209	2	-3.4	-0.213
2	-3.5	-0.235	2	-3.5	-0.216	2	-3.5	-0.208
2	-3.6	-0.213	2	-3.6	-0.219	2	-3.6	-0.224
2	-3.7	-0.167	2	-3.7	-0.231	2	-3.7	-0.185
2	-3.8	-0.174	2	-3.8	-0.213	2	-3.8	-0.195
2	-3.9	-0.181	2	-3.9	-0.193	2	-3.9	-0.190
2	-4	-0.171	2	-4	-0.177	2	-4	-0.170
2	-4.1	-0.127	2	-4.1	-0.137	2	-4.1	-0.158
2	-4.2	-0.110	2	-4.2	-0.128	2	-4.2	-0.132
2	-4.3	-0.106	2	-4.3	-0.119	2	-4.3	-0.131
2	-4.4	-0.107	2	-4.4	-0.115	2	-4.4	-0.128
2	-4.5	-0.136	2	-4.5	-0.109	2	-4.5	-0.118
2	-4.6	-0.084	2	-4.6	-0.098	2	-4.6	-0.107
2	-4.7	-0.079	2	-4.7	-0.125	2	-4.7	-0.103
2	-4.8	-0.065	2	-4.8	-0.080	2	-4.8	-0.067
2	-4.9	-0.048	2	-4.9	-0.071	2	-4.9	-0.027
2	-5	-0.039	2	-5	-0.075	2	-5	0.003
2	-5.1	-0.027	2	-5.1	-0.062	2	-5.1	0.060
2	-5.2	-0.025	2	-5.2	-0.019	2	-5.2	0.083
2	-5.3	0.012	2	-5.3	0.020	2	-5.3	0.078
2	-5.4	-0.011	2	-5.4	0.055	2	-5.4	0.031
2	-5.5	-0.010	2	-5.5	0.035	2	-5.5	0.045
2	-5.6	-0.010	2	-5.6	0.022	2	-5.6	0.065
2	-5.7	0.015	2	-5.7	0.050	2	-5.7	0.080
2	-5.8	0.050	2	-5.8	0.095	2	-5.8	0.125
2	-5.9	0.099	2	-5.9	0.117	2	-5.9	0.127

2	-6	0.121	2	-6	0.140	2	-6	0.135

Table A2- 51. Line 2 (Test 7 and Test 8)

ORIGINAL PROFILE			AFTER TEST 7			AFTER TEST 8		
Long-shore distance (m)	**Cross-shore distance (m)**	**Depth relating to S.W.L. (m)**	**Long-shore distance (m)**	**Cross-shore distance (m)**	**Depth relating to S.W.L. (m)**	**Long-shore distance (m)**	**Cross-shore distance (m)**	**Depth relating to S.W.L. (m)**
4	-0.6	-0.429	4	-0.6	-0.427	4	-0.6	-0.429
4	-0.7	-0.430	4	-0.7	-0.447	4	-0.7	-0.447
4	-0.8	-0.436	4	-0.8	-0.439	4	-0.8	-0.426
4	-0.9	-0.423	4	-0.9	-0.409	4	-0.9	-0.411
4	-1	-0.406	4	-1	-0.414	4	-1	-0.409
4	-1.1	-0.422	4	-1.1	-0.408	4	-1.1	-0.411
4	-1.2	-0.400	4	-1.2	-0.397	4	-1.2	-0.400
4	-1.3	-0.383	4	-1.3	-0.396	4	-1.3	-0.405
4	-1.4	-0.394	4	-1.4	-0.383	4	-1.4	-0.388
4	-1.5	-0.393	4	-1.5	-0.379	4	-1.5	-0.387
4	-1.6	-0.374	4	-1.6	-0.378	4	-1.6	-0.379
4	-1.7	-0.364	4	-1.7	-0.376	4	-1.7	-0.372
4	-1.8	-0.346	4	-1.8	-0.352	4	-1.8	-0.350
4	-1.9	-0.336	4	-1.9	-0.344	4	-1.9	-0.339
4	-2	-0.321	4	-2	-0.328	4	-2	-0.297
4	-2.1	-0.306	4	-2.1	-0.322	4	-2.1	-0.319
4	-2.2	-0.305	4	-2.2	-0.296	4	-2.2	-0.295
4	-2.3	-0.297	4	-2.3	-0.292	4	-2.3	-0.289
4	-2.4	-0.293	4	-2.4	-0.286	4	-2.4	-0.281
4	-2.5	-0.282	4	-2.5	-0.290	4	-2.5	-0.285
4	-2.6	-0.270	4	-2.6	-0.282	4	-2.6	-0.265

4	-2.7	-0.256	4	-2.7	-0.260	4	-2.7	-0.256
4	-2.8	-0.247	4	-2.8	-0.256	4	-2.8	-0.254
4	-2.9	-0.241	4	-2.9	-0.232	4	-2.9	-0.233
4	-3	-0.216	4	-3	-0.232	4	-3	-0.225
4	-3.1	-0.204	4	-3.1	-0.231	4	-3.1	-0.213
4	-3.2	-0.185	4	-3.2	-0.206	4	-3.2	-0.199
4	-3.3	-0.185	4	-3.3	-0.195	4	-3.3	-0.192
4	-3.4	-0.168	4	-3.4	-0.178	4	-3.4	-0.181
4	-3.5	-0.156	4	-3.5	-0.159	4	-3.5	-0.163
4	-3.6	-0.158	4	-3.6	-0.155	4	-3.6	-0.160
4	-3.7	-0.150	4	-3.7	-0.183	4	-3.7	-0.149
4	-3.8	-0.133	4	-3.8	-0.169	4	-3.8	-0.136
4	-3.9	-0.130	4	-3.9	-0.136	4	-3.9	-0.144
4	-4	-0.120	4	-4	-0.131	4	-4	-0.139
4	-4.1	-0.119	4	-4.1	-0.125	4	-4.1	-0.141
4	-4.2	-0.082	4	-4.2	-0.110	4	-4.2	-0.137
4	-4.3	-0.071	4	-4.3	-0.101	4	-4.3	-0.139
4	-4.4	-0.059	4	-4.4	-0.087	4	-4.4	-0.130
4	-4.5	-0.056	4	-4.5	-0.089	4	-4.5	-0.129
4	-4.6	-0.045	4	-4.6	-0.102	4	-4.6	-0.120
4	-4.7	-0.035	4	-4.7	-0.078	4	-4.7	-0.113
4	-4.8	-0.004	4	-4.8	-0.077	4	-4.8	-0.111
4	-4.9	0.010	4	-4.9	-0.050	4	-4.9	-0.068
4	-5	0.013	4	-5	-0.068	4	-5	-0.061
4	-5.1	0.007	4	-5.1	-0.046	4	-5.1	-0.026
4	-5.2	0.005	4	-5.2	-0.035	4	-5.2	0.015
4	-5.3	0.021	4	-5.3	0.007	4	-5.3	0.077
4	-5.4	0.030	4	-5.4	0.044	4	-5.4	0.121
4	-5.5	0.025	4	-5.5	0.016	4	-5.5	0.049
4	-5.6	0.035	4	-5.6	0.045	4	-5.6	0.055

4	-5.7	0.057	4	-5.7	0.065	4	-5.7	0.065
4	-5.8	0.065	4	-5.8	0.050	4	-5.8	0.063
4	-5.9	0.045	4	-5.9	0.077	4	-5.9	0.085
4	-6	0.050	4	-6	0.085	4	-6	0.080

Table A2- 52. Line 3 (Test 7 and Test 8)

ORIGINAL PROFILE			AFTER TEST 7			AFTER TEST 8		
Long-shore distance (m)	**Cross-shore distance (m)**	**Depth relating to S.W.L. (m)**	**Long-shore distance (m)**	**Cross-shore distance (m)**	**Depth relating to S.W.L. (m)**	**Long-shore distance (m)**	**Cross-shore distance (m)**	**Depth relating to S.W.L. (m)**
5.64	-0.6	-0.439	5.64	-0.6	-0.426	5.64	-0.6	-0.427
5.64	-0.7	-0.447	5.64	-0.7	-0.427	5.64	-0.7	-0.423
5.64	-0.8	-0.442	5.64	-0.8	-0.413	5.64	-0.8	-0.419
5.64	-0.9	-0.421	5.64	-0.9	-0.405	5.64	-0.9	-0.396
5.64	-1	-0.392	5.64	-1	-0.387	5.64	-1	-0.379
5.64	-1.1	-0.385	5.64	-1.1	-0.376	5.64	-1.1	-0.372
5.64	-1.2	-0.379	5.64	-1.2	-0.371	5.64	-1.2	-0.348
5.64	-1.3	-0.373	5.64	-1.3	-0.366	5.64	-1.3	-0.361
5.64	-1.4	-0.364	5.64	-1.4	-0.358	5.64	-1.4	-0.360
5.64	-1.5	-0.367	5.64	-1.5	-0.364	5.64	-1.5	-0.344
5.64	-1.6	-0.363	5.64	-1.6	-0.347	5.64	-1.6	-0.350
5.64	-1.7	-0.400	5.64	-1.7	-0.334	5.64	-1.7	-0.341
5.64	-1.8	-0.365	5.64	-1.8	-0.330	5.64	-1.8	-0.322
5.64	-1.9	-0.357	5.64	-1.9	-0.318	5.64	-1.9	-0.311
5.64	-2	-0.323	5.64	-2	-0.314	5.64	-2	-0.306
5.64	-2.1	-0.314	5.64	-2.1	-0.294	5.64	-2.1	-0.289
5.64	-2.2	-0.302	5.64	-2.2	-0.288	5.64	-2.2	-0.291
5.64	-2.3	-0.286	5.64	-2.3	-0.285	5.64	-2.3	-0.278

5.64	-2.4	-0.285	5.64	-2.4	-0.269	5.64	-2.4	-0.267
5.64	-2.5	-0.270	5.64	-2.5	-0.255	5.64	-2.5	-0.258
5.64	-2.6	-0.258	5.64	-2.6	-0.243	5.64	-2.6	-0.245
5.64	-2.7	-0.269	5.64	-2.7	-0.249	5.64	-2.7	-0.246
5.64	-2.8	-0.255	5.64	-2.8	-0.243	5.64	-2.8	-0.248
5.64	-2.9	-0.264	5.64	-2.9	-0.236	5.64	-2.9	-0.237
5.64	-3	-0.266	5.64	-3	-0.230	5.64	-3	-0.243
5.64	-3.1	-0.270	5.64	-3.1	-0.199	5.64	-3.1	-0.222
5.64	-3.2	-0.204	5.64	-3.2	-0.189	5.64	-3.2	-0.197
5.64	-3.3	-0.191	5.64	-3.3	-0.163	5.64	-3.3	-0.168
5.64	-3.4	-0.175	5.64	-3.4	-0.163	5.64	-3.4	-0.172
5.64	-3.5	-0.172	5.64	-3.5	-0.159	5.64	-3.5	-0.161
5.64	-3.6	-0.186	5.64	-3.6	-0.143	5.64	-3.6	-0.147
5.64	-3.7	-0.132	5.64	-3.7	-0.137	5.64	-3.7	-0.154
5.64	-3.8	-0.128	5.64	-3.8	-0.115	5.64	-3.8	-0.133
5.64	-3.9	-0.120	5.64	-3.9	-0.109	5.64	-3.9	-0.125
5.64	-4	-0.129	5.64	-4	-0.110	5.64	-4	-0.129
5.64	-4.1	-0.145	5.64	-4.1	-0.111	5.64	-4.1	-0.115
5.64	-4.2	-0.105	5.64	-4.2	-0.118	5.64	-4.2	-0.123
5.64	-4.3	-0.092	5.64	-4.3	-0.086	5.64	-4.3	-0.119
5.64	-4.4	-0.068	5.64	-4.4	-0.080	5.64	-4.4	-0.111
5.64	-4.5	-0.060	5.64	-4.5	-0.098	5.64	-4.5	-0.108
5.64	-4.6	-0.082	5.64	-4.6	-0.084	5.64	-4.6	-0.110
5.64	-4.7	-0.055	5.64	-4.7	-0.079	5.64	-4.7	-0.120
5.64	-4.8	-0.075	5.64	-4.8	-0.074	5.64	-4.8	-0.125
5.64	-4.9	-0.069	5.64	-4.9	-0.078	5.64	-4.9	-0.109
5.64	-5	-0.053	5.64	-5	-0.077	5.64	-5	-0.096
5.64	-5.1	-0.052	5.64	-5.1	-0.044	5.64	-5.1	-0.085
5.64	-5.2	-0.029	5.64	-5.2	-0.005	5.64	-5.2	-0.081
5.64	-5.3	-0.023	5.64	-5.3	0.046	5.64	-5.3	-0.048

5.64	-5.4	-0.023	5.64	-5.4	0.037	5.64	-5.4	0.005
5.64	-5.5	-0.018	5.64	-5.5	0.030	5.64	-5.5	0.061
5.64	-5.6	0.013	5.64	-5.6	0.043	5.64	-5.6	0.041
5.64	-5.7	0.024	5.64	-5.7	0.048	5.64	-5.7	0.033
5.64	-5.8	0.020	5.64	-5.8	0.061	5.64	-5.8	0.035
5.64	-5.9	0.031	5.64	-5.9	0.066	5.64	-5.9	0.045
5.64	-6	0.055	5.64	-6	0.080	5.64	-6	0.065

Table A2- 53. Line 1 (Test 9 and Test 10)

ORIGINAL PROFILE			AFTER TEST 9			AFTER TEST 10		
Long-shore distance (m)	**Cross-shore distance (m)**	**Depth relating to S.W.L. (m)**	**Long-shore distance (m)**	**Cross-shore distance (m)**	**Depth relating to S.W.L. (m)**	**Long-shore distance (m)**	**Cross-shore distance (m)**	**Depth relating to S.W.L. (m)**
2	-0.6	-0.433	2	-0.6	-0.445	2	-0.6	-0.432
2	-0.7	-0.433	2	-0.7	-0.439	2	-0.7	-0.434
2	-0.8	-0.424	2	-0.8	-0.428	2	-0.8	-0.431
2	-0.9	-0.426	2	-0.9	-0.415	2	-0.9	-0.415
2	-1	-0.418	2	-1	-0.435	2	-1	-0.422
2	-1.1	-0.426	2	-1.1	-0.423	2	-1.1	-0.428
2	-1.2	-0.419	2	-1.2	-0.428	2	-1.2	-0.426
2	-1.3	-0.423	2	-1.3	-0.422	2	-1.3	-0.433
2	-1.4	-0.414	2	-1.4	-0.413	2	-1.4	-0.417
2	-1.5	-0.410	2	-1.5	-0.414	2	-1.5	-0.416
2	-1.6	-0.408	2	-1.6	-0.393	2	-1.6	-0.409
2	-1.7	-0.396	2	-1.7	-0.404	2	-1.7	-0.458
2	-1.8	-0.381	2	-1.8	-0.373	2	-1.8	-0.438
2	-1.9	-0.389	2	-1.9	-0.379	2	-1.9	-0.417
2	-2	-0.374	2	-2	-0.376	2	-2	-0.408

2	-2.1	-0.357	2	-2.1	-0.372	2	-2.1	-0.370
2	-2.2	-0.341	2	-2.2	-0.391	2	-2.2	-0.347
2	-2.3	-0.335	2	-2.3	-0.399	2	-2.3	-0.358
2	-2.4	-0.349	2	-2.4	-0.400	2	-2.4	-0.355
2	-2.5	-0.334	2	-2.5	-0.373	2	-2.5	-0.349
2	-2.6	-0.311	2	-2.6	-0.316	2	-2.6	-0.324
2	-2.7	-0.340	2	-2.7	-0.303	2	-2.7	-0.326
2	-2.8	-0.331	2	-2.8	-0.300	2	-2.8	-0.290
2	-2.9	-0.265	2	-2.9	-0.275	2	-2.9	-0.285
2	-3	-0.254	2	-3	-0.270	2	-3	-0.263
2	-3.1	-0.248	2	-3.1	-0.255	2	-3.1	-0.258
2	-3.2	-0.224	2	-3.2	-0.297	2	-3.2	-0.301
2	-3.3	-0.231	2	-3.3	-0.285	2	-3.3	-0.286
2	-3.4	-0.213	2	-3.4	-0.208	2	-3.4	-0.226
2	-3.5	-0.196	2	-3.5	-0.204	2	-3.5	-0.227
2	-3.6	-0.187	2	-3.6	-0.207	2	-3.6	-0.239
2	-3.7	-0.174	2	-3.7	-0.196	2	-3.7	-0.241
2	-3.8	-0.161	2	-3.8	-0.186	2	-3.8	-0.232
2	-3.9	-0.144	2	-3.9	-0.196	2	-3.9	-0.219
2	-4	-0.149	2	-4	-0.197	2	-4	-0.190
2	-4.1	-0.143	2	-4.1	-0.156	2	-4.1	-0.174
2	-4.2	-0.130	2	-4.2	-0.146	2	-4.2	-0.154
2	-4.3	-0.123	2	-4.3	-0.142	2	-4.3	-0.131
2	-4.4	-0.117	2	-4.4	-0.126	2	-4.4	-0.132
2	-4.5	-0.104	2	-4.5	-0.096	2	-4.5	-0.104
2	-4.6	-0.079	2	-4.6	-0.092	2	-4.6	-0.076
2	-4.7	-0.055	2	-4.7	-0.065	2	-4.7	-0.050
2	-4.8	-0.050	2	-4.8	-0.055	2	-4.8	-0.047
2	-4.9	-0.034	2	-4.9	-0.020	2	-4.9	-0.010
2	-5	-0.034	2	-5	-0.041	2	-5	0.040

2	-5.1	-0.027	2	-5.1	-0.021	2	-5.1	0.083
2	-5.2	-0.002	2	-5.2	0.017	2	-5.2	0.139
2	-5.3	0.015	2	-5.3	0.070	2	-5.3	0.203
2	-5.4	0.030	2	-5.4	0.115	2	-5.4	0.218
2	-5.5	0.042	2	-5.5	0.150	2	-5.5	0.153
2	-5.6	0.053	2	-5.6	0.108	2	-5.6	0.097
2	-5.7	0.099	2	-5.7	0.096	2	-5.7	0.115
2	-5.8	0.120	2	-5.8	0.095	2	-5.8	0.115
2	-5.9	0.130	2	-5.9	0.105	2	-5.9	0.120
2	-6	0.155	2	-6	0.120	2	-6	0.115

Table A2- 54. Line 2 (Test 9 and Test 10)

ORIGINAL PROFILE			AFTER TEST 9			AFTER TEST 10		
Long-shore distance (m)	**Cross-shore distance (m)**	**Depth relating to S.W.L. (m)**	**Long-shore distance (m)**	**Cross-shore distance (m)**	**Depth relating to S.W.L. (m)**	**Long-shore distance (m)**	**Cross-shore distance (m)**	**Depth relating to S.W.L. (m)**
4	-0.6	-0.431	4	-0.6	-0.427	4	-0.6	-0.433
4	-0.7	-0.408	4	-0.7	-0.429	4	-0.7	-0.431
4	-0.8	-0.428	4	-0.8	-0.420	4	-0.8	-0.420
4	-0.9	-0.419	4	-0.9	-0.418	4	-0.9	-0.417
4	-1	-0.417	4	-1	-0.405	4	-1	-0.414
4	-1.1	-0.410	4	-1.1	-0.411	4	-1.1	-0.416
4	-1.2	-0.400	4	-1.2	-0.401	4	-1.2	-0.401
4	-1.3	-0.395	4	-1.3	-0.401	4	-1.3	-0.401
4	-1.4	-0.386	4	-1.4	-0.384	4	-1.4	-0.389
4	-1.5	-0.388	4	-1.5	-0.370	4	-1.5	-0.383
4	-1.6	-0.376	4	-1.6	-0.384	4	-1.6	-0.381
4	-1.7	-0.364	4	-1.7	-0.352	4	-1.7	-0.375

4	-1.8	-0.338	4	-1.8	-0.352	4	-1.8	-0.339
4	-1.9	-0.333	4	-1.9	-0.340	4	-1.9	-0.339
4	-2	-0.330	4	-2	-0.306	4	-2	-0.310
4	-2.1	-0.300	4	-2.1	-0.323	4	-2.1	-0.319
4	-2.2	-0.294	4	-2.2	-0.295	4	-2.2	-0.302
4	-2.3	-0.291	4	-2.3	-0.292	4	-2.3	-0.301
4	-2.4	-0.279	4	-2.4	-0.284	4	-2.4	-0.294
4	-2.5	-0.271	4	-2.5	-0.291	4	-2.5	-0.300
4	-2.6	-0.273	4	-2.6	-0.280	4	-2.6	-0.281
4	-2.7	-0.243	4	-2.7	-0.259	4	-2.7	-0.269
4	-2.8	-0.253	4	-2.8	-0.250	4	-2.8	-0.262
4	-2.9	-0.235	4	-2.9	-0.245	4	-2.9	-0.246
4	-3	-0.226	4	-3	-0.238	4	-3	-0.227
4	-3.1	-0.218	4	-3.1	-0.206	4	-3.1	-0.211
4	-3.2	-0.214	4	-3.2	-0.225	4	-3.2	-0.229
4	-3.3	-0.206	4	-3.3	-0.222	4	-3.3	-0.224
4	-3.4	-0.189	4	-3.4	-0.196	4	-3.4	-0.213
4	-3.5	-0.167	4	-3.5	-0.179	4	-3.5	-0.224
4	-3.6	-0.154	4	-3.6	-0.172	4	-3.6	-0.216
4	-3.7	-0.140	4	-3.7	-0.155	4	-3.7	-0.213
4	-3.8	-0.149	4	-3.8	-0.160	4	-3.8	-0.220
4	-3.9	-0.150	4	-3.9	-0.173	4	-3.9	-0.217
4	-4	-0.155	4	-4	-0.177	4	-4	-0.212
4	-4.1	-0.139	4	-4.1	-0.180	4	-4.1	-0.218
4	-4.2	-0.129	4	-4.2	-0.171	4	-4.2	-0.207
4	-4.3	-0.115	4	-4.3	-0.171	4	-4.3	-0.205
4	-4.4	-0.120	4	-4.4	-0.172	4	-4.4	-0.191
4	-4.5	-0.096	4	-4.5	-0.161	4	-4.5	-0.169
4	-4.6	-0.084	4	-4.6	-0.143	4	-4.6	-0.163
4	-4.7	-0.055	4	-4.7	-0.135	4	-4.7	-0.129

4	-4.8	-0.055	4	-4.8	-0.125	4	-4.8	-0.125
4	-4.9	-0.045	4	-4.9	-0.065	4	-4.9	-0.050
4	-5	-0.043	4	-5	-0.085	4	-5	-0.095
4	-5.1	-0.034	4	-5.1	-0.049	4	-5.1	-0.085
4	-5.2	-0.020	4	-5.2	-0.032	4	-5.2	-0.050
4	-5.3	-0.003	4	-5.3	0.010	4	-5.3	-0.031
4	-5.4	0.020	4	-5.4	0.003	4	-5.4	0.151
4	-5.5	0.039	4	-5.5	0.140	4	-5.5	0.117
4	-5.6	0.051	4	-5.6	0.155	4	-5.6	0.172
4	-5.7	0.062	4	-5.7	0.115	4	-5.7	0.247
4	-5.8	0.065	4	-5.8	0.095	4	-5.8	0.208
4	-5.9	0.080	4	-5.9	0.090	4	-5.9	0.151
4	-6	0.105	4	-6	0.105	4	-6	0.138

Table A2- 55. Line 3 (Test 9 and Test 10)

ORIGINAL PROFILE			AFTER TEST 9			AFTER TEST 10		
Long-shore distance (m)	**Cross-shore distance (m)**	**Depth relating to S.W.L. (m)**	**Long-shore distance (m)**	**Cross-shore distance (m)**	**Depth relating to S.W.L. (m)**	**Long-shore distance (m)**	**Cross-shore distance (m)**	**Depth relating to S.W.L. (m)**
5.64	-0.6	-0.406	5.64	-0.6	-0.429	5.64	-0.6	-0.432
5.64	-0.7	-0.409	5.64	-0.7	-0.418	5.64	-0.7	-0.437
5.64	-0.8	-0.394	5.64	-0.8	-0.426	5.64	-0.8	-0.417
5.64	-0.9	-0.394	5.64	-0.9	-0.415	5.64	-0.9	-0.420
5.64	-1	-0.376	5.64	-1	-0.390	5.64	-1	-0.397
5.64	-1.1	-0.367	5.64	-1.1	-0.389	5.64	-1.1	-0.393
5.64	-1.2	-0.350	5.64	-1.2	-0.388	5.64	-1.2	-0.378
5.64	-1.3	-0.356	5.64	-1.3	-0.375	5.64	-1.3	-0.356
5.64	-1.4	-0.351	5.64	-1.4	-0.370	5.64	-1.4	-0.365

5.64	-1.5	-0.326	5.64	-1.5	-0.347	5.64	-1.5	-0.364
5.64	-1.6	-0.346	5.64	-1.6	-0.361	5.64	-1.6	-0.359
5.64	-1.7	-0.328	5.64	-1.7	-0.333	5.64	-1.7	-0.336
5.64	-1.8	-0.325	5.64	-1.8	-0.336	5.64	-1.8	-0.341
5.64	-1.9	-0.305	5.64	-1.9	-0.322	5.64	-1.9	-0.325
5.64	-2	-0.298	5.64	-2	-0.320	5.64	-2	-0.319
5.64	-2.1	-0.283	5.64	-2.1	-0.314	5.64	-2.1	-0.311
5.64	-2.2	-0.280	5.64	-2.2	-0.352	5.64	-2.2	-0.305
5.64	-2.3	-0.268	5.64	-2.3	-0.290	5.64	-2.3	-0.287
5.64	-2.4	-0.262	5.64	-2.4	-0.277	5.64	-2.4	-0.263
5.64	-2.5	-0.253	5.64	-2.5	-0.271	5.64	-2.5	-0.261
5.64	-2.6	-0.241	5.64	-2.6	-0.259	5.64	-2.6	-0.273
5.64	-2.7	-0.235	5.64	-2.7	-0.260	5.64	-2.7	-0.259
5.64	-2.8	-0.233	5.64	-2.8	-0.262	5.64	-2.8	-0.264
5.64	-2.9	-0.236	5.64	-2.9	-0.248	5.64	-2.9	-0.246
5.64	-3	-0.232	5.64	-3	-0.244	5.64	-3	-0.261
5.64	-3.1	-0.225	5.64	-3.1	-0.240	5.64	-3.1	-0.237
5.64	-3.2	-0.194	5.64	-3.2	-0.220	5.64	-3.2	-0.227
5.64	-3.3	-0.176	5.64	-3.3	-0.207	5.64	-3.3	-0.221
5.64	-3.4	-0.163	5.64	-3.4	-0.194	5.64	-3.4	-0.208
5.64	-3.5	-0.158	5.64	-3.5	-0.170	5.64	-3.5	-0.212
5.64	-3.6	-0.184	5.64	-3.6	-0.156	5.64	-3.6	-0.207
5.64	-3.7	-0.160	5.64	-3.7	-0.165	5.64	-3.7	-0.200
5.64	-3.8	-0.159	5.64	-3.8	-0.164	5.64	-3.8	-0.213
5.64	-3.9	-0.153	5.64	-3.9	-0.168	5.64	-3.9	-0.212
5.64	-4	-0.156	5.64	-4	-0.160	5.64	-4	-0.213
5.64	-4.1	-0.153	5.64	-4.1	-0.147	5.64	-4.1	-0.210
5.64	-4.2	-0.131	5.64	-4.2	-0.158	5.64	-4.2	-0.218
5.64	-4.3	-0.116	5.64	-4.3	-0.153	5.64	-4.3	-0.217
5.64	-4.4	-0.110	5.64	-4.4	-0.157	5.64	-4.4	-0.216

5.64	-4.5	-0.080	5.64	-4.5	-0.173	5.64	-4.5	-0.190
5.64	-4.6	-0.089	5.64	-4.6	-0.158	5.64	-4.6	-0.178
5.64	-4.7	-0.115	5.64	-4.7	-0.165	5.64	-4.7	-0.155
5.64	-4.8	-0.085	5.64	-4.8	-0.130	5.64	-4.8	-0.152
5.64	-4.9	-0.087	5.64	-4.9	-0.109	5.64	-4.9	-0.150
5.64	-5	-0.078	5.64	-5	-0.097	5.64	-5	-0.116
5.64	-5.1	-0.060	5.64	-5.1	-0.085	5.64	-5.1	-0.096
5.64	-5.2	-0.055	5.64	-5.2	-0.059	5.64	-5.2	-0.050
5.64	-5.3	-0.048	5.64	-5.3	-0.037	5.64	-5.3	-0.034
5.64	-5.4	-0.045	5.64	-5.4	0.015	5.64	-5.4	-0.034
5.64	-5.5	-0.024	5.64	-5.5	0.073	5.64	-5.5	0.055
5.64	-5.6	-0.005	5.64	-5.6	0.165	5.64	-5.6	0.090
5.64	-5.7	0.016	5.64	-5.7	0.126	5.64	-5.7	0.135
5.64	-5.8	0.015	5.64	-5.8	0.115	5.64	-5.8	0.175
5.64	-5.9	0.040	5.64	-5.9	0.095	5.64	-5.9	0.168
5.64	-6	0.080	5.64	-6	0.094	5.64	-6	0.170

APPENDIX III

A1. The application of Goda's breaking method in spreadsheet (Torrini and Allsop, 1999)

Goda's breaking method requires offshore wave conditions. In the event that the given wave height is not offshore, a synthetic one is produced, as explained below in the following:

The local wave height at a given water depth is given. The deepwater wavelength is calculated (Eq.A3- 1), and the breaker limit wave height is estimated using Goda's breaking criterion (Eq.A3- 2).

Eq.A3- 1 $$L_0 = \frac{gT_p^{\,2}}{2\pi}$$

where L_0= offshore wavelength

T_p= peak period

Eq.A3- 2 $$\frac{H_b}{L_0} = A\left\{1 - \exp\left[-1.5\frac{\pi d_b}{L_o}\left(1 + 15\left(\frac{1}{m}\right)^{\frac{4}{3}}\right)\right]\right\}$$

where H_b= breaking wave height

A = coefficient set equal to 0.12

m = bed slope (1:)

The given wave height is compared with the limiting wave height, and a warning is given if this has been exceeded; in this case, there is no need to proceed with the method.

If the initial wave height is smaller than the limiting wave height, the local wavelength is determined, using either Fenton's formula (Eq.A3- 3), for intermediate water, or the formula for shallow water (Eq.A3- 4).

Eq.A3- 3 $$L_{local} = L_0 \tanh\frac{2}{3}\left(\frac{2\pi h_{local}}{L_0}\right)^{\frac{3}{4}} \qquad 0.04 \le \frac{h_{local}}{L_{local}} \le 0.5$$

Eq.A3- 4 $$L_{local} = T\sqrt{gh_{local}} \qquad \frac{h_{local}}{L_{local}} < 0.04$$

where L_{local}= wavelength calculated at a given water depth

h_{local}= initial water depth

The shoaling coefficient K_s is then estimated. Since non-linear effects can be neglected in relative deep water (Goda, 1985), the shoaling coefficient is calculated here using the small amplitude wave theory (Eq.A3- 5).

Eq.A3- 5 $$K_s = \frac{1}{\sqrt{\left[1+\frac{\left(\frac{4\pi h_{local}}{L_{local}}\right)}{\sinh\left(\frac{4\pi h_{local}}{L_{local}}\right)}\right]\tanh\left(\frac{2\pi h_{local}}{L_{local}}\right)}}$$

From the relationship relating the offshore wave height to the local wave height (Eq.A3- 6) a synthetic offshore wave height is derived.

Eq.A3- 6 $$H_{s0} = \frac{H_{slocal}}{K_s}$$

The equivalent significant deepwater wave height (significant deepwater wave height after being refracted) is calculated (Eq.A3- 7).

Eq.A3- 7 $$H_{s0}' = K_r H_{s0}$$

where K_r= refraction coefficient

Coming inshore, the shoaling coefficient (Shuto's non-linear shoaling coefficient, as suggested in Goda (1985) is then estimated (Eq. A3-8) and the wave height is determined (Eq.A3- 9).

Eq.A3- 8
$$K_s = K_{si} \quad \text{for } h_{30} \le h$$
$$K_s = (K_{si})_{30}\left(\frac{h_{30}}{h}\right)^{\frac{2}{7}} \quad \text{for } h_{50} \le h \le h_{30}$$
$$K_s\left(\sqrt{K_s} - B\right) - C = 0 \quad \text{for } h < h_{50}$$

where h= water depth

K_{si} = shoaling coefficient for small amplitude wave (Eq.A3- 5)

h_{30} = water depth satisfying Eq.A3- 9

$(K_{si})_{30}$= shoaling coefficient for h_{30}

h_{50} = water depth satisfying Eq.A3- 10

B, C = constants defined in Eq.A3- 11 and Eq.A3- 12

Eq.A3- 9 $$\left(\frac{h_{30}}{L_0}\right)^2 = \frac{2\pi}{30}\frac{H_{s0}'}{L_0}(K_{si})_{30}$$

Eq.A3- 10 $$\left(\frac{h_{50}}{L_0}\right)^2 = \frac{2\pi}{50}\frac{H_{s0}'}{L_0}(K_{si})_{50}$$

Eq.A3- 11 $$B = \frac{2\sqrt{3}}{\sqrt{\frac{2\pi H_{s0}'}{L_0}}}\frac{h}{L_0}$$

Eq.A3- 12 $$C = \frac{C_{50}}{\sqrt{\frac{2\pi H_{s0}'}{L_0}}} \left(\frac{L_0}{h}\right)^{\frac{3}{2}}$$

where $(K_{si})_{30}$= shoaling coefficient at $h=h_{50}$

C_{50} = constant defined by Eq.A3- 13

Eq.A3- 13 $$C_{50} = (K_{si})_{50} \left(\frac{h_{50}}{L_0}\right)^{\frac{3}{2}} \left[\sqrt{2\pi \frac{H_{s0}'}{L_0} (K_{si})_{50}} - 2\sqrt{3}\frac{h_{50}}{L_0}\right]$$

The wave height is then estimated by shoaling, Eq.A3- 14 and compared with the breaker limit wave height, calculated using Goda's breaking criterion (Eq.A3- 2).

Eq.A3- 14 $$H_{si} = K_s H_{s0}'$$

When the limit is exceeded, breaking is initiated, the wave has entered the surf zone and Goda's braking method is applied (Eq.A3- 15).

Eq.A3- 15 $$H_{1/3} = \begin{cases} K_s H_{s0}' & \text{for } \frac{h}{L_0} \geq 0.2 \\ \min\{(\beta_0 H_{s0}' + \beta_1 h), \beta_{max} H_{s0}', K_s H_{s0}'\} & \text{for } \frac{h}{L_0} < 0.2 \end{cases}$$

where β_0, β_1, and β_{max} are defined as follow:

Eq.A3- 16 $$\beta\beta_0 = 0.028 \left(\frac{H_{s0}'}{L_0}\right)^{-0.38} \exp(20m^{1.5})$$

Eq.A3- 17 $$\beta_1 = 0.52e^{4.2m}$$

Eq.A3- 18 $$\beta_{max} = \max\left\{0.92, 0.32 \left(\frac{H_{s0}'}{L_0}\right)^{-0.29} e^{2.4m}\right\}$$

A2. Observation of the cross-shore currents, of each individual test and line, during the experiment

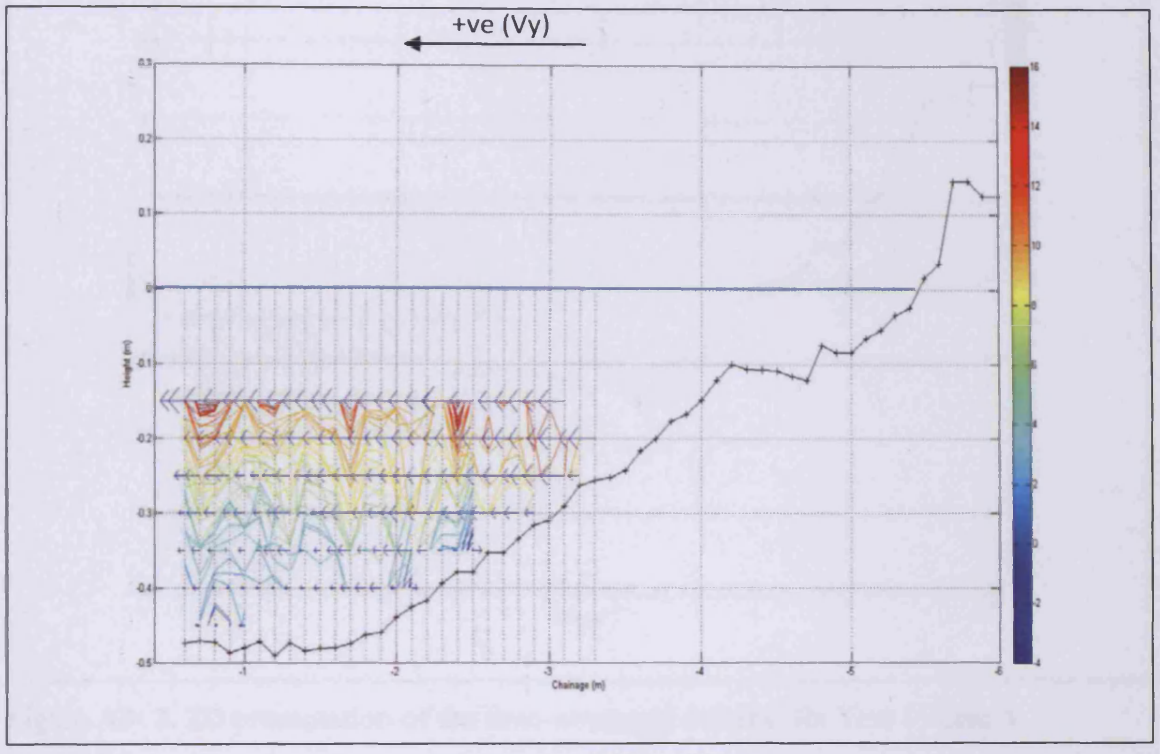

Figure A3- 1.2D presentation of the time-averaged currents for Test 1-Line 1

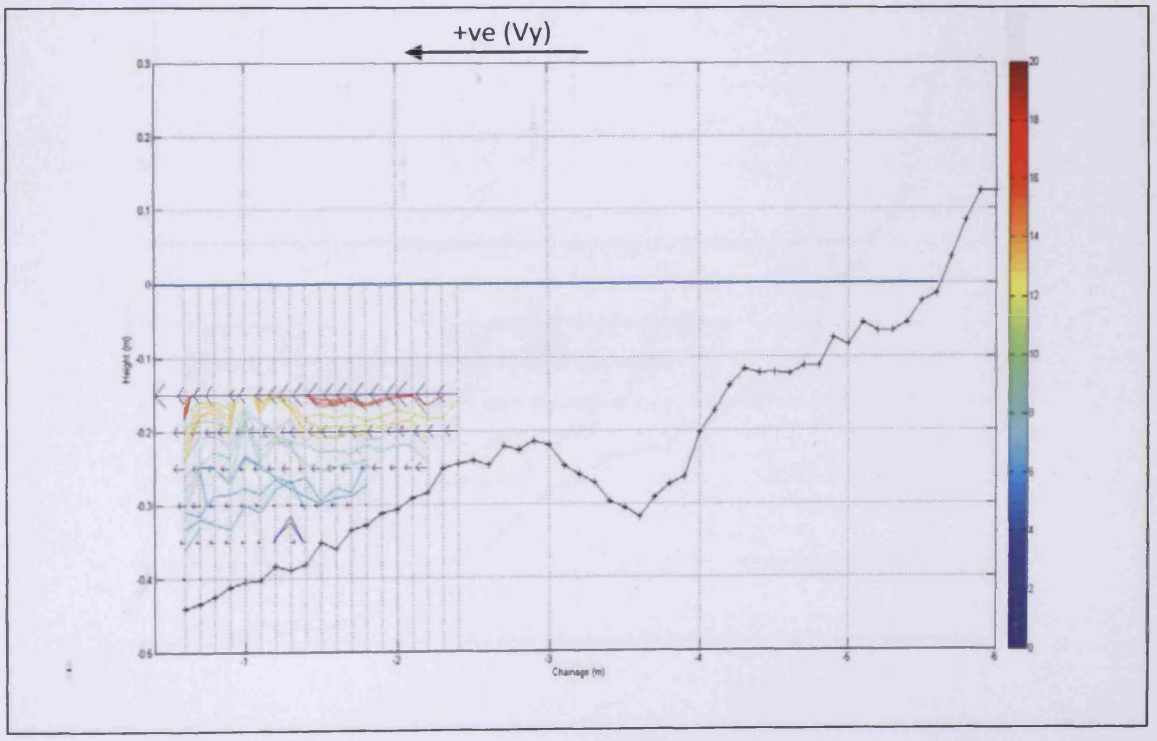

Figure A3- 2. 2D presentation of the time-averaged currents for Test 1- Line 2

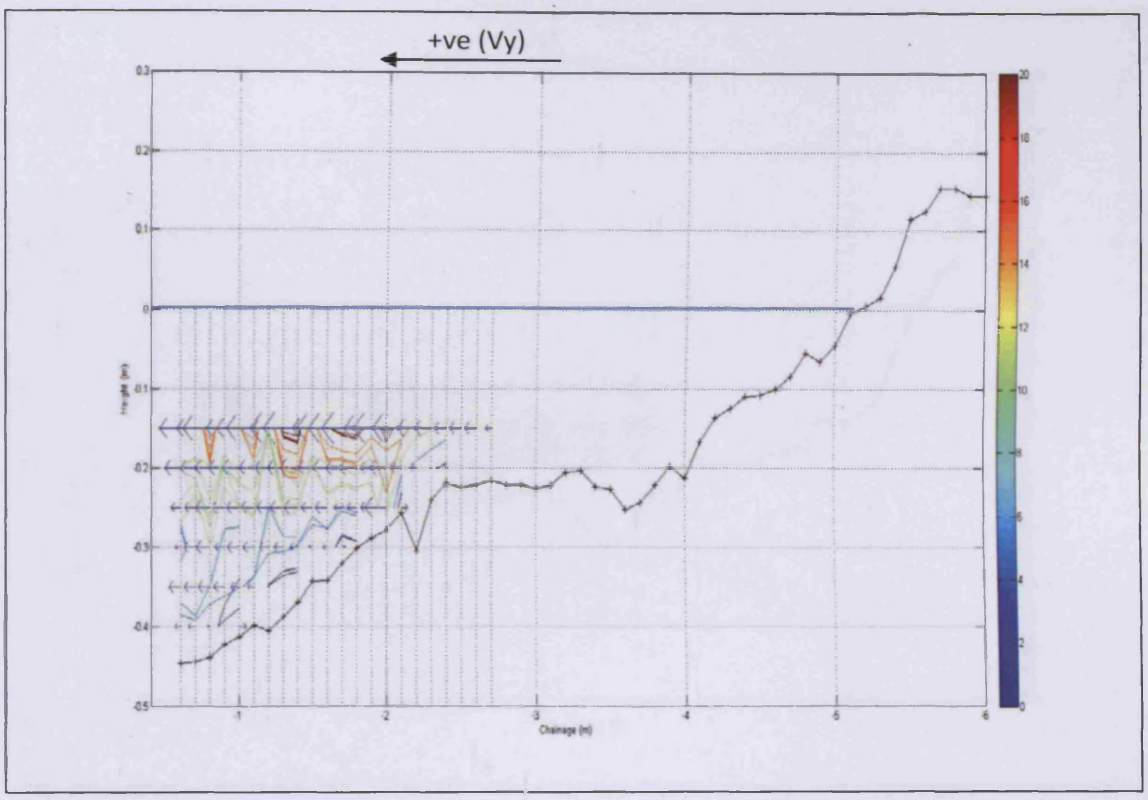

Figure A3- 3. 2D presentation of the time-averaged currents for Test 1- Line 3

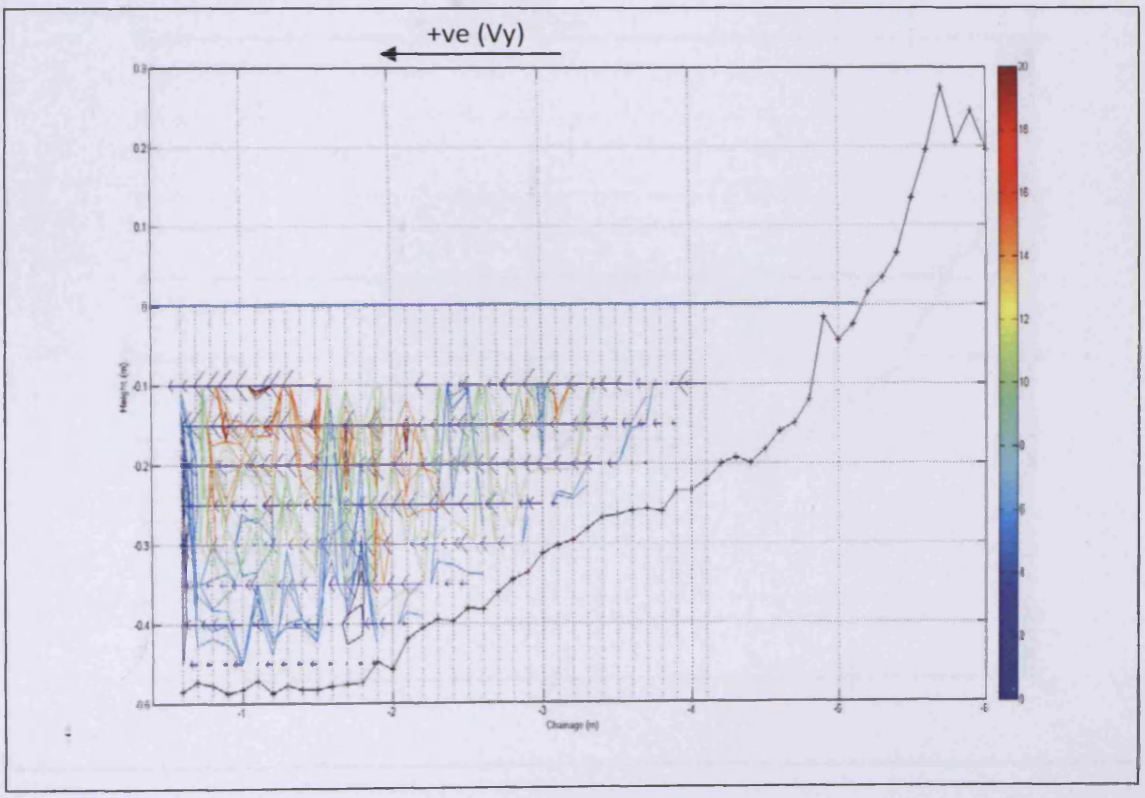

Figure A3- 4. 2D presentation of the time-averaged currents for Test 2- Line 1

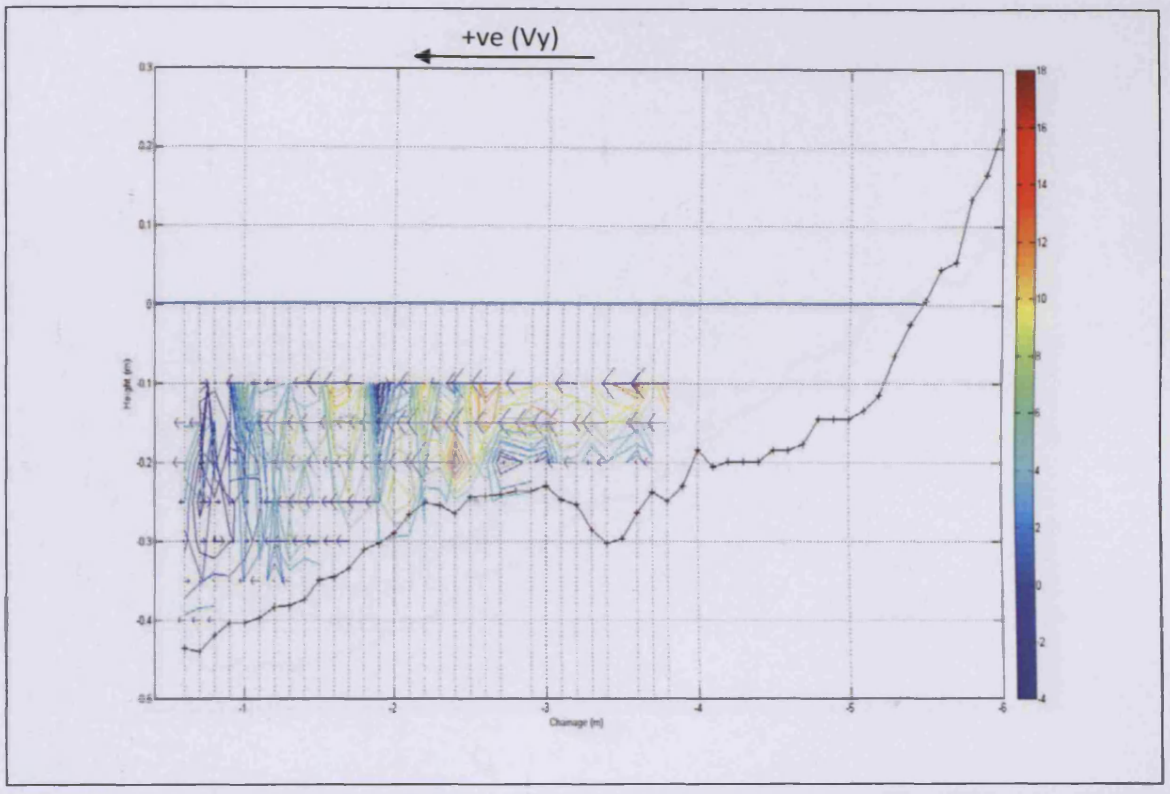

Figure A3- 5. 2D presentation of the time-averaged currents for Test 2- Line 2

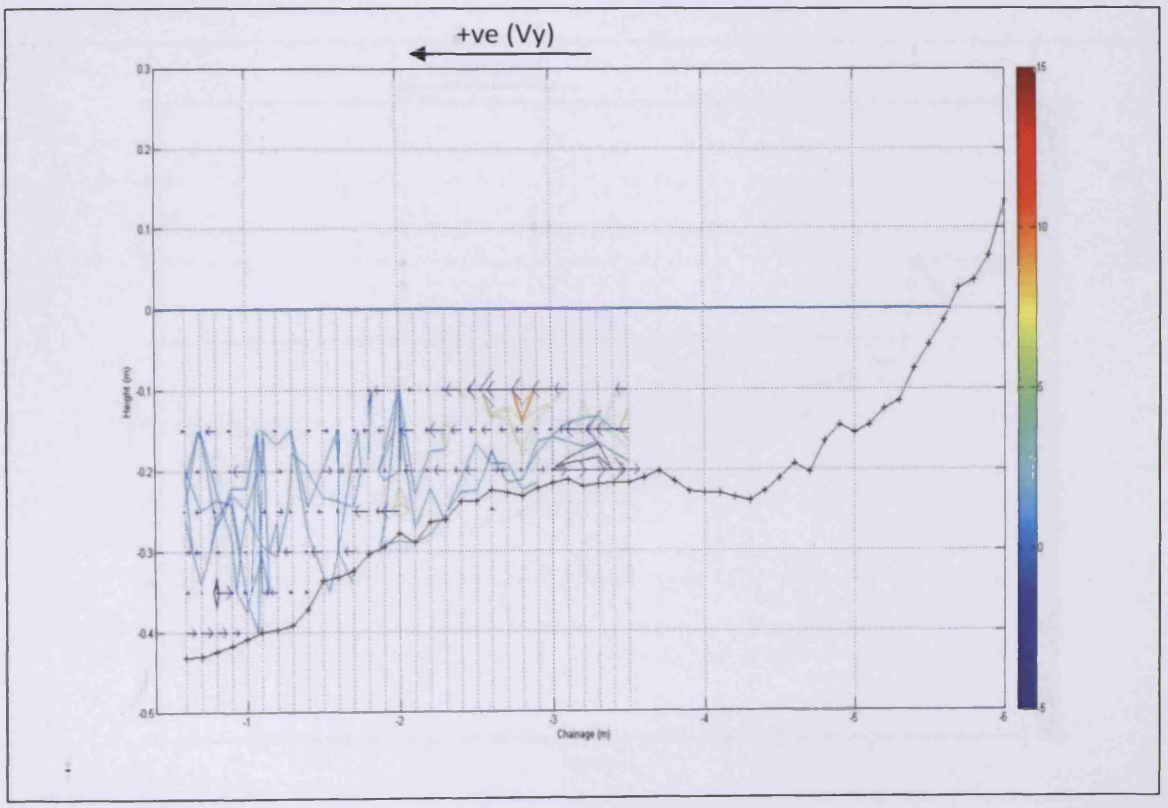

Figure A3- 6. 2D presentation of the time-averaged currents for Test 2- Line 3

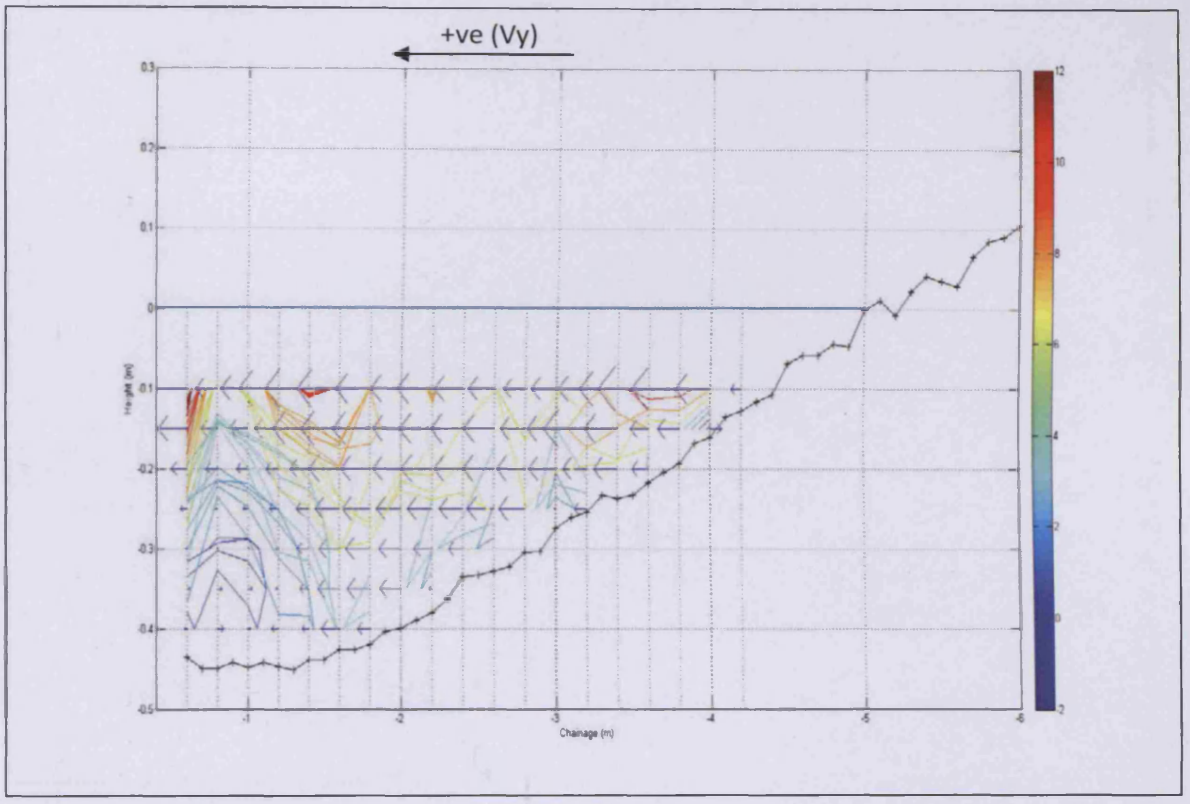

Figure A3- 7. 2D presentation of the time-averaged currents for Test 3- Line 1

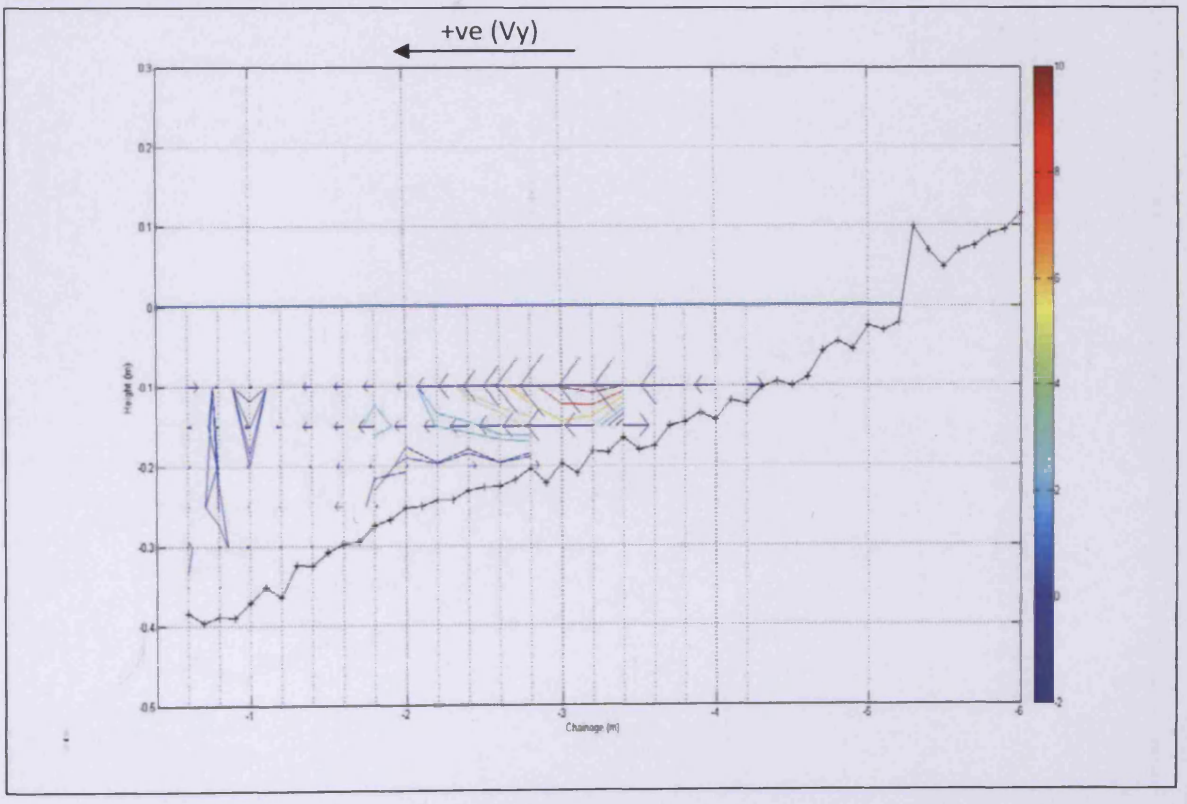

Figure A3- 8. 2D presentation of the time-averaged currents for Test 3- Line 2

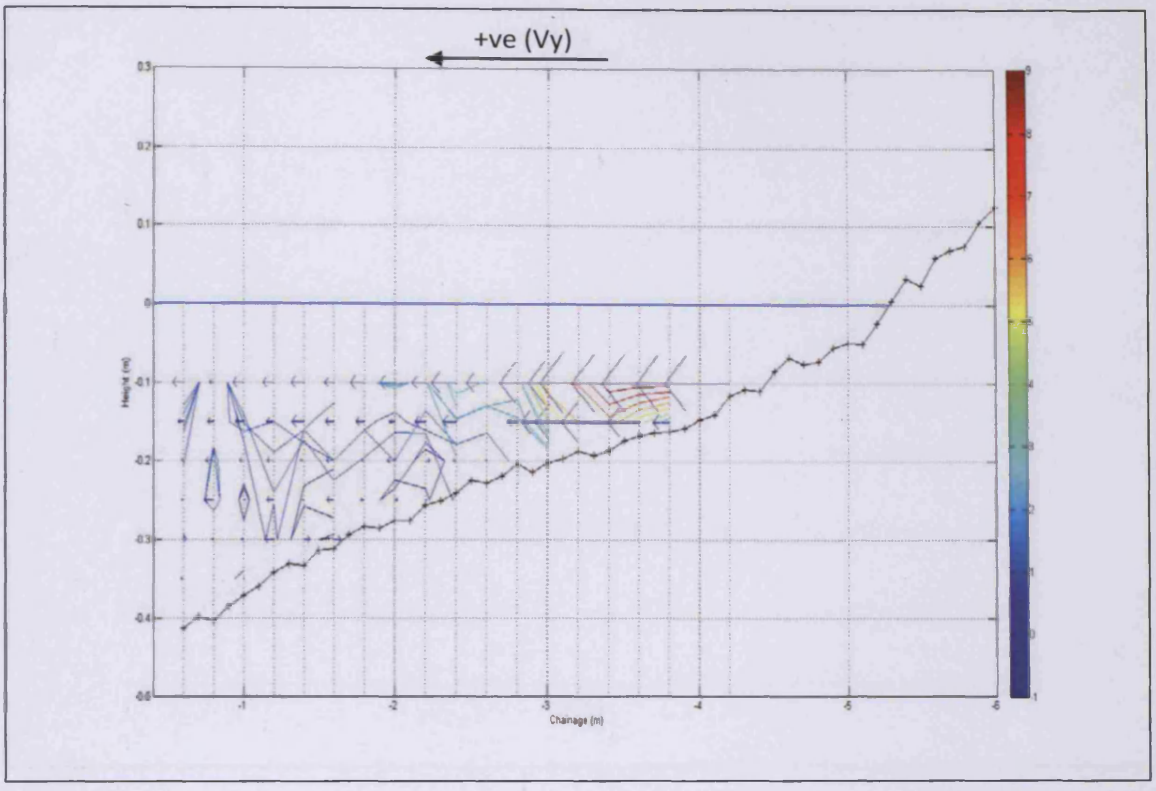

Figure A3- 9. 2D presentation of the time-averaged currents for Test 3- Line 3

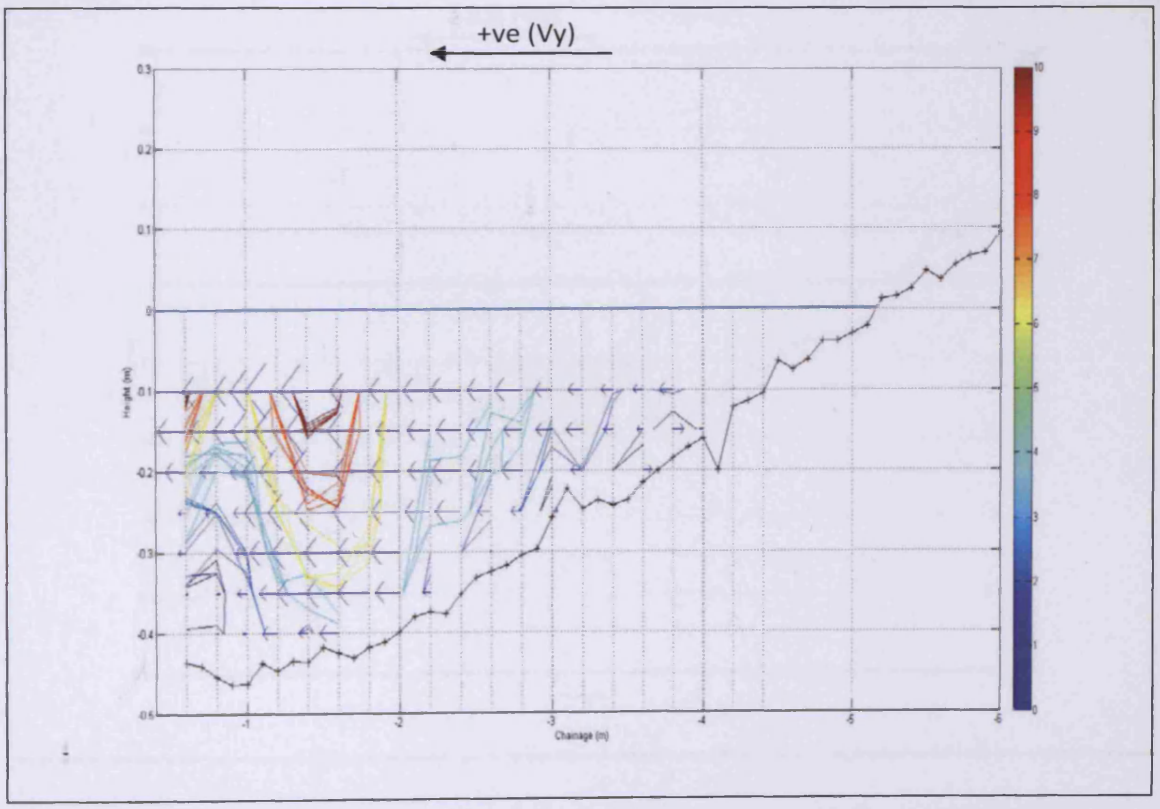

Figure A3- 10. 2D presentation of the time-averaged currents for Test 4- Line 1

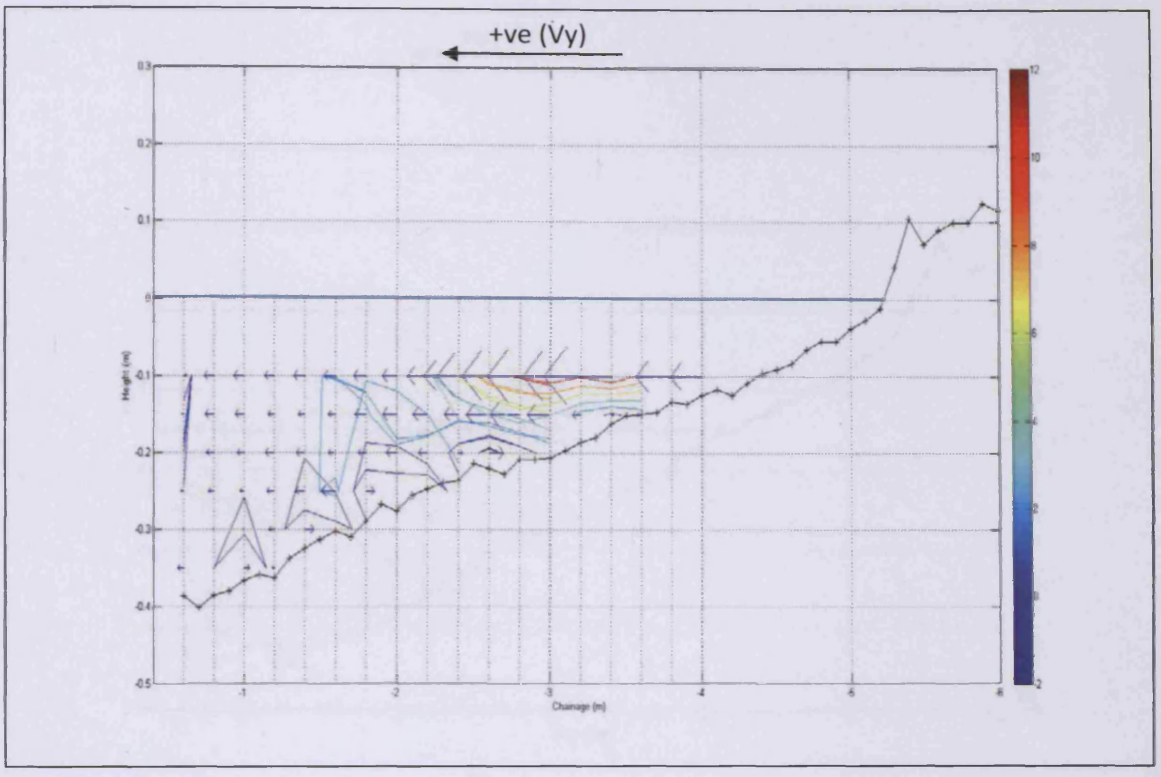

Figure A3- 11. 2D presentation of the time-averaged currents for Test 4- Line 2

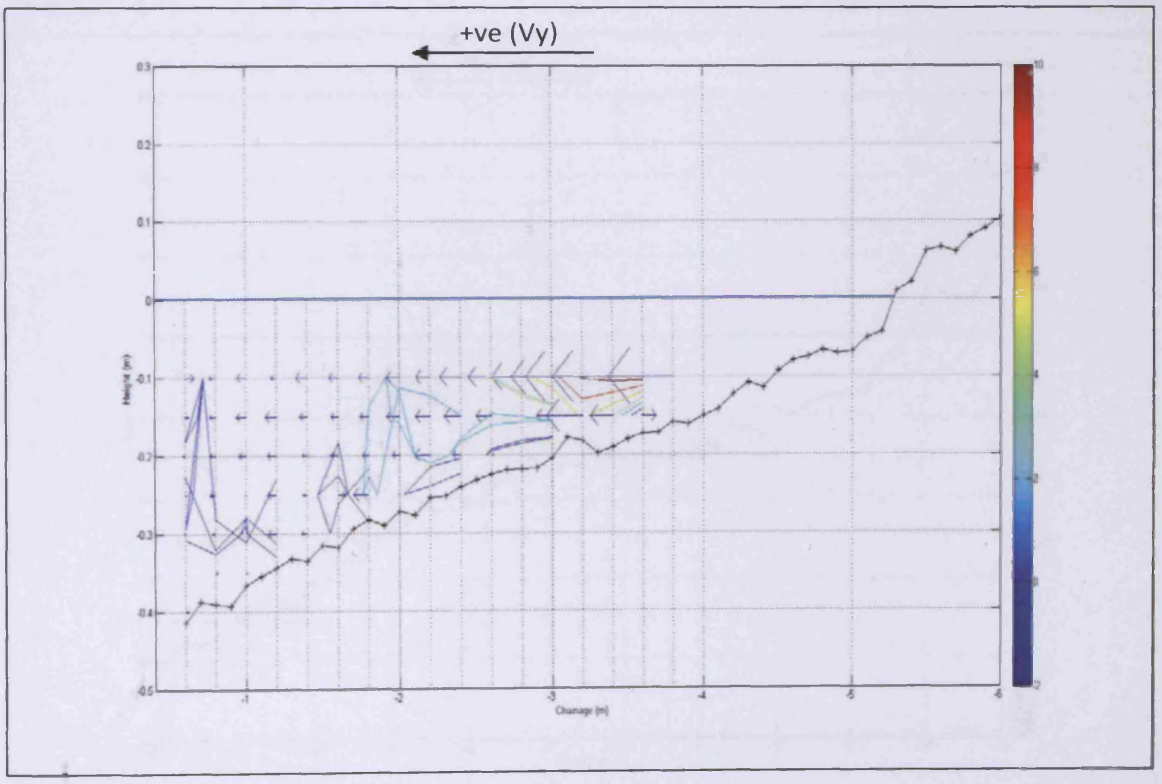

Figure A3- 12. 2D presentation of the time-averaged currents for Test 4- Line 3

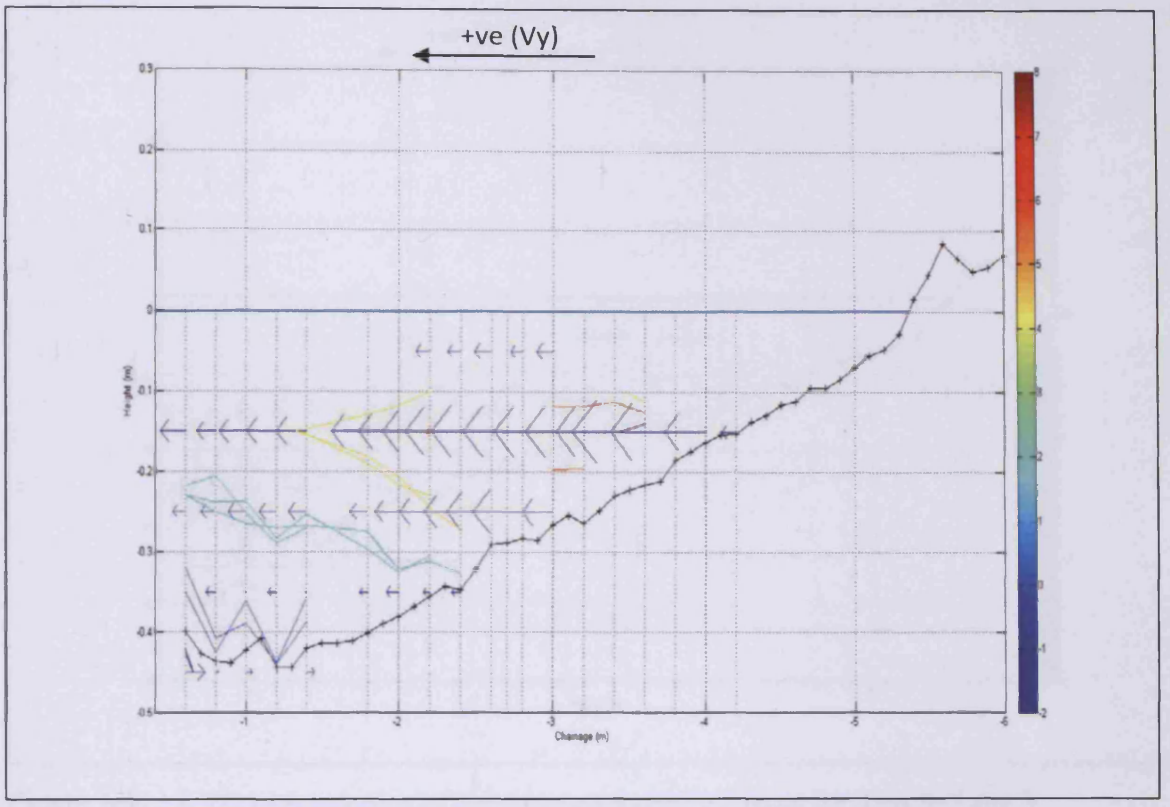

Figure A3- 13. 2D presentation of the time-averaged currents for Test 5- Line 1

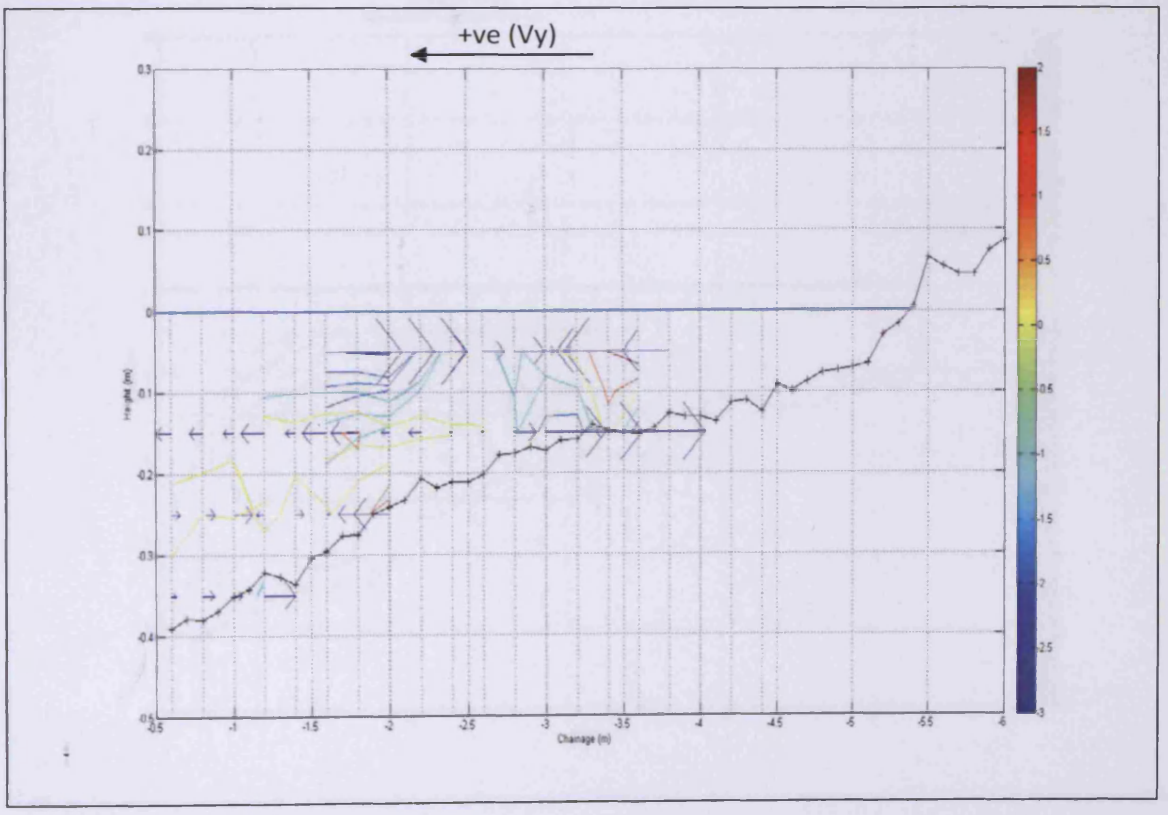

Figure A3- 14. 2D presentation of the time-averaged currents for Test 5- Line 2

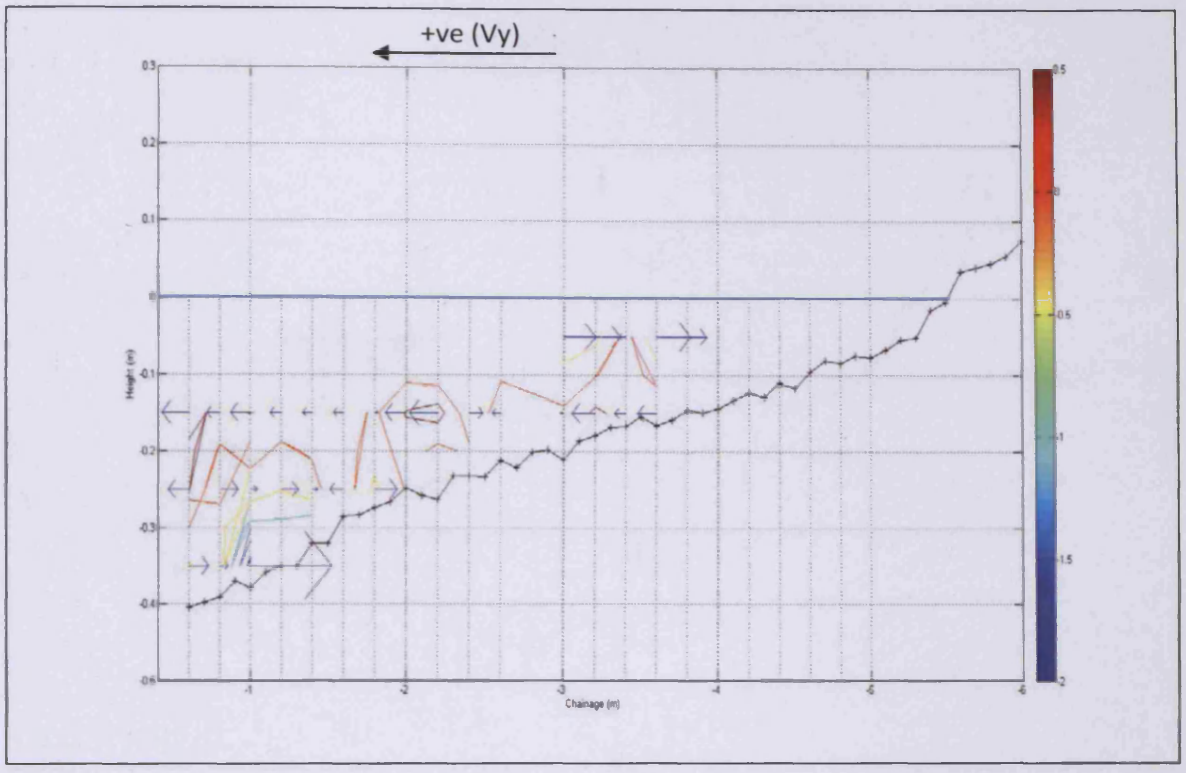

Figure A3- 15. 2D presentation of the time-averaged currents for Test 5- Line 3

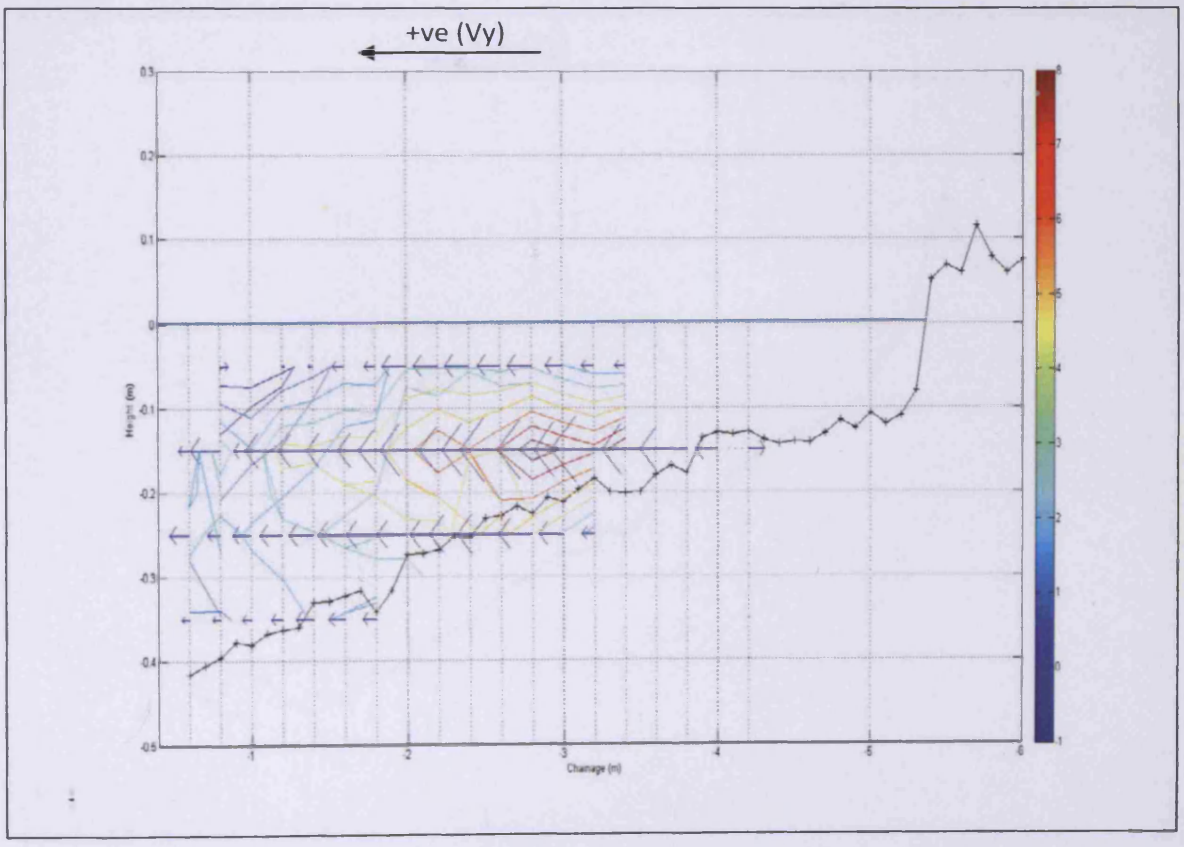

Figure A3- 16. 2D presentation of the time-averaged currents for Test 6- Line 1

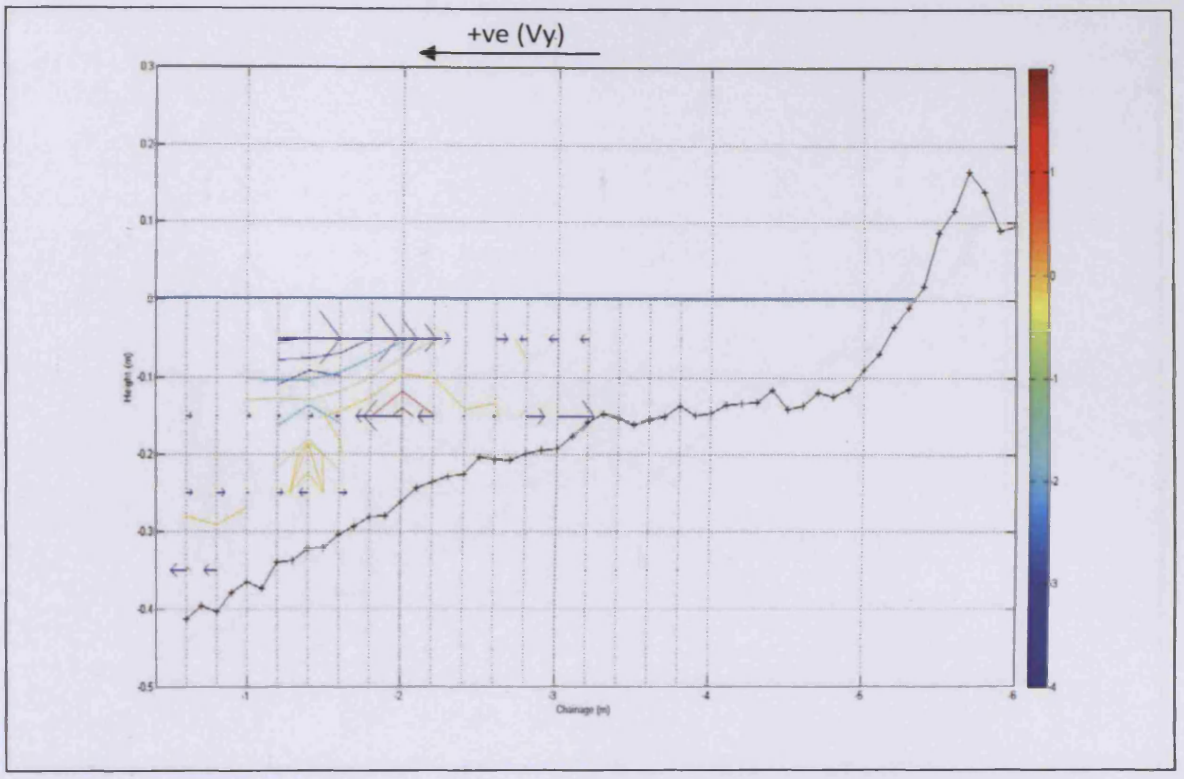

Figure A3- 17. 2D presentation of the time-averaged currents for Test 6- Line 2

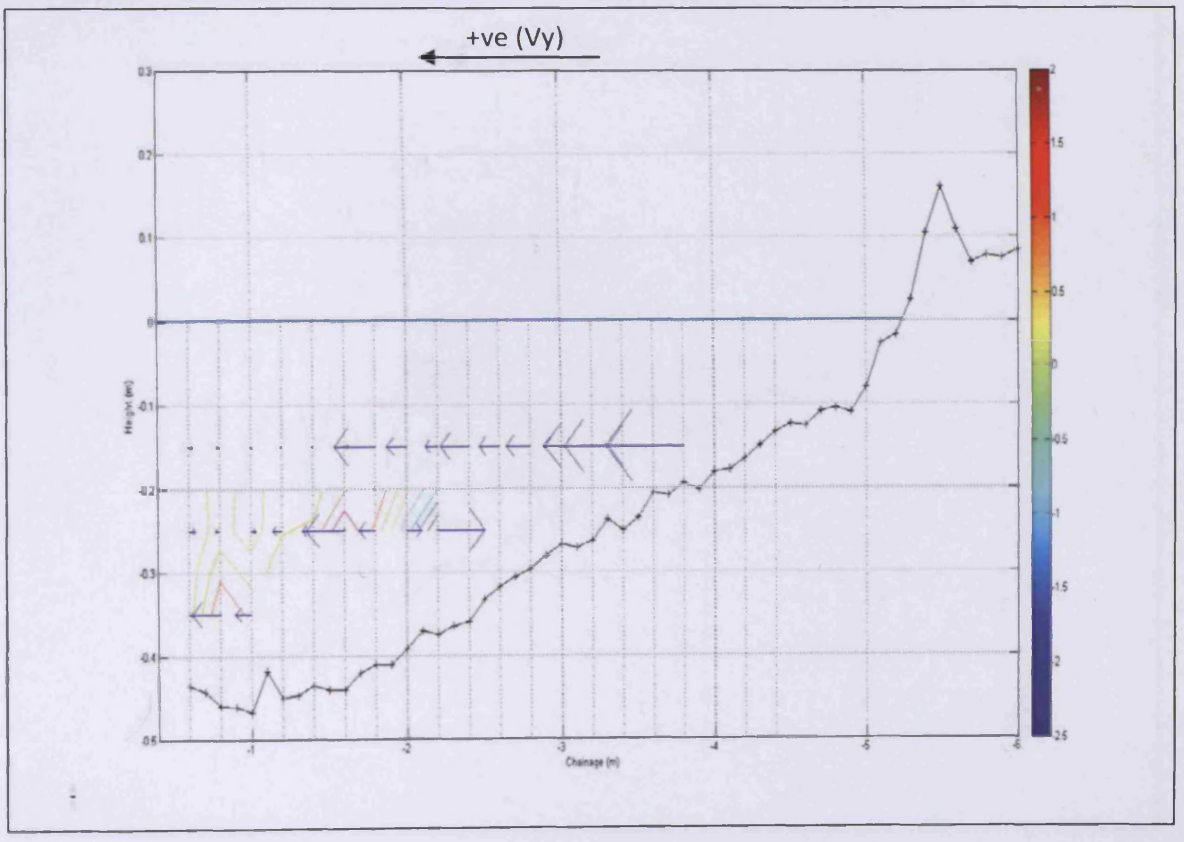

Figure A3- 18. 2D presentation of the time-averaged currents for Test 6- Line 3

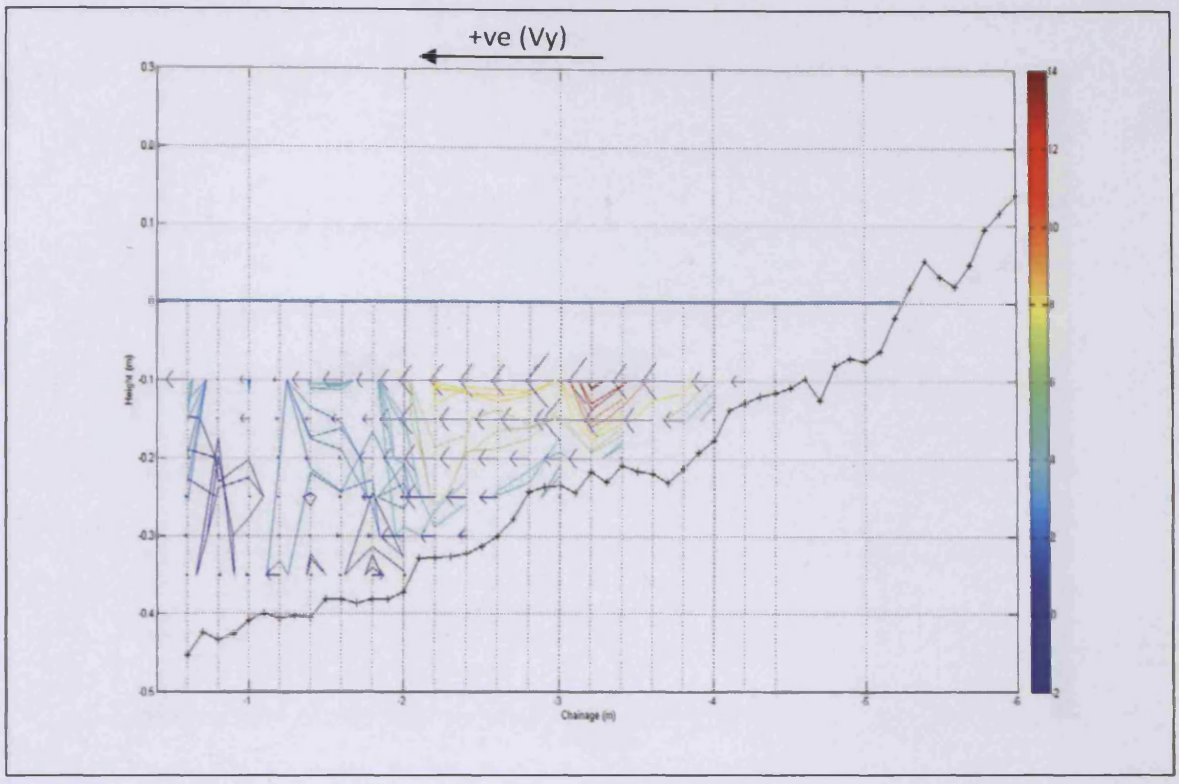

Figure A3- 19. 2D presentation of the time-averaged currents for Test 7- Line 1

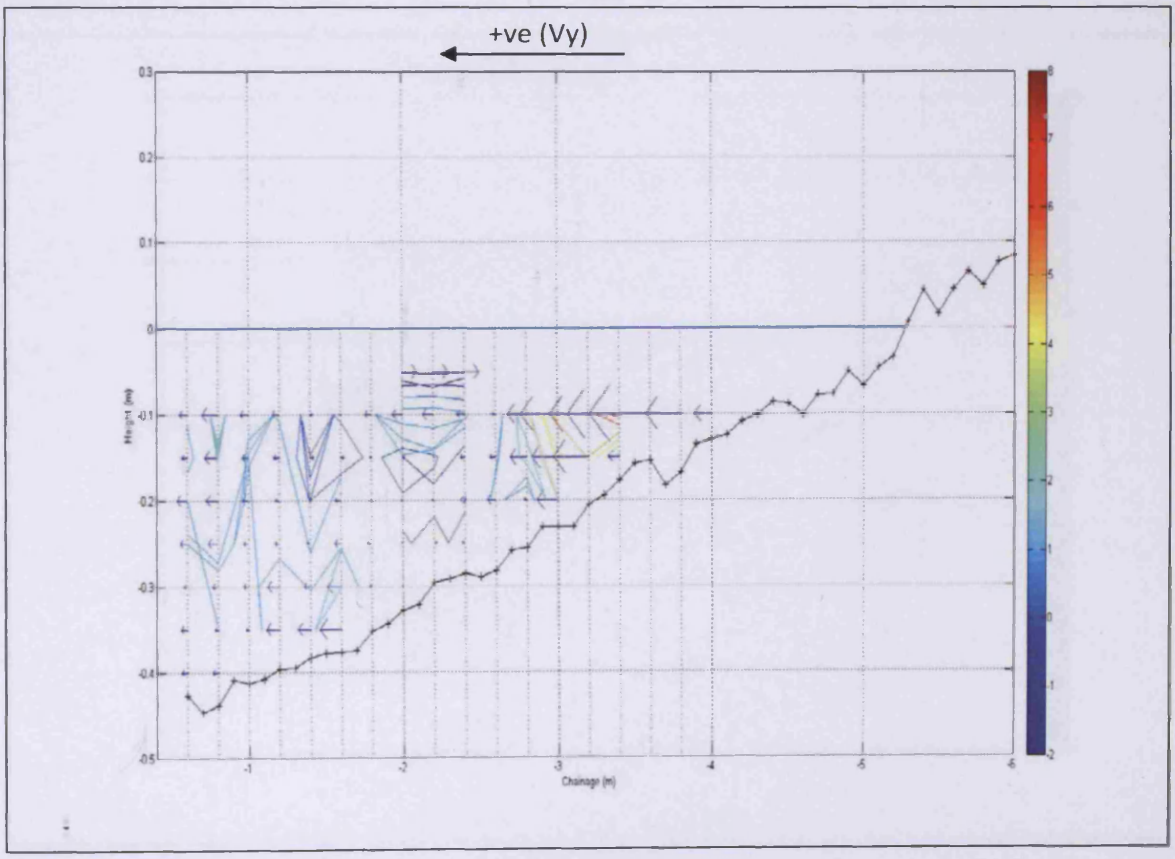

Figure A3- 20. 2D presentation of the time-averaged currents for Test 7- Line 2

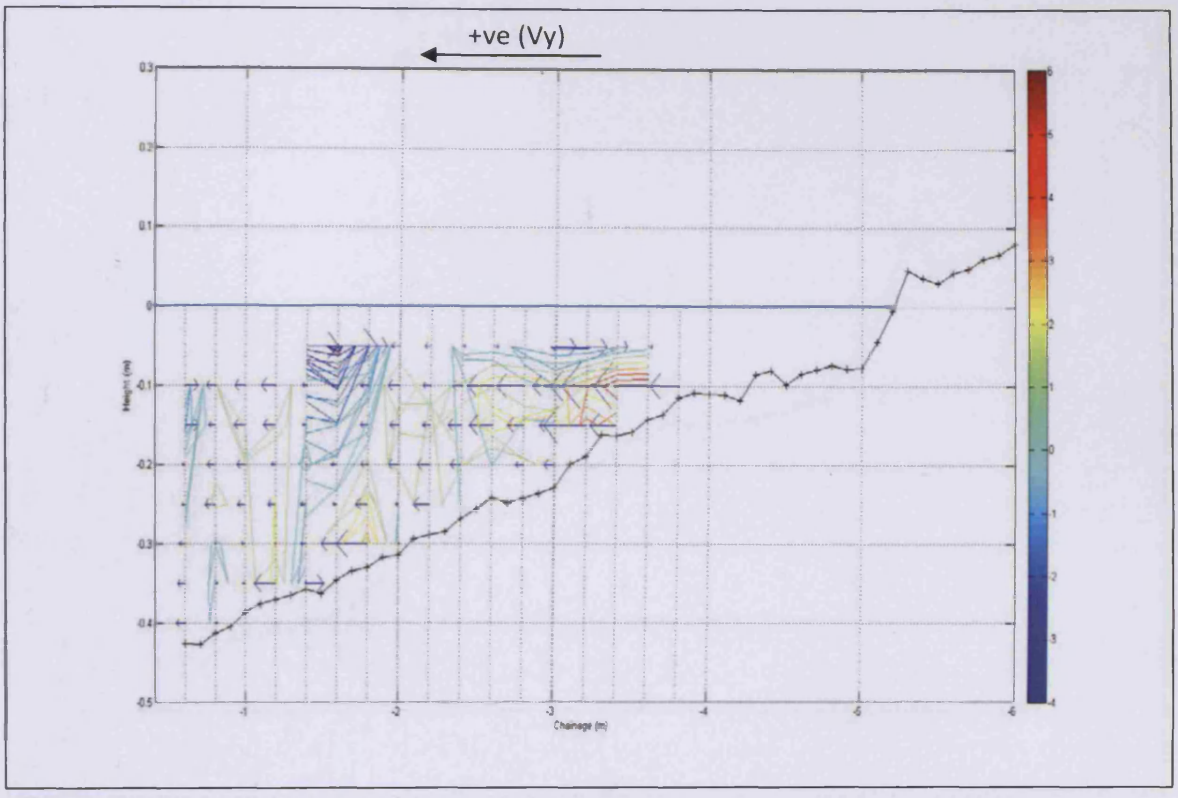

Figure A3- 21. 2D presentation of the time-averaged currents for Test 7- Line 3

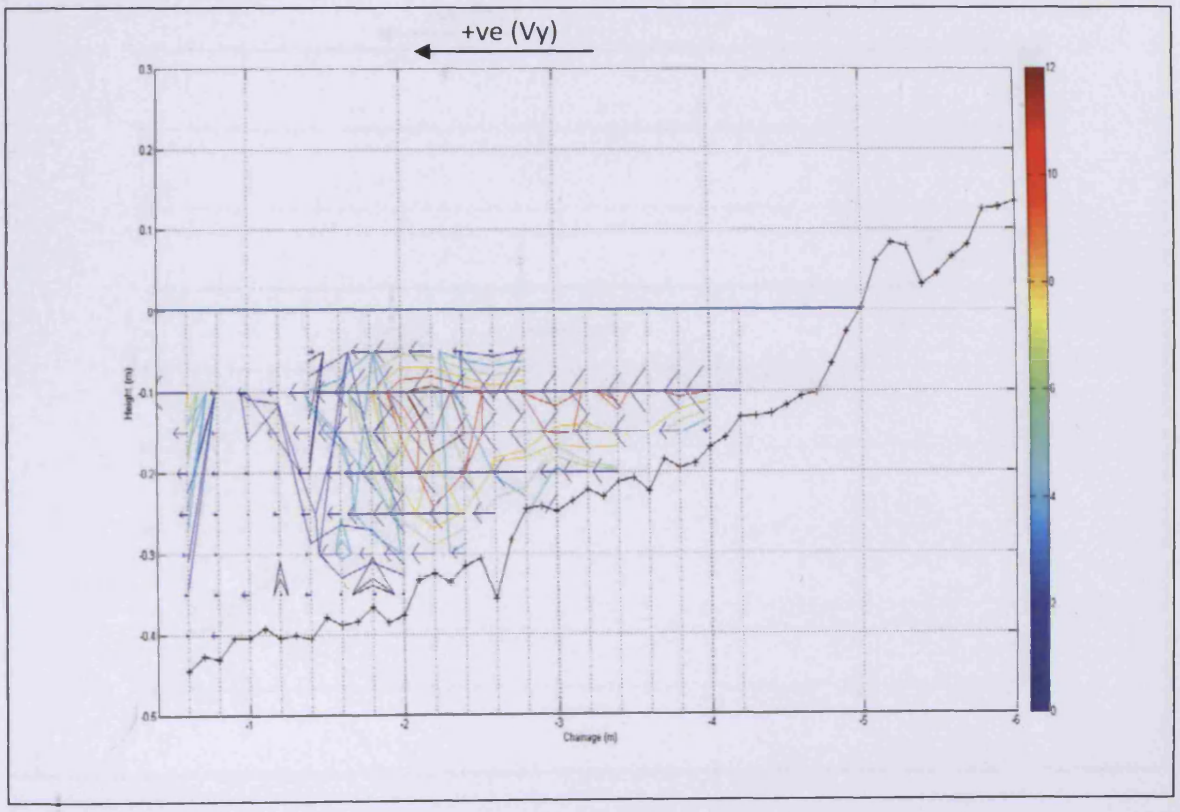

Figure A3- 22. 2D presentation of the time-averaged currents for Test 8- Line 1

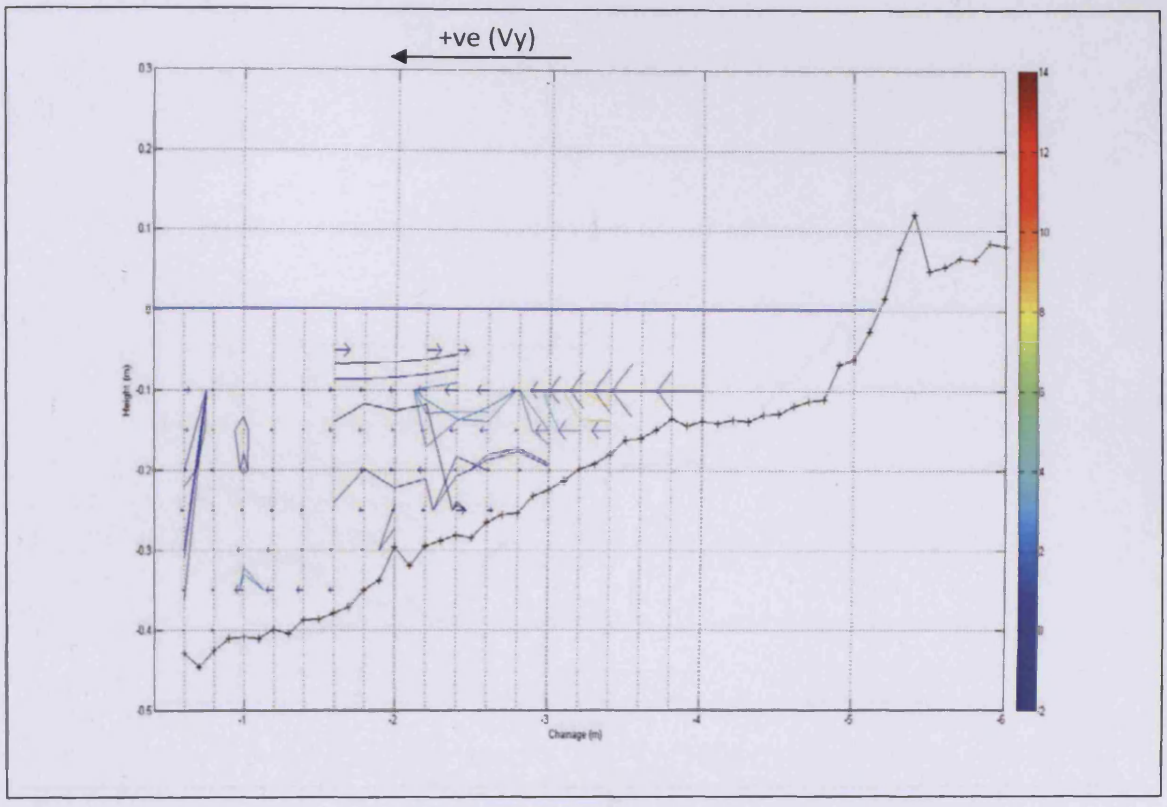

Figure A3- 23. 2D presentation of the time-averaged currents for Test 8- Line 2

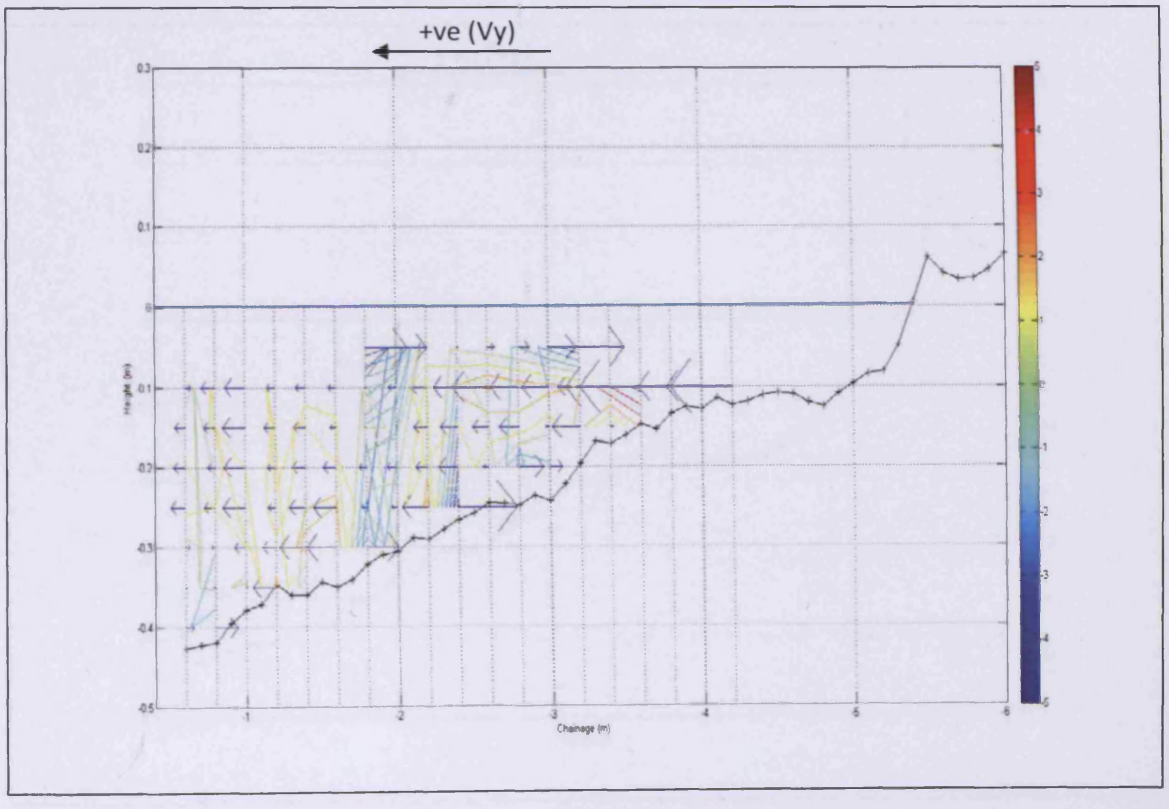

Figure A3- 24. 2D presentation of the time-averaged currents for Test 8- Line 3

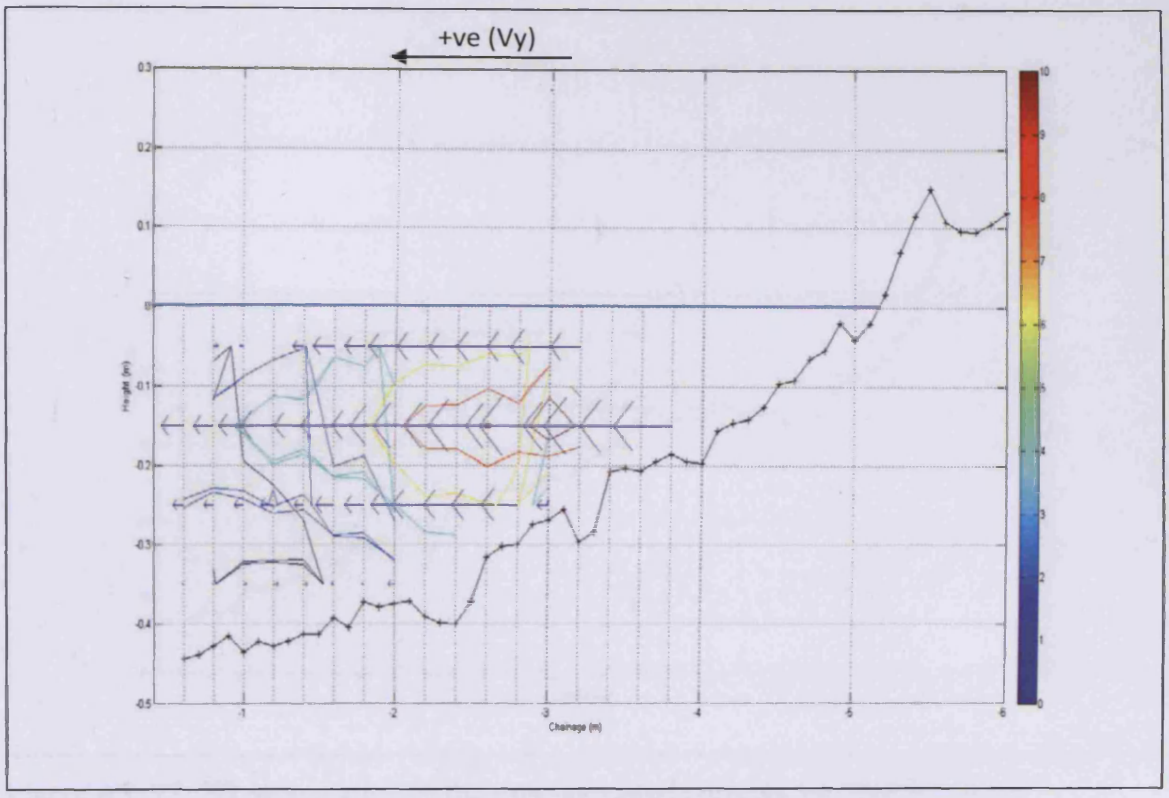

Figure A3- 25. 2D presentation of the time-averaged currents for Test 9- Line 1

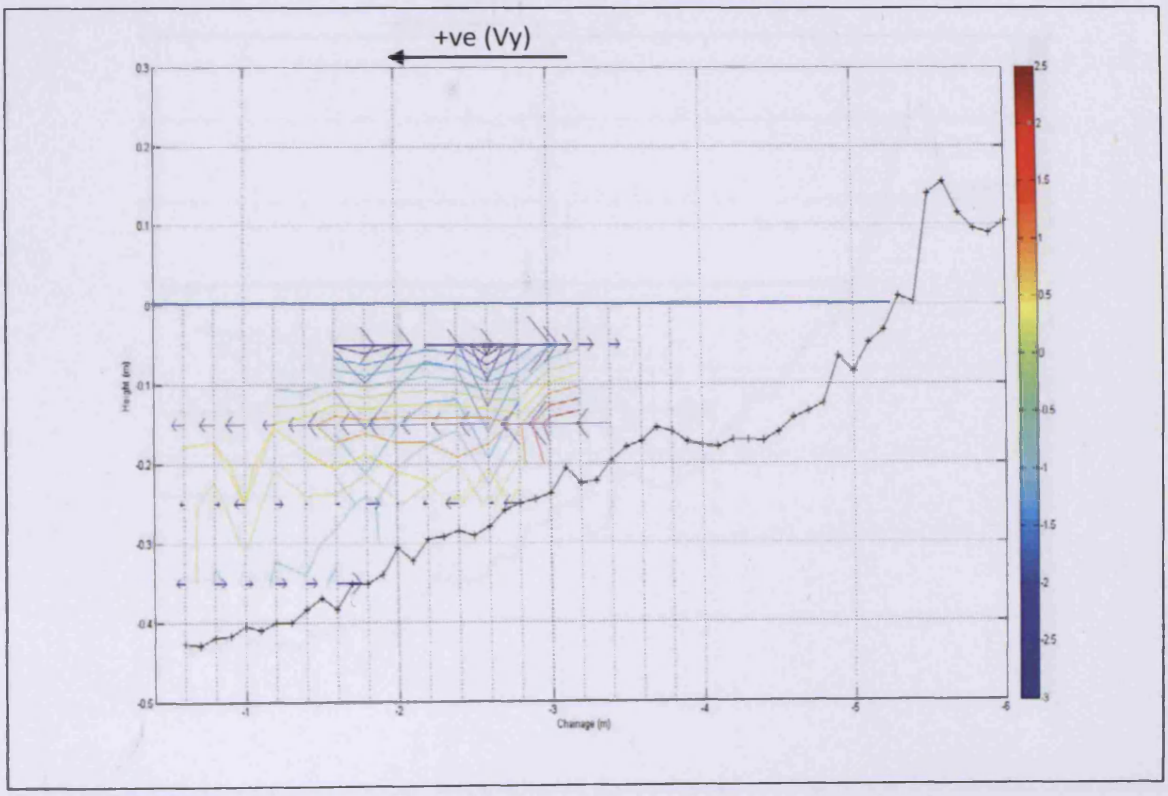

Figure A3- 26. 2D presentation of the time-averaged currents for Test 9- Line 2

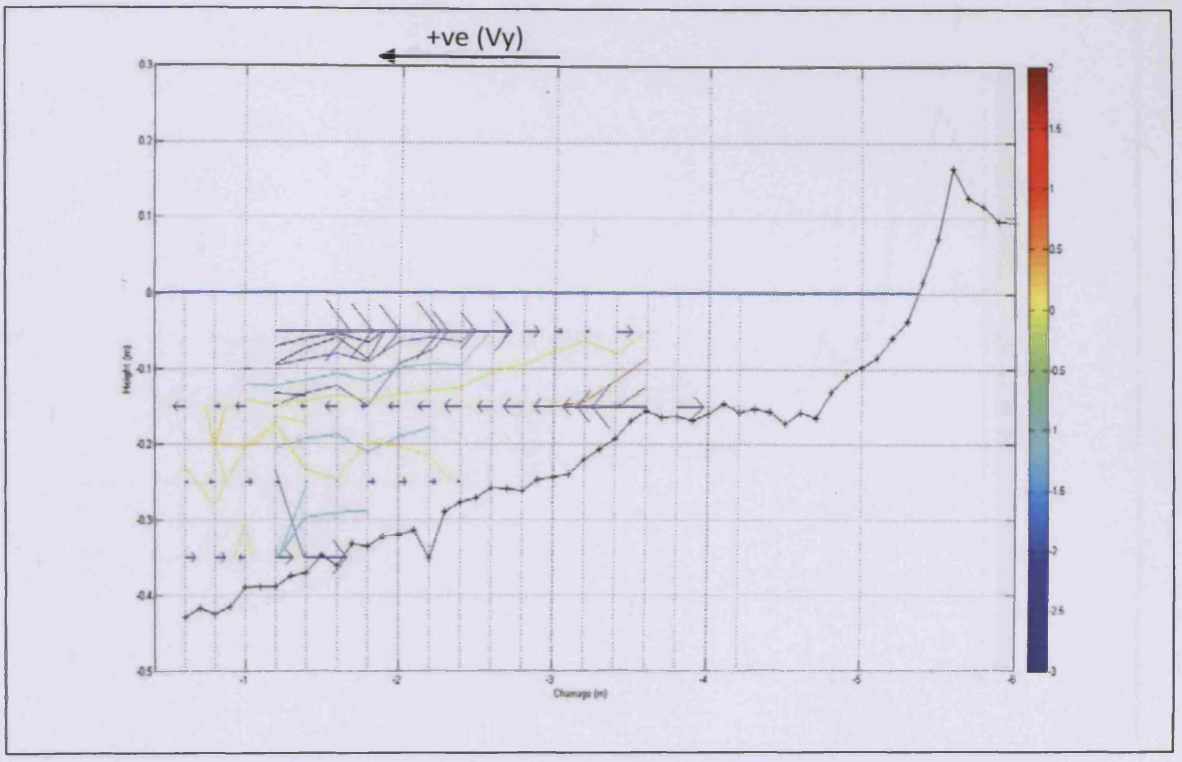

Figure A3- 27. 2D presentation of the time-averaged currents for Test 9- Line 3

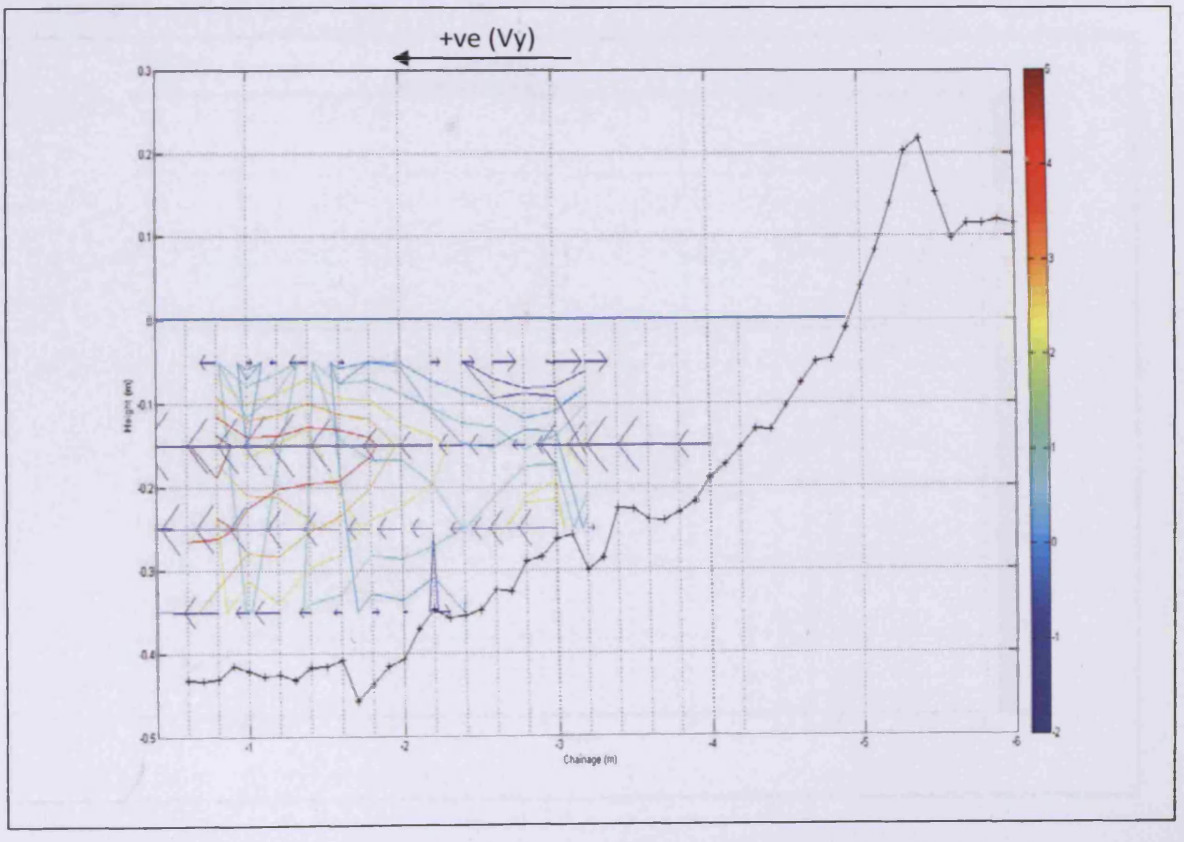

Figure A3- 28. 2D presentation of the time-averaged currents for Test 10- Line 1

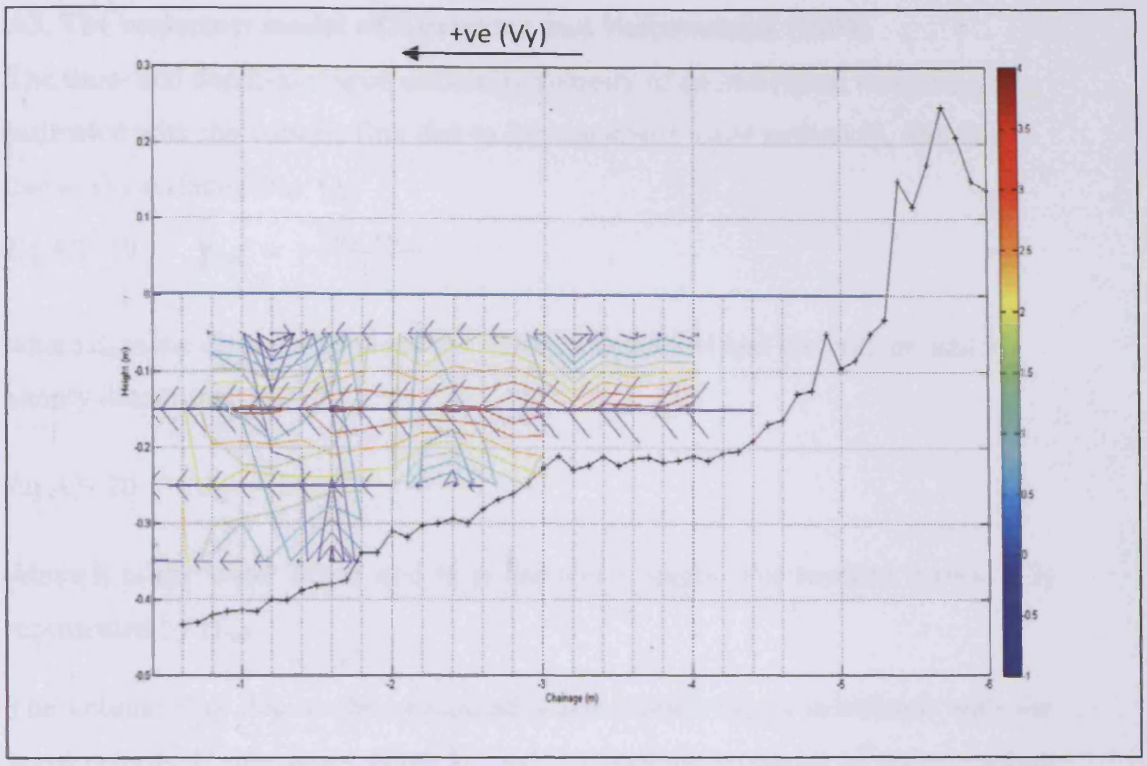

Figure A3- 29. 2D presentation of the time-averaged currents for Test 10- Line 2

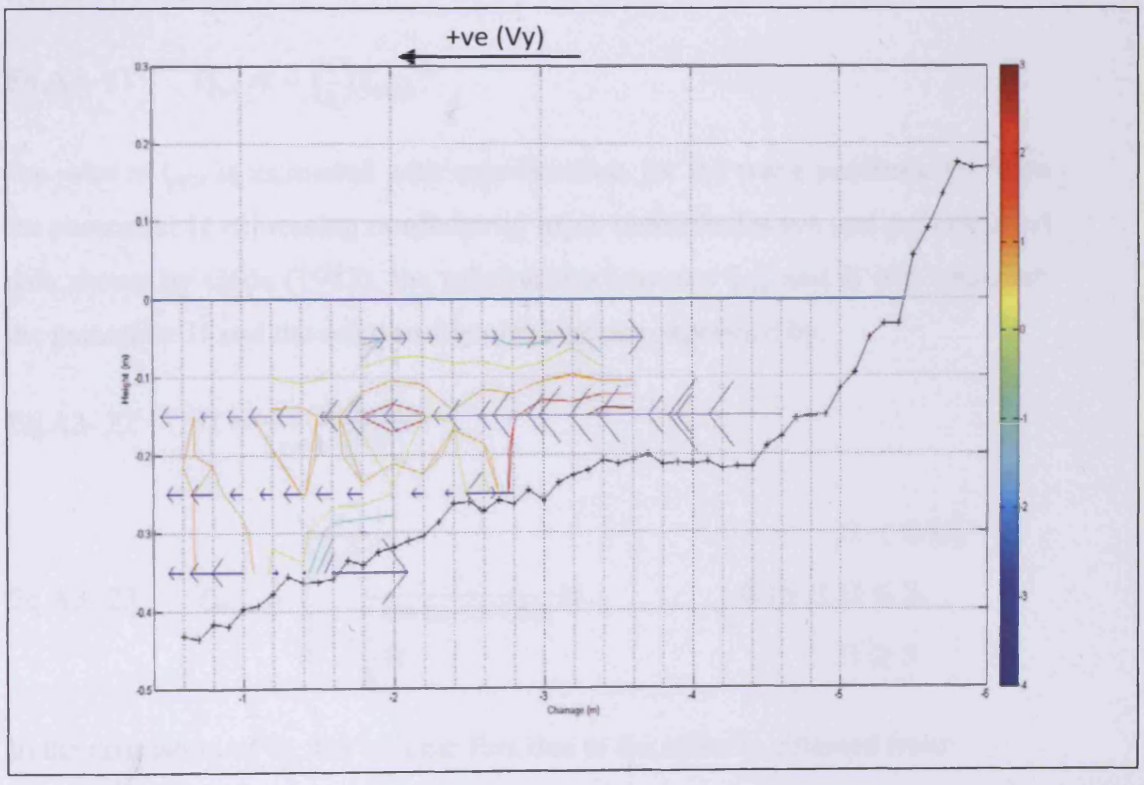

Figure A3- 30. 2D presentation of the time-averaged currents for Test 10- Line 3

A3. The undertow model of Kuriyama and Nakatsukasa (2000)

The time- and depth-averaged undertow velocity of an individual wave V_{ind} is estimated with the volume flux due to the organised wave motion Q_w and that due to the surface roller Q_r.

Eq.A3- 19 $$V_{ind} = -\frac{(Q_w + Q_r)}{d_{tr}},$$

where d_{tr} is the distance between the wave trough level and the bottom, and is simply determined as

Eq.A3- 20 $$d_{tr} = h - \frac{H}{2}$$

where h is the water depth and H is the wave height. For random waves H is represented by H_{m0}.

The volume flux due to the organized wave motion Q_w is calculated with the wave celerity C, the water depth h, and the root-mean-square of water surface elevation of an individual wave ζ_{rms} by the following equation proposed by Svendsen (1984a):

Eq.A3- 21 $$Q_w = -\left(\frac{C}{h}\right)\zeta_{rms}{}^2$$

The value of ζ_{rms} is estimated with consideration for the wave nonlinearity. With the parameter Π expressing nonlinearity of an individual wave and experimental data shown by Goda (1983), the relationship between ζ_{rms} and H was obtained; the parameter Π and the relationship obtained are expressed by:

Eq.A3- 22 $$\Pi = \frac{H}{L \cot h^3\left(\frac{2\pi h}{L}\right)}$$

Eq.A3- 23 $$\zeta_{rms} = \begin{cases} \frac{1}{2\sqrt{2}}, & \Pi < 0.15, \\ \frac{1}{1.668 \log \Pi + 4.204} H, & 0.15 \le \Pi \le 3, \\ \frac{1}{5} H, & \Pi \ge 3. \end{cases}$$

In the estimation of Q_r, the volume flux due to the roller is obtained from

Eq.A3- 24 $$Q_r = -\frac{A_r C}{2L},$$

where A_r is the area of the roller. The area of the surface roller is estimated on the basis of the assumptions mentioned below.

(1) The area of the surface roller is basically assumed to be proportional to the square of the wave height. The area A_{r1} is estimated with a dimensionless coefficient C_A from

Eq.A3- 25 $$A_{r1} = C_A H^2,$$

where C_A is given by

Eq.A3- 26 $$C_A = 17.0 \log \xi_b + 24.7,$$

where ξ_b is the surf similarity parameter at the wave breaking position and is estimated by

Eq.A3- 27 $$\xi_b = \frac{\tan \beta}{\sqrt{\left(\frac{H_{1/3,b}}{L_{1/3,0}}\right)}},$$

where tanβ is the bed slope, $L_{1/3,0}$ is the offshore wavelength corresponding to the significant wave period and $H_{1/3,b}$ is the significant wave height at the wave-breaking position and is estimated by

For random waves (Kuriyama, 1996):

Eq.A3- 28 $$\frac{H_b}{h_b} = C_{br}\left[0.16\frac{L_0}{h_b}\left[1 - \exp\left\{-0.8\pi\frac{h_b}{L_0}\left(1 + 15\tan\beta^{\frac{4}{3}}\right)\right\}\right] - \frac{}{0.96\tan\beta + 0.2}\right],$$

For regular waves (Seyama and Kimura, 1988):

Eq.A3- 29 $$H_b = 1.25 h_b\left[0.16\frac{L_0}{h_b}\left[1 - \exp\left\{-0.8\pi\frac{h_b}{L_0}\left(1 + 15\tan\beta^{\frac{4}{3}}\right)\right\}\right] - \frac{}{0.96\tan\beta + 0.2}\right]$$

where H_b is the wave breaking height, h_b is the wave breaking depth and L_0 is the wavelength in deep water. C_{br} is a dimensionless coefficient with a range from 0.7 to 1.2.

(2) The energy of the surface roller should not exceed the energy transferred from the organized wave motion. The roller area is therefore determined not to exceed the roller area A_{r2} estimated without the energy dissipation of the surface roller from the following equation:

Eq.A3- 30 $$\frac{\partial(E_w C_g)}{\partial y} + \frac{\partial(W_r C_g)}{\partial y} = 0,$$

where,

Eq.A3- 31 $$W_r = \frac{1}{8}\rho C^2 \frac{A_{r2}}{L}$$

Eq.A3- 32 $$\frac{\partial(E_w C_g)}{\partial y} = \frac{1}{4}\rho g \frac{1}{T}\frac{(BH)^3}{h},$$

where W_r is the energy of the roller having the distribution of the time-averaged velocity above the wave trough level, E_w is the energy of the organized wave motion ($=\rho g H^2/8$), C_g is the group velocity, ρ is the sea water density, T is the wave period, H is the wave height, h is the water depth, and B is a dimensionless coefficient determining the amount of energy dissipation. Kuriyama and Ozaki (1996) investigated the coefficient B with the experimental data of Seyama and Kimura (1988), and proposed the following formula:

Eq.A3- 33 $$B = C_B\left\{1.6 - 0.12\ln\left(\frac{H_0}{L_0}\right) + 0.28\ln(\tan\beta)\right\},$$

where H_0 is the wave height in deep water, and C_B is a dimensionless coefficient with a range from 0.7 to 1.1.

(3) The surface roller diminishes at the wave reforming point

In the actual calculation, A_{r1} and A_{r2} are estimated and the smaller value is assumed to be the area of the surface roller.

A4. The undertow model of Grasmeijer and Ruessink (2003)

The time- and depth-averaged undertow velocity $\bar{u}$ is derived from the mass flux due to the wave motion (Q_w) and the mass flux due to the surface roller (Q_r).

Eq.A3- 34 $$\bar{u} = -\frac{(Q_w + Q_r)}{h_{trough}},$$

where $h_{trough} = h - H/2$

where h is the water depth and H is the wave height. For random waves H is represented by H_{rms}.

Using linear theory, Qw is computed as

Eq.A3- 35 $$Q_w = \frac{E}{\rho c} = \frac{1}{8}\left(\frac{g}{c}\right) H^2 \cos\theta,$$

where E is the wave energy ($=\cos\theta\rho g H^2/8$) for obliquely waves, θ is the angle of incidence, ρ is the density of the water and c is the wave phase speed.

The roller distribution Q_r is computed as (Svendsen, 1984a)

Eq.A3- 36 $$Q_r = \frac{A}{T} = \frac{2E_r}{\rho c}\cos\theta$$

where A is the roller area, T is the wave period and Er is the roller energy density and is estimated by

Eq.A3- 37 $$E_r = \frac{\rho A c^2}{2L} = \frac{\rho A c}{2T}$$

A5. BREAKWAT (Van der Meer, 1988)

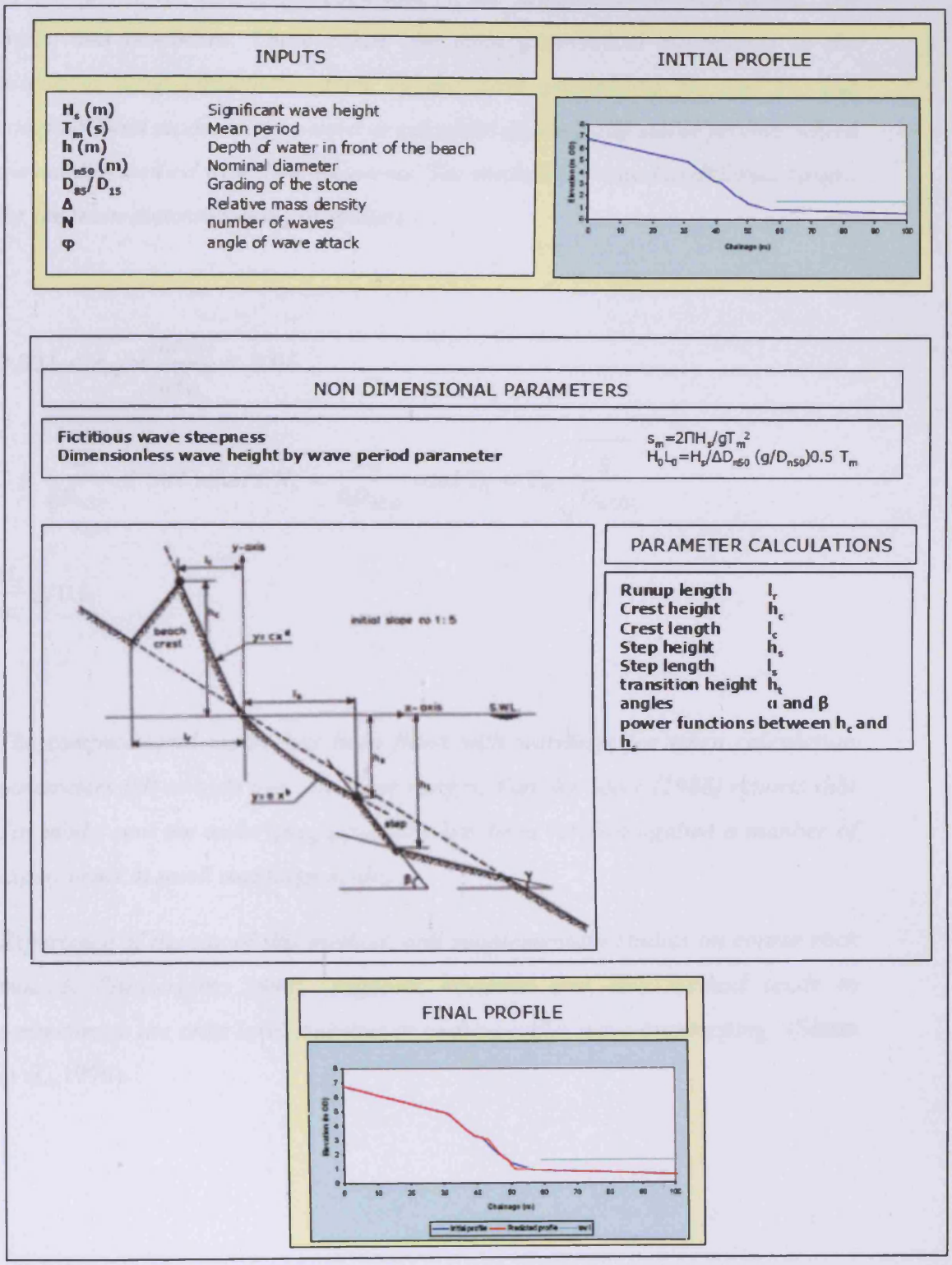

Figure A3- 31. Descriptive summary of BREAKWAT (taken from Lopez de San Roman-Blanco, 2003)

"The computational model of BREAKWAT uses empirical equations developed by Van der Meer (1988) for rock and riprap armouring on breakwaters, sea walls, and revetment. These relate the main geometrical parameters of the profile to wave conditions given by the wave parameters H_0 and T_0. The computational model may be used to calculate dynamically stable profiles where the manual method would be laborious. The method is limited to different ranges for the main dimensionless parameters:

$$0.001 < s_m = \frac{2\pi H_s}{g T_m{}^2} < 0.06$$

$$3 \leq \frac{H_s}{\Delta D_{n50}} \leq 500 \text{ where } N_s = \frac{H_s}{\Delta D_{n50}} \text{ and } T_0 = T_m \sqrt{\frac{g}{D_{n50}}}$$

$$\frac{H_s}{h_s} \leq 0.6$$

The computational model has been fitted with warnings for when calculation parameters fall outside these or other ranges. Van der Meer (1988) reports that this model and the underlying equations has been verified against a number of experiments at small and large scales.

Experience of the use of this method, and supplementary studies on coarse rock mounds (Sievwright, 1994), suggests however that this method tends to overestimate the crest level and thus to under-predict wave overtopping" (Simm et al., 1996).

A6. SHINGLE (Powell, 1990 and 1993)

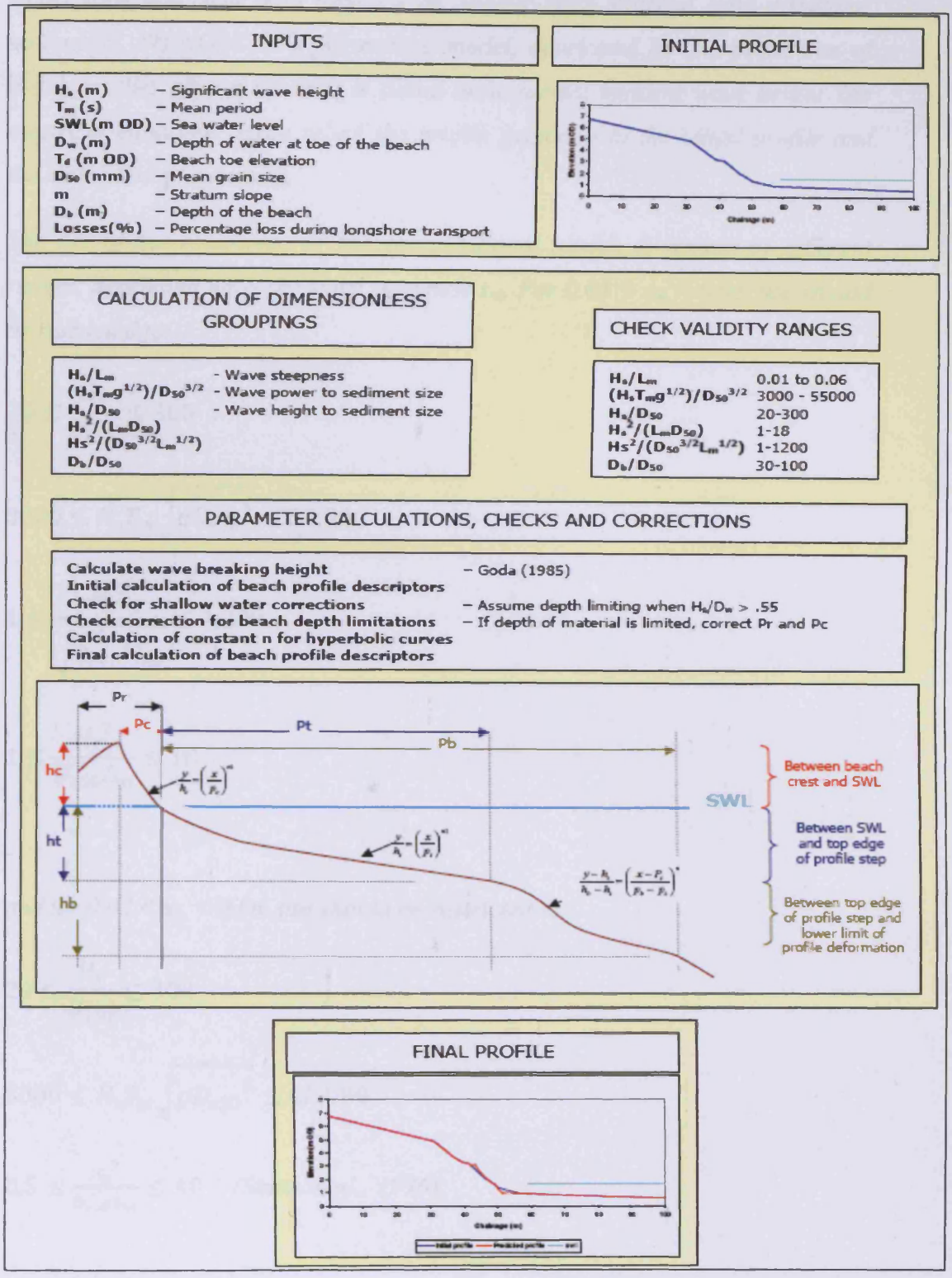

Figure A3- 32. Descriptive summary of SHINGLE (taken from Lopez de San Roman-Blanco, 2003)

"The SHINGLE model was developed by Powell (1990, 1993) from the results of model tests and field data analysis on shingle-sizes material (and dissimilar sediments). SHINGLE is a parametric model, developed for the prediction of beach profiles after a storm It is based on a normal incident wave height The empirical equations again relate the profile geometry to the initial profile and the main wave parameters.

The use of the equations, or the computational model, is limited to different ranges, depending upon the wave steepness s_m. For $0.01 < s_m < 0.03$, use should be restricted to:

$$20 \leq \frac{H_s}{D_{e50}} \leq 300$$

$$3000 \leq H_s T_m \sqrt{g {D_{e50}}^3} \leq 55{,}000$$

$$1 \leq \frac{{H_s}^2}{\sqrt{{D_{e50}}^3 L_m}} \leq 1{,}200$$

$$1 \leq \frac{{H_s}^2}{D_{e50} L_m} \leq 18$$

and for $0.03 < s_m < 0.06$, use should be restricted to:

$$20 \leq \frac{H_s}{D_{e50}} \leq 300$$

$$5000 \leq H_s T_m \sqrt{g {D_{e50}}^3} \leq 40{,}000$$

$$0.5 \leq \frac{{H_s}^2}{D_{e50} L_m} \leq 40$$ *" (Simm et al., 1996).*

APPENDIX IV

A1. Results of the predictions of the equations of the model (field data)

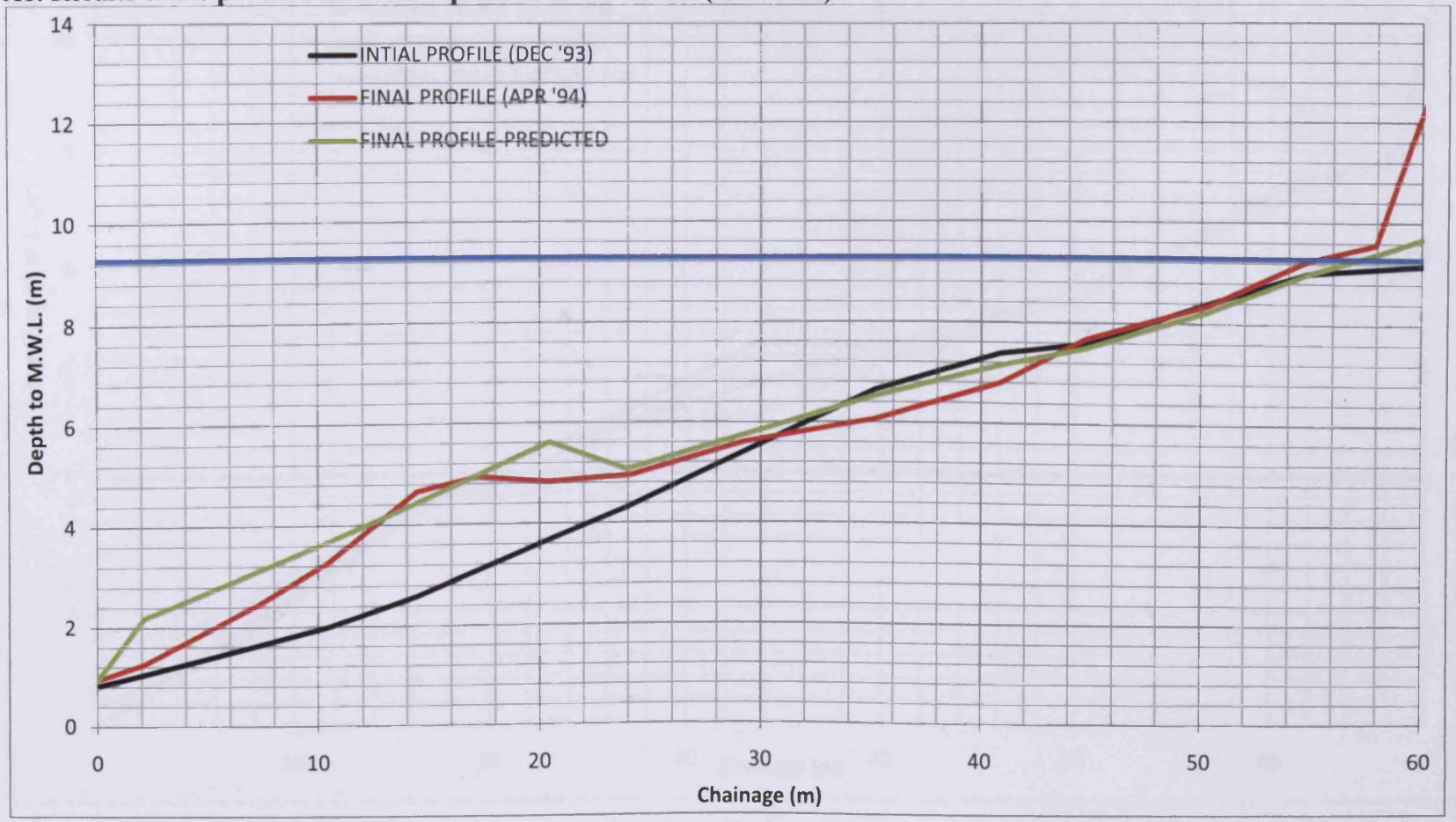

Figure A4- 1 Comparison of predicted and measured beach profile for location A-Middle (December '93-April '94)

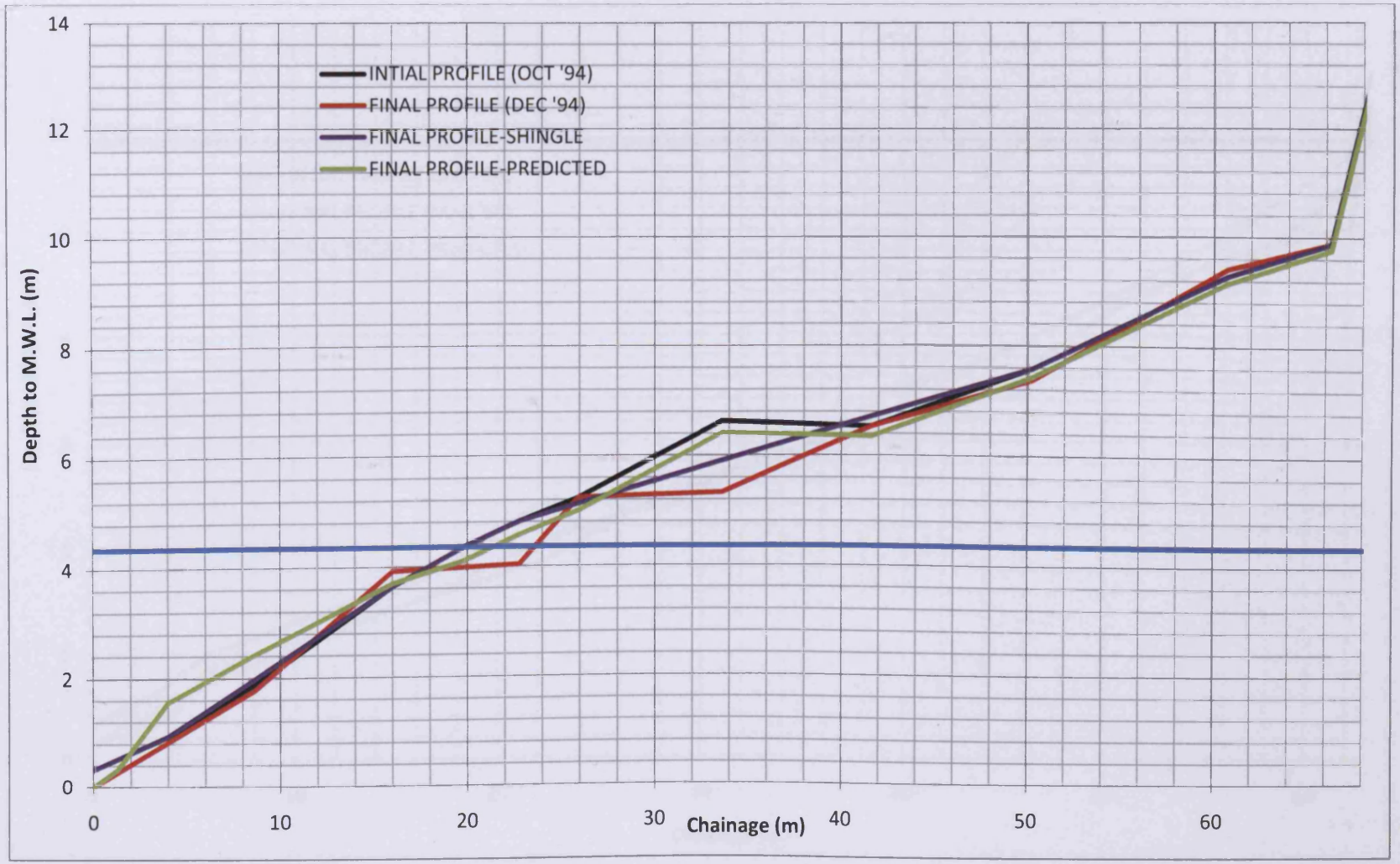

Figure A4- 2 Comparison of predicted and measured beach profile for location A-Middle (October '94-December '94)

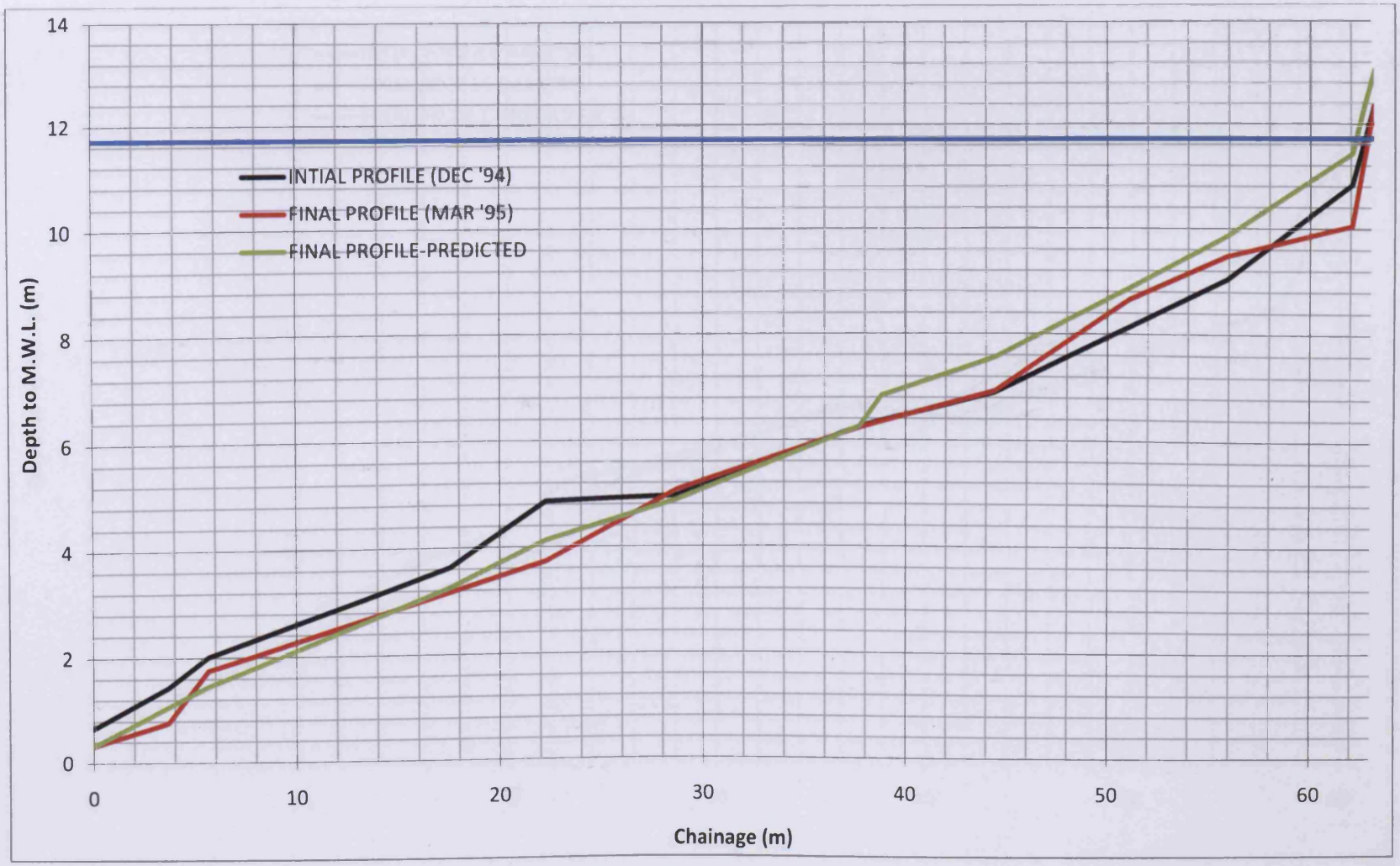

Figure A4- 3 Comparison of predicted and measured beach profile for location A-Middle (December '94-Mar '95)

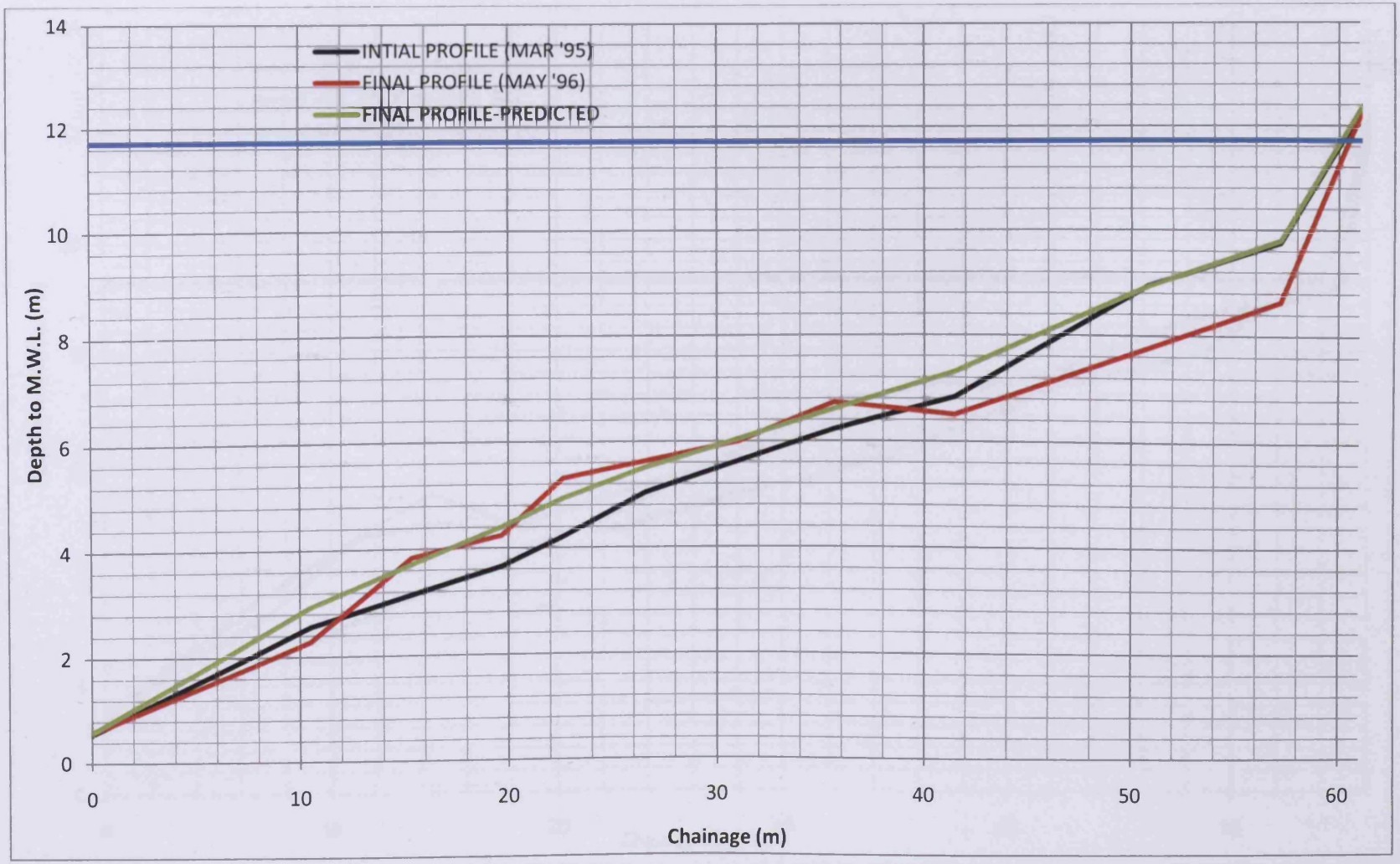

Figure A4- 4 Comparison of predicted and measured beach profile for location A-Middle (Mar '95-May '96)

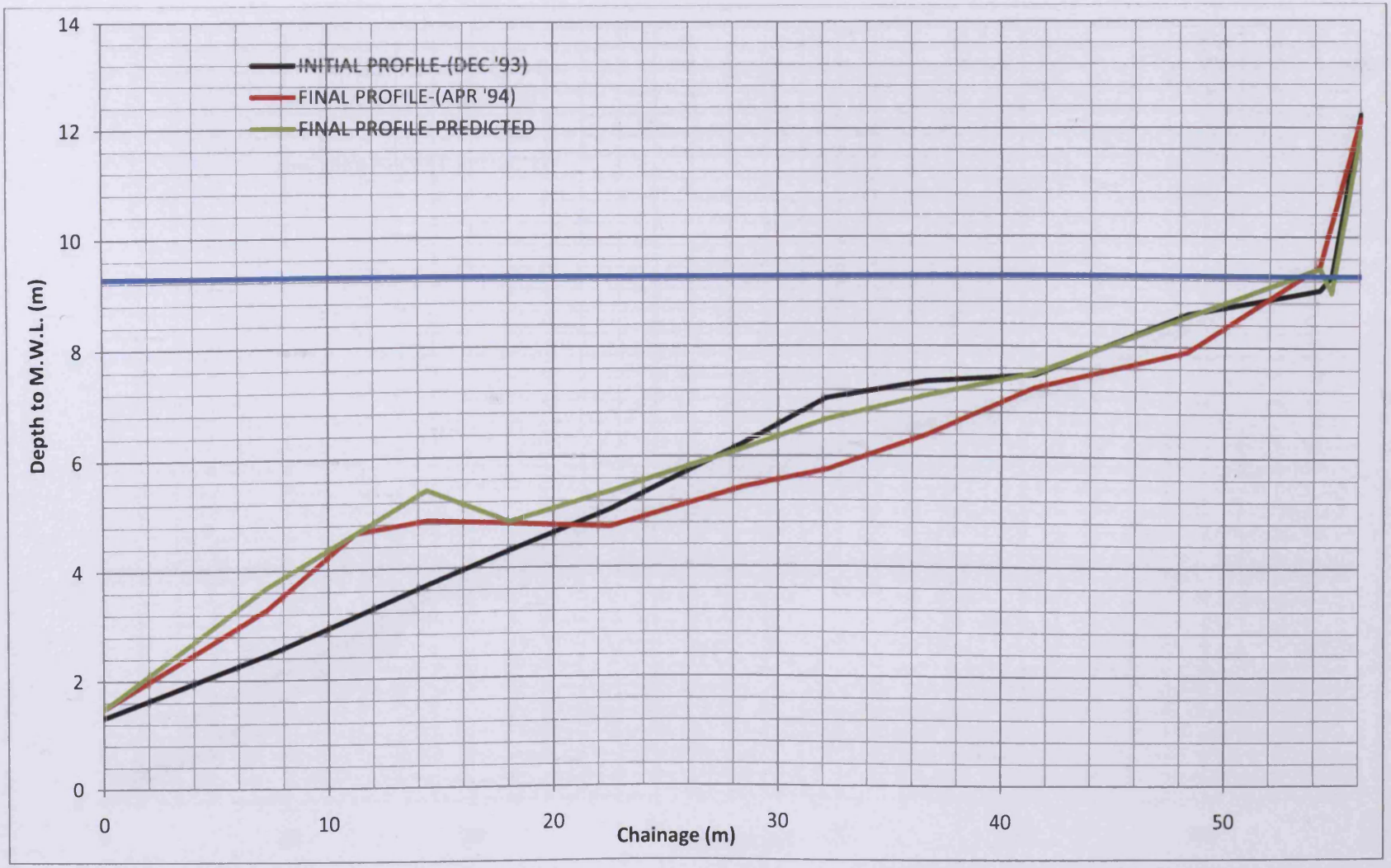

Figure A4- 5 Comparison of predicted and measured beach profile for location A-North (December '93-April '94)

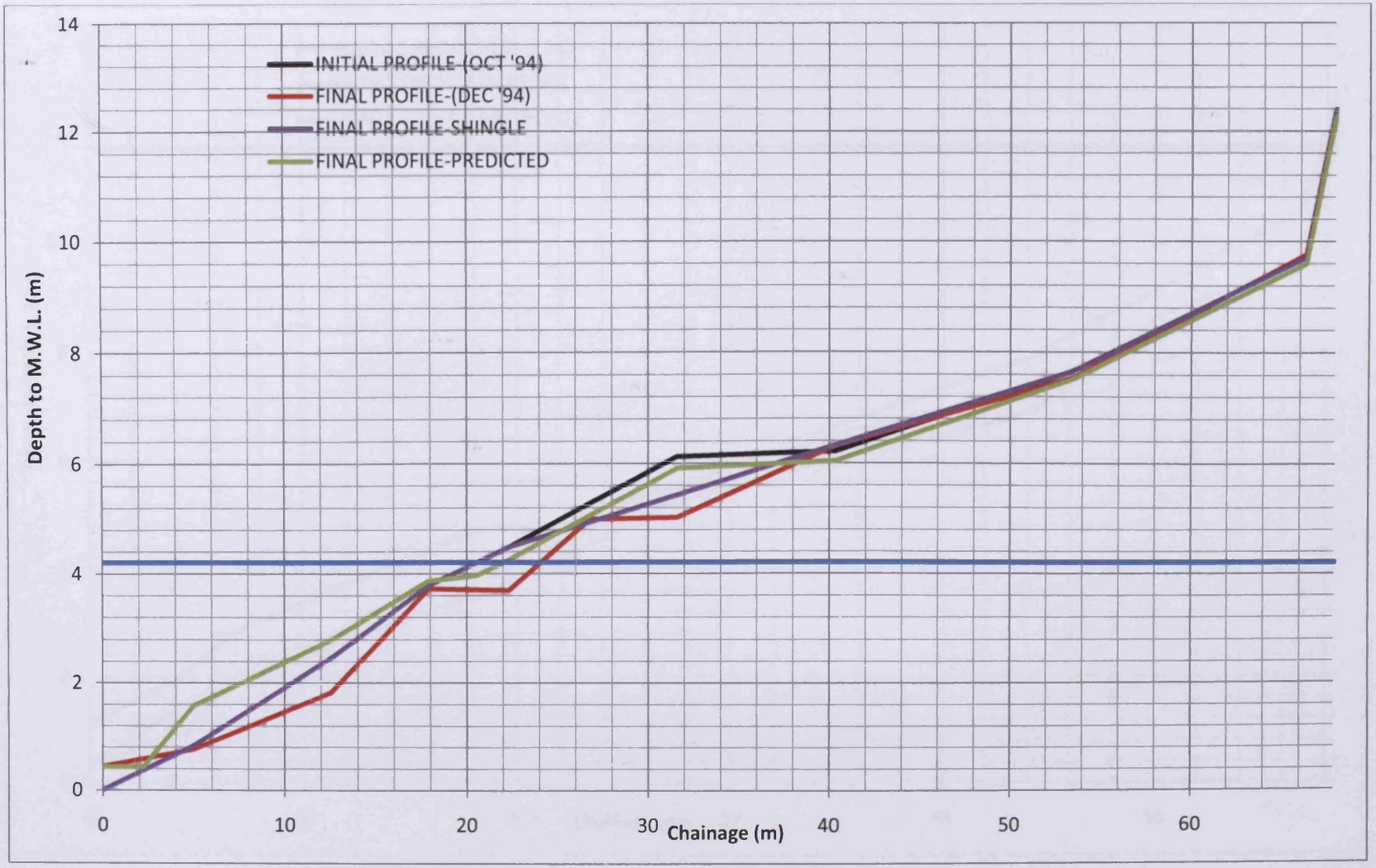

Figure A4- 6 Comparison of predicted and measured beach profile for location A-North (October '94-December '94)

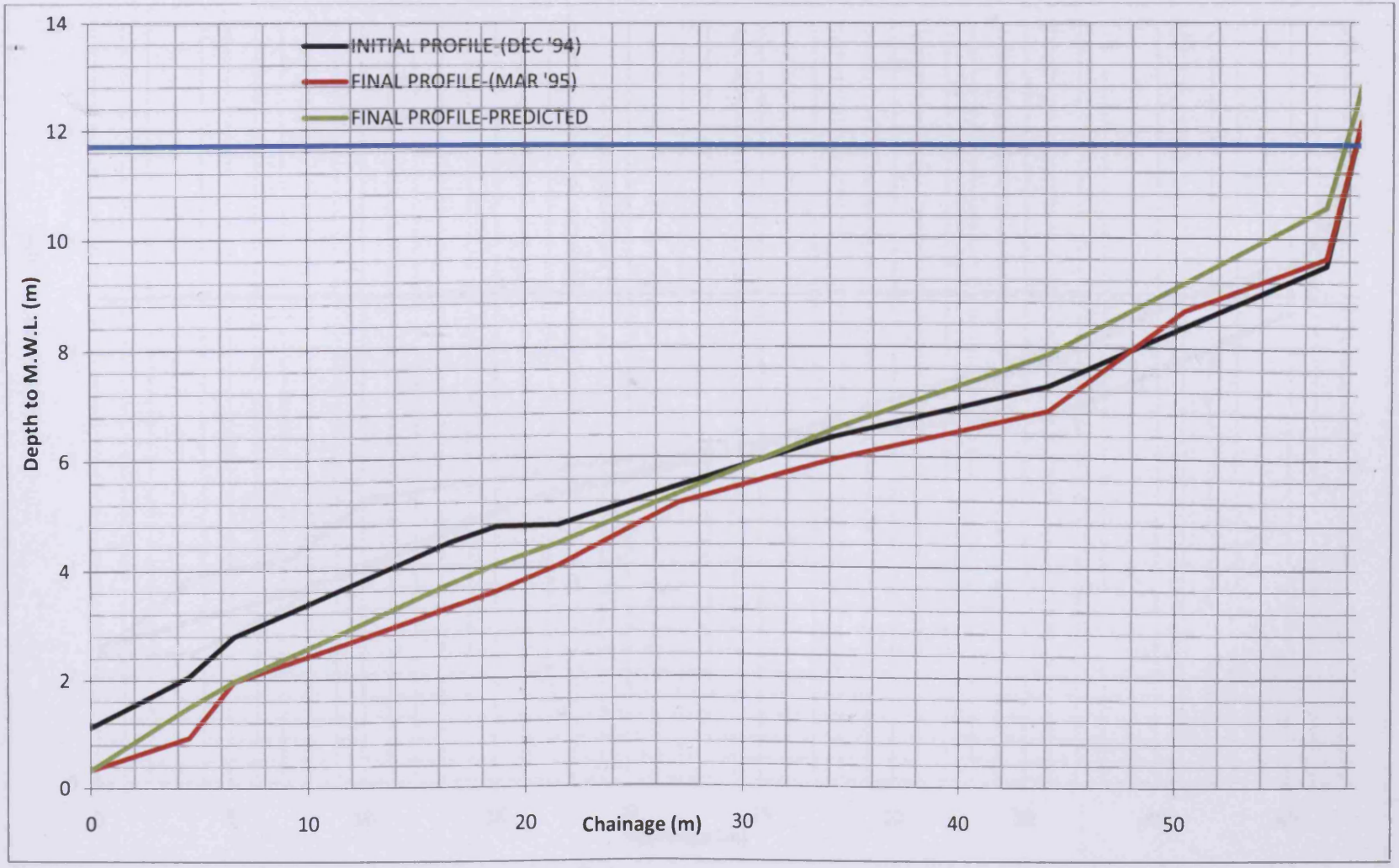

Figure A4- 7 Comparison of predicted and measured beach profile for location A-North (December '94-March '95)

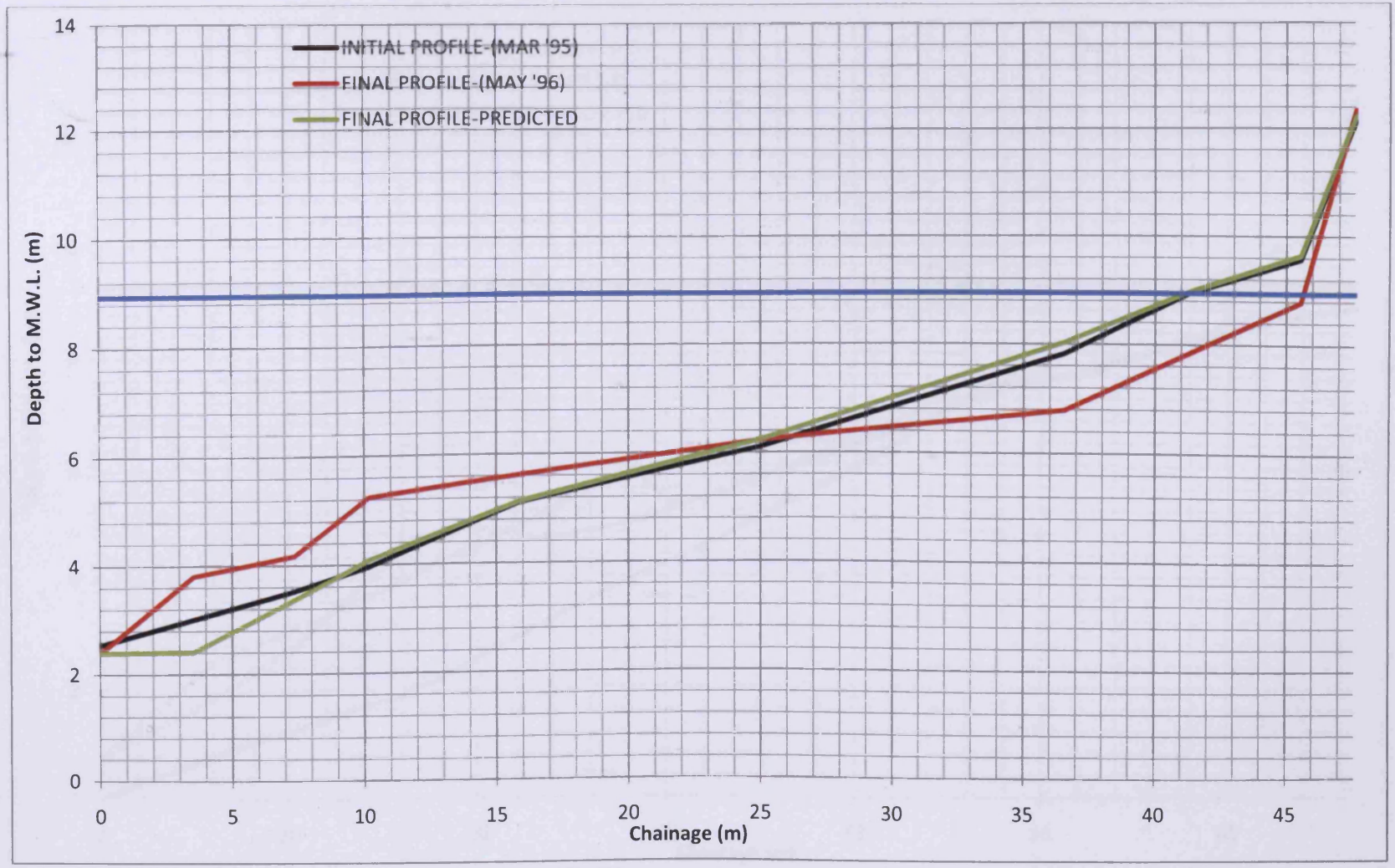

Figure A4- 8 Comparison of predicted and measured beach profile for location A-North (March '95-May '96)

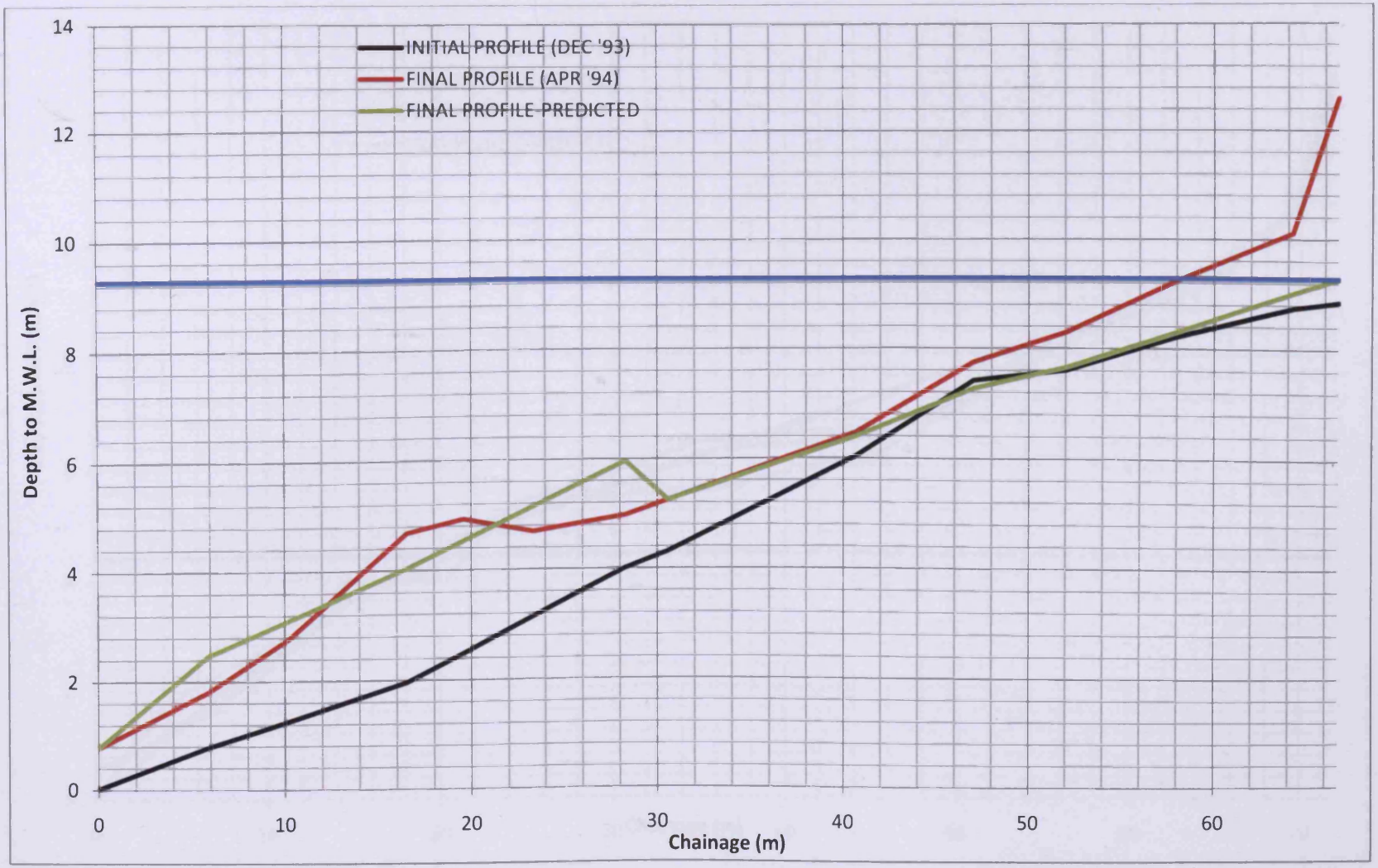

Figure A4- 9 Comparison of predicted and measured beach profile for location A-South (December '93-April '94)

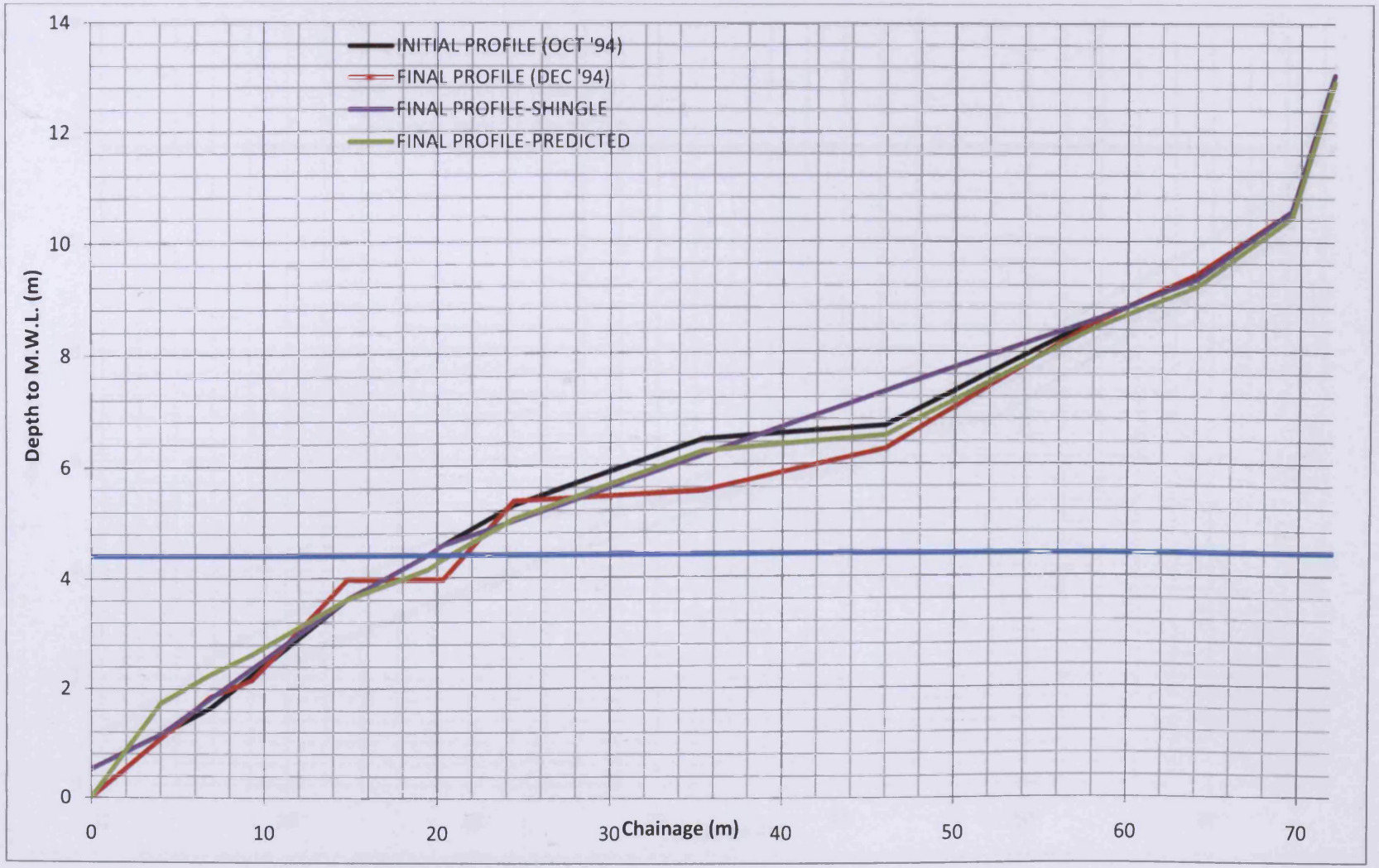

Figure A4- 10 Comparison of predicted and measured beach profile for location A-South (October '94-December '94)

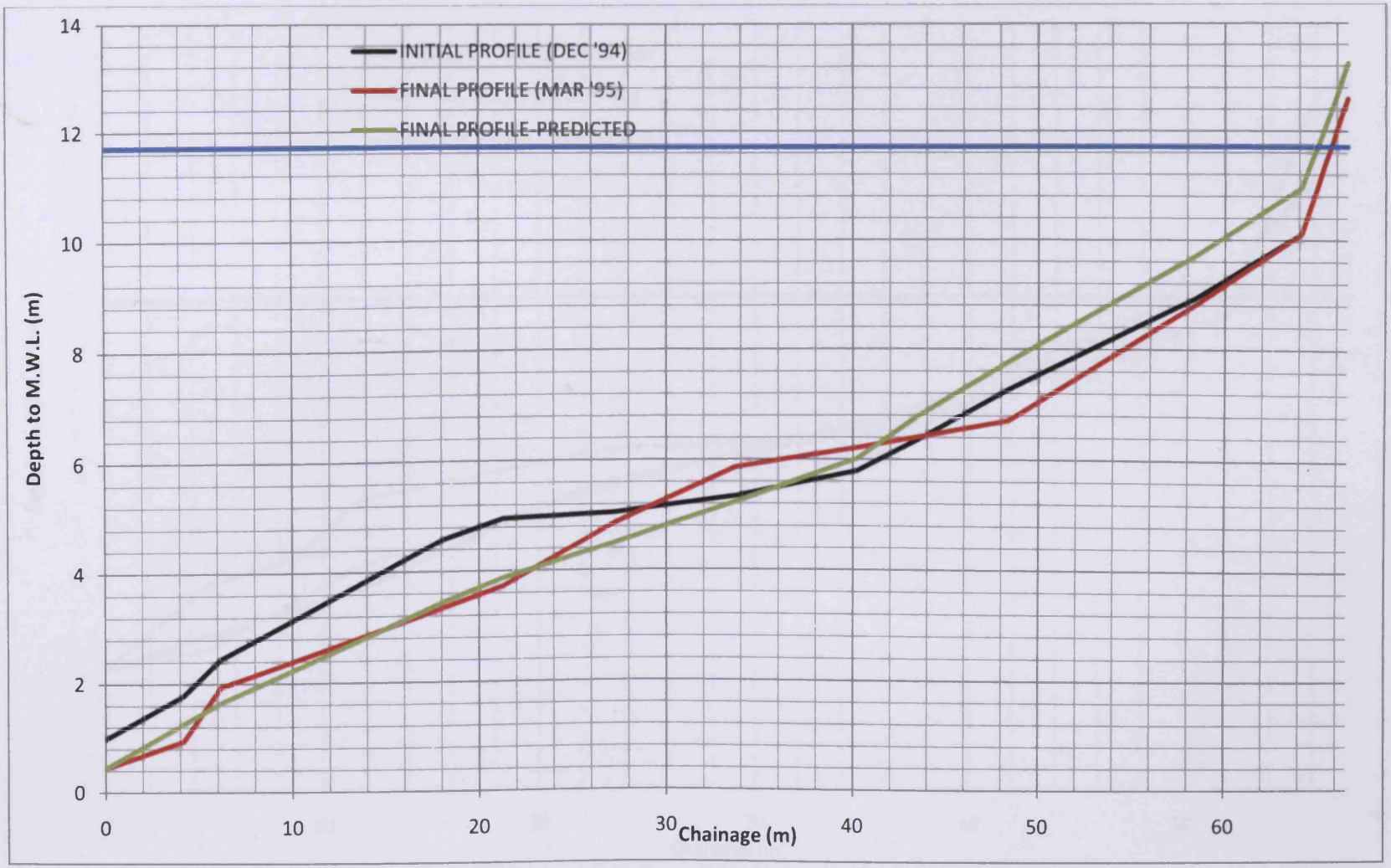

Figure A4- 11 Comparison of predicted and measured beach profile for location A-South (December '94-March '95)

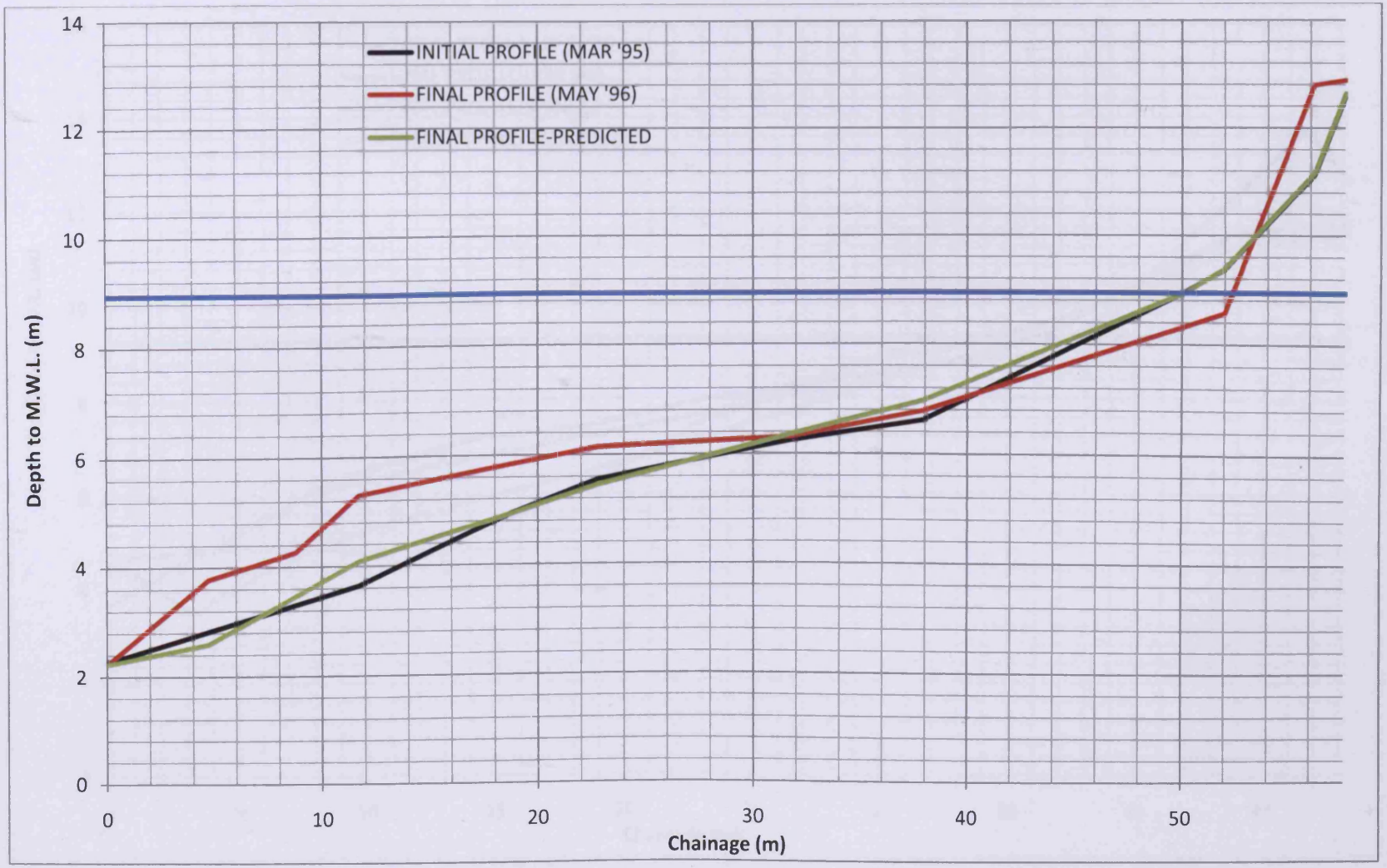

Figure A4- 12 Comparison of predicted and measured beach profile for location A-South (March '95-May '96)

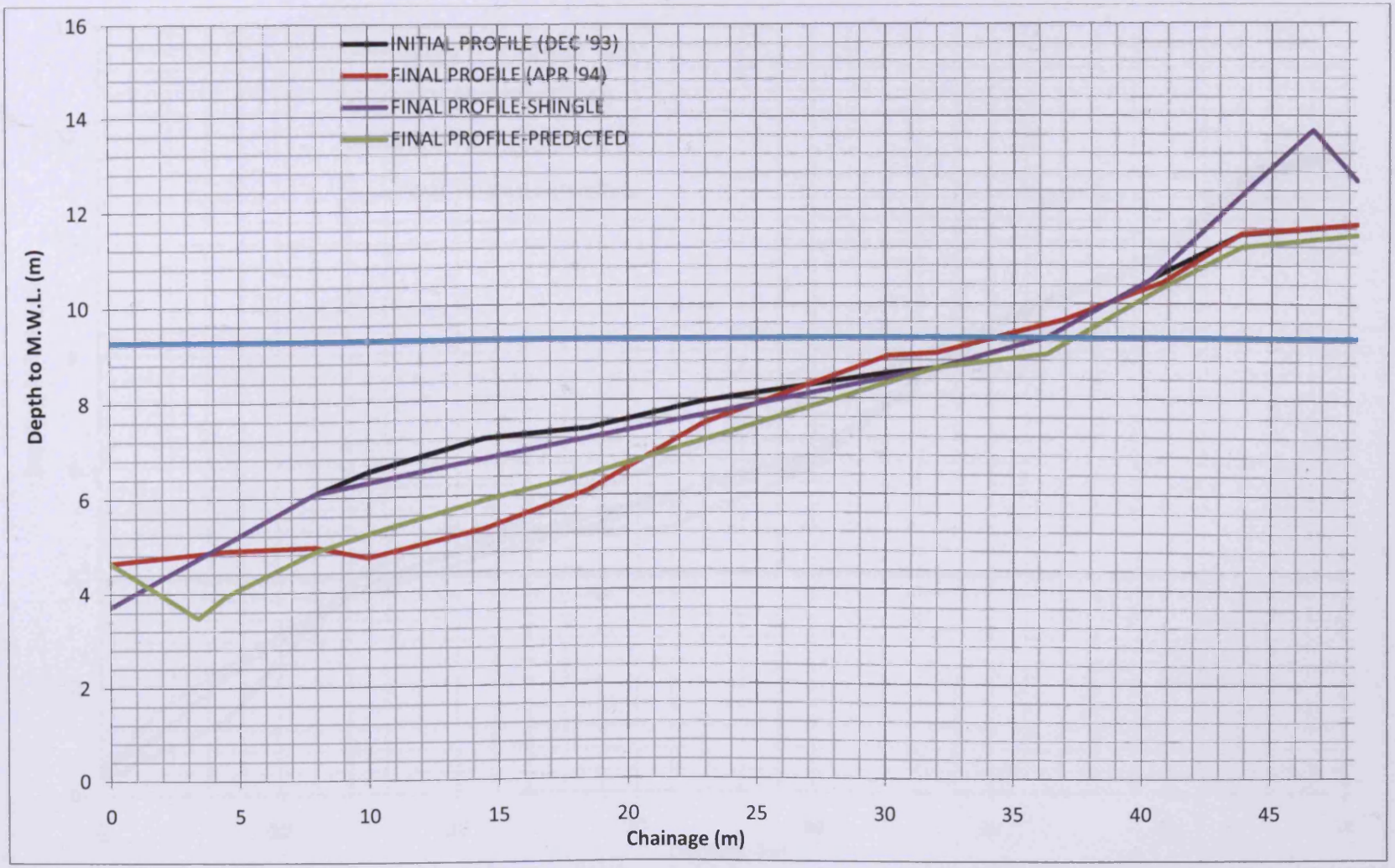

Figure A4- 13 Comparison of predicted and measured beach profile for location B-Middle (December '93-April '94)

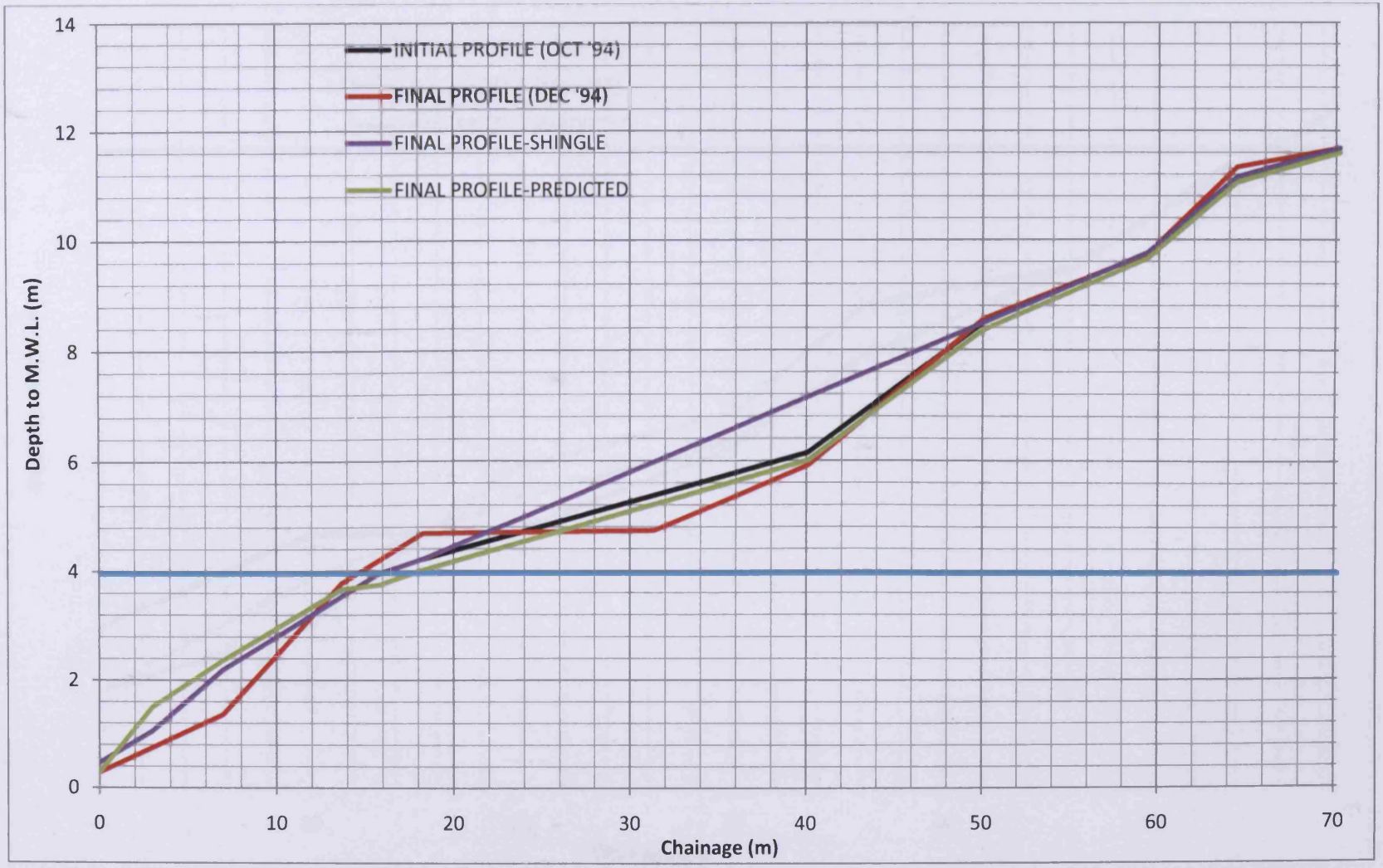

Figure A4- 14 Comparison of predicted and measured beach profile for location B-Middle (October '94-December '94)

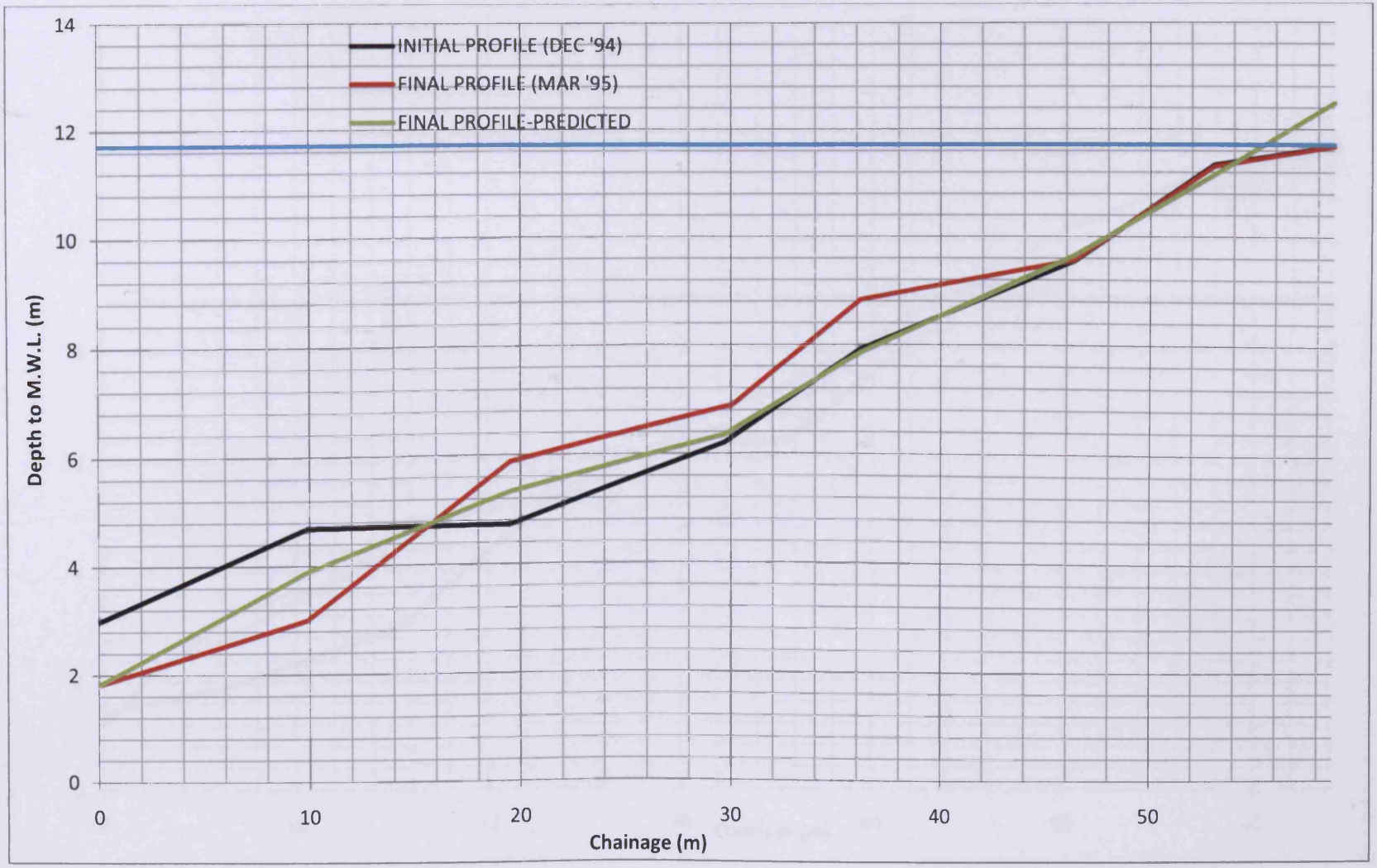

Figure A4- 15 Comparison of predicted and measured beach profile for location B-Middle (December '94-March '95)

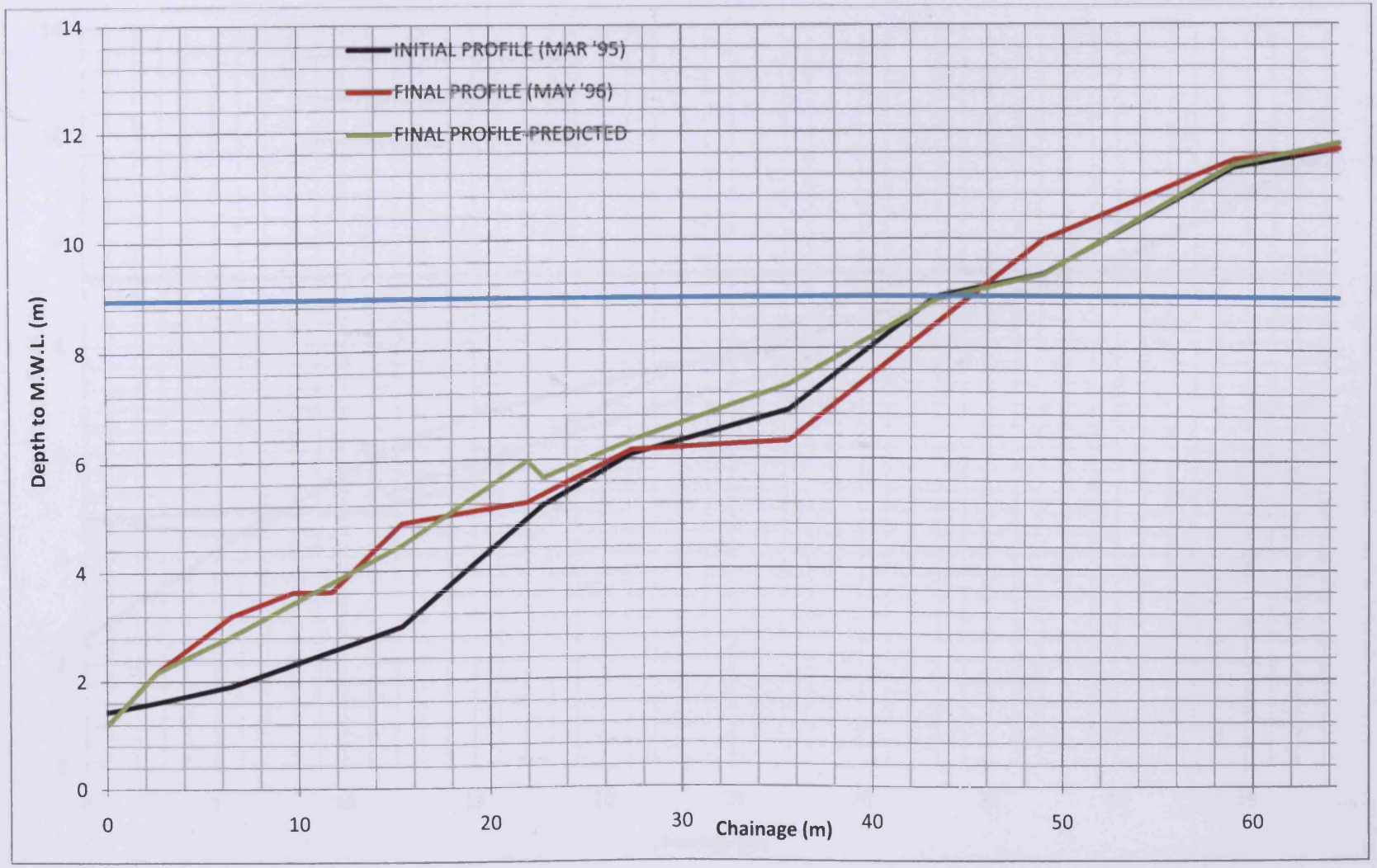

Figure A4- 16 Comparison of predicted and measured beach profile for location B-Middle (March '95-May '96)

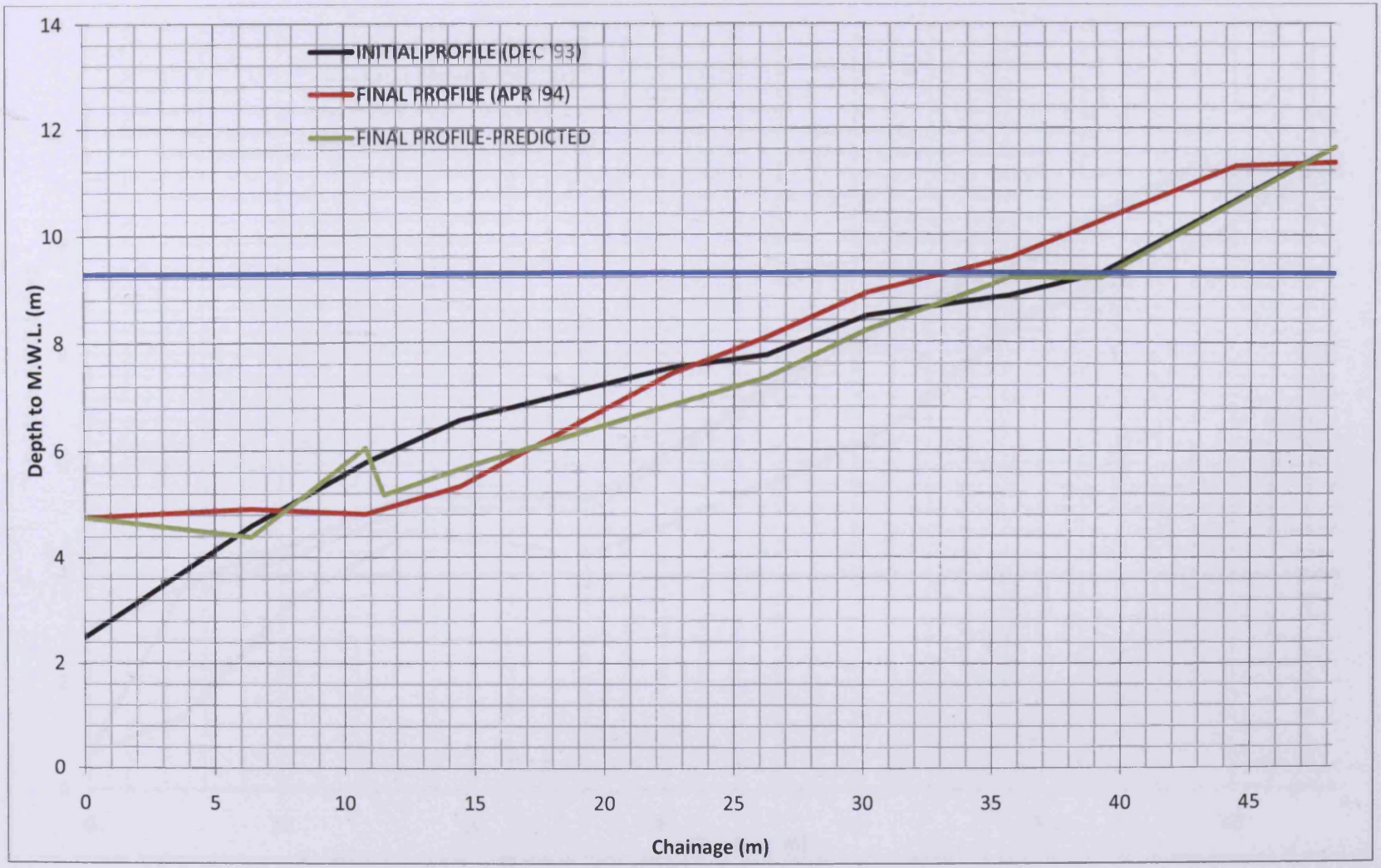

Figure A4- 17 Comparison of predicted and measured beach profile for location B-North (December '93-Apr '94)

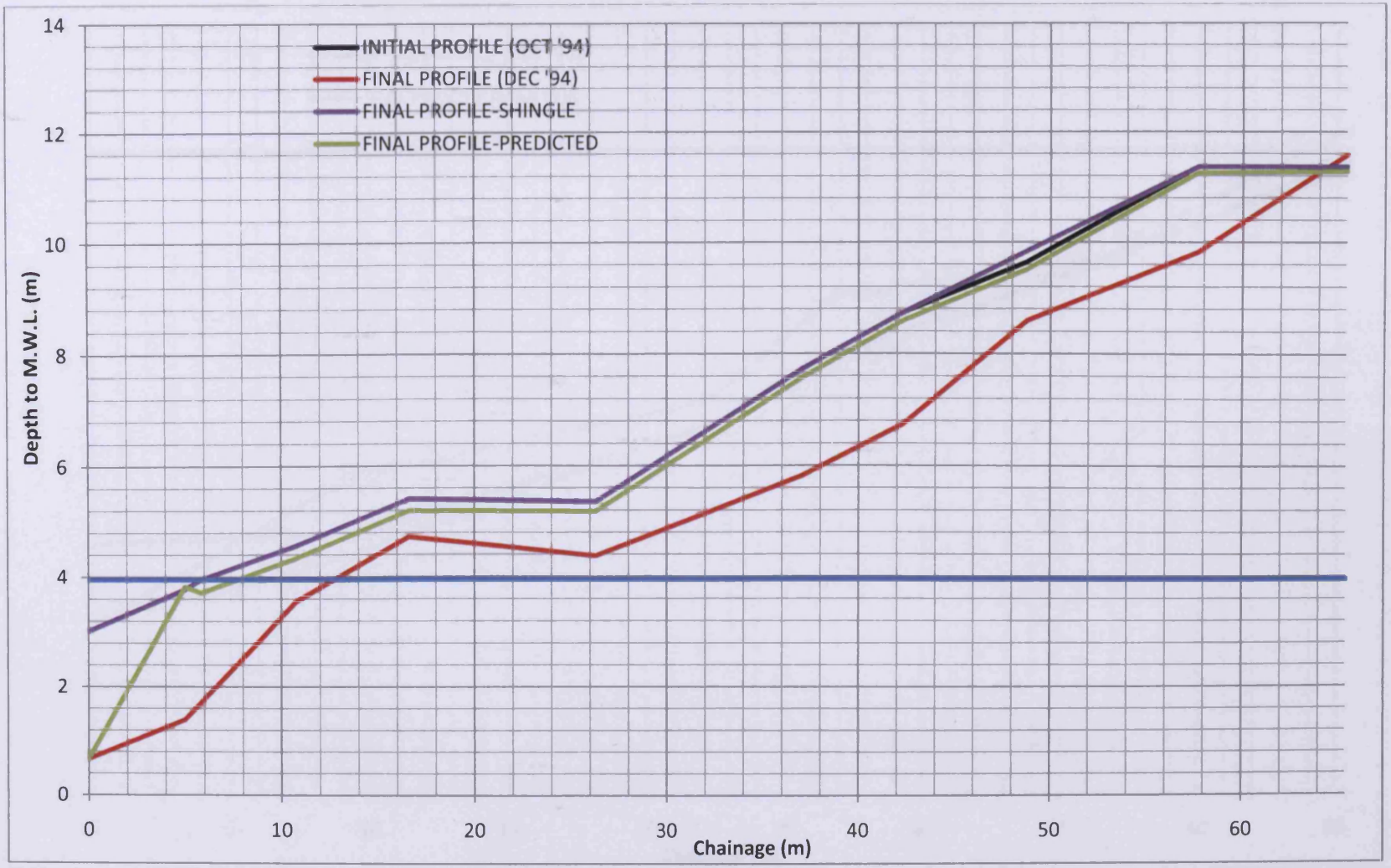

Figure A4- 18 Comparison of predicted and measured beach profile for location B-North (October '94-December '94)

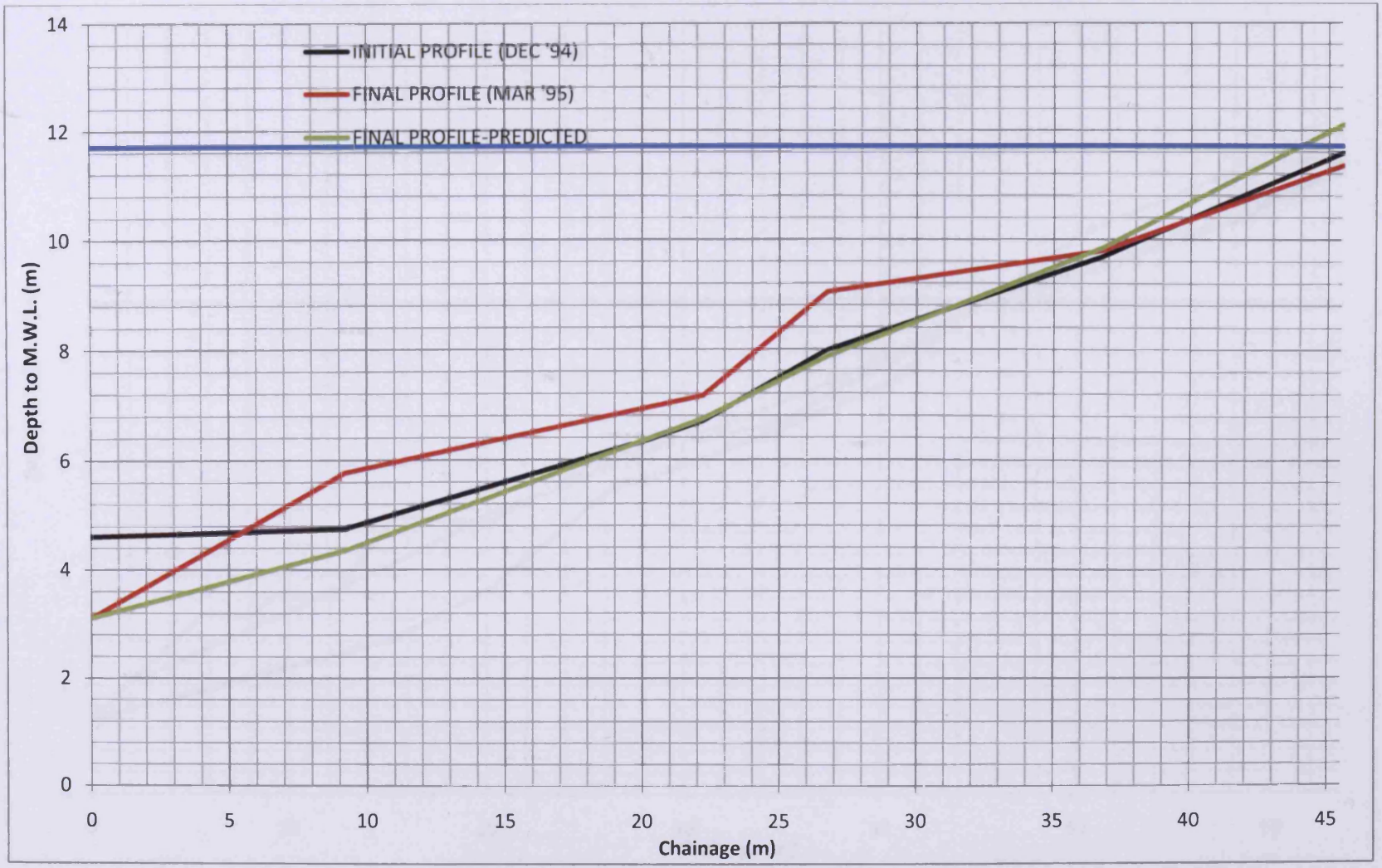

Figure A4- 19 Comparison of predicted and measured beach profile for location B-North (December '94-March '95)

Figure A4- 20 Comparison of predicted and measured beach profile for location B-North (March '95-May '96)

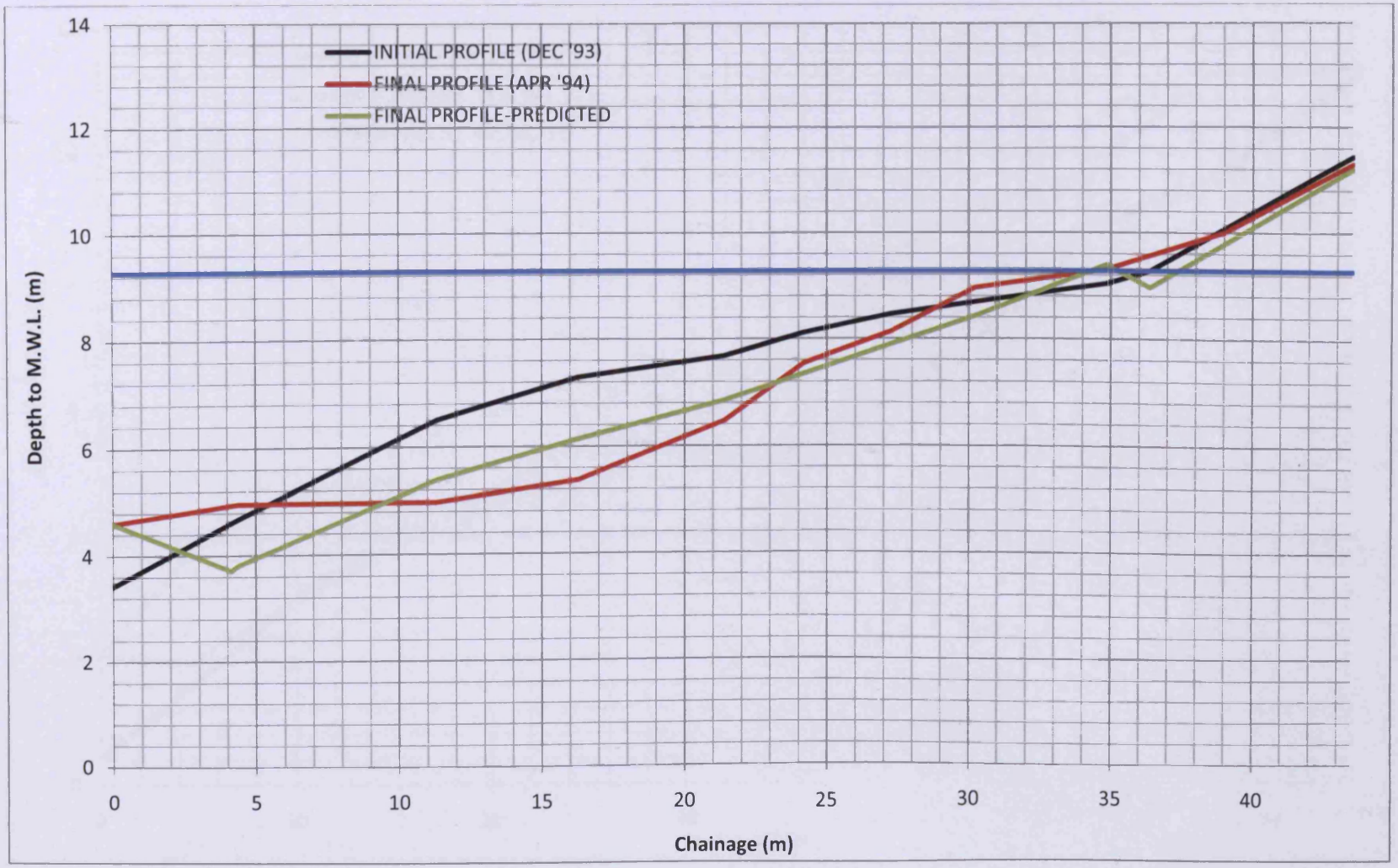

Figure A4- 21 Comparison of predicted and measured beach profile for location B-South (December '93-April '94)

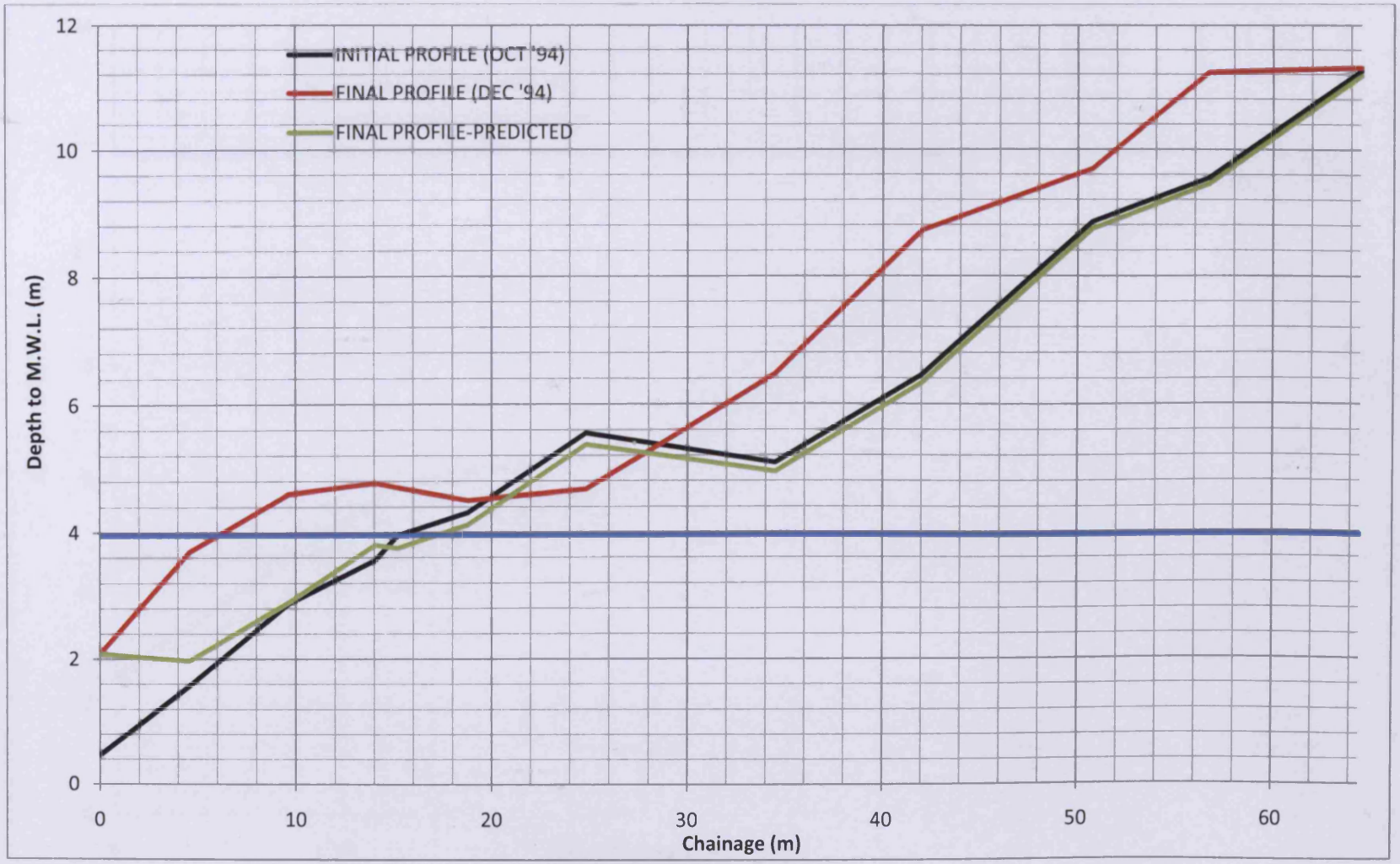

Figure A4- 22 Comparison of predicted and measured beach profile for location B-South (October '94-December '94)

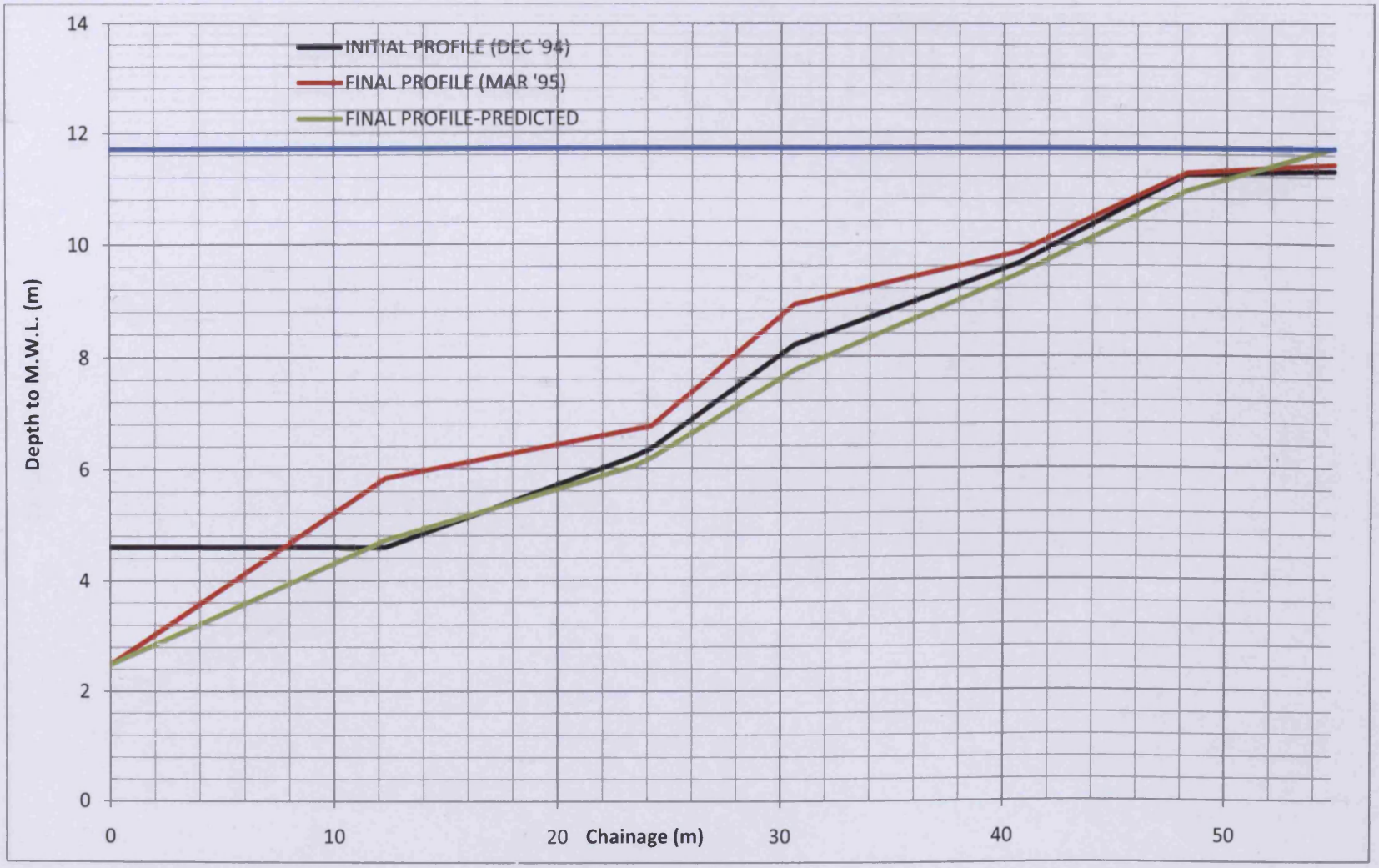

Figure A4- 23 Comparison of predicted and measured beach profile for location B-South (December '94-March '95)

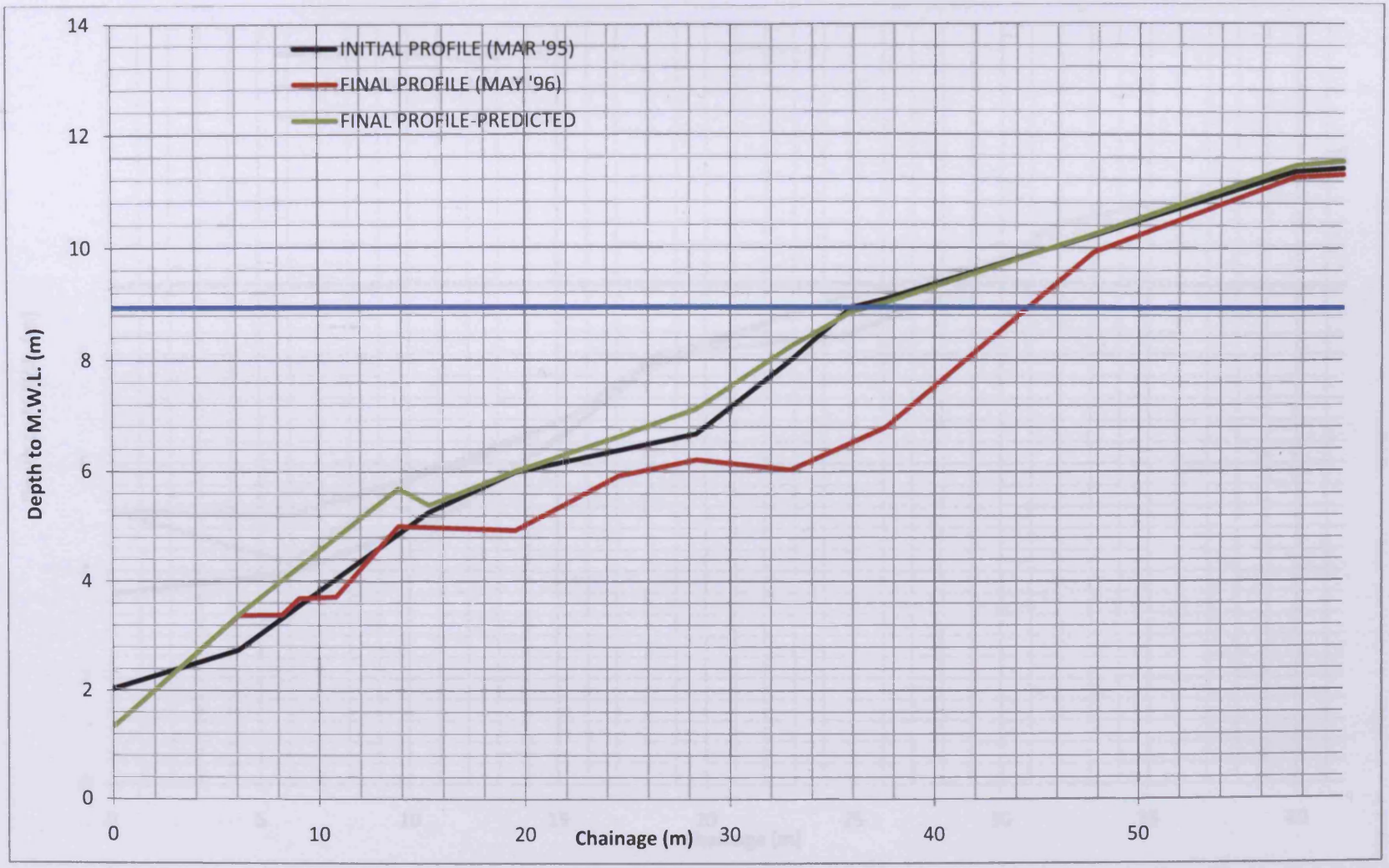

Figure A4- 24 Comparison of predicted and measured beach profile for location B-South (March '95-May '96)

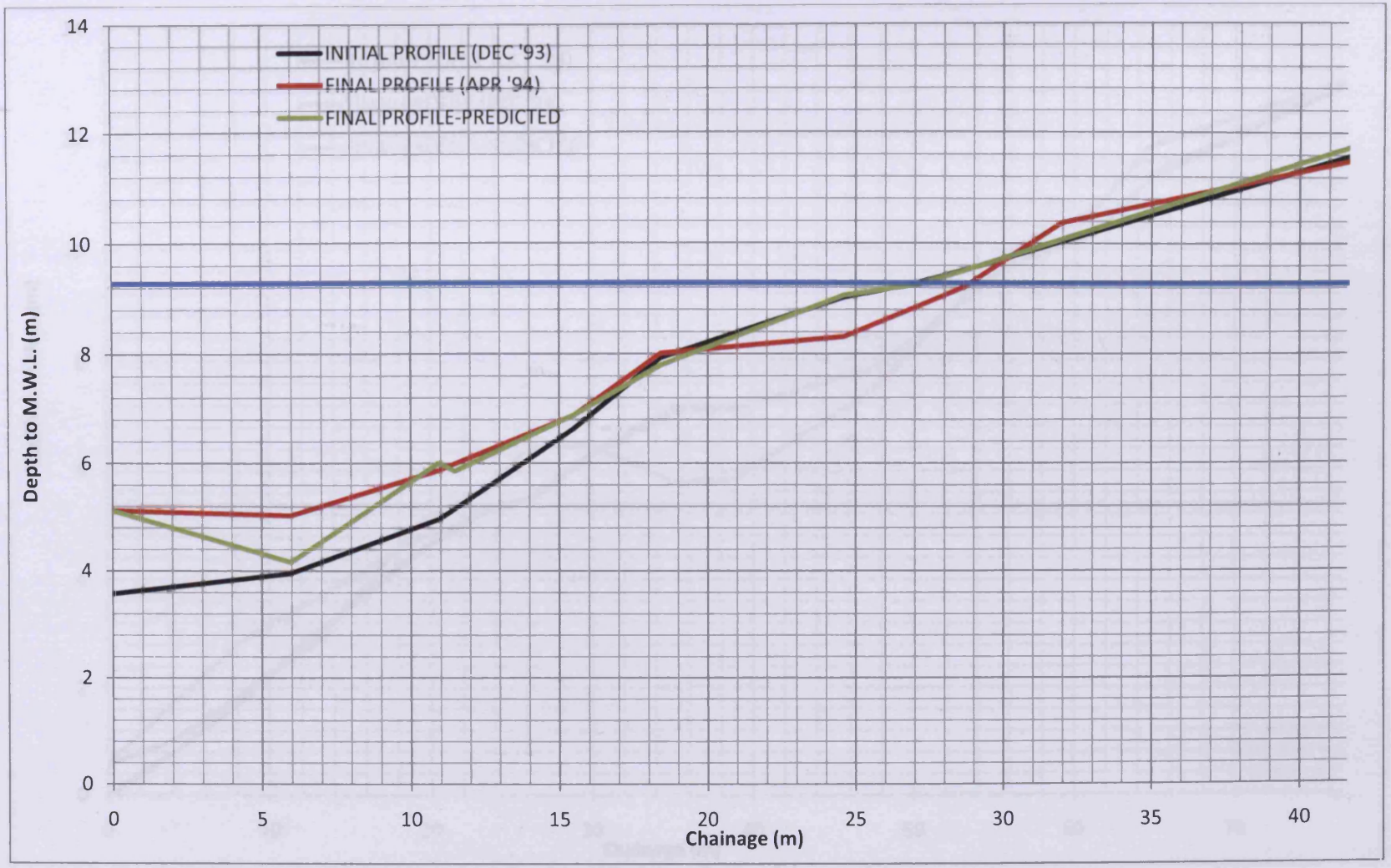

Figure A4- 25 Comparison of predicted and measured beach profile for location C-Middle (December '93-April '94)

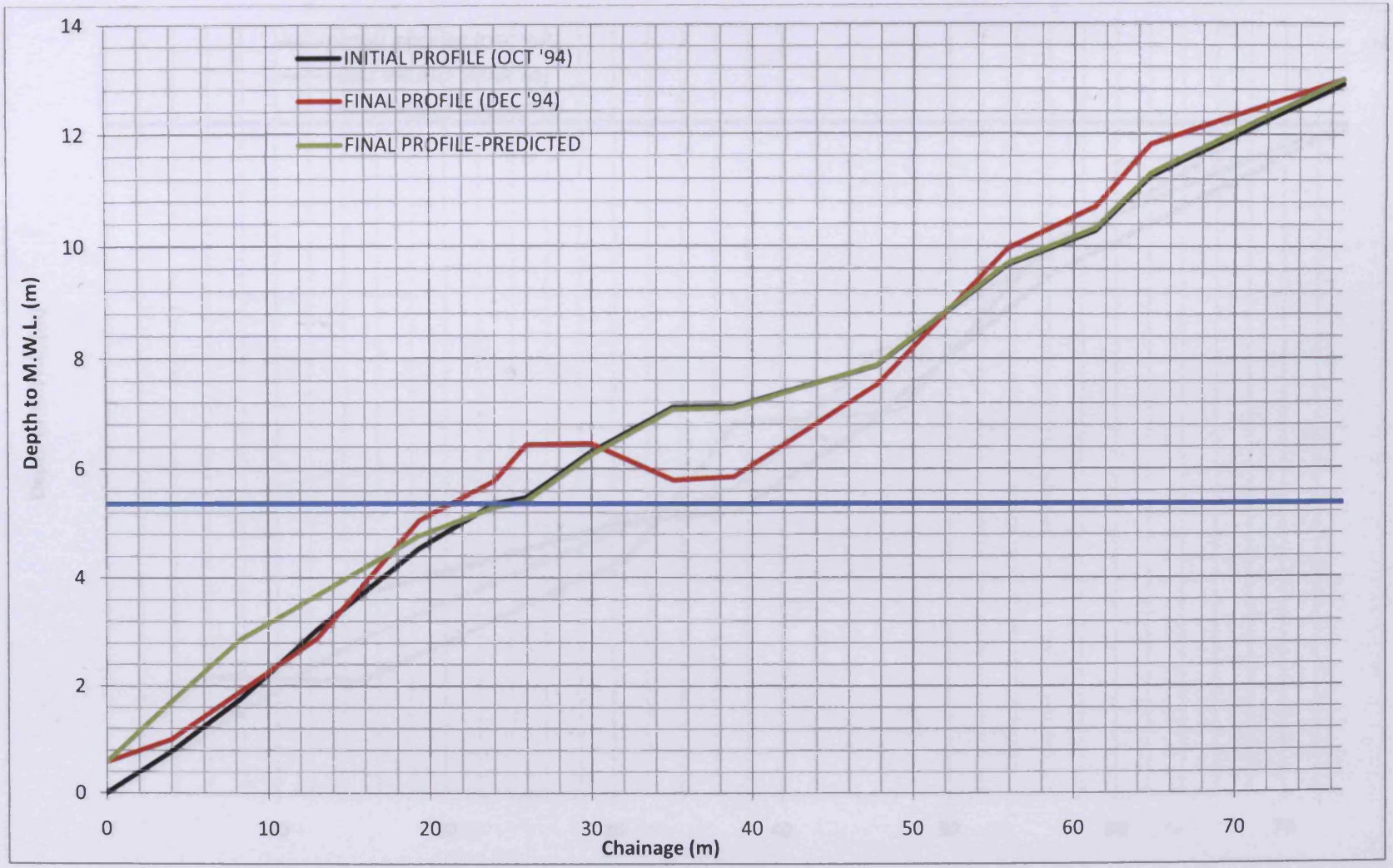

Figure A4- 26 Comparison of predicted and measured beach profile for location C-Middle (October '94-December '94)

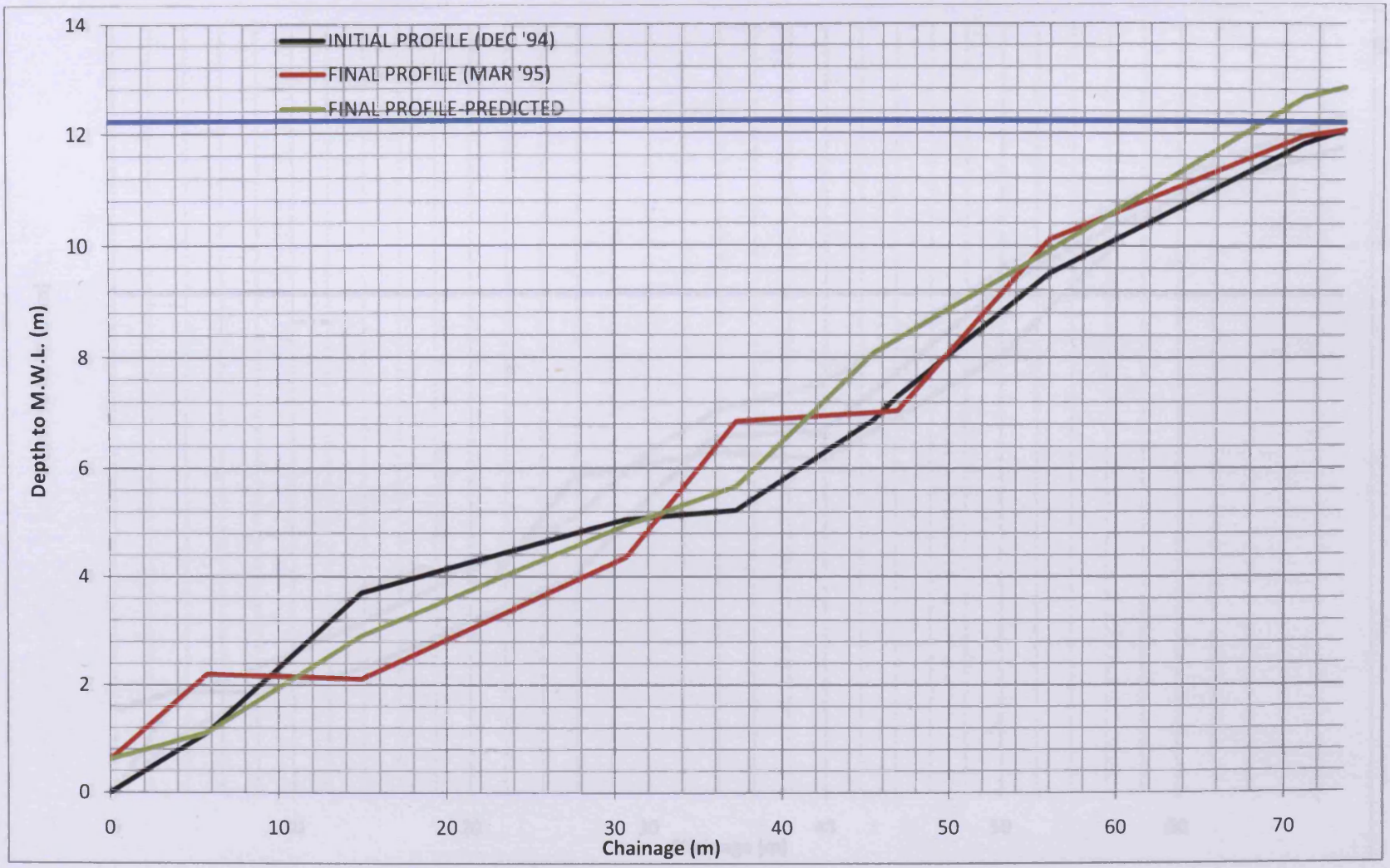

Figure A4- 27 Comparison of predicted and measured beach profile for location C-Middle (December '94-March '95)

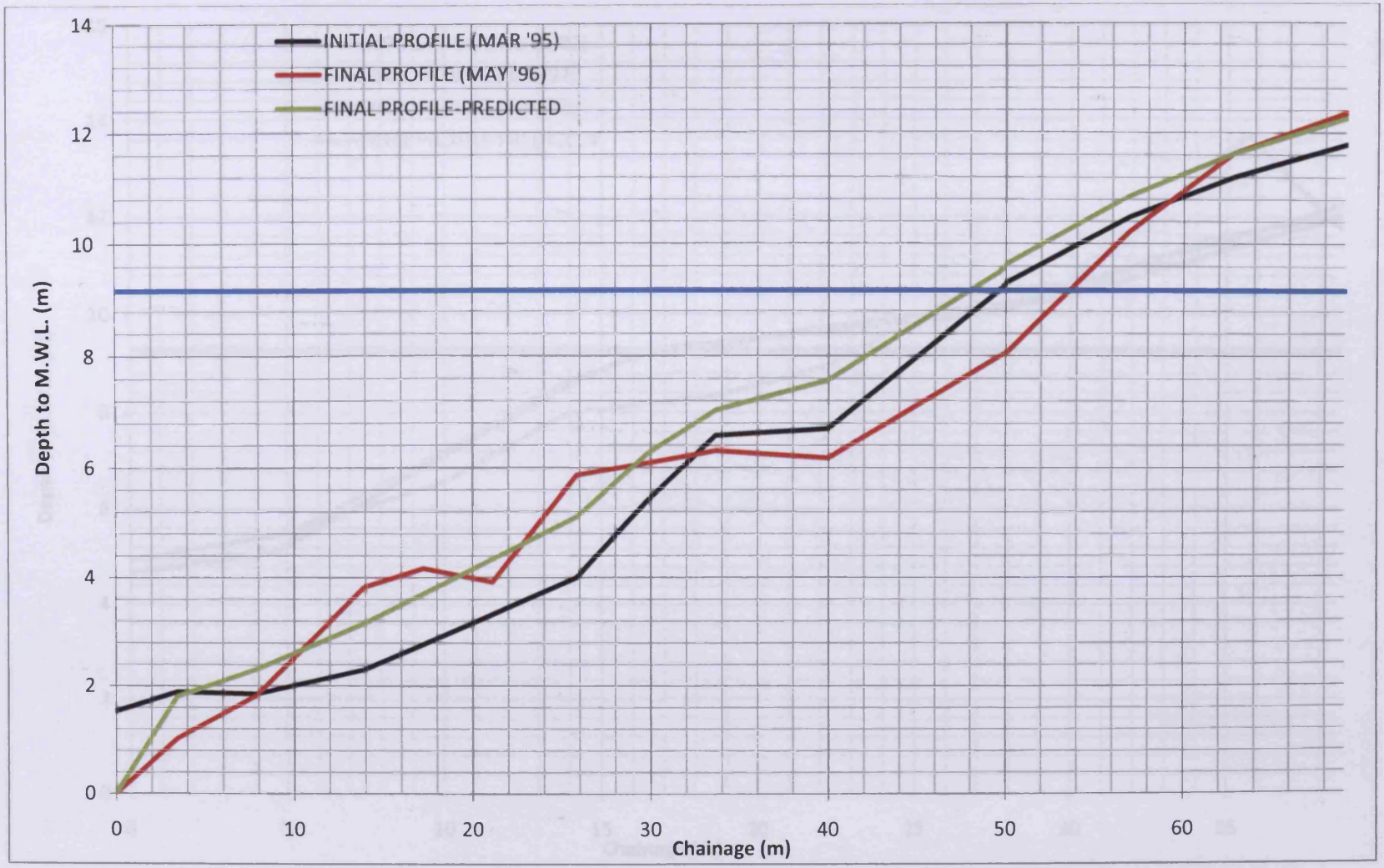

Figure A4- 28 Comparison of predicted and measured beach profile for location C-Middle (March '95-May '96)

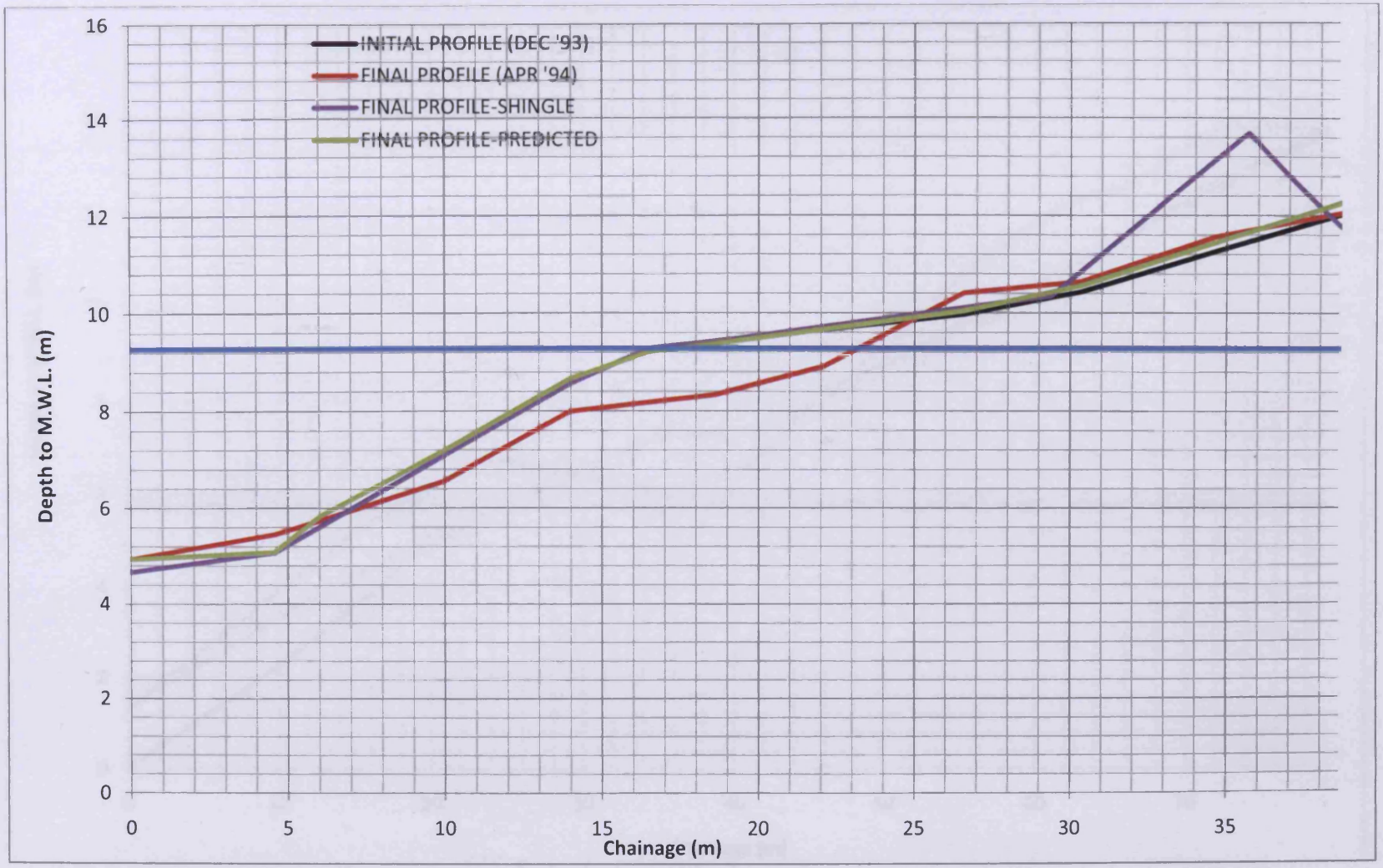

Figure A4- 29 Comparison of predicted and measured beach profile for location C-North (December '93-April '94)

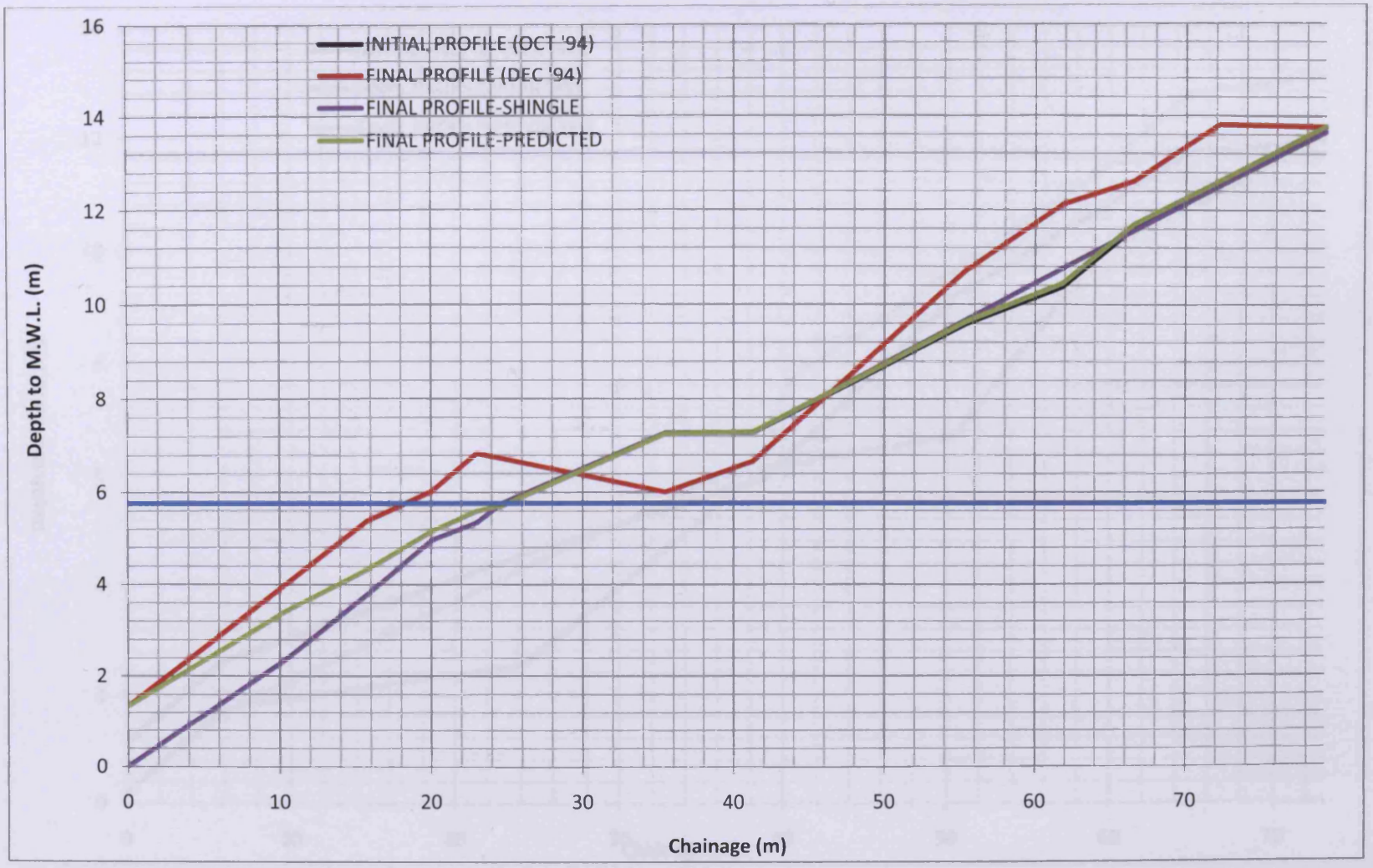

Figure A4- 30 Comparison of predicted and measured beach profile for location C-North (October '94-December '94)

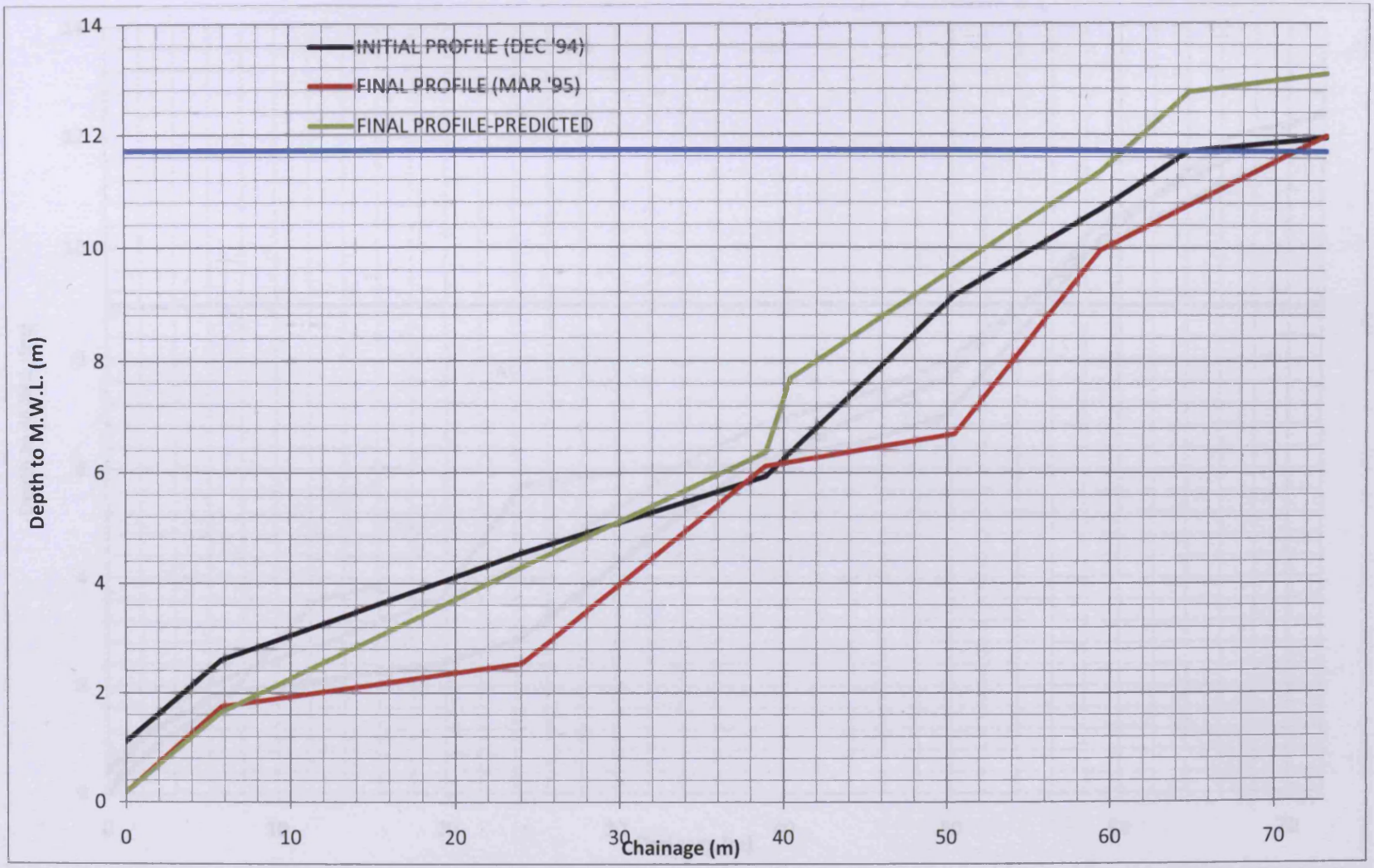

Figure A4- 31 Comparison of predicted and measured beach profile for location C-North (December '94-March '95)

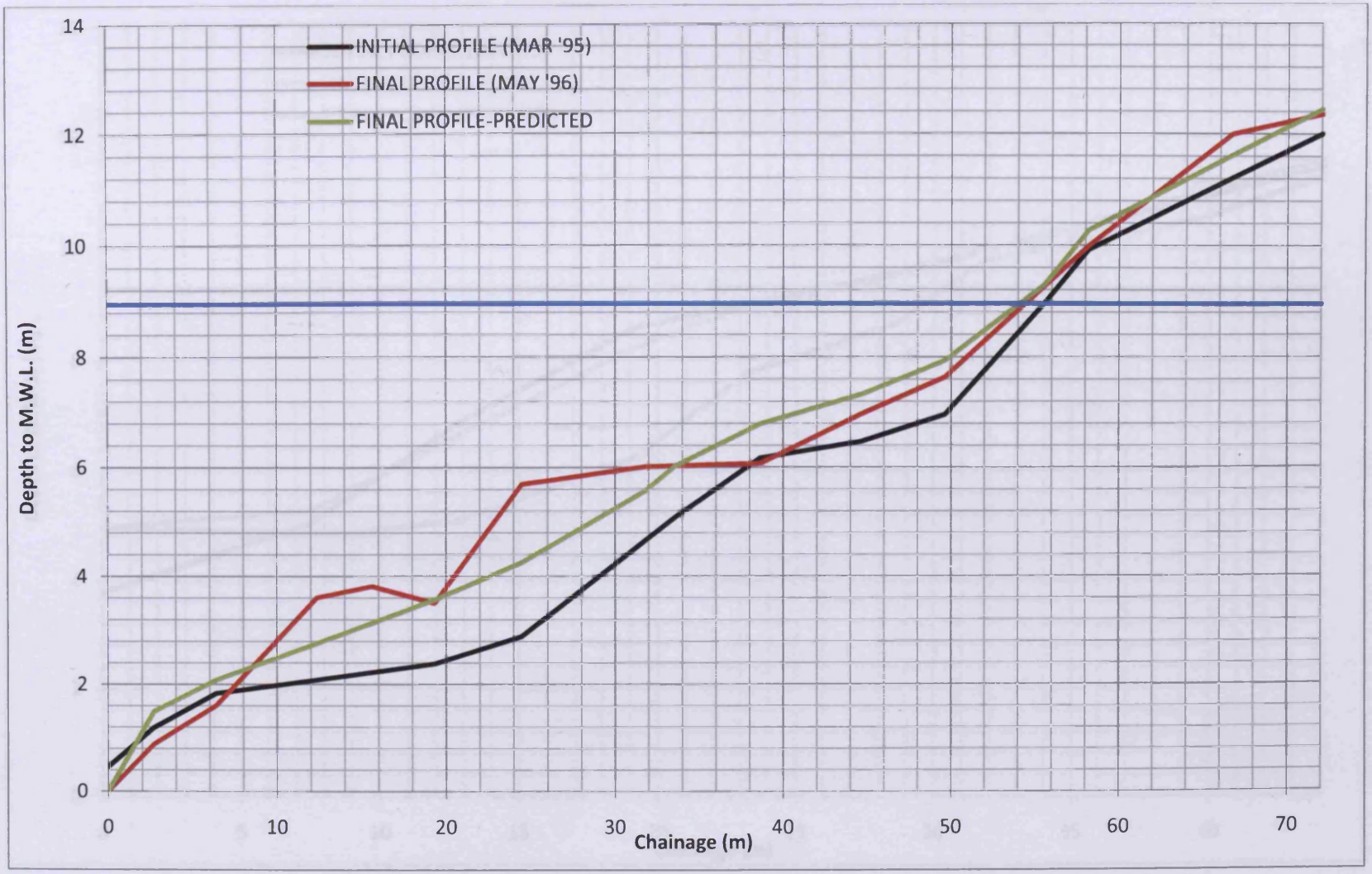

Figure A4- 32 Comparison of predicted and measured beach profile for location C-North (March '95-May '96)

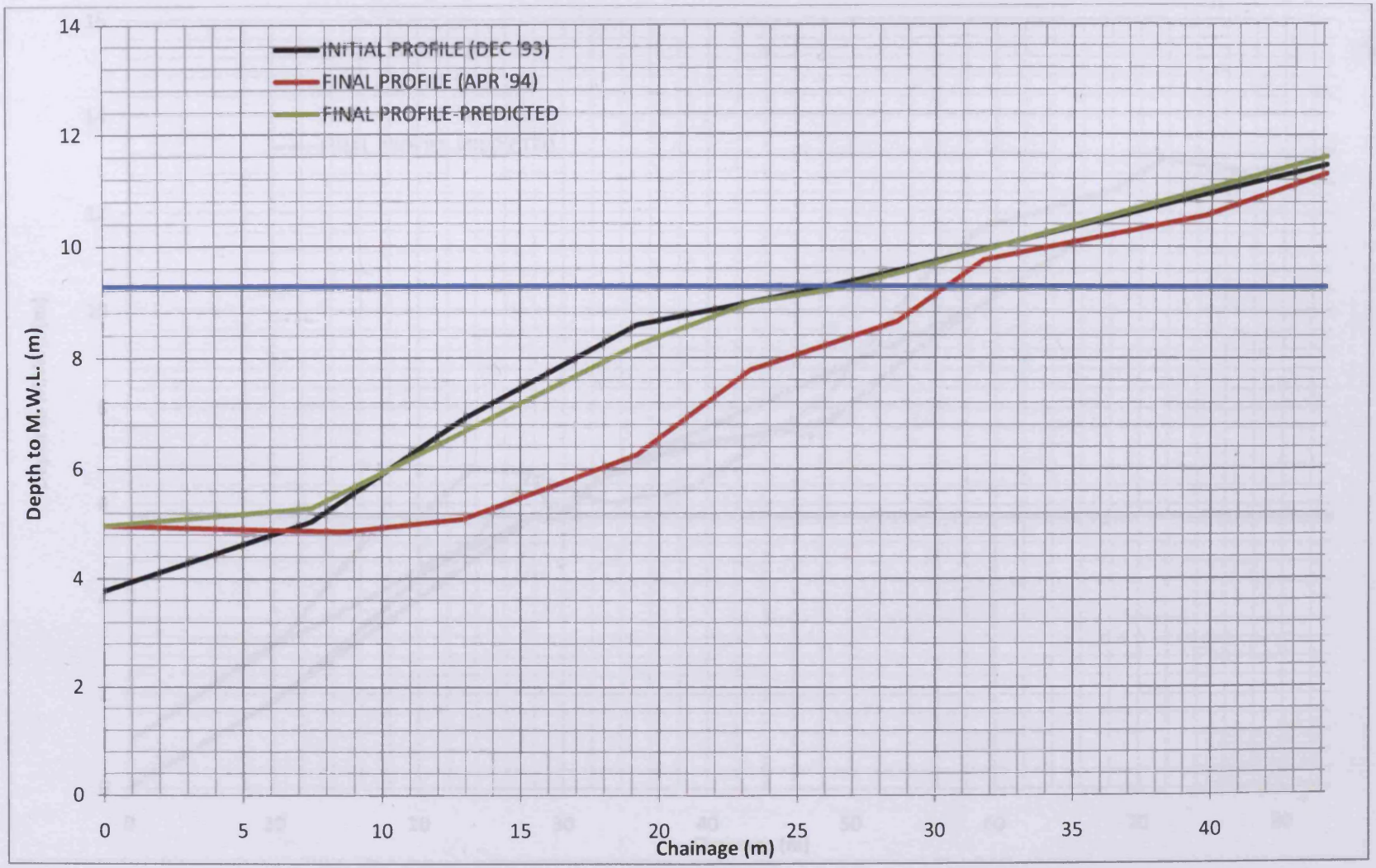

Figure A4- 33 Comparison of predicted and measured beach profile for location C-South (December '93-April '94)

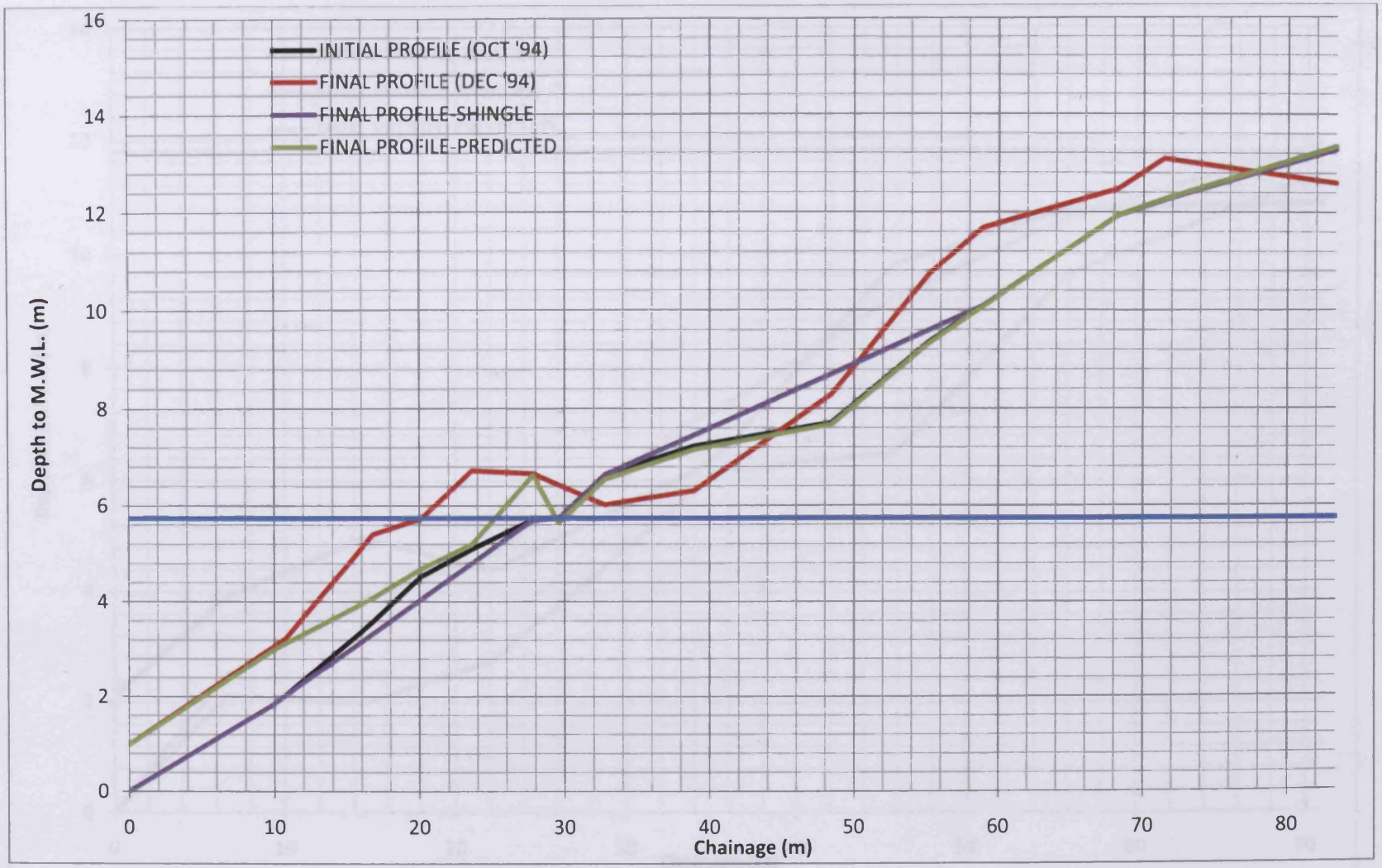

Figure A4- 34 Comparison of predicted and measured beach profile for location C-South (October '94-December '94)

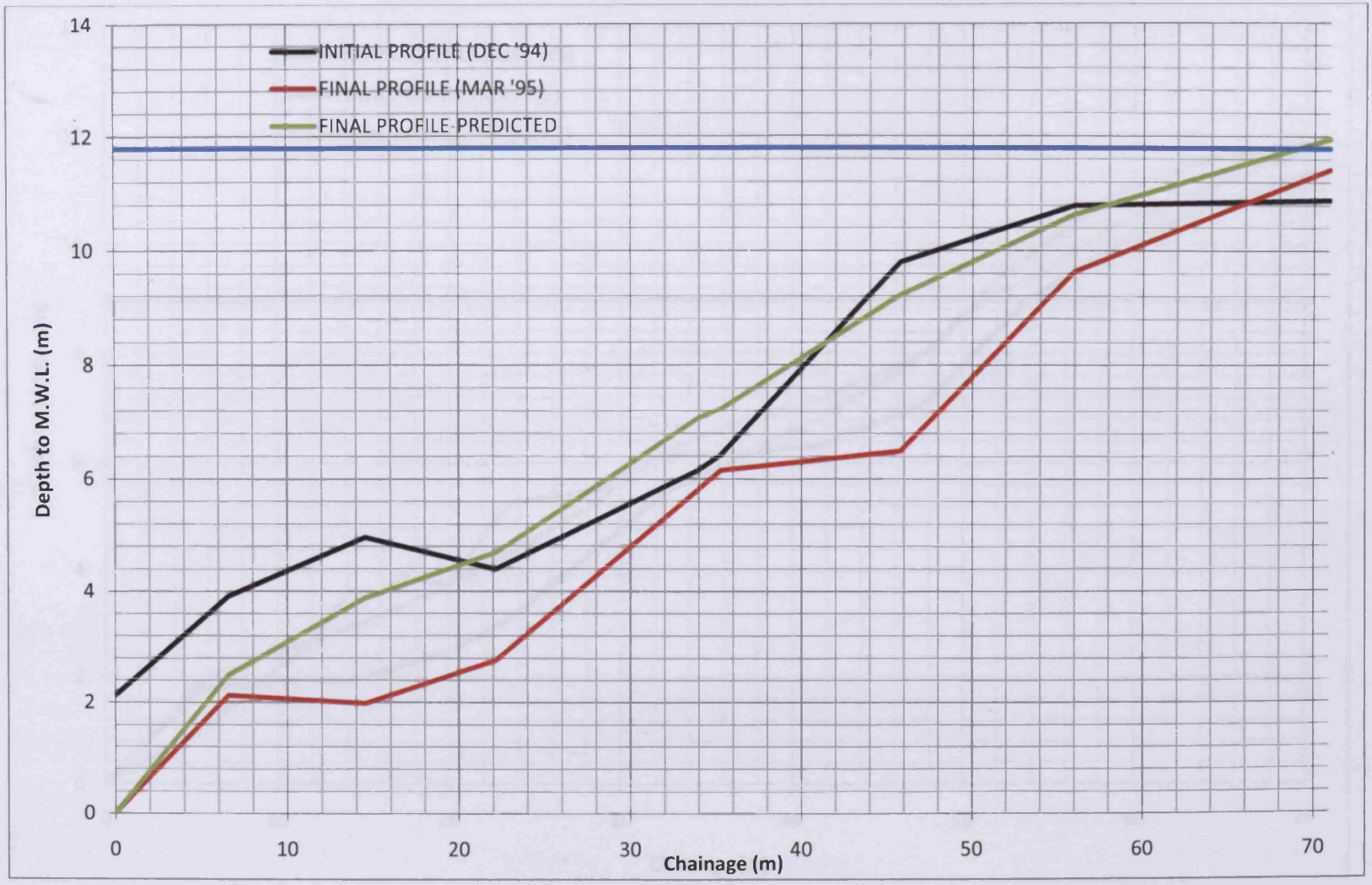

Figure A4- 35 Comparison of predicted and measured beach profile for location C-South (December '94-March '95)

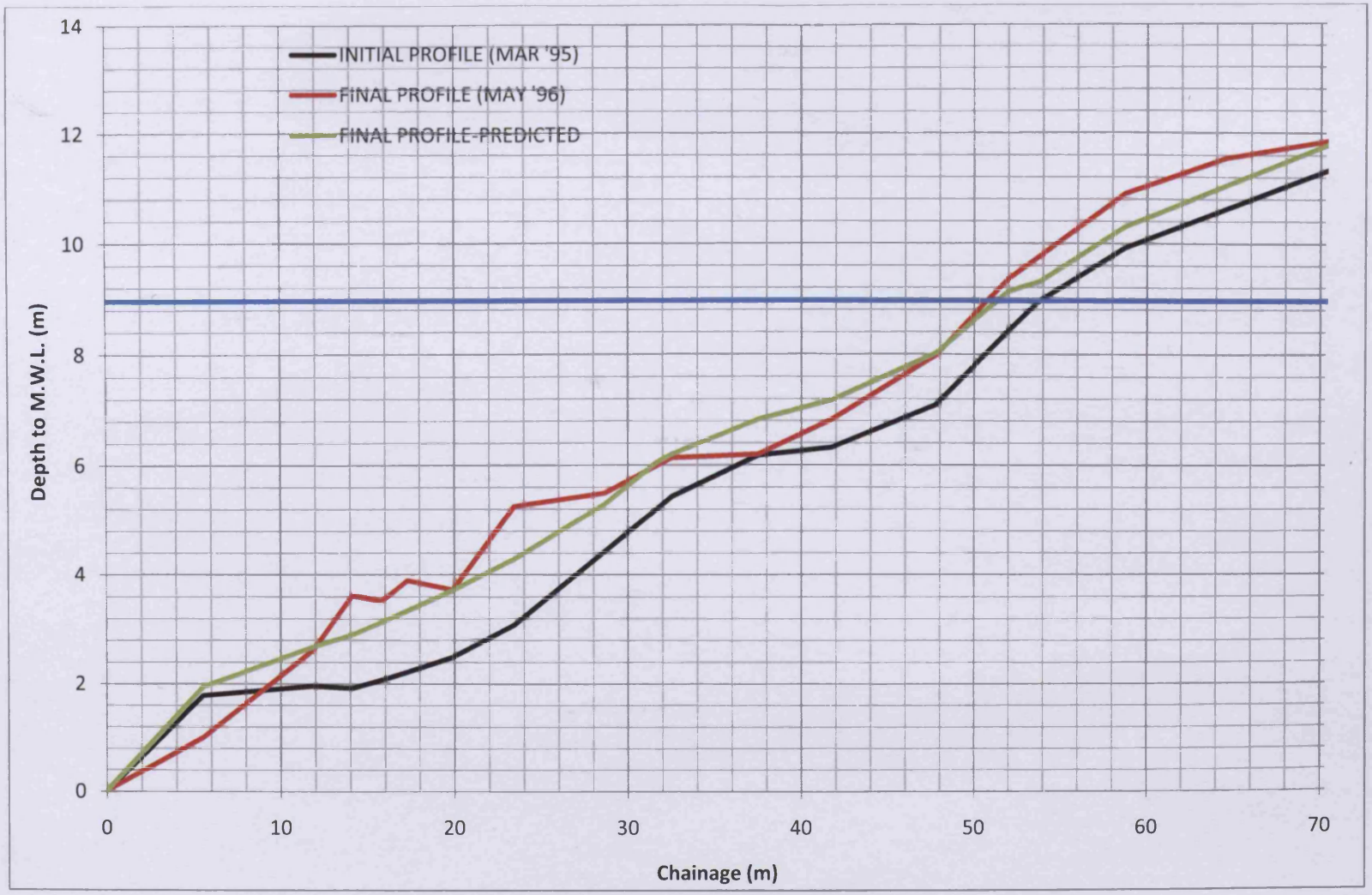

Figure A4- 36 Comparison of predicted and measured beach profile for location C-South (March '95-May '96)